West Virginia Super Circuit Project

Final Report

Submitted to:

U.S. Department of Energy

by:

Monongahela Power

May 30, 2014

DOE ACKNOWLEGEMENT
This material is based upon work supported by the Department of Energy under Award Number DE-FC26-08NT02868

This page is intentionally left blank

Contents

List of Figures

List of Tables

1.0 Executive Summary

The West Virginia Super Circuit (WVSC) project was proposed to demonstrate improved performance and reliability of electric supply through the integration of distributed resources and advanced technology.

1.1 Project Overview

The project objectives and five technologies are listed below. Project financial report information is in Appendix G.

Objectives

1. Achieve greater than 15% peak power reduction, cost competitive with capacity upgrades on a Mon Power circuit located in Morgantown, WV
2. Demonstrate the viability of advanced circuit control through multi-agent technologies
3. Leverage advanced wireless communications to address interoperability issues between control and protection systems and distributed energy resources
4. Demonstrate the benefits of the integrated operation of technologies such as rotary and inverter-based distributed generation, energy storage, Automated Load Control (ALC), advanced wireless communications, and advanced system control technologies
5. Demonstrate advanced operational strategies such as dynamic islanding and micro-grids to serve priority loads through advanced control strategies
6. Demonstrate the reliability benefits of Dynamic Feeder Reconfiguration across several adjacent feeders

Technologies

1. **Microgrid System**
   A microgrid system was designed, modeled and simulated with Mon Power circuit data in grid connected and islanded operation modes using the Distributed Energy Resources (DER). DERs were designed to be installed at a microgrid site including a natural gas fired generator, a solar photovoltaic system, an energy storage system, and a supporting communications system.

2. **Fault Location Isolation Restoration System**
   An agent-based Fault Location Isolation Restoration (FLIR) logic system using some of a pre-existing system was designed, modeled and simulated with Mon Power circuit data to improve system reliability.

3. **Fault Location Algorithm and Fault Prediction Algorithm**
   An intelligent fault location algorithm (FLA) and intelligent fault prediction algorithm (FPA) was developed by North Carolina State University (NCSU) utilizing data from field deployed sensors. These schemes were designed to extract fault current and type information from the field sensor data and using a system model estimated fault location.

4. **DER Dispatch for Peak Reduction**
   Distributed Energy Resource (DER) distributed generation from a local area hospital was designed to be used to enable peak load reduction on a single distribution feeder. Forecasted feeder load was designed to be used to reduce peak load levels. Hospital loads were designed and analyzed to be transferred to the distributed generator to affect 15% the load reduction on the distribution feeder.

5. **Advanced Communication System**
   An open architecture system was designed that incorporated an advanced communication system with access points and sensor network appliances that were procured fully capable of intelligent, distributed control located on selected distribution circuits.

Figure 1-1 shows a graphic of the proposed project site location.

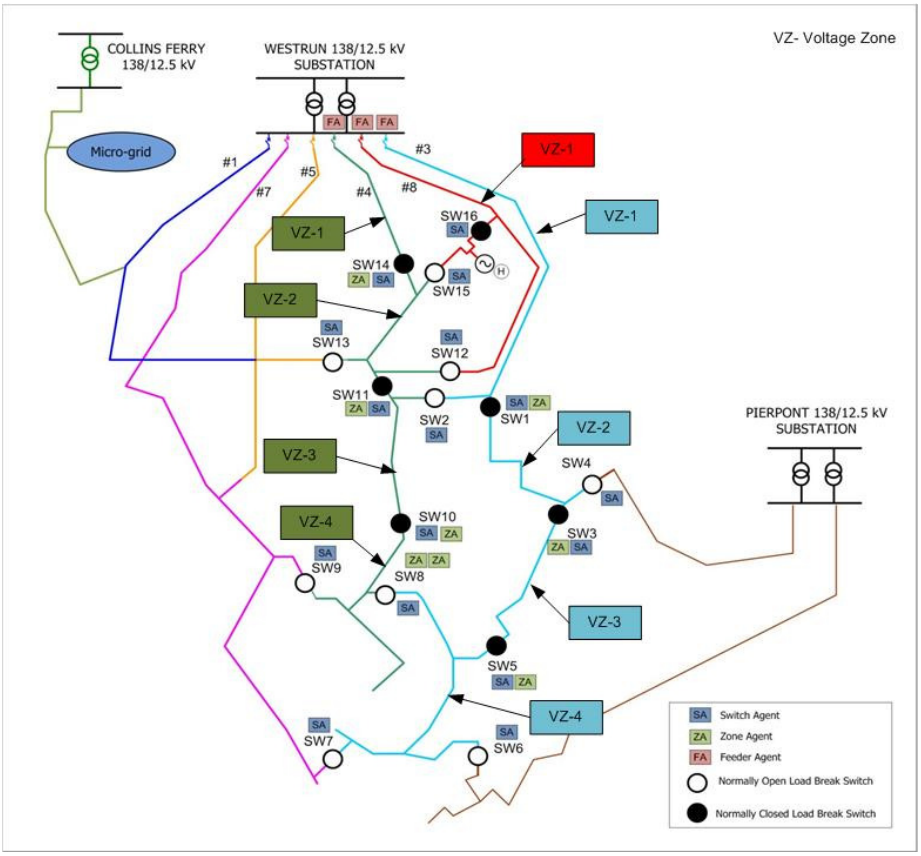

Figure 1-1: WVSC Site Graphic

1.2 Lessons Learned

The WVSC project work provided lessons learned that indicated that significant investment in infrastructure and additional research is still needed for modernizing the electric distribution system and can inform future projects and activities. The lessons learned fall into three categories: technology, communications and siting as described in the Section 6.

The proposed WVSC project included systems design, modeling and simulation (M&S), data collection and demonstration tasks. The design, M&S tasks were successfully completed by project partners. The project was then re-evaluated per decision gate criteria and prior to the deployment/demonstration phase. The project utilized the requirements driven VEE process methodology as described in Section 4.0 for technology development at sub-system and system levels, and significantly higher costs were identified in order to realize utility level integration results. The evaluation gave Mon Power the understanding of the significant changes that were required. Due to significantly higher costs to achieve utility level integration, the project team, with the DOE review team, determined at the conclusion of the project period to proceed directly to develop a final report on the work already performed. The project design methodology, modeling and simulation results provide insights and learnings to support grid modernization.

Analysis and evaluation of the performance of each technology system to assess operational value and identify both expected and unexpected outcomes was tasked. A cost benefit analysis (CBA) of each technology deployed was also tasked, however because the systems were not deployed at a utility level, no actual CBA of the installed system was able to be performed. A university CBA study using hypothetical and estimated values was performed and is included in Appendix F.

1.2.1 Technology Lessons Learned

1.2.1.1 *Equipment*

The maturity of smart grid devices is still developing in the industry, resulting in a limited selection of off-the-shelf devices and the use of some devices that "almost do the job."

Unanticipated installation costs were encountered. The original budget estimates provided by potential vendors proved to be much lower than the quoted prices for installation when firm bids were requested, about 50% above the quoted costs obtained from vendors and that installing the project would not be cost effective within the budget. For example, the cost of the control house designed for the microgrid equipment increased drastically. Also, costs to reconfigure Utility facilities to accommodate the project systems were higher than anticipated. Due to significantly higher costs to utility level integration, the project team, with the DOE review team, determined at the conclusion of the project period, to proceed directly to develop a final report on the work already performed.

Microgrid simulations of the control design showed that the integration of the PV/BESS systems in the microgrid can support capacity firming and load following use cases.

1.2.1.2 *Modeling Tools*

Identifying a single power system modeling software that allowed simulation of different modeling scenarios was difficult. Each tool had different strengths and weaknesses, therefore, several power system software tools were used.

Dynamic simulations could be carried out using both MATLAB and PSCAD software, but PSCAD has a better library for power device models. Also, dynamic stability analysis of the microgrid using simplified system model in CYMSTAB produced similar results as of using full system model in MATLAB.

1.2.2 Communications Lessons Learned

Effective wireless Communications is still a key consideration. This was emphasized after the study of the previous wireless system indicated that a complete replacement of the system, rather than a rehabilitation was required.

The original communications technology solution proved to be unreliable due to lack of system enhancement, interference issues, and technological flaws. The original communications system lacked redundancy, was impacted by other communication systems noise and vegetation obstructions and had technical issues with the mesh algorithm, which all impacted reliability. Based upon the above issues and the recommendations, by DOE and other standards making organizations, not to use unlicensed Wi-Fi as it is not suitable for electric utility smart grid communications backhaul systems.

1.2.3 Siting Lessons Learned

Finding suitable locations and willing customers for the installation of Distributed Energy Resources proved more challenging than originally anticipated. Considerations included insurance, ongoing maintenance, liability, and possible damage to existing customer facilities and general managing customer expectations.

Also, commercial customers with existing Distributed Generation provided several hurdles to the project including difficulties in interconnecting to the customers' facilities. Their equipment was not assessable, but situated within their facilities making direct connection difficult, or expensive.

Customers were hesitant to give control of their generation to an outside group. Those that were agreeable wanted at least 24 hour notice before turning on their generation. This was a result of their requirement for internal load switching and the people needed to make appropriate changes to their systems.

2.0 Introduction

The U. S. Department of Energy (DOE) awarded the West Virginia Super Circuit (WVSC) project to Monongahela (Mon) Power through its Renewable and Distribution Systems Integration (RDSI) program in April 2008. WVSC is a smart grid demonstration project that is led by Mon Power and supported by Leidos Engineering (formerly SAIC), Intergraph (formerly Augusta Systems), Advanced Power and Electricity Research Center (APERC) and North Carolina State University (NCSU).

Mon Power worked closely with project partners and vendors to design a smart grid system through the integration of distributed resources and advanced technologies to improve efficiency, reliability, and security of electric supply.

The WVSC project was kicked off on June 1, 2010 with the attendance of all project stakeholders and project partners started working on their respective tasks as planned. During the Research and Development (R&D) phase of the project, there were developments that impacted the proposed system design in major ways. Committed to the goals of the smart grid demonstration project, the project scope was modified as needed by Mon Power, the DOE and project partners to achieve the intent of the project.

3.0 Project Overview

3.1 Project Objectives

The objectives of the WVSC project are listed below:

1. Achieve greater than 15% peak power reduction, cost competitive with capacity upgrades on a Mon Power circuit located in Morgantown, WV
2. Demonstrate the viability of advanced circuit control through multi-agent technologies
3. Leverage advanced wireless communications to address interoperability issues between control and protection systems and distributed energy resources
4. Demonstrate the benefits of the integrated operation of technologies such as rotary and inverter-based distributed generation, energy storage, Automated Load Control (ALC), advanced wireless communications, and advanced system control technologies
5. Demonstrate advanced operational strategies such as dynamic islanding and micro-grids to serve priority loads through advanced control strategies
6. Demonstrate the reliability benefits of Dynamic Feeder Reconfiguration across several adjacent feeders

3.2 Project Partners and Responsibilities

3.2.1 Monongahela Power

Monongahela Power (Mon Power) is one of the ten regulated distribution companies owned by FirstEnergy Corporation. Mon Power serves about 385,000 customers in 34 West Virginia counties. Stretching from the Ohio-Indiana border to the New Jersey shore, the companies operate a vast infrastructure of more than 194,000 miles of distribution lines and are dedicated to providing customers with safe, reliable and responsive service.

FirstEnergy is a diversified energy company with 16,500 employees dedicated to safety, reliability and operational excellence. Its 10 electric distribution companies form one of the nation's largest investor-owned electric systems, serving 6 million customers in Ohio, Pennsylvania, New Jersey, West Virginia, Maryland and New York. Its generation subsidiaries currently control more than 18,000 megawatts of capacity from a diversified mix of scrubbed coal, non-emitting nuclear, natural gas, hydro, pumped-storage hydro and other renewables.

Mon Power was the lead organization for the WVSC project. In this capacity, Mon Power managed the project budget and schedule and worked closely with project partners to ensure the project would meet the established objectives.

As being the host utility, Mon Power selected appropriate distribution feeders for the smart grid technologies. In addition, Mon Power supported project design and analysis tasks and provided all the data that was required.

3.2.2 Leidos - formerly SAIC

Leidos is among the nation's largest research and engineering companies, providing information technology, systems engineering and integration solutions to commercial and government customers. Leidos engineers and scientists solve complex technical problems in defense, homeland security, energy, the environment, space, telecommunications, health care and logistics. With annual revenues of $8.3 billion, Leidos has more than 20,000 employees in 150 cities worldwide. Leidos provides engineering, scientific, technical and policy expertise to government and commercial customers for the development of solutions in energy management, nuclear security and nonproliferation, food defense, transportation and emergency response planning, and environmental analyses.

Leidos served as the lead engineering company for the WVSC project. In this capacity, Leidos led the project technical team in engineering and design tasks. In addition, Leidos provided project management and project controls support to Mon Power to prepare and submit DOE required reports. Leidos engineers developed power system models and conducted simulation studies to support the design efforts and the cost benefit analysis.

3.2.3 Intergraph Corporation - formerly Augusta

Intergraph Corporation’s technologies power distributed intelligent networks. The technologies extend enterprise networks by enabling rapid integration, intelligent processing, and enterprise utilization of data from sensors, actuators, and other edge systems and devices. Intergraph products enable the most efficient and effective convergence and use of data from edge systems and devices for numerous applications, including security, monitoring, automation, and asset tracking, among others.

Based on the developed project design and assistance, Intergraph developed an implementation plan complementary to the overall project plan for the wireless communications network. Intergraph developed and functionally wireless network based on the requirements. Intergraph led integration activities related to physical and logical interfaces for system hardware.

3.2.4 Advanced Power and Electricity Research Center

The Advanced Power and Electricity Research Center (APERC) is a university-wide research center at West Virginia University (WVU) in Morgantown, WV. The interdisciplinary center team, which includes power and mechanical engineers, computer scientists, mathematicians and economists, addresses electric power system research areas important to the state and the nation. APERC capitalizes on the challenge of change, focusing on innovations in system-wide control, using operational and economic data to allow companies to be profitable in a competitive market. APERC has equal interest in controls to ensure system reliability and availability for large-scale systems, such as the transmission grid, and for small-scale systems, such as those found on submarines. Current projects are funded by the US Department of Energy (Integrated Computing, Communication and Distributed Control of Deregulated Electric Energy Systems)

and the Office of Naval Research (Intelligent Agents for Reliable Operation of Electric Warship Power Systems.)

APERC has put together a team of researchers comprised of computer science, electrical and mechanical engineering, mathematics, and resource economics faculty to develop a Multi-Agent Grid Management System (MGM) and to assess the economics of such a system. The focus of APERC's work is on the research and development of MGM and simulation of the system on the low voltage power simulator. As a part of this research, APERC studied the financial analysis of the proposed technology solutions using hypothetical benefits and estimated costs to serve peaks loads and enhance system reliability.

3.2.5 North Carolina State University

The Semiconductor Power Electronics Center (SPEC) at North Carolina State University (NCSU) is one of the few centers in the US focusing on power electronics for electric utility applications. The center has established an experimental facility for conducting research on power electronics based systems at power levels up to 5 MVA. Current industry and government agencies supporting the center include ABB, TVA, BPA, EPRI, DOE and Duke Power. Sponsored by these members, the center has three large projects which are integrative in that they involve development from components to the whole power electronic systems for field demonstrations. Current research focuses on the development of the high power semiconductor switch ETO (Emitter Turn-off Thyristor), new modular and scalable power converter systems and their control, new cooling system designs, and distribution level power management using new power electronics based systems and distributed generation.

NCSU conducted research to develop fault locating and fault prediction algorithms. Locating faults fast was considered to help the utility to respond to the outages that result due to faults quickly, and thus, is important for improving reliability of service. This project aimed to demonstrate the fault locating and prediction features by making use of the advanced monitoring systems.

3.3 Project Technologies and Site Locations

To meet the project objectives, the scope of the WVSC project was to design a smart grid demonstration project that would include the five technologies listed below:

1. **Microgrid System**
   A micro-grid system was designed, modeled and simulated using Mon Power circuit data to operate in grid connected and islanded modes using Distributed Energy Resources (DER). DERs chosen were a natural gas fired generator, a solar photovoltaic system, an energy storage system, and a supporting communications system.
2. **Fault Location Isolation Restoration (FLIR) System**

   An agent-based FLIR system based on a project developed under a prior project was augmented, modeled and simulated using Mon Power circuit data to improve system reliability.
3. **Fault Location Algorithm (FLA) and Fault Prediction Algorithm (FPA)**

   An intelligent fault location algorithm (FLA) and intelligent fault prediction algorithm (FPA) were designed utilizing data from field deployed sensors and Mon Power circuit data. These schemes were designed to extract fault current and type information from field sensor data to be used in a system model to estimate fault location.
4. **DER Dispatch for Peak Reduction**

   Distributed Generation (DG) from a local area hospital was designed and analyzed to enable peak load reduction on a single distribution feeder. Forecasted feeder load was used to reduce peak load levels. Hospital loads were designed to be transferred to the distributed generator to affect the load reduction on a specific distribution feeder.
5. **Advanced Communication System**
   An open architecture system was designed that incorporated an advanced communication system with access points and sensor network appliances capable of intelligent, distributed control located on selected distribution circuits.

Mon Power worked closely with the project partners and the DOE to select project sites for each technology. The initial project proposal had identified Morgantown WV substations and feeders as the project sites, which are the West Run 138/12.5 kV substation, Pierpont 138/12.5 kV substation, and Collins Ferry 138/12.5 kV substation.

3.3.1 Microgrid System

At the proposal stage, the microgrid site was planned to be at Research Park in Morgantown, WV. Research Park was a technology park that was under development by the West Virginia University (WVU) at the time. The intent of the Research Park microgrid was to utilize the distributed energy resources at Research Park and build a microgrid that would provide

improved reliability to the customer. At the same time, Research Park's energy resources would be utilized by Mon Power to reduce feeder peak by at least 15%.

Due to the extensive delays in Research Park construction and WVU's budgetary constraints, Mon Power needed to identify another microgrid site. The project team reached out to potential microgrid partners in the Morgantown area and held meetings with them to describe the goals of the project. As a result of these efforts, Mon Power was able to engage Research Ridge management to host the microgrid site in their office buildings that are located at Collins Ferry Rd., Morgantown, WV.

A lateral island microgrid was designed and analyzed for this project and was planned to be operated in two use cases 1) grid-connected peak shaving and 2) islanded operation. One natural gas generator (150 kW), a 40.2 kW solar PV system - 21 kW AC, 19.2 kW DC output, a 24 kW/52.8 kWh Li-Ion battery energy storage system (BESS), and load control devices were designed however, not deployed due to project constraints. An agent based microgrid management system (MGMS) was developed by WVU/APERC.

3.3.2 Fault Location Isolation Restoration System

A Fault Location Isolation Restoration System (FLIR) is a distribution automation functionality to provide the capability for fault location, isolation and service restoration to the upstream section as well as the downstream feeder. This part of the project was sited on 3 West Run circuits that are also networked with 2 Pierpont circuits. Agent based FLIR algorithms (MGMS) were developed, modeled and simulated using Mon Power circuit data. FLIR system was designed for peer-to-peer communication between software agents, which were to be located at switch locations, zones and DER locations.

3.3.3 Fault Location Algorithm & Fault Prediction Algorithm

The Fault Location Algorithm (FLA) was designed, modeled and simulated using Mon Power circuit data to identify the location of a fault on distribution systems including identifying the protective devices that may have operated in response to the fault. This aspect of the project was designed to be sited on three West Run circuits. A Fault Prediction Algorithm (FPA) was designed to predict the distribution system faults before they occur by analyzing the current and voltage waveform signatures of devices prior to failure. North Carolina State University (NCSU) was responsible for this aspect of the project.

3.3.4 DER Dispatch for Peak Reduction

Mon Power reached an agreement with Mon General hospital located in Morgantown, WV located on West Run circuit #8 that would allow them to demonstrate a peak load reduction methodology by using customer owned distributed energy resources (DER). The negotiations and discussions with the commercial and industrial customers illustrated the non-technical challenges of developing a microgrid system, which is also documented in this report.

Peak reduction would be accomplished through utilizing Mon General hospital's back-up generator during peak hours. Feeder load would be projected for the next day and DG owner would be informed about when and how long the back-up generator would be required to stay on in the next day.

3.3.5 Advanced Communications System

The WVSC project leveraged the network architecture that was put in place in the previous DFT project. Modifications to the existing architecture were to be made to accommodate new technologies.

It was planned that a WiMax based communications system provided by RuggedCom operating in the 3.65 GHz lightly licensed spectrum would be used. It could give connectivity between switches, West Run substation, and the DER equipment at Research Ridge, the technology solutions were not deployed.

3.4 Scope of Work

3.4.1 Develop Project Design

There was a design effort for each technology which included requirements and preliminary designs. Hardware and software specifications were developed and included the integration of university developed algorithms, distributed energy resource integration, monitoring and control systems, protection systems, and an advanced communication system.

A microgrid system was to be designed for grid connected, peak shaving and islanded operation of the distributed energy resources (DER). The technologies designed into the microgrid include a natural gas fired generators, a solar photovoltaic system, a battery energy storage system, and a supporting communications system.

A fault locating scheme was designed leveraging a previous Mon Power project that extracts fault current and type information from sensor data and uses a system model to estimate fault location. Data from multiple sensor locations was designed to be integrated with the ability to pinpoint fault locations evaluated against the use of single sensor location data. Fault prediction algorithms were also developed. The ability to predict faults through learning algorithms such as Artificial Neural Networks (ANNs) were designed, modeled, simulated and documented using Mon Power circuit data.

Intelligent fault prediction and location algorithms were developed by NCSU utilizing data from field deployed sensors.

A peak reduction capability was designed using distributed generation (DG) from a local area hospital that would enable peak load reduction on a single distribution feeder. Feeder load was forecasted in order to determine the DG schedule. A DG commitment schedule was prepared for when feeder load exceeds a certain threshold and provided to the DG owner so that they would start the unit to accomplish the peak load reduction.

An advanced communication system using an open architecture was designed with access points and sensor network appliances fully capable of intelligent, distributed control located on selected circuits.

3.4.2 Conduct Modeling & Simulation

Modeling tools were used that leveraged past modeling work and other commercially available software packages. The results of the modeling and simulation effort provided feedback to the technology designs.

3.4.3 Deploy Systems

Each of the technologies were to be deployed, however, due to post design evaluation, the systems were not installed.

A FLIR system was deployed on the Mon Power distribution system through a prior DOE funded demonstration project. Fourteen switches and two re-closers were installed to enable this system. In the WVSC project, additional equipment was to be added for the agent-based FLIR logic, which was designed, but not installed.

3.4.4 Report on Lessons Learned

Analysis and evaluation of the performance of each technology system to assess operational value and identify both expected and unexpected outcomes was tasked. A cost benefit analysis of each technology deployed was also tasked, however as no systems were installed, no performance evaluation and no formal CBA on the actual benefits and the actual costs of the project was performed. A university CBA study using hypothetical benefits and estimated equipment costs was performed.

4.0 Project Design

The project team followed a requirements-driven process to design each technology area of the smart grid project. The project design process was established in a way that it could be utilized in similar smart grid projects and addresses the use case development process, requirements gathering process, and modeling and simulation scenarios to support each technology area.

The WVSC design team followed Leidos' VEE model as illustrated in Figure 4-1: WVSC VEE Design Process. The VEE Model depicts the technical aspects of the project cycle where decomposition and definition make up the left leg of the VEE and integration and verification constitute the right leg of the VEE. At the bottom of the VEE is the construction of the atomic components of the system that are sequentially integrated to form the complete system.

In Figure 4-1, the VEE process has also been extended at the upper left and right sides to address operational aspects of the overall system lifecycle. The VEE is a true development/operations representation of the complete lifecycle. The notion of decomposition of the complex system into smaller elements, and the subsequent integration of the smallest elements into increasingly larger pieces of the system, is shown in the figure by the italicized text illustrating system decomposition/integration levels (e.g., Utility, System, Sub-system, and Component). The two axes in the figure are the vertical axis of Program Detail (or Program Aggregation Level) and the horizontal axis of Program Maturity. Progress in the system lifecycle is made by traversing the VEE from the upper left (User Needs), through the upper right (A user validated system employed for operational use). The emphasis on detailed elements of the system increases moving from the top to the bottom of the VEE and system maturity increases moving from left to right.

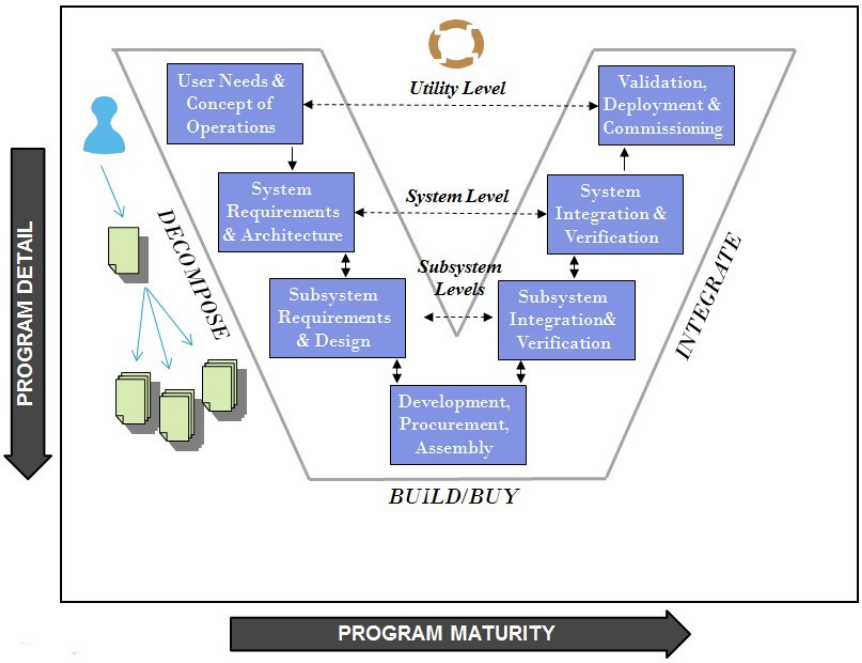

Figure 4-1: WVSC VEE Design Process

The first step in this process is to develop user needs and requirements. In order to accomplish this, the project team decided to develop functional use cases for each project technology area by collaborating with all the project partners. The developed use cases played a significant role in identifying detailed requirements of each project element.

A use case in software engineering and systems engineering is defined as "A description of a system's behavior as it responds to a request that originates from outside of that system. In other words, a use case describes 'who' can do 'what' with the system in question". Use cases are a valuable method of documenting applications and processes for purposes of defining requirements.

The project design team held several workshops to identify project use cases which are listed in Table 4-1. In these workshops, the project team developed details of each use case which were documented using standard templates. The use case documents developed are presented in Appendix A.

Table 4-1: WVSC Project Use Cases

Use Case #	Use Case Description
1	Multi-agent system automatically reconfigures after a feeder fault.
2	Multi-agent system dispatches DER to achieve 15% peak load reduction goal.
3	Fault location algorithm identifies the exact location of a fault.
4	Fault prediction algorithm predicts an equipment failure or a high impedance fault.
5	Microgrid islands in case of a power outage/disturbance or forecasted overload.

The second step in the VEE model is to collect system requirements based on user needs and use cases. The requirements were documented by technology using standard templates which are presented in Appendix B. The WVSC team believes that the requirement development process followed was very productive. The third step in the VEE model is the system and sub-system design process as described in the next sections.

4.1 Microgrid

A microgrid system was designed for peak shaving and islanded operation of distributed energy resources (DER), including a natural gas fired generator, solar photovoltaic and an energy storage system with supporting communications and control systems. It was modeled and simulated but not deployed or demonstrated in the field.

4.1.1 Microgrid Definition

One definition of a microgrid is sections of an electric distribution grid that includes DER matched with some or all of a designated set of customer loads. It can operate in parallel with

the grid or in islanded mode, disconnected from grid operation. IEEE Standard 1547.4 defines seven distinct microgrid configurations as illustrated in Figure 4-2. The WVSC microgrid design conforms to the IEEE Lateral Island definition. In a lateral island, an island is formed from load normally served from a distribution circuit lateral. Local generation and/or storage are used to serve the local load when the lateral switching device opens.

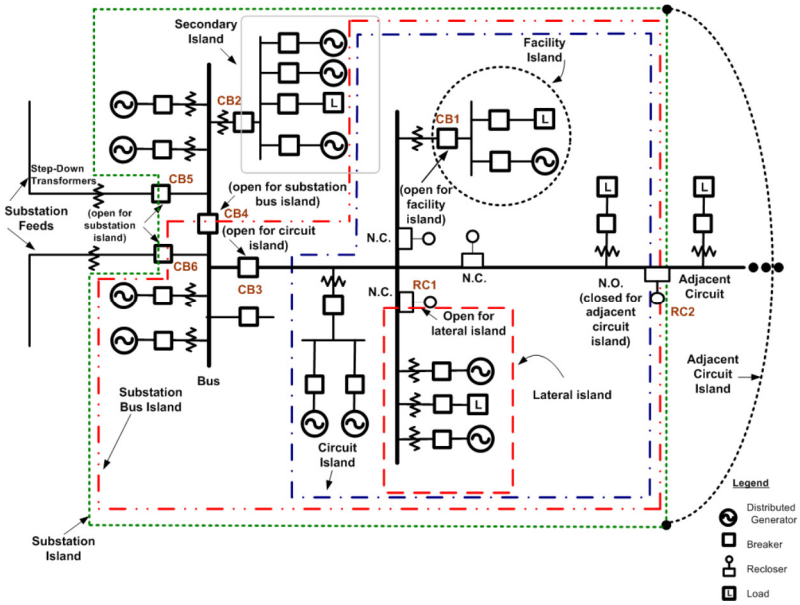

Figure 4-2: IEEE 1547.4 Microgrid Configurations

Microgrid islanding and resynchronization is accomplished with a switch, installed at the Point of Common Coupling (PCC). IEEE 1547-2003 standard requirements will apply to the PCC switch. During the islanded mode operation of the microgrid, one or more DERs may operate outside of voltage and frequency limits defined in IEEE Std. 1547-2003 requirements. The microgrid will have capability to operate in either grid connected or islanded modes of operation. In the grid connected mode, the microgrid follows grid voltage and frequency and does not regulate. In islanded mode, the microgrid control system takes local action to maintain voltage and frequency for the islanded system.

4.1.2 WVSC Microgrid Site

The WVSC microgrid is designed to be attached off of a 12.5 kV lateral circuit in Morgantown, WV that serves a portion of the Research Ridge office complex. There are two office buildings on the lateral, each building having its own pad-mounted distribution transformer. Each transformer has 112.5 kVA installed capacity and is fed by three-phase 12.5 kV underground cabling (#2 Al). The microgrid one-line diagram is illustrated in Figure 4-5. All DER resources were planned to be placed in empty green place between two office buildings as shown in the Figure 4-3.

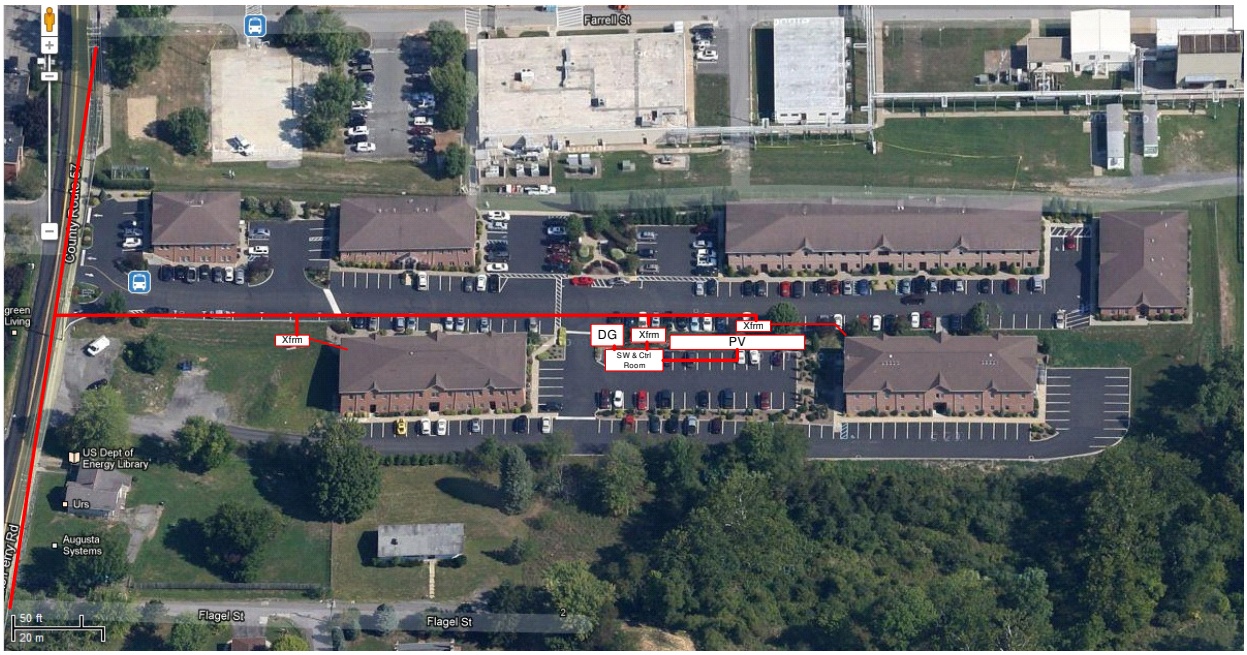

Figure 4-3: Proposed Microgrid Site Satellite View

4.1.3 WVSC Microgrid Load

Each of the two office buildings (#3592 and #3596) that were to be served by the microgrid has approximately 75-100 kW of peak summer load when fully occupied. Some offices are currently vacant therefore measured peak demand is less than expected. Air conditioning load is the primary load for these buildings.

A smart meter was already installed at building 3592. 15 minute average consumption data was available for year 2011. The peak day for 2011 was on 07/22/2011. Daily load profile of the 2011 peak day is illustrated in Figure 4-4. Typical summer and winter weekday/weekend load profiles are presented in Appendix C.

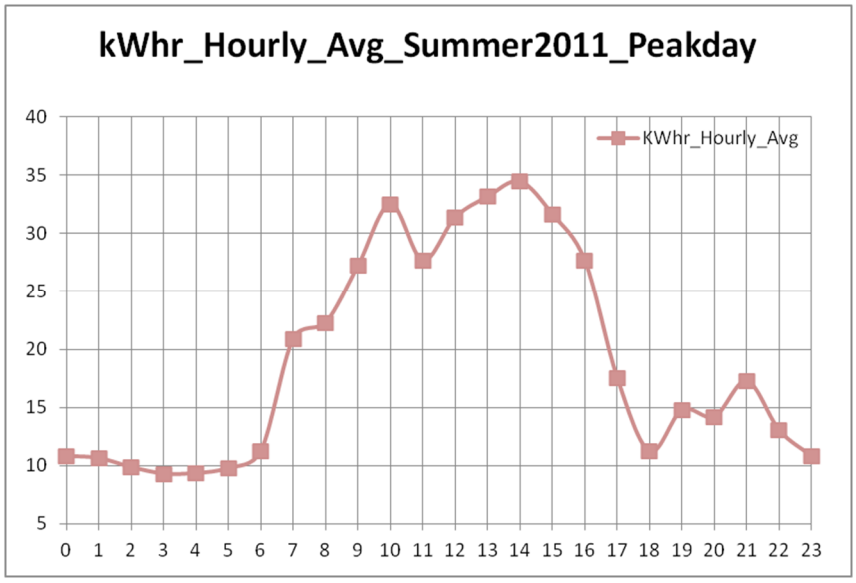

Figure 4-4: Summer Peak Day Load Profile

4.1.4 Microgrid Distributed Energy Resources

The microgrid DER includes a natural gas generator, an energy storage system with Li-ion batteries, and a PV system. Table 4-2 lists the DER equipment and their technical specifications.

Table 4-2: Microgrid Distributed Energy Resources

DER Type	Rating (kW)	Quantity	Total Capacity (kW)
Natural Gas Generator	150	1	150
Solar PV	19.2	78 (240W panels)	19.2
Solar PV (w/ Micro Inverters)	21	87 (240W panels)	21
Energy storage System with Li-ion Batteries(2hrs)	8 each	3	24
TOTAL			**214.2**

4.1.5 Microgrid Electrical Diagrams

Figure 4-5 shows a detailed one-line diagram of the microgrid. All DER resources indicated in Table 4-2 are connected to a common low voltage (LV) bus in an outdoor electrical control room. This control room is used to house the energy storage units and required switchgear. Figure 4-6 is a detailed three line diagram showing the connections of DER resources to the LV bus in the control room. A visible and lockable load break disconnect switch is installed outside the control room for the purpose of isolating the DER resources by utility personnel in the event of emergency. This LV assembly is connected to the medium (MV) system via a 225kVA step-up power transformer. A breaker is installed at the PCC point with required protection and synchronizing capabilities.

The PCC Breaker and CB1 have the following protection features in compliance with IEEE 1547, UL 1741 and FirstEnergy's DG Interconnection requirements.

a. 27 Under Voltage Relay
b. 59 Over Voltage (phase-to-ground) Relay
c. 59G Over Voltage (zero-sequence) Relay
d. 81 Over and Under Frequency Relay
e. 25 Synchronism Check Relay
f. 67 AC Directional Overcurrent and/or 32 Directional Power (reverse power)

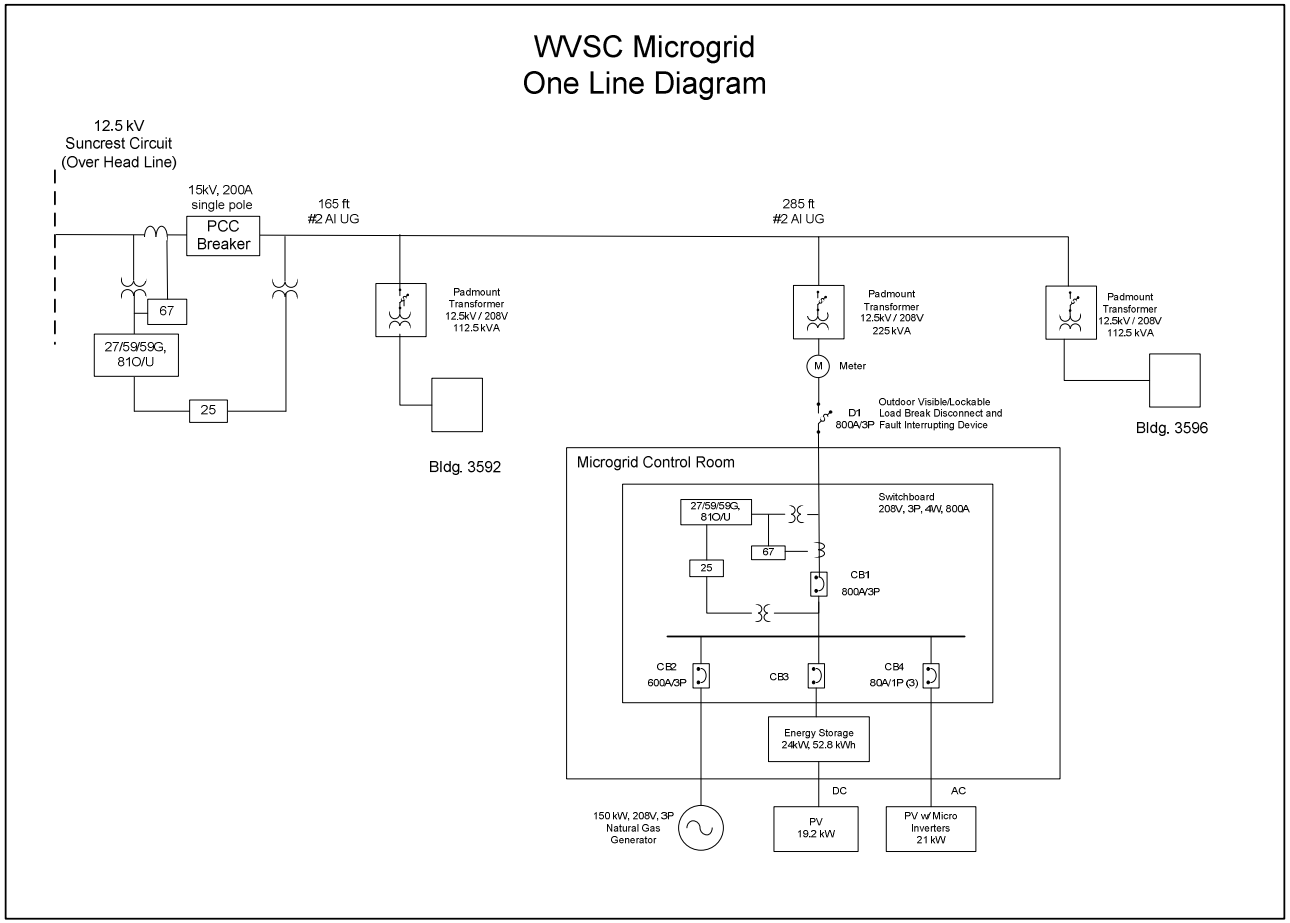

Figure 4-5: Microgrid One Line Diagram

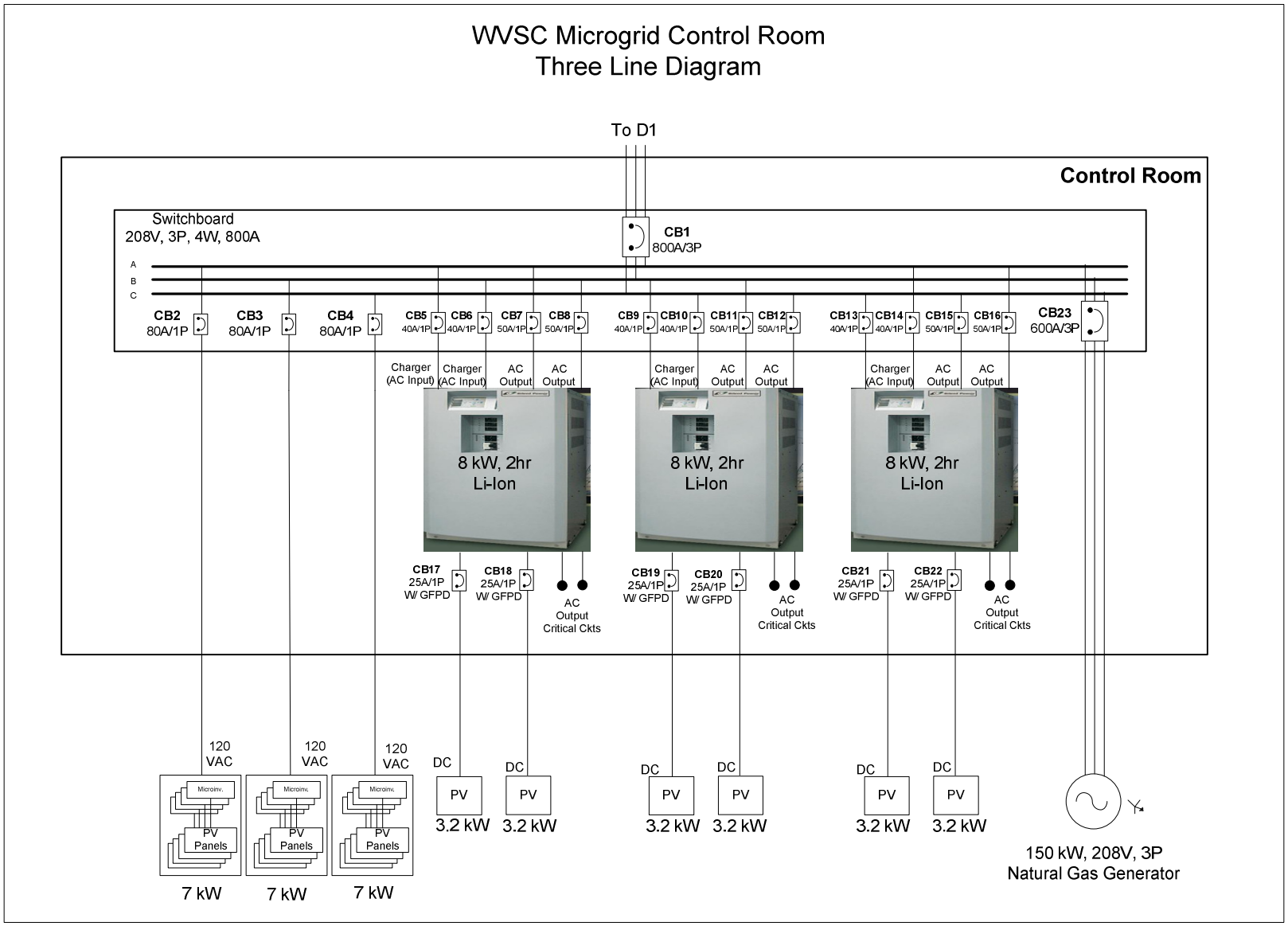

Figure 4-6: Microgrid Three Line Diagram

4.1.6 Modeled Microgrid Modes of Operation

Microgrids can have different modes of operations such as islanding mode, utility reconnection mode, grid connected mode, and islanded mode. The operation of equipment may change based on the microgrid operational mode. The sequence of events for each modeled mode of microgrid operation is described below. A microgrid controller would manage and control these events.

Islanding Mode (Transition from Grid-Connected Mode to Islanded Mode)

WVSC microgrid would transition into the islanded mode of operation when utility power is lost at the PCC breaker or any abnormal voltage/frequency conditions prevail as stated in 1547 requirements. During this transition, all loads experience a short outage except the critical loads that are served by the energy storage. Microgrid loads are designed to be energized soon after the power is lost. A draft sequence of events of microgrid islanding is listed below. Controllers are utilized to enable this control sequence.

Microgrid Islanding Initiation:

1. Utility power at PCC is lost for a predefined duration (e.g., 30 seconds) and/or abnormal voltage/frequency conditions prevailed as stated in 1547 requirements.
2. 1547 compliant generation resources (energy storage units and PV with micro-inverters) in the microgrid cease energizing the utility grid.
3. PCC breaker opens to initiate the microgrid islanding process.

Serving Critical Load:

1. When utility power is lost, energy storage units can provide power to single or two phase loads. These loads have to be connected to the storage units via automatic transfer switches (ATS). Each ATS will switch to the energy storage as soon as the loss of voltage is detected.

Load Restoration:

1. Natural gas generator will turn on and energize the bus bar. This will energize the MV part of the microgrid and supplies power to the building loads.
2. Critical load automatic transfer switches will switch to ‘N’ position to serve the load from natural gas generators.
3. Energy storage units and PV micro inverters will synchronize to the generator reference voltage and reconnect to the microgrid.

Utility Reconnection Mode (Transition from Islanded Mode to Grid-Connected Mode)

Microgrid utility reconnection is initiated when utility power is restored at the PCC breaker for a minimum of 5 minutes. A draft sequence of events using controllers for the utility reconnection is listed below.

1. The microgrid generator synchronizes with the utility grid voltage and frequency via local controls.

2. PCC breaker closes. Note: This close transition has the microgrid loads served by both utility grid and microgrid DER.
3. Natural gas generator releases loads and turns off.
4. BESS and PV with micro-inverters stay connected and paralleled with the utility grid as the inverters of these resources are 1547 compliant.

Grid-Connected Mode of Operation

When microgrid is operating in utility grid connected mode, the natural gas generator, the BESS and the solar PV system operate in compliance with Mon Power interconnection requirements are not designed to regulate frequency or voltage in grid connected mode of operation. The design steps are:

1. The natural gas generator runs in speed droop control scheme to load share with the utility grid.
2. The natural gas generator Automatic Voltage Regulator (AVR) is not designed to actively regulate the voltage at the PCC regardless that the voltage at the PCC point goes beyond the requirements of ANSI C84.1-1995, Range A.
3. BESS may charge/discharge real power based on the control mode. VAR control is disabled in grid connected mode.
4. PV system with micro-inverters supply available kW into the system. VAR control is disabled in grid connected mode.

Islanded Mode of Operation

When microgrid is islanded from the utility grid, frequency and voltage has to be maintained within certain limits. In the islanded mode of operation, IEEE 1547 frequency and voltage limits do not apply, however voltage and frequency regulation is still needed because all loads are designed to operate within certain limits. In the WVSC microgrid, a natural gas generator, a BESS and a solar PV system has been designed to operate as discussed below to provide frequency and voltage regulation functions.

Frequency Regulation

The 150 kW natural gas generator was designed equipped with a generator controller to provide frequency regulation in the microgrid. A controller is designed to utilize the BESS in frequency regulation, which is to send command signals to the BESS local controller.

Voltage Regulation

The voltage regulation design in the islanded mode of operation operates:

1. Generator: Automatic Voltage Regulator (AVR) of natural gas generator is designed to regulate the voltage of the microgrid. The controller is to regulate voltage at the connection points and provide reactive power to meet load requirements.

2. Micro-inverters with embedded controls have been designed to provide dynamic VAR support. Target power factor has been designed to be set by the operator or by an external controller. Micro-inverters are designed to supply reactive power to the full capacity of device operation, both leading and lagging and to operate in fixed VAR or Automated Volt/VAR modes. In fixed VAR mode, the micro-inverters are to limit real power output as needed to achieve the requested VAR output. In automated Volt-VAR mode, the micro-inverters provide voltage regulation support by sinking reactive power if the line voltage is higher than the selected maximum voltage and by sourcing reactive power if the line voltage drops below the selected minimum voltage. No operator intervention is required other than to configure the applicable voltage range as percentages of nominal line voltage from 80% to 110%.
3. The BESS inverter is also designed to provide VAR support. The boundaries for the VAR support have been specified under IEEE 1547, that is Vmin = 88% of V nominal, and Vmax = 110% of V nominal. Qmax = current VAR capability, and may be positive (+, capacitive) or negative (-, inductive). It is the kVA capability left after supporting kW demand.

4.1.7 Battery Energy Storage System Control

The battery energy storage system (BESS) is designed to have local controls to enable five different use cases as listed in the table below. An external controller or operator is utilized to switch between use cases.

Table 4-3: Energy Storage System Use Cases

Use Case	Description	Grid-Connected	Islanded
Solar PV Capacity Firming	BESS shall charge/discharge the battery in real-time based on varying solar PV output to keep the combined (solar PV and battery) power output level constant over a specified period of time. Designation of such time period and the charge/discharge behavior mode shall be selectable via an external controller.	Yes	Yes
Voltage Support	BESS shall be able to inject reactive power into the microgrid to provide voltage support and power factor correction	No	Yes
Renewable Energy Time Shift	BESS shall charge energy storage with PV power, then discharge energy storage later to reduce building's peak demand.	Yes	Yes
Electric Service Reliability for Microgrid Support	When microgrid transitions to islanded mode, BESS shall provide rated energy output to ride through a power outage. Maximum power requirement shall be limited to the BESS rating. On site generation shall be turned on as soon as an outage is detected.	No	Yes

Load Following	BESS shall be dispatched to follow the load in the microgrid. An external controller shall issue these control signals. BESS shall be able to receive these signals and adjust its output accordingly.	Yes	Yes

4.1.8 Monitoring and Control

The ENMAC system at Greensburg Control Center was planned to be utilized to monitor and control the WVSC microgrid including the energy resources, sensors and switches.

4.1.9 Vendor Selection Process

WVSC team developed technical specifications for hardware and software to solicit vendor proposals for project purchased. Once received, the proposals and costs were evaluated against the technical specifications.

4.2 Fault Location Isolation Restoration

Fault Location Isolation Restoration (FLIR) is a distribution automation functionality that provides capabilities for fault location, isolation and service restoration to the entire upstream section of the feeder and as much of the downstream feeder as possible. A FLIR system was deployed on the West Run #3 and West Run #4 circuits through the previous DOE demonstration project, Morgantown Developmental Field Test (DFT) and as shown in Figure 4-7. Fourteen switches and two re-closers were installed to enable the DFT system. In this WVSC project, APERC developed an agent-based FLIR logic model for the West Run #3, #4 and #8 circuits. The new agent-based FLIR system leveraged some of the DFT hardware and software and is described in section 4.2.1.

4.2.1 Morgantown DFT FLIR System

This section describes the existing FLIR system architecture, system hardware/software including substation and feeder assets, and the existing logic used to locate faults and restore the system.

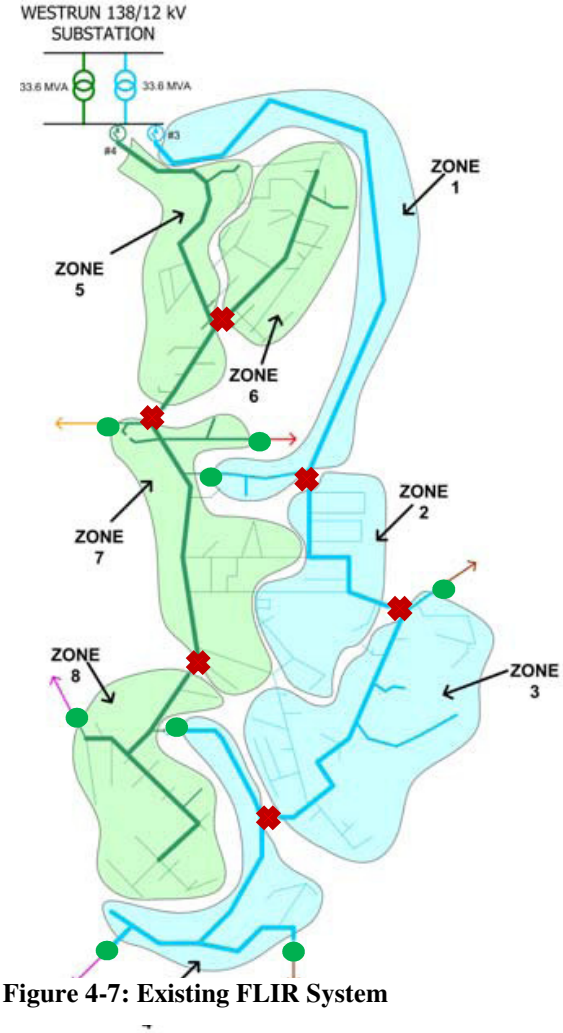

Figure 4-7: Existing FLIR System

DFT System Assets and Architecture

The West Run Substation has eight feeders, of which West Run #3 and West Run #4 are monitored for faults. Once a fault is detected, the logic, when in automatic mode, will isolate the faulted zone and restore power to the unaffected zones. Two additional feeders are connected to circuits #3 & #4 from Pierpont Substation. These, along with three other West Run feeders, are used to restore power to isolated zones. Once the fault is cleared, the logic is programmed to automatically return the entire feeder to its normal state. In manual mode, the logic will detect a fault but perform no control actions to isolate and recover zones. Once a zone is recovered, the program will continue to monitor the source feeder to determine if the source has exceeded its thermal limits. If so, the program will disconnect the zone and attempt to recover from another source.

Each substation has a Microsol RTU. The West Run RTU communicates with the Pierpont RTU, the Feeder USP RTUs and the Systems Master Station HMI using DNP TCP/IP.

The Substation RTU communicates with the SEL351A relays. These provide the feeder metering information for all feeders other than feeders #3 & #4, which communicate with Cooper Form6 reclosers for their metering and status data. Hardwired input/output modules on the West Run RTU provides breaker control for circuits #3 & #4 and substation Local/Remote indication. The RTU at Pierpont Substation communicates with the West Run Substation RTU, providing information on Circuits #5 & #6. The West Run RTU has a DNP TCP/IP master to all 14 feeder RTUs and the Pierpont RTU. A DNP TCP/IP slave communicates with the HMI Master Station.

In total, there are 14 feeder switching points: eight normally-open ties and six normally-closed zone isolation switches. Each switching point has a Microsol USP RTU communicating with a Microsol AIM-020 meter, which functions as a meter and a fault (over-current) detection device.

The USP provides control and indication along with communications to the West Run Microsol Substation RTU.

The Substation RTU connects to an existing Ethernet 100BaseT (RJ45) access point for Feeder RTU and Master Station communications using DNP TCP/IP. Two RS485 ports are used to connect to the SEL351A relays and in the case of Feeders 3 & 4, the Cooper Form 6s using DNP Serial.

The 14 Feeder RTUs connect to a serial to IP converter then to the systems Ethernet communications system using serial DNP. The Feeder RTU communicates to the AIM meter using serial Modbus.

DFT Project Substation Intelligent Electronic Devices

Existing intelligent electronic devices in West Run and Pierpont substations are illustrated in Figure 4-8. The black lines in the figure represent the existing equipment and red lines represent designed new equipment.

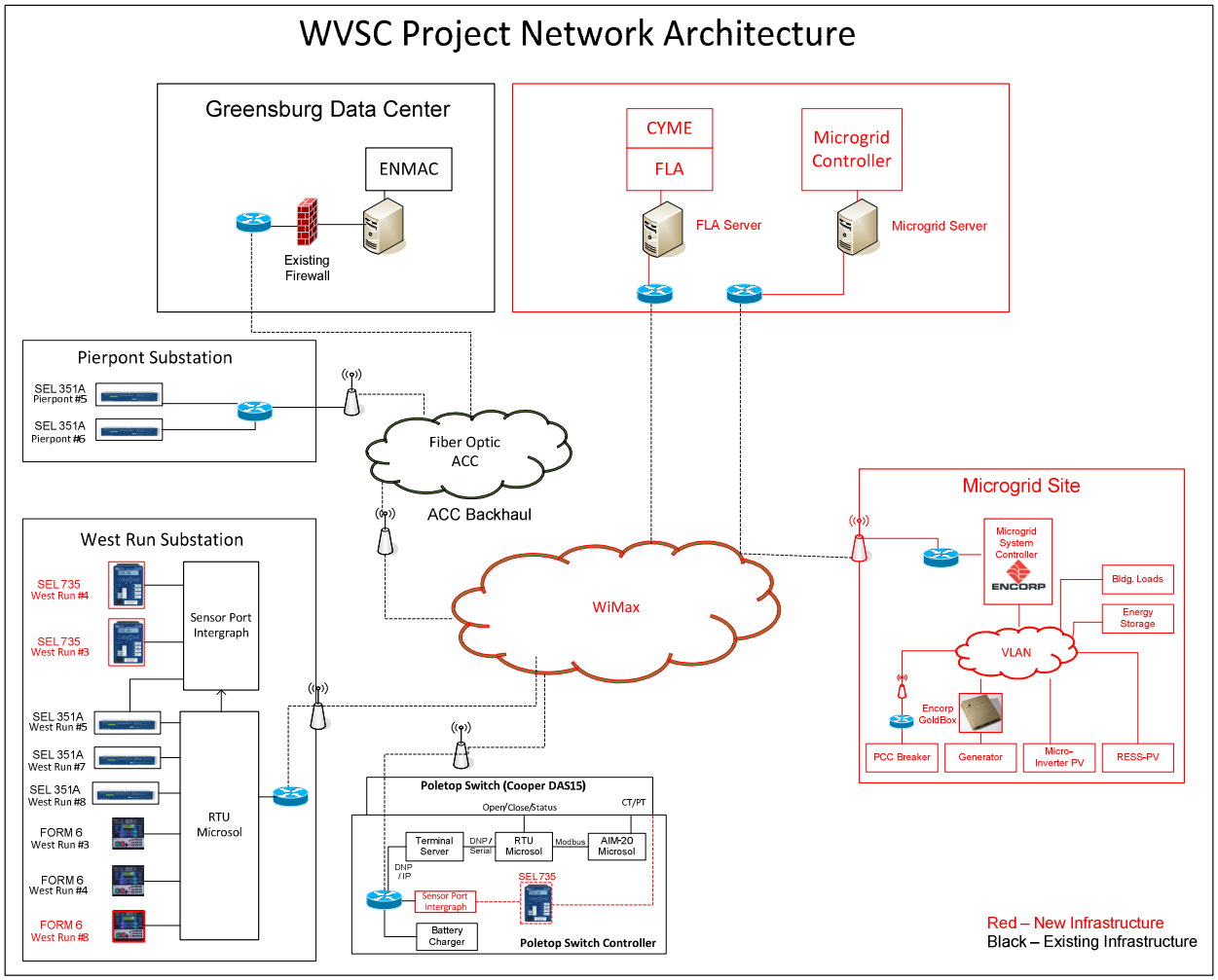

Figure 4-8: WVSC FLIR Network Architecture

DFT Project Substation Reclosers

All circuits connecting at the West Run substation are equipped with reclosers. Circuits #3 and #4 have 560A, 15.5 kV Cooper electronic reclosers with Form 6 controllers. Circuits #5, #7 and #8 have hydraulic reclosers which are not suitable for remote control.

The system design, when there is a fault trips and closes the recloser. The FLIR system then initiates the fault location, isolation and restoration process following a recloser lock-out signal. The FLIR is not designed to take any action when recloser trips on a temporary fault and remains closed after a recloser operation.

Figure 4-9: Electronic Reclosers at West Run substation

Time Current Characteristic (TCC) information at two current levels for Circuit #3 and #4 reclosers is given in Table 4-4. These reclosers are programmed to operate three times before locking out. The first reclosing operates on A-curve and the following two reclosings operate on D-curve. The approximate clearing times for A-curve and D-curve are also listed. The reclosers wait for 60 cycles between the each reclosing operation.

Table 4-4: Recloser Settings for West Run Circuits #3 and #4

TCC	A curve		D curve	
Current	2000A	6000A	2000A	6000A
Clearing Time	5 cycles	3 cycles	43 cycles	8 cycles

DFT Project Pole-Top Load Break Switches

The DFT project has 14 load-break switches installed, which are Cooper DAS-15 type three-phase vacuum switches with 15kV, 630 A ratings and is shown in Figure 4-10. A three-phase current transformer set is embedded in these switches, and a three-phase set of potential transformers are installed externally on one side of the switch (either on source side or load side) which is given in Table 4-5.

Figure 4-10: Pole-Top Load Break Switch

Table 4-5: PT Connections at Switch Locations

Switch ID	PT Connection
4_SW13	All PTs are connected on the source end (WR ckt#4)
4_SW14	All PTs are connected on the source end (WR ckt#4)
4_SW11	All PTs are connected on the source end (WR ckt#4)
4_SW12	All PTs are connected on the load end (WR ckt#8)
3_SW2	All PTs are connected to the source end (WR ckt#3)
3_SW1	All PTs are connected to the source end (WR ckt#3)
3_SW3	All PTs are connected to the source end (WR ckt#3)
3_SW4	All PTs are connected to the source end (WR ckt#3)
3_SW5	All PTs are connected to the source end (WR ckt#3)
3_SW6	All PTs are connected to the Load end (PP ckt#6)
4_SW9	All PTs are connected on the source end (WR ckt#4)
3_SW7	All PTs are connected to the Load end (WR ckt # 7)
3_SW8	All PTs are connected to the source end (WR ckt#3)
4_SW10	All PTs are connected to the Load end (WR ckt#4)

DFT Project Automation Logic

The existing DFT FLIR system has a fault detection logic algorithm running that looks for an over-current followed by a no voltage condition. The meter that detects the fault has two outputs, one for no voltage on one or all phases, and one for a fault on one or all phases. These outputs are connected to the USP status inputs to be reported back to the West Run RTU Feeder Automation logic. The meter also passes metering values to the USP via Modbus, then to the West Run RTU by the USP using DNP protocol.

Fault Detection occurs after an over-current event followed by a loss of voltage event within the Fault Detection Validation Time (FD_VT) period. An over-current event occurs when the current level goes above the over-current threshold (OC_FT) longer than the over-current validation time (OC_FV). A Loss of Voltage event occurs when the voltage level goes below the Voltage Loss Threshold (VD_LT) longer than the Voltage Loss Validation Time

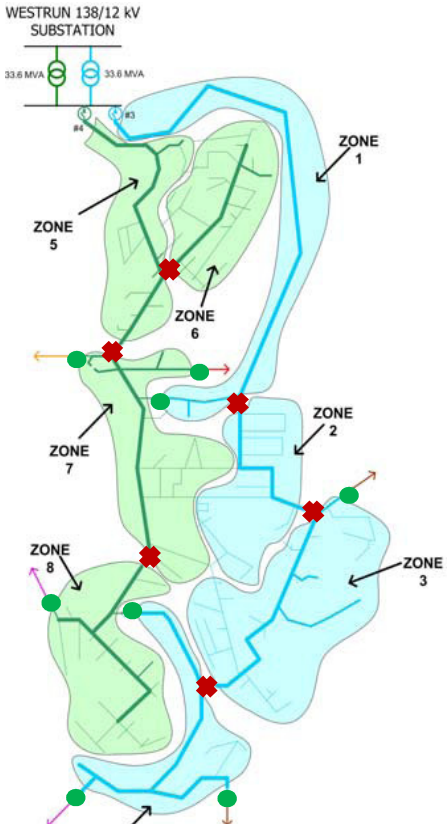

Figure 4-11: Existing FLIR System

(VD_LV). Figure 4-12 illustrates how the fault detection logic works based on these parameters.

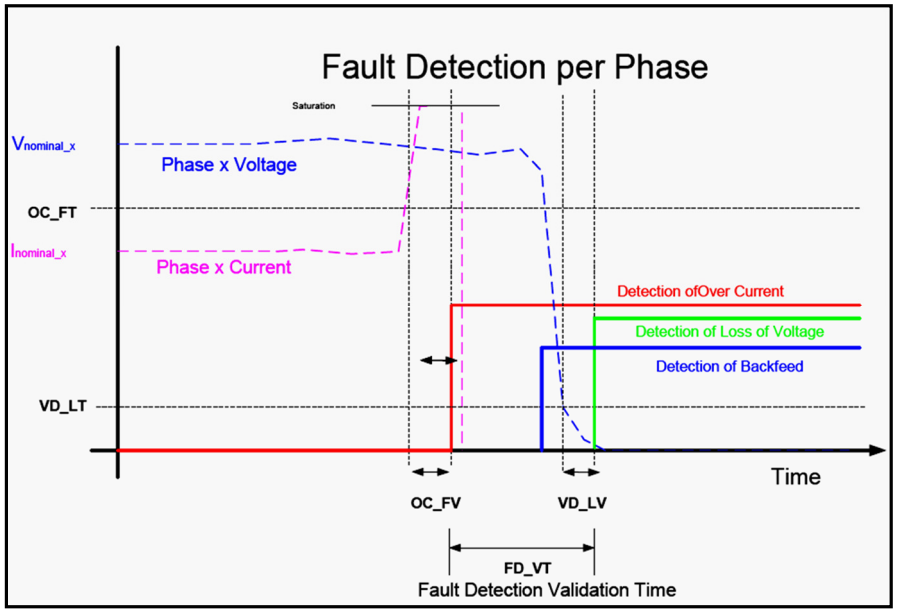

Figure 4-12: Existing Fault Detection Logic

4.2.2 New FLIR Technology Description

This section describes the designed FLIR system architecture, system hardware/software adding in the proposed new equipment and the resulting architecture including substation and feeder assets, and the existing logic used to locate faults and restore the system.

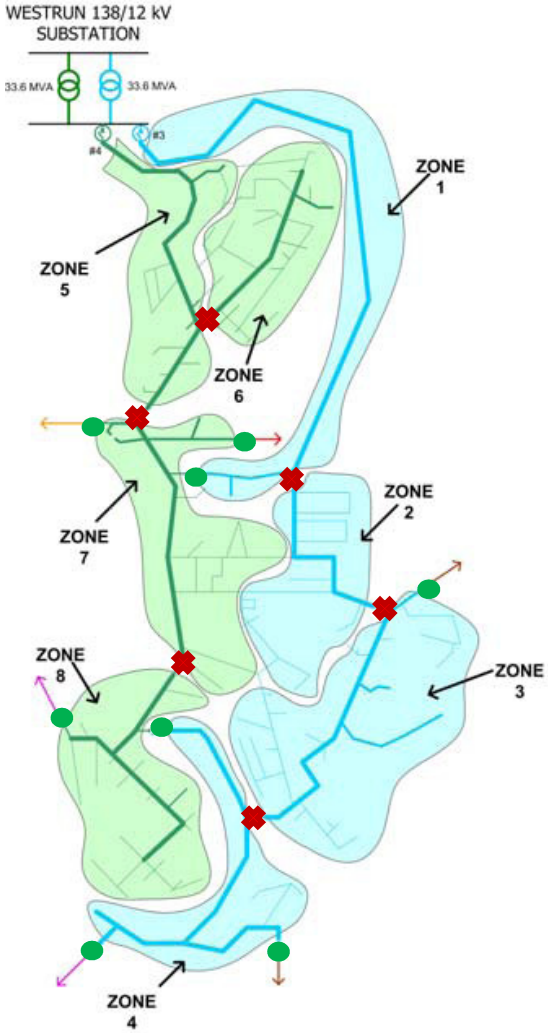

Figure 4-13: FLIR System with New Equipment

New FLIR System Assets and Architecture

The new FLIR system has been designed to be implemented using different system architectures including decentralized (distributed) and centralized system architectures. Each approach has its advantages and disadvantages.

In a decentralized system the decisions have been designed to be made locally in the field based on peer-to-peer device communication. The main advantage of this architecture is improved system reliability. Distributed control architectures does not rely on a single component; therefore, failure of one component usually does not take the entire DA system down. However, decentralized systems usually pose more challenges to maintain and operate compared to centralized systems. Decentralized systems are better suited for large systems where it becomes very challenging to take centralized control actions. Although intelligence is decentralized, these solutions will require a Human Machine Interface (HMI) at the control center for monitoring and control purposes.

In centralized system architecture all decisions are made by a central entity. This architecture requires a master-slave relationship where all system data is transmitted to a master where all actions are being made. Centralized systems usually are easier to maintain and operate. The decisions can be taken using the entire system information which usually will yield a better solution. Another advantage is that a network model can be integrated into the solution with real-time power flow capability, which enables running simulations and reviewing system responses before taking any action.

In the WVSC project, agent-based FLIR (FLIR-A) algorithms were developed by WVU/APERC as a component of the Multi-Agent Grid Management System (MGMS). The FLIR-A system employed a decentralized system architecture as was described above and would require peer-to-

peer communication between software agents. These agents would located at switch locations, zones and substations, as depicted in Figure 4-14.

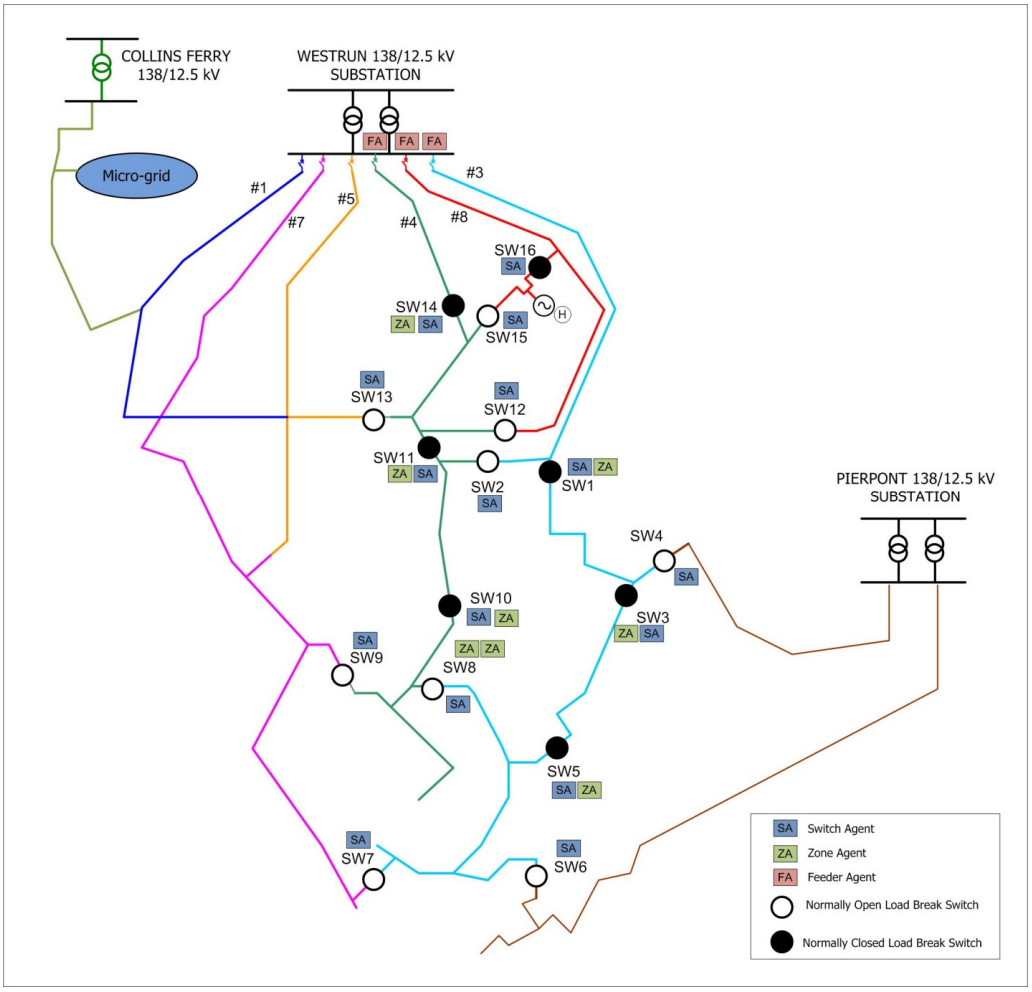

Figure 4-14 - FLIR Agents

New Recloser and Pole Top Switches

As part of the WVSC project, the #8 feeder recloser was planned to be retrofitted to enable remote control. Also, two additional load break switches (SW15 and SW16) were specified be procured and installed onto the #8 circuit. The new equipment was not deployed.

New Switch Controllers

Existing switch controllers were designed to be reconfigured to accommodate new hardware and software. There were three switch controllers designed to be used:

> **Type-1 Switch Controller:** A PQ monitor, agent platform (both described below the Figure) and Wi-Max hardware were designed to be added to existing switch controllers as illustrated in Figure 4-15.

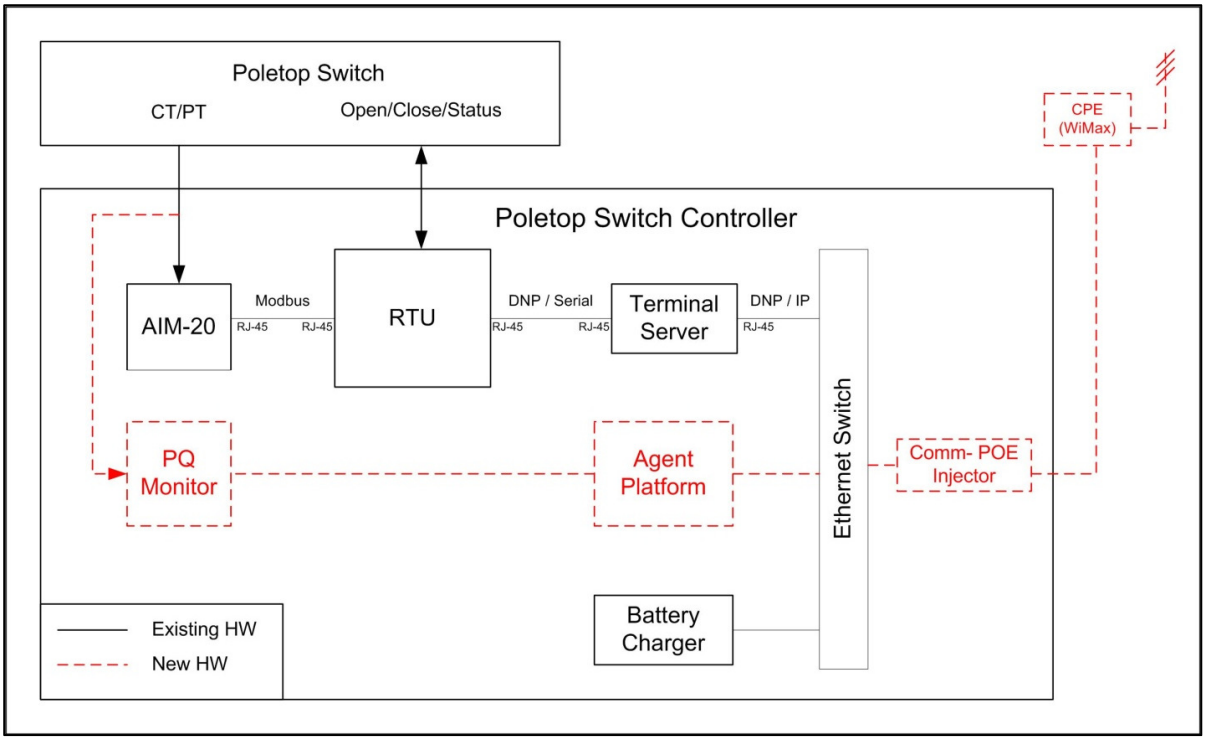

Figure 4-15: Type-1 Switch Controllers

New Power Quality (PQ) Monitors

PQ monitors were designed to be installed at Type 2 switch controller locations. The data that was to be collected were to be used by both APERC agents and FLA/FPA algorithms. The microprocessor-based power quality meter was to measure kilowatts, kilovars, voltage (rms), current (rms), power factor, harmonics and synchronized phasor measurements for voltage and current. The meter was designed to measure kilowatt-hours delivered or received as well as kilovar-hours leading and lagging for power delivered and received. The meter was to capture voltage and current waveforms with programmable logic triggers. The meter was also meant to include self-diagnostic functions to alarm upon detected failure.

Agent Platform

The agent platform is an embedded PC which has been designed to accommodate software agents developed by APERC. The operating system and communications protocol conversion software was designed for the agent platform. The Agent platforms were designed to support:

- Advanced distributed algorithm execution using software agents associated with switches, zones, and Distributed Energy Resources (DERs)
- Substation and field data collection to support modeling, training of algorithms, and system operations

- Data interpretation encoded using various protocols including DNP 3.0, Modbus and IEC 61850
- Data translation from one message type to another to support integration of components utilizing multiple formats and protocols
- Data storage in the field supporting archival and optimum communications
- Evaluation and debugging activities
- Remote asset monitoring
- Operating system execution of functional source code including C, JAVA, C++, and .NET

Type-2 Switch Controller: An agent platform and Wi-Max hardware were designed to be added to existing controllers as illustrated in Figure 4-16.

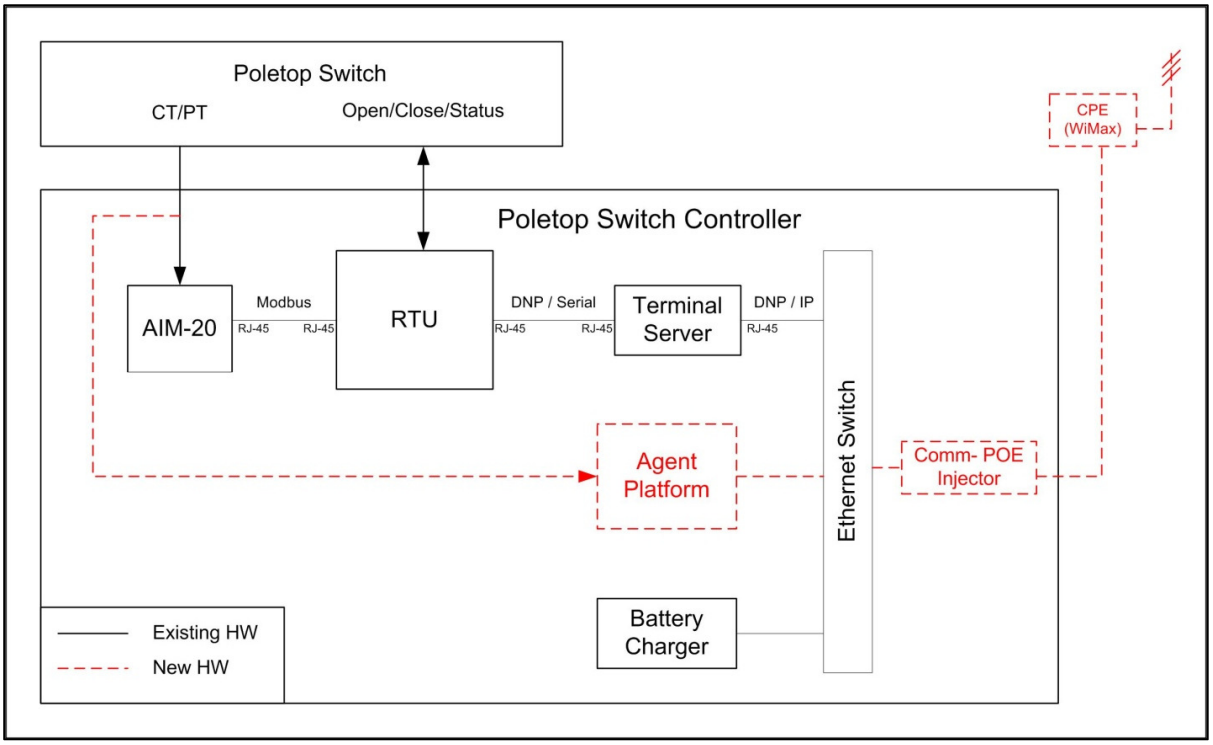

Figure 4-16: Type-2 Switch Controller

Type-3 Controllers: These controllers were designed for the new switches.

Table 4-6: Switch Controller Types (see Figure 4-14 for switch locations)

Switch ID	Switch Controller Type
SW1	Type 1
SW2	Type 2
SW3	Type 1
SW4	Type 2
SW5	Type 1

SW6	Type 2
SW7	Type 2
SW8	Type 1
SW9	Type 2
SW10	Type 1
SW11	Type 1
SW12	Type 2
SW13	Type 2
SW14	Type 1
SW15	Type 3
SW16	Type 3

4.2.3 Agent Based FLIR – APERC Research

The research and development work done by APERC on Multi-Agent System is presented here. APERC developed several agent based approaches for FLIR in power distribution systems which were presented and demonstrated in the laboratory environment. When there is a fault in a Power Distribution System, the proposed Multi-Agent System quickly isolates the fault and restores the service to fault-free zones.

Three Multi-Agent system architectures were evaluated: Hierarchical, Decentralized and Hybrid. Advantages and disadvantages of each architecture are discussed below.

For Fault Location and Isolation applications, three algorithms are developed based on either sequence currents, or impedance, or using a distributed Multi-Agent System method. For the Restoration, an Immune System based method and Optimization based restoration techniques are presented.

4.2.3.1 *Multi-Agent Systems: Background*

In order to explore the potential benefits of Multi-Agent Systems (MAS) to power system applications, the basic concepts and approaches associated with multi-agent systems need to be understood. A brief background on Agent and Multi-Agent System is given in this section.

Definition of an Agent

The computer science community has produced a myriad of definitions for what an agent is. All the definitions share a basic set of concepts: the notion of an agent, its environment, and the property of autonomy.

An agent is merely “a software (or hardware) entity that is situated in some environment and is able to autonomously react to changes in that environment” [18]. The environment is external to the agent. In order to be situated in an environment, at least part of the environment must be observable to, or alterable by, the agent. The environment may be physical (e.g., the power system), and therefore observable through sensors, or it may be the

computing environment (e.g., data sources, computing resources, and other agents), observable through system calls, program invocation, and messaging. An agent may alter the environment by taking some action: either physically (such as closing a normally-open switch to reconfigure a network), or otherwise (e.g., storing diagnostic information in a database for others to access).

An agent which displays flexible autonomy, i.e., an intelligent agent, has the following three characteristics [18].

- **Reactivity:** an intelligent agent is able to react to changes in its environment in a timely fashion, and takes some action based on those changes and the function it is designed to achieve.
- **Pro-activeness:** intelligent agents exhibit goal-directed behavior. Goal-directed behavior means that an agent will dynamically change its behavior in order to achieve its goals. For example, if an agent loses communication with another agent whose services it requires to fulfill its goals, it will search for another agent that provides the same services. This pro-activeness is described as an agent's ability to "take the initiative."
- **Social ability:** intelligent agents are able to interact with other intelligent agents. Social ability means more than the simple passing of data between different software and hardware entities, something many traditional systems do. It brings the ability to negotiate and interact in a cooperative manner. That ability is normally underpinned by an Agent Communication Language (ACL), which allows agents to converse rather than simply pass data.

While an agent displays the characteristic of reactivity, in order to be classed as an intelligent agent, an agent must also have a form of pro-activeness and a form of social ability. It is the goal-directed behavior of individual agents and the ability to flexibly communicate and interact that sets intelligent agents apart.

Definition of a Multi-Agent System

A Multi-Agent System (MAS) is a system comprising two or more agents or intelligent agents. It is important to recognize that there is no overall system goal, simply the local goals of each separate agent. The designer's intentions for the system can only be realized by including multiple intelligent agents, with local goals corresponding to subparts of that intention.

Depending on the definition of the agency adhered to, agents in a multi-agent system may or may not have the ability to communicate directly with each other. However, intelligent agents must have social ability and therefore must be capable of communicating with each other. This work focuses on MAS where this communication is supported.

MAS Architecture

In order to manage and control a power distribution system more efficiently, multi-agent systems have been employed recently to solve challenging problems more efficiently and in a timely manner. MAS are used for fault diagnostics, system monitoring, reconfiguration and restoration, protection, etc. There are two types of MAS structures: centralized and decentralized strategies. In the following, more details about both centralized and decentralized approaches and their application in power systems self-healing are presented [23].

It is important to have a common language for Agent Communication, without which, the coordination and negotiation will hardly be successful. There are some standards for agents' communication languages (ACL) for MAS. The most notable ones are the Knowledge Query and Manipulation Language (KQML) and the Foundation for Intelligent Physical Agents (FIPA) [19]. In these languages the message types are standardized and the message intent is specified. A FIPA ACL message will contain one or more message parameters, according to the requirements of the agent application.

In some MAS architecture, agents have different functionalities and responsibilities such as training agents, fault locating agents and coordinating agents where the tasks are divided among the agents to process. In this work, agents have all the functionalities and are considered to be autonomous.

There are different strategies for controlling agents in MAS; centralized and decentralized, hierarchical and hybrid. Figure 4-17 shows these architectures which are described in the following.

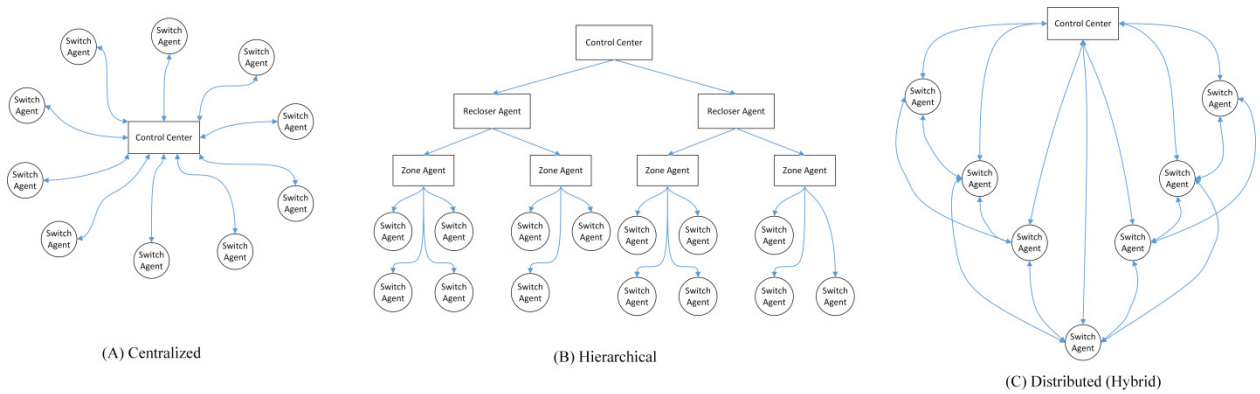

Figure 4-17: MAS Architectures

Centralized

Centralized is the conventional approach and are inadequate for the power systems of the future due to lack of robustness, openness, flexibility, and single points of fault. In

centralized approaches, a coordinator agent is responsible for managing a group of sub-agents. In this architecture, all the agents send their data to a control center and wait for commands. The control center runs the fault location and isolation algorithms and makes decisions. Commands are then sent back to corresponding agents through the communication channel.

Decentralized

With the introduction of distributed power generation, load control, market operations, increasing complexity in the distribution network, and an increased number of interconnections, the operation of a modern power system is extremely complex. Multi-agent systems provide a technology for flexibly controlling this power system, which is an approach that provides intelligent, fast, and adaptable local control and decision making is required [20]. By distributing management and control functionality using intelligent agents, decision-making for network restoration, reconfiguration, the dispatch of generation, and the management of loads can be locally managed. Local decision-making requires agents to perform a range of actions, such as monitoring local conditions, controlling switches and other devices, and coordinating with other regions of the network.

In this architecture, all agents are in the same level of functionality and communicate with its neighbors in a specified neighborhood. The agents make decisions based on the local condition and in the case of malfunction of any agent, other agents continue operating. The agent's link to the control center is considered as supervisory monitoring. Although decentralized approaches are more robust and flexible than a centralized design, the disadvantage with the decentralized strategies is centered on the agent's ability to communication to only its neighbors.

Hierarchical

In this strategy agents work at different levels of decision making. Agent's levels from high to low are the control center agent, recloser agent, zone agent and switch agent. Each zone agent is in charge of a group of switch agents. Low level agents do not have authority and communicate only with higher level agents. Higher level agents have a broader view of the network condition and can use their upstream agents' comments in their decision making process. The information flow in this architecture is bottom–up, and the comments and commands originate from higher level agents. This architecture considers zone agents as decision makers that ask the recloser agent for its permission before sending commands to switch agents.

The disadvantage with this architecture is that a higher level agent's malfunction can create critical situations for all of the sub-agents.

Hybrid

Hybrid MAS structures can leverage both centralized and decentralized approaches with good restoration results. This architecture enables MAS to work in a decentralized manner with the added benefit that agents have access to information form more than their immediate neighbors and the control center plays a role in decision making, thus better decisions are made.

A multi-agent system is composed of several of this kind of agents interacting with each other to achieve a global goal which is beyond their individual capabilities. Hence, this type of technology can allow us to distribute and localize the control of power systems. By incorporating intelligence at the device level, the reliability of the system should improve dramatically since there is no single point of failure as compared to the centralized control. MAS can be depicted as shown in Figure 4-18 below.

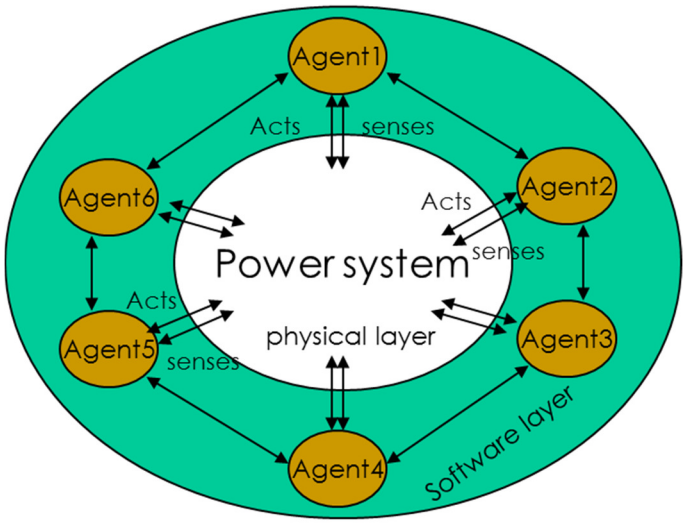

Figure 4-18 : Multi-agent System Power System Graphic

In addition, an agent has to be autonomous, which means that an agent can operate without direct human intervention. The agent can decide on its own, the required actions to be taken in order to achieve system objectives. The MAS has to be autonomous for it to be an intelligent system. MAS without intelligence is no different to another software application, where the decision making process is designed by the programmer and if any unexpected situation other than a planned event occur, the system would crash.

4.2.3.2 *WVSC FLIR Multi-Agent System Architecture*

In this section, information about the WVSC FLIR multi-agent hybrid; hierarchical-decentralized design system architecture is described in Figure 4-20. The West Run Substation has eight feeders, two of which, WR#3 and WR#4 are monitored for faults. The substation feeders are equipped with reclosers. When there is a fault in the system, the recloser will go through its trip and close operations as configured. The entire number of agents in a power distribution system substation corresponds to the overall number of substations reclosers and switches. The WVSC

FLIR system is divided into different zones connected through 16 controllable switches, shown with circles in Figure 4-19.

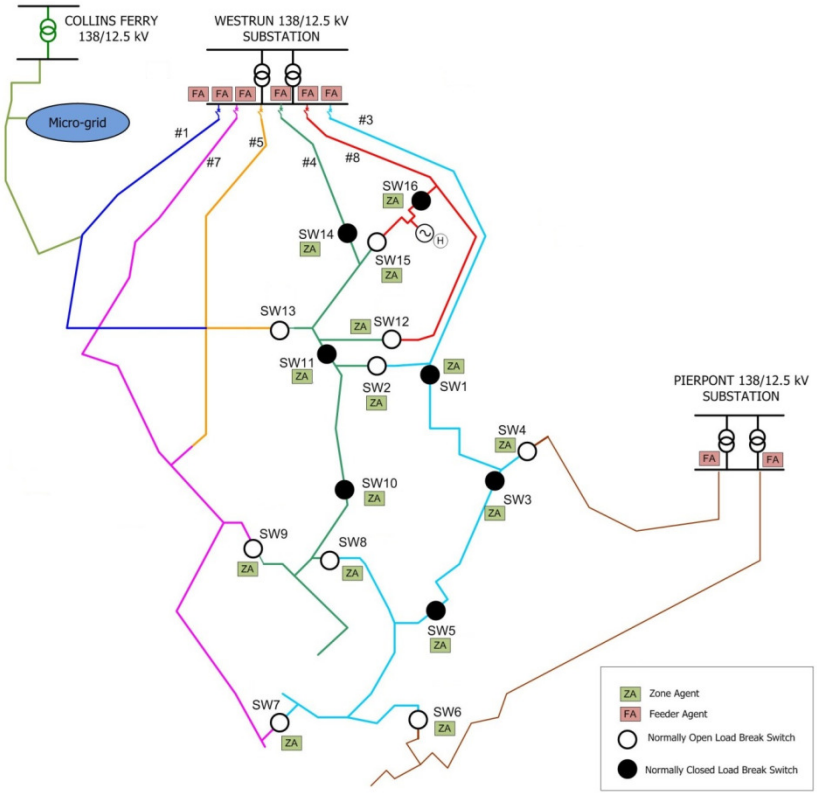

Figure 4-19: WVSC FLIR System Design

The switches along the feeder are for data acquisition and their role is restricted to record voltage and current waveforms as well as fault location and isolation. Agents are computers with high protection standards and powered by uninterruptible power supplies (UPS) that are installed at some switch locations. MAS is embedded in these computers.

To perform the FLIR for a self-healing power delivery system, the hierarchical-decentralized MAS framework is employed. As shown in Figure 4-20, there are three type of agents in the proposed MAS; recloser, zone and switch agents. These agents are intelligent units that have problem solving capabilities and can communicate, resolve, coordinate and debate with other agents and make decisions.

Recloser Agents (RA) keep track of the status of the recloser at the substation and informs the Zone Agents (ZA) in various zones when the recloser locks out. The ZA and Switch Agent (SW) are agents that are responsible for managing each zone in the power distribution system. Each ZA has one associated SW for that particular zone.

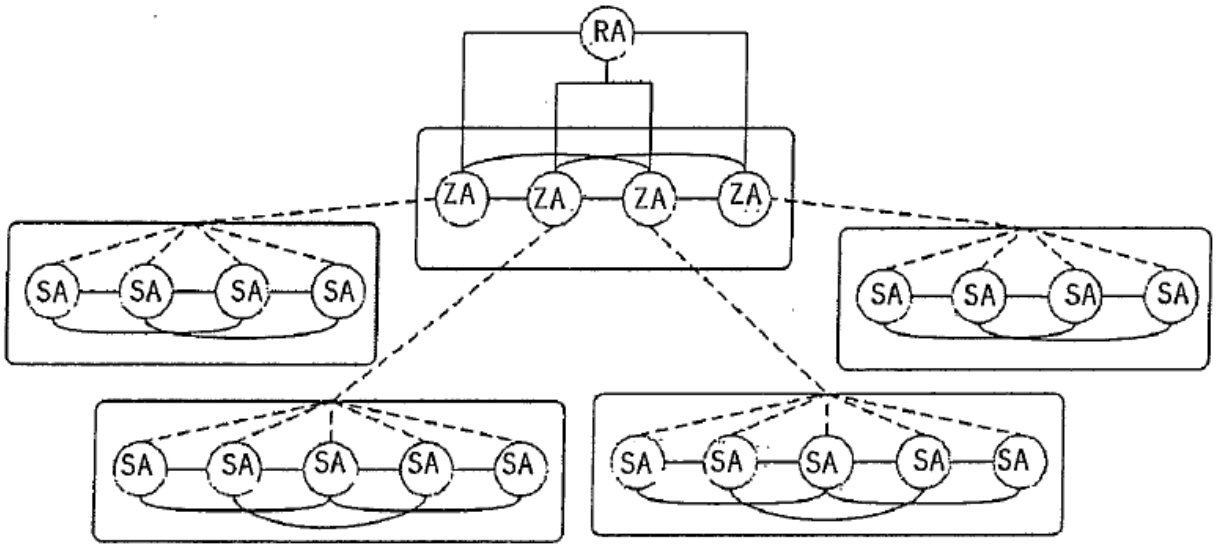

Figure 4-20: Multi-Agent Hybrid; Hierarchical-Decentralized Architecture

The main responsibility of each agent is described below:

- Recloser Agent (RA): This agent keeps track of the status of the Recloser at the substation and informs the Zone Agents in various zones when the recloser locks out. After the lock out, the tripping off action of the recloser is implemented by opening the substation transformer in the test system. So, the Recloser Agent sees negligible current in all phases of substation transformer element that has been opened and informs the zonal agents about the lock out.
- Zone Agent (ZA): These agents inform their corresponding Switch Agents about the recloser lock out and ask them to check for faulty condition and implement the fault location algorithm.
- Switch Agent (SW): This agent is the most important entity in this agent architecture since it implements the fault location and isolation after receiving information about the recloser lock out from its corresponding zone agent. This agent has information of the power flows, sequence current magnitudes and phase angle of all the lines in its zone. The values of symmetrical current components are obtained directly from the simulation of the test system in OpenDSS software.

When a permanent fault occurs in the system, the recloser tries multiple times to close and then locks out, upon which the recloser agent informs the zone agents of the lock out. Then, the ZA informs its corresponding SA to check for a fault condition on the circuits in its zone and implements the fault location algorithm. The zone and switch agents are designed with local distribution line information, such as power flow and sequence current magnitude and phase angle in their respective zones.

The agents obtain information regarding sequence, current magnitudes, and phase angles from protective relays. Zone and switch agents implement fault location in a decentralized manner upon receiving the recloser lock out signal from the recloser agent.

4.2.3.3 *Fault Location Algorithm Design*

The fault location process is described in this section. There are two stages in the fault location, 1) Identifying the type of fault whether the fault is single line-to-ground, line-to-line or three phase-to-ground and 2) Determining the fault location.

Fault Type Identification

Each fault type can be identified based on the magnitudes of the current sequence components. The two current sequence components are positive sequence current (I1), negative sequence current (I2) and zero sequence current (I0). Each component shows violation depending on the kind of fault occurring in the system. For identifying single line to ground fault, 3-phase to ground fault and line to line faults the residual current or zero sequence (Ir), positive sequence current (I1) and negative sequence current (I2) magnitudes respectively are used. The residual current is the sum of positive, negative, and zero sequence currents. The reason for using sequence current magnitudes for fault detection is that when a fault occurs, depending on its type of corresponding sequence, current magnitudes are high in the affected lines. These values are substantial even for faults in an islanded microgrid. Thus the sequence current magnitudes give a rough estimate of where the fault exists.

Residual currents are used for identifying single line-to-ground faults, positive sequence current is used for three phase-to-ground fault, and negative sequence is used for line-to-line faults. The thresholds (0th, 1th, and 2th) are set for these sequence currents and all the lines violating the limit are suspected of having a fault in them. The switch agent first checks all the lines that exceed these thresholds.

In order to determine these thresholds, a detailed short circuit analysis at every node of the test system has to be performed. The thresholds have been determined for different penetration levels of the distributed generation units in the microgrid. The penetration levels considered are 25%, 50%, 75% and 100%.

Determining the Fault Location

The next phase of the fault location algorithm is identifying the fault location, which is dependent on the location of the faulty node, whether the node has a two way power flow or a unidirectional flow. For a node which has two way current flow during a fault, current reversal shall be checked. The reason to check for current reversal is because of the two way power flow and that when fault occurs in a system, all the generation units will feed this fault. When a fault occurs in a node between two lines such that on either side of that node a generation unit exists, the unit will have to feed the fault and thus, the adjoining lines of the node will have current flowing in opposite directions. This demonstrates that the fault can be located based on current reversal.

The current direction for a single line to ground fault is determined by looking at the change in the phase angles of zero sequence currents of the lines. For a fault located between two lines, these angles magnitudes are of the opposite sign. While for multi-phase faults like 3-phase and line-to-line faults, the current direction can be determined from the values of real power. For a 3 phase fault, the real power values will be of opposite signs in all the 3 phases. For a line-to-line fault, this would be the case in the two faulted phases in the lines attached to the faulty node. To add further credibility for the determination of fault location in the case of 3 phase fault and line-to-line faults, the phase angles of the corresponding sequence components can be used. This applies to a fault type that is a positive sequence component for 3 phase fault and one that is a negative sequence current for line-to-line faults. Similar to single line-to-ground, these phase angles in the adjacent lines of the faulty node will be in opposite sign.

In the scenario where the fault occurs in a node/line where there is unidirectional power flow, the condition for current reversal will not be satisfied. The faulty node can be determined by the condition for negligible residual current and is considered for faults in terminal nodes/lines where there is no two way power flow. It has been observed from simulation that in these nodes/ lines the residual currents become negligible during a fault and this is being used for fault identification. The complete flow chart of the fault location algorithms is provided in Figure 4-21, below.

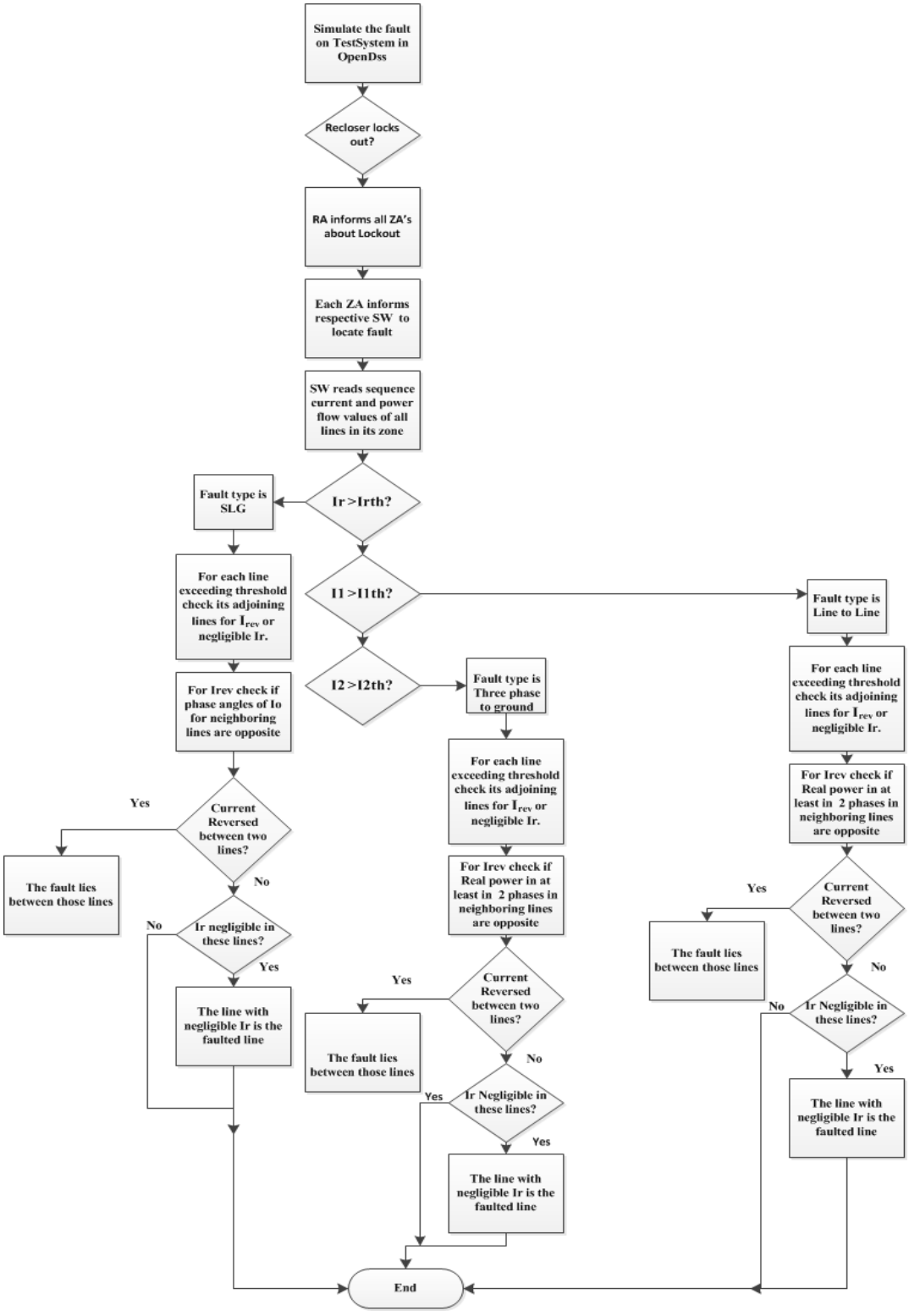

Figure 4-21: Flow Chart for Fault Location

Fault Location Isolation Algorithm using Zone Current Usage[23]

Figure 4-23 shows the fault location, isolation algorithm flowchart. In normal operation, agents update their load profile data and also update their neighbor's data. Agent's pull out the meters recorded data during the last recloser trial with highest resolution and compare the data with recent normal operation data.

Each agent has access to its neighbor agent's data and can calculate the current injected to area between itself and upstream or downstream agents by using the Kirchhoff's law as follows:

$$\sum_{i=1}^{n} I_{Enterance_i} - \sum_{j=1}^{m} I_{Exit_j} = I_{Zone}$$

where, $I_{Entrance_i}$ is the Ith current entering the zone, I_{Exit_j} is the Jth exiting current and I_{Zone} is the zone current. Figure 4-22 shows the sketch of the message exchange between two agents.

In an engineering context, "inform" and "request" could relate the agent's data transferring where the message contents contain the information (Figure 4-22). After "inform" and sending each data packet, agents wait for acknowledgement. The data should be resent if the acknowledgment is not received; because agents need the synchronized data of their neighbors for decision making process.

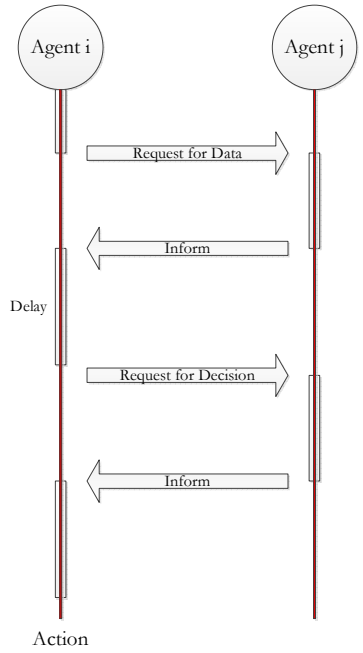

Figure 4-22: Message Exchange Sketch

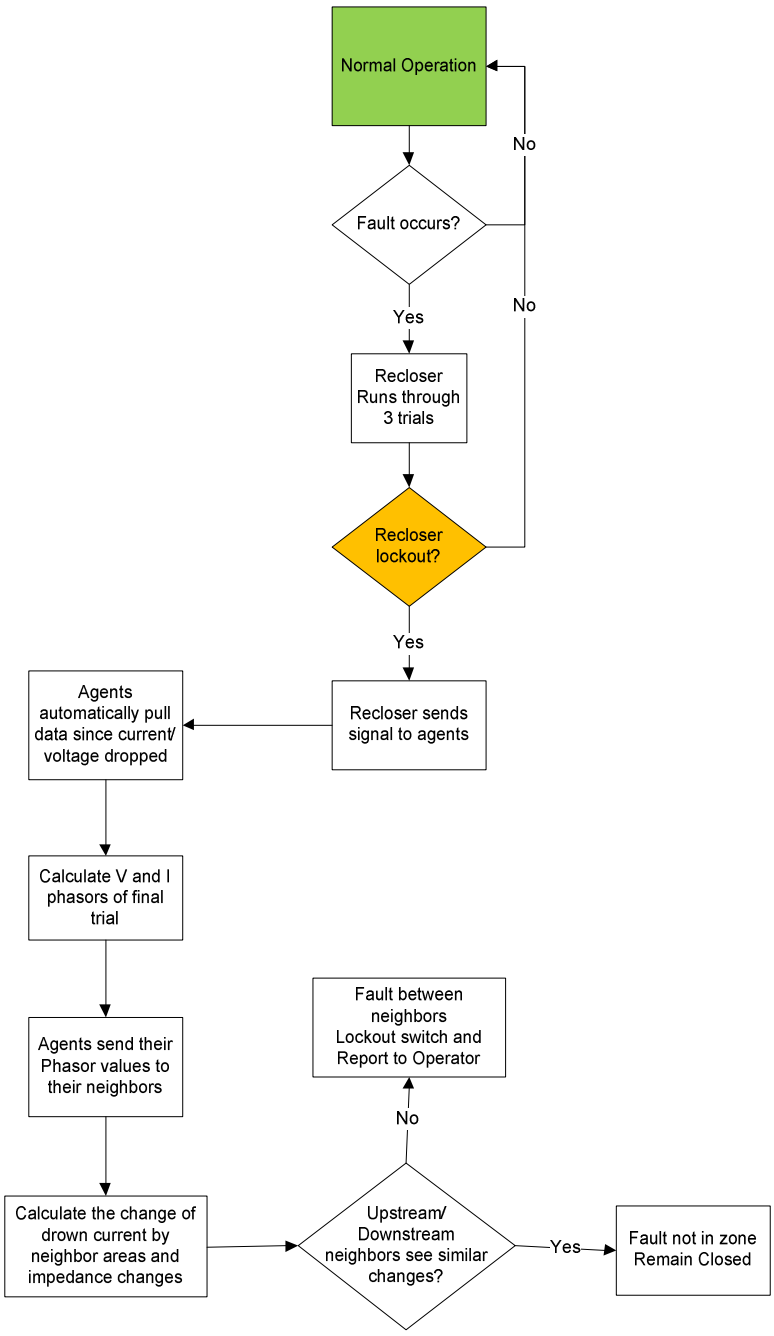

Figure 4-23: Fault Location, Isolation Algorithm Flowchart

4.3 Fault Location Algorithm / Fault Prediction Algorithm

4.3.1 Fault Location Algorithm

FLA algorithms that were developed by North Carolina State University (NCSU) were designed to identify the fault location on distribution system. In addition to providing distance to fault with precision, the FLA algorithm also identifies the protective device (e.g. fuse) that may have operated in response to a fault. The FLIR system developed by APERC also finds the fault

location, but FLIR can only identify in which Zone the fault is in and cannot give any more specific information.

Mon Power, through its OMS software predicts the fault location based on customer calls and the utility crew is dispatched to drive the faulted circuit to manually find the fault location. The FLA system improves system reliability by decreasing the time needed for fault location.

The high-level architecture and the major components of the FLA system are shown in Figure 4-24.

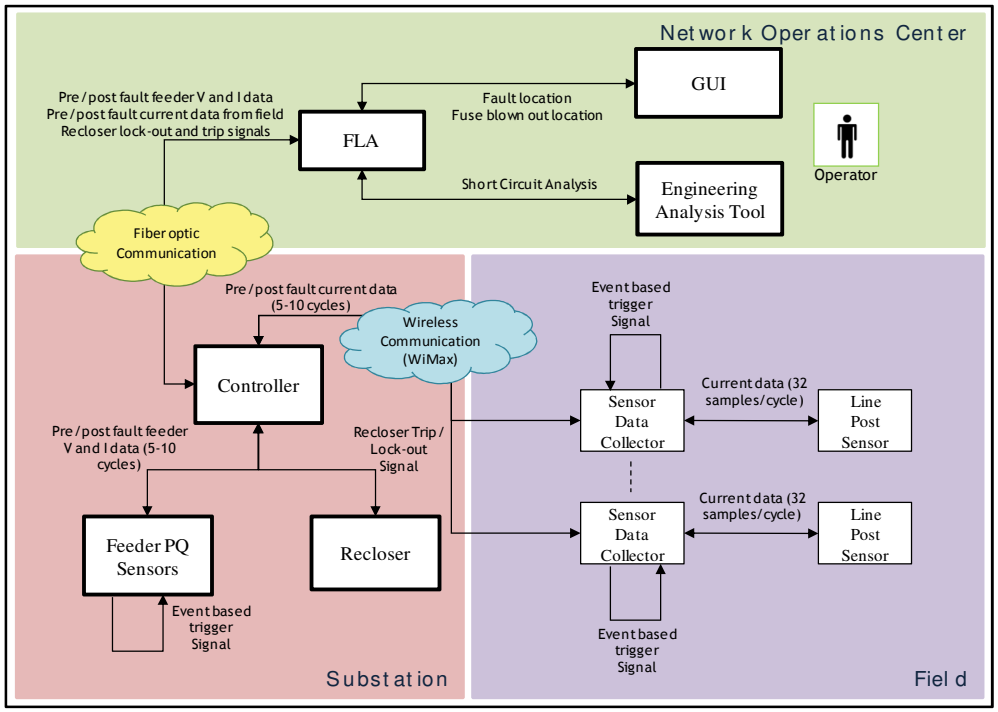

Figure 4-24: FLA System Architecture

Fault Location Methodology

The Fault Locating Method (FLM) developed uses the current waveforms from Power Quality (PQ) Monitors located on distribution feeders to determine the location of a permanent fault. The method is model based in that it uses a detailed feeder model to estimate the fault currents and compares it with the data obtained from PQ monitors.

The designed FLM aims at estimating the location of a fault which caused a Protection Device (PD) operation to clear a permanent fault on a distribution feeder. A PQ monitor located at the substation captures the fault current waveform and sends it to the distribution operation center to determine the fault location, which is then displayed to a system dispatcher who is coordinating the response to the resulting outage.

The proposed FLM has four main steps:

Step 1: Data Extraction: Using the fault current waveform, extract the data about the fault: fault current level, fault type, duration of fault, and the load current rejected, i.e., change in load current before and after the fault is cleared.

Step 2: Identify the PD Operated: Using the fault current and the database about PD devices on the feeder, identify the candidate PDs which may have cleared the fault. This is achieved by comparing the estimated operating time of the PDs with the fault duration extracted from fault data.

Step 3: Identify candidate fault locations: Use a fault analysis method to calculate the fault current levels the PDs will see by simulating the faults along the feeder. Compare the calculated fault currents with the extracted fault current to identify the locations that provide a good match between these two currents.

Step 4: Process data from other PQ monitors: If there is data available from other PQ monitors on the feeder use this data to further localize the location of the fault.

These steps are elaborated further below.

Step 1: Data Extraction from Fault Current

The fault current waveform obtained from the monitoring device is first used to obtain the corresponding root mean square (rms) profile. Figure 4-25 shows a typical profile. The rms profile is then used to extract the three main features about the fault: fault current level, I_f, time it took for the PD to operate to clear the fault, T_{cl}, and the pre-fault and post-fault current levels. Figure 4-26 shows these parameters.

The difference between the instant of fault inception and the time that the protective operated is the total clearing time.

$$T_{cl} = T_{open} - T_{inception} \quad \text{---- (1)}$$

To determine the type and the phase(s) on which the fault occurred, the fault current magnitude from each phase and the neutral is compared to its corresponding overcurrent threshold. These overcurrent thresholds are set for each of the three phases and the neutral. Threshold values are typically 1.5 times that of the peak load current levels.

Next, the pre-fault, fault, and post-fault currents are calculated. For the pre-fault current, current before the fault inception time $T_{inception}$ is considered. The fault current, I_f, is taken as the current immediately following the initial transient. The post-fault current is calculated by using the part of the waveform after the fault has been cleared. Finally, the load rejection for each phase is calculated as the difference between the pre-fault and post-fault values of the current.

$$I_{rej} = I_{pre-fault} - I_{post-fault} \quad \text{---- (2)}$$

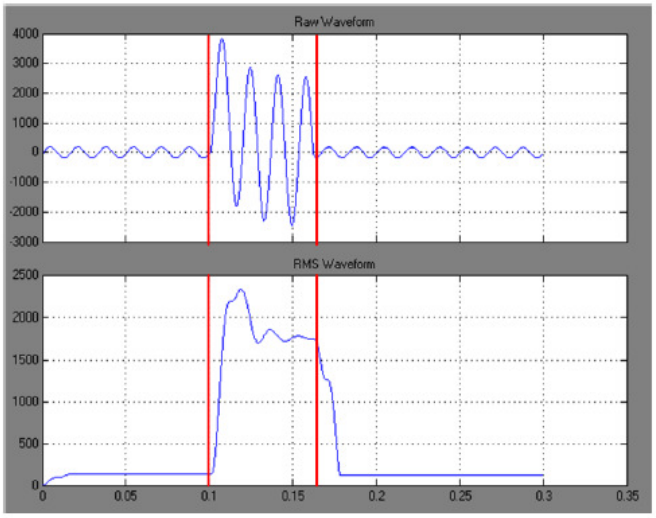

Figure 4-25: Instantaneous and RMS Waveforms

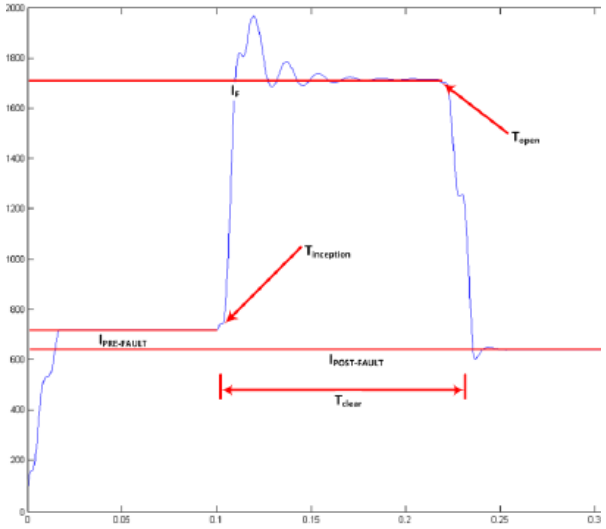

Figure 4-26: Parameters extracted from a fault current RMS profile.

Step 2. Identification of the Protective Device (PD)

It is known that the PDs (relay controlled switches or fuses) on the feeder must have operated to clear the fault. These devices have inverse time-current characteristics (TCC) which can be used to estimate the time it will take for them to operate if they have seen the fault current I_f extracted in step 1.

For example, FLM can calculate the total clearing time (T_{CC}) for a fuse with the TCC characteristics shown in Figure 4-27, for the given I_f. This is repeated for each candidate PD, and the estimated clearing time, $T_{CC,}$ is calculated. Then these values are compared with the measured clearing times, $T_{cl,}$ that are obtained in step 1 to determine the devices with close match between estimated and measured values. To quantify the match, the percentage difference between T_{CC} and the measured total clearing time (T_{cl}) is calculated as the Time Error. The PDs with lowest *Time Error* is more likely the one that actually operated.

$$TimeErr = \frac{T_{CC} - T_{cl}}{T_{cl}} \text{ ---- (3)}$$

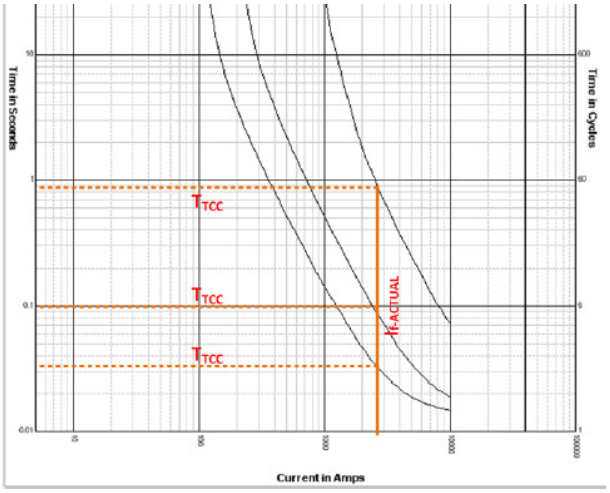

Figure 4-27: TCC Characteristics of Fuses

An estimate load drop by each candidate PD is obtained by using power flow analysis. The pre-fault current at substation end is used to estimate the loading condition on the feeder. Using a detailed feeder model and power flow program, the current through each PD is calculated. This current drop, $I_{pf,}$ is what the PQ monitor observe after the PD operates to isolate the fault. These values are then compared with the measured load rejection current, $I_{rej,}$ to identify the PDs that better match. This is done by calculating the mismatch errors as follows:

$$Lderr(i) = \frac{|I_{pf}(i) - I_{rej}|}{I_{rej}} \text{ ---- (4)}$$

where i is the index for all the PDs on the feeder.

A fault analysis is then performed on the feeder and then calculated are the fault currents each PD will see. This is done by simulating the fault at every node within each candidate PD's zone of protection. These calculated fault currents are then compared with the measured fault current to determine the likelihood that the fault is within the candidate PD's zone of protection. If there is a fault current that matches the measured fault current, I_f, then the corresponding PD is kept as the candidate. Otherwise, it is eliminated from the list. Here, a 3%-25% match is used to account for inaccuracies in the model and to account for measurement and communication errors.

Finally, the time error and load drop errors are combined by taking an average of these two errors:

$$PDErr(i) = \frac{TimeErr(i) + LdErr(i)}{2} \text{ ---- (5)}$$

This measure is used to rank and determine the most likely PDs that operated to clear the fault.

Step 3. Identification of Faulted Nodes

The measured fault current I_f is compared with the fault current values obtained from short circuit analysis done in the previous step. Since we simulate the fault at every node *n* within a candidate PDs zone of protection, I_{fnode}, one can compare this value with I_f and identify the candidate nodes that provide a close match:

$$CurrentErr(n) = \frac{I_f - I_{fnode}(n)}{I_f} \quad \text{---- (6)}$$

where, *n* is the node index. Based on this measure, FLM ranks the nodes within a candidate PD's zone of protection to indicate the most likely fault locations.

Step 4. Filtering Nodes Based on Additional Measurements

If there are additional PQ monitors (PQMs) on a feeder, data from these monitors can also be used to further localize the location of the fault. Data from these PQMs will first help to determine which PQM has seen the fault. This information can be used to eliminate the PDs which are not downstream of the PQMs. If there are few PQMs that are strategically placed along a feeder, it can help fault localization considerably. This is illustrated in the test results section.

4.3.2 FLA Integration with CYME

When the FLA algorithm runs, it analyzes the load flow and short-circuit results which are developed using an external power system simulation software. The topology and loading used in the simulation need to be identical with the actual values when the fault happened. Since Mon Power used CYME as their power system simulation software, an interface is designed between CYME and FLA. FLA was integrated with CYME software in order to run simulations and obtain results.

Figure 4-28 illustrates the interfaces required between FLA and CYME. The Fault Location Algorithm which can be developed in C, C++, or C# languages, can access the CYME software via the CYME COM interface that was developed in C#. FLA/FPA algorithms can seamlessly integrate with CYME software with the help of the CYME COM Interface to run short circuit and load flow analysis and getting the results back in desired formats. Depending upon the request from the CYME COM interface, particular CYME circuit models are fetched into the CYME software for performing requested analyses.

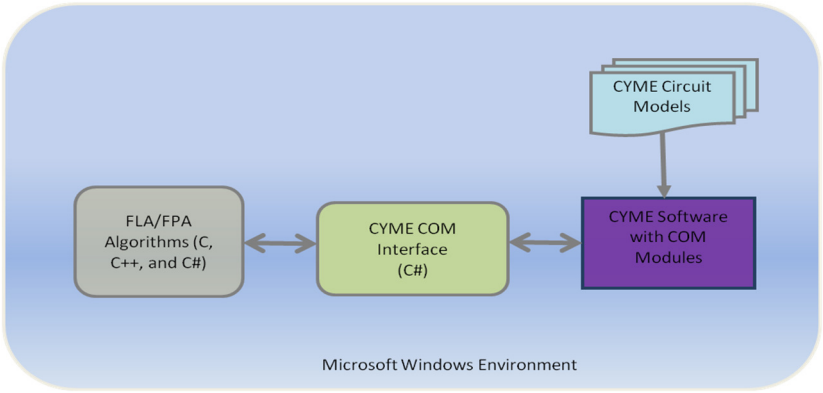

Figure 4-28: FLA Integration with CYME

4.3.3 Fault Prediction Algorithm

Fault Prediction Algorithms (FPS) were developed by NCSU. The main purpose of these algorithms is to predict distribution system faults before they actually occur by analyzing the fault signatures in the current and voltage waveforms. The high-level architecture and the major components of FPA system are shown in Figure 4-29.

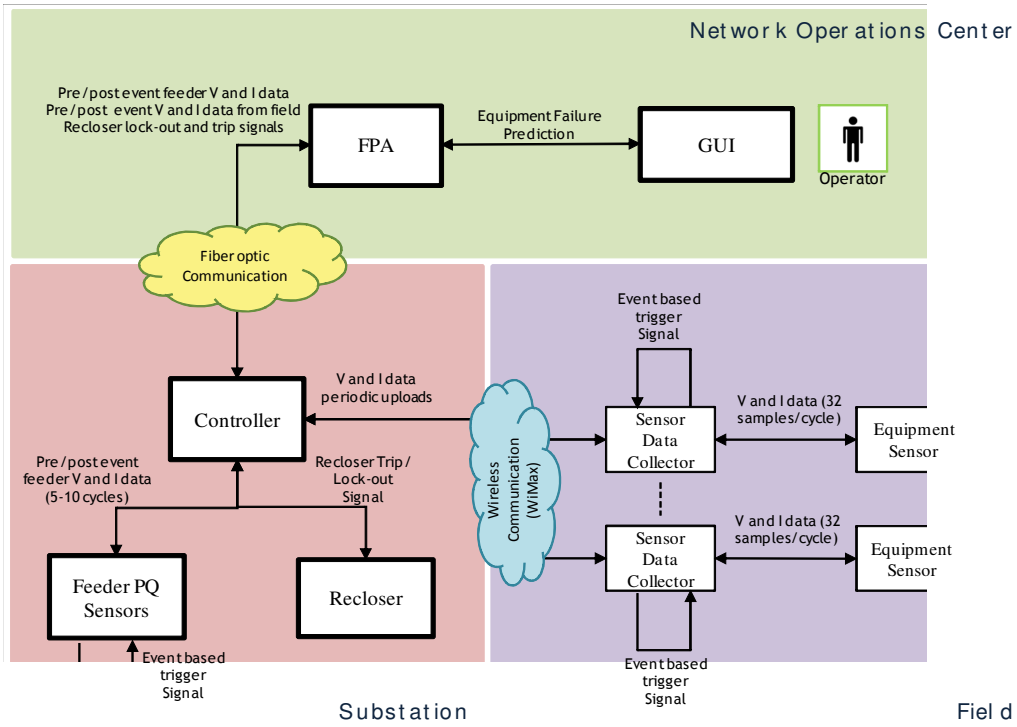

Figure 4-29: FPA System Architecture

Fault Prediction Methodology

Recent studies have tried to capture the signatures that can be observed from voltage and current monitors when distribution feeder assets: transformer, arrestor, circuit breaker and capacitor bank. As assets age, they experience a higher rate of incipient faults leading up to asset failure.

Methods have been developed to capture these signals and alert system operators about possible asset failure. These studies mainly use monitoring data from a single location.

This project improved upon existing methods by using monitoring data from several feeder locations. The closer the sensor is located to the asset(s) being monitored, the better the signature is expected to be. NCSU developed an Artificial Neural Network (ANN) based method for this purpose. Previous investigations have indicated that ANNs can identify signatures very effectively.

For each asset under study, an ANN is trained to recognize failure signatures and the incipient faults that indicate premature failure. For ANN training and testing, a large PQ database was used that has been collected through Electric Power Research Institute (EPRI) sponsored projects, and also the data collected on Mon Power systems from previous projects. This ANN-based program can provide the following prognosis for the equipment on a feeder: surge arrestor discharge, voltage regulator failure, capacitor bank failure or partial failure, distribution transformer problems, and underground cable partial failure.

4.4 DER Dispatch for Peak Reduction

WVSC project planned to demonstrate a feeder peak load reduction solution using customer owned distributed energy resources. During the process to make application to the DOE for the WVSC project, WVSC project team participated in negotiations with the WVU Research Park group. At that time, Research Park had agreed to provide access to their planned generations resources for peak reduction on West Run #3 circuit. Research Park offered the following as their part of the project:

1) A letter of intent to participate and provide cost share toward the project
2) A business plan that would provide for installation and participation in the project with "the purchase of 1.5 MWs of distributed Energy Resources (micro-turbines, diesel generators [biodiesel/other renewable fuel sources], solar cells, batteries, etc.) in the years 2008-2012."
3) An estimation of funding in the order of $2.25 million.

Research Park's DERs were designed to be lumped together and available for direct grid connection and be available for control by Mon Power, with certain contract restrictions.

At a later date, due to economic downturns and the resultant lack of clients for the Research Park, they decided that they could not install the DERs and as a result, dropped out of the project.

After a search was performed, Mon General Hospital was approached to participate in the project with their back-up generation as a resource. A study of their facilities was performed to determine their ability to meet the original goals of the project. During this review, several operating realities were discovered.

1) Mon General Hospital's generators could not be connected directly to the grid due to the internal wiring configuration used.
2) Mon General Hospital was not willing or able to allow direct control of their generation by the project (Mon Power).
3) Mon General Hospital requested a 24 hour notice prior to reducing their utility consumption by starting their generation to replace "shore" power.

The final agreement between Mon Power and Mon General Hospital was signed on June 25, 2013. According to this agreement, Mon General Hospital DERs would be dispatched to reduce peak power on the West Run #8 circuit. The project team would forecast the #8 circuit load for the next day based on historical data.

Once the peak load is predicted for the next day, Mon General Hospital personnel would be contacted by phone and informed about when and how long the back-up generator would be required to stay on the next day.

The project team analyzed the load profile of the West Run #8 circuit to estimate the hours that DER would be dispatched in order to provide 15% load reduction on the circuit. The load duration curve for the West Run #8 circuit is presented in Figure 4-30. This analysis showed that the top 15% of the feeder load occurs only 150 hours a year, therefore it would be enough to dispatch DERs for 150 hours for the 15% peak load reduction goal.

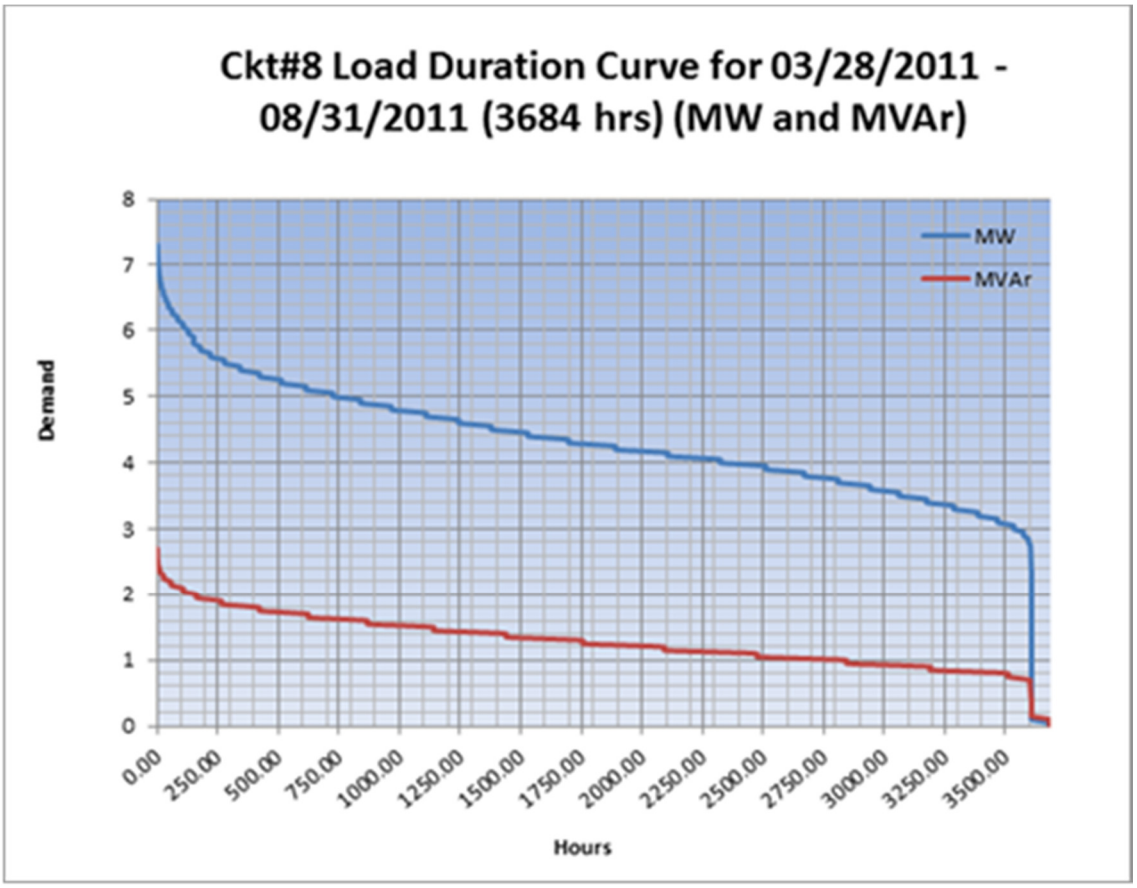

Figure 4-30: Circuit # 8 Load Duration Curve

4.5 Network Architecture and Communications

4.5.1 Network Architecture

The WVSC project leveraged the network architecture that was put in place in the previous DFT project. Modifications to the existing architecture were to be made to accommodate new technologies. Figure 4-31 illustrates the existing network architecture and the new technologies that were designed.

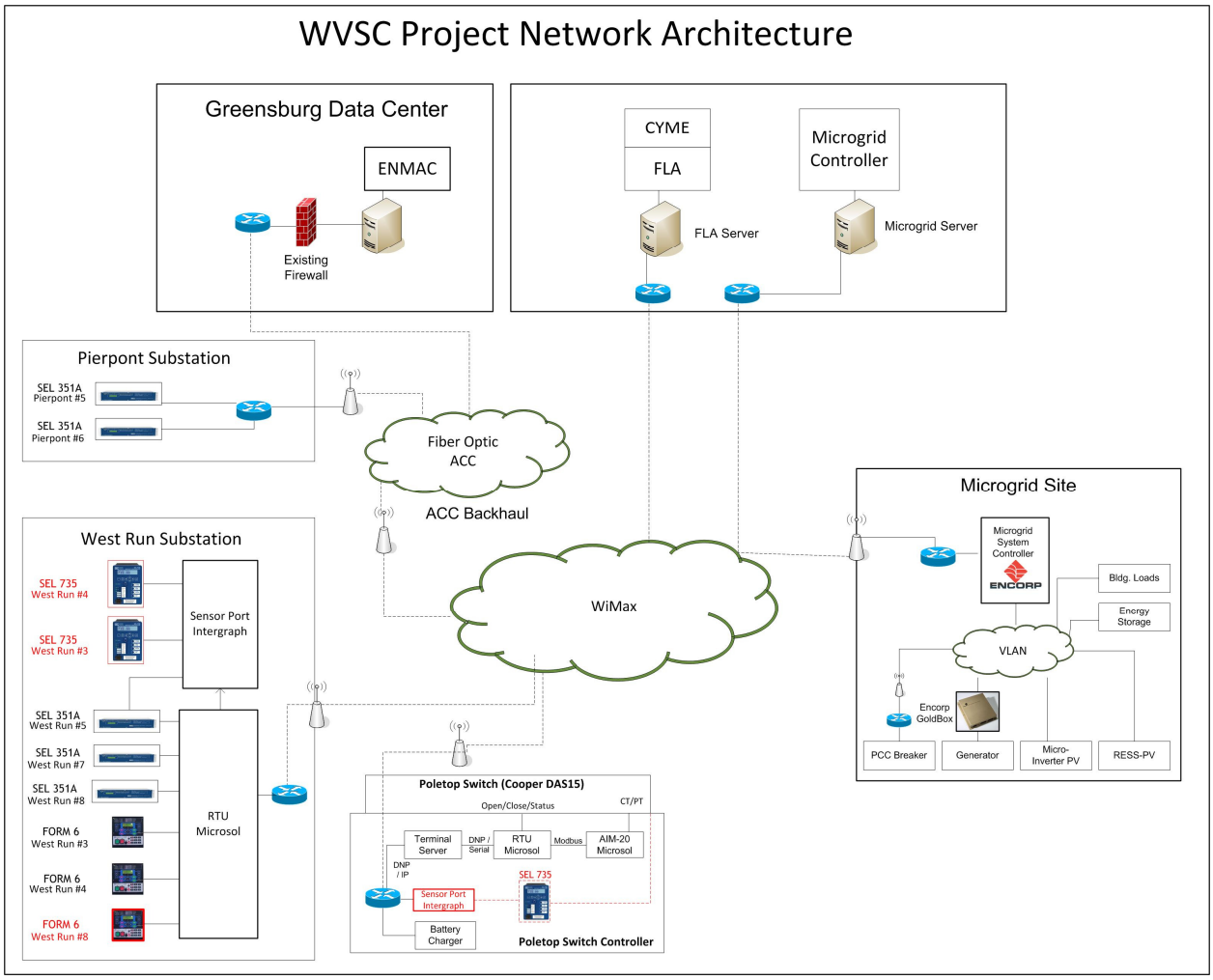

Figure 4-31: WVSC Network Architecture

4.5.2 Wireless Communications System

4.5.2.1 *Legacy Morgantown DFT Wireless Communications*

The communications system planned to be used by the WVSC project was originally installed in an earlier DOE sponsored project, the Morgantown Developmental Field Test (DFT). The DFT project started in 2006 and was completed the end of 2009. The WVSC project was proposed in 2007 and awarded by the DOE in 2008.

The WVSC project communications system was based on the DFT system being operational. Due to the overlap in the two projects, problems arose and are discussed below.

After the DFT system was installed and prior to being placed in production, operating characteristics weaknesses in the communications system were discovered and due to these problems, the system was not implemented. To understand the problems, an analysis was undertaken so that corrective action could be taken as described in the following sections.

Morgantown DFT Wireless Communications History

In 2006, an unlicensed Wi-Fi (2.4 GHz and 5 GHz) wireless technology was chosen to serve as the communications backbone for fourteen (14) distributed automation switches installed for two (2) feeder circuits originating from West Run substation.

This technology was selected by DFT team project managers to adopt open/unlicensed Wi-Fi technology due, to adhere with then existing standards, and to provide the potential for internet access within the coverage area for future development.

This technology solution proved to be unreliable due to lack of system enhancement, interference issues, and technological flaws. Specifically:

- With system enhancement, as originally planned, the implementation of the DFT communications system was to provide limited redundancy available within the DFT budget limitations with further expansion to increase redundancy and reliability to occur as part of the West Virginia Super Circuit (WVSC) project activities that were expected to follow on shortly after the DFT project completion.

- Related to growing interference, other 2.4 GHz and 5 GHz transceivers have been detected in the coverage zones resulting in noise levels which reduce the communications links' reliability. Additionally, construction of new buildings and additional tree growth has obstructed some communications paths that were not obstructed three/four years ago. These new obstructions were tolerated by WiFi technologies especially without redundancy at the end points.

- Related to technological flaws, the DFT program product was flawed in several technological respects leading to unreliable links to many coverage areas. The major flaw was associated with the meshing algorithm used to determine optimal communications path among available paths. When determining the optimal path, when certain conditions existed, the algorithm shifted communications paths or, in some cases, failed to select a path, altogether.

Based upon the above issues and the current recommendations, by DOE and other standards making organizations, not to use unlicensed Wi-Fi as it is not suitable for electric utility smart grid communications backhaul systems, a recommendation was made to replace the legacy communications network entirely under the WVSC project activities rather than enhance it as originally planned.[1]

4.5.2.2 *Design Features of the Planned WVSC Communications System*

Intergraph, formerly known as Augusta Systems, Inc., was charged with researching the replacement communications technologies and proposing an appropriate system. Their work resulted in the system that was specified and included the following requirements and findings.

Communications Design Requirements

[1] PNNL-19084, A Survey of Wireless Communications for the Electric Power System, Prepared for the U.S. Department of Energy under Contract DE-AC05-76RL01830, January 2010, Page IV

- Coverage area - Approximately 2 mile x 2 mile area
- Approximately 50 end points, consisting of:
  - 14 - Existing switches
  - 1 - West Run substation
  - 1 - Backhaul point
  - 5 - Additional switches for added circuits
  - 2- 4 - Switches supporting microgrid
  - Other points for DER locations

Other Communications System Recommendations

- Consistent with the technology selection process described by the NIST Priority Action Plan 2 (PAP2), Guidelines for Assessing Wireless Standards for Smart Grid Applications
- NIST advocates selecting a wireless solution for a smart grid project based on an initial screening of the wireless technologies against the smart grid business functional and volumetric requirements
- USDOE assessment in January 2010, recommended using WiMAX and cellular technologies for feeder reconfiguration applications and notes WiFi as not suitable

Selection Process Used

- Minimum requirements for consideration of technology/vendor: throughput and latency
  - Greater than 1Mbps at each endpoint
  - No more than 500 ms latency
- Review and ranking of candidate technologies
- Review and ranking of vendors associated with selected technologies including interviews
- Vendor supplied basic list of materials and budgetary estimates
- Bench and field testing of selected vendor solutions
- Final ranking based on vendor reviews and field performance

Wireless Performance Criteria

- Throughput
- Latency
- Coverage/Distance
- Network Based
- Security
- Redundancy
- Licensed/Unlicensed
- Deployment Logistics

Several vendors in the field were researched and the top potential candidates were determined. Those potential vendors were reviewed with greater scrutiny and were further interviewed and

tested to determine the best source for the new communications system being specified for the WVSC project.

Field and Bench Testing

The following tests were performed to determine the best candidate for the communications system.

- Bench-top Testing – Performance baseline under perfect conditions
- Research Ridge Testing – NLOS/multi-path testing (not distance testing)
- Research Ridge Testing – LOS distance testing
- Field/Deployment Testing – NLOS/multi-path & distance testing

After review and testing, the solution offered by RuggedCom best met the requirements for the communications system. Their solution offered the following characteristics:

- WiMax – 3.65 GHz
  - 2 base station locations (3 base stations per location)
  - Approximately 50 end points
- Coverage appears to meet the area extent
  - Extensible with additional base stations
  - Extensible with additional endpoints
- Expectations
  - Throughput (at ~10ft height with omni-directional antennas)
    - 1.5-3.5 Mbps uplink, 2-3 Mbps downlink (Exceeds basic criteria)
  - Latency
    - 10 – 40 ms endpoint to endpoint based on 10 ms delay through each base station point (Exceeds basic criteria)
  - Reliability
    - Robust utility grade hardware
    - Easily installed with minimal connections, i.e. integrated antennas, POE powering
  - Redundancy
    - Endpoints switch between base stations within communications range
    - Dual endpoints can be used at the takeout point ensuring that both base station locations can be reached
  - Other
    - Low noise frequency band
    - Better foliage/obstruction penetration than higher frequencies
    - Licensing normally without difficulty

4.5.2.3 *WVSC Wireless Communications*

It was planned that a WiMax based communications system provided by RuggedCom operating in the 3.65 GHz lightly licensed spectrum would be used. It could give connectivity between

switches, West Run substation, and the DER equipment at Research Ridge. Below in Figure 4-32 a bird's eye view shows the communications network equipment location.

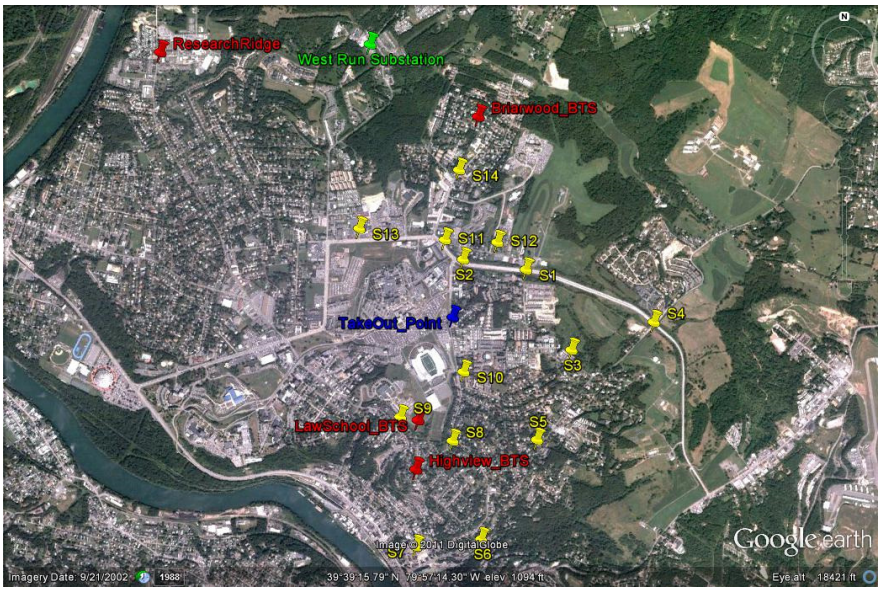

Figure 4-32: Location of Equipment Associated with the WVSC Communications Network

In the above figure,

- Yellow markers indicate the location of communication endpoints.
- Red markers indicate the location of base station sites.
- The blue marker is the location of the Fiber Takeout point.
- The green marker is the location of West Run substation.
- There are two additional endpoints located at the Highview site and the Briarwood site to accommodate backhaul.

The communications equipment that was to be supplied by RuggedCom includes base stations (BSTs), endpoints (CPEs), and the battery backup cabinets associated with the base stations.

The base station consists of a RuggedCom WiN7200 Base Station which is a small form factor, outdoor, long range, secure, IEEE 802.16e-2005 mobile WiMAX broadband wireless platform as shown below.

The subscriber unit consists of a WiN5200 Subscriber Station which is a high performance

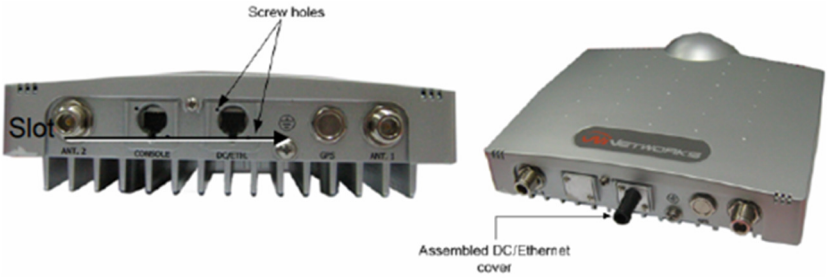

Figure 4-33 : Wimax Broadband Wireless Platform

outdoor Subscriber Station (SS), providing complete 802.16e mobile WiMAX broadband wireless access functionality as shown below.

Figure 4-34 : Subscriber Station

At each communications equipment installation point, except for West Run and Research Ridge, a battery backup and weather proof enclosure was required. At existing switch locations, the originally installed cabinets and battery backup solutions will provide battery backup and weather proof installation locations for required equipment. At each base station location, a new cabinet would be installed providing both a battery backup solution and a weather proof location for networking equipment. The general layout of the base station cabinets is shown below.

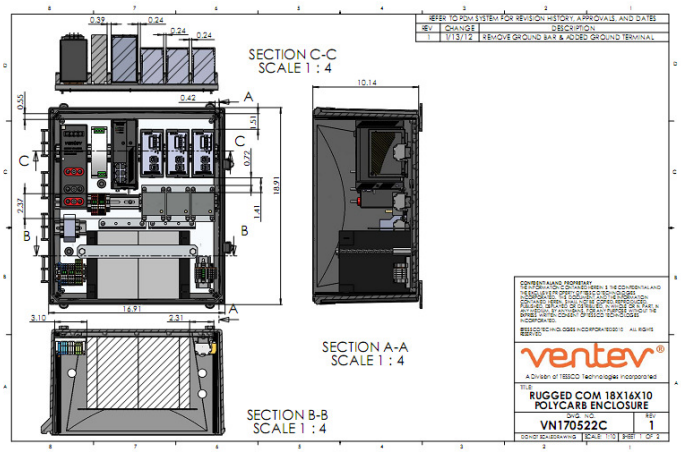

Figure 4-35: Layout of Base station Cabinet

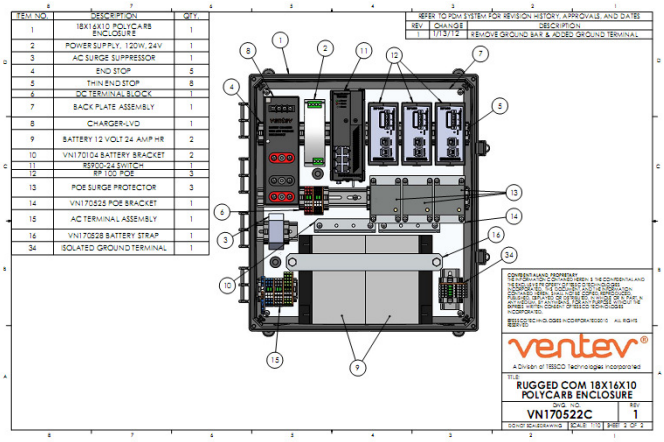

Figure 4-36: Layout of Base station Cabinet

The backbone of the network consists of five chained BTSs providing connectivity between all base stations and the fiber takeout point. All CPEs connect to one of the five base station locations. The overall backbone architecture is shown below.

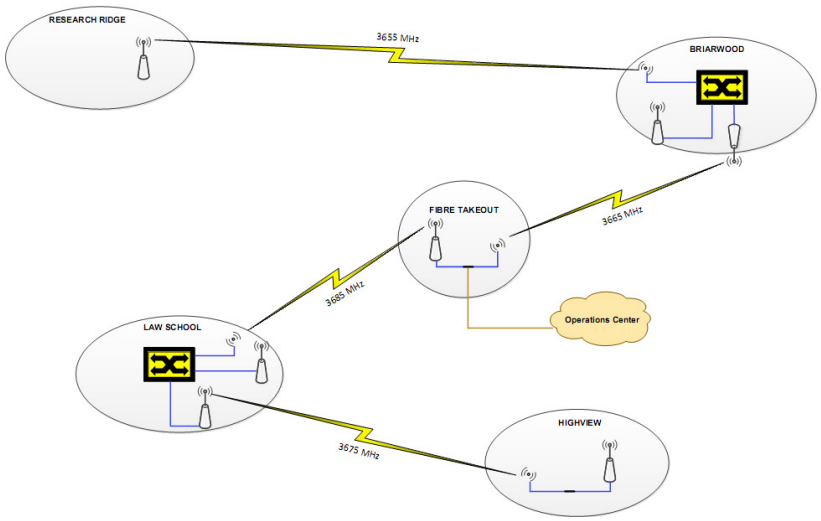

Figure 4-37: Communications Backbone Architecture

4.6 Data Collection

Baseline data was designed to be collected for the project. The table below lists data sets that were to be collected. The table also indicates the purpose of the data collection and describes how each data set was to be used. Some of the data collected provided feedback to finalize system designs, to size the microgrid generation resources, to determine feeder peak shaving requirements, to develop FLA/FPA algorithms, and to configure distribution system models.

Table 4-7: Data Collected for WVSC Project

Dataset	Purpose/Usage
SCADA data from West Run, Pierpont, Collins Ferry Substation Transformers	Determined substation transformer and feeder load profiles and load duration curves
SCADA data from feeder load break switches	Used as test data for FLA development
Event data from West Run and Pierpont Substation Relays	Used as test data for FPA development
Line Monitor Data from Suncrest Circuit	Determined load profile of Suncrest Circuit
Meter data from Research Ridge Building	Determined building load profile

A plan for future data monitoring and collection was developed for after project deployment, which was not implemented. Table 4-8 below lists the data to be collected, monitored, and provides the purpose for its collection. A data flow graphic between the project components is shown in Figure 4-38.

Table 4-8: Future Data that was to be Collected and Monitored

Dataset	Purpose/Usage
SCADA data from West Run and Pierpont Substation	• FLIR system operations • Monitoring and control of FLIR system • DER dispatch for peak shaving • DOE Metrics and Benefits reporting
SCADA data and event data from feeder load break switch PQ monitors (voltage/current rms data; 16 and 32 samples per cycle data)	• FLIR system operations • Monitoring and control of FLIR system • FLA/FPA system operations • DOE Metrics and Benefits reporting
SCADA data from Collins Ferry substation (Suncrest circuit)	• Microgrid operations • Monitoring and control of Microgrid • DOE Metrics and Benefits reporting
SCADA data from Microgrid generation resources and switchgear	• Microgrid operations • Monitoring and control of Microgrid • DOE Metrics and Benefits reporting

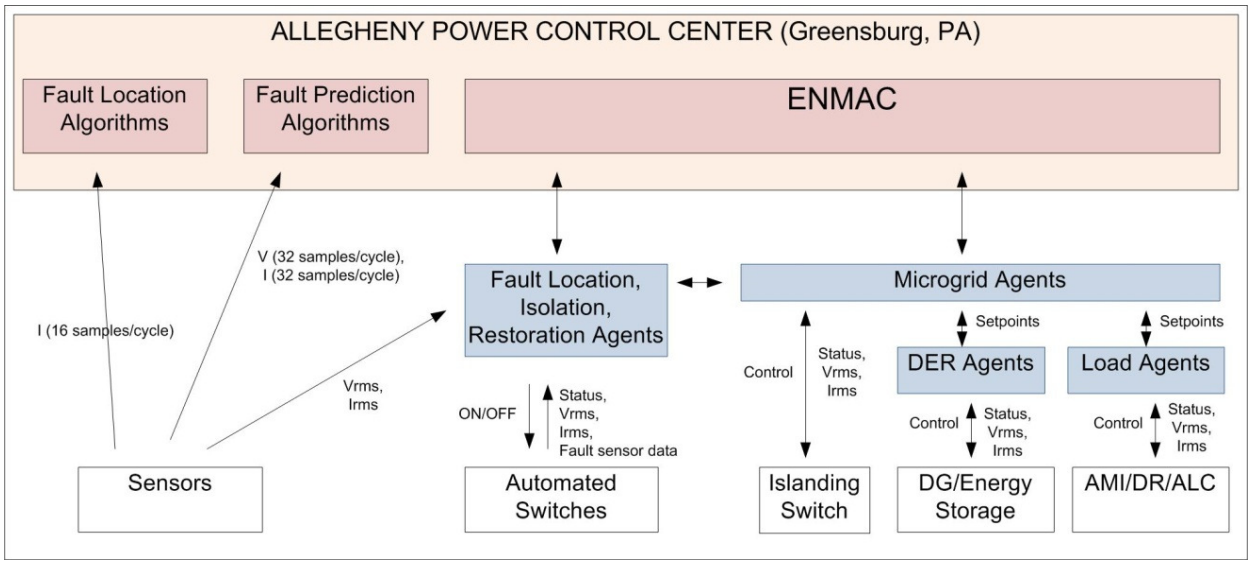

Figure 4-38: High-level Data Flow

5.0 Modeling and Simulation

WVSC project partners Leidos, APERC and NCSU conducted modeling and simulation (M&S) studies to analyze project technologies and to provide feedback to the design. This section presents the modeling, simulation and analysis efforts for each technology with information on the simulation tools used and the analyses conducted.

Leidos' microgrid modeling and simulation efforts focused on the design and configuration of the proposed technologies, which were used to optimize the microgrid system design and is presented in section 5.3. Leidos conducted various simulation studies as listed below to provide feedback to the design process.

- Reconfiguration study
- Microgrid Load Flow and Long-Term Dynamic Analysis
- Microgrid Short Circuit and Protection Coordination Study
- Microgrid Dynamic Stability Study

APERC conducted M&S to support the reconfiguration study and the FLIR agent software development to establish a test environment, which is presented in section 5.4.

Throughout the project, the Leidos team coordinated the M&S efforts among partners to avoid redundancy. The models developed by each partner were made available to other partners to increase productivity.

The WVSC project technologies can impact the way distribution systems are designed and operated. Operational and design challenges are mainly due to the presences of two-way power flows, rotary and inverter based distributed energy resources, islanded operation of microgrid and agent-based control algorithms. Modeling and simulation studies were necessary to determine design aspects of the project technologies, to ascertain performance requirements of the agent-based control algorithms, and to design the protection systems.

A detailed modeling and simulation plan was created to guide this effort that also helped engaging the project members in establishing the requirements and goals of this effort. Also, the modeling and simulation plan helped to identify a set of modeling software requirements. After a careful evaluation of these requirements, Leidos chose CYME and Matlab/Simpower software for the modeling and simulation tasks of WVSC project. Models were built using electric system data provided by Mon Power. The models developed were validated using test simulations and compared against the results of Mon Power's existing distribution modeling software (Distribution Engineering Workstation).

The study process was designed to run a series of analyses to assist in designing the WVSC project technology systems (FLIR, FLA/FPA, and Microgrid systems) and to ensure proper distribution operation. The analyses are outlined below:

5.1 Modeling and Simulation Plan

Power Flow – Power flow is a steady state analysis focused on the balance of power in the system and the thermal and voltage based limitations of equipment. The primary goal of this evaluation was to simulate the FLIR system feeders to see if any system violations such as thermal limits and voltage regulation exist in normal operating configurations and all possible reconfigured configurations. The simulation results can be used to prepare the reconfiguration plan. In the microgrid system, power flow simulations help identify the system violations (loading limits and voltage limits) in both grid connected and islanded modes of microgrid operation for the proposed microgrid DER capacities.

Short Circuit – This evaluation focused on determining current levels for various types of faults in the system. It is based upon a model constructed from a series of assumptions to reduce the complexity of the solution. This was also checked when evaluating the type and size of generation and its locations. This was done in order to assess the impact on withstand and interrupting capacities and the possible changes in fault current flow in the system along with its effect on the proper detection and selectivity of applied protective relaying. The major goal of this study was to compute the fault levels in an islanded microgrid to check if fault levels are enough to operate the proposed protective devices.

Dynamic Stability – This evaluation simulates the short-term (up to approximately 20 seconds) responsive behavior of applied controls and the dynamic characteristics of loads, branches, transformers and, most importantly, generators/energy sources. The primary goal of was to assess the capability of the microgrid to remain stable and within reasonable voltage and frequency targets when the main grid source is lost, as well as its ability to remain stable for individual events when already islanded.

Protection and Coordination –This study looks at the results provided by the system studies such as the maximum and minimum available fault current, over/under voltage conditions, power swings, and critical clearing times to check the specific characteristics of applied relays. The major goal of this study was to check the capability of protective devices to clear the faults in the islanded microgrid.

5.2 Modeling & Simulation Tools

Leidos developed a set of high-level requirements for the modeling tools needed for WVSC project's modeling and simulation tasks, which are listed below. After reviewing these requirements, Leidos chose CYME and Matlab/SimPower software for their M&S efforts.

1. Software shall perform dynamic simulations with single phase loads and generators, such as the loss of one single phase lateral along with its load and generation contribution, and its effect on other single phase loads and generators connected elsewhere. Simulating loss of the normal transmission source and transition to islanded operation was also important.

2. Software shall be capable of running system condition variations and events automatically and in reasonable processing times.
3. Models for devices and equipment within the software shall be detailed enough for accurate determination of the system response.
4. Optimally, a single software package/model for dynamic stability, short circuit and load flow will allow more accurate representation of contingencies.
5. Software shall be capable of representing changes in the operating mode of a machine – for example in simulating a loss of the grid the islanded generator would switch voltage regulation modes.
6. Software shall be capable of performing complex logical operations in order to simulate behavior of the MGMS/FLIR/FLA.
7. Dynamic representation of automatic protective devices improves the speed with which multiple events can be screened by decreasing the amount of manual review of output data looking for conditions that might yield a trip, and once set-up, should be more accurate and less likely to miss a critical event.

MATLAB® & PSCAD®

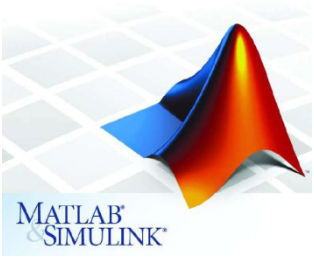

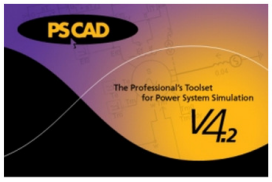

The microgrid simulation tools used are the MATLAB/SIMULINK® software and the PSCAD® software. At first, the system is modeled in detail using the MATLAB/SIMULINK® software.
MATLAB® (matrix laboratory) is a multi-paradigm numerical computing environment Developed by MathWorks, MATLAB® allows matrix manipulations, plotting of functions and data, implementation of algorithms, creation of user interfaces, and interfacing with programs written in other languages. Simulink developed by MathWorks, is a data flow graphical programming language tool for modeling, simulating and analyzing multi-domain dynamic systems. Its primary interface is a graphical block diagramming tool and a customizable set of block libraries. In this work, MATLAB Simpower is used to model the power system circuits, and user defined S-functions are used for Multi Agent System Simulations. The software PSCAD®, a general-purpose time domain simulation tool for studying transient behavior of electrical networks, was used and provided much better results.

CYME

The CYME Power Engineering software is a suite of applications composed of a network editor, analysis modules, and user-customizable model libraries from which one can choose to get the most powerful solution. In this work, CYME is used for voltage drop studies for the restoration scenario evaluation.

OPENDSS

The OpenDSS is an electric power Distribution System Simulator (DSS) for supporting distributed resource integration and grid modernization efforts which in this work is used for power system simulation and fault studies.

JADE

Jade software is for the development of agents implemented in Java. JADE supports coordination between several agents and provides a standard implementation of the communication language FIPA-ACL, which facilitates the communication between agents. In this work Jade is used for MAS communication modeling.

5.3 Modeling and Simulation for the Microgrid

5.3.1 Modeling and Simulation for the Microgrid by Leidos

Dynamic models of the designed microgrid system were created in both CYME and Matlab/Simpower software for running stability analyses. Leidos compared the dynamic stability results from a simplified model developed in CYME to a detailed model developed in Matlab/Simpower. The comparison assisted Leidos in identifying problem areas more precisely.

5.3.1.1 *Model for Microgrid Steady State Analysis*

A microgrid model was developed in CYMDist to conduct steady state analyses such as load flow analysis, long term dynamic study (time-series load flow), short circuit study, and protection and coordination study. Figure 5-1 below shows the CYMDist model developed for the microgrid.

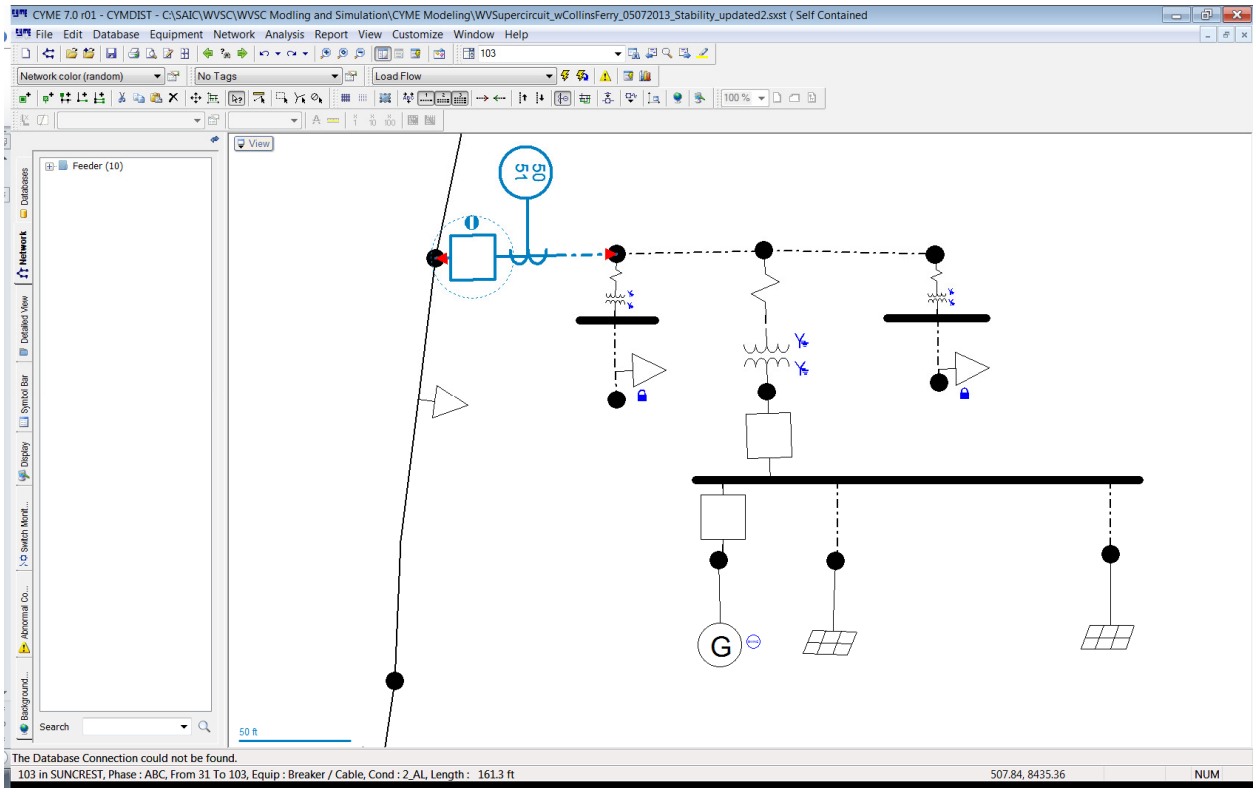

Figure 5-1: CYMDist Microgrid Steady State Model

5.3.1.2 *Model for Microgrid Dynamic Stability Analysis*

The microgrid system dynamic stability analysis model was created in CYME using the CYMSTAB module. Single phase inverters and source models were not supported by CYMSTAB, therefore three phase models were used to develop the model. Figure 5-2 shows the model created.

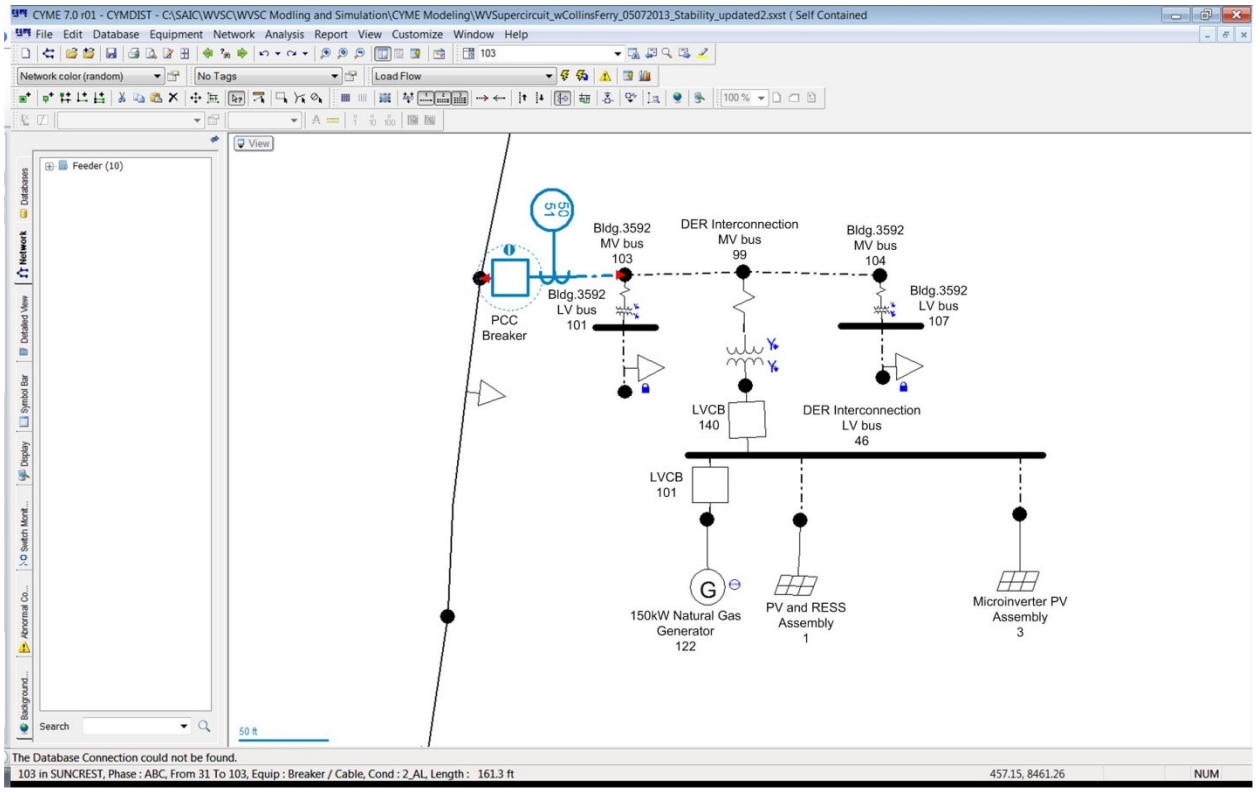

Figure 5-2: CYMSTAB Microgrid Dynamic Stability Model

This dynamic model was built using the following assumptions.

1. Three-phase Natural Gas Generator of 150 kW (Figure 5-3) was modeled as a Synchronous Generator of Type-3 Salient pole with Transient and Sub-Transient effects with appropriate Exciter and Turbine models.

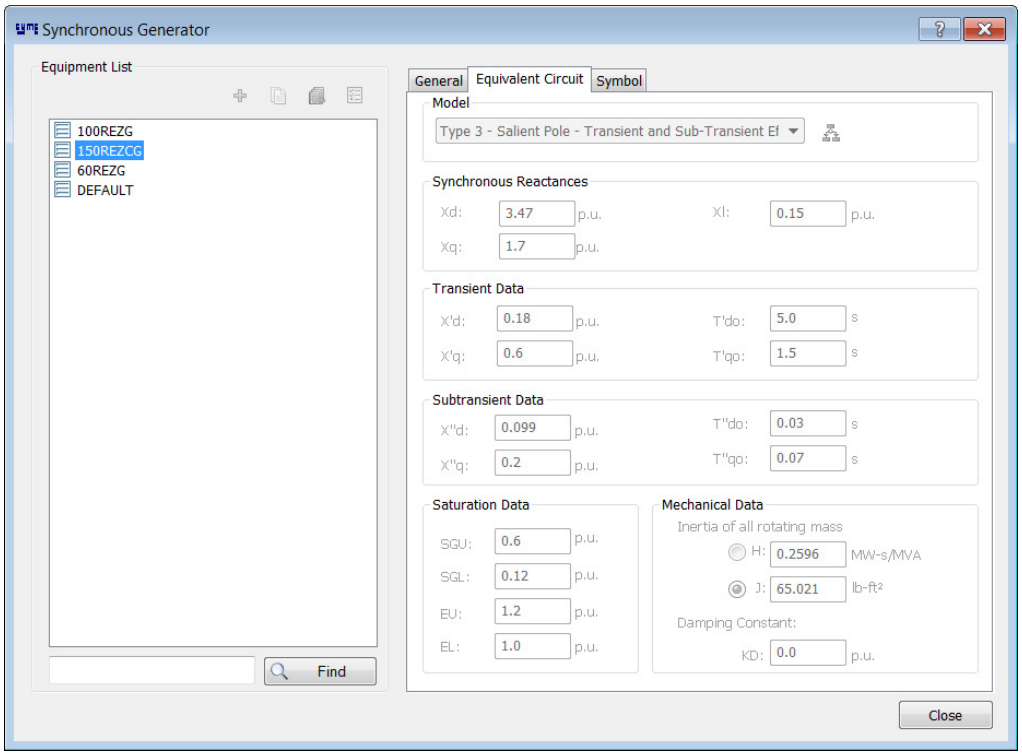

Figure 5-3: 150 kW Synchronous Generator Parameters

2. Battery Energy Storage System (BESS) with PV system (Figure 5-4) was modeled as a single three-phase 24kW PV dynamic system. Solar irradiation was kept constant at 1000 W/m2 during the simulation.

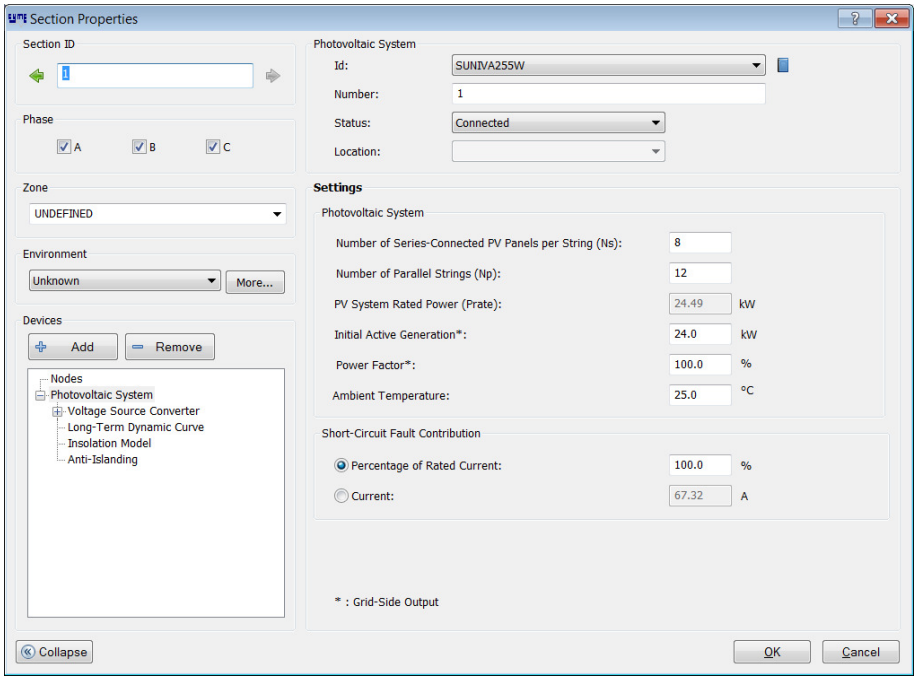

Figure 5-4: BESS PV System Parameters

3. Micro-inverter system was modeled as a single three-phase 21 kW PV dynamic system. Solar irradiation was kept constant at 1000 W/m2 during the simulation.
4. Microgrid building loads were allocated based on their recorded peak loadings.
5. Additionally, it was necessary to model a voltage and frequency dependence for system loads (Figure 5-5). Leidos relied upon research conducted by Rochester Gas & Electric in 1982, which is widely accepted in stability studies nationwide, as the source for the voltage and frequency load dependency. The window below shows the network data added to the model for use in stability simulations. Specifically, this model dictates that loads within the model be evaluated for their frequency and voltage dependence using exponential relationships. Thus typically the method for specifying the degree of frequency and voltage dependence for real and reactive power components is to provide the exponents in the equation, nP and nQ and bP, bQ:

$$P = P0x\left(\frac{V}{Vbase}\right)^{nP} x(1 + Pfreqx\Delta f)$$

$$Q = Q0x\left(\frac{V}{Vbase}\right)^{nQ} x(1 + Qfreqx\Delta f)$$

where:

nP = 0.78 Pfreq = 0.69

nQ = 3.29 Qfreq = -8.89

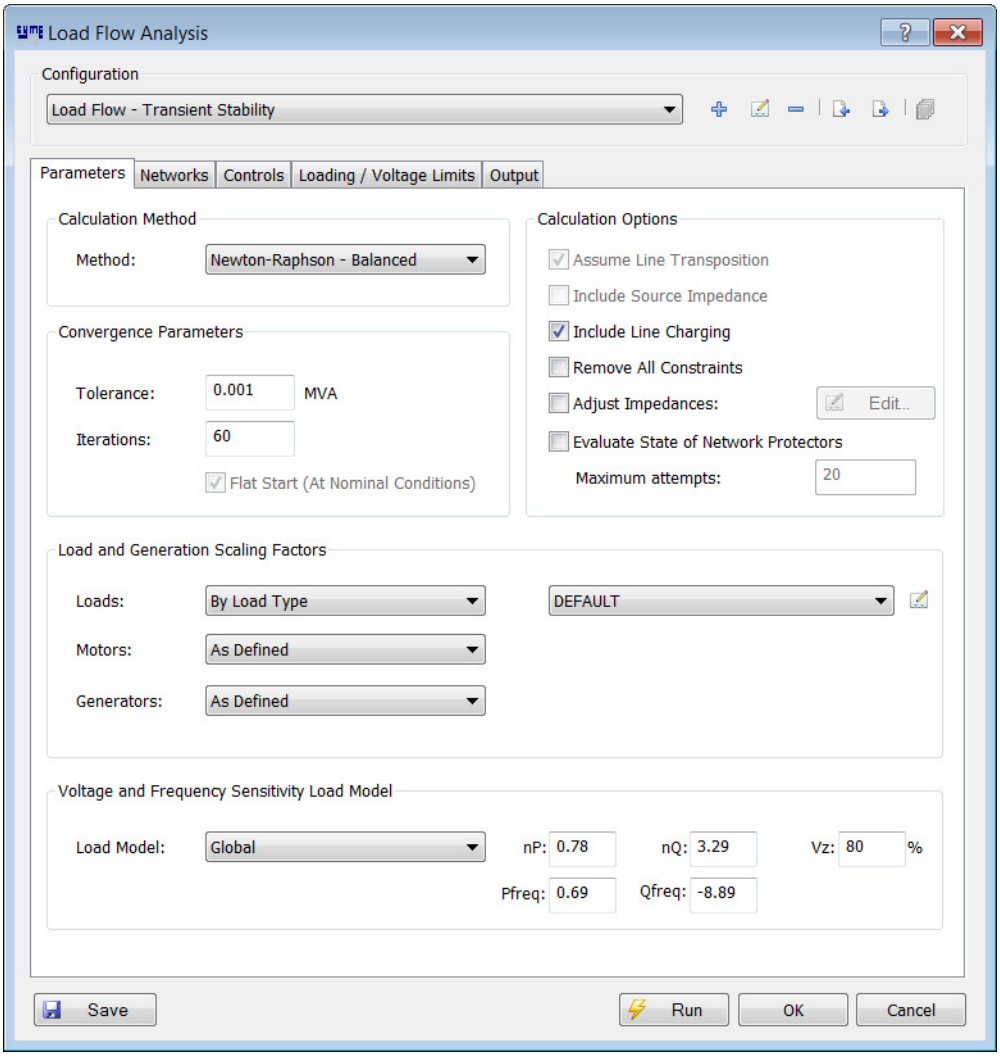

Figure 5-5: Voltage and Frequency Load Dependency Parameters

5.3.1.3 *Dynamic Stability Model in Matlab/Simpower*

Leidos developed a detailed dynamic model of microgrid comprising of all the required single phase and three phase detail dynamic models of DER in the microgrid (BESS, PV, and natural gas generator) in Matlab/Simpower. The Figure 5-6 shows the model created for the WVSC microgrid.

This Simulink modeling platform uses "Average Models" to simulate the average dynamics of the power electronics: BESS and PV micro-inverter system. An average model simulates the general response of a power electronic circuit without considering the switching dynamics of the circuit. Generally, an average model takes into account the power balance of the circuit (i.e., power input = power output + losses) and the overall control response of the circuit which generally incorporates PI loops to simulate the slower (compared to the switching frequency) response of the circuit. The average models can be "upgraded" as necessary to include more precise response characteristics. An average model-based platform permits large, complicated

electrical networks to be simulated with reasonable computation times while yielding average responses that may need to be modeled. For example, fault protection coordination in a large network seldom depends upon characterizing the dynamics associated with the switching frequency of the circuit.

As shown in Figure 5-6, the WVSC microgrid model is composed of various Simulink sub-models. These sub-models are explained in the following section.

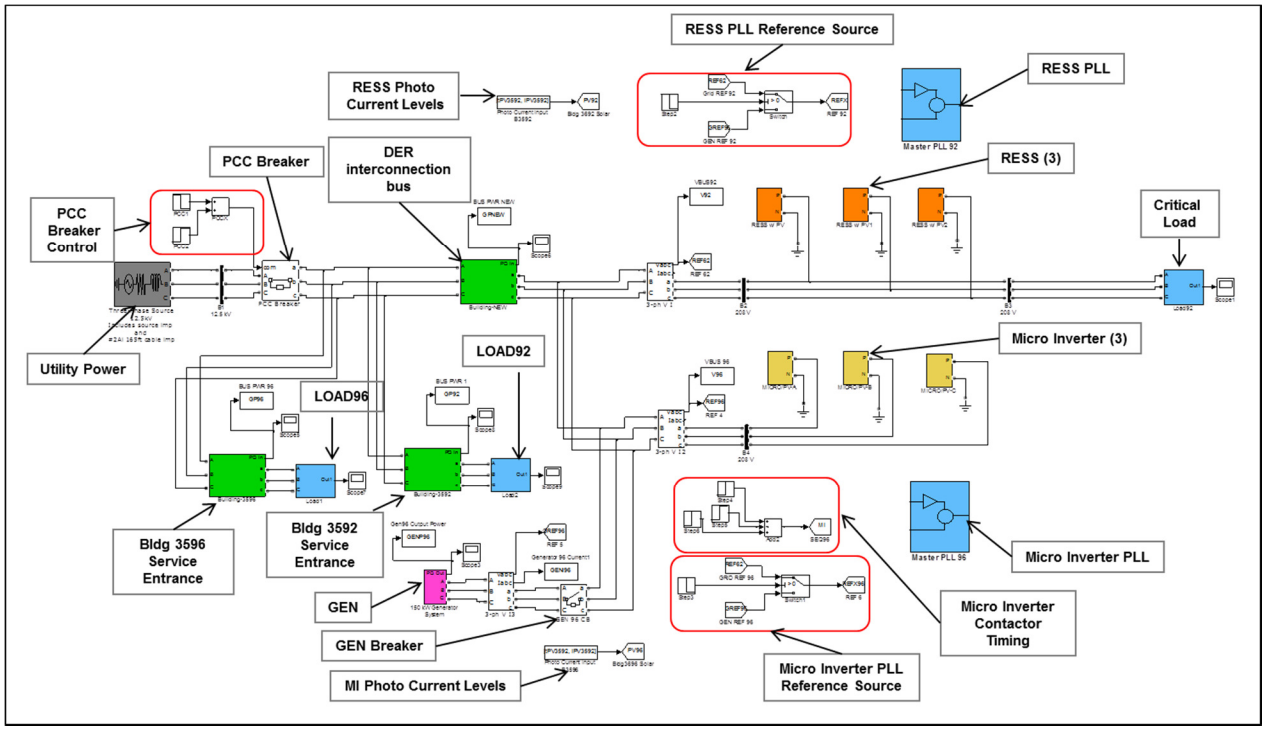

Figure 5-6: Matlab/Simpower Microgrid model

BESS Unit Sub-Model

The BESS unit sub-model is one single-phase BESS unit Simulink sub-model as shown Figure 5-7. When there is a utility power failure, the BESS unit operates to provide up to 7 kW per phase to loads that are connected to the critical load bus. Non-critical loads remain unpowered during a utility failure until the 150 kW generator engages and picks up both the critical and non-critical loads. When the utility is providing power, or when power is provided by the 150 kW generator, the BESS unit accepts power from a PV array and delivers the power to the DER interconnection bus, up to 7 kW per phase.

First-order PV Array Model:

- Simulates the IV Curve of the PV array as a whole.

PV Array Charge Controller:

- Seeks to maintain PV voltage at the V_{MPP} level by controlling the current that is being drawn from the PV array.

- Defines the power that is delivered to the DER interconnection bus by the BESS when operating in the "Non-Power Loss" (grid connected mode).

BESS Inverter Controller:

- Controls the output voltage (output power) of the power inverter (amplitude control, frequency control)

BESS:

- Simulates the dynamics of the battery that is used to supply the BESS during a Power Loss (islanded mode).

Power Output Section:

- Simulates 120 V, 60 Hz, Single-phase BESS Inverter Output

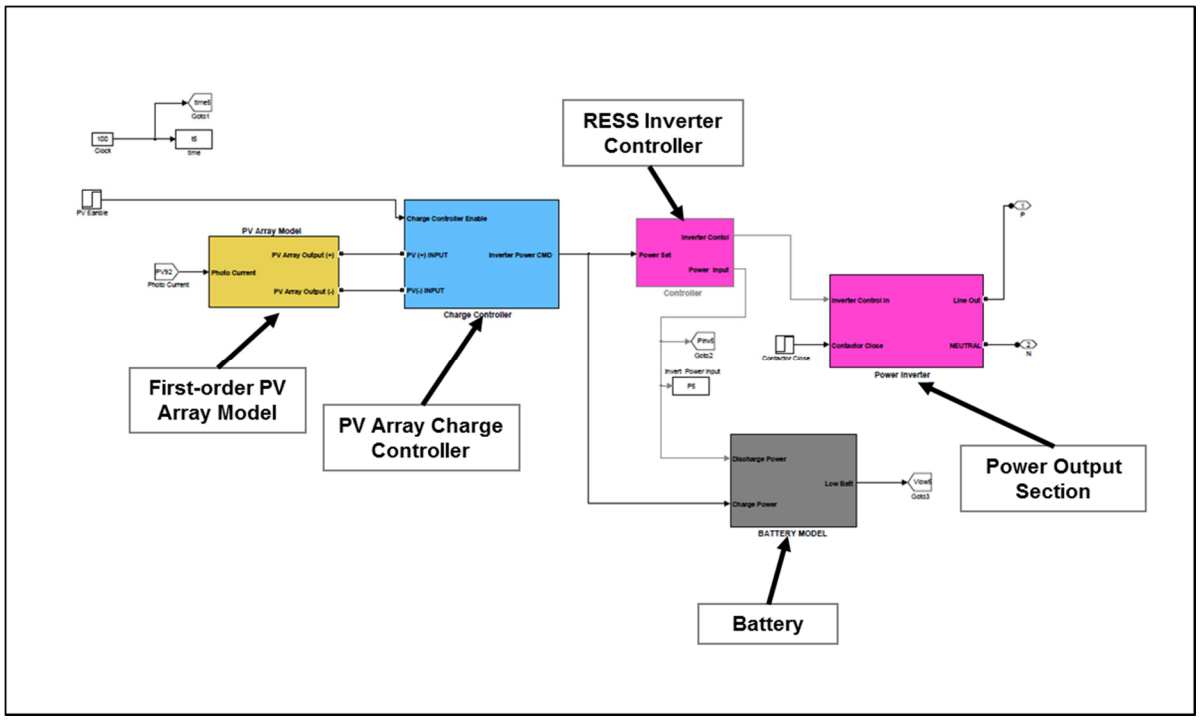

Figure 5-7: Single Phase BESS Unit Simulink Sub-Model

PV Micro-inverter Unit Sub-Model

The PV micro-inverter unit sub-model is composed of individual micro-inverters associated with each phase and were modeled as one inverter unit. Figure 5-8 shows one single-phase PV micro-inverter unit Simulink sub-model. The micro-inverters only provide power to the DER interconnection bus when the bus is powered from another source, i.e. the utility or the 150 kW generator. Each micro-inverter will process up to 7 kW per phase combining the power derived from the PV arrays, thus offsetting load demand from the utility or the 150 kW generator.

First-order PV Array Model:

- Simulates the IV Curve of the PV array as a whole.

PV Array Charge Controller:

- Seeks to maintain PV voltage at the V_{MPP} level by controlling the current that is being drawn from the PV array.
- Defines the power that is delivered to the DER interconnection bus by the micro-inverter.

Inverter Controller:

- Controls the output voltage (output power) of the power inverter (amplitude control, frequency control)

Power Output Section:

- Simulates 120 V, 60 Hz, Single-phase micro-inverter output.

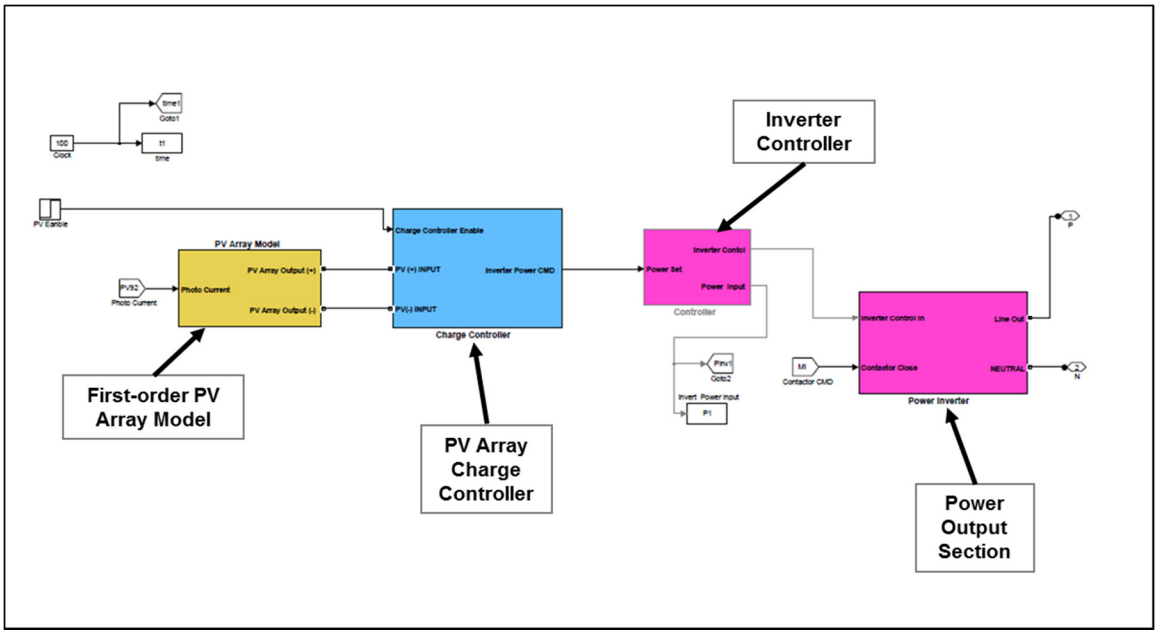

Figure 5-8: Single-Phase PV Micro-inverter Unit Simulink Sub-Model

Generator Unit Sub-Model

A three phase synchronous generator (208V, 60 Hz, 150 kW, 4 pole) is modeled in Simulink as shown in Figure 5-9. The engine model has a simple PI loop controller which seeks to hold the speed of the generator set at a constant 900 RPM. The output voltage of the generator is proportional to the rotational speed of the machine.

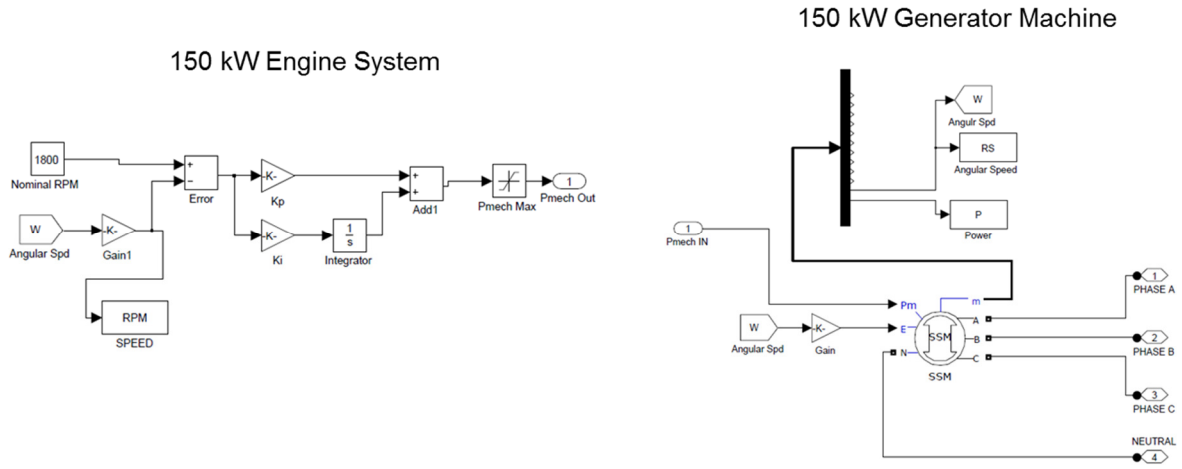

Figure 5-9: 150kW Generator Simulink Sub-Model

PV Array Average Model

The first order characteristics of a PV array can be modeled as shown in Figure 5-10. This simple model produces abrupt transitions, however, reasonable accuracy still can be achieved using this model that servers our modeling goals. Additional accuracy can be achieved by adding more branches in parallel with Iphoto. The V-I characteristics and the V-P characteristics produced using this model are shown in Figure 5-11. From the V-P characteristics, it is clear that the PV array should be operated close to V_{MPP} (~200V) to achieve the maximum power output from PV array.

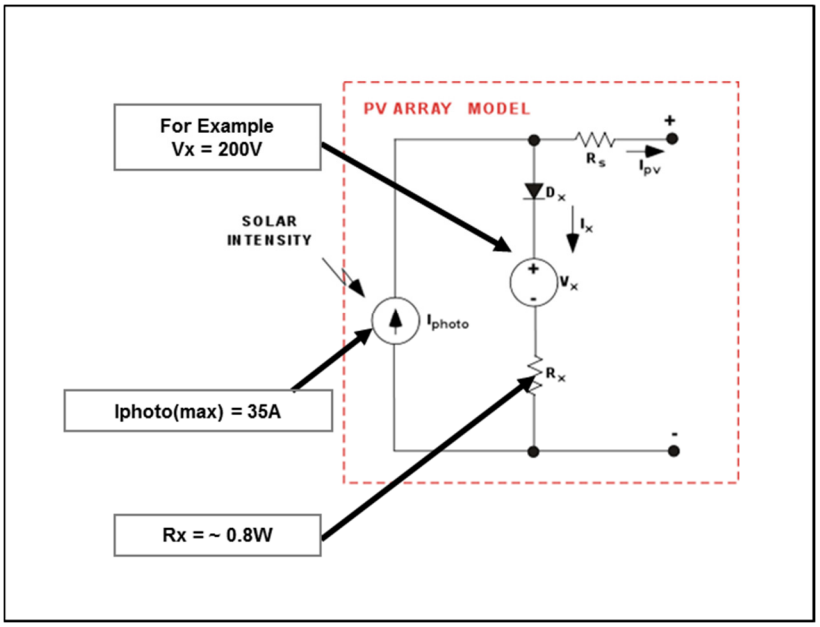

Figure 5-10: PV Array Average Model

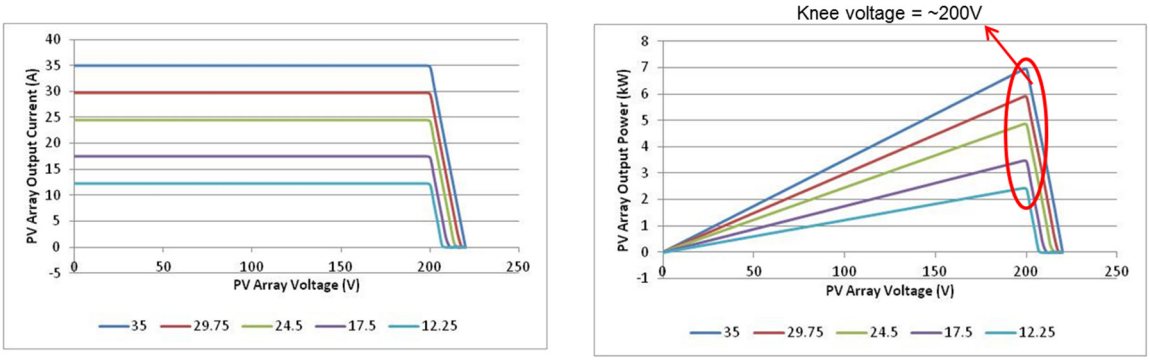

Figure 5-11: V-I and V-P Characteristics of PV Model

5.3.1.4 *Microgrid Load Flow and Long-Term Dynamic Analysis*

Leidos performed snapshot and time series load flow analyses for the scenarios listed in Table 5-1. The snapshot analysis considered annual peak load of the Suncrest feeder whereas the time series analysis considered Suncrest feeder profile for an entire peak day. The snapshot load flow summary results are shown in Table 5-2 and Table 5-3, which reveal that there would be no voltage and loading violations in the system due to the microgrid operation. Figure 5-12 and Figure 5-13 show the time-series voltage profiles of few selected points within microgrid for Scenario-4 and Scenario-5. These charts reveal that there would be no voltage violations when the microgrid operates in either the grid connected mode or islanded mode. Detailed results along with time series charts of building loading profiles, generation profiles, and voltage profile of selected microgrid nodes are presented in Appendix-E.

Table 5-1: Load Flow Scenarios

Snapshot Load flow	
Scenario-1	Base system with no microgrid generation connected to the feeder
Scenario-2	Grid connected microgrid
Scenario-3	Islanded microgrid
Long-Term Dynamic Analysis (Time Series Load flow)	
Scenario-4	Grid connected microgrid
Scenario-5	Islanded microgrid

Table 5-2: Scenario-1 Load Flow Summary Results

Total Summary	kW	kVAR	kVA	PF(%)
Source – CollinsFerry2	4838	1630	5105	94.8
Generators	0	0	0	0
Total Generation	**4838**	**1630**	**5105**	**94.8**
Total Loads	**4779**	**1391**	**4977**	**96**
Line Losses	35.29	93.3	99.75	-
Cable Losses	7.28	8.93	11.52	-
Transformer Load Losses	2.18	164.9	164.9	-
Transformer No-Load Losses	14.31	0	14.31	-
Total Losses	**59.06**	**267.1**	**273.6**	**-**

Table 5-3: Scenario-2 Load Flow Summary Results

Total Summary	kW	kVAR	kVA	PF(%)
Source – CollinsFerry2	4642.6	1618.5	4916.63	94.43
Generators	194.42	0.05	194.42	100
Total Generation	**4837.02**	**1618.55**	**5100.63**	**94.83**
Total Loads	**4778.72**	**1390.76**	**4976.98**	**96.02**
Line Losses	34.71	91.24	97.62	-
Cable Losses	7.96	9.04	12.05	-
Transformer Load Losses	1.33	156.35	156.36	-
Transformer No-Load Losses	14.31	0	14.31	-
Total Losses	**58.3**	**256.64**	**263.17**	**-**

Table 5-4: Scenario-3 Load Flow Summary Results

Total Summary	kW	kVAR	kVA	PF(%)
Source – CollinsFerry2	4764	1618.97	5056.66	94.74
Generators	73	0	73	100
Total Generation	**4837**	**1618.97**	**5129.66**	**94.29**
Total Loads	**4776.68**	**1386.16**	**4973.74**	**96.04**
Line Losses	35	92.31	98.72	-
Cable Losses	7.19	8.72	11.31	-
Transformer Load Losses	1.7	160.09	160.1	-
Transformer No-Load Losses	14.31	0	14.31	-
Total Losses	**58.21**	**261.13**	**267.53**	**-**

Table 5-5: Capacity and Voltage Conditions

Total Summary	Maximum Loading (%)	Maximum Voltage (%)	Minimum Voltage (%)
Scenario 1	60.8	103.11	99.7
Scenario 2	64.7	103.16	99.73
Scenario 3	60.8	103.14	98.98
Note: Values include conductors, cables, and transformers.			

Figure 5-12: Voltage Profiles for Microgrid Grid Connected Operation (Scenario-4)

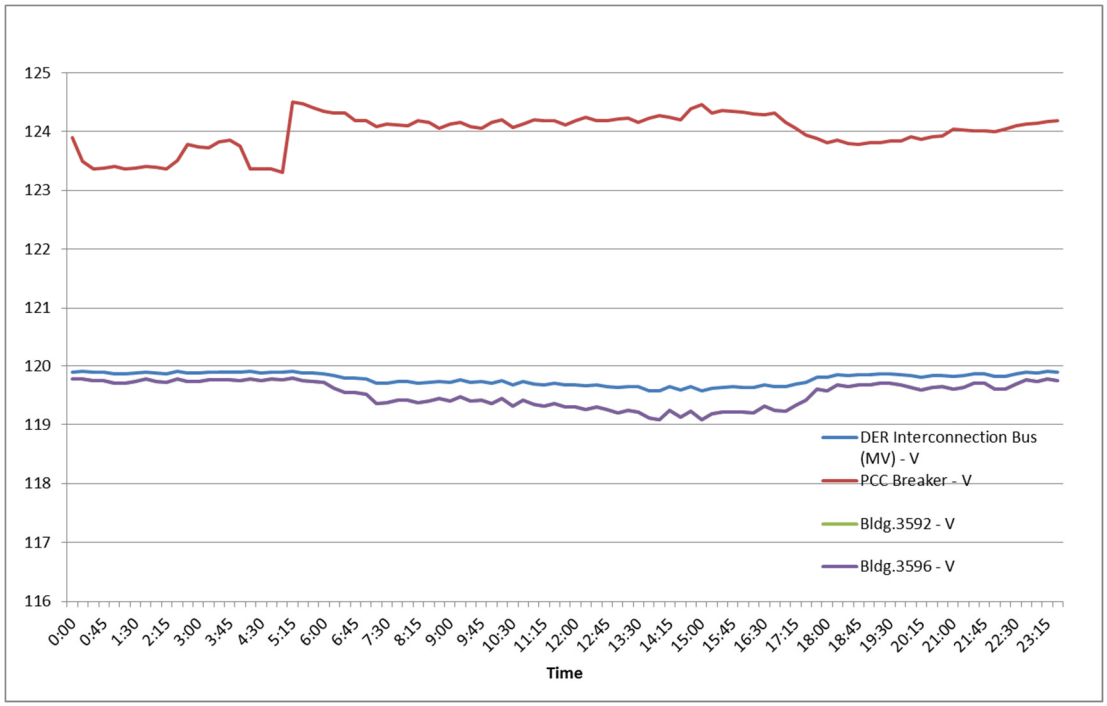

Figure 5-13: Voltage Profiles for Microgrid Islanded Operation (Scenario-5)

5.3.1.5 *Microgrid Short Circuit and Protection Coordination Study*

Leidos performed short circuit and protection coordination studies on WVSC microgrid using the CYMEProtec module of CYME software. The primary goals of the short circuit and protection coordination study were the following:

- To test fault levels against equipment capabilities
- To confirm and evaluate whether the operation of proposed protective devices during islanded operation is satisfactory for equipment protection, system stability, safety, and reliability.

It is important to clarify that the goal of this assessment is to evaluate at a high level what the proposed protective devices are capable of during islanded operation, and not to assess exact coordination at every point in the system, as the exact size, make/model of many low voltage protective devices was not precisely known at the time the study was conducted.

Table 5-6 shows the maximum and minimum fault currents at selected points within the microgrid system during islanded mode of operation.

Table 5-6: Short circuit summary – microgrid islanded mode

Node Name	Voltage (kV) LN	3-Phase Fault (A)		Line to Line to Ground Fault (A)		Line to Line Fault (A)		Line to Ground Fault (A)	
		Max	Min	Max	Min	Max	Min	Max	Min
Bldg. 3592 MV bus	7.2	72	72	79	79	62	62	74	74
Bldg. 3596 MV bus	7.2	72	72	79	79	62	62	74	74
DER Interconnection MV bus	7.2	72	72	79	79	62	62	74	74
Bldg. 3592 LV bus	0.1	3309	3309	3552	3552	2842	2842	3387	3387
Bldg. 3596 LV bus	0.1	3309	3309	3552	3552	2842	2842	3387	3387
DER Interconnection LV bus	0.1	4895	4895	5415	5415	4186	4186	5038	5038

Medium Voltage (12.47-kV) System Faults

Fault study results are presented in

Table 5-6 for islanded microgrid scenario. As can be seen in the fault summary, fault currents on the medium voltage system are very low, in the order of 80 Amps, and are very flat (i.e. they do not differ significantly from one point of the MV system to the other). This was an expected result since only significant fault contribution comes from the 150kW synchronous generator and the rest of the inverter based sources (PV) only can supply fault contribution up to one per unit of rated capacity. The transformer fuses located at the high-side of the transformer see these faults but will take a longer time to operate on the faults, having a detrimental impact to system stability. However, the generator circuit breaker and the LV Circuit Breaker (LVCB) located at the DER interconnection point are capable of clearing the faults anywhere in MV system quickly. Figure 5-14 is a snapshot of the sequence of events showing a three phase fault at Bldg. 3596 MV bus cleared by the generator LVCB (101) and the DER interconnection LVCB (140).

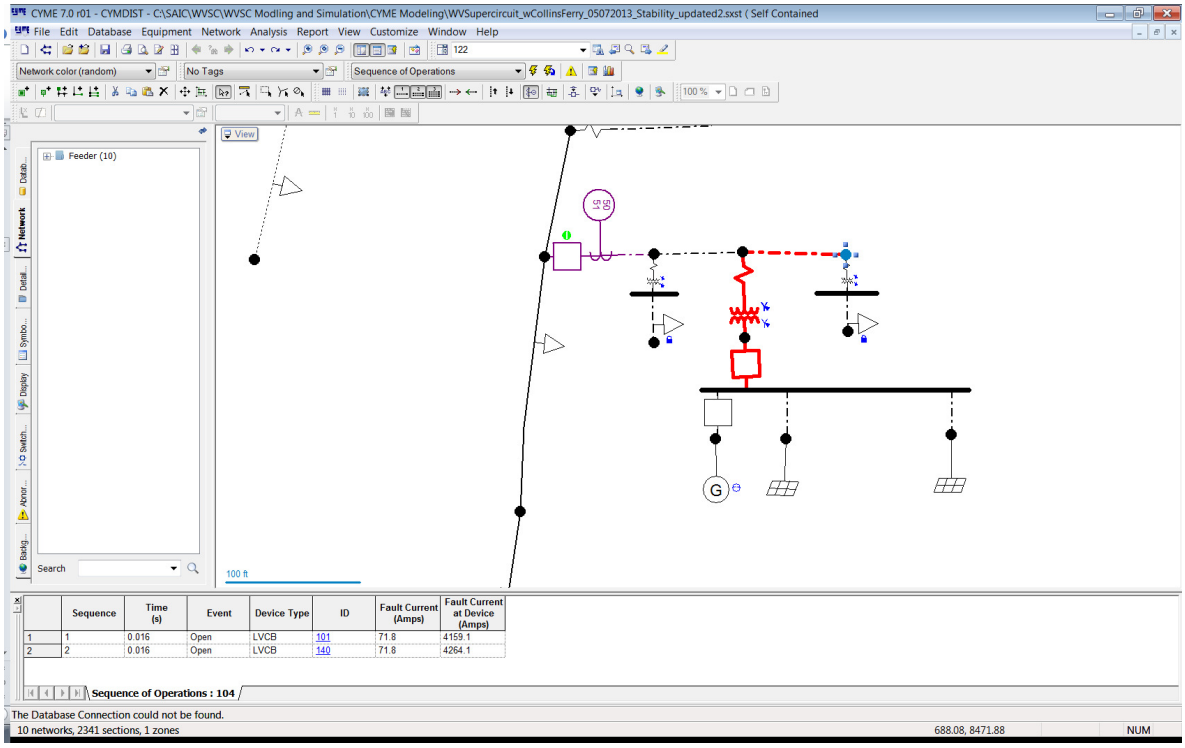

Figure 5-14: Sequence of Events Showing Three Phase Fault Clearance at Bldg. 3596 MV Bus

Low Voltage Faults

As can be seen from the fault current summary table, fault currents on low voltage buses are generally high enough for protective devices to operate quickly. Even in this case, the generator and DER interconnection LVCBs operate faster than the transformer high-side fuses. Figure 5-15 shows a snapshot of the sequence of events showing a three phase fault at Bldg. 3592 LV bus cleared by the generator LVCB (101) and the DER interconnection LVCB (140).

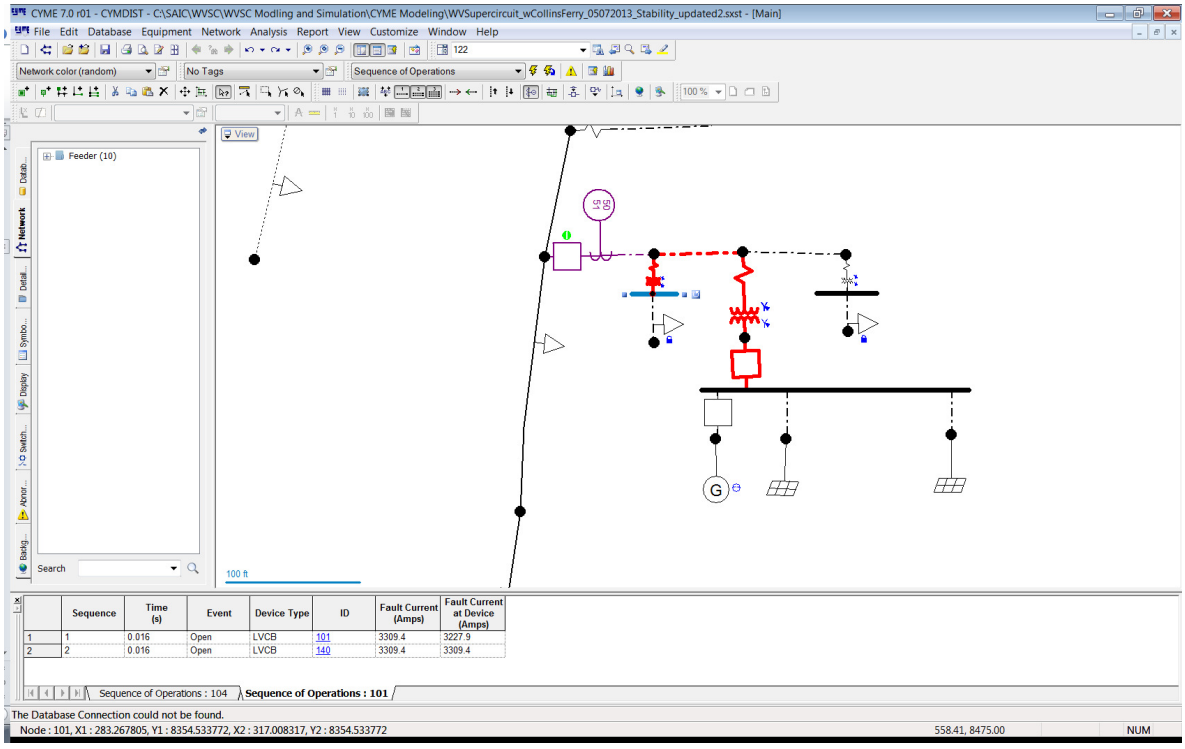

Figure 5-15: Sequence of Events Showing Three Phase Fault Clearance at Bldg. 3592 LV Bus

5.3.1.6 *Microgrid Dynamic Stability Study*

Dynamic stability simulations were conducted as a high-level rotor angle analysis in support of the final microgrid resource sizing and the design. Dynamic models created in CYME and Matlab/Simpower programs were used for this analysis. Simulations conducted identified system voltage and frequency response to faults and to loss of a large load or generator in order to assess the risk to WVSC microgrid loads during micro-grid operation and to confirm the acceptable sizes for the proposed units. The intended goal of this analysis was to study the dynamic stability behavior of microgrid for vulnerable situations like faults, generation loss, and step increase/decrease in loads to propose remedies to these vulnerabilities that can be achieved through modifications to the design. This analysis was also helpful to see if the proposed design is compliant with the DER Interconnection requirements stated by Mon Power.

CYME Dynamic Stability Results:

Based upon the anticipated operating procedures and methods for the microgrid, Leidos prepared a list of events for analysis. In general the goal of the analysis was to assess the stability of the system as proposed, any vulnerability that exists, and any remedies to these vulnerabilities that can be achieved through modifications to the design. The events evaluated are listed below in Table 5-7 along with the simulation results for each scenario determining whether the system is stable or not. Detailed analysis results are presented in Appendix E.

Table 5-7: CYME Dynamic Stability Results

Events	Simulation Result
10 cycle fault at Bldg. 3592 LV Bus	Unstable
5 cycle fault at Bldg. 3592 LV Bus	Stable
10 cycle fault at Bldg. 3592 MV Bus	Unstable
5 cycle fault at Bldg. 3592 MV Bus	Stable
10 cycle fault at Bldg. 3596 LV Bus	Unstable
5 cycle fault at Bldg. 3596 LV Bus	Stable
10 cycle fault at Bldg. 3596 MV Bus	Unstable
5 cycle fault at Bldg. 3596 MV Bus	Stable
10 cycle fault at generator interconnection bus	Unstable
5 cycle fault at generator interconnection bus	Stable
Loss of 24kW BESS PV System	Stable
Loss of 21 kW Micro-inverter System	Stable
Simultaneous loss of 24kW BESS PV System and 21 kW Micro-inverter System	Stable

System Faults

Fault simulations conducted included tests of 10 cycle and 5 cycle faults on various points in the microgrid system. The microgrid was consistently not able to withstand a 10 cycle fault on the system, which is somewhat expected of a network with small generators and little inertia. Figure 5-16 and Figure 5-17 below show the system frequency and voltage response following a 5 cycle fault at Bldg. 3592 MV bus confirming the stable operation of microgrid.

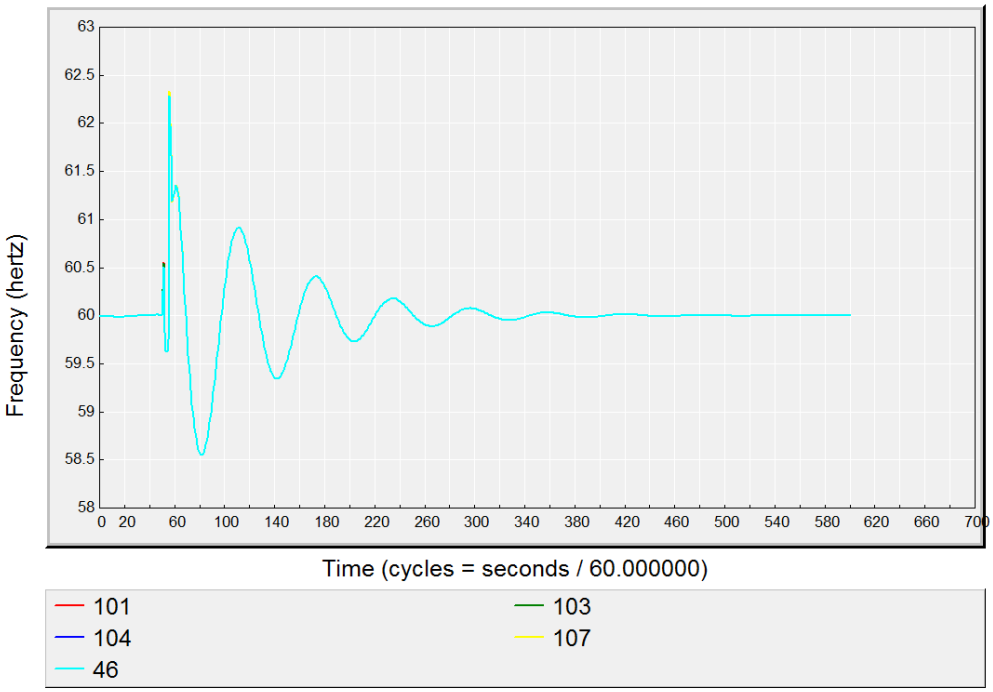

Figure 5-16: System Frequency Following a 5 Cycle Fault at Bldg. 3592 MV Bus.

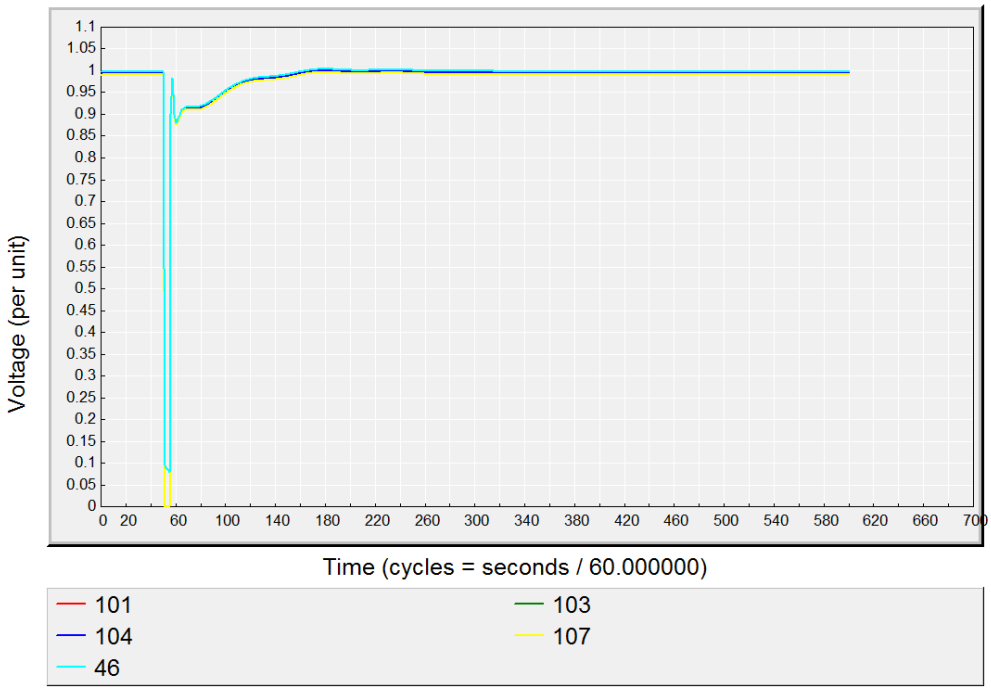

Figure 5-17: Bus Voltages Following a 5 cycle Fault at Bldg. 3592 MV Bus.

Legend: 103 - Bldg. 3592 MV bus; 104 - Bldg. 3596 MV bus; 99 – DER Interconnection MV bus;

101 - Bldg. 3592 LV bus; 107 - Bldg. 3596 LV bus; 46 – DER Interconnection LV bus;

Figure 5-18 and Figure 5-19 below show the system frequency and voltage response following a 10 cycle fault at Bldg. 3592 MV bus confirming unstable operation of microgrid.

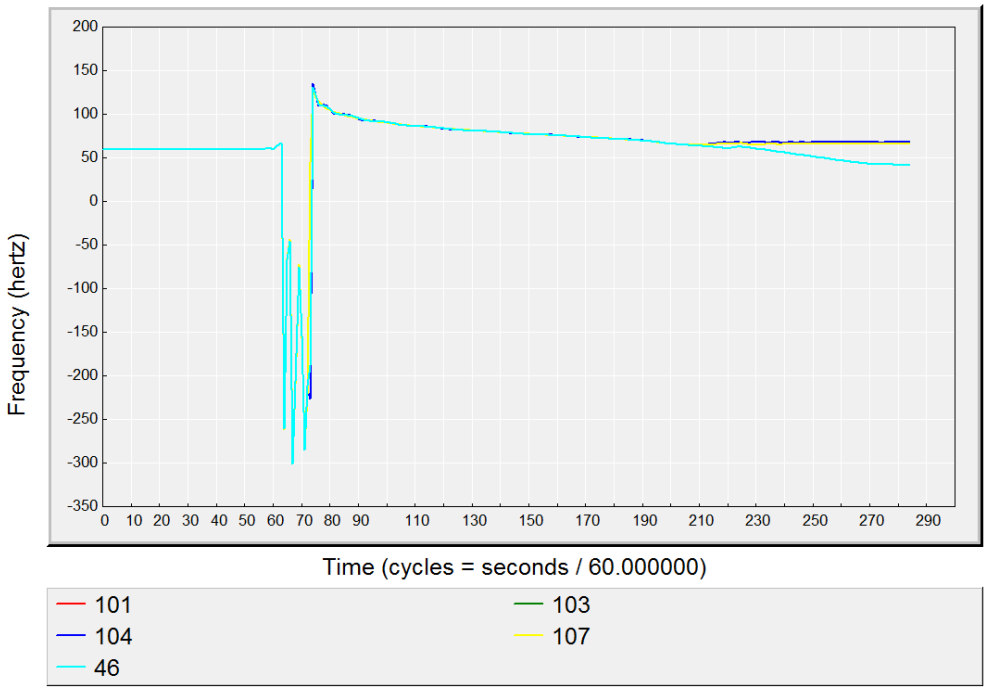

Figure 5-18: System Frequency Following a 10 Cycle Fault at Bldg. 3592 MV Bus.

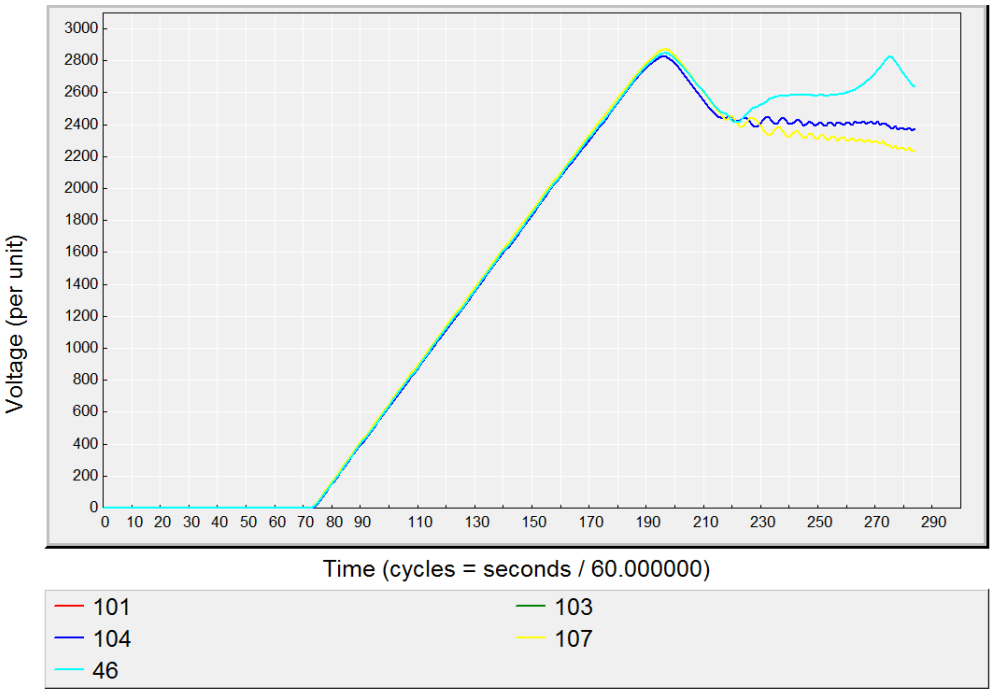

Figure 5-19: Bus Voltages Following a 10 Cycle Fault at Bldg. 3592 MV Bus.

Loss of Generators

Leidos modeled the loss of PV generation units during islanded microgrid operation. As can be seen in the summary table, system stability is maintained in any of the events: loss of 24kW BESS PV System, 21kW PV micro-inverter system, and simultaneous loss of both units. However, in most cases voltage or frequency violations were observed. It is self-evident that loss of 150kW natural gas generator will collapse the microgrid as this generator is the only source to provide phase reference to other resources (PV and BESS) of the microgrid for synchronization. Therefore this event was not included in the scenario list.

Figure 5-20 and Figure 5-21 show the system frequency and voltage response following the simultaneous loss of 24kW BESS PV System and 21kW PV micro-inverter system.

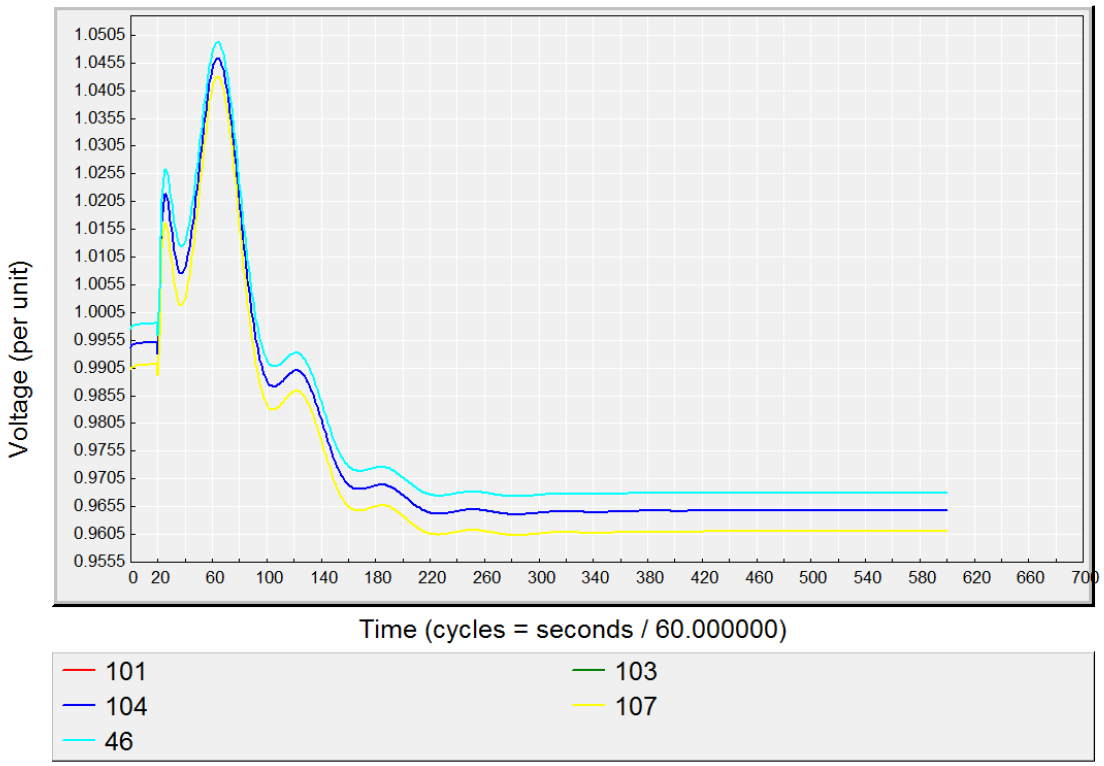

Figure 5-20: System Frequency Following Simultaneous Loss of 24kW BESS PV System and 21kW Micro-inverter System

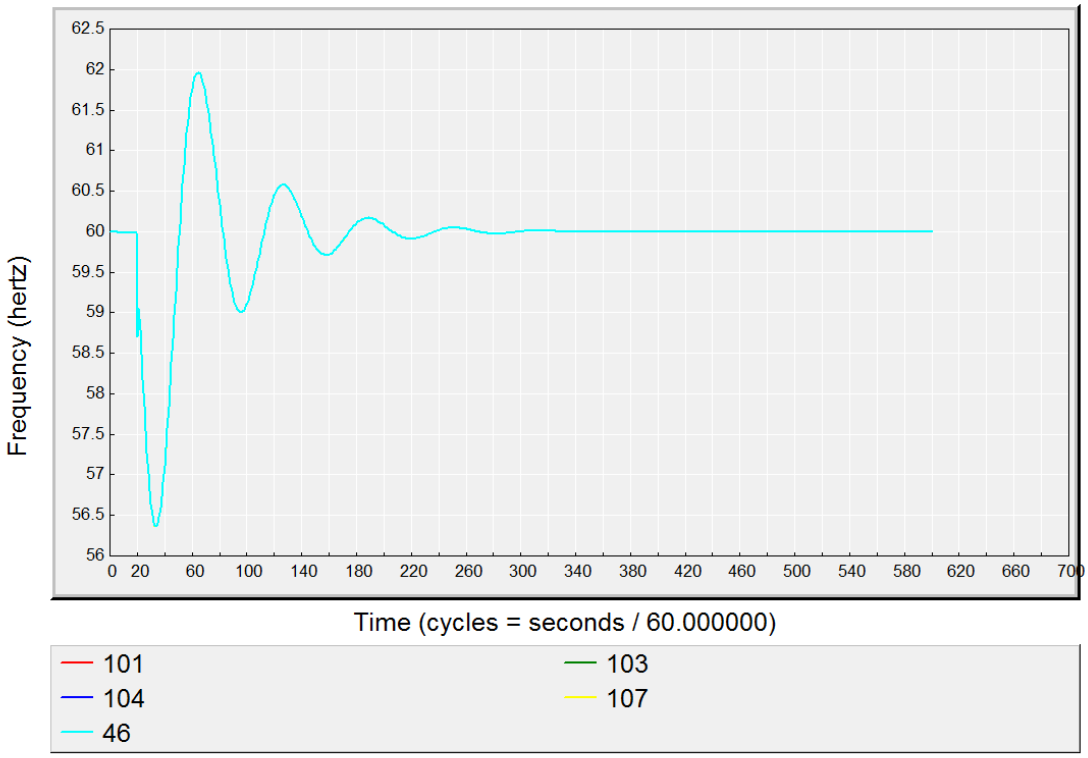

Figure 5-21: Bus Voltages Following Simultaneous Loss of 24kW BESS PV System and 21 kW Micro-inverter System.

Matlab/Simulink Dynamic Stability Results:

Dynamic stability of the WVSC microgrid was also studied using the Matlab/Simulink dynamic model. Similar scenarios described in the previous section were analyzed. Table 5-8 lists the contingences evaluated and presents summary of study results. Detailed analysis results are presented in Appendix E.

Table 5-8: Matlab/Simulink Dynamic Stability Results

Case #	Scenario	Conclusion
1	5 cycle fault at generator bus	Unstable, poorly damped response.
2	10 cycle fault at generator bus	Unstable, poorly damped response.
3	5 cycle fault at MV bus	Stable, poorly damped response.

4	10 cycle fault at MV bus	Unstable, poorly damped response.
5	5 cycle fault at Bldg. 3592 LV bus	Stable, poorly damped response.
6	10 cycle fault at Bldg. 3592 LV bus	Unstable, poorly damped response.
7	Loss of MI source	Stable
8	Step load increase at Bldg. 3592	Stable
9	Step load increase at Bldg. 3596	Stable

System Faults

Similar to the stability results using the simplified dynamic stability model in CYME, dynamic stability analysis using the detailed microgrid model revealed that the microgrid recovers from most of the 5 cycle faults on the system unlike the 10 cycle faults. However, faults occurring at the generator bus seem to be severe in nature and it takes very long time for the system to recover even from a 5 cycle fault. Thus, the microgrid system is vulnerable to the faults happening at the generator bus. The faults happening at the LV load buses of the system seem to be less severe in nature and the microgrid successfully recovers from 5 cycle faults at LV buses.

Figure 5-22 show the system frequency and voltage response following a 5 cycle fault at Bldg. 3592 LV bus (at 40 Seconds point) confirming the stable operation of the microgrid.

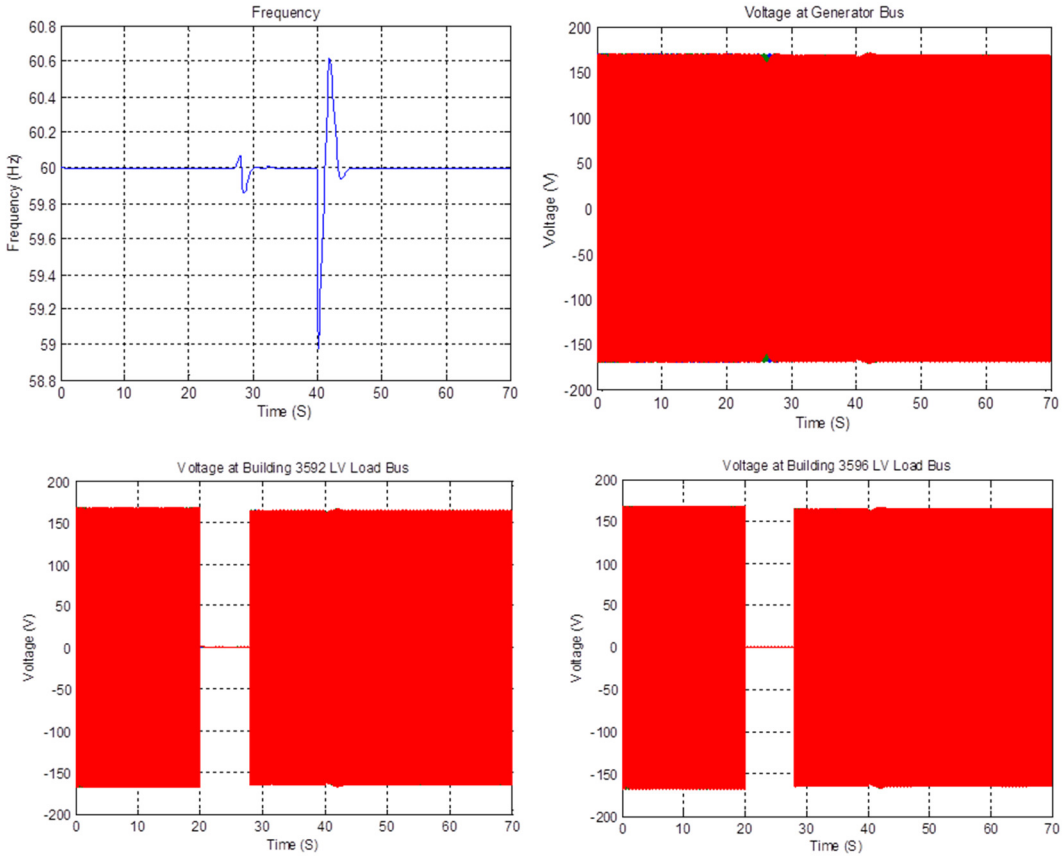

Figure 5-22: System Frequency and Voltage Response Following a 5 Cycle Fault at Bldg. 3592 LV Bus

Loss of Generators and Step Load Increase

Leidos evaluated contingency events such as loss of PV micro-inverter system and step load increase at buildings 3592 and 3596. As shown in the summary table, the analysis revealed that the microgrid system successfully recovers from all of these events.

Figure 5-23 shows system frequency and voltage response following the loss of PV micro-inverter system at 40 seconds point, confirming the stable operation of the microgrid.

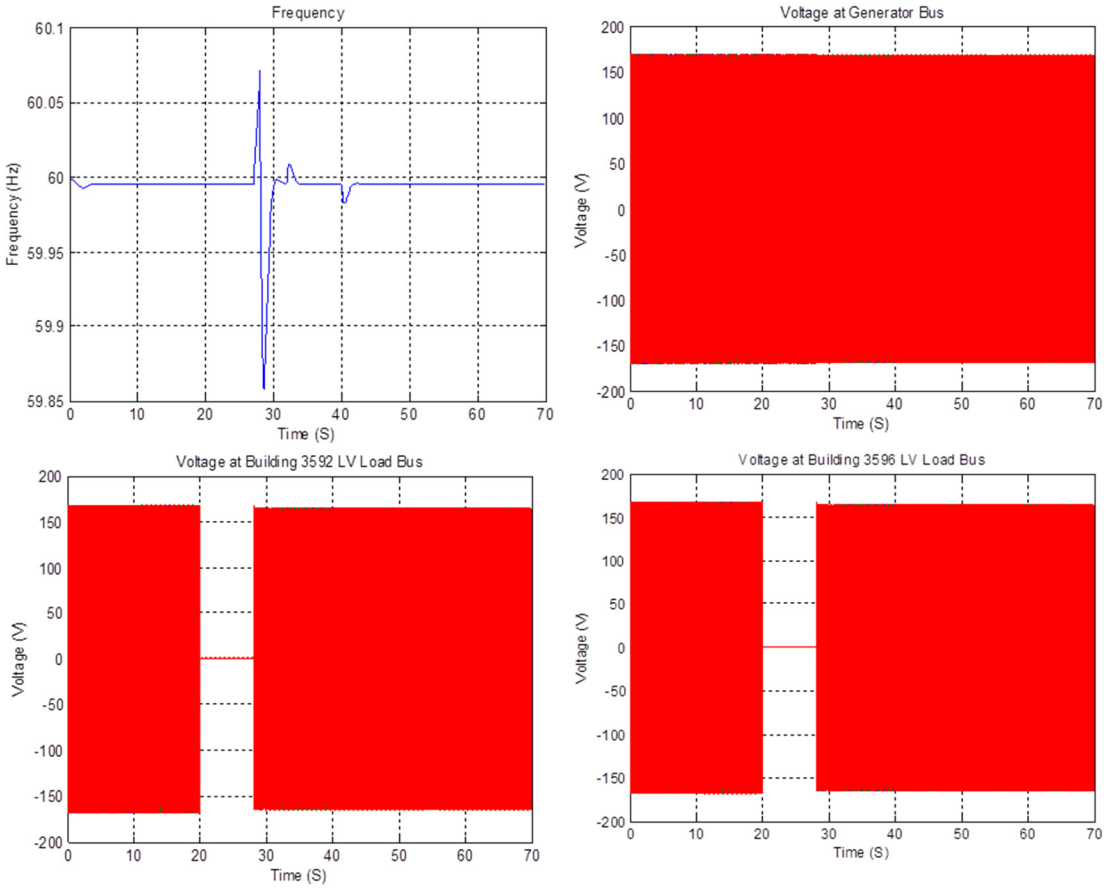

Figure 5-23: System Frequency and Voltage Response Following the Loss of PV Micro-inverter System

Figure 5-24 shows system frequency and voltage response following the step load increase (150%) at Bldg. 3592 (at 40 seconds point) confirming the stable operation of the microgrid.

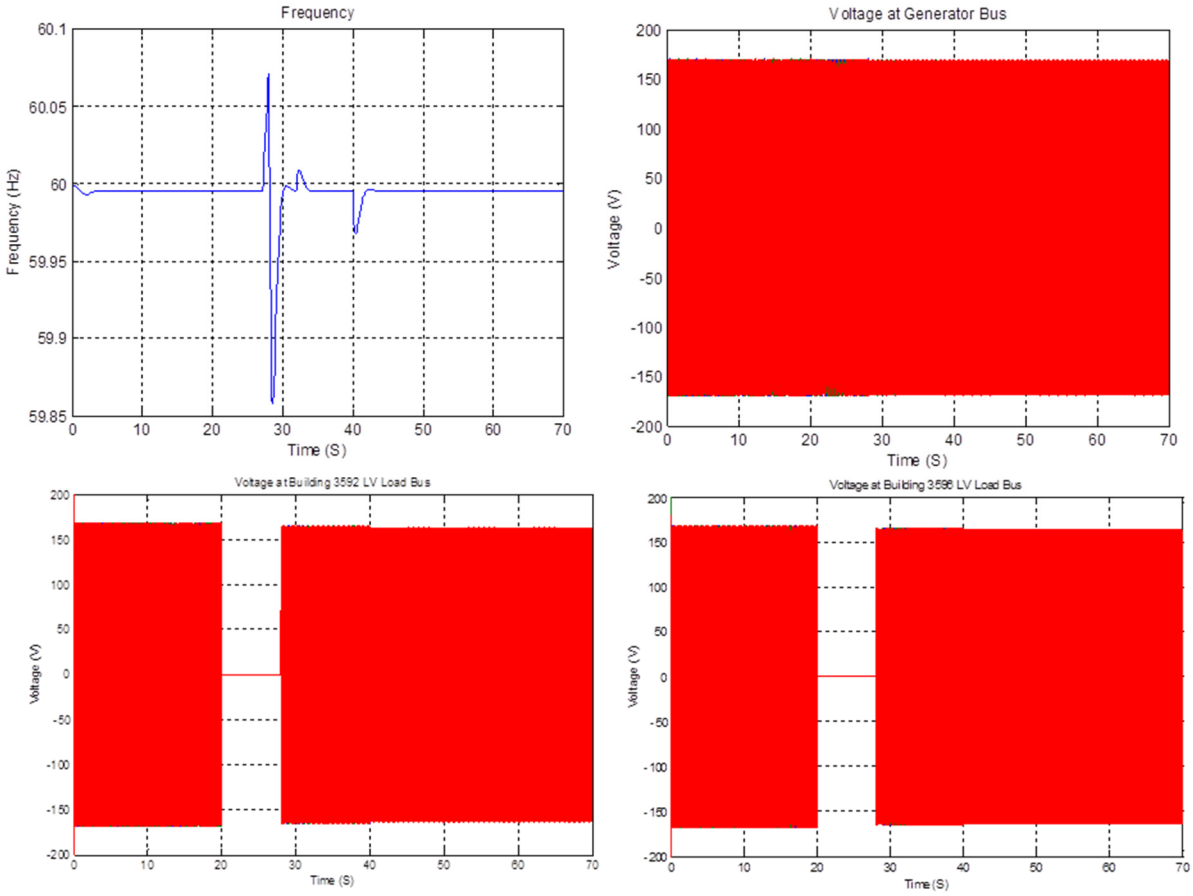

Figure 5-24: System Frequency and Voltage Following the Step Load Increase at Bldg. 3592

5.3.2 Modeling and Simulation for the Microgrid by APERC

The concept of a Microgrid incorporates three area of electrical engineering: power systems, power electronics, and electric energy conversion systems. The devices that are involved have different time scales, e.g. fast electronics and slow rotating machines, which make the simulation of such systems a difficult task. In this report, simulation has been performed in a MATLAB/SIMULINK® environment as well as in PSCAD®: Power System Computer Aided Design. PSCAD® allows detailed simulation of fast components, but the simulation time is then limited by the computing facility. Fortunately in this case, using an average modeling approach for the power electronics in PSCAD® has resulted in extending the simulation time without compromising the accuracy. The specific microgrid that was studied in this report consists of a Photovoltaic (PV) source coupled with a Battery Energy Storage System (BESS), and a rotating synchronous generator. Energy management in terms of capacity firming, as well as a load frequency control mechanism, have been developed to determine the output of the different

sources. It takes into account their characteristics while maintaining the frequency within an acceptable range. The capacity firming has been done in simulation, showing the management of battery system to follow the reference power. Load frequency control has been implemented to show the load tracking in the studied microgrid.

5.3.3 Microgrid M&S in MATLAB® Software Environment

5.3.3.1 *Microgrid System*

A schematic of the microgrid system studied is shown below. It has two generating units: a Photovoltaic (PV) source coupled with a Battery Energy Storage System (BESS), and a rotating synchronous generator as shown schematically in Figure 5-25

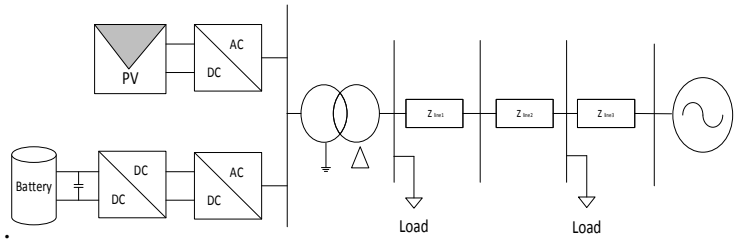

Figure 5-25: Schematic of the Microgrid Studied

In our study, a single phase as well as a three phase microgrid system is examined. The three-phase microgrid block in Figure 5-27 comprises a Phase-Locked Loop (PLL) that ensures that the output currents of the block are in phase with the generator's terminal voltages There are three pairs of PV panel/battery systems, each of which are connected as shown in Figure 5-26 to form a single phase of a three phase system.

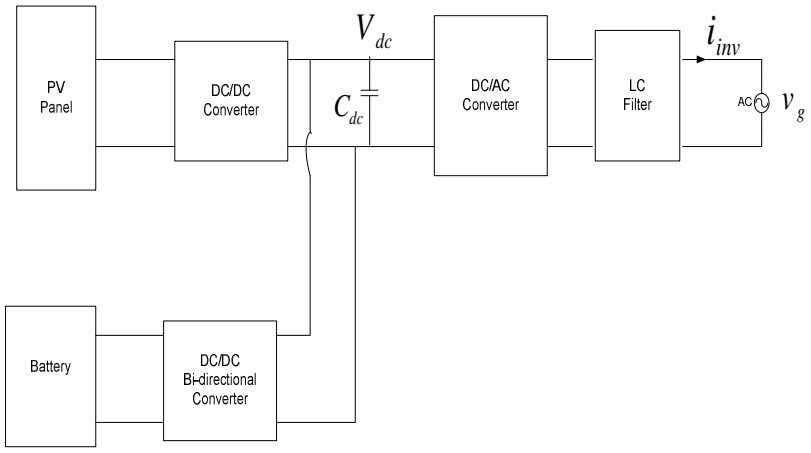

Figure 5-26: Schematic Block Diagram of a Single Phase Microgrid System

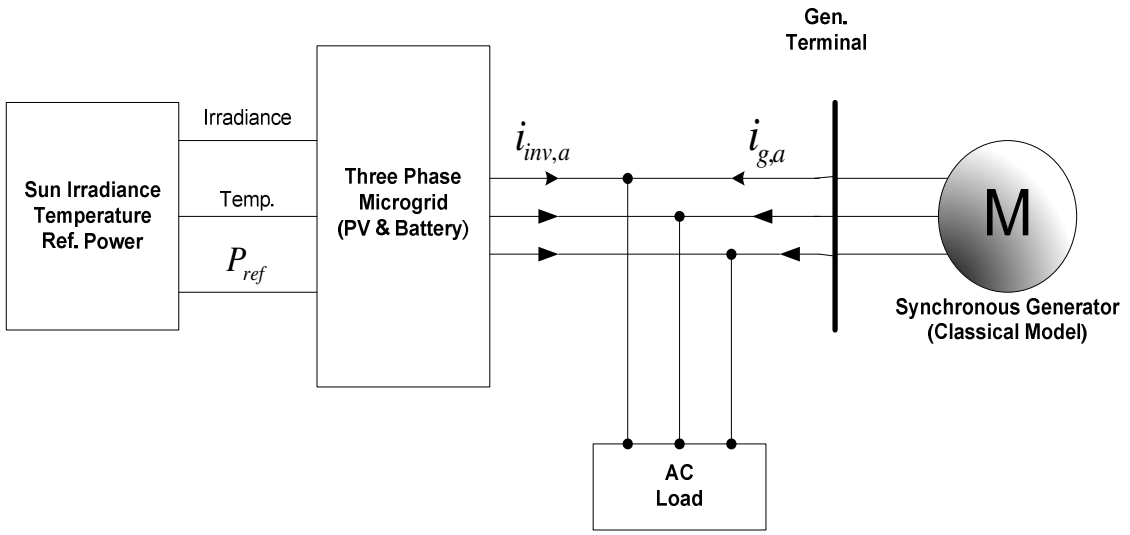

Figure 5-27: Schematic Block Diagram of a Three Phase Microgrid System

The single phase system, or each phase in the three phase system, contains a hybrid of sources. These sources consist of a Photovoltaic Energy Conversion System (PVECS), a Battery Energy System (BESS), and their corresponding converters.

The objective of this work is to utilize the PV/Battery system for (1) capacity firming and/or (2) energy time shift. The hybrid system is to generate a pre-defined or reference value of active power. This value can either be delivered to the grid or it can be used to supply a native load.

When there is excess in power generation from the sun with respect to the pre-defined value, the excess power is used to charge the battery. But, if the power generated by the PV is less than the pre-defined value, the BESS will discharge (provided it is charged) to cover the deficiency.

5.3.3.2 *Modeling of the Photovoltaic Module*

The PV module is modeled using a single exponential model as depicted in Figure 5-28. The PV module is represented by a current source I_{ph} in parallel with a shunt resistance R_P. The output DC voltage V is in series with the internal resistance R_S. The current flowing through the internal resistance is designated as I. The current I_{ph} is expressed in terms of voltage (V), current (I) and temperature (T) by the given equation:

$$I = I_{ph} - I_{sat}(e^{\frac{q(V+IR_S)}{n_c AkT}} - 1) - \frac{V + IR_S}{R_P} \qquad (3.1)$$

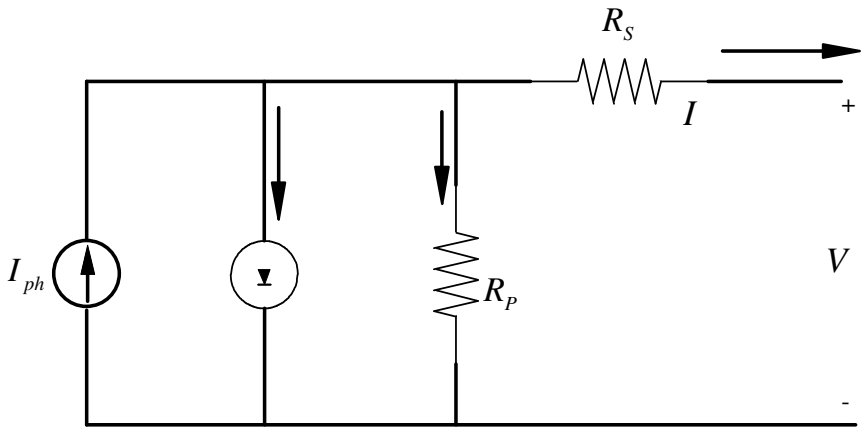

Figure 5-28: The Single Exponential Model of a Photovoltaic Module

The data which is required for PV modeling and the collection process are described in section 3.2.5.

5.3.3.3 *Modeling and control of BESS and DC bus*

Several BESS models have been proposed for simulating its charging and discharging dynamics [6,7]. A battery is generally represented by a set of nonlinear equations denoting the current delivered or absorbed by the battery as a function of its state of charge (SOC), internal resistance and capacitance. The built in SimPowerSys™ block model of Lithium Ion battery in MATLAB® is used in this work. The BESS is modeled as a constant resistance connected in series with a controlled voltage source as shown in Figure 5-29 [7]. The capacity of each of the lithium ion type BESS is 10 kWh at a terminal voltage of 84.0 Volts. The charge and discharge characteristics of the battery are defined by the following equations:

$$E_{ch\arg e}(it, i^*, i) = E_0 - \Sigma\frac{Q}{it + 0.1Q}i^* - \Sigma\frac{Q}{Q - it}it + A\exp(-B.it) \qquad (3.2)$$

$$E_{disch\arg e}(it, i*, i) = E_0 - \Sigma\frac{Q}{Q - it}i* - \Sigma\frac{Q}{Q - it}it + A\exp(-B.it) \qquad (3.3)$$

where:

A : The exponential zone amplitude (V)

B : The exponential capacity $(Ah)^{-1}$

it : extracted capacity (Ah)

i : Battery current (A)

$i*$: Low frequency current dynamics (A)

Σ : Polarization constant (Ah^{-1}) or polarization resistance (Ω)

Q : Maximum battery capacity (Ah)

E_0 : Battery constant voltage (V)

The voltage at the DC bus V_{dc} is designed to be within the range 190-210 Volts. The DC buses consist of capacitances that collect energy from different sources. For our study, the objective is to obtain a constant pre-defined active power value from the combination of PVECS/BESS in the single phase microgrid system or for each of the phases in the three phase microgrid system.

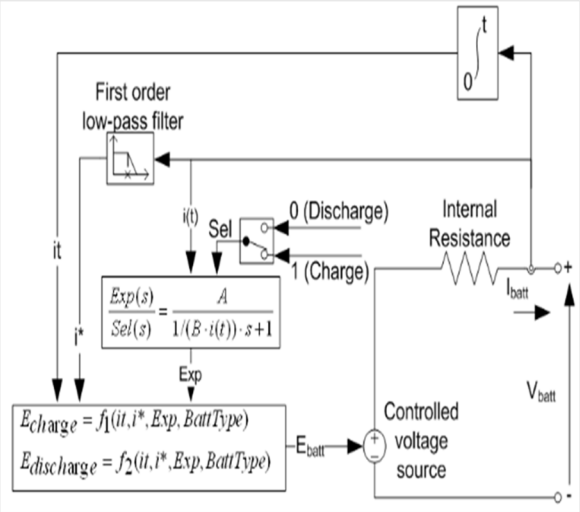

Figure 5-29: Schematic Diagrams of Battery Model

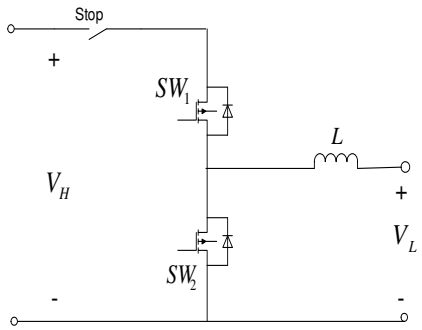

Figure 5-30: Bi-Directional DC/DC Converter

Since the value of the terminal voltage of each BESS is lower than the minimum value of the desired dc voltage value, a bi-directional DC/DC converter is placed or positioned between the BESS and the dc bus. The schematic diagram of the battery's bi-directional converter is depicted in Figure 5-30. In order to prolong the lifespan of the battery, the state of charge (SOC) of the battery is kept within a safe range (25-95 percent). The low and the high voltage sides of the converter are connected to the BESS and the dc bus respectively. When the power generated by the PVECS is greater than the specified value, the converter operates in buck or charge mode (SW1 is ON, SW2 is OFF) to charge the battery based on the battery SOC. When the power generated by the PVECS is less than the specified power, SW1 is turned OFF and SW2 is turned ON (boost mode) for the battery to supply the required power. During any of these conditions, the stop switch is CLOSED. The stop switch is opened in order to prevent the battery from either overcharging or discharging more than desired. The Simulink model for the battery management system is depicted in Figure 5-31. The Simulink battery control block is given in the Appendix-F. Cascade control is employed so as to limit the amount of current flowing into or out of the battery.

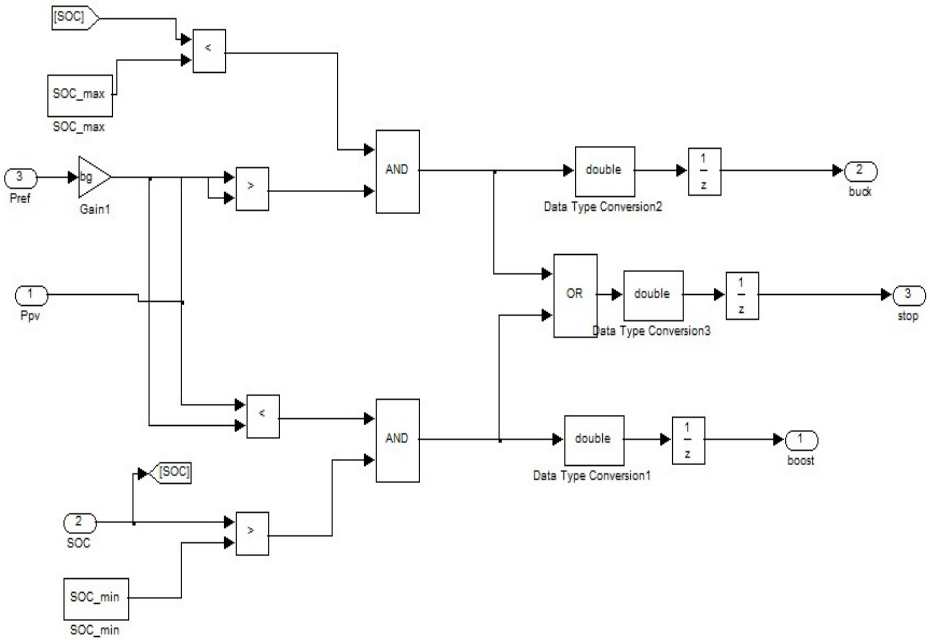

Figure 5-31: Simulink Model of the Battery Management System

5.3.3.4 *Modeling and Control of the Inverter*

The DC bus collects energy from the PVECS and the BESS and supplies it through a single phase inverter. The inverter is controlled using a bipolar Sinusoidal Pulse Width Modulation (SPWM) [8] technique to ensure that its load current (the current after filtering) is in phase with the grid voltage. Figure 5-32 shows the single phase inverter topology used in our study.

Assuming the grid voltage is represented by a sinusoidal signal given as:

$$v_g = v_{g,a}(t) = V_m \sin(\omega t) \tag{3.4}$$

where V_m is the amplitude of the sinusoidal voltage signal. Since the main objective of the inverter control is to transfer the power at the dc bus to the ac side with a unity power factor, the inverter's reference or desired output current can be assumed to be a fraction of the terminal voltage of the generator i.e.:

$$i^*_{inv}(t) = i^*_{inv,a}(t) = \mu v_g(t) = \mu v_{g,a}(t) \tag{3.5}$$

The transferred sinusoidal output power and its steady state values are given by:

$$p_{out}(t) = v_{g,a}(t).i_{inv,a}(t) = \frac{\mu V_m^2}{2}(1-\cos(2\omega t)) \tag{3.6}$$

$$P_{out} = \frac{1}{T}\int_0^T p_{out}(t)dt = \frac{\mu V_m^2}{2} \qquad (3.7)$$

Assuming a lossless operation and denoting the power at the dc bus (summation of the power generated by the PVECS and BESS) by P_{dc}, the value of μ can be obtained as:

$$P_{dc} = P_{out} \Rightarrow \mu = \frac{2P_{dc}}{V_m^2} \qquad (3.8)$$

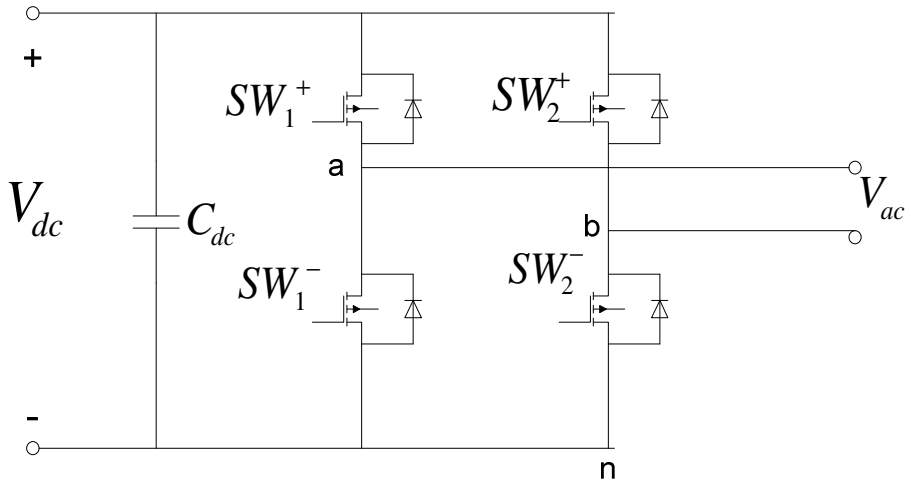

Figure 5-32: Schematic Diagram of Single Phase Inverter

The output voltage of the inverter is given by

$$v_{ac} = V_{dc}M_a.\sin(\omega t) + harmonics \qquad (3.9)$$

where M_a is the modulation of the inverter. Therefore, the peak or amplitude of the fundamental component has a value $V_{dc}M_a$ with $0 \le M_a \le 1$. The design practice is operating the inverter within the linear region, i.e. its modulation should be less or equal to 1. So in order to obtain an RMS voltage value of 120.0 Volts at the output of the inverter, the minimum value of V_{dc} has to be $120\sqrt{2}$ Volts.

5.3.3.5 *Modeling and Control of the Generator*

The classical model of the generator is used for this work. The schematic block diagram of the generator is depicted in Figure 5-33. The dynamics of the system are given by the swing equation. These equations are given by [9]:

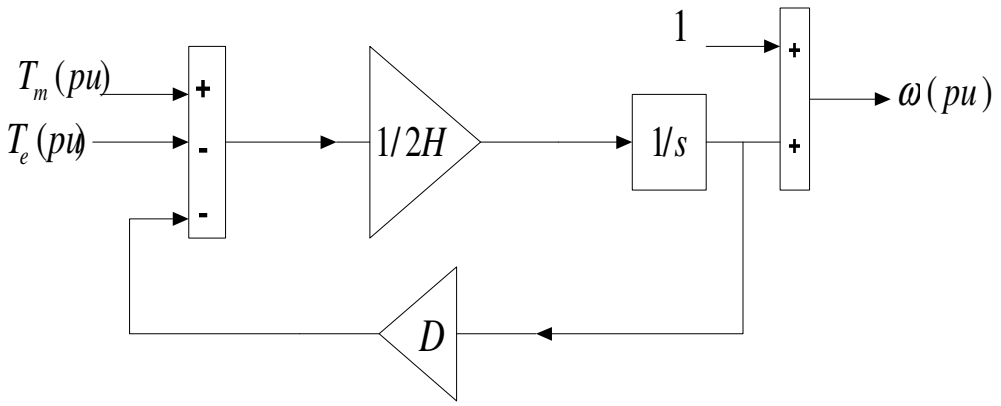

Figure 5-33: Schematic Block Diagram of the Generator

$$\Delta\omega(t) = \frac{1}{2H}\int_0^t (T_m - T_e)dt - D\Delta\omega(t) \qquad (3.10)$$

$$\omega(t) = \Delta\omega(t) + \omega_0 \qquad (3.11)$$

where:

$\Delta\omega$: Speed variation with respect to speed of operation (or synchronous speed)

H : Constant of inertia

T_m : Mechanical torque

T_e : Electrical torque

D : Damping factor

$\omega(t)$: Mechanical speed of the rotor

ω_0 : Nominal Speed (1 p.u.)

The objective of the control is to keep the speed of the generator constant at 1.0 p.u. The generator's speed deviation is measured and a PI controller is used to bring the speed error to 0.

5.3.4 Modeling and Simulation with the PSCAD® Software

PSCAD® stands for Power System Computer Aided Design. It is the software selected to model and analyze the PV inverter system in this research. The simulation environment includes a default master library that includes typical circuit components of a Spice library, but goes further in complexity by also including items ranging from advanced power electronic devices to rotating machine models such as a synchronous generator. The strength and uniqueness of the program is the ability to integrate complex power electronic circuits with large power systems and view the system responses in the time and frequency domains.

5.3.4.1 *PWM Inverter Modeling*

The inverter modeled in PSCAD is shown in Figure 5-34. The only additional inverter components are snubber circuits connected in parallel to each IGBT, and a clamping diode. Values selected for the snubber component were unchanged from the default value assigned by PSCAD®. They are shown in Figure 5-35.

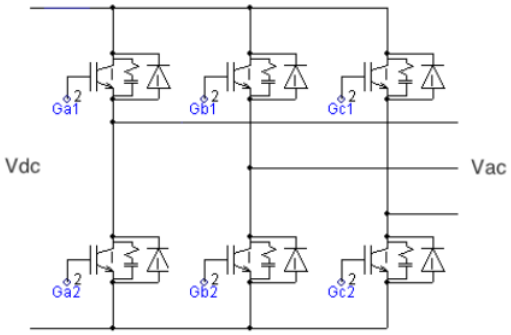

Figure 5-34: Inverter Modeled in PSCAD

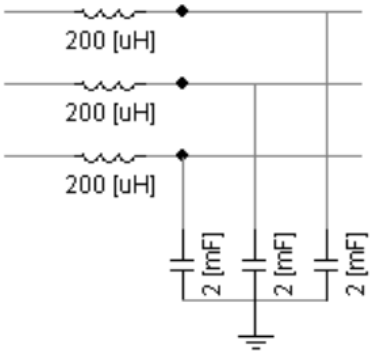

Figure 5-35: Snubber Circuit

After creating the three reference sine waves and the triangle carrier signal, the reference waves are each fed into a driving block that will finally turn on and off the IGBTs.

5.3.4.2 *PV Modeling*

The characteristic of a PV has been discussed previously. The PV module in PSCAD® is built using FORTRAN coding which is given in the Appendix-F. The PV array used in this modeling is shown in Figure 5-36.

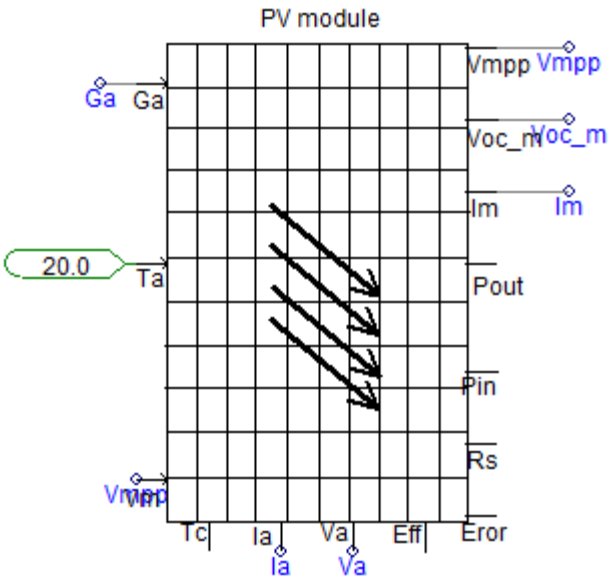

Figure 5-36: PV Module Used in PSCAD

The PV/BESS system has been implemented in PSCAD® to compare with the previous results and also to increase the simulation time.

The system contains three main parts:

1. PV and DC/DC
2. Battery
3. Inverter

Each part is simulated as a subsystem. The Figure 5-37 shows this system.

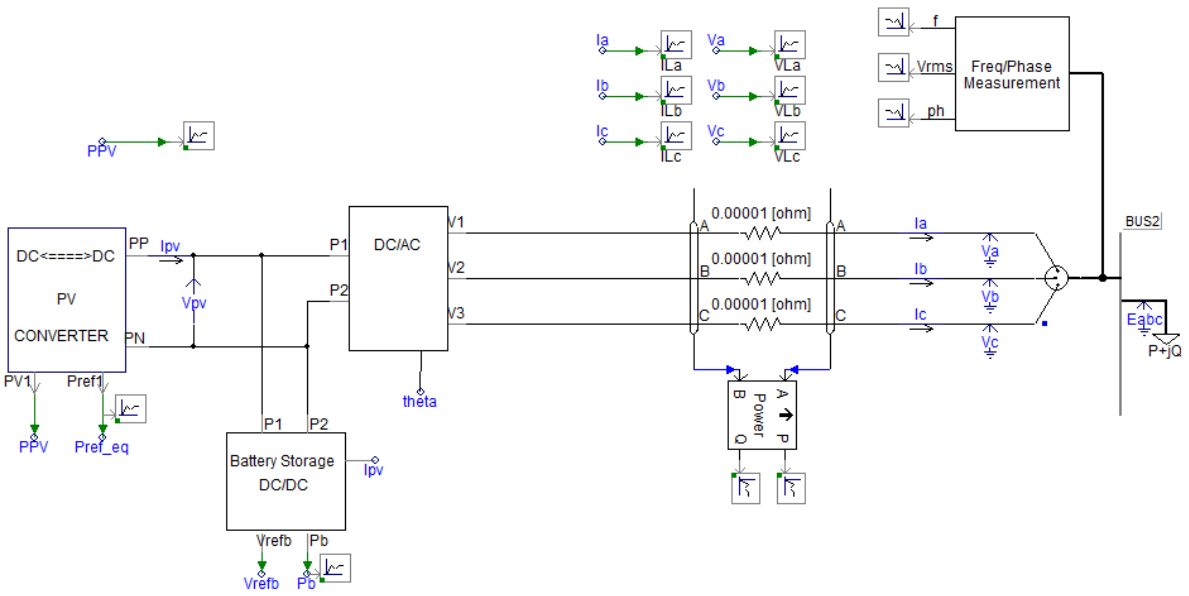

Figure 5-37: System Main Component

All other components and the control system for the BESS and PV inverter are given in the Appendix E.

Data Collection Process, Challenges and Assumptions

In this study the main data which was required to be collected was the data related to the solar panel. The data collection process for the PVECS is described below.

Modeling and Collection of Required Parameter of PVECS

The sun is the basic source of the earth's energy. It radiates electromagnetic waves, in the form of ultraviolet, visible and infrared energy. Most of the emitted energy is in the form of a short wave that is utilized in the planet's weather cycle, heat cycle, wind and waves. A small fraction of the energy is used for photosynthesis in plants and the remaining portion of the solar energy is radiated back into the space [1]. Sunlight is defined by irradiance. This implies the radiant energy of the sun. 1 sun is defined as the brightness to supply an irradiance of about 1 kilowatt (kW) per square meter (m^2) at sea level and 0.8 sun about $800W/m^2$. One sun's energy has 523 watts of infrared light, 445 watts of visible light and 32 watts of ultraviolet light.

The solar energy is directly converted into electrical energy by solar cells, also known as photovoltaic (PV) cells. PV cells are made of silicon materials (crystalline silicon (c-Si)). The striking of sunlight on the PV cell emancipates electrons from the surface of the cell. These electrons are guided toward the front of the surface, thereby causing current to flow between the negative and the positive sides of the cell. A PV module is referred to as the connected series solar cells. The data sheet of PV manufacturers always provides information of the PV module. The typical information will include the number of cells that were connected in series to form 1 module, the open circuit voltage and the short circuit current of the module, the maximum power and the values of voltage and current at the point of maximum power and so on. The typical

numbers of cells that constitute a module are 36, 50, 60 and 72. The voltage produced by each of the c-Si cells is about 0.5 – 0.7 V. For a module consisting of 60 of such cells, with each cell providing 0.5 V of voltage, the voltage of the PV module is 30 V. For a PV system, modules are connected in series to provide a higher operating voltage, and in parallel to supply a higher operating current. By connecting a number of PV modules in series, we form a string. A number of strings connected in parallel make an array. Both series and parallel connections may be required to generate or construct a PV system of desired specification. For instance, using the data sheet provided by the manufacturer Upsolar [2], the following information is obtained.

Maximum power point of the module, $P_{MPP} = 225\,W$

Voltage at P_{MPP}, $V_{MPP} = 29.2\,V$

Current at P_{MPP}, $I_{MPP} = 7.71\,A$

Short Circuit Current, $I_{SC} = 8.27\,A$

Open Circuit Voltage, $V_{OC} = 37.0\,V$

Number of cells connected in series is 60.

The values given above are the characteristics of the module under Standard Test Conditions (STC) ($1000\,W/m^2$ irradiance, AM 1.5 solar spectrum and $25\,^oC$ module temperature).

Photovoltaic Characteristics

As sun irradiance energy is captured by a PV Module, the open-circuit voltage of the module increases. This point is delineated in Figure 5-38 by V_{OC} with zero-input current. I_{SC} is the current flowing as the module is short-circuited. As indicated in this Figure, the voltage at this point is zero. The point on the I versus V characteristic where maximum power (P_{MPP}) can be reduced lies at a current I_{MPP} and the corresponding voltage point, V_{MPP}. The PV fill factor, FF is defined as a measure of how much solar energy is captured. It is defined by PV module open-circuit voltage and short-circuit current as:

$$FF = \frac{V_{MPP} I_{MPP}}{V_{OC} I_{SC}} \qquad (3.12)$$

The maximum power that can be extracted by the module and the efficiency of the module are given as:

$$P_{\max} = P_{MPP} = FF V_{OC} I_{SC} = V_{MPP} I_{MPP} \qquad (3.13)$$

$$\eta = \frac{P_{MPP}}{P_S} \qquad (3.14)$$

where P_S is the surface area of the module. The PV module efficiency can also be defined as:

$$\eta = \frac{P_{MPP}}{\int_0^{\infty} P(\lambda) d\lambda} \qquad (3.15)$$

where $P(\lambda)$ is the solar power density at wavelength λ.

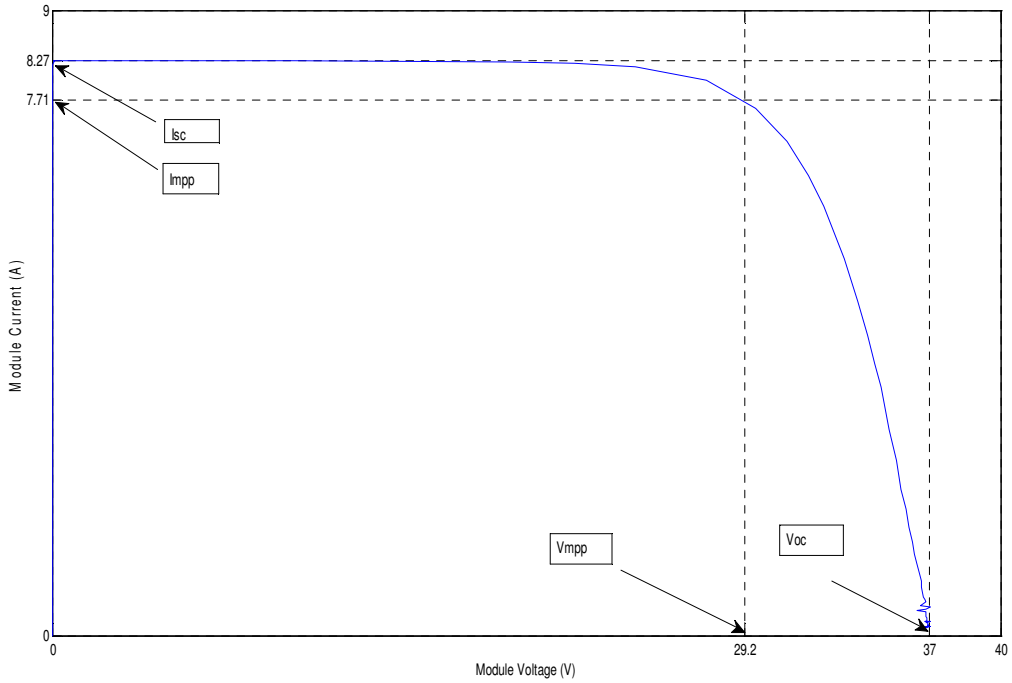

Figure 5-38: The Operating Characteristics of a Photovoltaic Module

5.3.4.3 *Modeling of the Photovoltaic Module*

As it was mentioned in a previous section, The PV module is modeled using a single exponential model as depicted in Figure 5-38.

The current flowing through the internal resistance is designated as I. The current I_{ph} is expressed in terms of voltage (V), current (I) and temperature (T) by the following equation:

$$I = I_{ph} - I_{sat}(e^{\frac{q(V+IR_S)}{n_c AkT}} - 1) - \frac{V + IR_S}{R_P} \qquad (3.16)$$

The other parameters are the diode quality factor (A), whose value varies between one and two. The number of cells in the module is n_c, the electronic charge (q), $1.6\times10^{-19}\ C$; Boltzmann's constant (k), $1.38\times10^{-23}\ J/K$, and the ambient temperature (T) is in Kelvin.

The equation given above is nonlinear and its parameters I_{ph}, I_{sat}, R_S, R_P and A are functions of temperature, irradiation and manufacturing tolerance. The values of these parameters are unknown and are supposed to be estimated using the data sheet obtained from the manufacturer. The accuracy of the simulation of the model depends on how well their estimates are close to the actual values. As we have mentioned earlier, these parameters are to be approximated using $P_{MPP}, I_{MPP}, V_{MPP}, I_{SC}$ and V_{OC}. Since A is between one and two, its value can be assumed. In our study, the value is taken to be 1.5. The estimates of the remaining unknown parameters are obtained from the equation given below [3]:

$$I_{pv} = (I_{SC} + k_i \Delta T)\frac{I_r}{I_{rr}} \tag{3.17}$$

where I_r is the surface irradiance, $\mathrm{I_{rr}}(1000 W/m^2)$ is the irradiance under STC, $\Delta T = T - T_{STC}$ (in Kelvin) and k_i is the short-circuit current coefficient. The temperature that describes the saturation current is given by [3]:

$$I_{sat} = \frac{I_{SC\_STC} + k_i \Delta T}{e^{\frac{V_{OC\_STC} + k_v \Delta T}{n_c A V_T}} - 1} \tag{3.18}$$

where V_T $(= \frac{kT_{STC}}{q})$ is the diode thermal voltage, I_{SC_STC} and V_{OC_STC} are PV module short-circuit current and open-circuit voltage at STC.

The remaining two unknown parameters, R_S and R_P, are obtained through iteration. The idea is to minimize the difference between the calculated maximum power (3.20) and the experimental (from the manufacturer's data sheet) maximum power $P_{MPP,E}$ by iteratively increasing the value of R_S and simultaneously computing the value of R_P. Using (3.16), at maximum power point I_{MPP} and P_{MPP} can be expressed as:

$$I_{MPP} = I_{ph} - I_{sat}(e^{\frac{V_{MPP} + I_{MPP} R_S}{n_c A V_T}} - 1) - \frac{V_{MPP} + I_{MPP} R_S}{R_P} \tag{3.19}$$

$$P_{MPP,C} = I_{MPP}V_{MPP} = V_{MPP}(I_{ph} - I_{sat}(e^{\frac{V_{MPP}+I_{MPP}R_S}{n_c AV_T}} - 1) - \frac{V_{MPP} + I_{MPP}R_S}{R_P}) \quad (3.20)$$

The expression of R_P can be expressed from (3.20) as:

$$R_P = \frac{V_{MPP}(V_{MPP} + I_{MPP}R_S)}{V_{MPP}(I_{ph} - I_{sat}(e^{\frac{V_{MPP}+I_{MPP}R_S}{n_c AV_T}} - 1)) - P_{MPP,E}} \quad (3.21)$$

The initial conditions of R_S and R_P are set as:

$$R_S = 0; \qquad R_P = \frac{V_{MPP}}{I_{SC} - I_{MPP}} - \frac{V_{OC} - V_{MPP}}{I_{MPP}} \quad (3.22)$$

Using these values, $P_{MPP,C}$ is computed using (3.20). This value is compared with the experimental value. The iteration continues until both values are equal or their difference is within a pre-defined tolerance value.

The PV panels used in this work are about 10 KW each. Each panel has 9 strings connected in parallel, each string comprises of 6 modules connected in series, and is constructed using the data sheet provided in [2]. The power–voltage and the current-voltage characteristics of the panel at constant temperature of $25\ ^oC$ and for different values of sun irradiance are depicted in Figure 5-39 and Figure 5-40 respectively.

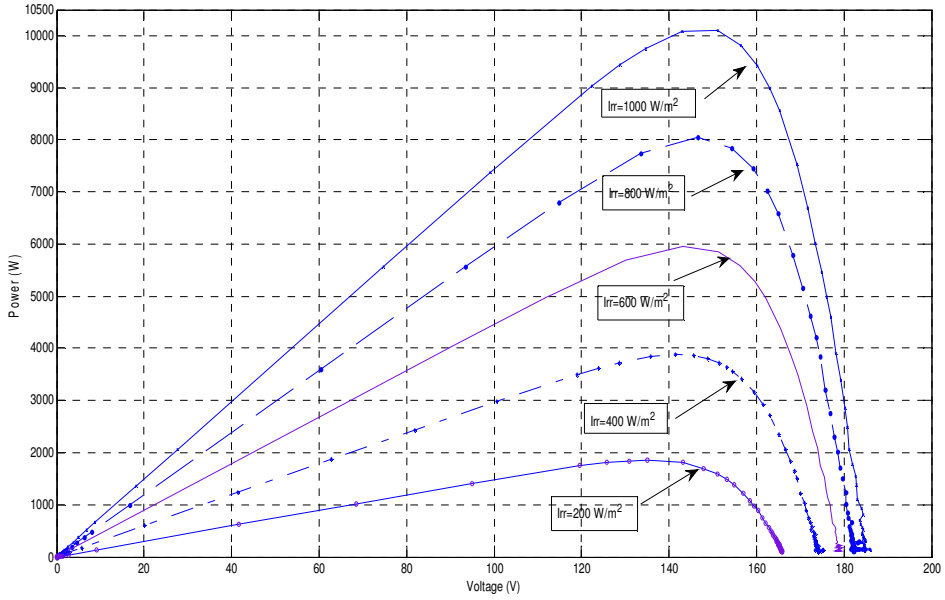

Figure 5-39: Panel P-V Characteristics at 25^0C and Changing Irradiance

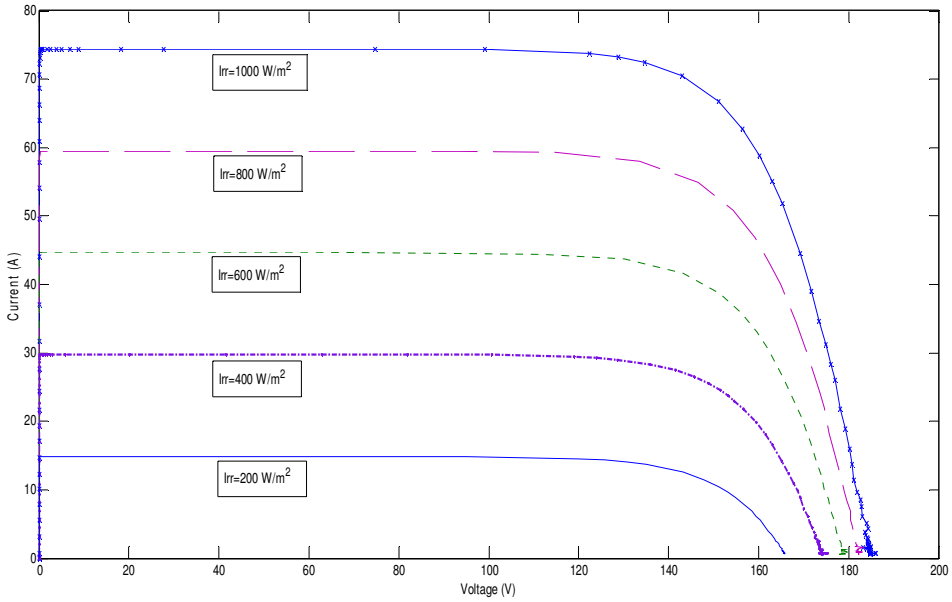

Figure 5-40: Panel I-V Characteristics at 25^0C and Changing Irradiance

From these Figures we can see that at STC (which is $25 \circ c$), the open circuit voltage and the short circuit current are about 185 Volts and 74.5 Amps, and the V_{mpp} of the panel is about 150 Volts. This implies that the panel has to operate close to the point at which its voltage is 150 Volts in order to extract or obtain maximum power from it. The panel's DC/DC boost converter is equipped with a Maximum Power Point Tracking (MPPT) algorithm. The purpose of the MPPT

algorithm is to ensure that maximum power is drawn from the PV panel. This is achieved by altering the duty cycle of the boost converter in order to track the maximum power point. Many MPPT are available in the literature among which are the popular Perturbation and Observation algorithm that we adopted in this work [4,5]. The other function of the boost converter is to raise the PV panel's voltage level to a level high enough to obtain a root mean square (rms) value of 120 Volts at the output of the inverter.

5.3.4.4 *Detailed versus Average Model*

As it was mentioned in previous sections, the running time of microgrid in Matlab with detailed modeling was very slow with small simulation time. So the different power electronic parts of the PV subsystem are then replaced by their average model for having a longer duration and faster run time. This section discusses simulation results using average model vs. detailed model.

In Figure 5-42 it is assumed that the PV is generating about 3000 Watts of power and the reference power is 6000 Watts. The battery should supply the load by injecting the extra needed amount of power. The diagram of PV/Battery system is shown in Figure 5-41. The output results for the detailed model are shown in Figure 5-42 and the average model in Figure 5-43.

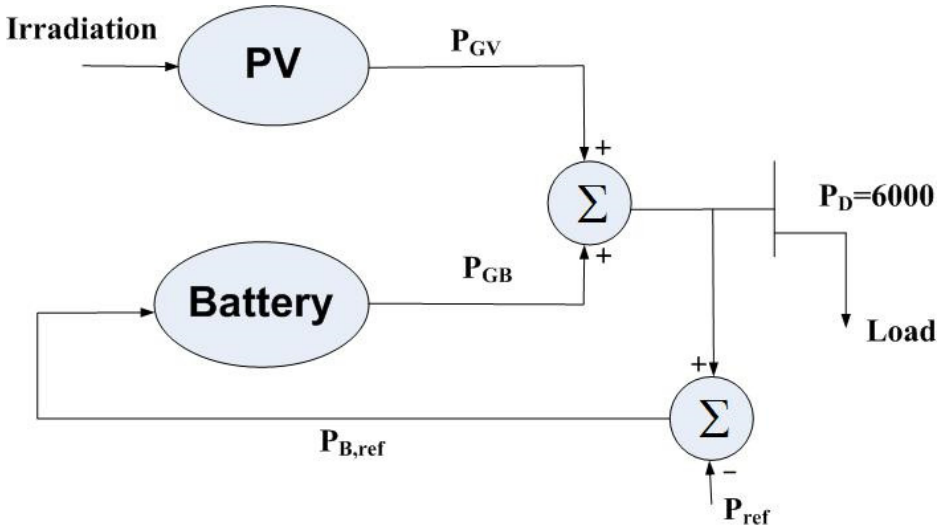

Figure 5-41: PV/BESS

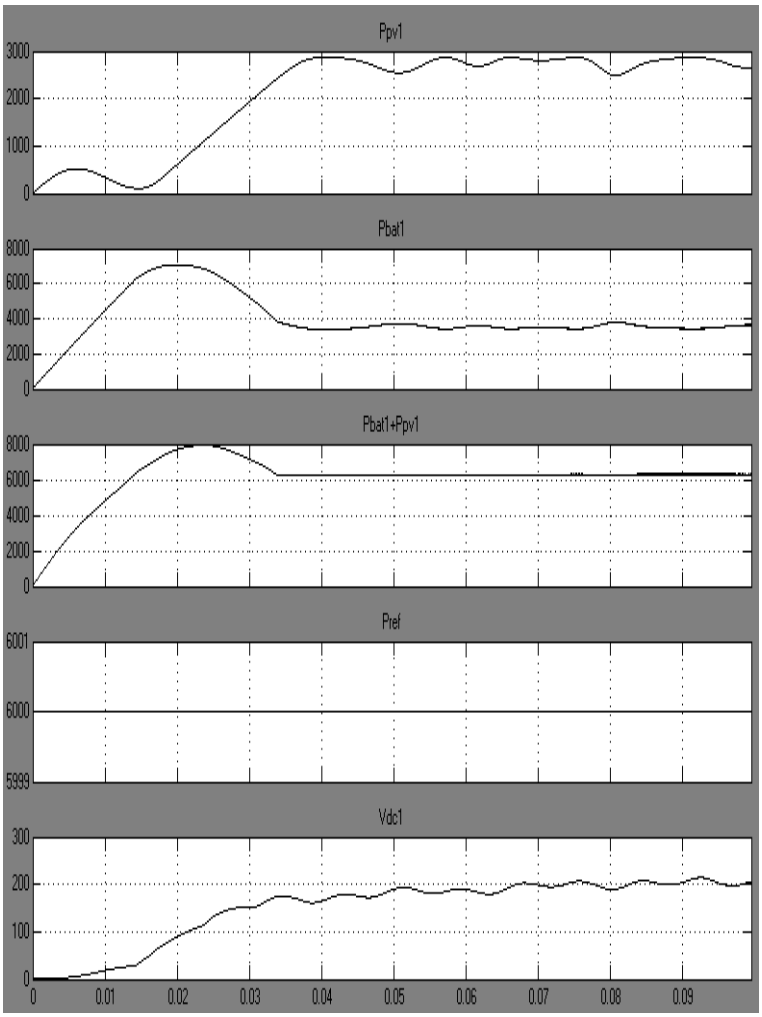

Figure 5-42: Output Result of PV System Using the Detailed Model (PV Generate 3000 W)

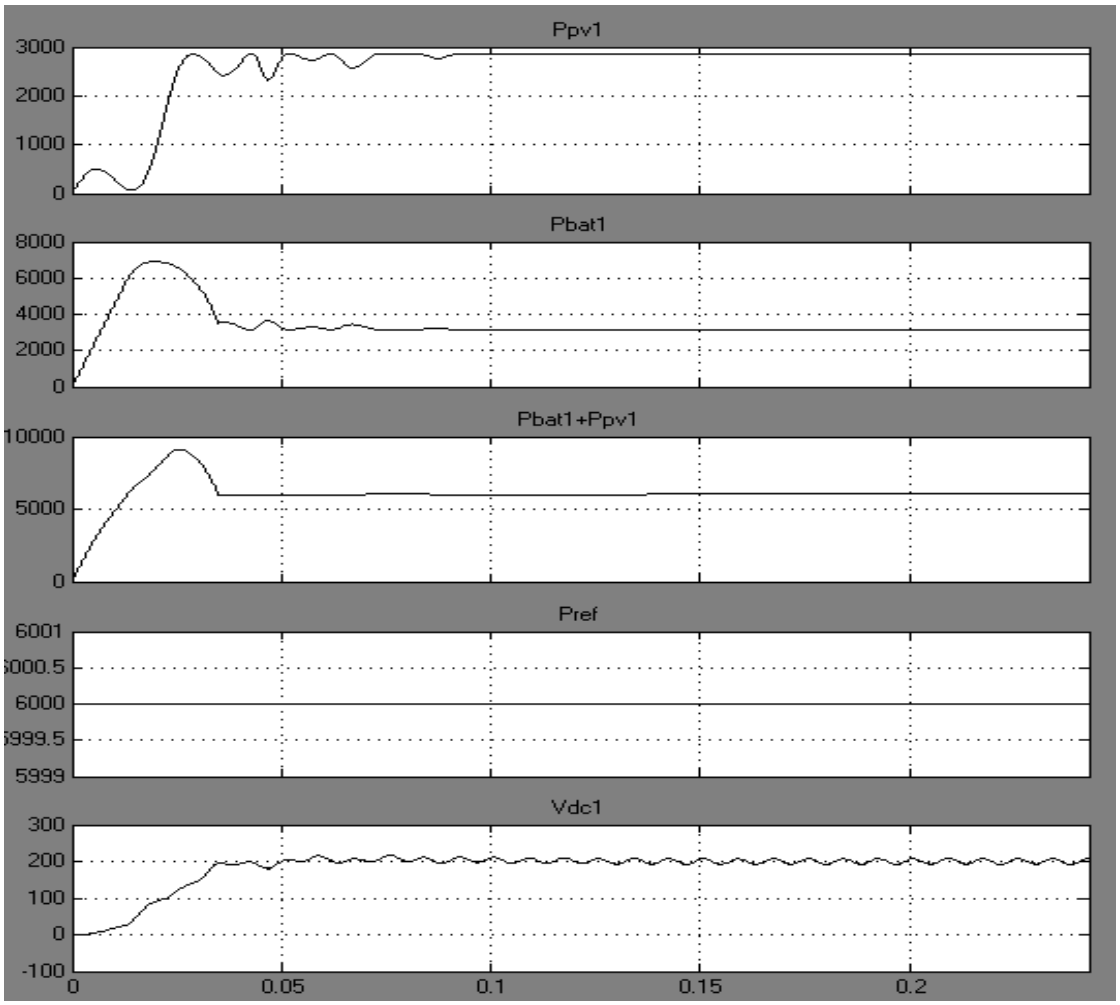

Figure 5-43: Output Result of PV System Using the Average Model (PV Generates 3000 W)

When comparing Figure 5-42 and Figure 5-43, it is evident that the average model gives similar results as the detailed model, but runs more than 10 times faster.

5.3.5 Simulation Scenarios

This section describes the simulation scenarios.

5.3.5.1 *Capacity Firming and Load Following (Matlab®)*

Two different cases are depicted for Capacity Firming and Load Following in a standalone microgrid:

1. Capacity Firming and Load Following in a Single Phase Microgrid System
2. Capacity Firming and Load Following in a Three Phase Microgrid System

The schematic diagram of this system can be seen in Figure 5-44. A switching frequency of 20 KHz is employed for the converters. The perturbation and observation algorithm is employed for maximum Power Point Tracking (MPPT) because of its simplicity and popularity.

5.3.5.2 *Frequency Control (PSCAD®)*

In this part of the simulation, the frequency of a microgrid, that contains PV generation and battery energy storage, is controlled. This study presents a new approach for Load Frequency Control (LFC) in a microgrid by considering the low voltage microgrid as an artificial multi area network and providing a new strategy which can significantly improve the frequency regulation of the microgrid.

A Virtual Area Control Error (VACE) is introduced which utilizes a virtual tie-line and includes the State of Charge (SOC) of the battery to take into consideration the realistic characteristics of the device. The system is simulated using PSCAD. The results show a good improvement in frequency deviation.

Controlling the inverters in a microgrid is a key point. For a microgrid with single inverters, most of traditional approaches use voltage-frequency (v-f) scheme in isolated operation or active power- reactive power (P-Q) control scheme in grid connected. It means that in an islanded mode the inverter should change its policy so that it can maintain the voltage and frequency at their nominal values. The paper [10] describes control strategies which can be adapted for inverters of a microgrid in an isolated mode. The two kinds of control strategies which can be used to operate an inverter are described as PQ inverter control and Voltage Source Inverter (VSI) control. Paper [10] also shows two possible control approaches for microgrids: Single master operation and Multi master operation. In these approaches the VSI inverters act as masters and the other inverters operating in PQ modes are slaves and produce their constant set point during transient situation. The previously mentioned control strategies paper [11] tries to implement a new power and voltage control (P-V) scheme for a single inverter that operates in an island to handle the active power sharing among parallel inverter-interfaced distributed energy resources.

Paper [12] is trying to restore the frequency of a microgrid to the nominal value while ensuring proper power sharing between multiple DGs considering the rating and dynamic characteristics of various energy sources. This paper uses the power vs. frequency droop control, since it enables decentralized control of multiple distributed generations. The author believes that the

power droop control alone is not enough for the microgrid because of continuous variation of load demand. He suggests two different secondary load frequency controls. The first one uses a central controller which sets the power reference signal of each DG, and second one adds an integral controller to the existing droop controller. The second method is used by the author [12] because of locally measured signal without additional communication.

In [13] a power storage system is used with solar photovoltaic, diesel generator and wind power generation for load frequency control of a power system. The microgrid system at Aichi Institute Technology in Japan is used as a simulation model. The load frequency method was performed using two different methods. The first one is power demand estimation and the second one is proportional control which uses the frequency deviation. In proportional control the purpose is bringing the frequency deviation back to zero, which may not be the best solution when the load is fluctuating. The author uses proportional control in absence of a storage device. The results are then compared to the situation in which there is storage in the system, and the load demand estimation method is applied for load frequency control. In the load demand estimation the load fluctuation of an area is estimated (the estimation of some generation units like PV and wind is also needed) and it has been used for the output set point of storage so that it can compensate for this change. The drawback of the load demand estimation method is that the load change is not always available in a microgrid.

Kourosh, in [14] introduced a Distribution System Error (DSE) to formulate the frequency control problem. Two control loops are proposed: the first one guarantees that the fuel cell is protected by maintaining its cell utilization within its admissible range, and the second one is for tracking the load and regulating the frequency. The DSE error is used by the secondary control loop. In this paper, the author tries to present a distributed load frequency problem with its own distribution system error. Fuel cell is used as DG here, which is an inverter based generation unit, and its output power can be controlled by adjusting the firing angle of the inverter. The secondary loop controller is designed for the fuel cell to correct the frequency deviations by tuning the inverter firing angle. In this paper a number of distributed generators are supplying a portion of native load while the remaining power is provided by the substation.

In this study a microgrid load frequency control has been developed which can significantly improve the frequency response to load fluctuations. The proposed approach is trying to divide the microgrid into virtual areas and control the frequency of the Microgrid. The control of frequency is accomplished by using the tie line error, called Virtual Area Control Error (VACE), rather than using the frequency deviation error.

In the following sections the modeling of the PV and the battery are described briefly, the problem is stated and finally, simulation results are presented and analyzed.

Microgrid System Configuration

The studied microgrid along with the power directions is shown in Figure 5-44. The main components of the system are the PV generator, the battery energy storage, the load demand, the

microgrid and the power electronics components. As it can be seen in Figure 5-44, the PV and battery are connected to the microgrid through a DC/AC inverter. Controlling the inverters in a microgrid is a key point. In this study the frequency of a microgrid has been controlled by sending appropriate control signal to the inverters.

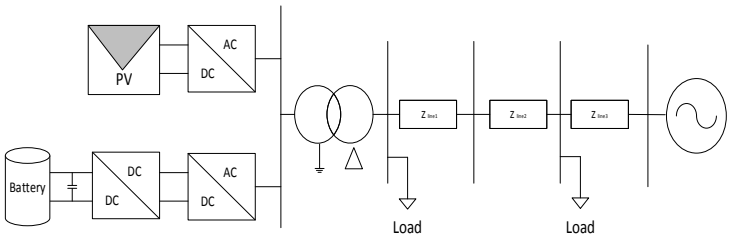

Figure 5-44: Schematic of the Studied Microgrid

Load Frequency Control Mechanism

In this section, load frequency control strategies in a microgrid are discussed. For a microgrid with single inverters, most traditional approaches use voltage-frequency (v-f) scheme in isolated operation or active power- reactive power (P-Q) control scheme in grid connected. As a result, an inverter in islanded mode should change its policy so that it can maintain the voltage and frequency in the nominal value. Two kinds of control strategies can be used for inverters of a microgrid in isolated mode operation [10]:

PQ inverter control: the inverter should produce a pre-specified value for active and reactive power. These set points for P and Q can be defined locally (using a local control loop) or centrally from the MGCC (Micro Grid Central Controller). A group of micro sources which are connected to the main grid can all be operated in PQ mode because the reference voltage and frequency is available.

Voltage source inverter (VSI) control: the VSI imitates the behavior of a synchronous machine. It is controlled to feed the load with pre-defined values for voltage and frequency. As a result, despite of PQ inverters, the real and reactive power output is defined based on the load. The equation below describes the frequency and voltage droop in a VSI inverter:

$$\omega = \omega_0 - kP \quad (3.23)$$

$$v = v_0 - kQ \quad (3.24)$$

If a cluster of VSI operates in a standalone ac system, frequency variations lead automatically to power sharing. It is important to note that in the case of a short circuit, the PQ inverters provide only a small amount of short circuit currents.

Whenever there is a disturbance or load change in the microgrid i.e., in transient situations, the PQ inverters produce their constant set point and the VSI inverters change their output power based on the frequency error. So, all the load demand is compensated with the VSI inverters (usually the inverter of storage devices acts as VSI inverters due to its fast response). This situation is not a desired condition for steady state, because storage devices are responsible for

the primary load frequency control and they have a finite storage capacity. Therefore, correcting permanent frequency deviation during islanded operation needs a secondary load frequency control. Secondary control loops change the PQ inverters set point based on frequency deviations and allocate a new value for their set point considering their rating and capability of producing power. Figure 5-45 can properly show the application of PQ and VSI inverter in a microgrid.

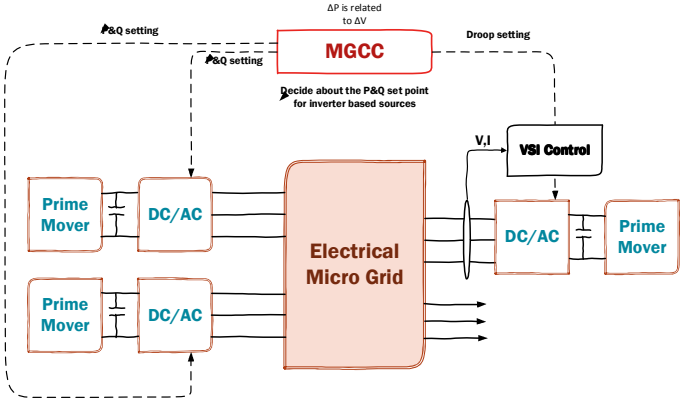

Figure 5-45: Control Scheme for SMO (Single Master Operation)

Another solution for adjusting frequency violation is using the frequency error as a common signal among DGs to balance active power generation based on their droop coefficient. It should be noted that the droop coefficient is usually determined by assuming that the load demand is shared among DGs proportional to their capacities of units. This approach is not as efficient as the previous one because in this strategy all of the DGs take part in the frequency regulation process. Due to the slow response of some of them, the transient response is poor compared to the transient response of the strategy in which only fast response devices take action in primary frequency loop control. Figure 5-46 shows the diagram related to the mentioned control loop approach.

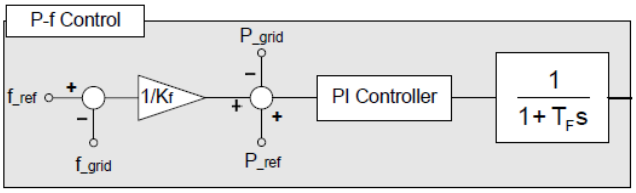

Figure 5-46: Power Controller of Inverter [15]

Novel Load Frequency Control Design

As it was mentioned previously, there are different approaches for controlling the frequency of microgrid; almost all of them consider the low voltage microgrid as one area and most of them use the frequency error as ACE. The main contribution of this paper is introducing a new approach for load frequency control. This approach suggests each of the fast response generating sources (like PV/BESS) take the responsibility of a virtual area around them and tries to support them in transient period which is caused by changing load in their own area. It is

important to note that the assigned ACE to each area may differ from other areas due to the characteristics of the power source of that area. In this research, a specific ACE is defined for PV/BESS system which can improve the load frequency control compared to the usual approaches.

Considering the configuration of the system which is used in this paper, the microgrid is divided into two areas. Figure 5-47 demonstrates the areas in this system.

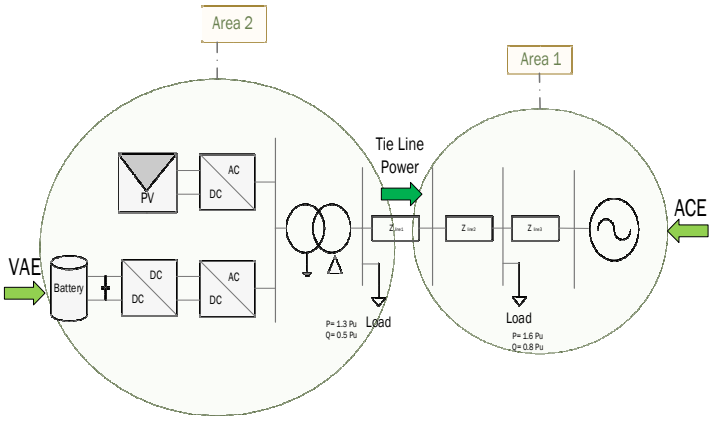

Figure 5-47: Dividing the System under Study into Two Areas

In fact in this case we have two assigned areas that each of them is supposed to take care of its own frequency, so whenever the load is changed in each area, that area does its best to control the frequency. In this case there is an imaginary tie line which tries to have a predetermined value for its power flow. The error of tie line power from the predetermined value is added as ACE to the set point of PV/BESS system. So the important term which defines our new ACE is a coefficient of tie line error, but this term alone cannot work for a long period due to the finite amount of power which battery is producing. As a result, we need another term which can bring the characteristic of battery into the defined ACE. The ACE should be multiplied by the battery's state of charge and subtracted by the minimum SOC.

This new measure to assess performance is called "Virtual Area Error" (VACE) and is introduced below:

$$VACE = (\alpha \Delta f + \Delta Ptie)\,(SOC - 20\%)^2 \qquad (3.25)$$

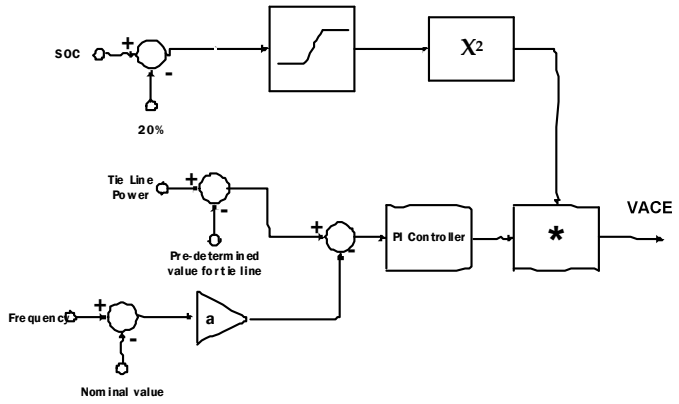

Figure 5-48: Virtual Area Error (VACE) Diagram

The term of SOC-20% helps the area (PV/BESS) to consider its own situation additional to frequency condition. The effectiveness of this approach is shown in the simulation section.

5.3.5.3 *Simulation Scenario Description*

In order to investigate the application of the above strategy, it has been tested on a detailed model of microgrid consisting of PV and battery energy storage in PSCAD environment.

Three different scenarios have been tested and the results are compared together in the next section.

First Scenario

In the first scenario, the PV/Battery is assumed to produce a 1.5 p.u. power which is constant during the simulation. It is working as a PQ inverter. In this case the synchronous generator, which is a rotating machine with inertia, is responsible for the microgrid load frequency control.

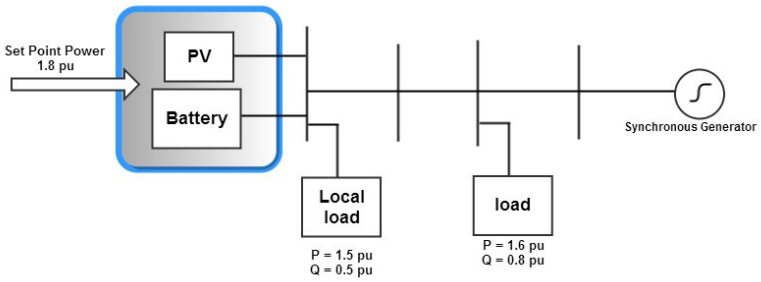

Figure 5-49: Load Frequency Control in First Scenario

Second Scenario

In the second scenario, a common ACE of a microgrid which is the frequency error compared to the reference value is also sent to the PV/Battery system so the PV/Battery helps the synchronous machine to bring the frequency back to the nominal value. The simulation results

shown in the next section show that there is an improvement in the frequency deviation compared to the first scenario. A better result is achieved through the proposed approach discussed in this report as the third scenario. The second and third cases are compared with the first one to show the improvement in frequency control.

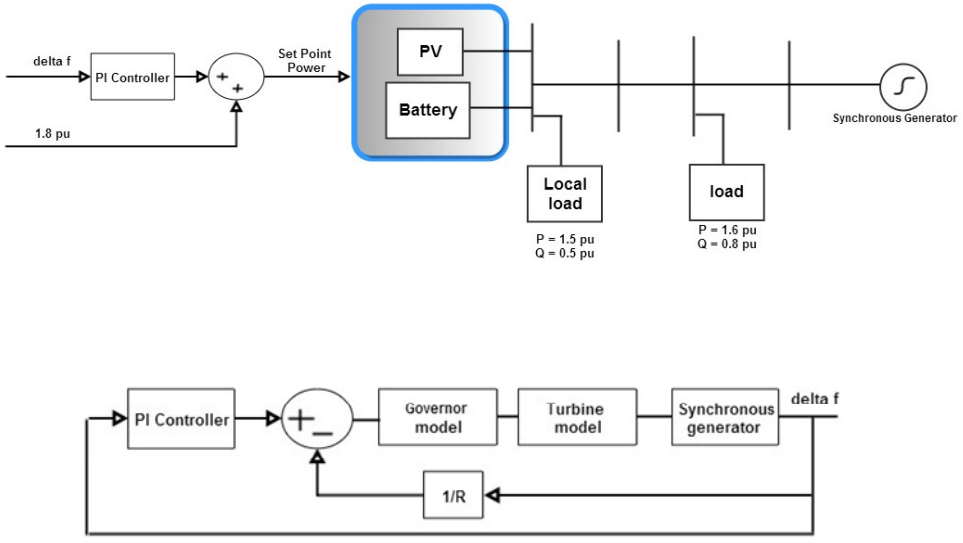

Figure 5-50: Load Frequency Control in Second Scenario

Third scenario

In third case the ACE which has been used to adjust the PV/BESS set point power, is changed from frequency deviation to VACE (which is tie line error of virtual area considering the state of charge of battery). In fact, in this case there are two assigned areas that are supposed to take care of frequency, so whenever the load is changed in each area, that area does its best to control the frequency. In this case there is an imaginary tie-line which tries to have a predetermined value for its power flow. The error of tie-line power from the predetermined value is added as ACE to the set point of PV/BESS system. Finally, the BESS is used by multiplying a term including battery's state of charge to the ACE.

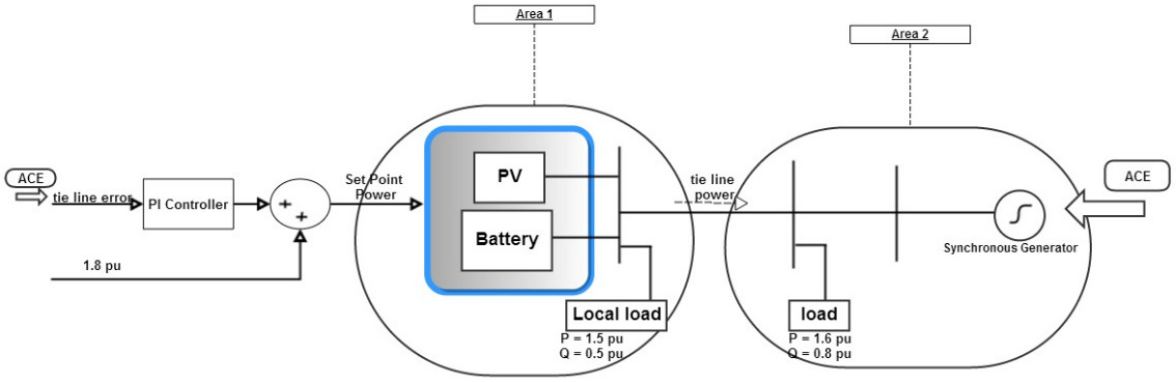

Figure 5-51: Load Frequency Control in Third Scenario

5.3.5.4 *System Configuration*

The studied micro grid along with the power directions are shown in Figure 5-52. The main components of the system are the PV generator, the batteries energy storage, the loads demand, the micro grid and the power electronics components. Power balance in the system is obtained from equation 3.26.

$$P_{net} = P_{PV} + P_{bat} + P_{load} \qquad (3.26)$$

Ppv is positive value, Pload is negative and Pbatt can be both positive and negative based on the decision.

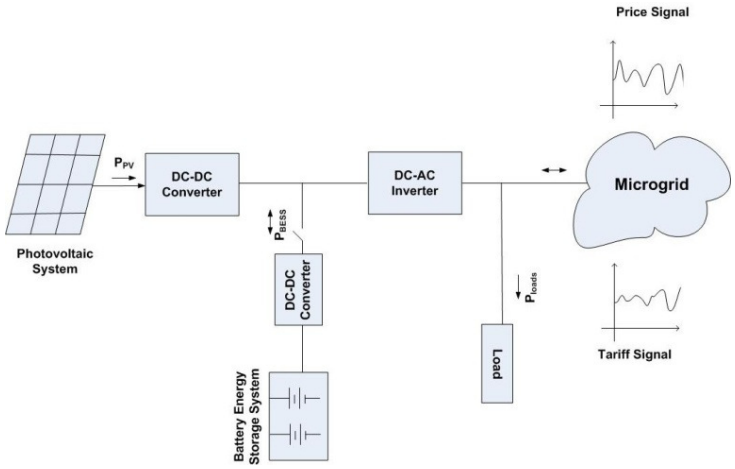

Figure 5-52: Schematic of the Studied Microgrid

In a normal operation, the PV feeds load demand. The production of the PV depends on how much solar energy is available. There is probability of not having enough PV power to supply the consumption. In case of the lack of power produced by PV, batteries or the grid will provide the remaining power. Conversely, when PV power is higher than demand, the extra generated power is injected to the battery and/or grid.

The stored energy in the battery comes from the PV and this storage can be used to supply the load. Therefore, the flows of the batteries are not going to feed the microgrid. In this hybrid system, electricity can be traded between PV and the microgrid.

The objective of the modeled microgrid is to minimize the cost of the consumer bill while supplying load demand. Based on different parameters such as availability of the PV power, price of the electricity, and profile of the local load, the consumer's electricity bill can be obtained. Having these parameters as control variables, this paper aims to find the best schedule for the operation of the batteries to minimize the total cost. In each step, it defines the condition of the batteries including charging, discharging, or resting, in order to supply the load with minimum cost.

5.3.5.5 *Decision Algorithm*

At each time two cases may happen based on the load and the PV generated power. The PV generated power can be more or less than the load power.

a. Ppv>Pload

If the PV's power was more than load, the following situations will occur:

1. The extra power which is generated by PV can be stored in the battery (the benefits of this operation appear during batteries discharge in future when the load power is higher than PV's). Equation 3.27 shows the benefit of this situation.

$$Benefit = \Delta P \times Price\ (t+\Delta t) \qquad (3.27)$$

2. The extra power can be injected to the grid and the benefit is as follows: (In this case the battery would rest.)

$$Benefit = \Delta P \times Tariff\ (t) \qquad (3.28)$$

3. The third situation occurs if the battery does not have enough space for storing extra power so the remaining power would be injected to the grid.

In situations where the PV is generating more than Load, the different choices should be compared and the one with more benefit chosen.

Based on equations 3.29 and 3.30, if the price of power in any time in future is higher than the current tariff the economic solution is to save the power in battery for further use.

$$\Delta P \times Price(t+\Delta t) > \Delta P \times Tariff(t) \qquad (3.29)$$

$$Price\ (t+\Delta t) > Tariff(t) \qquad (3.30)$$

b. Ppv<Pload

If the power of PV was less than load power, which means the generated power by PV is not sufficient for load so we will face these situations for the system:

1. The total lack of power can be obtained from the microgrid. (This case happens when the microgrid power price is low). The cost of this choice is explained in equation 3.31.

$$Cost = \Delta P \times Price(t) \quad (3.31)$$

2. The total lack of power can be supplied by the battery (in this case the battery needs to have enough charge for supplying the load). Equation 3.32 shows the cost of this choice.

$$Cost = \Delta P \times Price(t + \Delta t) \quad (3.32)$$

3. The total lack is obtained from both the microgrid and the battery. (When based on calculations, it is decided that extra power is needed from the battery, but the battery is not charged enough to support the load alone by itself.)

4. In addition to load, the battery may also be charged by the grid. (This happens due to the low price of power in the microgrid so the battery is charged with low price for further use.)

The cost for the consumer is shown in equation 3.33. In this case, the consumer is responsible for paying the price for both battery charging and the load supplying.

$$Cost = (\Delta P + Pbatt) \times Price(t + \Delta t) \quad (3.33)$$

To make a decision where the PV is generating less than Load, the cost of different choices should be compared and the one with less is chosen. Based on equation 3.34, if the price of power any time in the future is higher than the current price, the economic solution is to save the power in the battery for further use. If the price of power in the future is the same as the present price, the battery will not be charged to avoid battery fatigue.

$$Price(t + \Delta t) > Price(t) \quad (3.34)$$

In order to investigate the application of the above algorithm, a detailed model of microgrid consisting of PV and battery energy storage was tested in a PSCAD environment.

Two different case studies took place. In case A, the algorithm which uses the predefined price and tariff signals is applied to the system. In case B, a price change is considered and the adaptive algorithm is compared with the predefined one.

5.3.6 Simulation Results for Each Scenario

5.3.6.1 *Capacity Firming and Load Following*

Capacity Firming and Load Following in a Single Phase Microgrid System

The reference power is 6.0 kW from 0 to 0.6s and it is increased to 8.0 kW. Figure 5-53 shows the amount of irradiation of the sun, the reference power, and the actual power supplied by the microgrid into the grid. The output power extracted from the PV, the battery output power, and the voltage at the input of the inverter is shown in Figure 5-54. The state of battery charge and its voltage and current values are depicted in Figure 5-55. Figure 5-56 depicts the output voltage and current of the inverter. During 0 to 0.6 which has fixed reference power, the capacity firming is done by managing the battery to produce in a way that the output power becomes equal to the reference value and also the load following is done by changing the reference power based on load changes.

Capacity Firming and Load Following in a Three Phase Microgrid System

The schematic diagram for this case is depicted in Figure 5-52. As it can be seen in Figure 5-57, the sun irradiance is assumed to be 400 W/m^2 between 0 and 0.45 sec. This value increases linearly to 1000 W/m^2 at 0.5 sec and is kept constant at 1000 W/m^2 from 0.5 sec to 1.05 seconds. The reference value of the active power is 6.0 kW between 0 and 0.75 sec and 8.0 kW between 0.75 sec and 1.05 seconds. The total ac – load is 36.0 kW. Half of the load is to be supplied by the microgrid system between 0 and 0.75 sec and the remaining half should be supplied by the generator. The output of the microgrid system is to be increased to 24.0 kW at 0.75 sec. This implies that the power supplied by the generator is reduced to 12 kW.

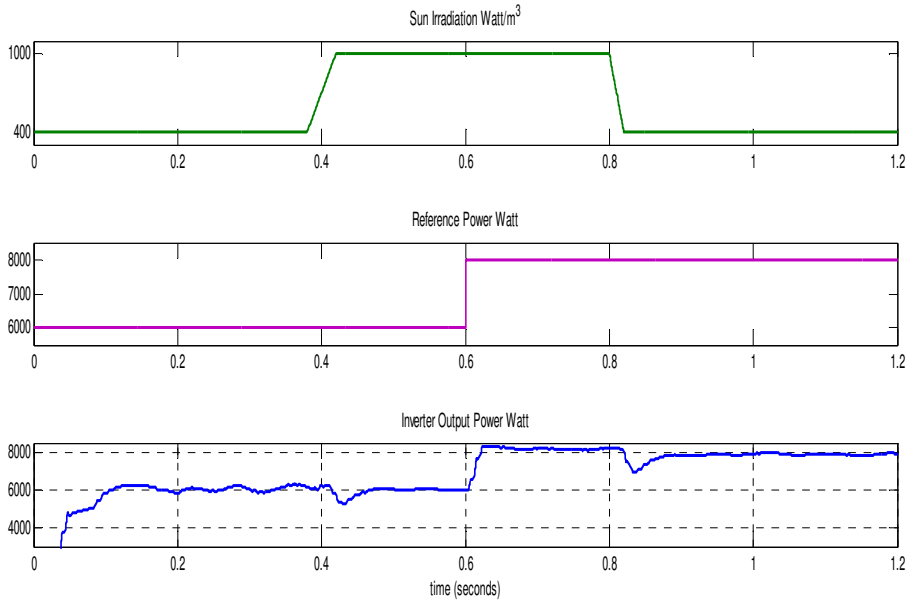

Figure 5-53: (a) Solar Irradiation, (b) Reference or Pre-specified Power, and(c) Microgrid Actual Power for Single Phase Microgrid System

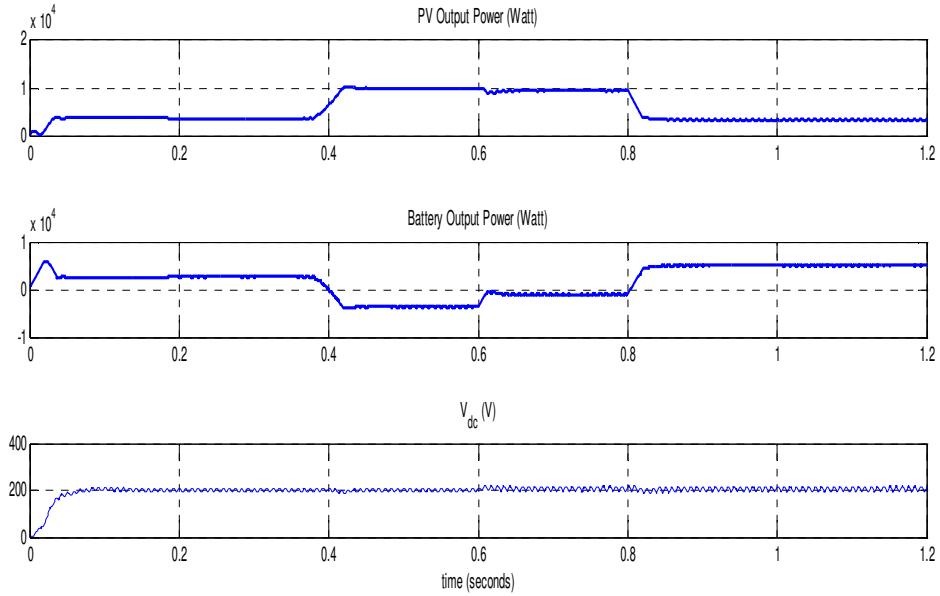

Figure 5-54: (a) PV Output Power, (b) Battery Output Power, and (c) Voltage at the Input of the Inverter for Single Phase Microgrid System

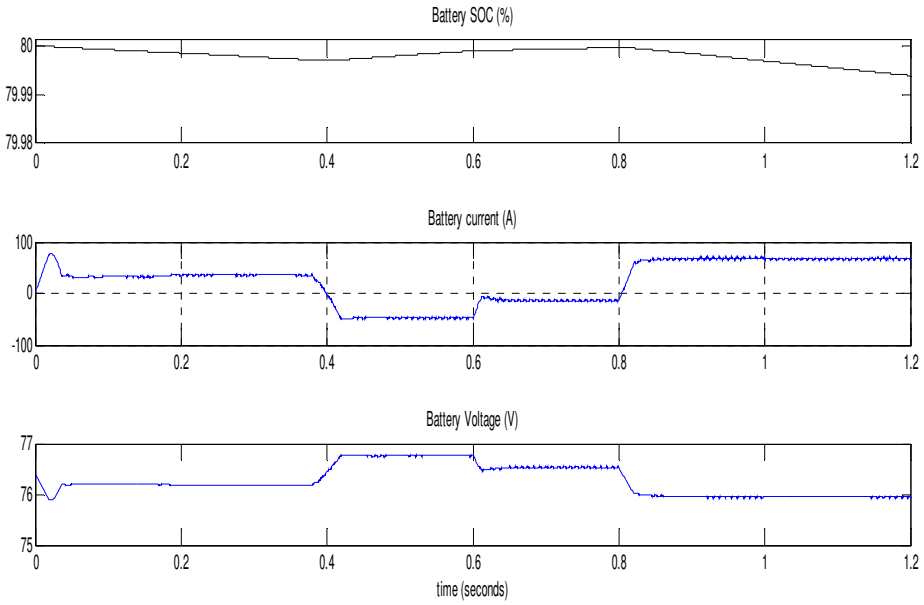

Figure 5-55: (a) Battery State of Charge (SOC), (b) Battery Current, and (c) Battery Voltage for Single Phase Microgrid System

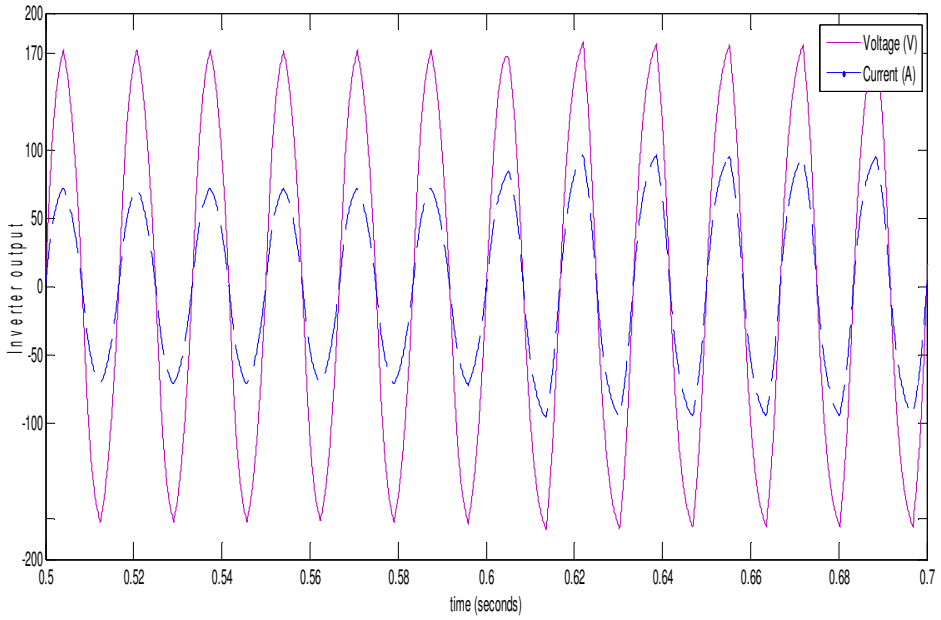

Figure 5-56: Inverter Output Voltage and Current for Single Phase Microgrid System

Figure 5-57 shows the graphs of the sun irradiance, the reference power and the power generated by the PVECS and BESS.

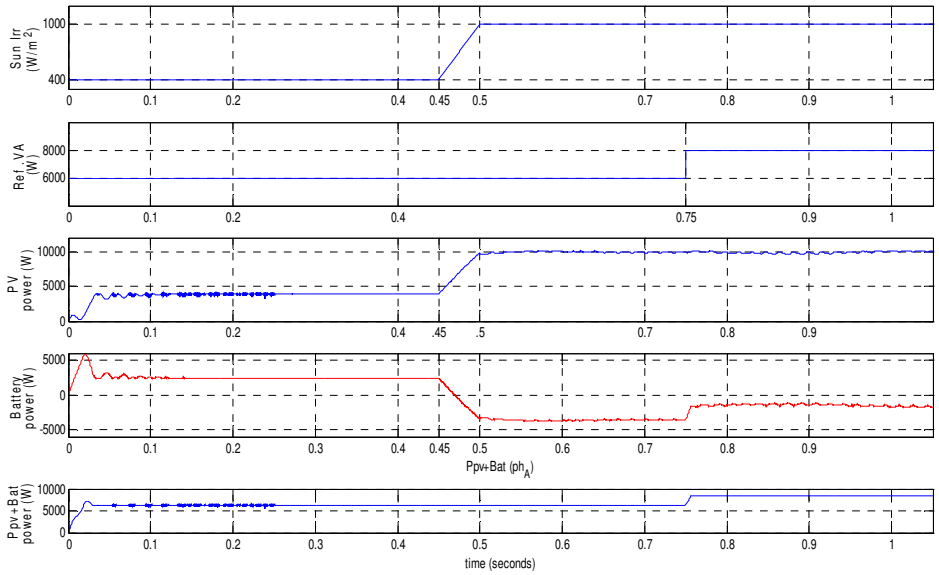

Figure 5-57: (a) Sun Irradiance, (b) Reference Power, (c) PV Generated Power, (d) Battery Power, (e) Summation of the PV Generated Power and Battery Power for Phase A of the 3-phase Microgrid System

From this Figure, we can see that the photovoltaic panel system generated about 4.0 kW between 0 and 0.45 sec. This value is less than the reference value, thus the battery has to be discharged to balance the remaining power. As the sun irradiance increases, the power generated by the PV also increases leading to a decrease in the power supplied by the battery. At the point at which the power generated by the PV equals the reference power (t=0.475 sec), the battery power is equal to 0. When the power generated by the PV panel is greater than the reference power ($t \geq 0.475\,\text{sec}$), the excess power is used to charge the battery.

The power supplied by the microgrid and the generators are depicted in Figure 5-58. The microgrid 3-phase voltage and current and the voltages at the dc buses are shown in Figure 5-59 and Figure 5-60 respectively. The SOC of each of the BESS and Total Harmonic Distortion (THD) of the microgrid's 3-phase voltage and current are shown in Figure 5-61 and Figure 5-62. The simulation results show that the designed controller performed exceptionally well for both cases considered in this report.

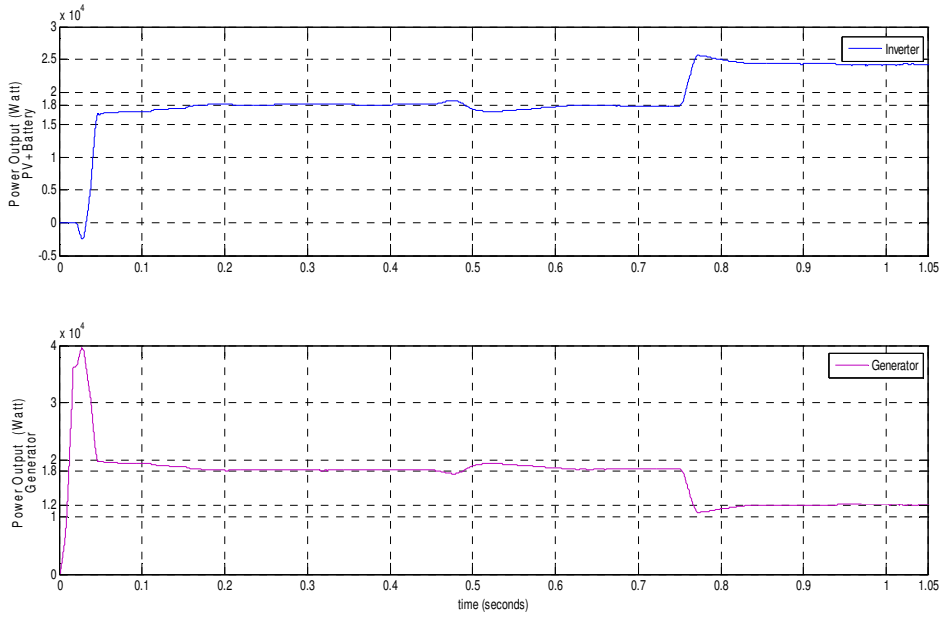

Figure 5-58: (a) Microgrid Power, (b) Generator Power

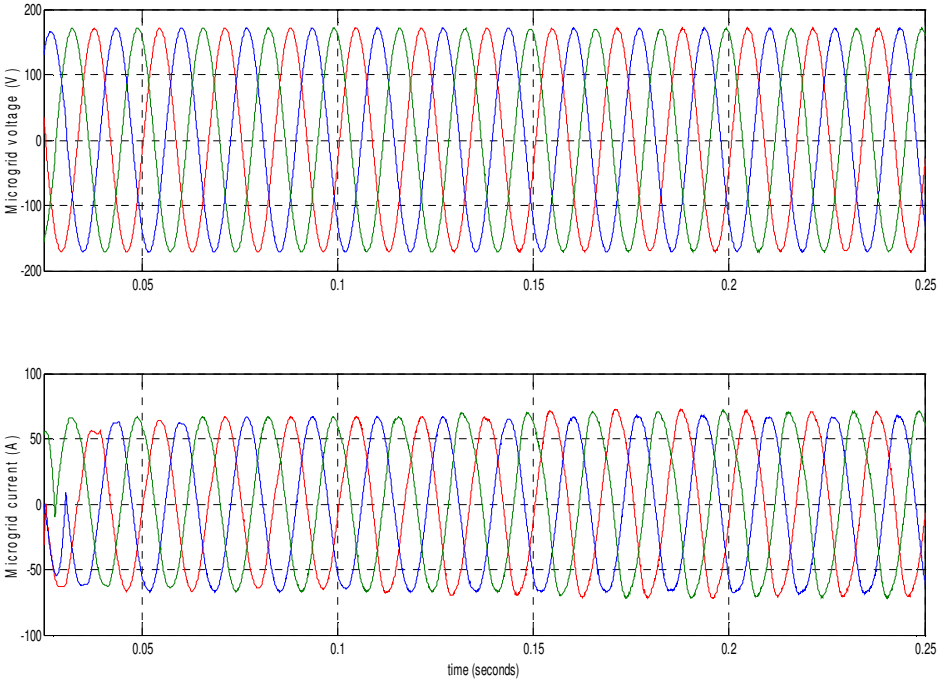

Figure 5-59: Microgrid 3-phase Voltage and Current

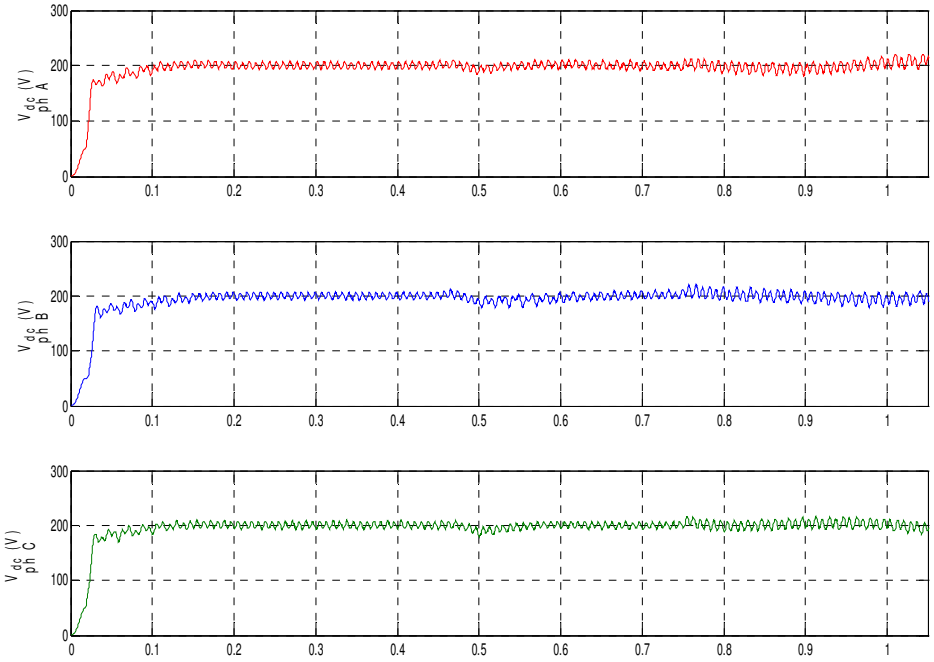

Figure 5-60: The DC Buses' Voltages

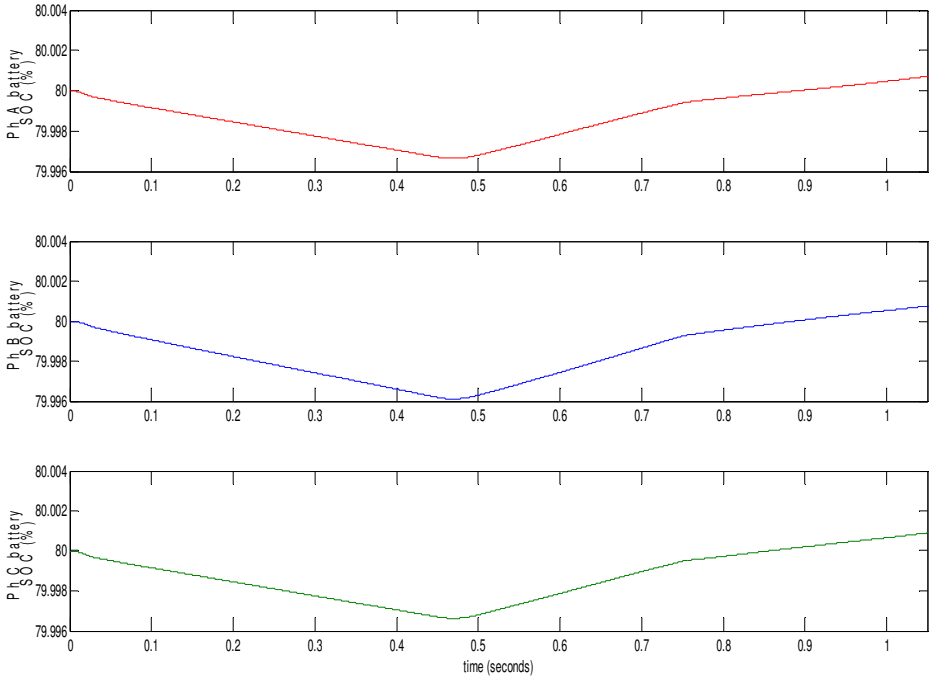

Figure 5-61: Batteries State of Charge (SOC)

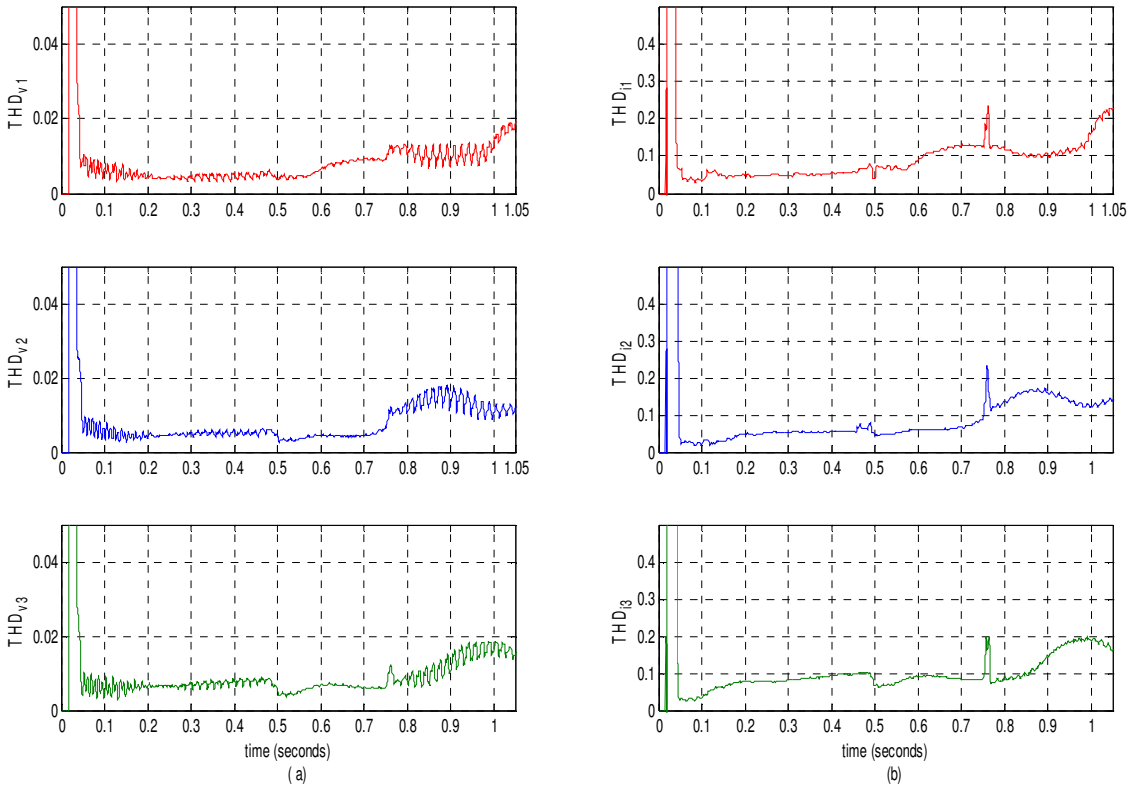

Figure 5-62: Total Harmonic Distortion of (a) Microgrid Voltage, (b) Microgrid Current

5.3.6.2 *Load Frequency Control*

The results show that this approach can have a significant improvement in controlling the frequency of the microgrid. To have better frequency control, each fast response inverter based microsource is supposed to be responsible for a group of loads near its location, forming an area which is connected to the microgrid via an imaginary tie line. So if any load in their dominant area changes, the microsources can change their set point to keep the tie line power flow constant equal to its pre-determined value. However, the characteristic of the microsource can prompt changes in the final VACE given to that microsource.

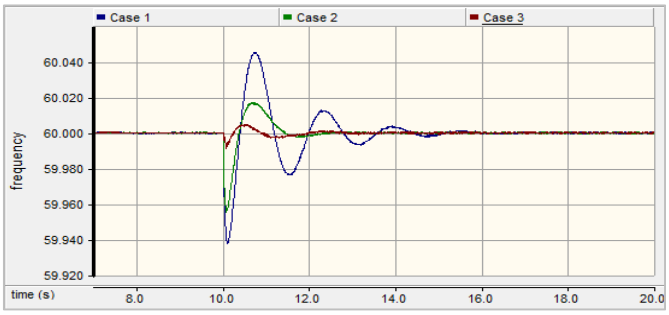

Figure 5-63: Comparing Frequency Fluctuation in Three Cases.

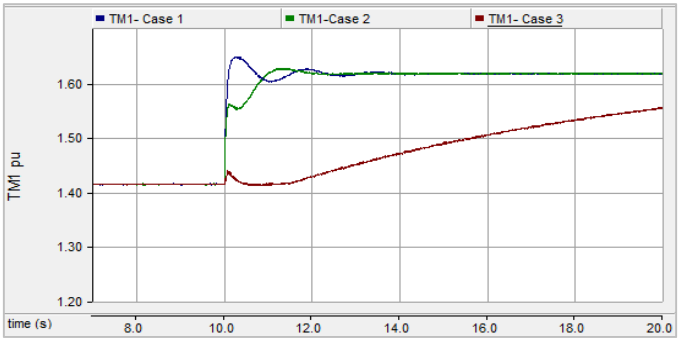

Figure 5-64: Comparing Torque of Synchronous Machine in Three Cases.

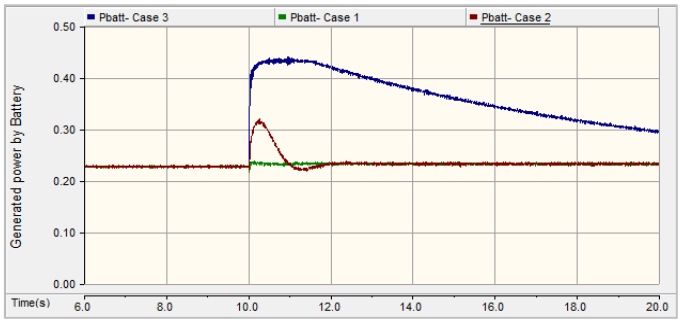

Figure 5-65: Power Generated by Battery in Three Cases.

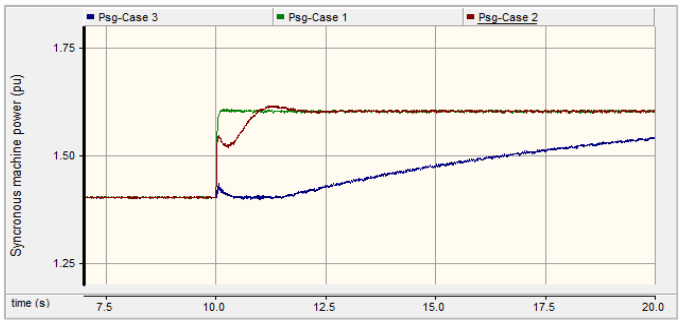

Figure 5-66: Power Generated by Synchronous Machine in Three Cases.

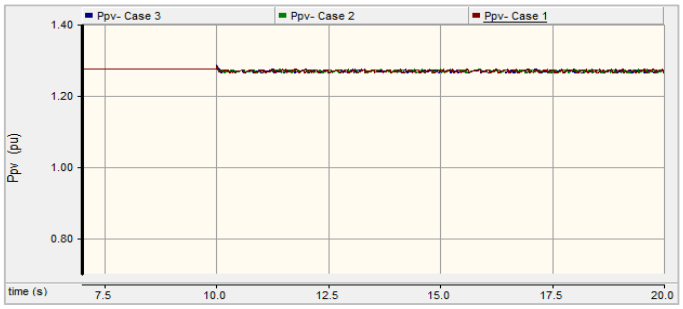

Figure 5-67: Generated Power by PV in Three Cases.

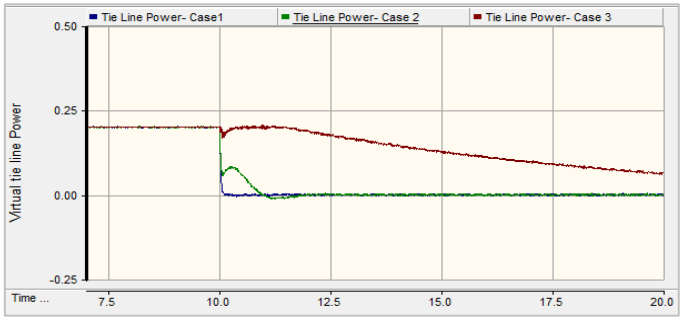

Figure 5-68: Virtual Tie Line Power in Three Cases.

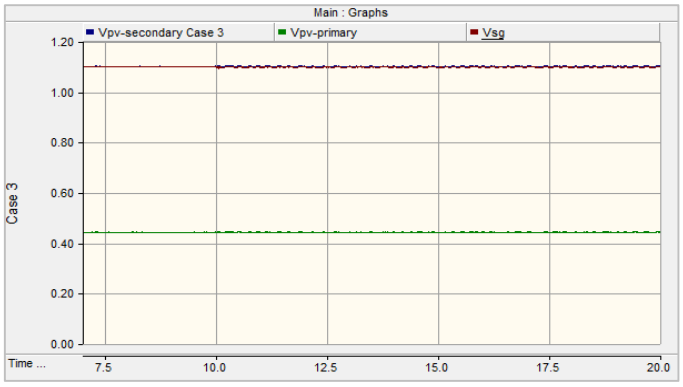

Figure 5-69: Output Voltage of Synchronous Machine and PV

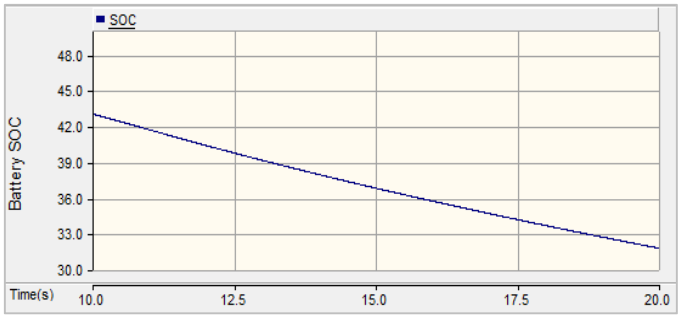

Figure 5-70: SOC of Battery in Third Case.

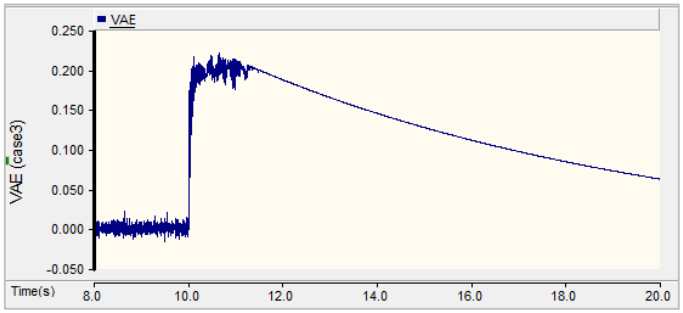

Figure 5-71: Virtual Area Error (In Third Case)

The above Figures show the results of the simulation. Figure 5-71 shows that the frequency in case-3 is much better than in the other two cases.

5.3.7 Microgrid Modeling Conclusions

A hybrid microgrid consisting of a photovoltaic energy source, battery energy storage and a synchronous generator along with demand load has been studied in this report. The modeling has been carried out in PSCAD and Matlab simulator using Mon Power circuit data.

System configuration and designed approach for Load Following and Load Frequency Control (LFC) have been explained in different sections. There are different approaches for controlling the frequency of the microgrid. Most approaches consider the low voltage microgrid as a one area and most use the frequency error as ACE. In this study, a new approach for LFC in microgrid is designed and the low voltage microgrid is considered as a two area network. In fact, the power of a virtual tie line is used with the term of ACE to improve the frequency fluctuation due to load change. Additionally, the characteristic of the generating unit have been considered by using the SOC of battery in VACE signal. There are different case studies analyzed in the Simulation Results section. The results show a good improvement in frequency deviation. This strategy can significantly improve the frequency regulation of the microgrid.

5.3.8 Lessons Learned from Microgrid Simulations

For simulation purposes, both MATLAB and PSCAD are useful tools, but PSCAD has a better library for power device models. The average model of the power electronics components is adequate for the studies that are performed. The integration of the PV/Battery system in the microgrid could provide some capacity firming and load following with appropriate control schemes. The control design that was designed and proposed could enable integration.

5.4 Modeling and Simulation for FLIR/FLA/FPA

5.4.1 Model for FLIR/FLA/FPA System Steady State Analysis Using CYME

All FLIR circuit models were developed using the circuit GIS maps provided by Mon Power. The models were developed using CYMDIST module of CYME software. Following are circuits that have been modeled in CYME.

- West Run Circuit#3 - Stewart Street
- West Run Circuit#4 – Pine View
- Pierpont Circuit#5 – Easton
- West Run Circuit#5 – Van Voorhis
- Pierpont Circuit#6 – Mile Ground
- West Run Circuit#7 – University Ave
- West Run Circuit#8 – Mon Hospital

The above circuits modeled in a detailed fashion to include components such as LTC (Load Tap Changer) transformers, reclosers, automated switches, parallel spacer cables, capacitor banks, and spot loads. Figure 5-72 below shows the CYME model of FLIR circuits.

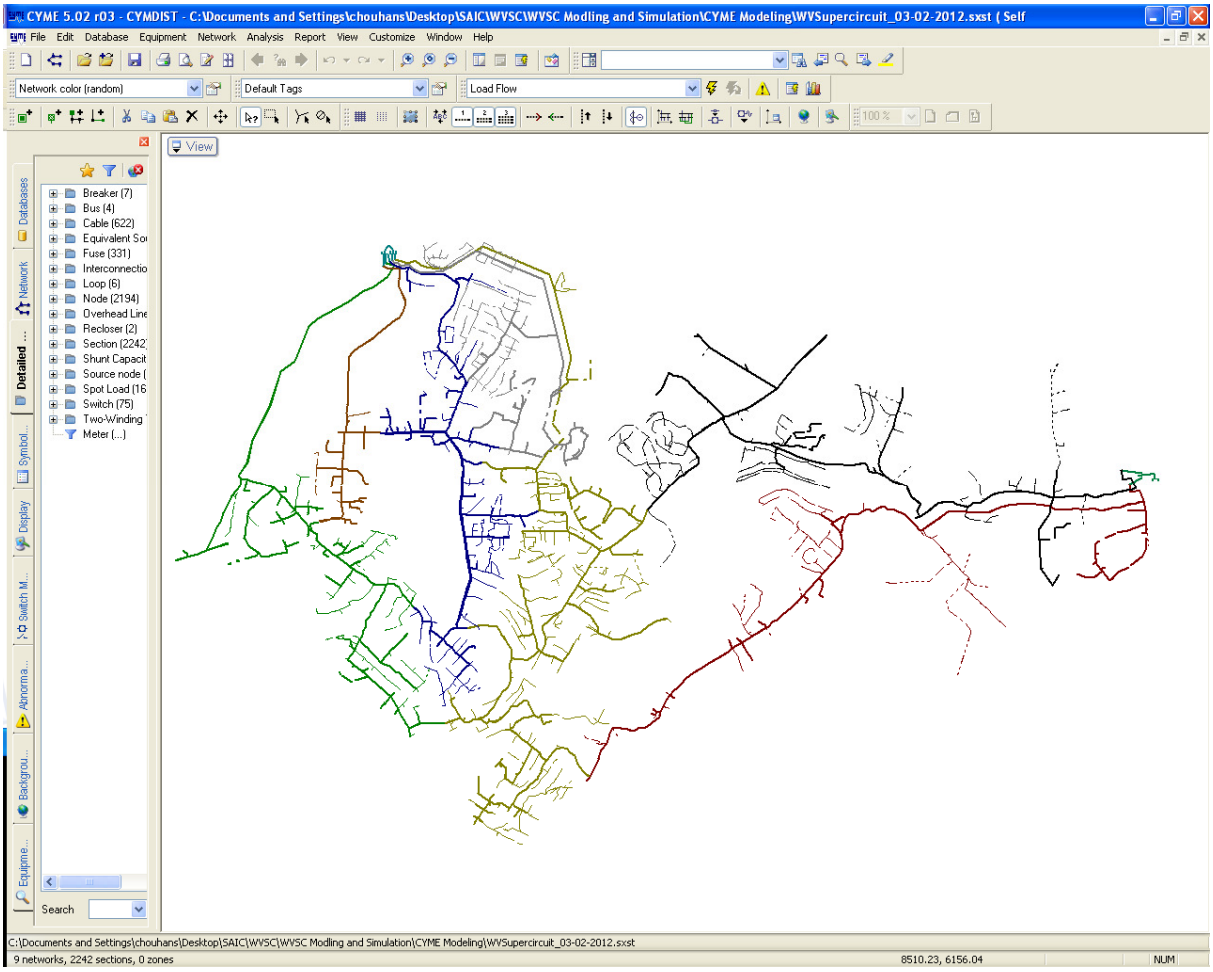

Figure 5-72: WVSC Circuit Models in CYMDist

DEW and CYME model comparison

In order to verify the accuracy of CYMDist circuit models, they were compared to existing DEW models. Load flow analysis was performed on each circuit using both software programs. The results were found to be very similar when a comparison was made, therefore no modification was needed.

5.4.2 FLIR/FLA/FPA Test System Modeling & Simulation using OpenDSS

Prior to performing the modeling & simulation on the WVSC, APERC performed a test model and simulation. An IEEE 37 Bus Test Feeder model was selected that represents an actual underground radial distribution feeder in California operating at 4.8kV under heavy phase imbalances. It is configured as a three-wire delta system and therefore it has only delta connected loads but no wye connected loads. It does, however, have many different line-to-line loads that contribute to unbalanced conditions. All conductors in the 37-Node model are assumed to be of the three-wire, delta configuration. In addition, they are buried underground with a Spacing ID of 515, corresponding to configuration in the following Figure 5-73:

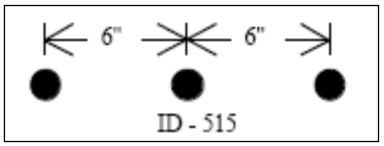

Figure 5-73: Cable Spacing

The microgrid simulation was implemented in OpenDSS software. To achieve the microgrid, the standard IEEE 37 bus system was modified by adding distribution generation units at various nodes in the circuit. The various nodes where distributed generation added are 724,718,742,729,731,736 and 741.The distribution generation unit considered here is solar. The default PV model of the solar generation available in OpenDSS has been used in the simulation. The capacity of these distributed generation units depends on the penetration level considered in the microgrid. The penetration levels considered are 25%, 50%, 75% and 100%.

In order to implement the Multi agent system, the Modified IEEE 37 bus system has been divided into three zones such that the distributed generation units in that zone can supply a part of or the full load in that zone. The Zone1 considered has 15 distribution lines (L1-L15), 9 loads demanding 779 KW and 344 KVar, and 3 solar distribution generation units connected at nodes 718,724,742. Zone 2 has 10 distribution lines (L16-L25), 8 loads demanding 549 KW and 267 KVar, and 2 distribution generation units of solar at 729,731. Zone 3 has 9 distribution lines (L26-L34), 7 loads demanding 567 KW and 275 KVar, and 2 distribution generation units at 736,741. The modified IEEE 37 bus system is shown in Figure 5-74 and Figure 5-75.

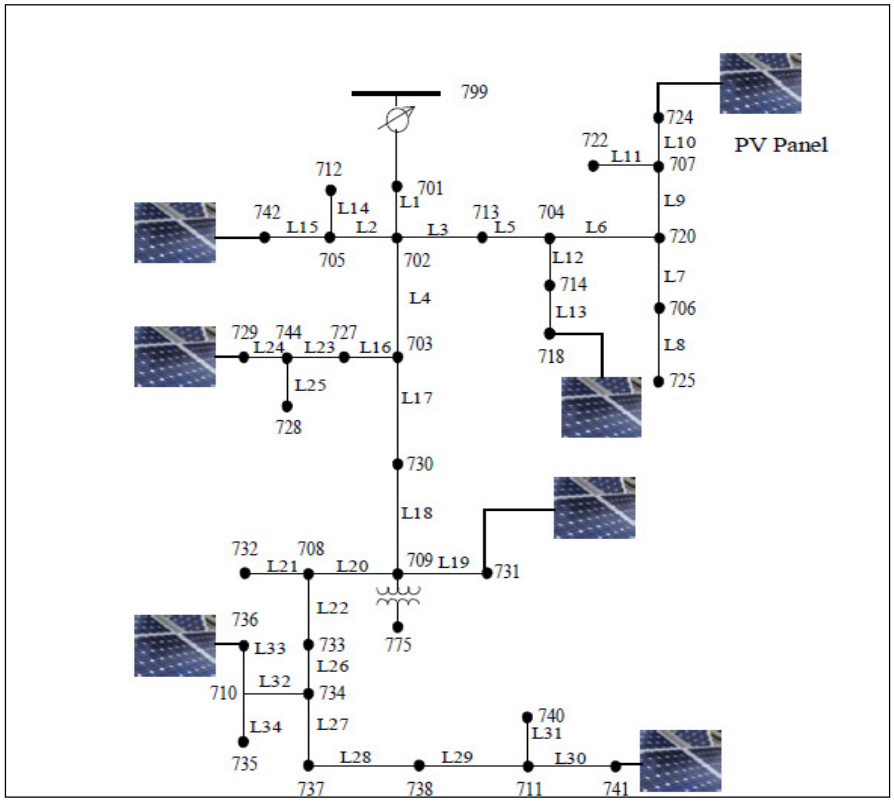

Figure 5-74: Modified IEEE Test System

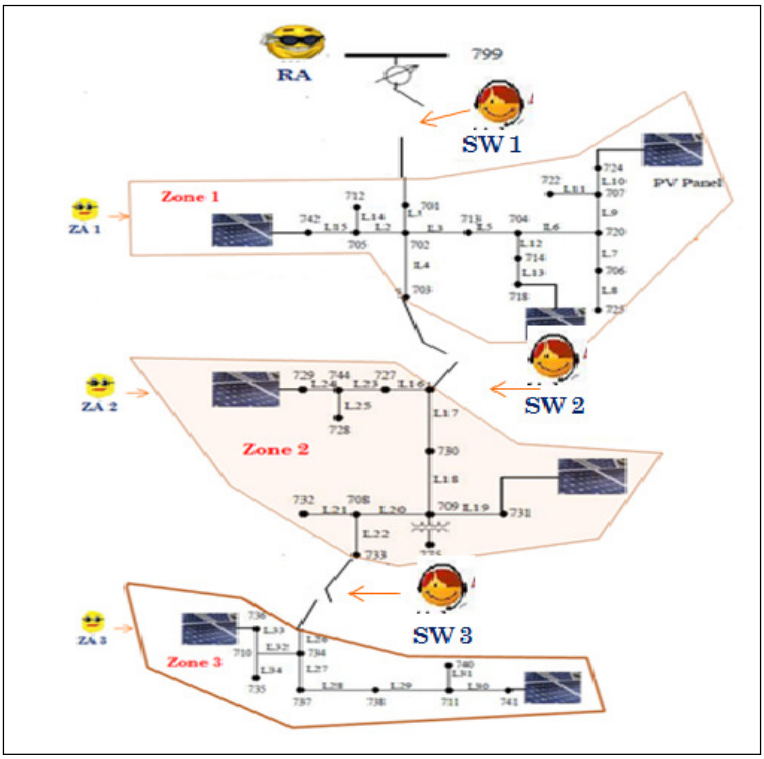

Figure 5-75: Test System with Agent

Fault Location Test Cases

The algorithm to implement the fault location is embedded in the switch agents. These switch agents only act upon receiving recloser lock out signal from its zone agent, which in turn receives the signal from the recloser agent.

The first step in the simulation process is to create the fault at a particular node in the OpenDSS software. Once the fault simulation is done, the power flow results along with values of sequence currents of all the lines along their phase angles at the instant before opening substation transformer are written to an excel file in .csv format.

In order to mimic the locking out action of the recloser action the substation transformer is opened after the fault simulation. The recloser agent, seeing no current in the substation transformer, will inform each of the zone agents about the lock out. The zone agents will in turn inform their respective switch agents in their zones which then implement the fault location based on the information exported to the .csv file.

The algorithm for fault location has been implemented for different penetration level of distributed generation like 25%, 50%, 75% and 100%. The only difference observed between these penetration levels is the change in the threshold values of the sequence current magnitudes, while the remainder of the observations discussed in the algorithm for fault location still hold true. In the following section, the various test cases for the fault location for 50% penetration level are presented.

Single Line to Ground Fault in Node 707

A single line to ground fault is simulated in OpenDSS. Following, the power flow results, along with the values of sequence currents of all the lines along their phase angles at the instant after opening the substation transformer, are written to an excel file in .csv format. The recloser agent informs all the zonal agents ZA1, ZA2 &ZA3 of its locking out action. Those agents in turn pass the message to their corresponding switch agent in their respective zone. Then, each of these agents starts reading the sequence current magnitudes of the lines in their zone. Upon reading these values, since the faulted node considered falls in Zone1, SwitchAgent1 observes that threshold for the residual current is violated by the lines L6 and L9. It then checks the L6 and L9 for any current reversal or if residual current magnitude is negligible. The current reversal is determined by looking at the phase angle of the zero sequence current (Io) for neighboring lines. It should be opposite if the fault exists at a node located between them and both the lines are fed by a DG unit. For L6 and L9, there is no reversal or negligible residual. Thus, the switch agent checks for L9 and observes a current reversal between L9 and L11 and confirms that the fault exists between the lines at the node 707. The output screen of the jade output in the command prompt is shown in the figure below, Figure 5-76:

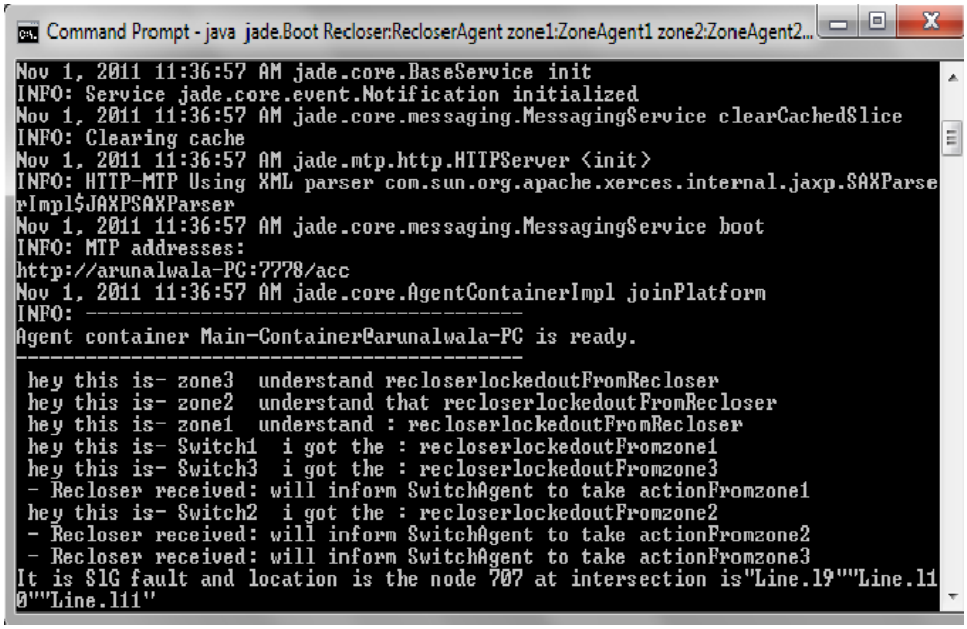

Figure 5-76: Jade Output for Fault at 707 Node

Single Line to Ground Fault in Node 706

Upon receiving the lock out signal information from their respective zone agent the switch agent starts looking for threshold limit violations in the magnitude of sequence current components in all the distribution lines in its zone. Since this is a single line to ground fault in Zone 1, SwitchAgent1 sees a violation in the residual current magnitude and the threshold limit is violated in lines L6 and L7. The agent then looks for either power reversal or negligible residual current, and does not see either for line L6.Then

upon checking the values in the line L8 that exists after L7, it observes that line L8 has negligible residual current and decides that fault exists between L7 and L8 that is in the node 706. The output screen of the jade output in the command prompt is shown in the figure below, Figure 5-77:

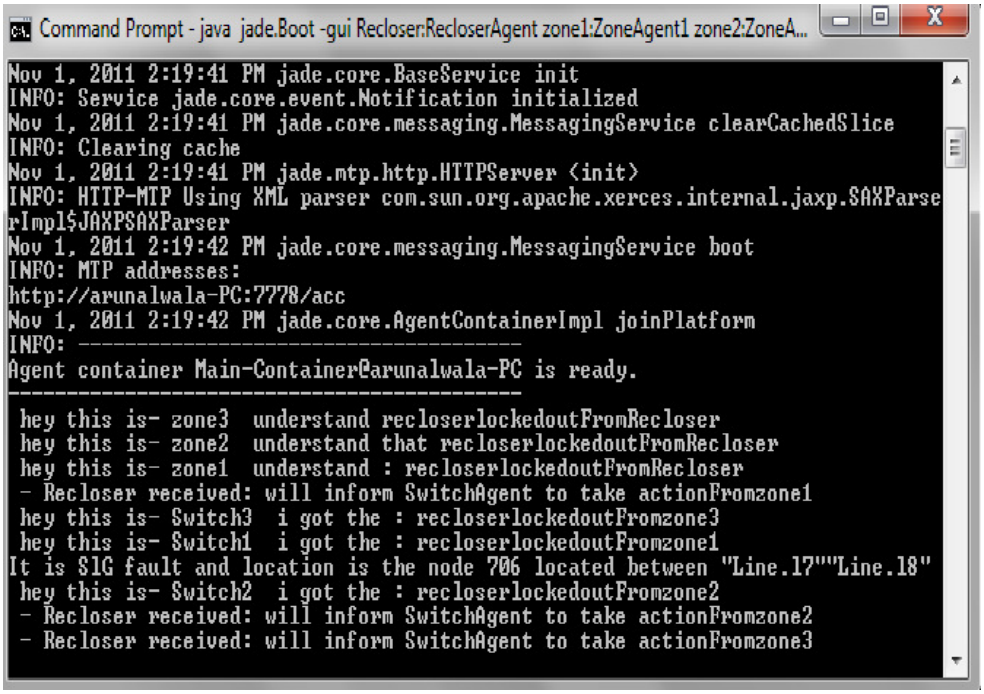

Figure 5-77: Jade Output for Fault at 706 Node

The agent message passing for fault location in zone1 is represented from sniffer agent GUI shown in Figure 5-78. Indication of the Switch Agent that is implementing the fault location is shown in it.

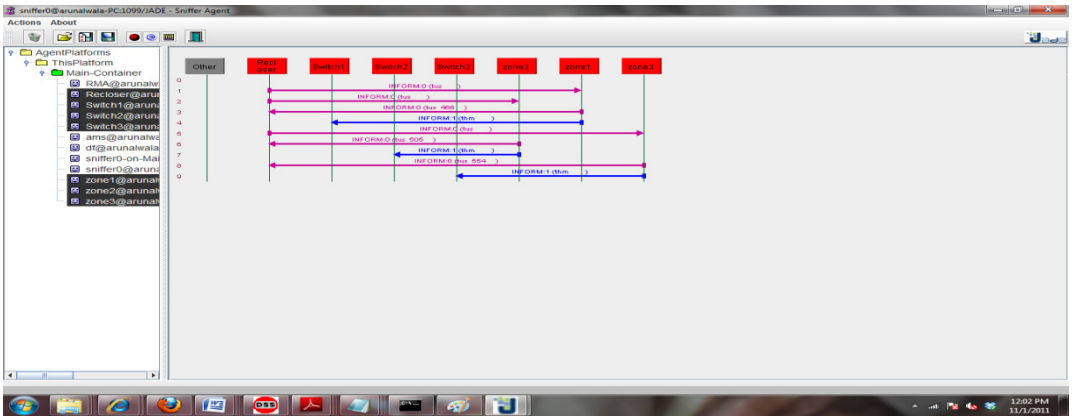

Figure 5-78: Agent Message Exchange for Fault

Three Phase to Ground Fault in Node 730

In this test case the fault simulated is zone2 and is a three phase fault. The Switch agents will find a violation in threshold of positive sequence current. The switch agents in all the zones start checking sequence current magnitudes and SwitchAgent2 notices violation in

threshold magnitude of positive sequence current of L17. It then starts checking for fault identification condition for a three fault in the neighboring lines of L17, L16 and L18 for current reversal or for negligible residual current value. The current reversal for three phase fault is determined by checking direction of real power in all three phases of the distribution line. The power flow direction is reversed in all three phases. The agent sees that the condition for currents reversal is satisfied for lines L17 and L18, and locates the fault to be between both of them. Even the phase angles of the positive sequence current of lines L17 and L18 are the opposite sign, and L16 and L17 are of the same sign. The jade output for this case is shown in Figure 5-79 below:

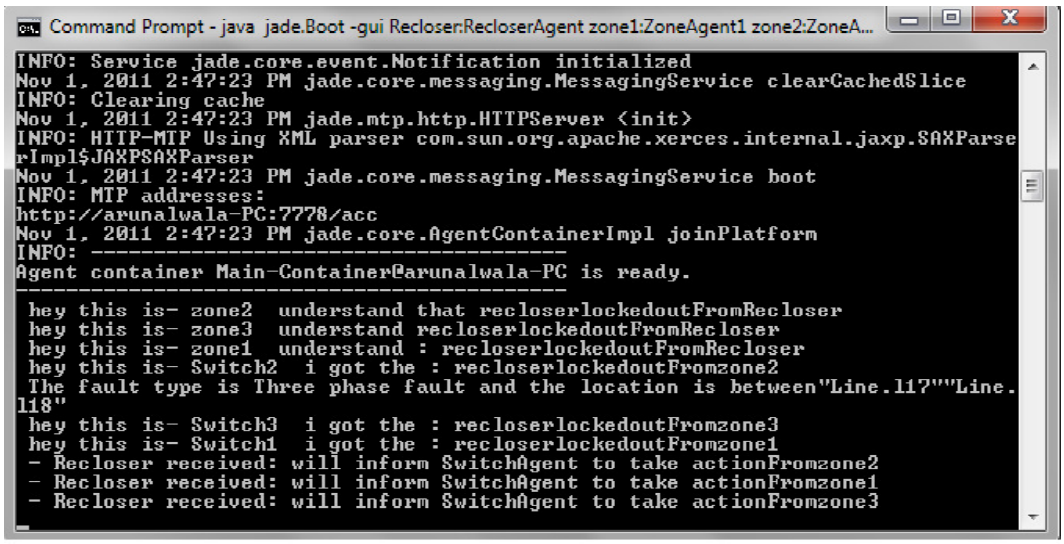

Figure 5-79: Jade Output for Fault at 730 Node

5.4.3 FLIR/FLA/FPA Simulation Using MATLAB Simpower

The simulation model has two parts. The first part is for simulating power system distribution network which is the WVSC by MATLAB Simpower Toolbox. The second part is the multi agent system which is implemented in Simulink by using user defined S-functions. In the following both parts are discussed in detail.

5.4.3.1 *Power System Model*

Three West Run feeders, WR#3, WR#4, and WR#8 which are shown in Figure 5-80 are modeled in MATLAB using Simpower Toolbox. There are 16 switches and 2 reclosers installed in these three feeders to enable the system. Switches are Cooper DAS-15 type three-phase vacuum switches with 15kV, 630 A ratings. Seven switches are normally closed and the other 9 switches are used for reconfiguration and restoration applications. Transformers in each feeder are 138/12.5 kV and 33.6 MVA. Simulation results are calculated based on per unit values. The base MVA, voltage values are 6 MVA, 12.5 kV.

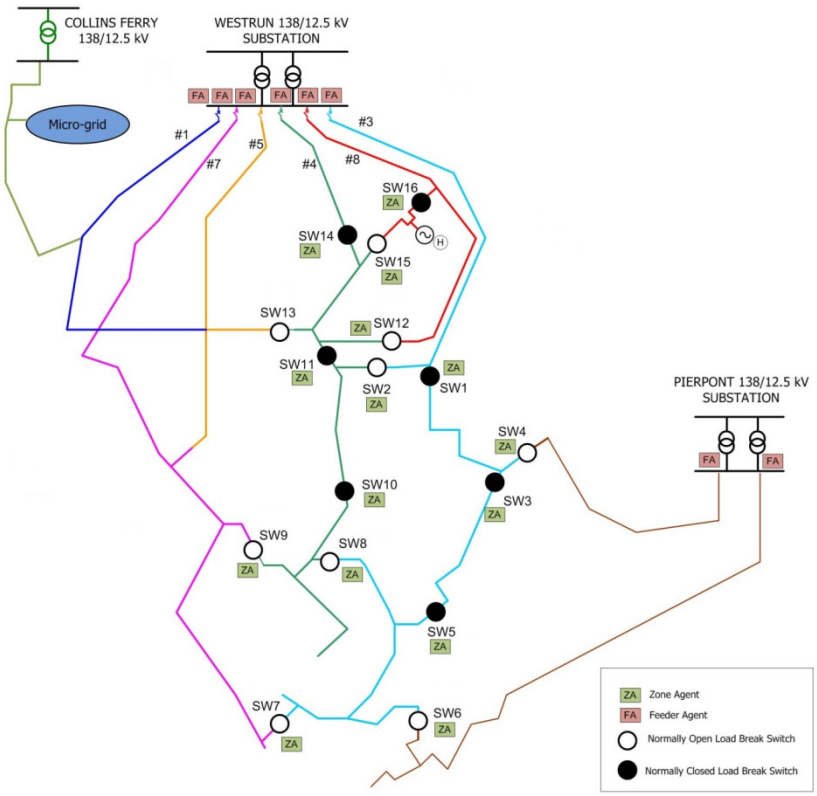

Figure 5-80: West Run Circuit Map

A block is designed to generate reclosers operation. Whenever recloser senses overcurrent, it locks out after three operations according to the time periods mentioned in Table 5-9: Recloser Setting for WR-3 AND WR-4, if the fault is not cleared.

TCC	A curve		D curve	
Current	2000A	6000A	2000A	6000A
Clearing Time	5 cycles	3 cycles	43 cycles	8 cycles

Table 5-9: Recloser Setting for WR-3 AND WR-4

Lines are modeled based on the positive, negative and zero sequence impedance values. Different types of faults such as single line to ground, line to line, and three phase faults are modeled with a fault block in Simpower Toolbox and ground resistance is considered to be 0.1 ohm. Feeder loads are modeled with active and reactive power. DGS are also modeled as a three phase source in series with R-L branch. The power system model could simulate in discrete, continuous or phasor modes. Since continuous model is more accurate, the power system is modeled using the continuous mode.

5.4.3.2 *Simulation Results*

In order to investigate the effect of DG sources on the fault location and isolation application, different penetration level of DG sources from 0 to more than 50 percent are simulated. Figure 5-81 shows the calculated I-zone for zones 1, 2 and 3 while a single line-to-ground fault is located in zone 2 and without the DG penetration. Figure 5-82 shows the results for the same scenario but with the 50% DG penetration. In this scenario DG is located in zone 2 and 4. The red line shows the faulty phase.

The I-zone index just increased in the faulty zone and in the other zones the index is decreased in both cases with or without DG generation.

Figure 5-83 shows the I-zone index for DG penetration of 50% with a line-to-line fault in zone 2. I-zone index increased in both zone 1 and 2, but change percentage in zone 2 is much larger than zone 1. Table 5-10 depicts results for other scenarios.

Table 5-10: I zone Change for Different Scenarios

Scenario		**5-** zone 1 Change Percentage	**5-** zone 2 Change Percentage	**5-** zone 3 Change Percentage
1	DG Penetration =0% Single line to ground Fault at Zone 1	90%	-65%	-65%
2	DG Penetration =50% Single line to ground Fault at Zone 1	60%	-35%	-40%
3	DG Penetration =0% Single line to ground Fault at Zone 3	-50%	-65%	150%
4	DG Penetration =50% Single line to ground Fault at Zone3	-15%	-50%	120%
5	DG Penetration =50% line to line Fault at Zone3	200%	-100%	600%

6	DG Penetration =50% Three phase to ground Fault at Zone2	400%	1400%	-100%

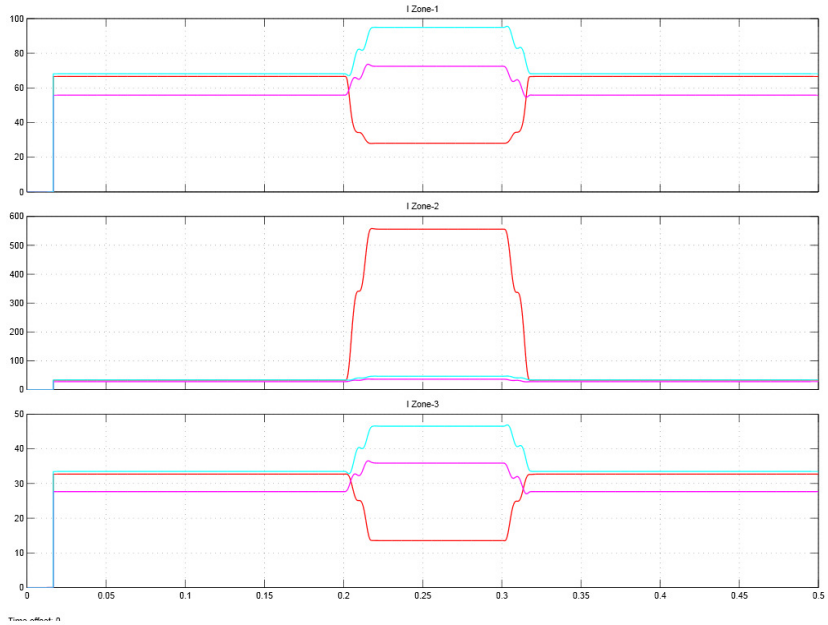

Figure 5-81:. Calculated Index for DG Penetration of 0%

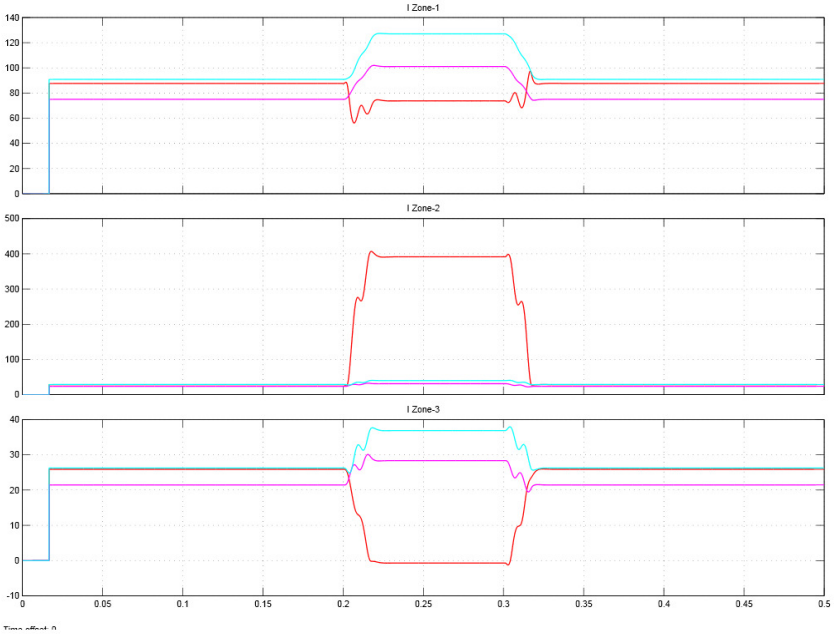

Figure 5-82: Calculated Index for DG Penetration of 50 %

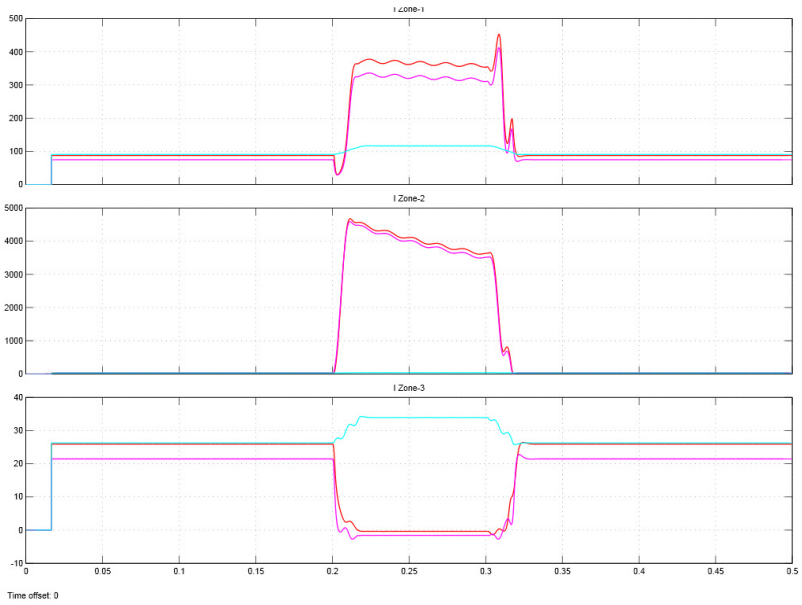

Figure 5-83: Calculated Index for DG Penetration of 50 %

5.4.3.3 *Additional FLIR Simulations: Impedance Based Fault Location Results*

Case I: Phase-to-Ground Fault between Switch 2 and 3

At time 20 seconds a single phase-to-ground fault occurs between switch 2 and 3 according to Figure 5-84: Recloser Operation, which detects the over current and then locks out. During the three recloser operations, data are communicated among the agents and the agents detect the fault type and zone, based upon the changes in current and impedance values change. Figure 5-84 shows the recloser operation after fault occurrences. Figure 5-85 and Figure 5-86 show the current and impedance change from recloser point of view.

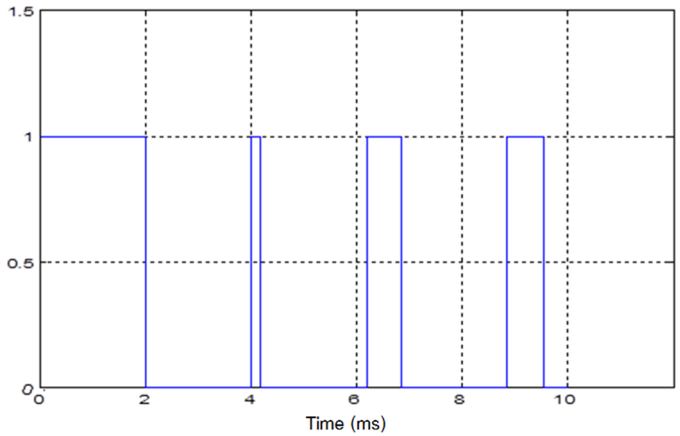

Figure 5-84: Recloser Operation

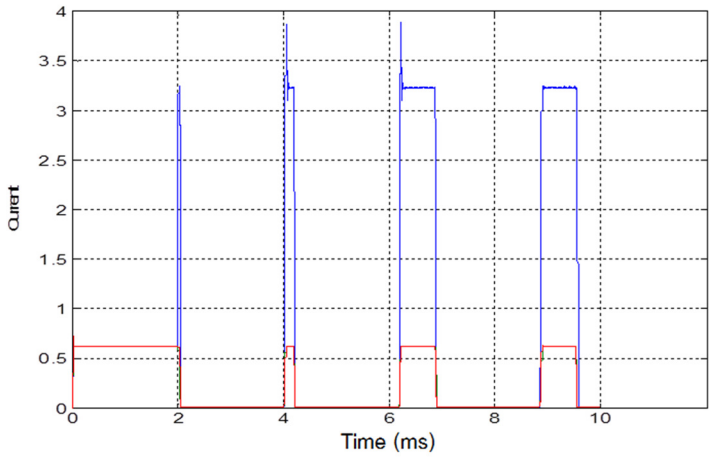

Figure 5-85: Current Changes for Switch 1 During and Before Fault (Per unit)

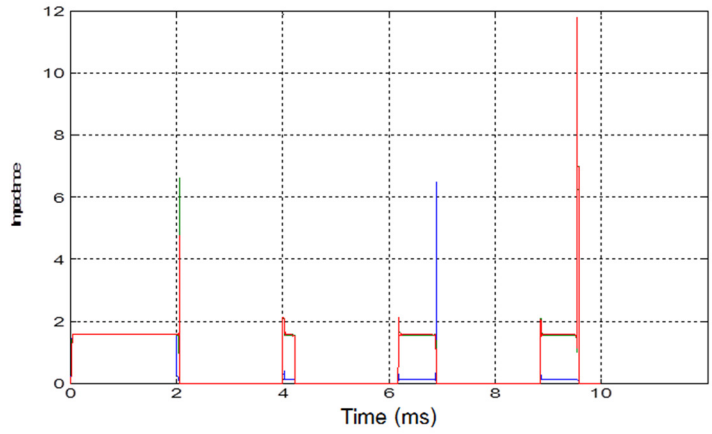

Figure 5-86: Impedance Changes for Switch 1 During and Before Fault (Per unit)

In this case, impedance values for the switches after the switch 3 in feeder WR#3 does not change after fault occurrences. This way, agents know that the faults are not downstream from switch 3. Another criterion which agents use to locate the fault is the difference between the input and output current of zone 1, where the fault occurs.

Case II: Phase-to-Phase Fault Between Switch 2 and 3

A phase A to phase B fault occurs at the 20 second time slot. Figure 5-87 and Figure 5-88 show the current and impedance changes before and after the fault and during the recloser operations. In this case, both phase A and B current increased and the impedance decreased.

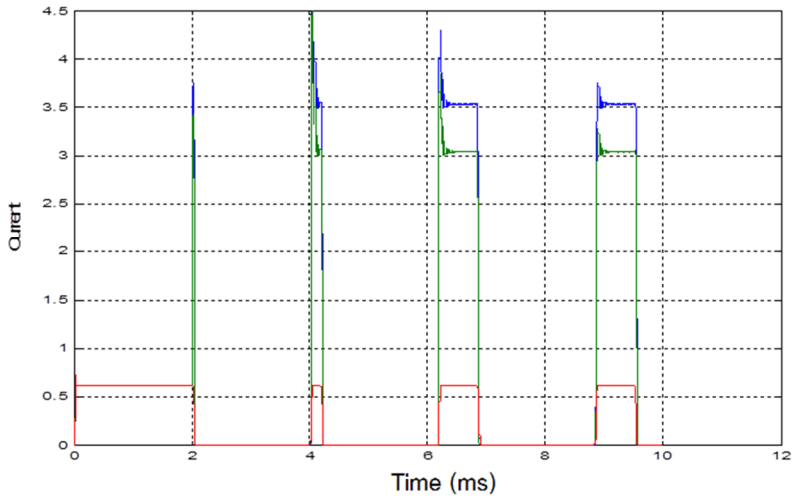

Figure 5-87: Current Changes for Switch 1 During and Before Fault (Per unit)

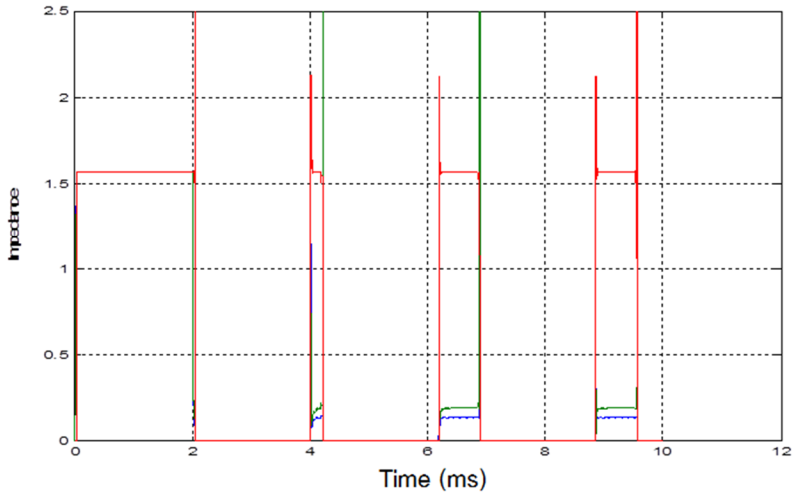

Figure 5-88: Impedance Changes for Switch 1 During and Before Fault (Per unit)

5.4.3.4 *Reconfiguration Study*

Reconfiguration study has been carried out to explore all the possible scenarios (circuit configurations) in which a healthy portion of a faulted circuit can be fed by the available adjacent feeders. Load flow analysis and fault analysis have been carried out for all of these circuit configurations to examine if there are any configurations that violate the voltage or thermal constraints of the system. Major intention of this study was to find out at least a single configuration in which a fault occurring on a feeder can be restored using the available adjacent circuit without violating any system constraints. Figure 5-89 shows the zones defined in circuit #3 - Stewart Street, circuit #4 – Pine View, and circuit #8 – Mon Hospital.

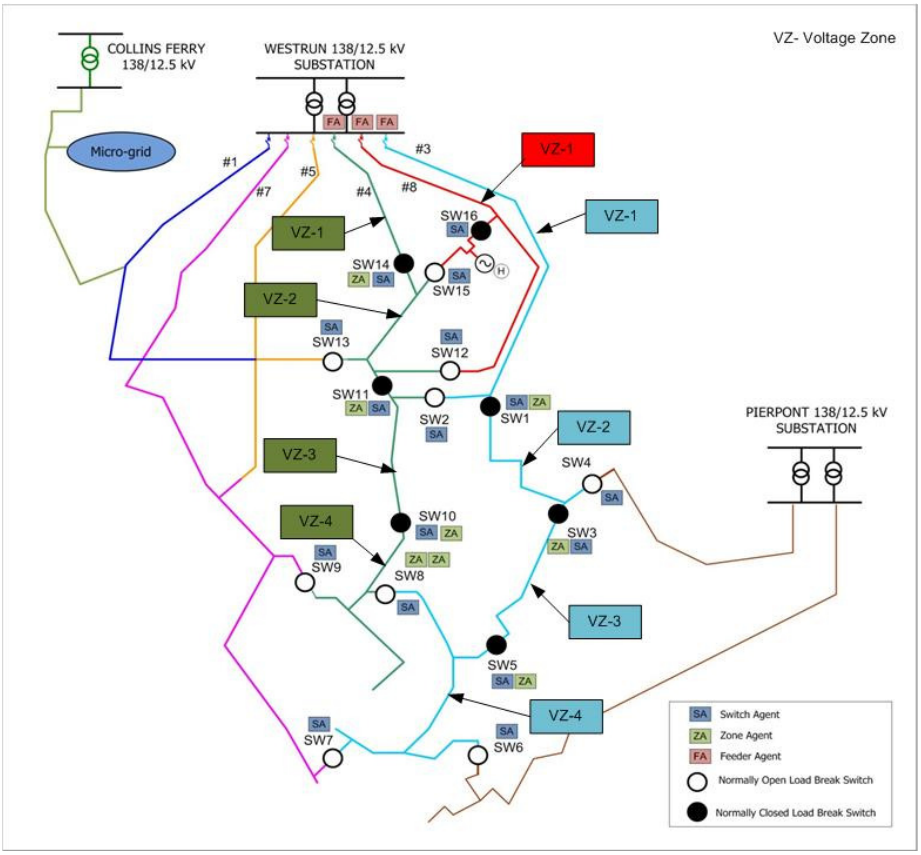

Figure 5-89: Voltage Zones of Circuits # 3, 4 and 8.

Table 5-11 below identifies the circuit configurations that do not violate the system constraints when a fault occurs in each of the voltage zones of feeders #3, 4 and 8. For example, if a fault occurs in VZ-1 of circuit #3, then transferring the healthy zones in circuit#3 to circuit # 5 (Easton) would restore the circuit with no system violations. Analysis results are presented in detail in Appendix C.

Table 5-11: Reconfiguration Study Summary

	Faulted Zone	Load Transferred To	Thermal or Voltage Violations
Circuit # 3	VZ-1	Pierpont #5 Easton	No
	VZ-2	West Run #4 Pineview	No
	VZ-3	Pierpont #6 Mileground	No
		West Run #4 Pineview	No
Circuit # 4	VZ-1	West Run #8 Mon Hospital	No
		West Run #5 Van Voorhis	No
		West Run #7 University Ave	No
	VZ-2	West Run 7 University Ave	No
	VZ-3	West Run #7 University Ave	No
Circuit # 8	VZ-1	West Run #4 Pineview	No

5.4.4 FLIR/FLA/FPA Modeling Conclusions

In order to support FLIR, FLA and FPA development, Mon Power data from WVSC project feeders were modeled in CYME distribution analysis software. This model was used by project partners to run steady state analyses and validate the algorithms. A reconfiguration study has been conducted to analyze all possible scenarios (circuit configurations). In these scenarios, thermal and voltage constraints are checked after a healthy section of a faulted circuit is fed by an adjacent feeder. The study revealed that there is at least one configuration exists for each feeder (Circuit#3, Circuit#4, and Circuit#8) in which power to the unfaulted zones can be restored without violating the system constraints.

The Multi Agent System (MAS) design for fault location and isolation is based on sequence current magnitudes and current direction. This design is tested on the IEEE-37 bus system with distributed generation added at specific locations. The test system and its fault simulations have been carried out in OpenDSS distribution simulation software. Simulation results revealed that various fault types including single-line-to-ground, line-to-line and three-phase-to-ground faults can be successfully located by the developed agent system.

Another MAS design which is based on zonal currents for fault location and isolation is tested on WVSC project feeders. In this MAS design, agents located throughout the feeder communicate with their neighbors and use local differential current information to locate the faulty zone. Agents exchange their voltage and current phasor data with their neighbors. In this design scenario, the distributed generation penetration is considered to be up to 50 percent. The multi-agent models are simulated in Matlab® Simulink using user defined s-functions and the power system is modeled using the Simulink Simpower toolbox. The simulation results show that both faulted zone and fault type can be identified successfully using the proposed agent system.

5.4.5 FLIR/FLA/FPA Simulation Lessons Learned

Fault location and isolation simulations require real-time dynamic modeling of the power system. Although, CYME is a well-established distribution analysis software for distribution planning, it lacks the dynamic simulation capability. Due to this fact, Matlab Simulink software has been used for the power system dynamic simulations. The MAS is also modeled in Matlab Simulink, and therefore, there is no need for an interface between the power system and MAS models. This provided a simpler and more accurate simulation model for investigating MAS applications in power systems.

6.0 Project Lessons Learned

The WVSC project work provided lessons learned that indicated that significant investment in infrastructure and additional research is still needed for modernizing the electric distribution system and can inform future projects and activities.

The proposed WVSC project included systems design, modeling and simulation (M&S), data collection and demonstration tasks. The design, M&S tasks were successfully completed by project partners. The project was then re-evaluated per decision gate criteria and prior to the deployment/demonstration phase. The project utilized the requirements driven VEE process methodology as described in Section 4.0 for technology development at sub-system and system levels, and significantly higher costs were identified in order to realize utility level integration results. The evaluation gave Mon Power the understanding of the significant changes that were required. Due to significantly higher costs to achieve utility level integration, the project team, with DOE review team, determined at the conclusion of the project period to proceed directly to develop a final report on the work already performed. The project design methodology, modeling and simulation results provide insights and learnings to support grid modernization.

The lessons learned fall into three categories: technology, communications, and siting as described below.

6.1 Technology Lessons Learned

6.1.1 Equipment

The maturity of smart grid devices is still developing in the industry, resulting in a limited selection of off-the-shelf devices and the use of some devices that "almost do the job."

Unanticipated installation costs were encountered. The original budget estimates provided by potential vendors proved to be much lower than the quoted prices for installation when firm bids were requested, about 50% above the quoted costs obtained from vendors and that installing the project would not be cost effective with the budget. For example, the cost of the control house designed for the microgrid equipment increased drastically. Also, costs to reconfigure Utility facilities to accommodate the project systems were higher than anticipated. Due to significantly higher costs to utility level integration, the project team, with DOE, determined at the conclusion of the project period, not to proceed and to develop a final report on the work performed.

Microgrid simulations of the control design showed that the integration of the PV/BESS systems in the microgrid can support capacity firming and load following use cases.

6.1.2 Modeling Tools

Identifying a single power system modeling software that allowed simulation of different modeling scenarios was difficult. Each tool had different strengths and weaknesses, therefore, several power system software tools were used.

Dynamic simulations could be carried out using both MATLAB and PSCAD software, but PSCAD has a better library for power device models. Also, dynamic stability analysis of the

microgrid using simplified system model in CYMSTAB produced similar results as of using full system model in MATLAB.

For simulation purposes, both MATLAB and PSCAD are useful tools, but PSCAD has a better library for power device models. The average model of the power electronics components is adequate for the studies that are performed. The integration of the PV/Battery system in the microgrid could provide some capacity firming and load following with appropriate control schemes. The control design that was designed and proposed could enable integration.

Fault location and isolation simulations require real-time dynamic modeling of the power system. Although, CYME is a well-established distribution analysis software for distribution planning, it lacks the dynamic simulation capability. Due to this fact, Matlab Simulink software has been used for the power system dynamic simulations. The MAS is also modeled in Matlab Simulink, and therefore, there is no need for an interface between the power system and MAS models. This provided a simpler and more accurate simulation model for investigating MAS applications in power systems.

6.2 Communications Lessons Learned

Effective wireless Communications is still a key consideration. This was emphasized after the study of the previous wireless system indicated that a complete replacement of the system, rather than a rehabilitation was required.

The original communications technology solution proved to be unreliable due to lack of system enhancement, interference issues, and technological flaws. The original communications system lacked redundancy, was impacted by other communication systems noise and vegetation obstructions and had technical issues with the mesh algorithm, which all impacted reliability. Based upon the above issues and the recommendations, by DOE and other standards making organizations, not to use unlicensed Wi-Fi as it is not suitable for electric utility smart grid communications backhaul systems.

6.3 Siting Lessons Learned

Finding suitable locations and willing customers for the installation of Distributed Energy Resources proved more challenging than originally anticipated. Considerations included insurance, ongoing maintenance, liability, and possible damage to existing customer facilities and general managing customer expectations.

Also, commercial customers with existing Distributed Generation provided several hurdles to the project including difficulties in interconnecting to the customers' facilities. Their equipment was not assessable, but situated within their facilities making direct connection difficult, or expensive.

Customers were hesitant to give control of their generation to an outside group. Those that were agreeable wanted at least 24 hour notice before turning on their generation. This was a result of

their requirement for internal load switching and the people needed to make appropriate changes to their systems.

Appendix A- Use Cases

User Definitions

Users are associated with each use case. The identifiers listed below represent the users for this system. A user will typically be associated with multiple use cases.

WVSC	West Virginia Super Circuit
FLIR	Fault Location Isolation and Restoration
MGMS	Multi Agent Grid Management System
PLR	Peak Load Reduction
FLA	Fault Location Algorithm
FPA	Fault Prediction Algorithm
DER	Distributed Energy Resources
SCADA	Supervisory Control and Data Acquisition System
RTU	Remote Terminal Unit
OMS	Outage Management System
HMI	Human Machine Interface
PPN	Policies, Procedures and Notifications
GUI	Graphical User Interface

A.1 Use Case #1 - Fault Location Isolation Restoration using Multi-Agent Grid Management System

The WVSC Multi-Agent Grid Management System (MGMS) for Fault Location Isolation Restoration (FLIR) is a hybrid; hierarchical-decentralized multi-agent control system to locate, isolate and restore the system after an occurrence of a fault in the system.

Narrative

There are two different scenarios in this use case.

Scenario#1: This scenario explains the sequence of steps to locate, isolate and restore the system after a fault in the system.

Scenario#2: This scenario explains the sequence of steps to bring back the system to original configuration.

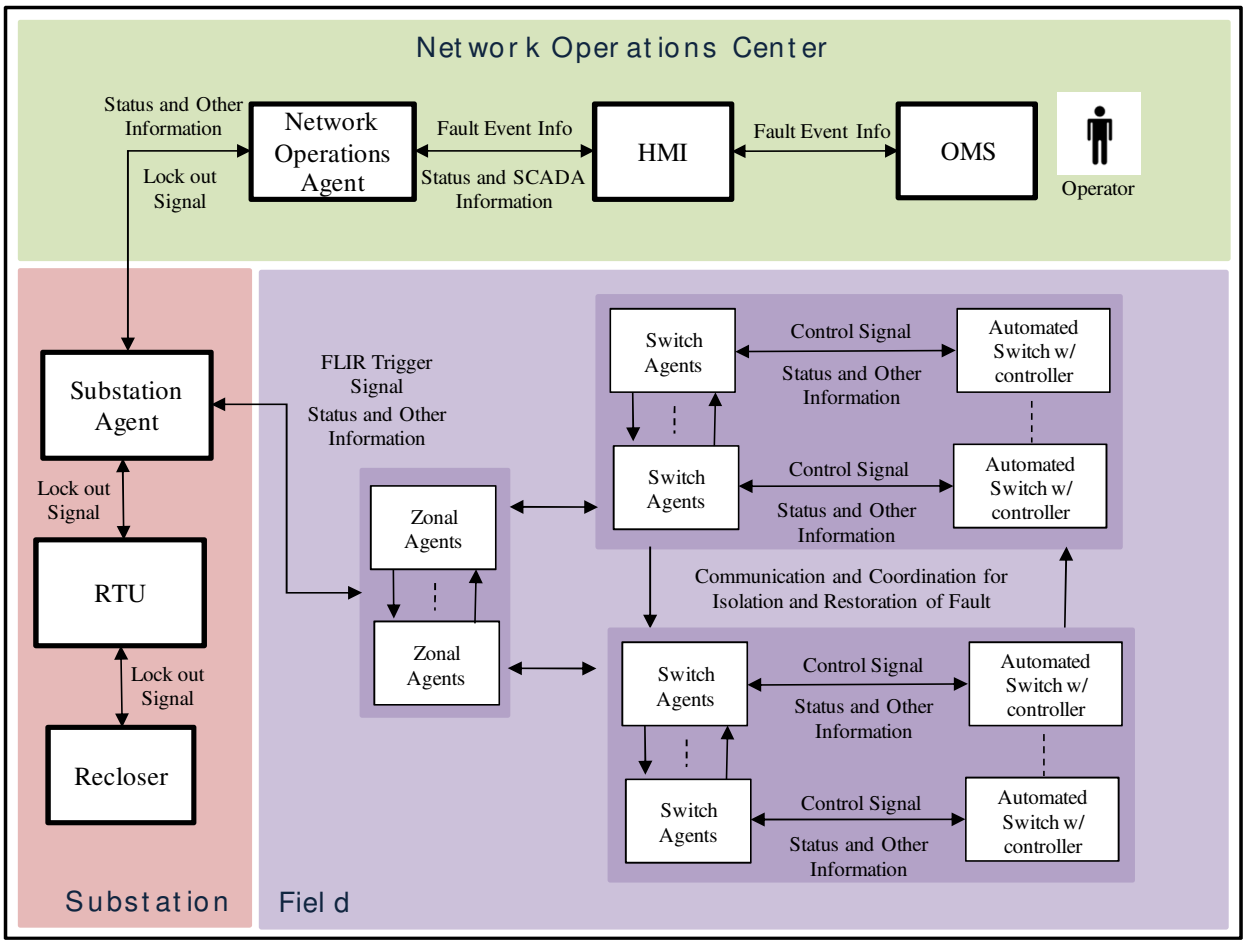

Figure A - 1: Context Diagram for MGMS FLIR Scenario #1

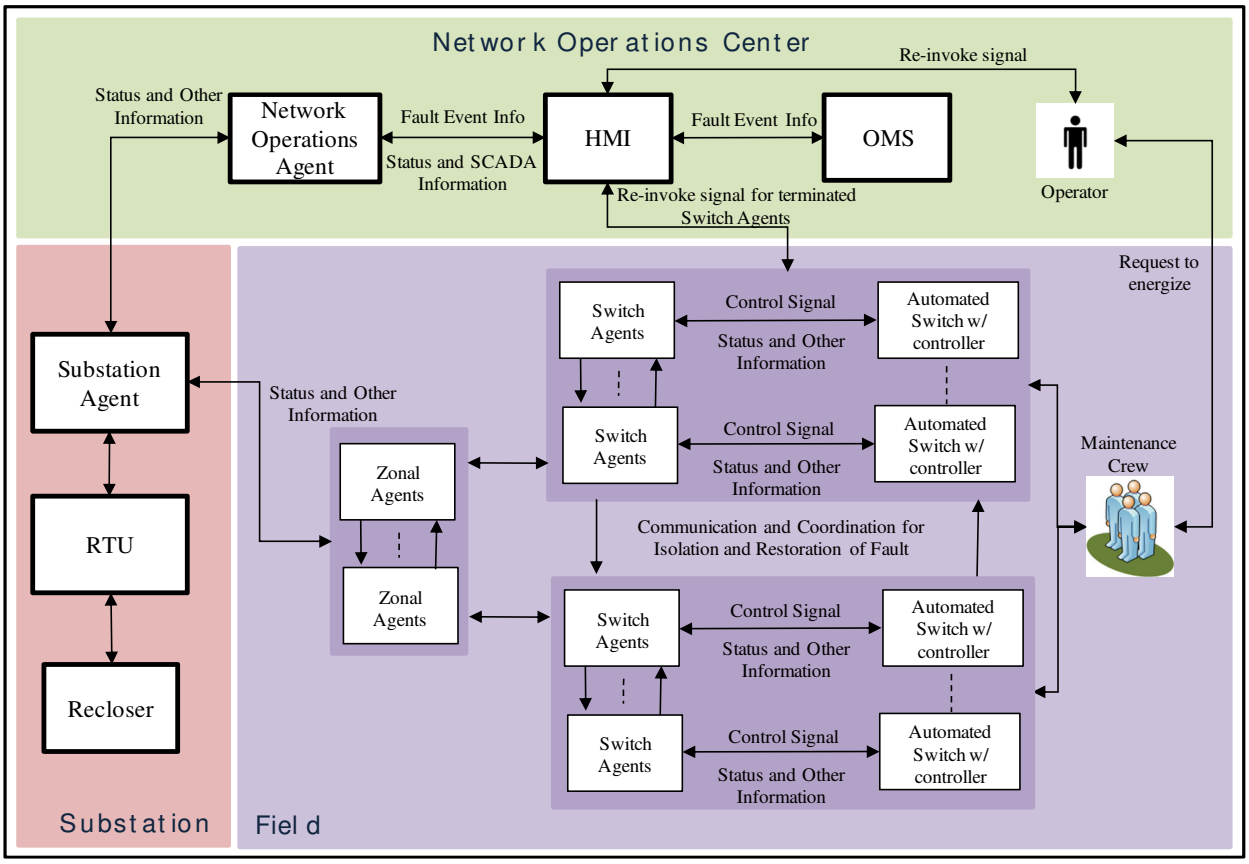

Figure

Figure A - 2: Context Diagram for MGMS FLIR Scenario #2

Actor (Stakeholder) Roles

Grouping (Community)		*Group Description*
Actor Name	*Actor Type (person, organization, device, system, or subsystem)*	*Actor Description*
Recloser	Device	This device isolates the faults to protect the system components.
Network Operations Agent	Device	This is a software agent residing at Networks operations center for monitoring the FLIR activities carried out by field agents.
Human Machine Interface	System	HMI will monitor and control the distribution system elements

Grouping (Community)		*Group Description*
Actor Name	*Actor Type (person, organization, device, system, or subsystem)*	*Actor Description*
Switch Agents	Device	This is a software agent resides at every automated switch.
Substation Agent	Device	This is a software agent resides at substation monitoring substation equipment especially the Recloser operations.
Remote Terminal Unit (RTU)	Device	This device receives and sends the SCADA information.
Automated Switches with Controller	Device	Automated Switches can be controlled by Switch Agents.
Operator	Person	Person who is responsible for distribution operations.
Zonal Agent	Device	This is a software agent resides at every predefined zone for monitoring the zone agents
OMS	System	Outage Management System keeps record of all the outages in the system
Maintenance Crew	Person	People responsible for clearing the faults in the system

Information exchanged

Describe any information exchanged in this template.

Information Object Name	*Information Object Description*
Lock-out Signal	Signal generated by Recloser when it's permanently lock-out on a fault.
FLIR Trigger Signal	Trigger signal to start the FLIR activities
SCADA and Status Information	SCADA monitoring data from Automated switches
Updated SCADA and Status Information	Updated SCADA monitoring data from Automated switches
Switching Commands	Switching Commands includes turn-on and turn-off signals to Automated switches
Acknowledgment	Communication acknowledgement confirming that the commands/messages received without any errors
Capacity Trigger Signal	Signal Indicating that there is not enough capacity to supply the unfaulted portion of the grid after reconfiguration

Information Object Name	*Information Object Description*
Confirmation Signal	Signal indicating that there is enough capacity available from adjacent feeders to restore the unfaulted circuit
Fault event Information	Fault Information
Request to energize	This is the request from maintenance crew to re-energize the faulted section of the circuit after the fault in the system is rectified.
Accept/Reject	This indicates the consent of the operator on dispatch plan.

Step by Step Analysis of Function

Steps to implement function – Name of Sequence

Automatic reconfiguration of Single Fault

Preconditions and Assumptions

Actor/System/Information/Contract	*Preconditions or Assumptions*
Switch Agents	Switch Agents should continuously monitor the automated switches and regularly update the loading and status information.
Zonal Agents	Zonal Agents should continuously monitor Switch agents in a zone and regularly update the zone loading information
Substation Agent	Substation Agents should continuously monitor Reclosers and regularly update the loading and status information.

Steps – Name of Sequence

#	Event	Primary Actor	Name of Process/Activity	Description of Process/Activity	Information Producer	Information Receiver	Name of Info Exchanged	Additional Notes	IECSA Environment
#	*Triggering event? Identify the name of the event.*[2]	*What other actors are primarily responsible for the Process/Activity? Actors are defined in section0.*	*Label that would appear in a process diagram. Use action verbs when naming activity.*	*Describe the actions that take place in active and present tense. The step should be a descriptive noun/verb phrase that portrays an outline summary of the step. "If …Then…Else" scenarios can be captured as multiple Actions or as separate steps.*	*What other actors are primarily responsible for Producing the information? Actors are defined in section0.*	*What other actors are primarily responsible for Receiving the information? Actors are defined in section0.* *(Note – May leave blank if same as Primary Actor)*	*Name of the information object. Information objects are defined in section 0*	*Elaborate architectural issues using attached spreadsheet. Use this column to elaborate details that aren't captured in the spreadsheet.*	*Reference the applicable IECSA Environment containing this data exchange. Only one environment per step.*
1	Recloser clears the fault (lock-out)	Recloser	Clear and send lock out to RTU	Recloser clears the fault and sends the lock out signal to RTU	Recloser	RTU	Lock-out Signal		
2		RTU	Send lock out signal to Substation Agent	RTU sends the lock out signal to Substation Agent	RTU	Substation Agent	Lock-out Signal		
3		Substation Agent	Send lock out to Network Operations Agent	The Substation Agent sends the lock out signal to Network Operations Agent	Substation Agent	Network Operations Agent	Lock-out Signal		
4		Substation Agent	Send FLIR trigger to Zonal Agents	The Substation Agent sends the FLIR trigger signal to the Zonal Agents	Substation Agent	Zonal Agents	FLIR Trigger Signal		
5		Zonal Agents	Send FLIR trigger to Switch Agents	Zonal Agents will communicate the trigger signal to their Switch Agents	Zonal Agents	Switch Agents	FLIR Trigger Signal		

[2] Note – A triggering event is not necessary if the completion of the prior step – leads to the transition of the following step.

#	Event	Primary Actor	Name of Process/Activity	Description of Process/Activity	Information Producer	Information Receiver	Name of Info Exchanged	Additional Notes	IECSA Environment
6		Switch Agents	Communicating and determining Isolation Plan	Switch Agents find the fault location and determine the isolation plan by utilizing fault data,	Switch Agents	Switch Agents	Fault data (Switch SCADA and Status Information)		
7		Switch Agents	Send Switching Commands to Automated Switches	Switch Agents send the isolation commands to Automated Switches	Switch Agents	Automated Switches w/ Controller	Switching Commands for Isolation		
8		Automated Switches w/ Controller	Send Acknowledgement to Switch Agents	Automated Switches acknowledge the commands.	Automated Switches w/ Controller	Switch Agents	Acknowledgment		
9		Automated Switches w/ Controller	Send updated SCADA and Status info to Switch Agents	Automated Switches perform switching activities to isolate the faulted section of the grid and send the updated status information to Switch Agents	Automated Switches w/ Controller	Switch Agents	Updated SCADA and Status Information		
10		Switch Agents	Terminate the isolated Switch Agents	The Switch Agents corresponding to open automated switches for isolation process are terminated and are sent to sleep mode.	Switch Agents	Switch Agents			

#	Event	Primary Actor	Name of Process/Activity	Description of Process/Activity	Information Producer	Information Receiver	Name of Info Exchanged	Additional Notes	IECSA Environment
11		Switch Agents	Communicating and determining reconfiguration Plan	Switch Agents calculate the reconfiguration plan	Switch Agents	Switch Agents	SCADA and Status Information		
12		Zonal Agents	Verify Capacity	Zonal Agents verify if there is enough capacity to supply the unfaulted portion of the grid. If there is enough capacity go to step **16**	Zonal Agents				
13		Zonal Agents	Send Capacity Trigger Signal	If there is not enough capacity available from adjacent feeders, Zonal Agents communicate the capacity trigger signal to the substation agent.	Zonal Agents	Substation Agent	Capacity Trigger Signal		
14		Substation Agent	Send Capacity Trigger Signal	Substation Agent communicates the capacity trigger signal to Network Operations Agent.	Substation Agent	Network Operations Agent	Capacity Trigger Signal		
15		Network Operations Agent	Send Capacity Trigger Signal	Network Operations Agent communicates the capacity trigger signal to HMI.	Network Operations Agent	HMI	Capacity Trigger Signal		

#	Event	Primary Actor	Name of Process/Activity	Description of Process/Activity	Information Producer	Information Receiver	Name of Info Exchanged	Additional Notes	IECSA Environment
16		Zonal Agents	Send confirmation signal to Switch Agents	Zonal Agent sends the confirmation signal to Switch Agents to reconfigure the circuit if there is enough capacity available from adjacent feeders.	Zonal Agents	Switch Agents	Confirmation signal		
17		Switch Agents	Send Switching Commands to Automated Switches	Switch Agents send the reconfiguration commands to Automated Switches	Switch Agents	Automated Switches w/ Controller	Switching Commands		
18		Automated Switches w/ Controller	Send Acknowledgement to Switch Agents	Automated Switches acknowledge the commands to Switch Agents	Automated Switches w/ Controller	Switch Agents	Acknowledgment		
19		Automated Switches w/ Controller	Send updated SCADA and Status info to Switch Agents	Automated Switches perform the activities to restore the unfaulted portion of the grid and send the updated status information to Switch Agents	Automated Switches w/ Controller	Switch Agents	Updated SCADA and Status Information		
20		Switch Agents	Send updated SCADA and Status info to Zonal Agents	Switch Agents send status updates and SCADA information to Zonal Agent	Switch Agents	Zonal Agents	Updated SCADA and Status Information		

#	Event	Primary Actor	Name of Process/Activity	Description of Process/Activity	Information Producer	Information Receiver	Name of Info Exchanged	Additional Notes	IECSA Environment
21		Zonal Agents	Send updated SCADA and Status info to Substation Agent	Zonal Agents send status updates and SCADA information to Substation Agent	Zonal Agents	Substation Agent	Updated SCADA and Status Information		
22		Substation Agent	Send updated SCADA and Status info to Networks Operations Agent	Substation Agent send status updates and SCADA information to Networks Operations Agent	Substation Agent	Networks Operations Agent	Updated SCADA and Status Information		
23		Networks Operations Agent	Send updated SCADA and Status info to HMI	Networks Operations Agent send status updates, SCADA and Fault Event information to HMI	Networks Operations Agent	HMI	Updated SCADA and Status Information		
24		HMI	Send Fault Event info to OMS	HMI sends the Fault Event Information to OMS	HMI	OMS	Fault Event Information		

Post-conditions and Significant Results

Actor/Activity	*Post-conditions Description and Results*
MGMS FLIR	Fault is cleared and supply to the unfaulted portion of the grid restored.

Diagram

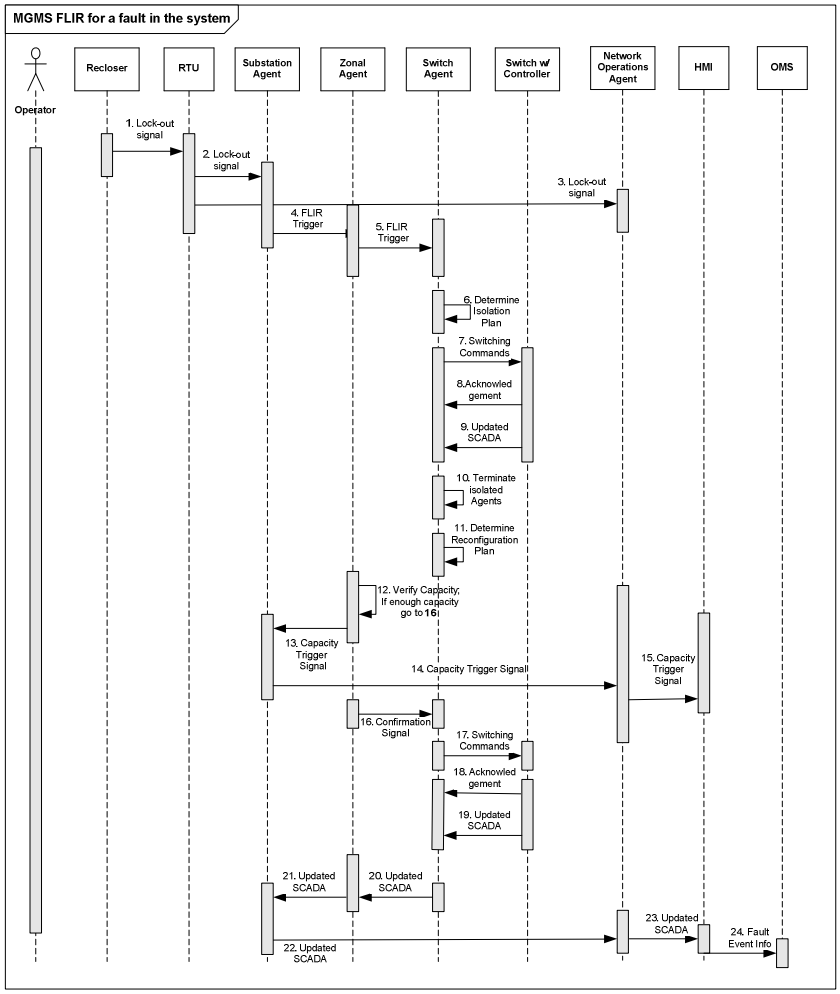

Figure A - 3: Sequence Diagram for Scenario #1

Step by Step Analysis of Function

Steps to implement function – Name of Sequence

Returning to original configuration after removing the fault form the system

Preconditions and Assumptions

Actor/System/Information/Contract	*Preconditions or Assumptions*
Switch Agents	Switch Agents should continuously monitor the automated switches and regularly update the loading and status information.
Zonal Agents	Zonal Agents should continuously monitor Switch agents in a zone and regularly update the zone loading information
Substation Agent	Substation Agents should continuously monitor Reclosers and regularly update the loading and status information.

Steps – Name of Sequence

#	Event	Primary Actor	Name of Process/Activity	Description of Process/Activity	Information Producer	Information Receiver	Name of Info Exchanged	Additional Notes	IECSA Environment
#	*Triggering event? Identify the name of the event.*[3]	*What other actors are primarily responsible for the Process/Activity? Actors are defined in section0.*	*Label that would appear in a process diagram. Use action verbs when naming activity.*	*Describe the actions that take place in active and present tense. The step should be a descriptive noun/verb phrase that portrays an outline summary of the step. "If …Then…Else" scenarios can be captured as multiple Actions or as separate steps.*	*What other actors are primarily responsible for Producing the information? Actors are defined in section0.*	*What other actors are primarily responsible for Receiving the information? Actors are defined in section0.* *(Note – May leave blank if same as Primary Actor)*	*Name of the information object. Information objects are defined in section 0*	*Elaborate architectural issues using attached spreadsheet. Use this column to elaborate details that aren't captured in the spreadsheet.*	*Reference the applicable IECSA Environment containing this data exchange. Only one environment per step.*
1	Operator dispatches the Maintenance crew	Operator	Dispatching Maintenance crew	Operator dispatches maintenance crew to repair/clear the faulted portion of the circuit	Operator	Maintenance crew			

[3] Note – A triggering event is not necessary if the completion of the prior step – leads to the transition of the following step.

#	Event	Primary Actor	Name of Process/Activity	Description of Process/Activity	Information Producer	Information Receiver	Name of Info Exchanged	Additional Notes	IECSA Environment
2		Maintenance crew	Perform fault repairing activities	Maintenance crew will perform the fault clearing activities and clear the fault	Maintenance crew				
3		Maintenance crew	Send request to re-energize	Maintenance crew will send request to re-energize the faulted portion of the circuit to Operator	Maintenance crew	Operator	Request to energize		
4		Operator	Send Re-invoke signal to HMI	Operator will re-invoke the terminated Switch Agents by sending the re-invoke signal to HMI	Operator	HMI	Re-invoke Signal		
5		HMI	Send Re-invoke signal to terminated Switch Agents	HMI sends the re-invoke signal to Switch Agents	HMI	Switch Agents	Re-invoke Signal		
6		Switch Agents	Communicating and determining switching plan	Switch Agents will communicate and coordinate among them to determine the switching plan to bring back the circuit to the original configuration.	Switch Agents	Switch Agents	SCADA and Status Information		
7		Switch Agents	Send Switching Commands to Automated Switches	Switch Agents send the switching commands to Automated Switches	Switch Agents	Automated Switches w/ Controller	Switching Commands		

#	Event	Primary Actor	Name of Process/Activity	Description of Process/Activity	Information Producer	Information Receiver	Name of Info Exchanged	Additional Notes	IECSA Environment
8		Automated Switches w/ Controller	Send Acknowledgement to Switch Agents	Automated Switches acknowledge the commands.	Automated Switches w/ Controller	Switch Agents	Acknowledgment		
9		Automated Switches w/ Controller	Send updated SCADA and Status info to Switch Agents	Automated Switches perform the activities to bring the circuit to original status and send the updated status information to Switch Agents	Automated Switches w/ Controller	Switch Agents	Updated SCADA and Status Information		
10		Switch Agents	Send updated SCADA and Status info to Zonal Agents	Switch Agents send status updates and SCADA information to Zonal Agent	Switch Agents	Zonal Agents	Updated SCADA and Status Information		
11		Zonal Agents	Send updated SCADA and Status info to Substation Agent	Zonal Agents send status updates and SCADA information to Substation Agent	Zonal Agents	Substation Agent	Updated SCADA and Status Information		
12		Substation Agent	Send updated SCADA and Status info to Networks Operations Agent	Substation Agent send status updates and SCADA information to Networks Operations Agent	Substation Agent	Networks Operations Agent	Updated SCADA and Status Information		

#	Event	Primary Actor	Name of Process/Activity	Description of Process/Activity	Information Producer	Information Receiver	Name of Info Exchanged	Additional Notes	IECSA Environment
13		Networks Operations Agent	Send updated SCADA and Status info to HMI	Networks Operations Agent send status updates, SCADA and Fault Event information to HMI	Networks Operations Agent	HMI	Updated SCADA and Status Information		

Post-conditions and Significant Results

Actor/Activity	*Post-conditions Description and Results*
MGMS FLIR	The circuit is returned to its original configuration

Diagram

FUTURE USE

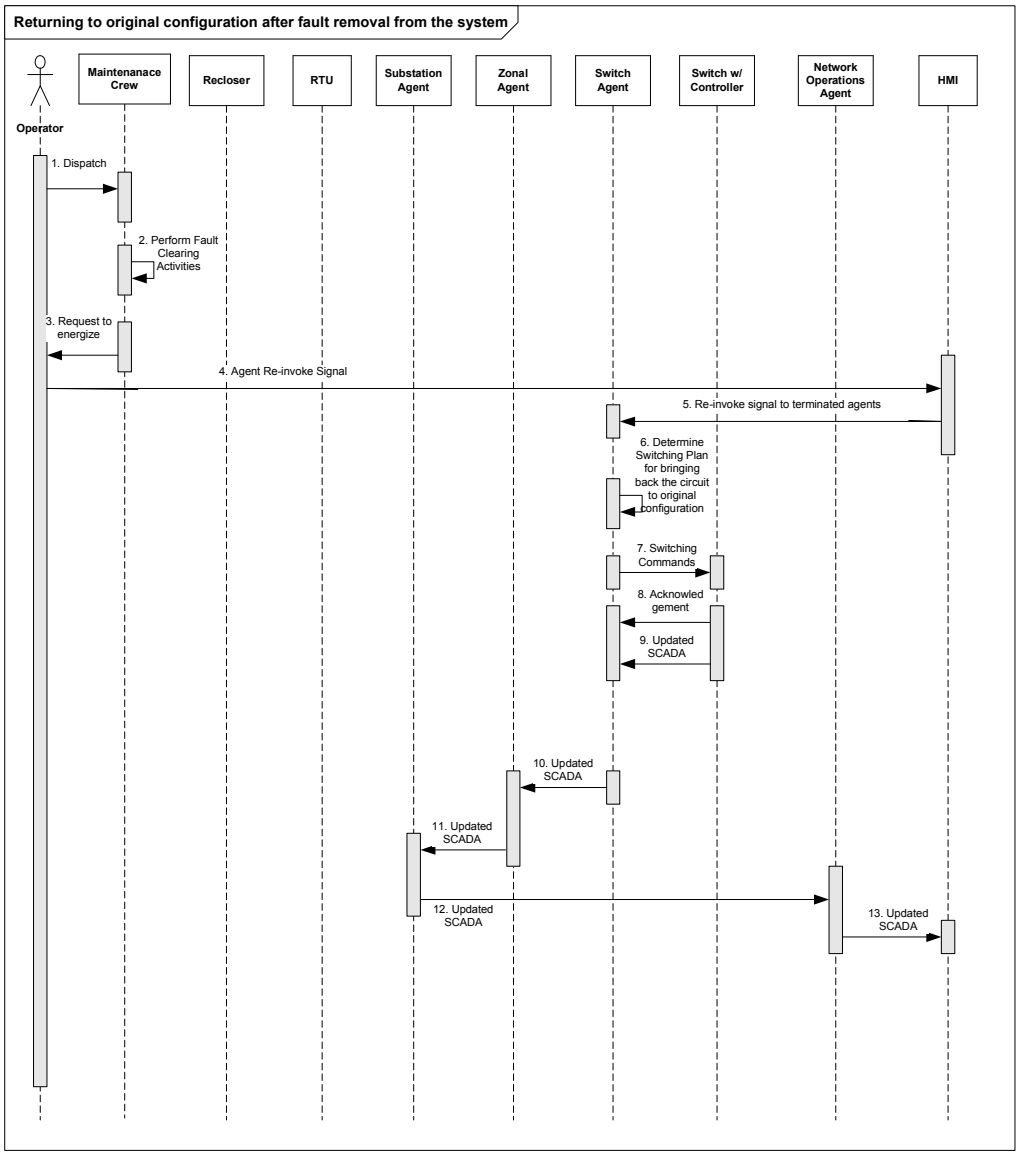

Figure

Figure A - 4: Sequence Diagram for Scenario#2

A.2 Use Case #2 - 15% Peak Load Reduction with DER using MGMS

In this use case, MGMS dispatches DER in order to reduce the system peak load by 15%.

Narrative

There is one scenario in this use case.

Scenario#1: This scenario explains the sequence of steps to reduce the system peak load by 15%.

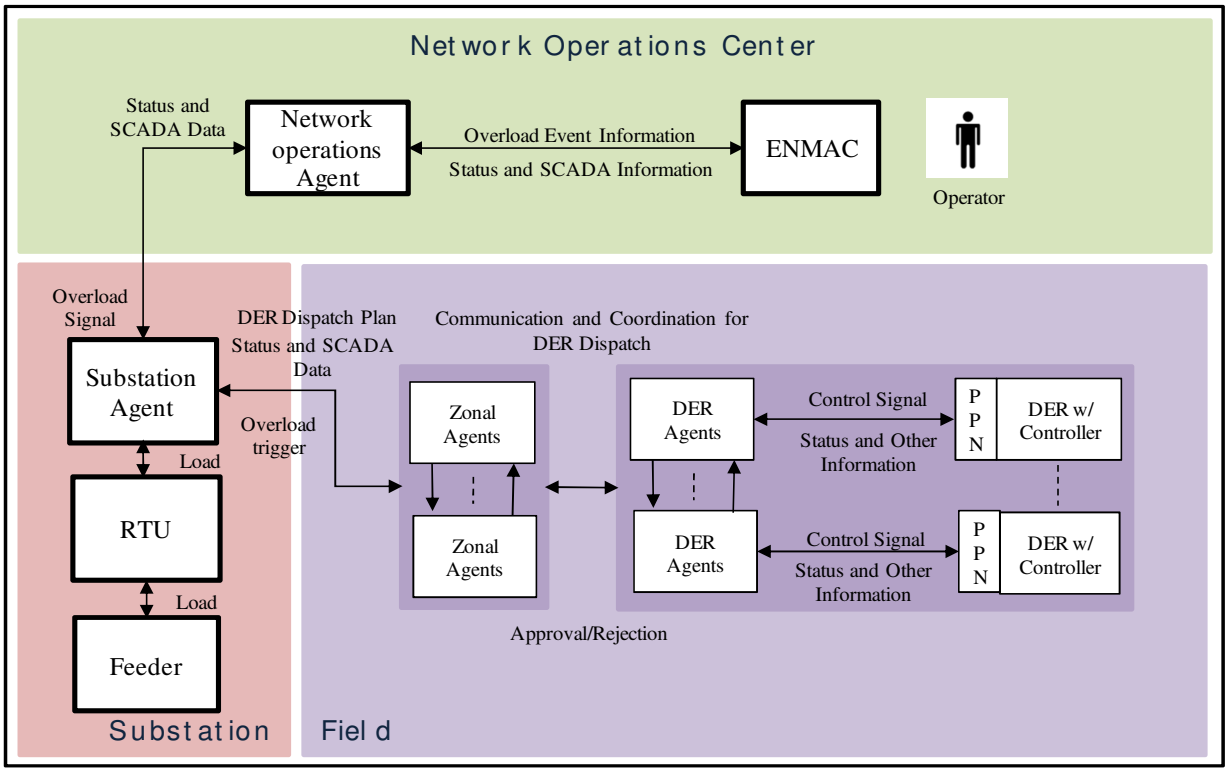

Figure A - 5: Context Diagram for MGMS PLR

Actor (Stakeholder) Roles

Grouping (Community)		*Group Description*
Actor Name	*Actor Type (person, organization, device, system, or subsystem)*	*Actor Description*
Feeder	Device	Distribution line used to transport the power from substation to load points
Network Operations Agent	Device	This is a software agent residing at Networks operations center for monitoring the activities carried out by field agents.
ENMAC	System	ENMAC is the distribution SCADA for monitoring and control of field devices.

Grouping (Community)		*Group Description*
Actor Name	*Actor Type (person, organization, device, system, or subsystem)*	*Actor Description*
DER Agent	Device	This is a software agent resides at every DER in the system.
DER Policies, Procedures, and Notification (PPN) Entity	Sub-system	This represents the various standards and policies in handling the DERs at customer sites.
Substation Agent	Device	This is a software agent resides at substation for monitoring substation equipment especially the Recloser operations.
Remote Terminal Unit (RTU)	Device	This device receives and sends the SCADA information.
DER with Controller	Device	DER residing at customer premise.
Operator	Person	Person who is responsible for distribution operations.
Zonal Agent	Device	This is a software agent resides at every predefined zone for monitoring the agents in that particular zone

Information exchanged

Describe any information exchanged in this template.

Information Object Name	*Information Object Description*
Overload Signal	Signal indicating the feeder overload condition.
Overload subside Signal	Signal indicating the normal loading condition of feeder.
SCADA and Status Information	SCADA monitoring data from DERs
Updated SCADA and Status Information	Updated SCADA monitoring data from DERs
Acknowledgment	Communication acknowledgement confirming that the commands/messages received without any errors
DER Dispatch Plan	Optimal dispatch set points for DER
DER Control Commands	This includes DER turn-on and turn-off commands.
Overload event Information	Overload Information

Step by Step Analysis of Function

Steps to implement function – Name of Sequence

Peak reduction through DER dispatch

Preconditions and Assumptions

Actor/System/Information/Contract	*Preconditions or Assumptions*
DER Agents	DER Agents should continuously monitor DERs and regularly update the DER output and status information.
Zonal Agents	Zonal Agents should continuously monitor DER agents in a zone and regularly update the zone loading information
Substation Agent	Substation Agents should continuously monitor Feeder load and regularly update the loading information.

Steps – Name of Sequence

#	Event	Primary Actor	Name of Process/Activity	Description of Process/Activity	Information Producer	Information Receiver	Name of Info Exchanged	Additional Notes	IECSA Environment
#	*Triggering event? Identify the name of the event.*[4]	*What other actors are primarily responsible for the Process/Activity? Actors are defined in section0.*	*Label that would appear in a process diagram. Use action verbs when naming activity.*	*Describe the actions that take place in active and present tense. The step should be a descriptive noun/verb phrase that portrays an outline summary of the step. "If …Then…Else" scenarios can be captured as multiple Actions or as separate steps.*	*What other actors are primarily responsible for Producing the information? Actors are defined in section0.*	*What other actors are primarily responsible for Receiving the information? Actors are defined in section0.* *(Note – May leave blank if same as Primary Actor)*	*Name of the information object. Information objects are defined in section 0*	*Elaborate architectural issues using attached spreadsheet. Use this column to elaborate details that aren't captured in the spreadsheet.*	*Reference the applicable IECSA Environment containing this data exchange. Only one environment per step.*
1	Substation Agent detects the overload on a feeder	Substation Agent	Send Overload Signal to Network Operations Agent	Substation Agent sends the overload signal to Network Operations Agent when the system overloads above a predefined threshold.	Substation Agent	Network Operations Agent	Overload Signal		
2		Substation Agent	Send Overload Signal and Overload Information to Zonal Agent	Substation Agent sends the overload signal to Zonal Agent	Substation Agent	Zonal Agent	Overload Signal and Overload Information		
3		Zonal Agent	Send Overload Trigger and Overload information to DER Agents	Zonal Agents send Overload Trigger and Overload information to DER Agents	Zonal Agent	DER Agents	Overload Signal and Overload Information		

[4] Note – A triggering event is not necessary if the completion of the prior step – leads to the transition of the following step.

#	Event	Primary Actor	Name of Process/Activity	Description of Process/Activity	Information Producer	Information Receiver	Name of Info Exchanged	Additional Notes	IECSA Environment
4		DER Agents	Communicating and determining DER dispatch Plan	DER agents communicate the DER SCADA and status information and coordinate among them to determine the DER dispatch plan for 15% peak load reduction.	DER Agents	DER Agents	SCADA and status information		
5		DER Agents	Send DER dispatch Plan to Operator	DER Agents send this dispatch plan to the operator for approval.	DER Agents	Operator	DER Dispatch Plan		
6		DER Agents	Send DER Control Commands to DER PPN Entity	Once the Operator approves the plan, DER Agents send the dispatch commands to DER Policies, Procedures and Notification (PPN) entity.	DER Agents	DER PPN Entity	DER Control Commands		
7		DER PPN Entity	Send Acknowledgement to DER Agents	DER Policies, Procedures and Notification (PPN) entity will acknowledge the dispatch commands from DER Agents	DER PPN Entity	DER Agents	Acknowledgment		
8		DER PPN Entity	Dispatch DER	DER PPN Entity makes sure that DER will get dispatched accordingly.	DER PPN Entity	DER w/ Controller	DER Control Commands		

#	Event	Primary Actor	Name of Process/Activity	Description of Process/Activity	Information Producer	Information Receiver	Name of Info Exchanged	Additional Notes	IECSA Environment
9		DER w/ Controller	Send updated SCADA and Status info to DER Agents	DERs w/ controller send the updated SCADA and status information to DER Agents	DER w/ Controller	DER Agents	Updated SCADA and Status Information		
10		DER Agents	Send updated SCADA and Status info to Zonal Agents	DER Agents send status updates and SCADA information to Zonal Agent	DER Agents	Zonal Agents	Updated SCADA and Status Information		
11		Zonal Agents	Send updated SCADA and Status info to Substation Agent	Zonal Agents send status updates and SCADA information to Substation Agent	Zonal Agents	Substation Agent	Updated SCADA and Status Information		
12		Substation Agent	Reevaluates the overload	Substation agent reevaluates if the peak reduction has been achieved or not. If the objective has met go to step **16**	Substation Agent				
13		Substation Agent	Send Overload Signal and Overload Information to Zonal Agent	If the objective has not been satisfied then Substation Agent resends the trigger signal with updated overload information to Zonal Agents for dispatching the additional resources.	Substation Agents	Zonal Agents	Overload Signal and Updated Overload information		

#	Event	Primary Actor	Name of Process/Activity	Description of Process/Activity	Information Producer	Information Receiver	Name of Info Exchanged	Additional Notes	IECSA Environment
14			Repeat steps **3** to **12**	Steps **3** to **12** repeat until peak reduction is achieved.					
15		Substation Agent	Send Updated SCADA and Status Information to Network Operations Agent	Substation Agent send Updated SCADA and Status Information to Network Operations Agent	Substation Agent	Network Operations Agent	Updated SCADA and Status Information		
16		Network Operations Agent	Send SCADA and Status Information and Overload event information to ENMAC	Network Operations Agent Send Updated SCADA and Status Information to ENMAC	Network Operations Agent	ENMAC	SCADA and Status Information and Overload event information		

Post-conditions and Significant Results

Actor/Activity	*Post-conditions Description and Results*
MGMS PLR	Specified peak load reduction is achieved.

A.3 Use Case #3 - Fault Location Algorithm Determining Fault Location

FLA locates faults in a system based upon the fault current data received from line sensors.

Narrative

Recloser and Fuses may react differently for various temporary and permanent faults. These faults may create fault currents above the thresholds however they may or may not operate a protective device. Below table displays the possible states of reclosers and fuses in response to permanent or temporary faults. FLA will analyze only the permanent faults (temporary fault data are processed by FPA algorithms).

Protective Device	**Permanent Faults**				**Temporary Faults**	
Case #	1	2	3	4	5	6
Recloser	Lock-out	Lock-out	No Trip/No Lock-out	Trip/No Lock-out	No Trip/No Lock-out	Trip/No Lock-Out
Fuse	Blown-out	No Blown-out	Blown-out	Blown-out	No Blown-out	No Blown-out

Use cases are analyzed in two scenarios:

Scenario #1: This scenario explains the sequence of steps for cases where recloser locks out (Case 1 and Case 2).

Scenario #2: This scenario explains the sequence of steps for cases where a fuse is blown out without a recloser lock out (Case 3 and Case 4).

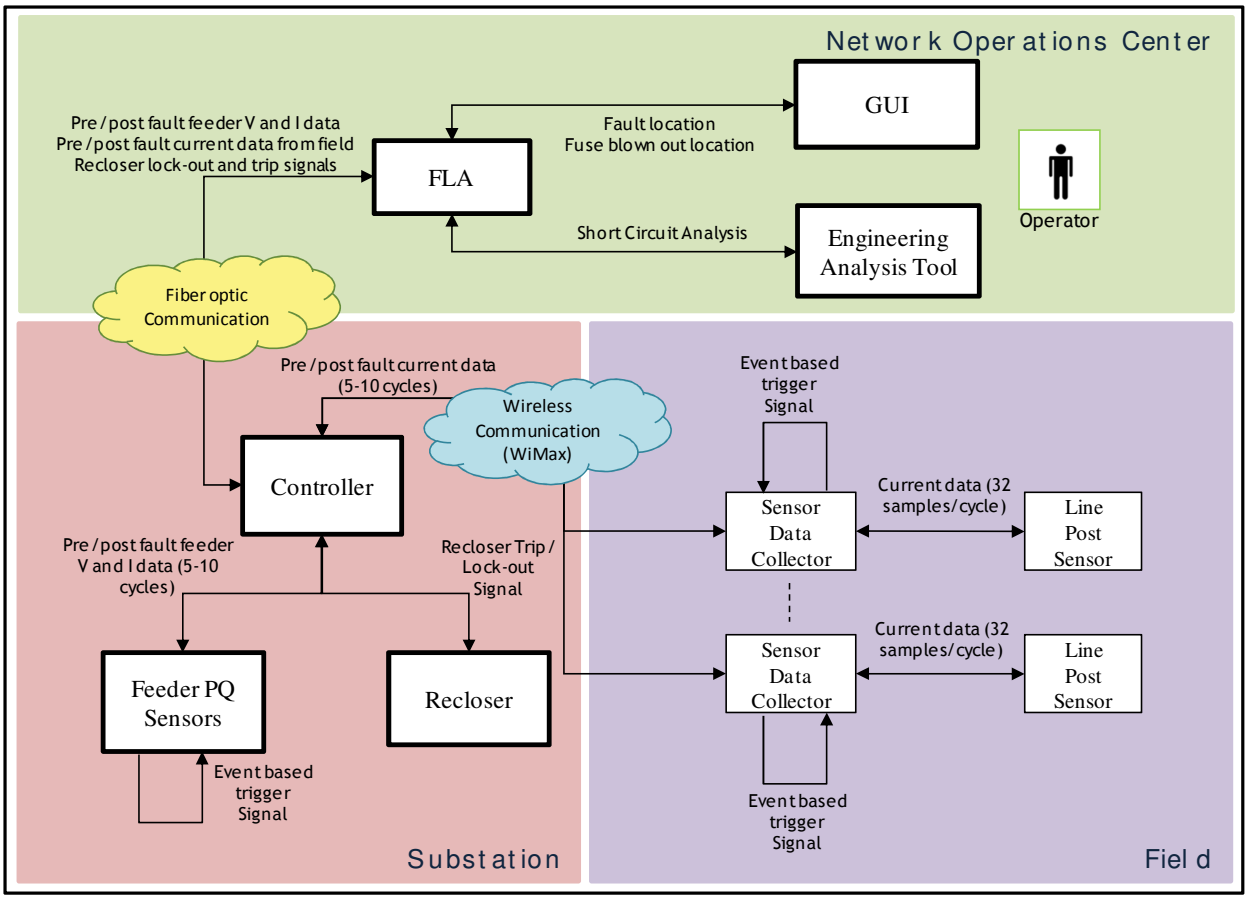

Figure A - 6: Context Diagram for FLA

Actor (Stakeholder) Roles

Grouping (Community)'		*Group Description*
Actor Name	*Actor Type (person, organization, device, system, or subsystem)*	*Actor Description*
Fault Location Algorithm (FLA)	System	This application consists of several intelligent algorithms to precisely find the fault location in the system.
Recloser	Device	This device isolates the faults to protect the system components.
Controller	Device	This is similar to Remote Terminal Unit (RTU) has the functionalities of monitoring the Feeder PQ sensors and Recloser. This can communicate the information to applications residing at Network Operations Center.
GUI	Device	This is the place where FLA outputs the fault location results.

Grouping (Community)		*Group Description*
Actor Name	*Actor Type (person, organization, device, system, or subsystem)*	*Actor Description*
Line Post Sensor	Device	Senses current and voltage quantities of a power line.
Sensor Data Collector	Device	Collects the data form line post sensors. Assumed to have some processing capability which allows logic setting to create the trigger for fault event capturing. Assumed to have local storage for event data logging.
Feeder PQ Sensors	Device	Senses current and voltage quantities of a feeder going out of substation.
Engineering Analysis Tool	System	Distribution analysis tool capable of performing fault analysis
Operator	Person	Person who is responsible for distribution operations.

Information exchanged

Describe any information exchanged in this template.

Information Object Name	*Information Object Description*
Line current data	Predefined (5-10 cycles) window line current data
Event based trigger	Trigger signal indicating that a monitoring quantity (e.g., fault current) exceeding the threshold.
Feeder voltage and current data	Predefined (5-10 cycles) window Feeder voltage and current data
Trip Signal	Signal indicating that the Recloser has operated for a temporary fault.
Lockout Signal	Signal indicating that the Recloser has locked out open on a permanent fault.
Acknowledgment	Communication acknowledgement confirming that the commands/messages received without any errors
Fault Information	Fault information like fault current magnitude, time of fault and etc.
Fault Analysis Results	Fault Analysis Results provided by Engineering Analysis Tool
Fault Location	Fault location in terms of pole locations/IDs.
Fuse Locations	Fuse IDs which are blown on a fault

Step by Step Analysis of Function

Steps to implement function – Name of Sequence

Recloser locks out on a permanent fault (Case#1 and Case#2)

Preconditions and Assumptions

Actor/System/Information/Contract	*Preconditions or Assumptions*
Engineering Analysis Tool	The model in the Engineering Analysis Tool is assumed to be updated frequently and should replicate the real system at all times.
Line Post Sensors	Line Post Sensors should continuously sense the line current and communicate this information to Sensor Data Collector
Sensor Data Collector	Sensor Data Collector should continuously sample the data from Line post sensors and check if the monitored quantity exceeds the threshold limit set by the operator.

Steps – Name of Sequence

#	Event	Primary Actor	Name of Process/Activity	Description of Process/Activity	Information Producer	Information Receiver	Name of Info Exchanged	Additional Notes	IECSA Environment
#	*Triggering event? Identify the name of the event.*[5]	*What other actors are primarily responsible for the Process/Activity? Actors are defined in section0.*	*Label that would appear in a process diagram. Use action verbs when naming activity.*	*Describe the actions that take place in active and present tense. The step should be a descriptive noun/verb phrase that portrays an outline summary of the step. "If …Then…Else" scenarios can be captured as multiple Actions or as separate steps.*	*What other actors are primarily responsible for Producing the information? Actors are defined in section0.*	*What other actors are primarily responsible for Receiving the information? Actors are defined in section0.* *(Note – May leave blank if same as Primary Actor)*	*Name of the information object. Information objects are defined in section 0*	*Elaborate architectural issues using attached spreadsheet. Use this column to elaborate details that aren't captured in the spreadsheet.*	*Reference the applicable IECSA Environment containing this data exchange. Only one environment per step.*

[5] Note – A triggering event is not necessary if the completion of the prior step – leads to the transition of the following step.

#	Event	Primary Actor	Name of Process/Activity	Description of Process/Activity	Information Producer	Information Receiver	Name of Info Exchanged	Additional Notes	IECSA Environment
1	Monitoring quantity will exceed the threshold value set in Sensor Data Collector	Sensor Data Collector	Generate the event based trigger	The logic (exception based on over current, harmonic distortion or etc.) embedded in the sensor data collector will trigger the event capturing.	Sensor Data Collector	Sensor Data Collector	Event based trigger		
2		Sensor Data Collector	Captures the Fault current data	Sensor data collector collects the predefined (5-10 cycles) window line current data and stores it.	Sensor Data Collector	Sensor Data Collector	Line current data		
3		Sensor Data Collector	Send Line current data to Controller	Sensor data collector sends the predefined (5-10 cycles) window line current data to the controller at substation	Sensor Data Collector	Controller	Line current data		
4		Feeder PQ sensors	Generate event based trigger	The logic (exception based on over current, harmonic distortion or etc.) embedded in the Feeder PQ sensors will trigger the event capturing.	Feeder PQ sensors	Feeder PQ sensors	Event based trigger		

#	Event	Primary Actor	Name of Process/Activity	Description of Process/Activity	Information Producer	Information Receiver	Name of Info Exchanged	Additional Notes	IECSA Environment
5		Feeder PQ sensors	Send Feeder voltage and current data to Controller	Feeder PQ sensors send the predefined (5-10 cycles) window feeder voltage and current data to the controller at substation	Feeder PQ sensors	Controller	Feeder voltage and current data		
6		Recloser	Send Lockout signal to Controller	Recloser sends the Lockout signal to the controller	Recloser	Controller	Lockout Signal		
7		Controller	Send event information to FLA	Controller sends all the data it received from Feeder PQ sensors, Sensor data Collectors, and Recloser to FLA	Controller	FLA	Line current data, Feeder voltage and current data, and Trip Signal		
8		FLA	Send fault information to Engineering Analysis Tool	FLA sends the required fault information to Engineering analysis tool for performing the fault analysis.	FLA	Engineering Analysis Tool	Fault Information		
9		Engineering Analysis Tool	Send analysis results to FLA	Engineering analysis tool sends the fault analysis results to FLA	Engineering Analysis Tool	FLA	Fault Analysis Results		

#	Event	Primary Actor	Name of Process/Activity	Description of Process/Activity	Information Producer	Information Receiver	Name of Info Exchanged	Additional Notes	IECSA Environment
10		FLA	Determines Fault Location and Fuse Locations	FLA performs the calculations using the data and determines the distance of the fault from substation and indicates the fault location in terms of pole location. It also determines the potential fuse blown outs.	FLA	FLA			
11		FLA	Send Fault Location and Fuse Locations	FLA sends the fault location and fuse blown out information to the GUI	FLA	GUI	Fault Location and Fuse Locations		
12		GUI	Display Fault Location and Fuse Locations	GUI displays the fault location and fuse blown out information	GUI				

Post-conditions and Significant Results

Actor/Activity	*Post-conditions Description and Results*
FLA	FLA determines the fault location and potential fuse blown out locations.

Step by Step Analysis of Function

Steps to implement function – Name of Sequence

Fuse blown out without a Recloser Lock-out (Case#3 and Case#4)

Preconditions and Assumptions

Actor/System/Information/Contract	*Preconditions or Assumptions*
Engineering Analysis Tool	The model in the Engineering Analysis Tool is assumed to be updated frequently and should replicate the real system at all times.
Line Post Sensors	Line Post Sensors should continuously sense the line current and communicate this information to Sensor Data Collector
Sensor Data Collector	Sensor Data Collector should continuously sample the data from Line post sensors and check if the monitored quantity exceeds the threshold limit set by the operator.

Steps – Name of Sequence

#	Event	Primary Actor	Name of Process/Activity	Description of Process/Activity	Information Producer	Information Receiver	Name of Info Exchanged	Additional Notes	IECSA Environment
#	*Triggering event? Identify the name of the event.*[6]	*What other actors are primarily responsible for the Process/Activity? Actors are defined in section0.*	*Label that would appear in a process diagram. Use action verbs when naming activity.*	*Describe the actions that take place in active and present tense. The step should be a descriptive noun/verb phrase that portrays an outline summary of the step. "If …Then…Else" scenarios can be captured as multiple Actions or as separate steps.*	*What other actors are primarily responsible for Producing the information? Actors are defined in section0.*	*What other actors are primarily responsible for Receiving the information? Actors are defined in section0.* *(Note – May leave blank if same as Primary Actor)*	*Name of the information object. Information objects are defined in section 0*	*Elaborate architectural issues using attached spreadsheet. Use this column to elaborate details that aren't captured in the spreadsheet.*	*Reference the applicable IECSA Environment containing this data exchange. Only one environment per step.*
1	Monitoring quantity will exceed the threshold value set in Sensor Data Collector	Sensor Data Collector	Generate the event based trigger	The logic (exception based on over current, harmonic distortion or etc.) embedded in the sensor data collector will trigger the event capturing.	Sensor Data Collector	Sensor Data Collector	Event based trigger		

[6] Note – A triggering event is not necessary if the completion of the prior step – leads to the transition of the following step.

#	Event	Primary Actor	Name of Process/Activity	Description of Process/Activity	Information Producer	Information Receiver	Name of Info Exchanged	Additional Notes	IECSA Environment
2		Sensor Data Collector	Sensor Data Collector Captures the Fault current data	Sensor data collector collects the predefined (5-10 cycles) window line current data and stores it.	Line Post Sensors	Sensor Data Collector	Line current data		
3		Sensor Data Collector	Send Line current data to Controller	Sensor data collector sends the predefined (5-10 cycles) window line current data to the controller at substation	Sensor Data Collector	Controller	Line current data		
4		Feeder PQ sensors	Generate event based trigger	The logic (exception based on over current, harmonic distortion or etc.) embedded in the Feeder PQ sensors will trigger the event capturing.	Feeder PQ sensors	Feeder PQ sensors	Event based trigger		
5		Feeder PQ sensors	Send Feeder voltage and current data to Controller	Feeder PQ sensors send the predefined (5-10 cycles) window feeder voltage and current data to the controller at substation	Feeder PQ sensors	Controller	Feeder voltage and current data		
6		Recloser	Send Trip signal to Controller	Recloser sends the trip signal to the controller	Recloser	Controller	Trip Signal		

#	Event	Primary Actor	Name of Process/Activity	Description of Process/Activity	Information Producer	Information Receiver	Name of Info Exchanged	Additional Notes	IECSA Environment
7		Controller	Send event information to FLA	Controller sends all the data it received from Feeder PQ sensors, Sensor data Collectors, and Recloser to FLA	Controller	FLA	Line current data, Feeder voltage and current data, Trip Signal, and Lockout Signal		
8		FLA	Send fault information to Engineering Analysis Tool	FLA sends the required fault information to Engineering analysis tool for performing the fault analysis.	FLA	Engineering Analysis Tool	Fault Information		
9		Engineering Analysis Tool	Send analysis results to FLA	Engineering analysis tool sends the fault analysis results to FLA	Engineering Analysis Tool	FLA	Fault Analysis Results		
10		FLA	Determines Fault Location and Fuse Locations	FLA performs the calculations using the data and determines the distance of the fault from substation and indicates the fault location in terms of pole location. It also determines potential fuse blown outs.	FLA	FLA			
11		FLA	Send Fault Location and Fuse Locations	FLA sends the fault location and fuse blown out information to the GUI	FLA	GUI	Fault Location and Fuse Locations		

#	Event	Primary Actor	Name of Process/Activity	Description of Process/Activity	Information Producer	Information Receiver	Name of Info Exchanged	Additional Notes	IECSA Environment
12		GUI	Display Fault Location and Fuse Locations	GUI displays the fault location and fuse blown out information	GUI				

Post-conditions and Significant Results

Actor/Activity	*Post-conditions Description and Results*
FLA	FLA determines the fault location and potential fuse blown out locations.

A.4 Use Case #4 - Fault Prediction Algorithm predicts potential faults

FPA predicts the fault in a system based upon the data received from various sensors in the field.

Narrative

This use case has only one scenario

Scenario#1: This scenario explains the sequence of steps in predicting the fault in a system

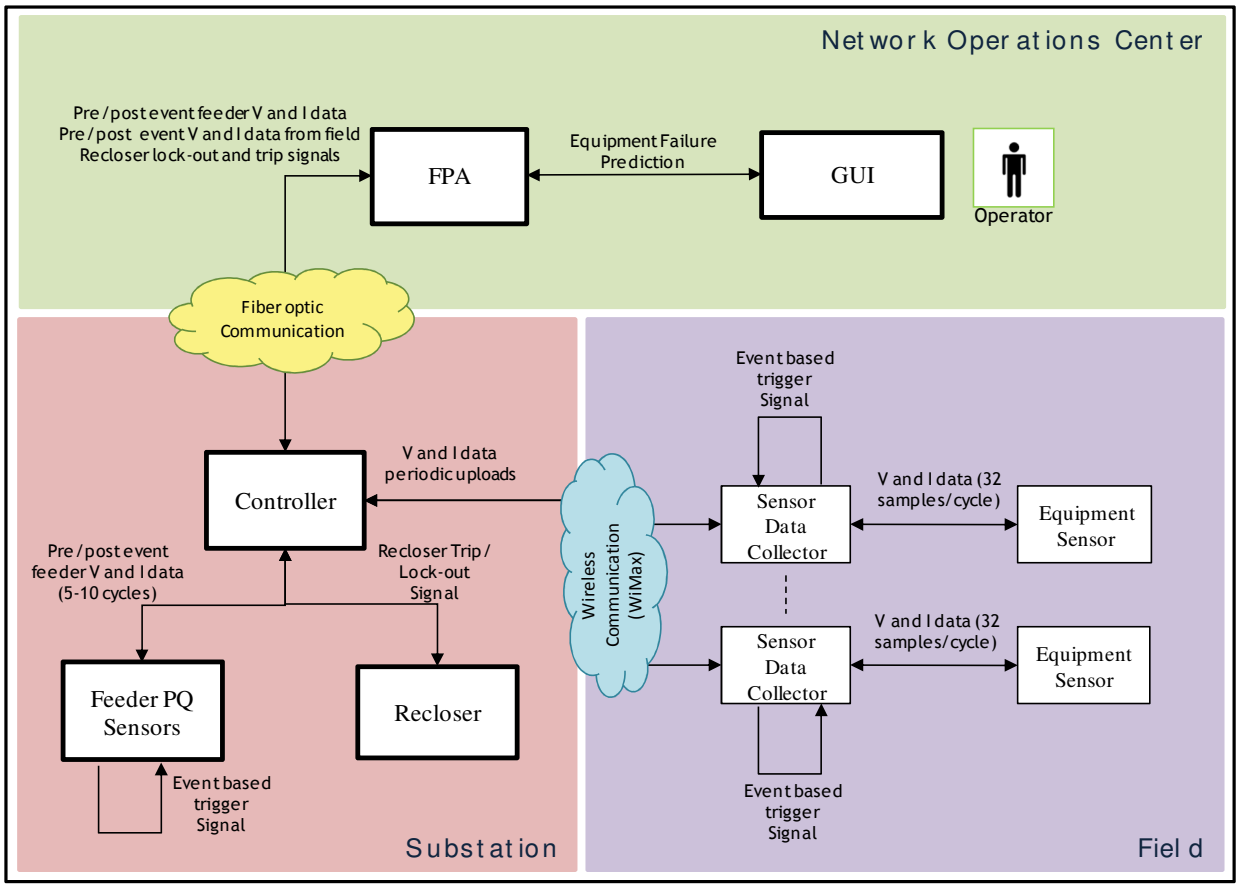

Figure A - 7: Context Diagram for FPA

Actor (Stakeholder) Roles

Grouping (Community)		*Group Description*
Actor Name	*Actor Type (person, organization, device, system, or subsystem)*	*Actor Description*
Fault Prediction Algorithm (FPA)	System	This application consists of several intelligent algorithms to predict the fault in the system.
Recloser	Device	This device isolates the faults to protect the system components.

Grouping (Community)		*Group Description*
Actor Name	*Actor Type (person, organization, device, system, or subsystem)*	*Actor Description*
Controller	Device	This is similar to Remote Terminal Unit (RTU) has the functionalities of monitoring the Feeder PQ sensors and Recloser. This can communicate the information to applications residing at Network Operations Center.
GUI	Device	This is the place where FPA outputs the fault location results.
Equipment Sensor	Device	Senses current and voltage quantities of an equipment.
Sensor Data Collector	Device	Collects the data form equipment sensors. Assumed to have some processing capability which allows logic setting to create the trigger for fault event capturing. Assumed to have local storage for event data logging.
Feeder PQ Sensors	Device	Senses current and voltage quantities of a feeder going out of substation.
Operator	Person	Person who is responsible for distribution operations.

Information exchanged

Information Object Name	*Information Object Description*
Voltage and Current Data	Predefined (5-10 cycles) window voltage and current data of an equipment
Event based trigger	Trigger signal indicating that a monitoring quantity (e.g., fault current) exceeding the threshold.
Feeder voltage and current data	Predefined (5-10 cycles) window Feeder voltage and current data
Trip Signal	Signal indicating that the Recloser has operated for a temporary fault.
Lockout Signal	Signal indicating that the Recloser has locked out open on a permanent fault.
Lockout Signal	Signal indicating that the Recloser has locked out open on a permanent fault.
Fault Prediction	Predicted fault information

Step by Step Analysis of Function

Steps to implement function – Name of Sequence

Predicting the fault in the system

Preconditions and Assumptions

Actor/System/Information/Contract	*Preconditions or Assumptions*
Equipment Sensors	Equipment Sensors should continuously sense the voltage and current quantities and communicate this information to Sensor Data Collector
Sensor Data Collector	Sensor Data Collector should continuously sample the data from Equipment Sensors and check if the monitored quantity exceeds the threshold limit set by the operator.

Steps – Name of Sequence

#	Event	Primary Actor	Name of Process/Activity	Description of Process/Activity	Information Producer	Information Receiver	Name of Info Exchanged	Additional Notes	IECSA Environment
#	*Triggering event? Identify the name of the event.*[7]	*What other actors are primarily responsible for the Process/Activity? Actors are defined in section0.*	*Label that would appear in a process diagram. Use action verbs when naming activity.*	*Describe the actions that take place in active and present tense. The step should be a descriptive noun/verb phrase that portrays an outline summary of the step. "If …Then…Else" scenarios can be captured as multiple Actions or as separate steps.*	*What other actors are primarily responsible for Producing the information? Actors are defined in section0.*	*What other actors are primarily responsible for Receiving the information? Actors are defined in section0.* *(Note – May leave blank if same as Primary Actor)*	*Name of the information object. Information objects are defined in section 0*	*Elaborate architectural issues using attached spreadsheet. Use this column to elaborate details that aren't captured in the spreadsheet.*	*Reference the applicable IECSA Environment containing this data exchange. Only one environment per step.*
1	Monitoring quantity will exceed the threshold value set in Sensor Data Collector	Sensor Data Collector	Generate the event based trigger	The logic (exception based on over current, harmonic distortion or etc.) embedded in the sensor data collector will trigger the event capturing.	Sensor Data Collector	Sensor Data Collector	Event based trigger		
2		Sensor Data Collector	Sensor Data Collector Captures the Voltage and Current data	Sensor data collector collects the predefined (5-10 cycles) window Equipment Voltage and Current data and stores it.	Equipment Sensors	Sensor Data Collector	Voltage and Current Data		
3		Sensor Data Collector	Send Voltage and Current data to Controller	Sensor data collector sends the stored Equipment Voltage and Current data to the controller periodically (e.g., once in a day)	Sensor Data Collector	Controller	Voltage and Current Data		

[7] Note – A triggering event is not necessary if the completion of the prior step – leads to the transition of the following step.

#	Event	Primary Actor	Name of Process/Activity	Description of Process/Activity	Information Producer	Information Receiver	Name of Info Exchanged	Additional Notes	IECSA Environment
4		Feeder PQ sensors	Generate event based trigger	The logic (exception based on over current, harmonic distortion or etc.) embedded in the Feeder PQ sensors will trigger the event capturing.	Feeder PQ sensors	Feeder PQ sensors	Event based trigger		
5		Feeder PQ sensors	Send Feeder voltage and current data to Controller	Feeder PQ sensors send the predefined (5-10 cycles) window feeder voltage and current data to the controller at substation	Feeder PQ sensors	Controller	Feeder voltage and current data		
6		Controller	Send event information to FPA	Controller sends all the data it received from Feeder PQ sensors, Sensor data Collectors, and Recloser to FPA	Controller	FPA	Line current data, Feeder voltage and current data, Trip Signal, and Lockout Signal		
7		FPA	FPA predicts the fault	FPA performs the calculations using the data and predicts the fault in the system	FPA	FPA			
8		FPA	Send fault prediction to GUI	FPA sends the fault prediction information to the GUI	FPA	GUI	Fault Prediction		
9		GUI	Display fault prediction	GUI displays fault prediction	GUI				

Post-conditions and Significant Results

Actor/Activity	*Post-conditions Description and Results*
FPA	FPA predicts the fault in the system

Appendix B – Microgrid System Requirements

B.1 Functional Requirements

Reqmt ID	Requirement	Source
FR.1.1	MGMS algorithms shall find, isolate feeder faults, and restore service to un-faulted Zones.	UC #1
FR.1.2	MGMS algorithms shall be triggered by a recloser lock-out event.	UC #1
FR.1.3	Service restoration to un-faulted Zones shall be completed in less than five minutes after the recloser locks out.	UC #1
FR.1.4	MGMS algorithms shall adapt to the new system topologies and perform its entire functions.	UC #1
FR.1.5	MGMS algorithms shall handle multiple non-simultaneous contingencies which are apart from five minutes.	UC #1
FR.1.6	MGMS restoration algorithms shall not violate any thermal or voltage limits.	UC #1
FR.1.7	MGMS restoration algorithm shall restore as much load as possible depending upon the source capacity.	UC #1
FR.1.8	MGMS shall find faults in radial and non-radial (system configuration with multiple energy resources) configurations.	UC #1
FR.1.9	MGMS FLIR algorithms shall take distribution generation, energy storage and controllable load into account when determining the restoration plan.	UC #1
FR.1.10	MGMS shall provide the interface between the ENMAC™ system and the reclosers, automated switches and sensors.	UC #1
FR.1.11	MGMS shall be enabled/disabled by Mon Power operators remotely.	UC #1
FR.1.12	When MGMS is disabled, monitoring and manual control functions (by control center operators) shall still be allowed by the MGMS.	UC #1
FR.1.13	MGMS shall perform automatic switching operations to bring the system to the pre-fault configuration when a “Return to Pre-fault Configuration” signal is issued by the operator.	UC #1

Table B - 1: Use Case #1 Functional Requirements

Reqmt ID	Requirement	Source
FR.2.1	MGMS shall optimally dispatch distributed generation, energy storage, and controllable load to reduce the annual projected peak load by 15%. Projected load has been provided by Mon Power.	UC #2
FR.2.2	MGMS shall optimally dispatch distributed generation, energy storage, and controllable load when operators issue a command to initiate load reduction in the system. MGMS shall be able to accept the signal coming from the control center Human Machine Interface (HMI).	Team meeting
FR.2.3	MGMS shall dispatch DER with different cost functions optimally when excess capacity exists.	Team meeting
FR.2.4	MGMS shall make the islanding decision from the main grid.	Team meeting
FR.2.5	MGMS shall allow the islanded microgrid to reconnect to the main grid without taking an outage.	Team meeting
FR.2.6	MGMS shall dispatch DER to meet active and reactive power demand at all times in an islanded scenario.	Team meeting
FR.2.7	MGMS shall regulate the frequency of the islanded microgrid within [TBD] band.	Team meeting
FR.2.8	MGMS shall regulate the voltage of the islanded microgrid within 112-127 V (phase-to-neutral) band.	Team meeting
FR.2.9	MGMS shall be able to expand the borders of the microgrid when there is excess generating capacity present within the microgrid.	Team meeting

Table B - 2: Use Case #2 Functional Requirements

Reqmt ID	Use Case #3 Requirements	Source
FR.3.1	FLA shall determine the distance of faulted point from the substation by analyzing the fault data.	UC #3
FR.3.2	FLA shall be triggered by a fault which has been cleared by a protective device (recloser or fuse).	UC #3
FR.3.3	A local monitoring device (relay or power quality monitor) is needed to capture the data for FLA to analyze the fault.	UC #3
FR.3.4	FLA shall output the results as recommendations to the system operators. FLA shall not take any action with the results.	UC #3
FR.3.5	FLA will need at least the Current data from selected sensors. Additional Voltage data may improve the accuracy. Selected sensors shall provide 16/32 sample data per cycle.	UC #3
FR.3.6	FLA will require at least 5 cycles of fault data in order to determine fault locations. Therefore, fault monitors/sensors shall capture at least 5 cycles of fault data.	UC #3
FR.3.7	FLA shall determine the fault location as accurate as possible. Accuracy of 3-4 poles is expected based on prior efforts (600-800 ft.).	UC #3
FR.3.8	FLA shall identify which protective device (mainly fuse in this project) may have operated.	UC #3
FR.3.9	FLA shall be deployed into the existing computer hardware at Allegheny Control Center in Greensburg, PA.	UC #3
FR.3.10	FLA shall determine the location of faults in grid-connected mode.	UC #3
FR.3.11	FLA will look into the feasibility of developing fault location algorithms for an islanded mode assuming that the island large enough and enough data is provided to do the short circuit calculations.	UC #3
FR.3.12	In order to determine the exact fault location, FLA will need an accurate circuit model to conduct short circuit calculations. FLA also needs protective device information (fuse data, relay settings).	UC #3
FR.3.13	FLA shall determine the distance of faulted point from the substation by analyzing the fault data.	UC #3

Table B - 3: Use Case # 3 Functional Requirements

Reqmt ID	Use Case # 4 Requirements	Source
FR.4.1	FPA shall predict distribution equipment failures (transformer, arrestor, circuit breaker, capacitor bank) by processing the voltage and current waveform data. The equipment to be analyzed has been determined by the project team. Sensors are required for each monitored equipment.	UC #4
FR.4.2	FPA shall check for protection coordination.	UC #4
FR.4.3	FPA shall process current (I) and voltage (V) data from selected sensors which provide 32/64 sample data per cycle.	UC #4
FR.4.4	FPA shall use the same backbone communication system.	UC #4
FR.4.5	FPA shall be deployed into the existing computer hardware at Mon Power Control Center in Greensburg, PA.	UC #4
FR.4.6	FPA shall investigate the feasibility of detecting high impedance faults by using the data available from the sensors to be placed for fault current monitoring.	UC #4

Table B - 4: Use case #4 Functional Requirements

B.2 Communication System Requirements

WVSC project team followed a requirements development process recommended by NIST to develop the following communication requirements.

DETAILED COMMUNICATION REQUIREMENTS

Req ID	Event	Requirements	*Information Producer*	*Information Receiver*	Name of Info Exchanged	Reliability	Latency (response time one direction)	Payload size(bytes)	How Often?	How many at the same time?
MGMS-FLIR										

Req ID	Event	Requirements	*Information Producer*	*Information Receiver*	Name of Info Exchanged	Reliability	Latency (response time one direction)	Payload size(bytes)	How Often?	How many at the same time?
	Device status request	Substation agent shall be able to send device status request to Recloser/Switch	*Substation Agent*	*Recloser/Switch*	Device status request	%99.5	<4s	25	Every X seconds	
		Substation agent shall be able to send device status request to FAN Gateway	*Substation Agent*	*FAN Gateway*	Device status request	%99.5	<1s	25	Every X seconds	
		FAN Gateway shall be able to send device status request to Switch	*FAN Gateway*	*Switch*	Device status request	%99.5	<3s	25	Every X seconds	
		Substation agent shall be able to send device status request to RTU	*Substation Agent*	*RTU*	Device status request	%99.5	<1s	25	Every X seconds	
		RTU shall be able to send device status request to recloser	*RTU*	*Recloser*	Device status request	%99.5	<1s	25	Every X seconds	
	Device status response	Recloser/Switch shall be able to send device status response to Substation agent	*Recloser/Switch*	*Substation Agent*	Device status response	%99.5	<4s	50	Every X seconds	
		Recloser shall be able to send device status response to RTU	*Recloser*	*RTU*	Device status response	%99.5	<1s	50	Every X seconds	
		RTU shall be able to send device status response to Substation Agent	*RTU*	*Substation Agent*	Device status response	%99.5	<1s	50	Every X seconds	

Req ID	Event	Requirements	*Information Producer*	*Information Receiver*	Name of Info Exchanged	Reliability	Latency (response time one direction)	Payload size(bytes)	How Often?	How many at the same time?
		Switch shall be able to send device status response to FAN Gateway	*Switch*	*FAN Gateway*	Device status response	%99.5	<3s	50	Every X seconds	
		FAN Gateway shall be able to send device status response to Substation Agent	*FAN Gateway*	*Substation Agent*	Device status response	%99.5	<1s	50	Every X seconds	
	Device operate request	Substation Agent shall be able to send device operate request to Recloser/Switch	*Substation Agent*	*Recloser/Switch*	Device operate request	%99.5	<4s	25	On demand	
		Substation agent shall be able to send device operate request to FAN Gateway	*Substation Agent*	*FAN Gateway*	Device operate request	%99.5	<1s	25	On demand	
		FAN Gateway shall be able to send device operate request to Switch	*FAN Gateway*	*Switch*	Device operate request	%99.5	<3s	25	On demand	
		Substation agent shall be able to send device operate request to RTU	*Substation Agent*	*RTU*	Device operate request	%99.5	<1s	25	On demand	
		RTU shall be able to send device operate request to recloser	*RTU*	*Recloser*	Device operate request	%99.5	<1s	25	On demand	

Req ID	Event	Requirements	*Information Producer*	*Information Receiver*	Name of Info Exchanged	Reliability	Latency (response time one direction)	Payload size(bytes)	How Often?	How many at the same time?
	Acknowledgement	Recloser/Switch shall be able to send operate device acknowledgement to Substation Agent	*Recloser/Switch*	*Substation Agent*	Operate device acknowledgement	%99.5	<4s	25	On demand	
		Recloser shall be able to send operate device acknowledgement to RTU	*Recloser*	*RTU*	Operate device acknowledgement	%99.5	<1s	25	On demand	
		RTU shall be able to send operate device acknowledgement to Substation Agent	*RTU*	*Substation Agent*	Operate device acknowledgement	%99.5	<1s	25	On demand	
		Switch shall be able to send operate device acknowledgement to FAN Gateway	*Switch*	*FAN Gateway*	Operate device acknowledgement	%99.5	<3s	25	On demand	
		FAN Gateway shall be able to send operate device acknowledgement to Substation Agent	*FAN Gateway*	*Substation Agent*	Operate device acknowledgement	%99.5	<1s	25	On demand	
	Recloser lock-out	Recloser shall be able to send lock out signal to FEP	*Recloser*	*FEP*	Lock-out Signal	%99.5	<5s	50		
		Recloser shall be able to send lock out signal to RTU	*Recloser*	*RTU*	Lock-out Signal	%99.5	<1s	50	Event-based	

Req ID	Event	Requirements	*Information Producer*	*Information Receiver*	Name of Info Exchanged	Reliability	Latency (response time one direction)	Payload size(bytes)	How Often?	How many at the same time?
		RTU shall be able to send lock out signal to Substation Agent	*RTU*	*Substation Agent*	Lock-out Signal	%99.5	<1s	50	Event-based	
		Substation Agent shall be able to process and send lock out signal to FAN Gateway	*Substation Agent*	*FAN Gateway*	Lock-out Signal	%99.5	<1s	50	Event-based	
		FAN Gateway shall be able to process and send lock out signal to FEP	*FAN Gateway*	*FEP*	Lock-out Signal	%99.5	<2s	50	Event-based	
	FLIR trigger	Substation Agent shall be able to process lock-out signal and send FLIR trigger signal to Zonal/SW Agents	Substation Agent	Zonal/Switch Agents	FLIR Trigger Signal	%99.5	<4s	50		
		Substation Agent shall be able to process lock-out signal and send FLIR trigger signal to FAN Gateway	*Substation Agent*	*FAN Gateway*	FLIR Trigger Signal	%99.5	<1s	50	Event-based	
		FAN Gateway shall be able to process and send lock out signal to Zonal/Switch Agents	*FAN Gateway*	*Zonal/Switch Agents*	FLIR Trigger Signal	%99.5	<3s	50	Event-based	
	Fault Location, Isolation, Restoration	Zonal/Switch Agents communicate to each other	Zonal/Switch Agents	Zonal/Switch Agents						
		Step1								

Req ID	Event	Requirements	*Information Producer*	*Information Receiver*	Name of Info Exchanged	Reliability	Latency (response time one direction)	Payload size(bytes)	How Often?	How many at the same time?
		Step 2								
	Return to Previous Configuration	Zonal/Switch Agents communicate to each other	DMS	Zonal/Switch Agents						
		Step1								
		Step 2								
DER Dispatch										
	DER status request	DMS shall be able to send device status (voltage, real & reactive power, avail energy) request to DER (Renewable/Energy Storage/DG/Load controller)	*DMS*	*DER*		%99.5	<8s	25	On demand	
		DMS shall be able to send device status request to FEP	*DMS*	*FEP*		%99.5	<1s	25	On demand	
		FEP shall be able to send device status request to Substation Agent	*FEP*	*Substation Agent*		%99.5	<2s	25	On demand	
		Substation Agent shall be able to send device status request to Fan Gateway	*Substation Agent*	*FAN Gateway*		%99.5	<1s	25	On demand	

Req ID	Event	Requirements	*Information Producer*	*Information Receiver*	Name of Info Exchanged	Reliability	Latency (response time one direction)	Payload size(bytes)	How Often?	How many at the same time?
		Fan Gateway shall be able to send device status request to HAN Gateway	*FAN Gateway*	*HAN Gateway*		%99.5	<3s	25	On demand	
		HAN Gateway shall be able to send device status request to DER	*HAN Gateway*	*DER*		%99.5	<1s	25	On demand	
	DER status response	DER (Renewable/Energy Storage/DG/Load controller) shall be able to send device status (voltage, real & reactive power, avail energy) response to DMS	*DER*	*DMS*		%99.5	<8s	50	On demand	
		DER shall be able to send device status request to HAN Gateway	*DER*	*HAN Gateway*		%99.5	<1s	50	On demand	
		HAN Gateway shall be able to send device status request to Fan Gateway	*HAN Gateway*	*FAN Gateway*		%99.5	<3s	50	On demand	
		Fan Gateway shall be able to send device status request to Substation Agent	*FAN Gateway*	*Substation Agent*		%99.5	<1s	50	On demand	

Req ID	Event	Requirements	*Information Producer*	*Information Receiver*	Name of Info Exchanged	Reliability	Latency (response time one direction)	Payload size(bytes)	How Often?	How many at the same time?
		Substation Agent shall be able to send device status request to FEP	*Substation Agent*	*FEP*		%99.5	<2s	50	On demand	
		FEP shall be able to send device status request to DMS	*FEP*	*DMS*		%99.5	<1s	50	On demand	
	DER dispatch command	DMS/Substation Agent shall be able to send DER dispatch command to DER (Renewable/Energy Storage/DG/Load controller)	*DMS/Substation Agent*	*DER*		%99.5	<3s	25	On demand	
		DMS shall be able to send DER dispatch command to FEP	*DMS*	*FEP*		%99.5	<1s	25	On demand	
		FEP shall be able to send DER dispatch command to Substation Agent	*FEP*	*Substation Agent*		%99.5	<2s	25	On demand	
		Substation Agent shall be able to send DER dispatch command to Fan Gateway	*Substation Agent*	*FAN Gateway*		%99.5	<1s	25	On demand	
		Fan Gateway shall be able to send DER dispatch command to HAN Gateway	*FAN Gateway*	*HAN Gateway*		%99.5	<3s	25	On demand	

Req ID	Event	Requirements	*Information Producer*	*Information Receiver*	Name of Info Exchanged	Reliability	Latency (response time one direction)	Payload size(bytes)	How Often?	How many at the same time?
		HAN Gateway shall be able to DER dispatch command to DER	*HAN Gateway*	*DER*		%99.5	<1s	25	On demand	
	DER dispatch command acknowledgment	DER (Renewable/Energy Storage/DG/Load controller) shall be able to send DER dispatch command acknowledgment to DMS	*DER*	*DMS*		%99.5	<8s	25	On demand	
		DER shall be able to send DER dispatch command acknowledgment to HAN Gateway	*DER*	*HAN Gateway*		%99.5	<1s	25	On demand	
		HAN Gateway shall be able to send DER dispatch command acknowledgment to Fan Gateway	*HAN Gateway*	*FAN Gateway*		%99.5	<3s	25	On demand	
		Fan Gateway shall be able to send DER dispatch command acknowledgment to Substation Agent	*FAN Gateway*	*Substation Agent*		%99.5	<1s	25	On demand	
		Substation Agent shall be able to send DER dispatch command acknowledgment to FEP	*Substation Agent*	*FEP*		%99.5	<2s	25	On demand	

Req ID	Event	Requirements	*Information Producer*	*Information Receiver*	Name of Info Exchanged	Reliability	Latency (response time one direction)	Payload size(bytes)	How Often?	How many at the same time?
		FEP shall be able to send DER dispatch command acknowledgment to DMS	*FEP*	*DMS*		%99.5	<1s	25	On demand	
FLA										
	Pre/post fault line current data	Sensor collector shall be able to send the pre/post fault line current data (5-10 cycles) to the FLA/FPA when event happens.	*Sensor Collector*	*FLA/FPA*		%99.5	<12s	200	Event-based	
		Sensor collector shall be able to send the pre/post fault line current data (5-10 cycles) to the FAN Gateway.	*Sensor Collector*	*FAN Gateway*		%99.5	<5s	200	Event-based	
		FAN Gateway shall be able to send the pre/post fault line current data (5-10 cycles) to the RTU.	*FAN Gateway*	*RTU*		%99.5	<2s	200	Event-based	
		RTU shall be able to process and send the pre/post fault line current data (5-10 cycles) to the FEP.	*RTU*	*FEP*		%99.5	<3s	200	Event-based	

Req ID	Event	Requirements	*Information Producer*	*Information Receiver*	Name of Info Exchanged	Reliability	Latency (response time one direction)	Payload size(bytes)	How Often?	How many at the same time?
		FEP shall be able to send the pre/post fault line current data (5-10 cycles) to the FLA/FPA.	*FEP*	*FLA/FPA*		%99.5	<2s	200	Event-based	
	Pre/post fault feeder voltage and current data	Feeder PQ Sensor shall be able to send the pre/post fault feeder voltage and current data (5-10 cycles) to the FLA/FPA	*Feeder PQ Sensor*	*FLA/FPA*		%99.5	<7s	200	Event-based	
		Feeder PQ Sensor shall be able to send the pre/post fault feeder voltage and current data (5-10 cycles) to the RTU	*Feeder PQ Sensor*	*RTU*		%99.5	<2s	200	Event-based	
		RTU shall be able to send the pre/post fault feeder voltage and current data (5-10 cycles) to the FEP	*RTU*	*FEP*		%99.5	<3s	200	Event-based	
		FEP shall be able to send the pre/post fault feeder voltage and current data (5-10 cycles) to the FLA/FPA	*FEP*	*FLA/FPA*		%99.5	<2s	200	Event-based	

B.3 Control Center Systems – Monitoring, Control, Analysis

B.3.1 Real Time Monitoring and Control System (MCS) Requirements [e.g. ENMAC]

Reqmt ID	Requirement	Sour
	MCS shall have a Graphical User Interface (GUI) to illustrate the grid topology and DER connectivity.	Mon Pow
	Analog and digital data (status, current, voltage, active power, reactive power, apparent power) acquired from the field devices (reclosers, transformers, IEDs, switches, sensors, DER) shall be visualized on the MCS on a real-time basis.	Mon Pow
	MCS shall have a Graphical User Interface (GUI) to illustrate the grid topology and DER connectivity.	Mon Pow
	MCS shall allow distribution system operators to remotely control DER.	Mon Pow

B.3.2 Real-time Distribution System Analysis (DSA) Tool Requirements [e.g. DE

Reqmt ID	Requirement	Sour
	DSA shall be able to run short circuit and three phase unbalanced power flow analysis	UC #3
	DSA shall update the distribution system topology using real-time status data	UC #3
	DSA shall display the output of FLA/FPA system	UC #3

B.4 Distributed Energy Resources Requirements

B.4.1 Solar PV/Inverter (less than 30kW) Requirements

Reqmt ID	Requirement	Sour
	Solar PV/Inverter shall have capability for monitoring its connection status, real power output, reactive power output and voltage at the point of interconnection	Mon Pow
	The point of common coupling (PCC) shall be at secondary voltage	Mon Pow
	The generator shall be a single-phase, UL Listed inverter or converter	Mon Pow

B.4.2. Natural Gas-fired Generator Requirements

Reqmt ID	Requirement	Source
	Interconnection must comply with Mon Power's applicable standards.	Mon Power
	Emission requirements: NOx, SOx, COx emissions shouldn't exceed [TBD] ppmv	Mon Power
	Performance Requirements: Generator should at least have [TBD] % electrical efficiency.	Mon Power

B.4.3 Energy Storage/Inverter Requirements

Reqmt ID	Requirement	Source
	Energy Storage/Inverter shall have capability for monitoring its connection status, real power output, reactive power output and voltage at the point of interconnection	Mon Power
	Energy storage units should posses [TBD] nominal cycles of life.	Mon Power
	Energy storage units should posses [TBD] round trip efficiency.	Mon Power
	Energy storage unit size requirements [TBD]	Mon Power

B.4.4 DER Interconnection Requirements (less than 2MVA)

Reqmt ID	Requirement	Source
	The DER shall not actively regulate the voltage at the PCC.	Mon Power
	The DER installation shall not cause the AP service voltage at other customers to go outside the requirements of ANSI C84.1-1995 Range A or to exceed state or local regulations.	Mon Power
	The DER shall synchronize and parallel and/or transfer load with AP circuit without causing a voltage fluctuation at the point of common coupling greater than +/- 5% of the prevailing voltage level.	Mon Power
	The DER shall meet the voltage fluctuation and flicker requirements of IEEE 1453 – Recommended Practice for Measurement and Limits of Voltage Fluctuations and Associated Light Flicker on AC Power Systems during normal, paralleling or load transfer operation	Mon Power
	The DER shall not inject non-sinusoidal current nor adversely affect voltage, frequency or wave shape of power supplied at the point of common coupling.	Mon Power
	The DER shall meet both the voltage and current harmonic limit requirements of *IEEE 519 – Recommended Practices and Requirements for Harmonic Control in Electrical Power Systems*	Mon Power
	The DERs response to abnormal voltage and abnormal frequency shall meet requirements of *IEEE 1547 – Standard for Interconnecting Distributed Resources with electric Power Systems*	Mon Power

B.4.5 Automated Switches Requirements

Medium Voltage Switches (MVS)[e.g. automated switches for reconfiguration]

Reqmt ID	Requirement	Source
	MVS shall be a three-phase, pole mounted load-break switch with motor operator	Mon Power
	MVS shall have remote tripping capability	Mon Power
	MVS shall have capability of manual charging of operating springs.	Mon Power
	MVS shall have manual operation for OPEN and CLOSE. Lever shall be provided to disable close operation and lock unit in the open position	Mon Power
	Operation of MVS shall not be affected by icing or contaminated atmospheric conditions.	Mon Power
	MVS shall have mechanical counter to record operations.	Mon Power
	MVS shall be provided with pole mounting hanger	Mon Power
	Inboard and Outboard surge arrestor brackets to be provided	Mon Power
	MVS shall have local tripping capability such as a pushbutton or other means clearly identified for Allegheny personnel to operate as necessary	Mon Power
	MVS shall have the following ratings: Nominal Voltage Class: 14.4 Rated Maximum Voltage: 15.5 Basic Insulation Level (BIL), kV : 110 Continuous Current Rating (A): 600 Rated Load Interrupting Current: 600 Overload Current (A): 900 Fault Closing (A): 10,000 Momentary Rating, Asym (Amps): 10,000 Operating Temperature (F): -40 to +120	Mon Power

B.4.6 Microgrid Equipment Technical Specifications

Battery Energy Storage System (BESS) Technical Specifications

Functional Specifications

1. BESS shall have two single-phase 120/208VAC output voltage which will connect two phases of the 120/208 VAC three phase system.
2. Each BESS unit shall provide 8 kW output power.
3. BESS shall include a battery storage system based on the Lithium-Ion technology. The battery shall be sized to provide energy at 8 kW for minimum two (2) hours.

4. BESS shall be comprised of an integrated inverter system which includes ac/dc charger, dc/dc boost charger or charge controls, circuit breakers, contactors and other relevant equipment to satisfy the specifications defined on this document.
5. BESS shall accommodate solar PV panel DC output directly.
6. The BESS shall convert DC power produced by the PV and Energy Storage equipment into AC power at the voltage and frequency levels of the local grid conditions.
7. BESS shall have MPPT Tracking capability. The control system continuously adjusts the voltage to optimize the output of the PV arrays.
8. BESS shall allow connection of an AC source which may be electric grid or an AC generator. AC source can used to charge the battery or to inject power to the grid through AC/DC/AC conversion.
9. BESS shall be available in both NEMA 2 and 4/3R cabinets.
10. Switching components and the relative cooling system shall be sized in such a way the BESS can operate properly within the nominal temperature range.
11. The output voltage total harmonic distortion THDU% shall be <1% for loads at 100% rated output power and with linear load and <4% with nonlinear load.
12. The BESS shall be capable of delivering the rated power at a power factor of between 0.9 leading and 0.9 lagging and at the rated voltage, (these characteristics must be maintained even when the PV input DC voltage to the BESS is at its minimum value).
13. The BESS shall be able to withstand an overload and is equipped with its own output current-limiting circuit; so that components are not damaged in the event of short-circuit and the BESS is protected by a combination of electronic circuitry and fuses.
14. BESS shall have at least one Ethernet port for communications.
15. No additional software other than Microsoft Internet Explorer or standard windows operating systems shall be necessary to set parameters and operate the system. Systems requiring the purchase of additional software licenses are not permitted.
16. All parameters shall be accessible through via IEC61850, DNP3.0, Modbus Plus, XML or other industry standard communications protocol.
17. The BESS shall have an appropriate display on the front panel to display the instantaneous measurements.
18. The bidder shall provide the following technical specification for their proposed system.
    a. Capacity
    b. Roundtrip efficiency
    c. Life cycles and warranty period and details
    d. Recommended Maximum Depth of Discharge
    e. Charge rate
    f. Nominal discharge rate (kW/sec)
    g. Unit size (Length x Width x Height) and weight
    h. Nominal temperature range without derating
    i. Audible noise
19. BESS shall be dispatched for applications that are described below. BESS units shall be able to switch between these applications via an XML command signal generated by an external controller.
    a. Electric Service Reliability (UPS functionality): When Microgrid transitions to islanded mode, BESS shall provide rated energy output to ride through a power outage. Maximum

power requirement shall be limited to the BESS rating. On site generation shall be turned on by an external generator as soon as an outage is detected.

b. Load Following: BESS shall be dispatched to follow the load in the Microgrid. An external controller shall issue these control signals. BESS shall be able to receive these signals and adjust its output accordingly.
c. Renewable Energy Time Shift: BESS shall charge energy storage with PV power, then discharge energy storage later to reduce building's peak demand.
d. Voltage Support: BESS shall be able to inject reactive power into the Microgrid to provide voltage support and power factor correction
e. Solar PV Capacity Firming: BESS shall charge/discharge the battery in real-time based on varying solar PV output to keep the combined (solar PV and battery) power output level constant over a specified period of time. Designation of such time period and the charge/discharge behavior mode shall be selectable via an external controller.

20. BESS shall be able to charge the battery using AC generator output, solar PV output or electrical grid power. AC generator to be controlled by external controllers.
21. BESS shall have controls to support local charge/discharge schedule. BESS controls shall be programmed based on time and date for the battery charge/discharge schedule.
22. BESS shall be able to charge/discharge the battery and change the output power based on a signal received from external controllers.
23. BESS shall be able to receive remote control signals to change its output active and reactive power.
24. BESS shall have the controls to directly send the PV output to the grid bypassing the battery charging.
25. BESS shall put the battery in idle mode following an external signal or when the battery is fully charged. In this case, all PV output shall be injected to the electric grid.
26. The BESS shall have the capability to provide VAR support in islanded mode. VAR injection shall change based on the measured voltage at the BESS terminals.
27. When the power available from the PV array and Energy Storage is insufficient to supply the losses of the BESS, the BESS shall go to a standby/shutdown mode. The BESS control shall prevent excessive cycling during rightly shut down or extended periods of insufficient solar irradiance.
28. BESS shall restart after an over or under frequency shutdown when the utility grid voltage and frequency have returned to within limits for a minimum of five minutes.
29. The BESS shall restart after an over or under voltage shutdown when the utility grid voltage and frequency have returned to within limits for a minimum of five minutes.

Electrical Safety, Grounding and Protection

1. Internal Faults: Built-in protection for internal faults including excess temperature, commutation/gating failure, and overload and cooling fan failure (if fitted) is required.
2. Overvoltage Protection: Overvoltage protection against atmospheric lightning discharge to the PV array or electrical grid is required at AC terminals. Protection is to be provided against voltage fluctuations in the grid itself and internal faults in the power conditioner, operational errors and switching transients.

Installation, Training and Support Services

1. The bidder shall provide on-site training to Mon Power's and/or other partner organizations' personnel.
2. The bidder shall be responsible for system delivery, installation and electrical interface at customer location. The bidder shall describe their process for installation and commissioning of the BESS, including the process to hire subcontractors if needed.
3. Instruction books shall be furnished which shall contain the description of components, parts and accessories, detailed installation instructions, complete instructions covering operation and maintenance of equipment, complete replacement parts list with current pricing.
4. Manufacturer shall provide the BESS with spare parts for critical, long lead time, or high-failure components (such as air filters if necessary). Provide a list of available spare parts as part of the submitted bid.
5. Certified test shall be conducted in accordance with applicable standards. The supplier shall furnish two (2) copies of certified test reports for all tests covered by this specification to Mon Power within two (2) weeks of delivery.

Standards Compliance

1. BESS units shall be compliant with UL1741 and IEEE 1547. UL 1741 listing with a NRTC (Nationally Recognized Testing Laboratory) is required.
2. The equipment specified herein shall be designed, manufactured, assembled and tested in accordance with all applicable portions of all applicable ANSI, IEC, IEEE and NEMA standards including the latest revisions with respect to material, design and testing.

Microinverter-based Solar PV System Technical Specifications

Functional Specifications

1. Total solar PV capacity shall be 20 kW. This capacity shall be connected in three groups so that each group can be connected to one phase of the three-phase system. Each group is expected to provide ~6.6 kW AC output power.
2. Each individual solar panel shall embed a micro inverter and a communicator unit that should have the following features,
    a. Convert DC input into AC power at the voltage and frequency levels of the local grid conditions.
    b. Measure voltage and current quantities both on AC and DC side.
    c. Indicate health status of each individual panel.
    d. MPPT Tracking capability. The control system continuously adjusts the voltage to optimize the output of the PV arrays.
    e. Supply reactive power to the grid in the instances of islanded scenarios. VAR injection shall change based on the measured voltage at the bus terminals. NOTE – This operation is outside of UL1741 compliance and requires operator acknowledgement.
    f. Onboard communication module to communicate to a central communication unit for communication and control.
    g. Should use open standard communication protocol such as ZigBee or etc.
    h. Accept commands on the air to change real and reactive power output of the inverter.

Hardware/Software Specifications

1. Each Solar PV panels with micro inverter system shall be comprised of a solar module, micro inverter, and a communicator to meet the specifications listed in the above section.
2. The proposed system shall have an energy web portal-software that will archive the data from the solar panels and be able to present the various performance statistics on solar panels. This software feature is recommended but not necessary.
3. The proposed solution shall come with necessary racking and cabling system to mount the solar panels on the overhead structure to be built by the bidder,
4. The whole solar panel assembly shall be weather proofed and meet the specifications by NEMA 4 and/or other applicable standards.
5. The vendor shall provide the following technical specification for their proposed system.
    a. Capacity
    b. Microinverter efficiency
    c. DC power input
    d. AC output voltage
    e. RMS output current
    f. AC output frequency
    g. Total Harmonic Distortion (THD)
    h. AC Reactive power output
    i. Power factor
    j. Warranty period and details
    k. Unit size (Length x Width x Height) and weight
    l. Nominal temperature range without de-rating

Electrical Safety, Grounding and Protection

1. Internal Faults: Built-in protection for internal faults including excess temperature, commutation/gating failure, and overload and cooling fan failure (if fitted) is required.
2. Overvoltage Protection: Overvoltage protection against atmospheric lightning discharge to the PV panels is required. Protection is to be provided against voltage fluctuations in the grid itself and internal faults in the power conditioner, operational errors and switching transients.
3. Each solar panel with micro inverter assembly shall be able to withstand an overload and is equipped with its own output current-limiting circuit; so that components are not damaged in the event of short-circuit and the panel is protected by a combination of electronic circuitry and fuses.

Installation, Training and Support Services

1. The vendor shall provide on-site training to Mon Power's and/or other partner organizations' personnel.
2. The vendor shall be responsible for system delivery, installation and electrical interface at customer location. The vendor shall describe their process for installation and commissioning, including the process to hire subcontractors if needed.
3. Instruction books shall be furnished which shall contain the description of components, parts and accessories, detailed installation instructions, complete instructions covering operation and maintenance of equipment, complete replacement parts list with current pricing.

4. Manufacturer shall provide spare parts for critical, long lead time, or high-failure components. Provide a list of available spare parts as part of the submitted bid.
5. Certified test shall be conducted in accordance with applicable standards. The supplier shall furnish two (2) copies of certified test reports for all tests covered by this specification to Mon Power within two (2) weeks of delivery.

Standards Compliance

1. The equipment specified herein shall be designed, manufactured, assembled and tested in accordance with all applicable portions of all applicable ANSI, IEC, IEEE, NEMA and other applicable standards including the latest revisions with respect to material, design and testing.

NOTE – In order to provide dynamic VAR per section 7.4.6.2.1, micro-inverters shall support UL1741 features during standard (non-VAR) operation. These micro-inverters do not need to be UL1741 labeled or listed.

Solar PV DC system (only panels, no inverters) Technical Specifications

Functional Specifications

1. Each BESS unit allows two solar PV DC outputs (3.2 kW) to be connected. As there are 3 BESS units designed, a total of 6 solar PV arrays are designed at this building. Each array must be limited to 3200 watts with a maximum string voltage of 150VDC. Total PV capacity at this building shall be 19.2 kW.
2. Each PV array shall be wired separately up to the BESS units.

Hardware/Software Specifications

1. Each individual solar panel shall come with required racking and cabling system to mount on the cantilevered structure as provided by the bidder.
2. The whole solar panel assembly shall be weather proofed and meet the specifications by NEMA 4 and/or other applicable standards.
3. The vendor shall provide the following technical specification for their proposed system.
    a. Solar module type
    b. Power Rating
    c. Open circuit voltage
    d. Short circuit current
    e. Module efficiency
    f. Operating temperature range
    g. Power tolerance
    h. Warranty period and details
    i. Unit size (Length x Width x Height) and weight

Electrical Safety, Grounding and Protection

1. Ground Fault Supervision: DC arrays shall comply with ground fault detection requirements according to NEC and local electrical code requirements.

Installation, Training and Support Services

Same as section 7.4.6.2.4

Standards Compliance

1. The equipment specified herein shall be designed, manufactured, assembled and tested in accordance with all applicable portions of all applicable ANSI, IEC, IEEE, NEMA and other applicable standards including the latest revisions with respect to material, design and testing.

Control Room Technical Specifications

1. The control room shall accommodate switchboards, panels, controllers, protective relays, three (3) energy storage units, and PV connector boxes/auxiliaries.
2. The room shall be climate controlled within -4F to 104F range.
3. The room shall have proper NEMA rating.

Low Voltage Switchgear and Protective Relays Technical Specifications

One-line and three-line diagrams shown in Figure 4-5: Microgrid One Line Diagram and Figure 4-6: Microgrid Three Line Diagram illustrate a draft design of the low voltage switchgear. It's required that CB1 and CB2 in the one-line diagram are electrically operated circuit breakers. The switchgear shall have a communications interface (using a standard protocol) to allow remote monitoring and control.

Medium Voltage Switchgear (PCC breaker) Technical Specifications

The PCC breaker shall be a 15 kV, three-phase, 600A breaker with PTs on both sides and CTs on one side. Protective relays shall also be provided for protective functions illustrated in the one-line diagram as shown in Figure 4-5: Microgrid One Line Diagram. PCC breaker shall have the ability to perform a closed transition to the utility grid. The switchgear shall have a communications interface (using a standard protocol) to allow remote monitoring and control.

Natural Gas Generator Technical Specifications

The Natural Gas Generator shall be an outdoor, pad-mounted, 150 kW, 120/208V, 60 Hz, three-phase natural gas generator with a sound attenuated enclosure. The generator shall:

1. Shall have electronic governor and voltage regulator
2. Shall have remote start/stop capability.
3. Shall meet both voltage and current harmonic limit requirements of IEEE 519.
4. Shall provide a communications interface (using a standard protocol) to allow remote reading of generator operating parameters – Voltage, kW, kVAR, output frequency, status
5. Shall provide both isochronous and speed droop control functionalities. It shall have capability to change control modes locally or remotely.
6. Shall have protection features such as over/under voltage, over/under frequency, over speed, low oil pressure, etc.
7. Shall come with a line breaker with synchronization capability.

Appendix C - Microgrid Load Profiles

C.1. Summer Load Profiles:

May, June, July, and August months are considered as the summer months for generating the summer load profiles.

C.1.1. Summer Peak Day Load Profile, 07/22/2011 (Friday)

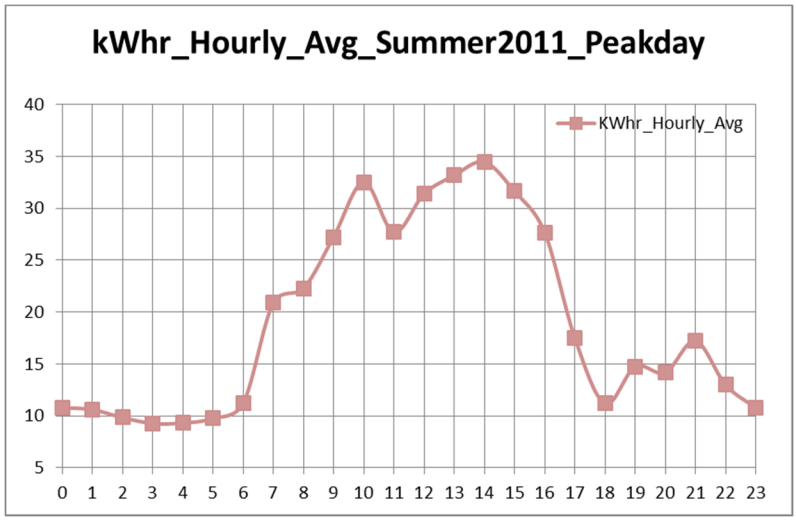

C.1.2. Typical Summer Weekday Load Profile

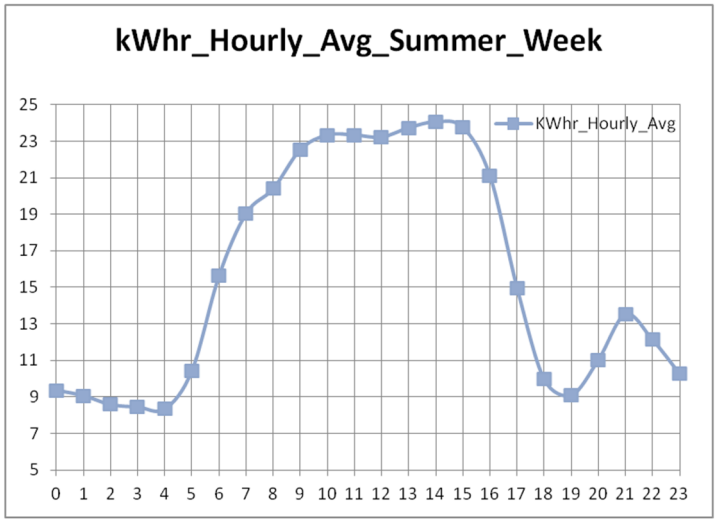

C.1.3. Typical Summer Weekend Load Profile

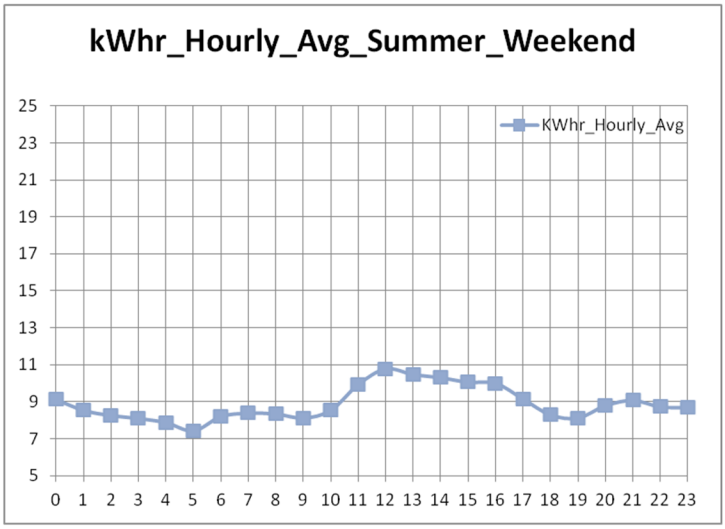

C.2. Winter Load Profiles:

January, February, November, and December months are considered as the winter months for generating the winter load profiles.

C.2.1 Winter Peak Day Load Profile, 02/23/2010 (Tuesday)

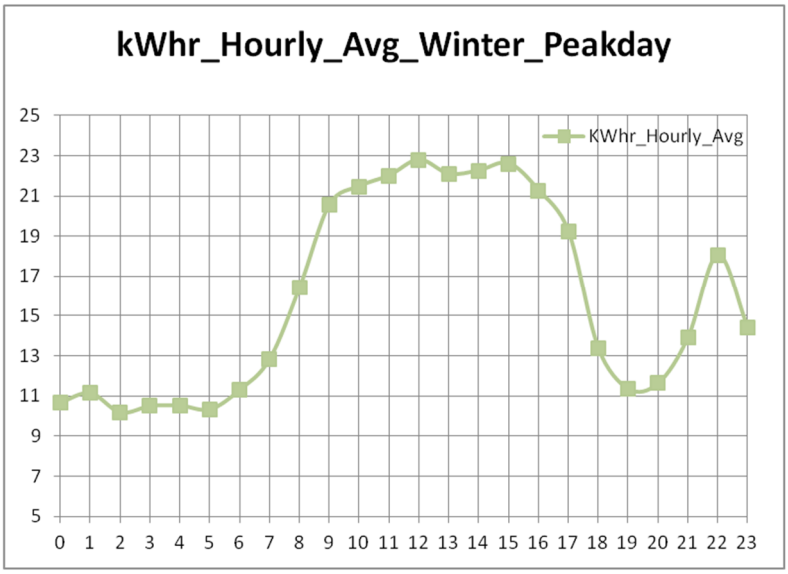

C.2.2. Typical Winter Weekday Load Profile

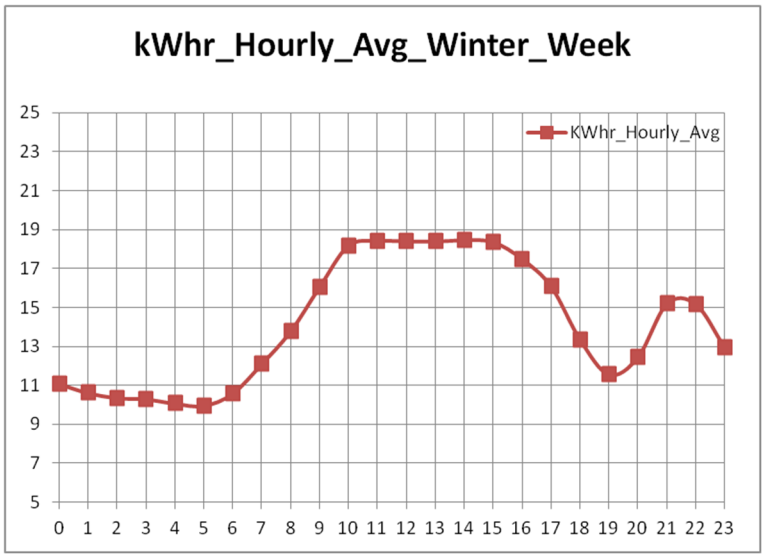

C.2.3. Typical Winter Weekend Load Profile

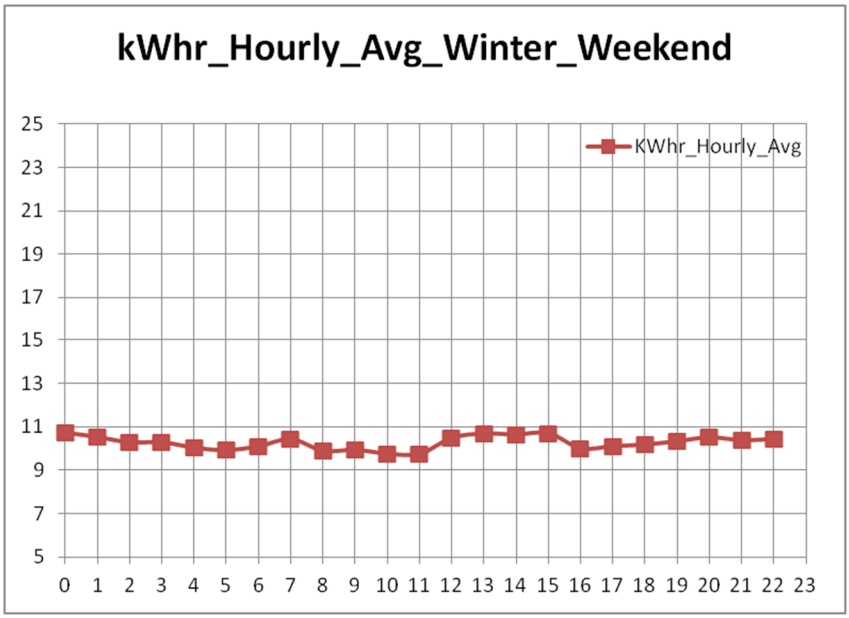

Appendix D- Leidos Modeling and Simulation Results

D.1 Reconfiguration Study Results

This appendix presents the detailed analysis results of reconfiguration study. Following figure shows the zones defined in circuit#3 – Stewart Street.

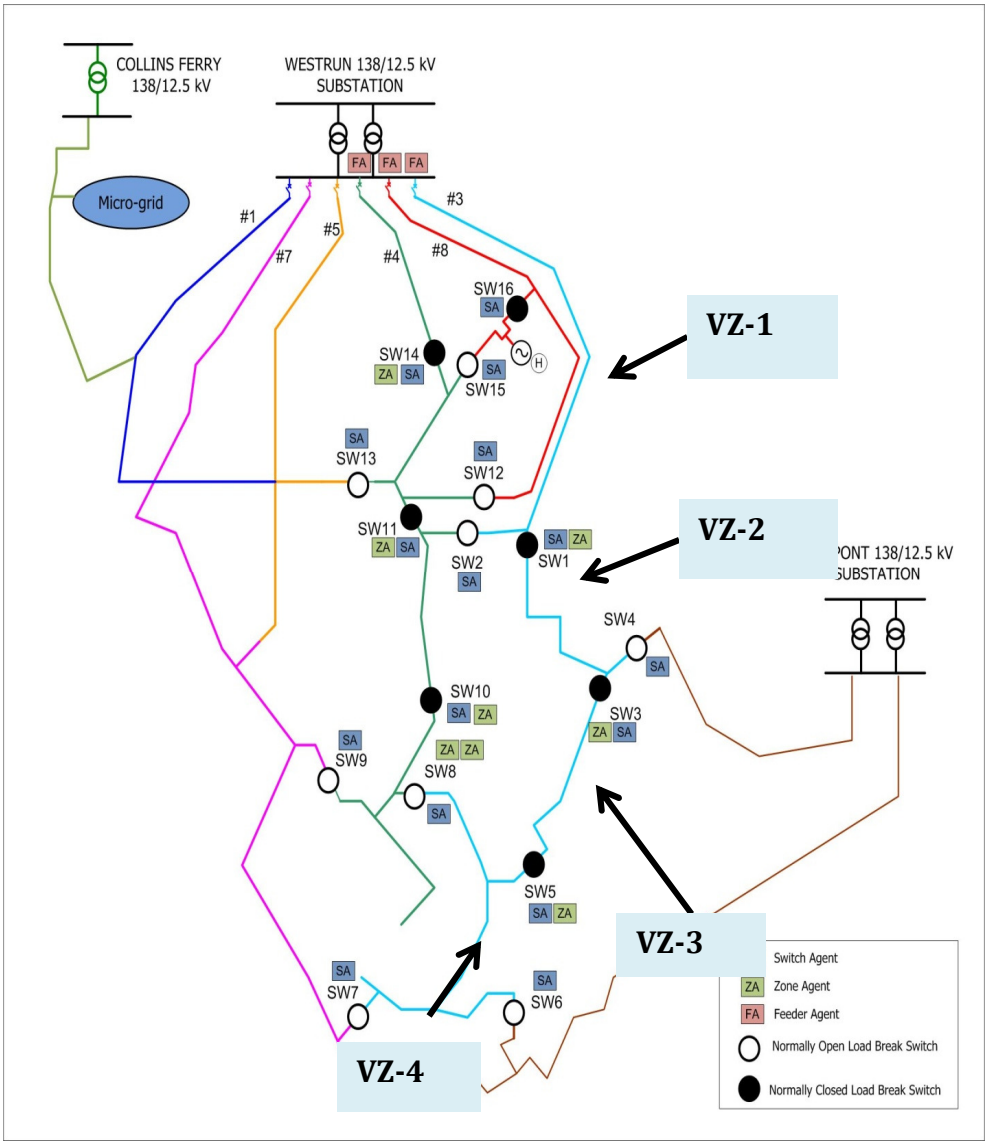

Figure E - 1: West Run Circuit #3 - Stewart Street

he switch status for all of the possible scenarios for faults in different zones of circuit#3 - Stewart Street.

Table E - 1: Switch Status of circuit#3 - Stewart Street

art		Switch Status								
	Load Transferred To	SW1	SW2	SW3	SW4	SW5	SW6	SW7	SW8	Notes
	NA	CLOSED	OPEN	CLOSED	OPEN	CLOSED	OPEN	OPEN	OPEN	
	#5 Easton	**OPEN**	OPEN	CLOSED	**CLOSED**	CLOSED	OPEN	OPEN	OPEN	
	#6 Mileground	**OPEN**	OPEN	CLOSED	OPEN	CLOSED	**CLOSED**	OPEN	OPEN	Low Voltage
	#7 University Ave	**OPEN**	OPEN	CLOSED	OPEN	CLOSED	OPEN	**CLOSED**	OPEN	Low Voltage
	#4 Pineview	**OPEN**	OPEN	CLOSED	OPEN	CLOSED	OPEN	OPEN	**CLOSED**	
	#6 Mileground	**OPEN**	OPEN	**OPEN**	OPEN	CLOSED	**CLOSED**	OPEN	OPEN	Low Voltage
	#7 University Ave	**OPEN**	OPEN	**OPEN**	OPEN	CLOSED	OPEN	**CLOSED**	OPEN	Low Voltage
	#4 Pineview	**OPEN**	OPEN	**OPEN**	OPEN	CLOSED	OPEN	OPEN	**CLOSED**	
	#6 Mileground	CLOSED	OPEN	**OPEN**	OPEN	**OPEN**	**CLOSED**	OPEN	OPEN	
	#7 University Ave	CLOSED	OPEN	**OPEN**	OPEN	**OPEN**	OPEN	**CLOSED**	OPEN	Low Voltage
	#4 Pineview	CLOSED	OPEN	**OPEN**	OPEN	**OPEN**	OPEN	OPEN	**CLOSED**	
	NA	CLOSED	OPEN	CLOSED	OPEN	**OPEN**	OPEN	OPEN	OPEN	

The following table shows the Load flow and Fault analysis results for the existing system.

Table E - 2: Load flow and Fault analysis results for the existing system

Feeder	Total kVA	Max Conductor Loading	Min Downline Voltage (%)	Min Downline Voltage (V)
#3 Stewart Street	4,801	69	99.1	118.92
#4 Pineview	3,887	40.6	102.87	123.444
#5 Easton	5,162	37.3	101.54	121.848
#5 Van Voorhis	1,330	24.6	103.31	123.972
#6 Mileground	3,049	45.9	102.73	123.276
#7 University Ave	2,762	30.2	102.06	122.472
#8 Mon Hosp	2,611	35.4	103.15	123.78

The following table lists the Minimum down line voltage and maximum conductor loading for each scenario of circuit#3 – Stewart Circuit.

Table E - 3: Minimum down line voltage and maximum conductor loading for each scenario of circuit#3 – Stewart Circuit

Fault	Scenarios - #3 Stewart Street	Load Transferred To	Total kVA	Max Conductor Loading	Min Downline Voltage (%)	Min Downline Voltage (V)
VZ-1	Scenario - 1	#5 Easton	9,668	67	97.1	116.52
	Scenario - 2	#6 Mileground	7,666	196.5	91.71	110.052
	Scenario - 3	#7 University Ave	7,350	98	96.24	115.488
	Scenario - 4	#4 Pineview	8,368	61	99.81	119.772
VZ-2	Scenario - 5	#6 Mileground	5,779	142.2	96.12	115.344
	Scenario - 6	#7 University Ave	5,515	72.9	96.85	116.22
	Scenario - 7	#4 Pineview	6,608	60.9	99.36	119.232
VZ-3	Scenario - 8	#6 Mileground	4,568	49.4	102.26	122.712
	Scenario - 9	#7 University Ave	4,290	60.1	100.53	120.636
	Scenario - 10	#4 Pineview	5,387	59.7	101.27	121.524
VZ-4	Scenario - 11	NA	NA	NA	NA	

The above results reveal that there is at least one successful scenario in which the circuit can be reconfigured and fed by one of the adjacent circuits when there is a fault in any of the zones.

Following figure shows the zones defined in circuit#4 –Pine View.

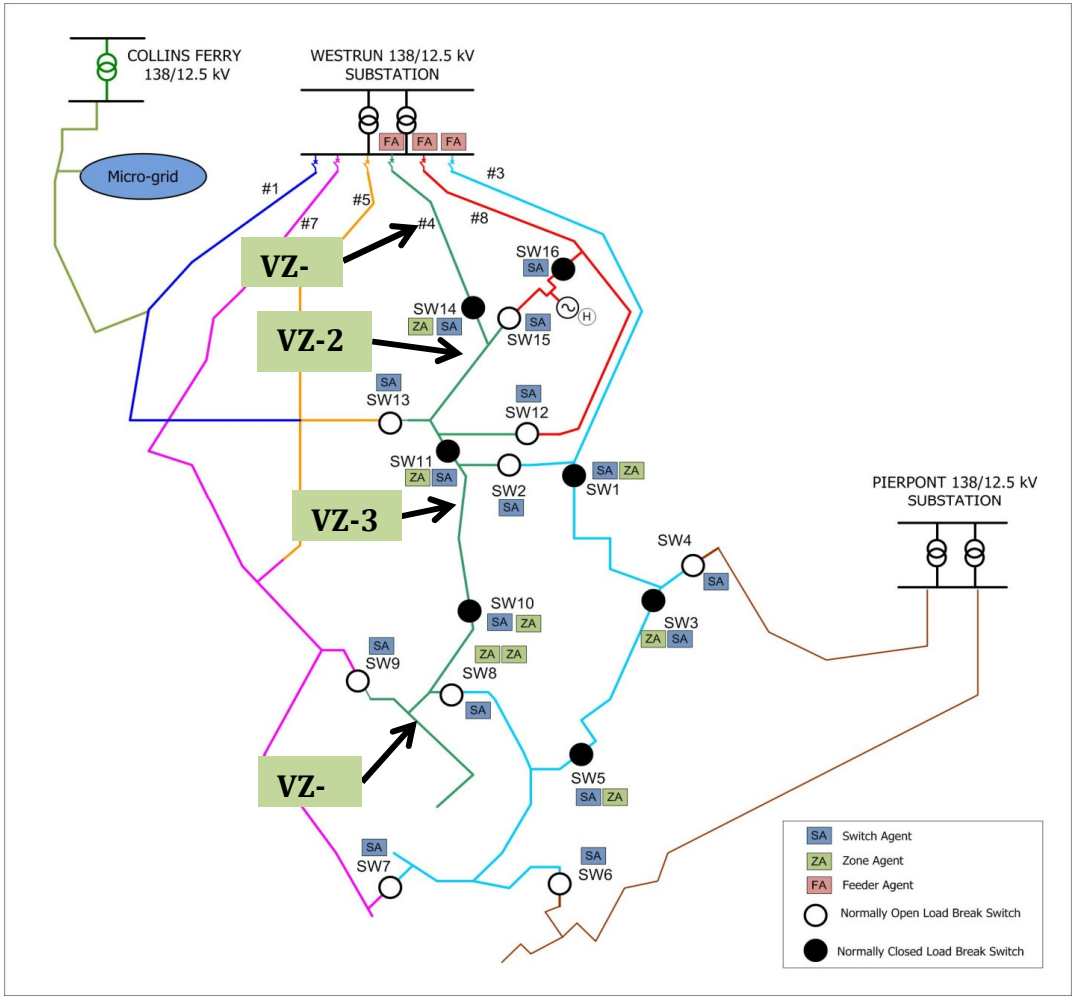

Figure E - 2: Circuit#4 –Pine View

Following table shows the switch status for all of the possible scenarios for faults in different zones of circuit#4 –Pine View.

Table E - 4: Switch Status in circuit#4 –Pine View

			Switch Status									
Fault	Scenarios - #4 Pineview	Load Transferred To	SW2	SW8	SW9	SW10	SW11	SW12	SW13	SW14	SW15	Notes
NA	Exisiting System	NA	OPEN	OPEN	OPEN	CLOSED	CLOSED	OPEN	OPEN	CLOSED	OPEN	
VZ-1	Scenario - 1	#8 Mon Hosp	OPEN	OPEN	OPEN	CLOSED	CLOSED	OPEN	OPEN	**OPEN**	**CLOSED**	
	Scenario - 2	#5 Van Voorhis	OPEN	OPEN	OPEN	CLOSED	CLOSED	OPEN	**CLOSED**	**OPEN**	OPEN	
	Scenario - 3	#7 University Ave	OPEN	OPEN	**CLOSED**	CLOSED	CLOSED	OPEN	OPEN	**OPEN**	OPEN	
	Scenario - 4	#3 Stewart Street	**CLOSED**	OPEN	OPEN	CLOSED	CLOSED	OPEN	OPEN	**OPEN**	OPEN	Low Voltage
VZ-2	Scenario - 5	#3 Stewart Street	**CLOSED**	OPEN	OPEN	CLOSED	**OPEN**	OPEN	OPEN	**OPEN**	OPEN	Low Voltage
	Scenario - 6	#7 University Ave	OPEN	OPEN	**CLOSED**	CLOSED	**OPEN**	OPEN	OPEN	**OPEN**	OPEN	
VZ-3	Scenario - 7	#3 Stewart Street	OPEN	**CLOSED**	OPEN	**OPEN**	**OPEN**	OPEN	OPEN	CLOSED	OPEN	Low Voltage
	Scenario - 8	#7 University Ave	OPEN	OPEN	**CLOSED**	**OPEN**	**OPEN**	OPEN	OPEN	CLOSED	OPEN	
VZ-4	Scenario - 11	NA	OPEN	OPEN	OPEN	**OPEN**	CLOSED	OPEN	OPEN	CLOSED	OPEN	

The following table lists the Minimum down line voltage and maximum conductor loading for each scenario of circuit#4 –Pine View.

Table E - 5: Minimum down line voltage and maximum conductor loading for each scenario of circuit#4 –Pine View

Fault	Scenarios - #4 Pineview	Load Transferred To	Total kVA	Max Conductor Loading	Min Downline Voltage (%)	Min Downline Voltage (V)
VZ-1	Scenario - 1	#8 Mon Hosp	5,683	75	101.23	121.5
	Scenario - 2	#5 Van Voorhis	4,315	40.8	102.26	122.7
	Scenario - 3	#7 University Ave	5,899	68.6	99.75	119.7
	Scenario - 4	#3 Stewart Street	7,907	70.9	99.63	119.6
VZ-2	Scenario - 5	#3 Stewart Street	7,107	70.2	99.05	118.9
	Scenario - 6	#7 University Ave	4,911	58.4	99.61	119.5
VZ-3	Scenario - 7	#3 Stewart Street	5,524	79.9	98.01	117.6
	Scenario - 8	#7 University Ave	3,405	39.6	101.45	121.7
VZ-4	Scenario - 11	NA				0.0

The above results reveal that there is at least one successful scenario in which the circuit can be reconfigured and fed by one of the adjacent circuits when there is a fault in any of the zones.

Following figure shows the zones defined in circuit#8 – Mon Hosp.

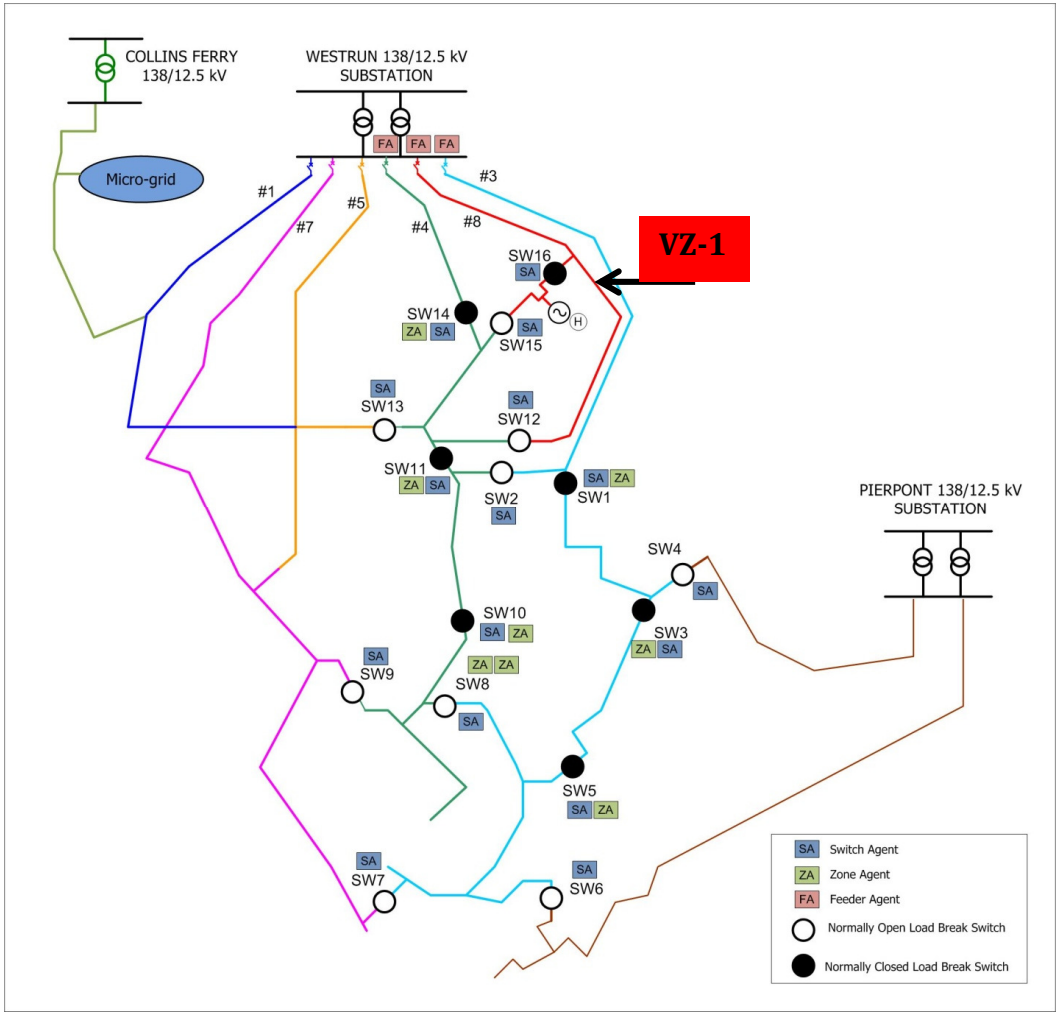

Figure E - 3: Circuit#8 – Mon Hosp

Table E - 6: Switch status in circuit#8 – Mon Hospital

			Switch Status			
Fault	Scenarios - #8 Mon Hosp	Load Transferred To	SW12	SW15	SW16	Notes
NA	Existing System	NA	OPEN	OPEN	CLOSED	
VZ-1	Scenario - 1	#4 Pineview	OPEN	**CLOSED**	**OPEN**	

The following table lists the Minimum down line voltage and maximum conductor loading for each scenario of circuit#8 – Mon Hospital.

Table E - 7: Minimum down line voltage and maximum conductor loading for each scenario of circuit#8 – Mon Hosp

Fault	Scenarios - #8 Mon Hosp	Load Transferred To	Total kVA	Max Conductor Loading	Min Downline Voltage (%)	Min Downline Voltage (V)
VZ-1	Scenario - 1	#4 Pineview	4,805	40.8	102.4	122.9

The above results reveal that there is at least one successful scenario in which the circuit can be reconfigured and fed by one of the adjacent circuits when there is a fault in any of the zones.

D.2 CYME Dynamic Stability Results

This appendix section provides all detailed CYME stability analysis results for all of the events mentioned in the table below. The figure below shows the CYME dynamic stability model of the WVSC microgrid. This figure displays all CYME nodes and node names, which are used in the stability result charts as legends.

Table D - 8: CYME Dynamic Stability Events and Results

Events	Simulation Result
10 cycle fault at Bldg. 3592 LV Bus	Unstable
5 cycle fault at Bldg. 3592 LV Bus	Stable
10 cycle fault at Bldg. 3592 MV Bus	Unstable
5 cycle fault at Bldg. 3592 MV Bus	Stable
10 cycle fault at Bldg. 3596 LV Bus	Unstable
5 cycle fault at Bldg. 3596 LV Bus	Stable
10 cycle fault at Bldg. 3596 MV Bus	Unstable
5 cycle fault at Bldg. 3596 MV Bus	Stable
10 cycle fault at generator interconnection bus	Unstable
5 cycle fault at generator interconnection bus	Stable
Loss of 24kW BESS PV System	Stable
Loss of 21 kW Microinverter System	Stable
Simultaneous loss of 24kW BESS PV System and 21 kW Microinverter System	Stable

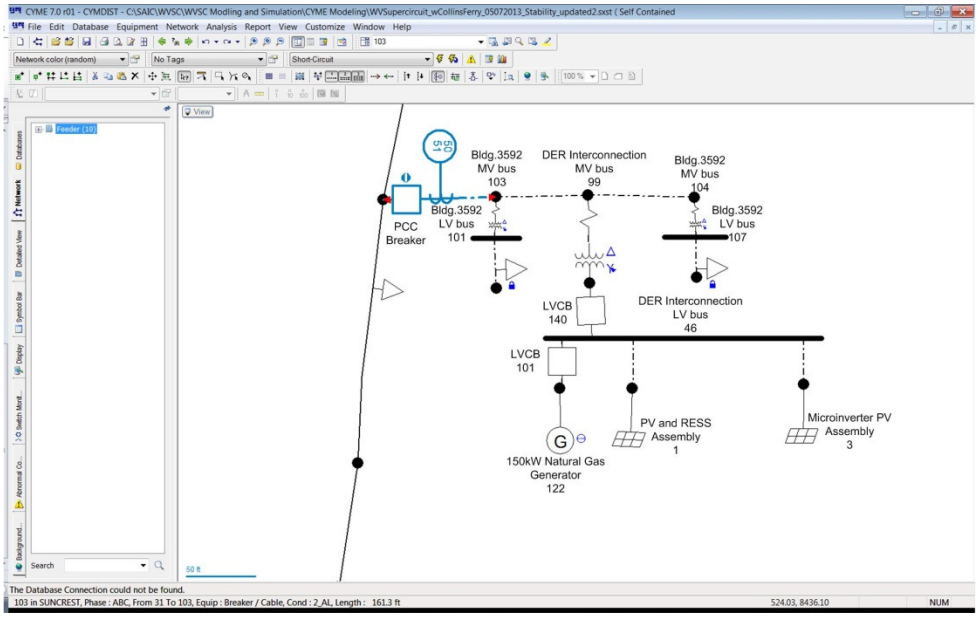

Figure E - 4: CYME Dynamic Microgrid Model

D.2.1 10 Cycle Fault at Bldg.3592 LV Bus (101):

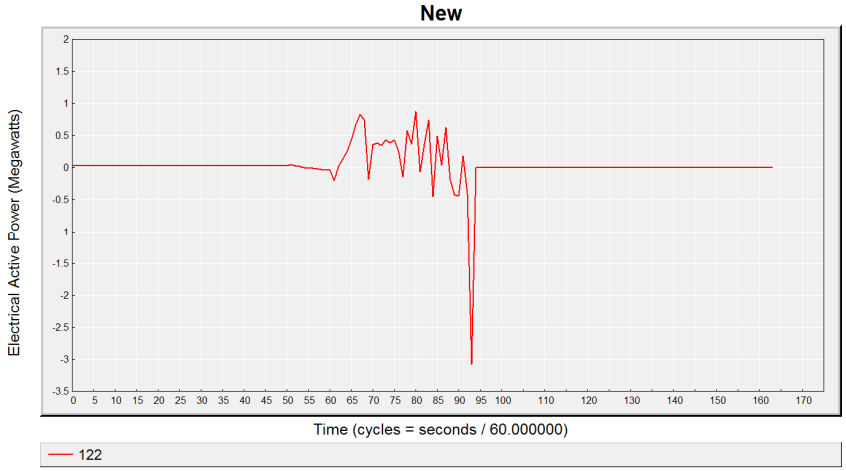

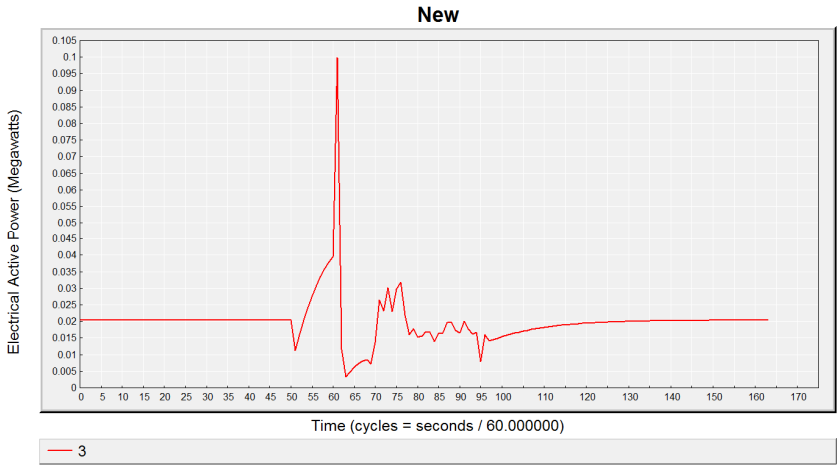

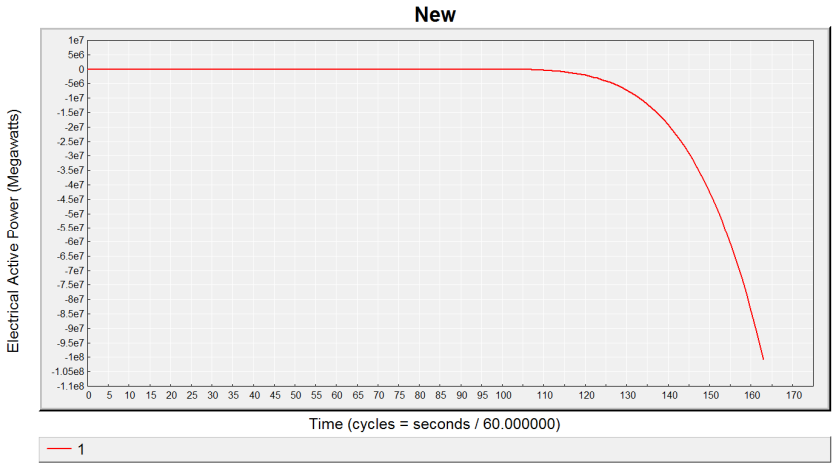

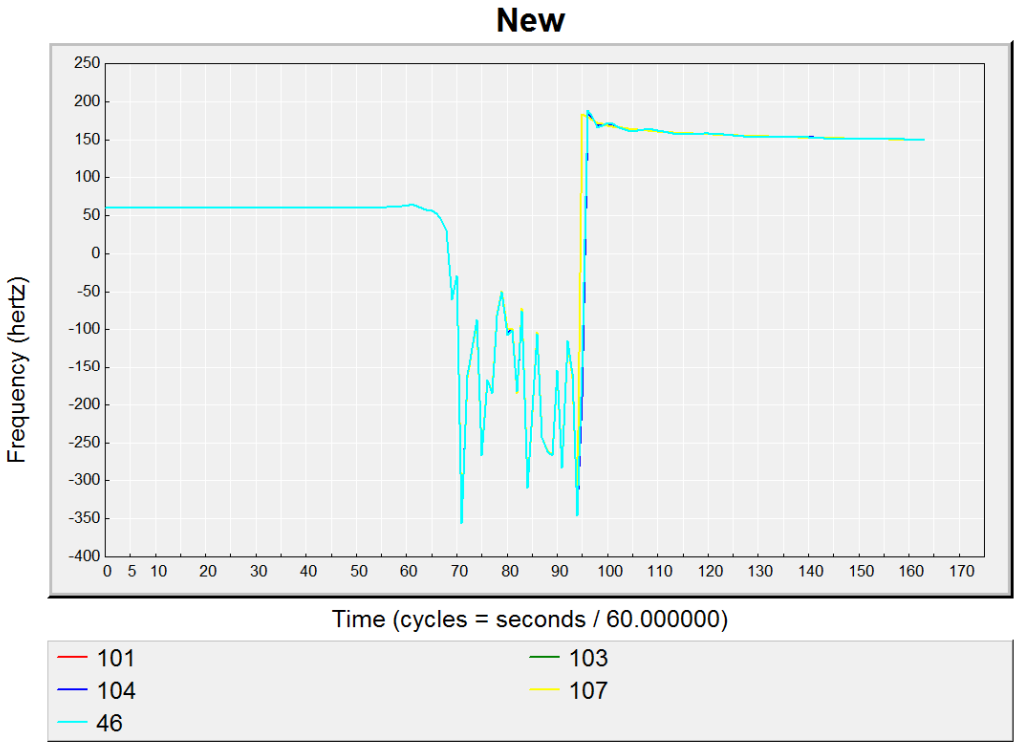
New
Frequency (hertz)
250
200
150
100
50
0
-50
-100
-150
-200
-250
-300
-350
-400
0 5 10 20 30 40 50 60 70 80 90 100 110 120 130 140 150 160 170
Time (cycles = seconds / 60.000000)
101
103
104
107
46

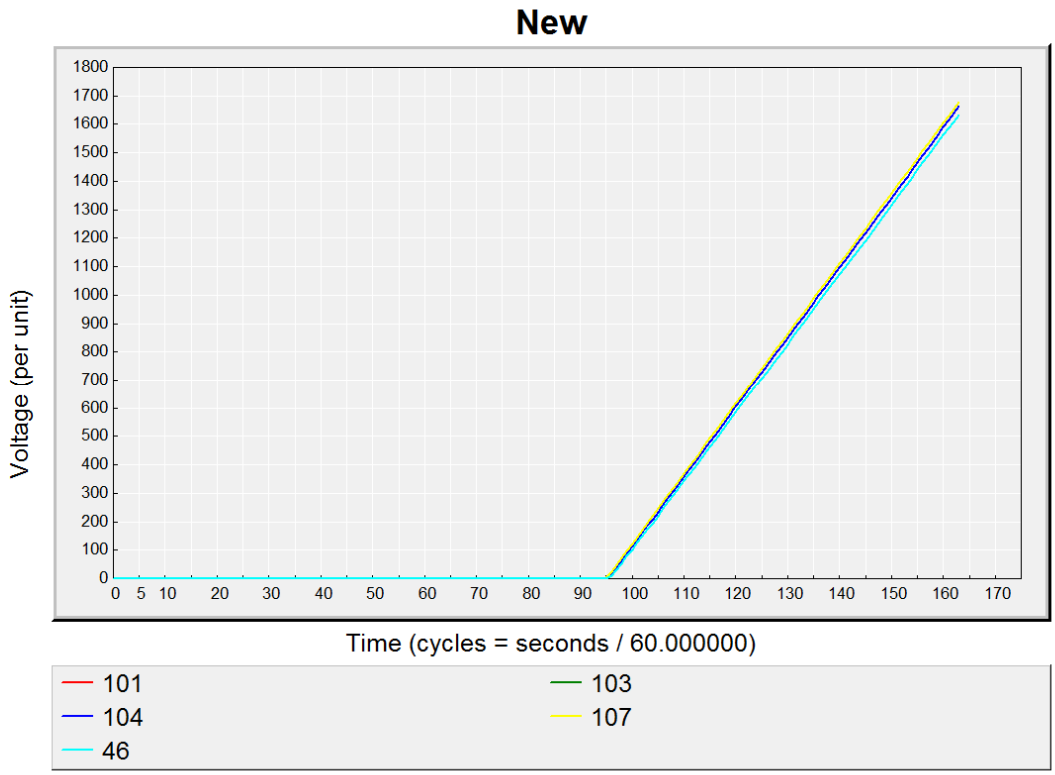
New
Voltage (per unit)
1800
1700
1600
1500
1400
1300
1200
1100
1000
900
800
700
600
500
400
300
200
100
0
0 5 10 20 30 40 50 60 70 80 90 100 110 120 130 140 150 160 170
Time (cycles = seconds / 60.000000)
101
103
104
107
46

D.2.2 5 Cycle Fault at Bldg.3592 LV Bus (101):

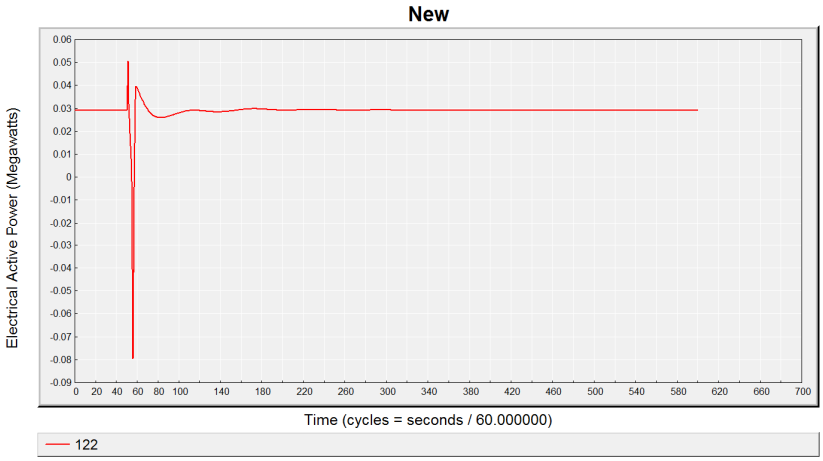

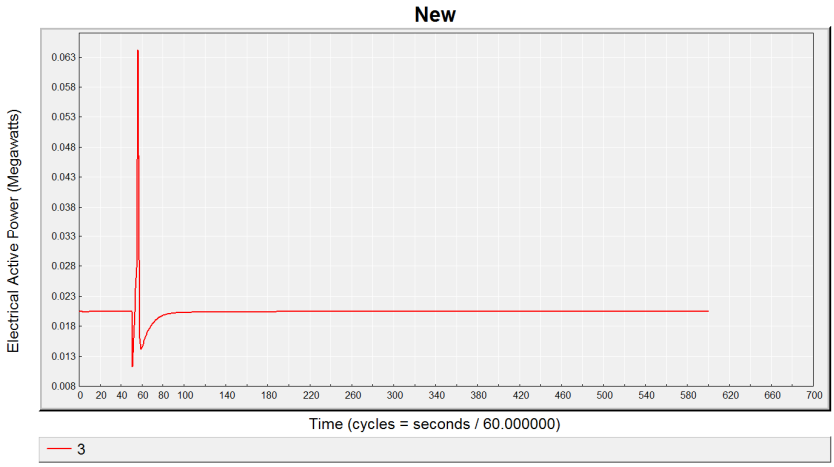

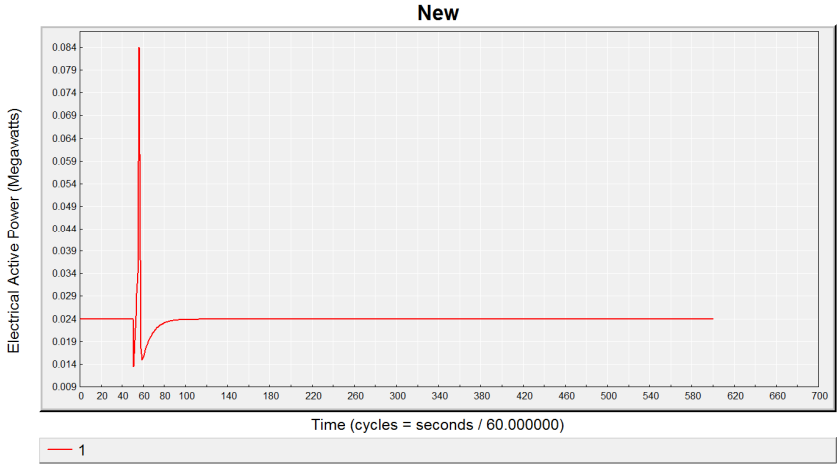

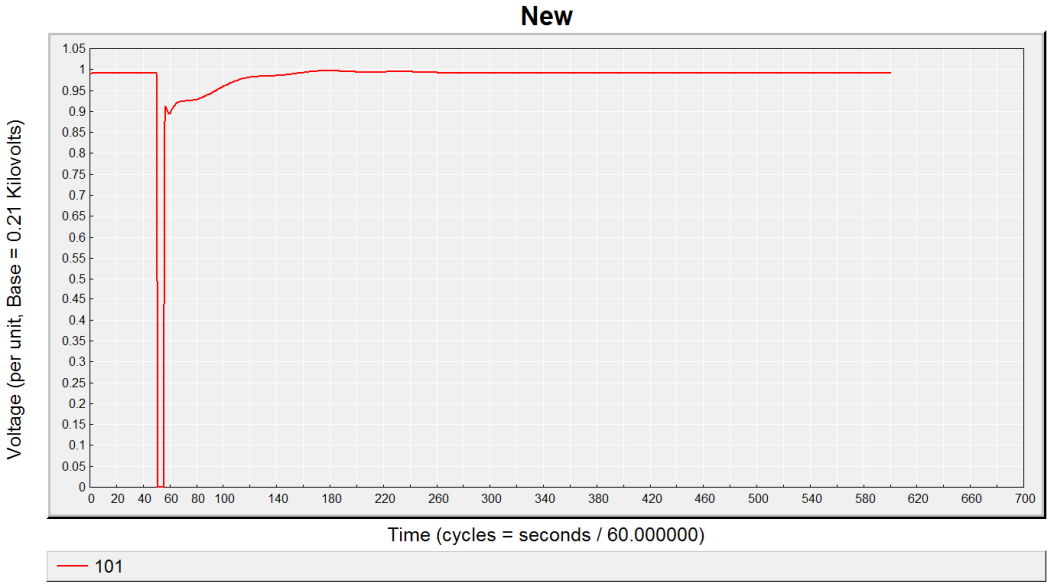
New
Voltage (per unit, Base = 0.21 Kilovolts)
1.05
1
0.95
0.9
0.85
0.8
0.75
0.7
0.65
0.6
0.55
0.5
0.45
0.4
0.35
0.3
0.25
0.2
0.15
0.1
0.05
0
0 20 40 60 80 100 140 180 220 260 300 340 380 420 460 500 540 580 620 660 700
Time (cycles = seconds / 60.000000)
101

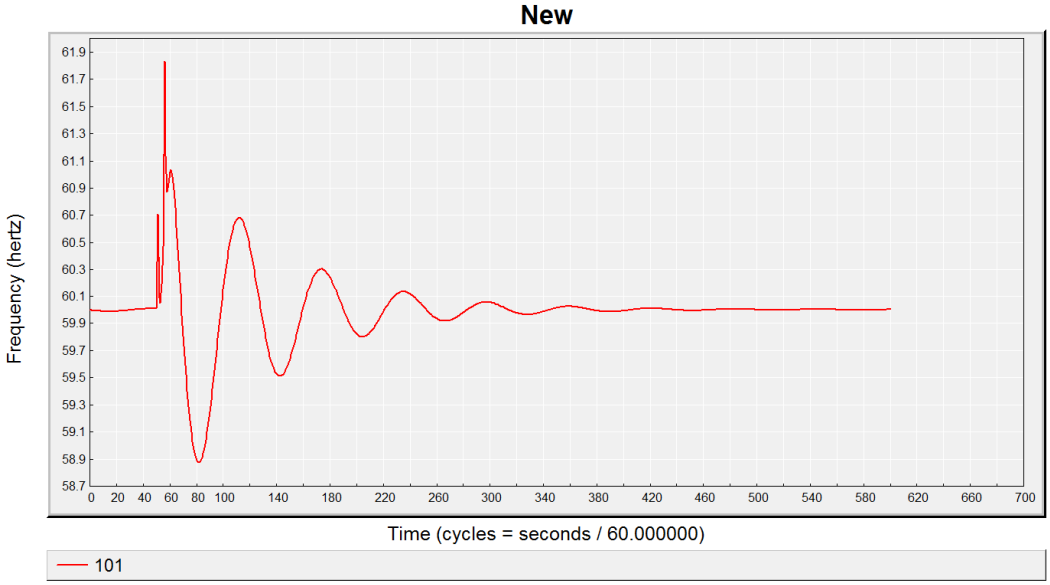
New
Frequency (hertz)
61.9
61.7
61.5
61.3
61.1
60.9
60.7
60.5
60.3
60.1
59.9
59.7
59.5
59.3
59.1
58.9
58.7
0 20 40 60 80 100 140 180 220 260 300 340 380 420 460 500 540 580 620 660 700
Time (cycles = seconds / 60.000000)
101

D.2.3 10 Cycle Fault at Bldg.3592 MV Bus (103):

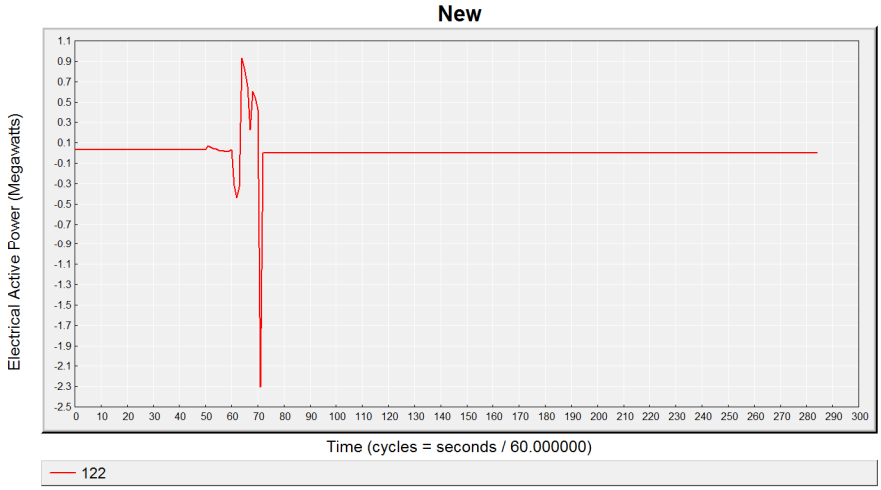

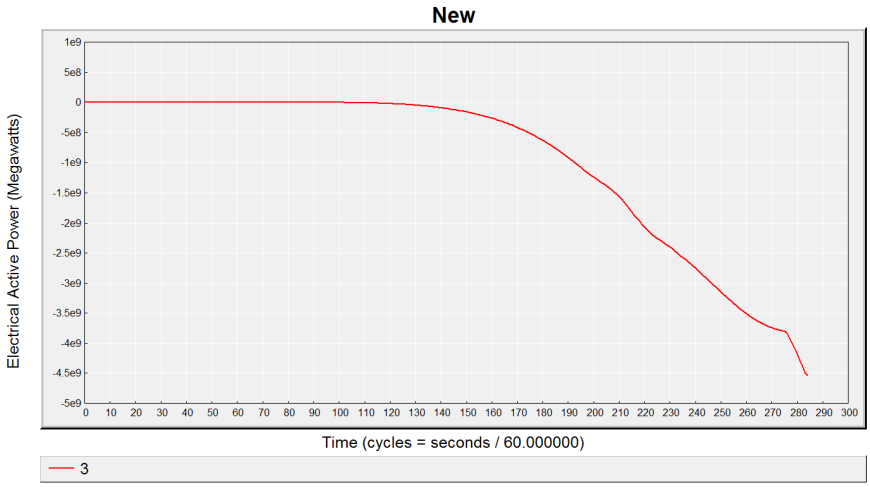

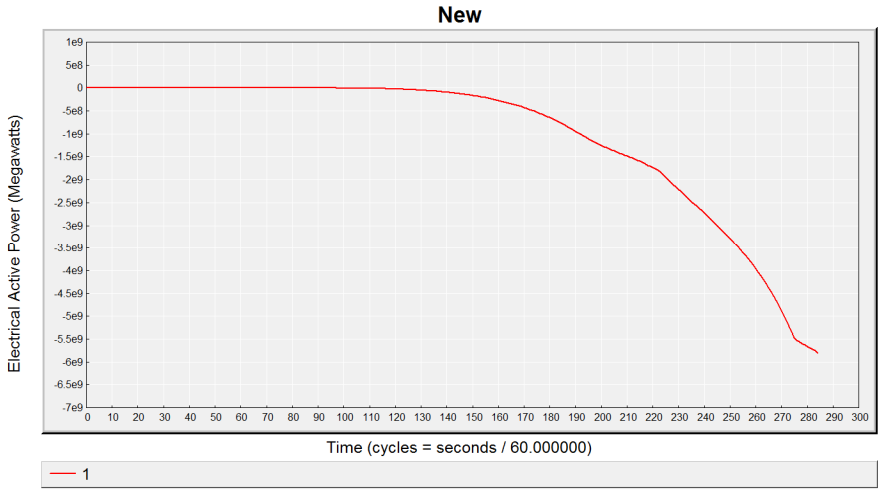

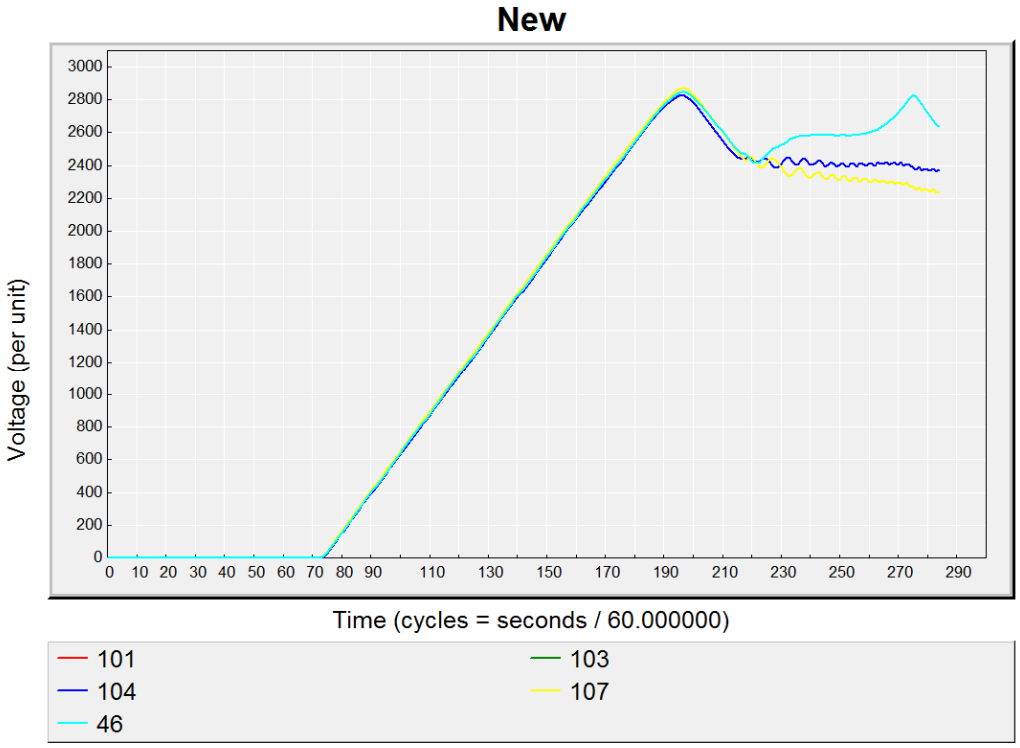
New
Voltage (per unit)
3000
2800
2600
2400
2200
2000
1800
1600
1400
1200
1000
800
600
400
200
0
0 10 20 30 40 50 60 70 80 90 110 130 150 170 190 210 230 250 270 290
Time (cycles = seconds / 60.000000)
101
103
104
107
46

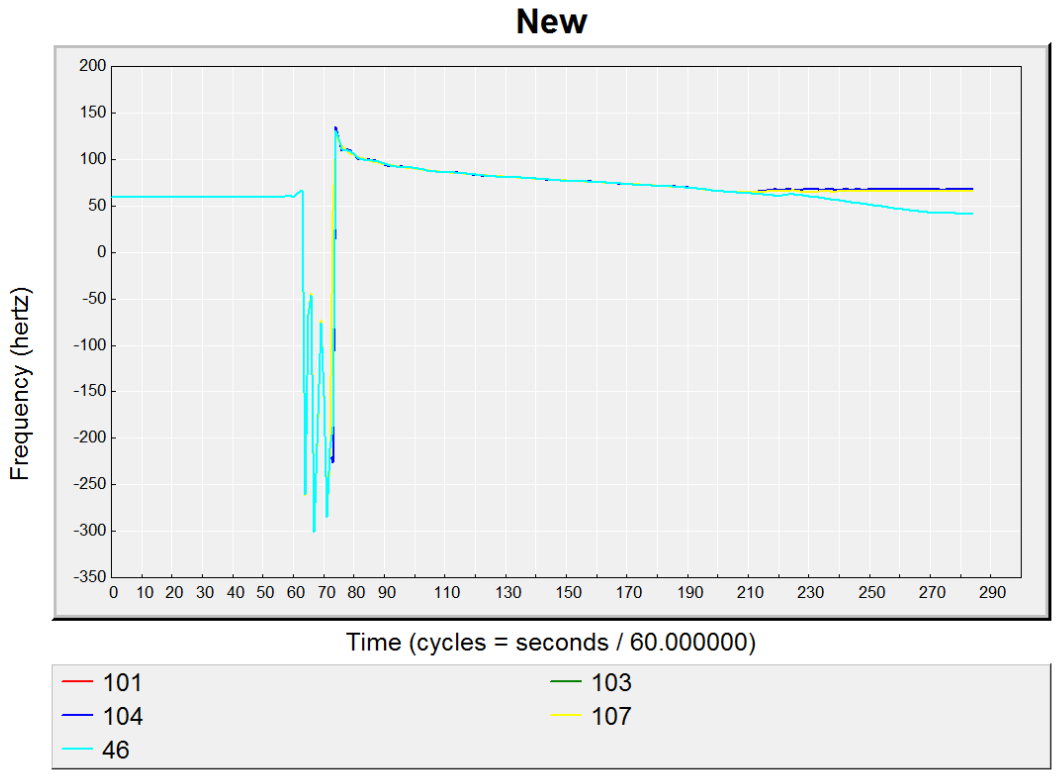
New
Frequency (hertz)
200
150
100
50
0
-50
-100
-150
-200
-250
-300
-350
0 10 20 30 40 50 60 70 80 90 110 130 150 170 190 210 230 250 270 290
Time (cycles = seconds / 60.000000)
101
103
104
107
46

D.2.4 5 Cycle Fault at Bldg.3592 MV Bus (103):

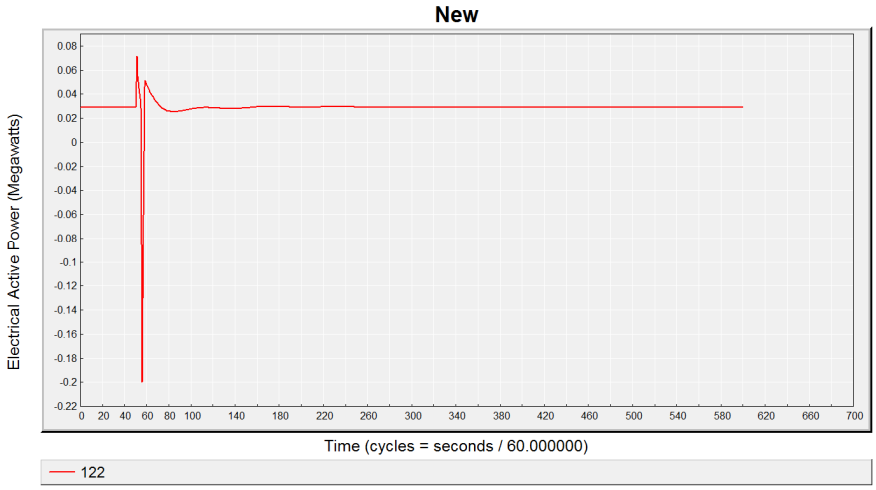

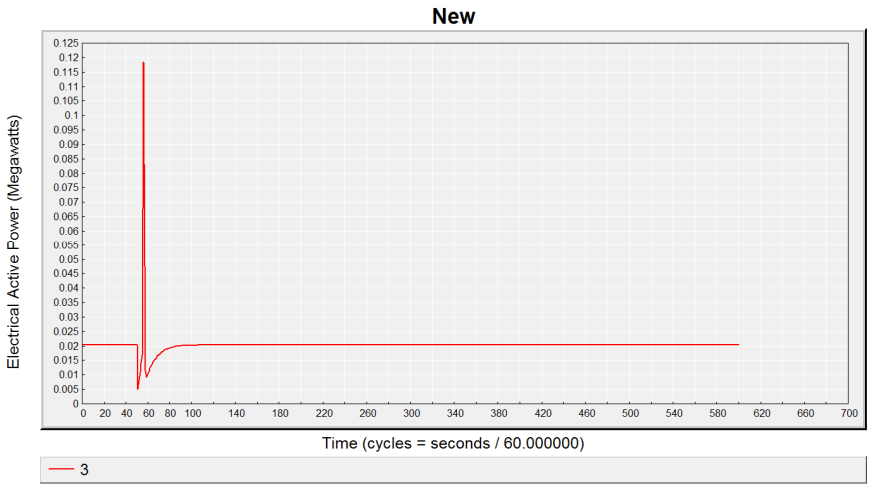

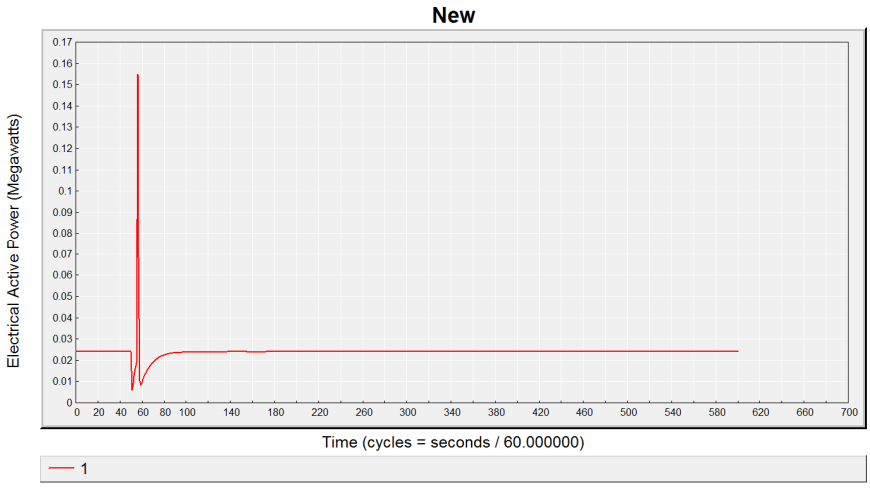

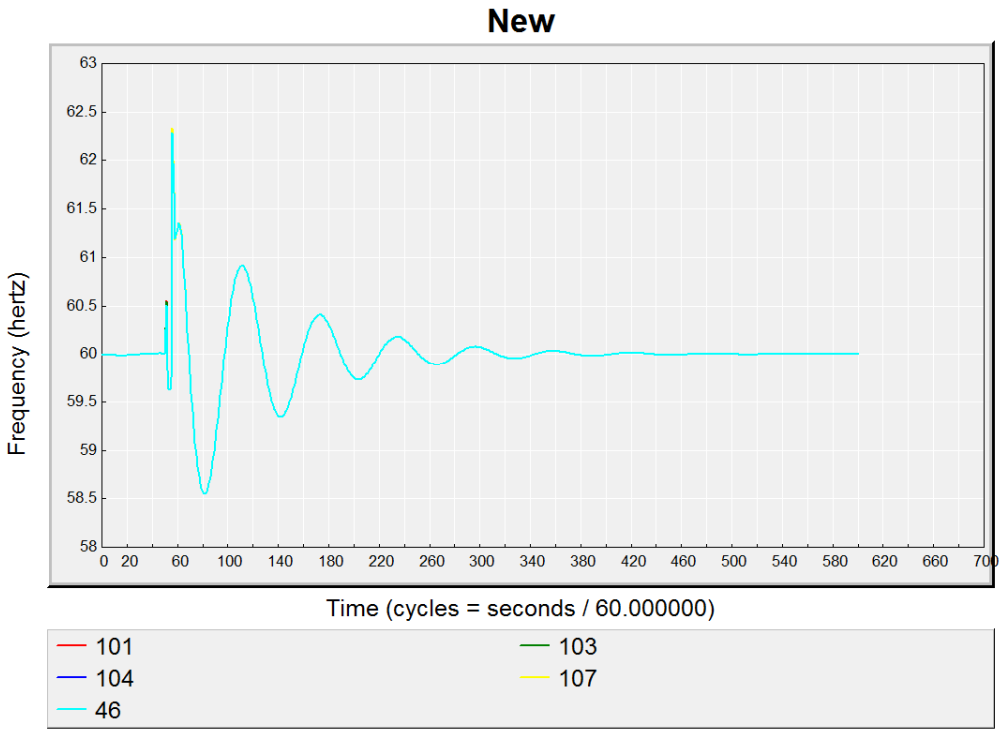
New
Frequency (hertz)
63
62.5
62
61.5
61
60.5
60
59.5
59
58.5
58
0 20 60 100 140 180 220 260 300 340 380 420 460 500 540 580 620 660 700
Time (cycles = seconds / 60.000000)
101
103
104
107
46

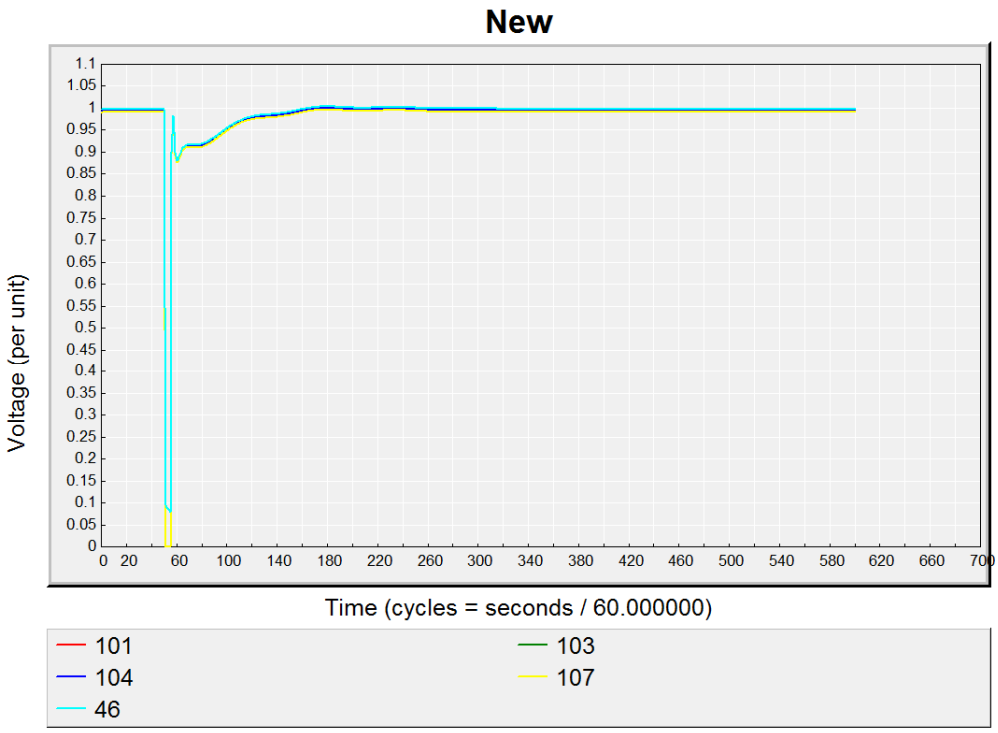
New
Voltage (per unit)
1.1
1.05
1
0.95
0.9
0.85
0.8
0.75
0.7
0.65
0.6
0.55
0.5
0.45
0.4
0.35
0.3
0.25
0.2
0.15
0.1
0.05
0
0 20 60 100 140 180 220 260 300 340 380 420 460 500 540 580 620 660 700
Time (cycles = seconds / 60.000000)
101
103
104
107
46

D.2.5 10 Cycle Fault at Bldg.3596 LV Bus (107):

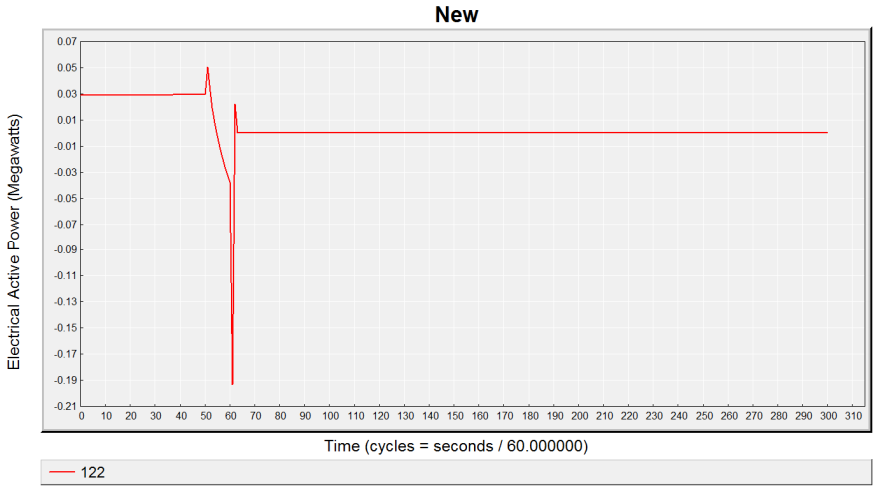

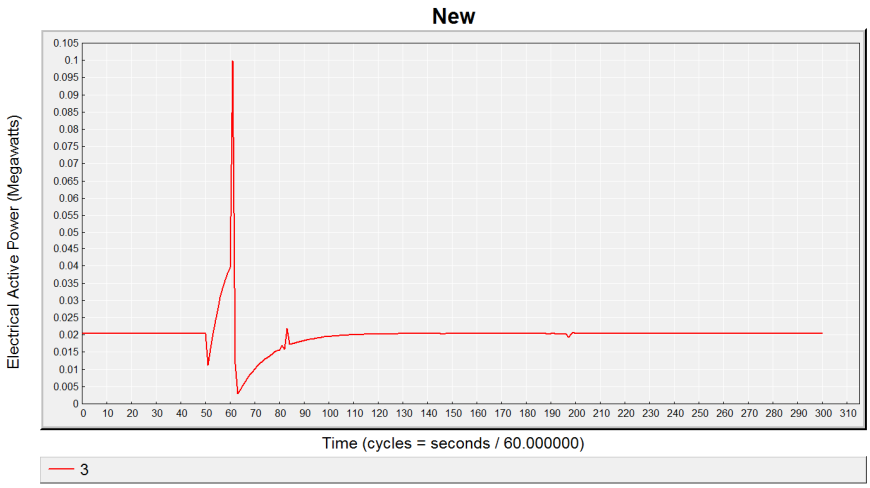

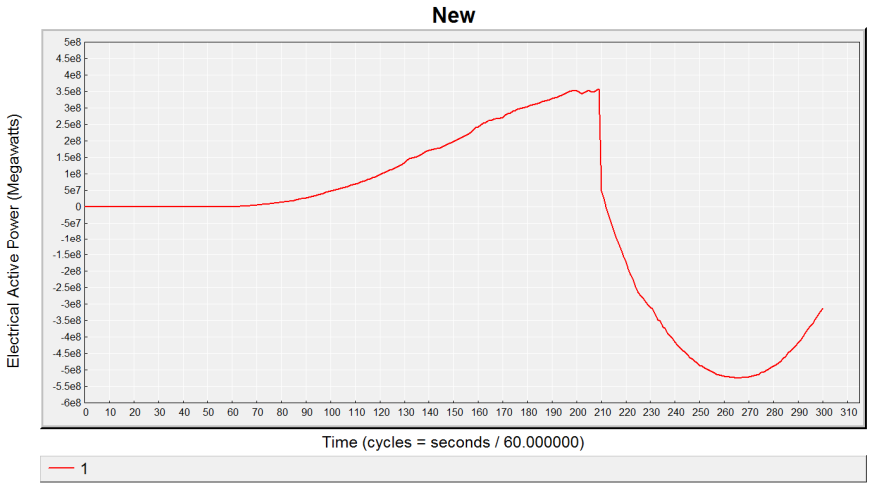

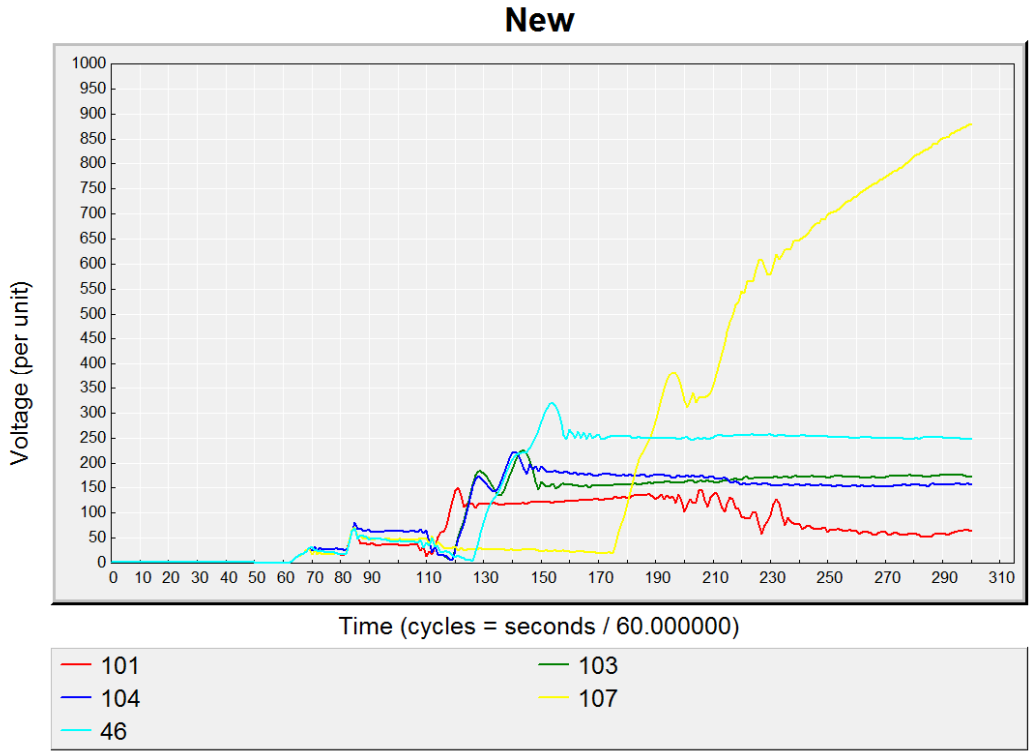
New
Voltage (per unit)
Time (cycles = seconds / 60.000000)
101
103
104
107
46

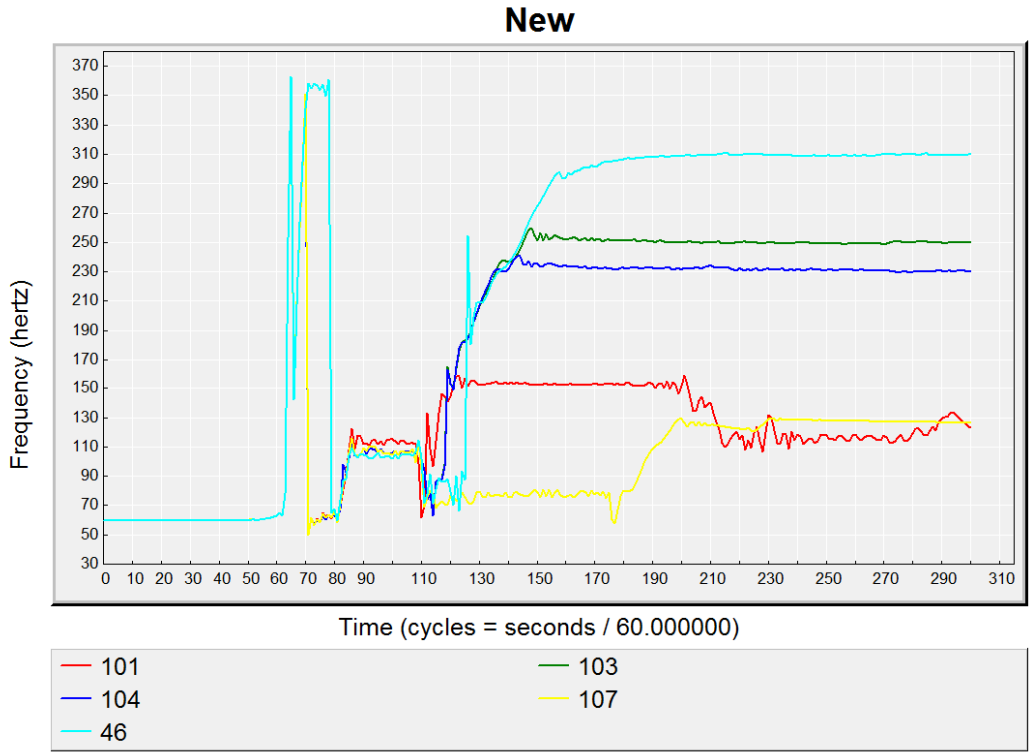
New
Frequency (hertz)
Time (cycles = seconds / 60.000000)
101
103
104
107
46

D.2.6 5 Cycle Fault at Bldg.3596 LV Bus (107):

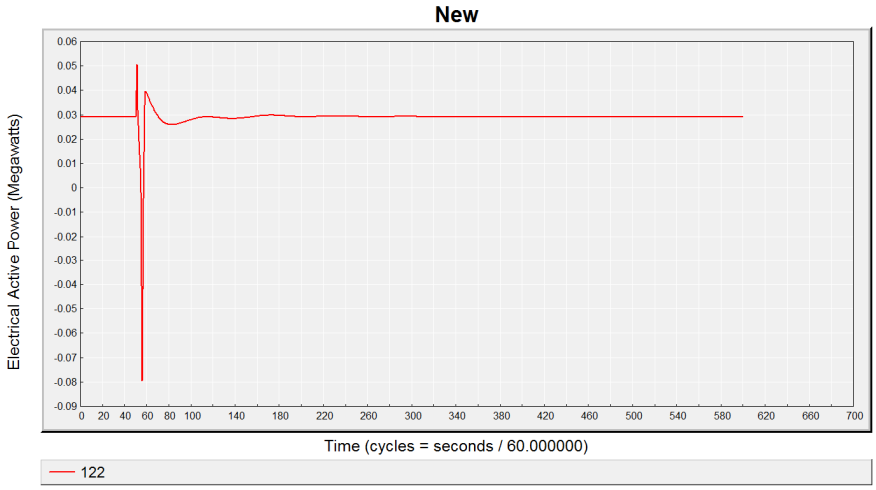

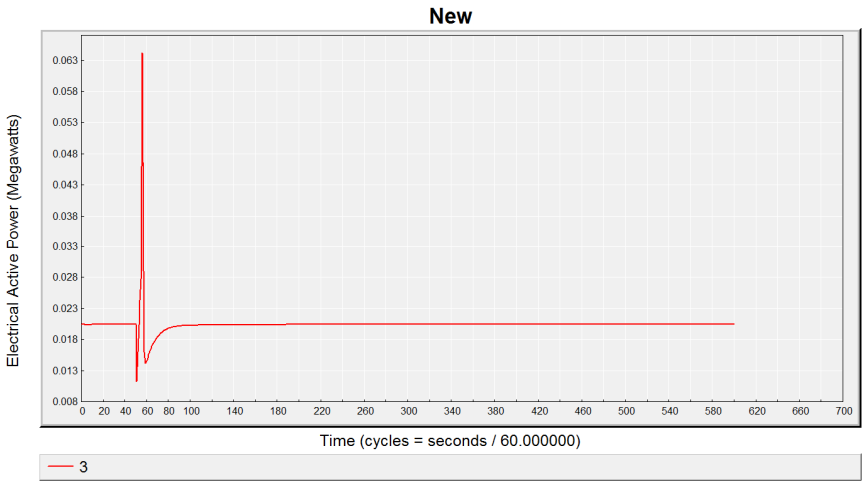

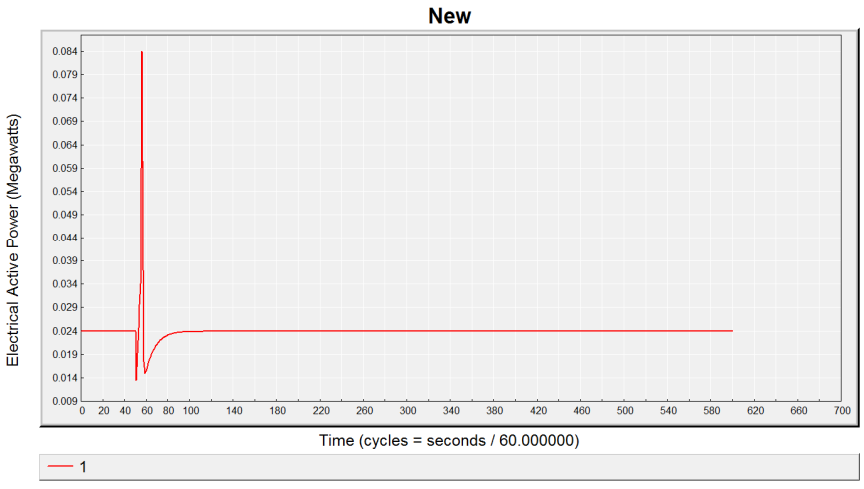

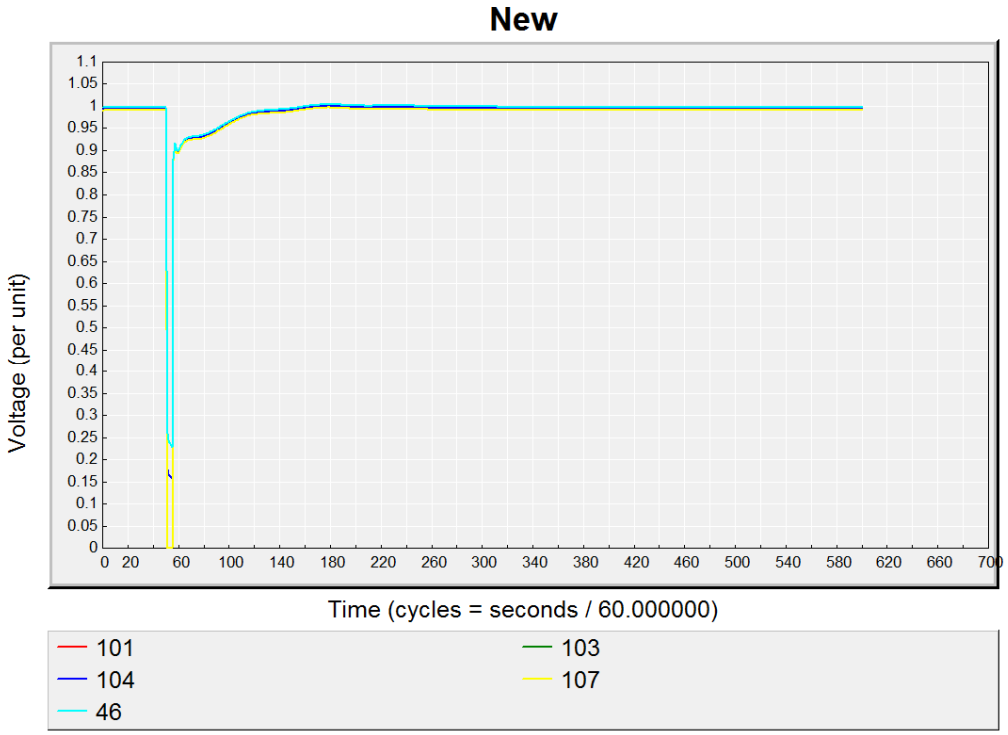
New
Voltage (per unit)
1.1
1.05
1
0.95
0.9
0.85
0.8
0.75
0.7
0.65
0.6
0.55
0.5
0.45
0.4
0.35
0.3
0.25
0.2
0.15
0.1
0.05
0
0 20 60 100 140 180 220 260 300 340 380 420 460 500 540 580 620 660 700
Time (cycles = seconds / 60.000000)
101
103
104
107
46


New
Frequency (hertz)
61.9
61.7
61.5
61.3
61.1
60.9
60.7
60.5
60.3
60.1
59.9
59.7
59.5
59.3
59.1
58.9
58.7
0 20 60 100 140 180 220 260 300 340 380 420 460 500 540 580 620 660 700
Time (cycles = seconds / 60.000000)
101
103
104
107
46

DE.2.7 10 Cycle Fault at Bldg.3596 MV Bus (104):

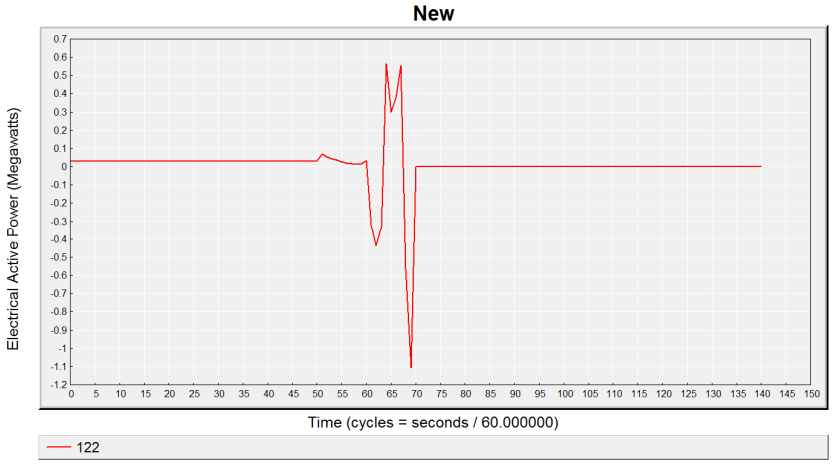

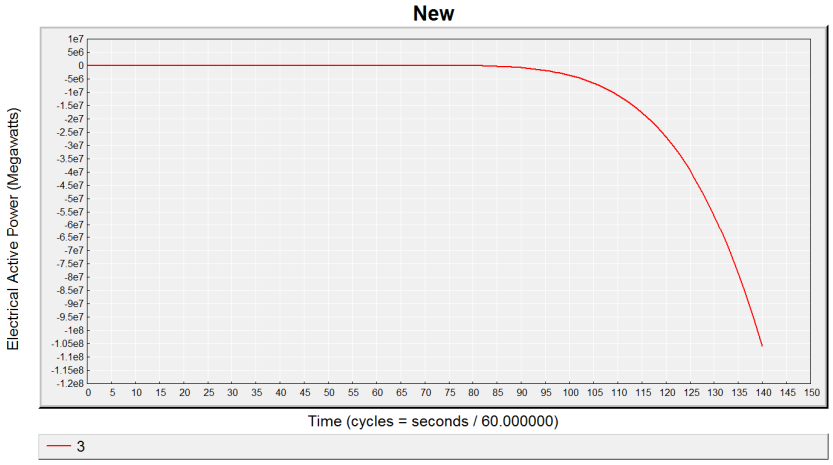

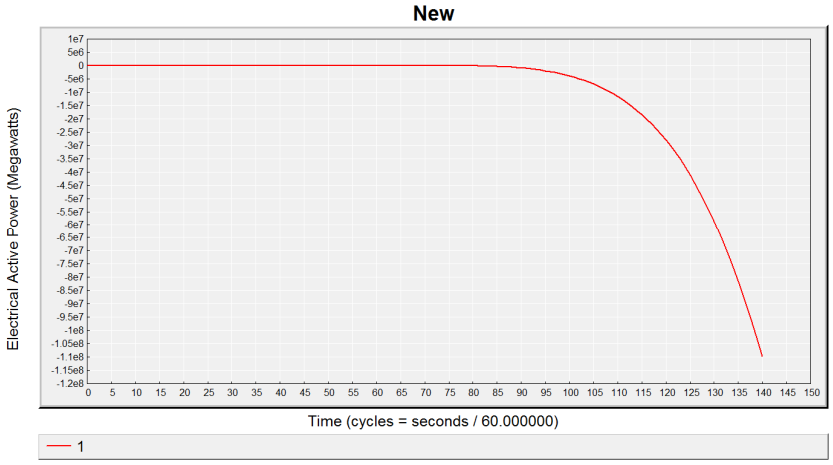

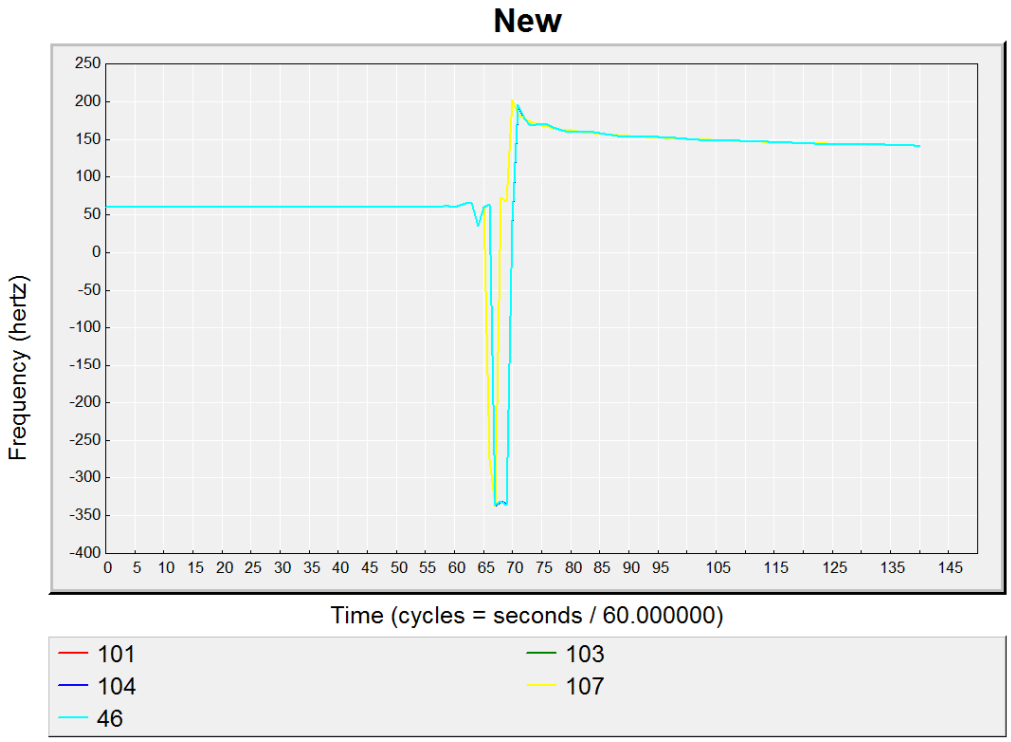
New
Frequency (hertz)
250
200
150
100
50
0
-50
-100
-150
-200
-250
-300
-350
-400
0 5 10 15 20 25 30 35 40 45 50 55 60 65 70 75 80 85 90 95 105 115 125 135 145
Time (cycles = seconds / 60.000000)
101
103
104
107
46

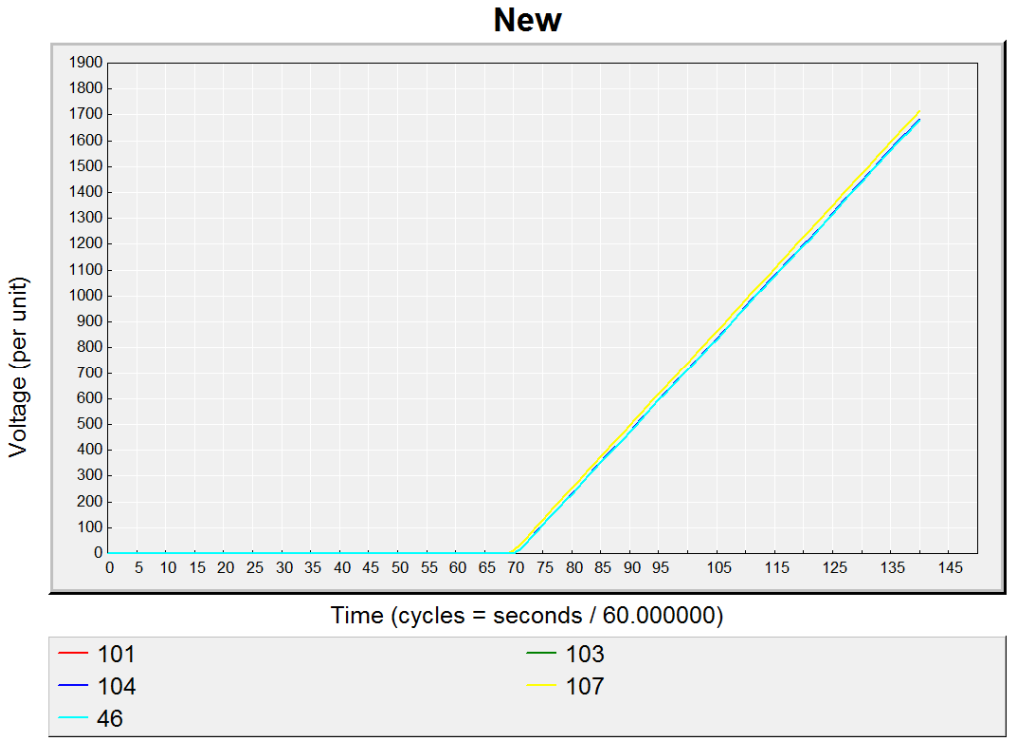
New
Voltage (per unit)
1900
1800
1700
1600
1500
1400
1300
1200
1100
1000
900
800
700
600
500
400
300
200
100
0
0 5 10 15 20 25 30 35 40 45 50 55 60 65 70 75 80 85 90 95 105 115 125 135 145
Time (cycles = seconds / 60.000000)
101
103
104
107
46

DE.2.8 5 Cycle Fault at Bldg.3596 MV Bus (104):

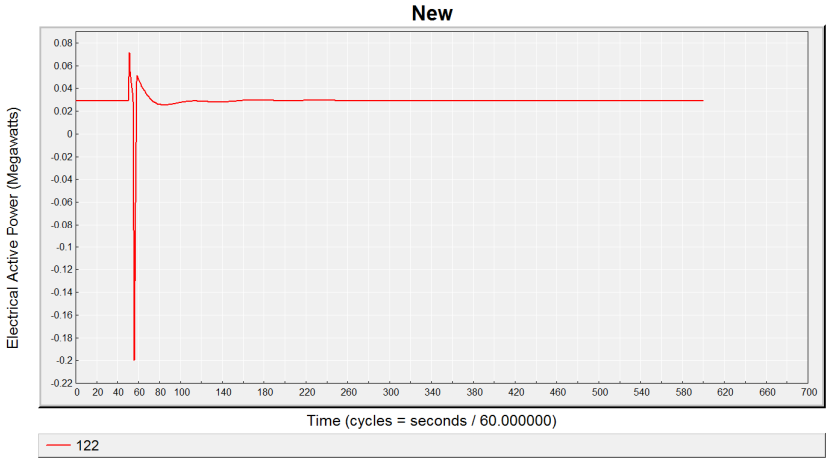

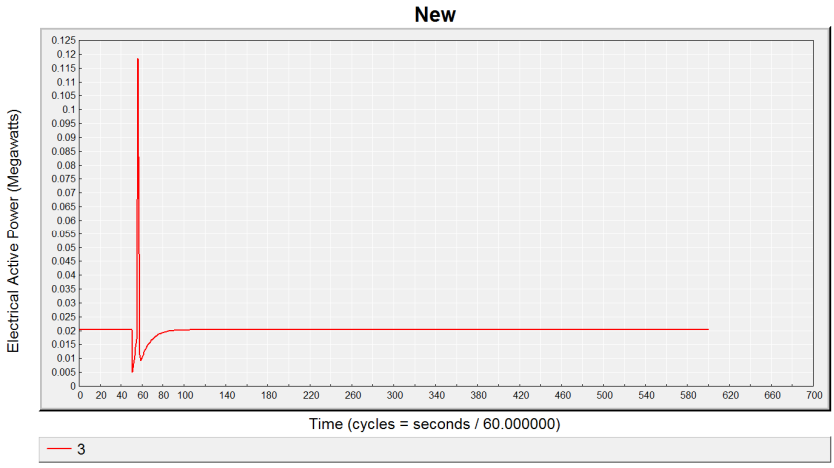

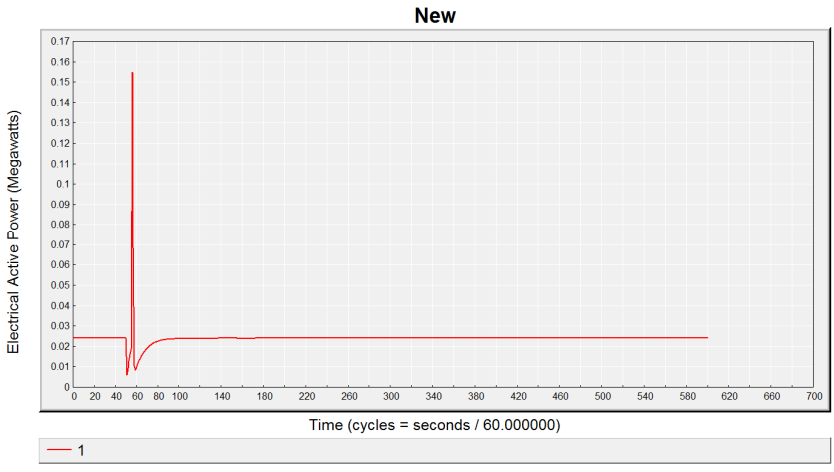

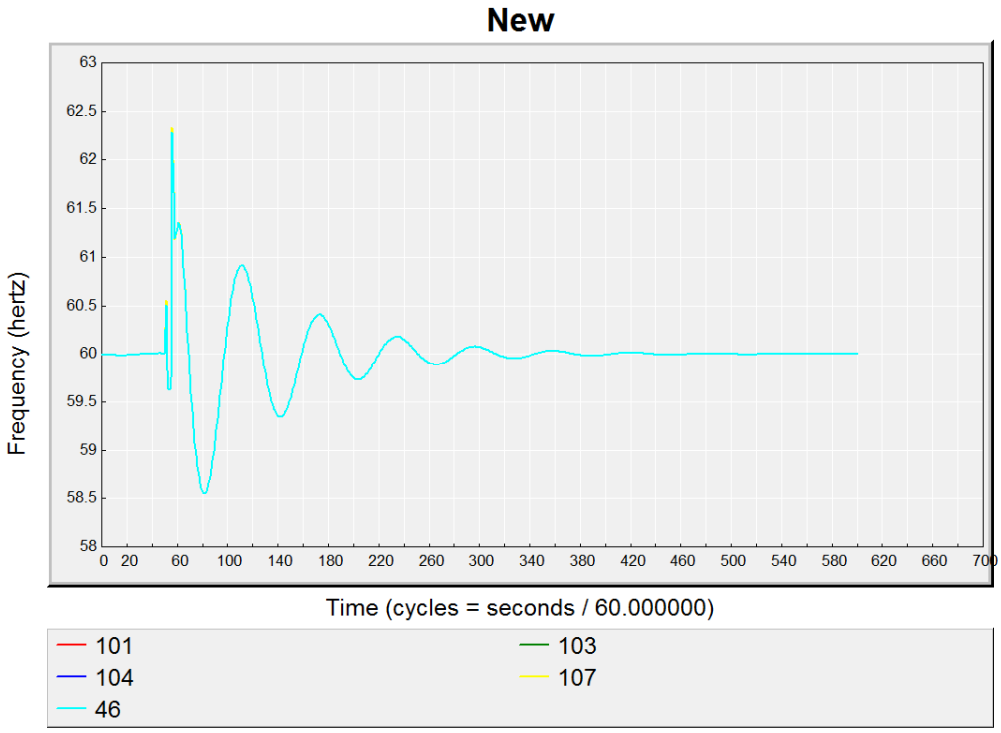
New
Frequency (hertz)
63
62.5
62
61.5
61
60.5
60
59.5
59
58.5
58
0 20 60 100 140 180 220 260 300 340 380 420 460 500 540 580 620 660 700
Time (cycles = seconds / 60.000000)
101
103
104
107
46

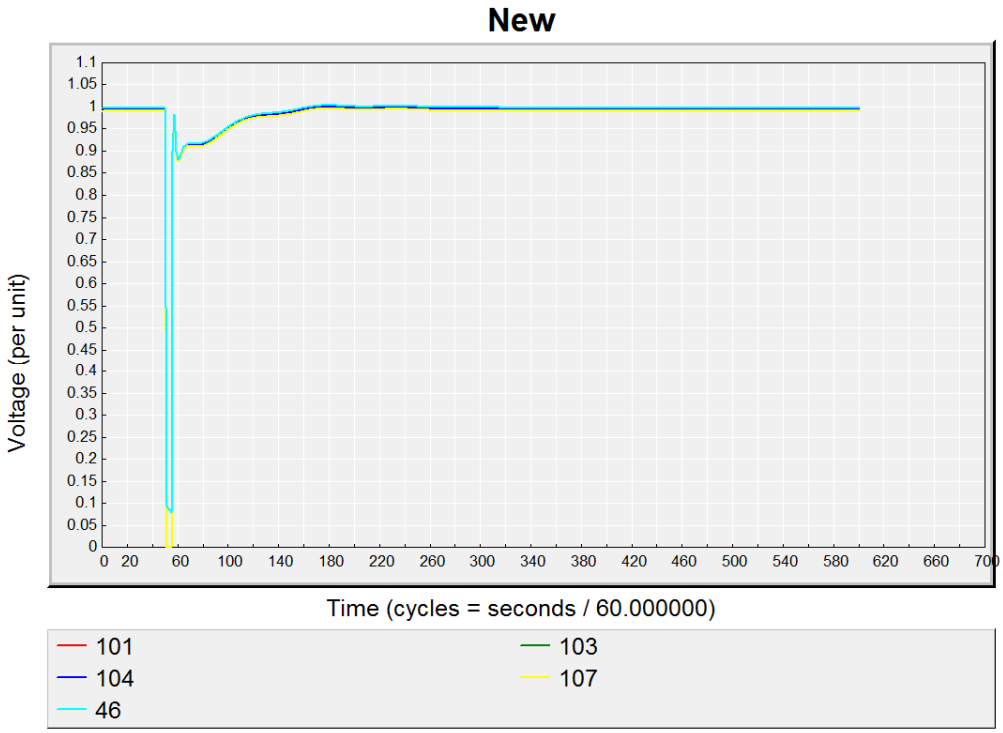
New
Voltage (per unit)
1.1
1.05
1
0.95
0.9
0.85
0.8
0.75
0.7
0.65
0.6
0.55
0.5
0.45
0.4
0.35
0.3
0.25
0.2
0.15
0.1
0.05
0
0 20 60 100 140 180 220 260 300 340 380 420 460 500 540 580 620 660 700
Time (cycles = seconds / 60.000000)
101
103
104
107
46

DE.2.9 10 Cycle Fault at generation interconnection LV bus:

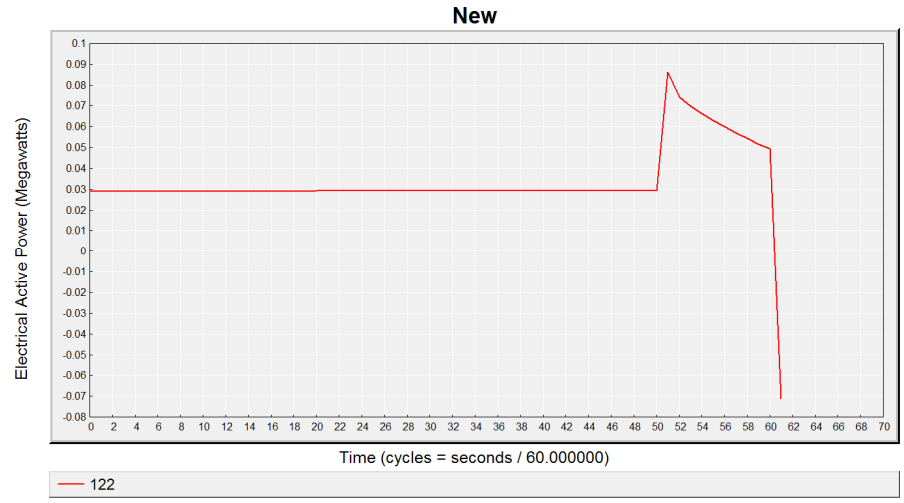

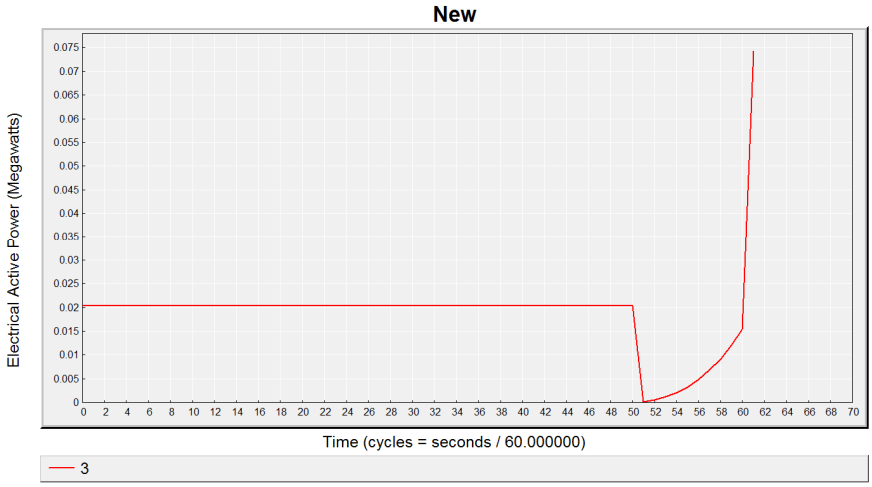

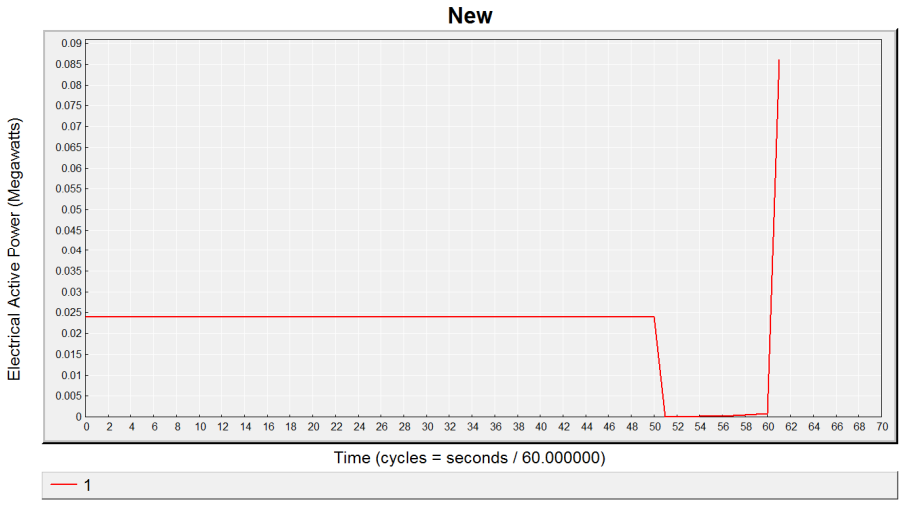

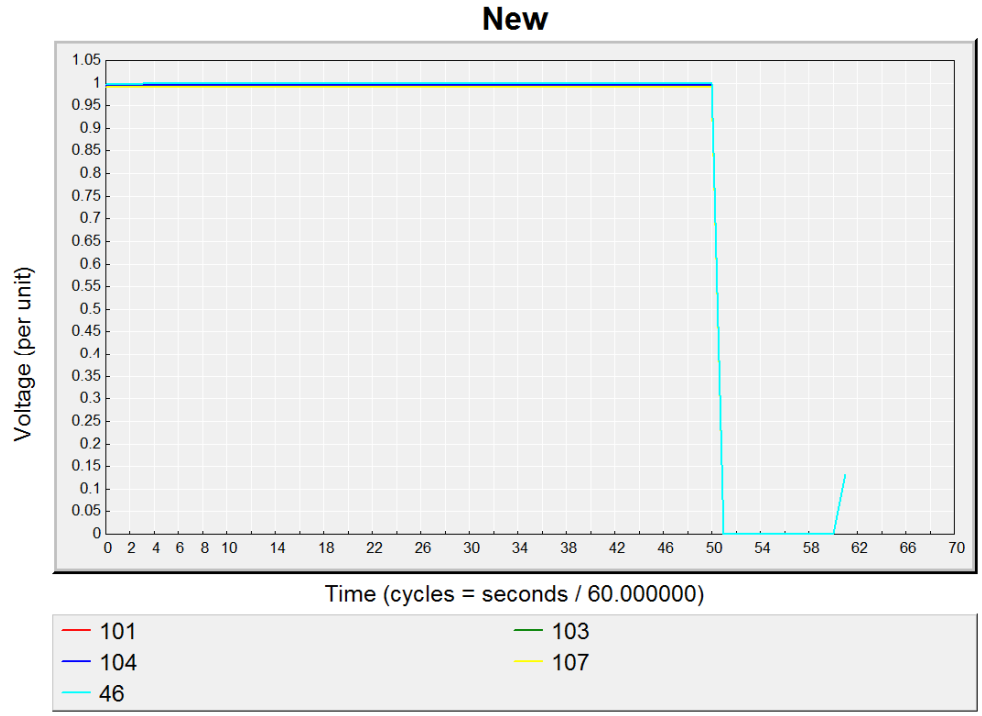
New
Voltage (per unit)
1.05
1
0.95
0.9
0.85
0.8
0.75
0.7
0.65
0.6
0.55
0.5
0.45
0.4
0.35
0.3
0.25
0.2
0.15
0.1
0.05
0
0 2 4 6 8 10 14 18 22 26 30 34 38 42 46 50 54 58 62 66 70
Time (cycles = seconds / 60.000000)
101
103
104
107
46


New
Frequency (hertz)
105
100
95
90
85
80
75
70
65
60
55
50
45
40
35
30
25
20
15
10
5
0
0 2 4 6 8 10 14 18 22 26 30 34 38 42 46 50 54 58 62 66 70
Time (cycles = seconds / 60.000000)
101
103
104
107
46

D.2.10 5 Cycle Fault at generation interconnection LV bus:

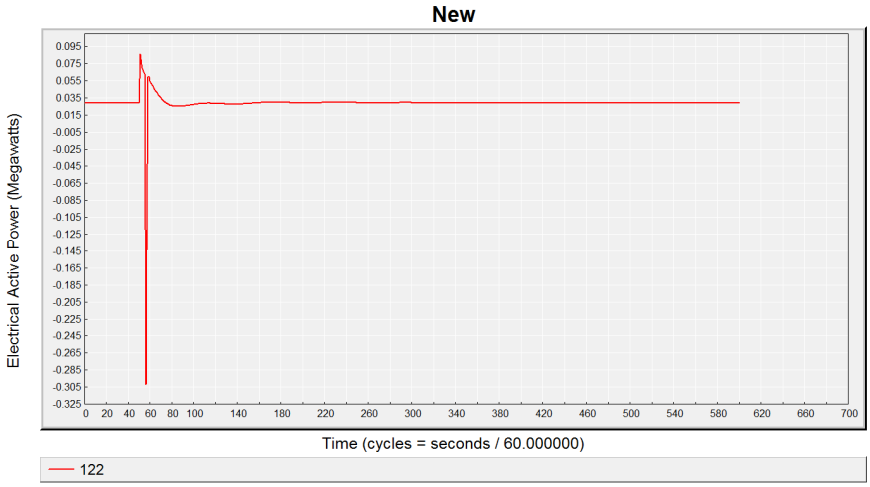

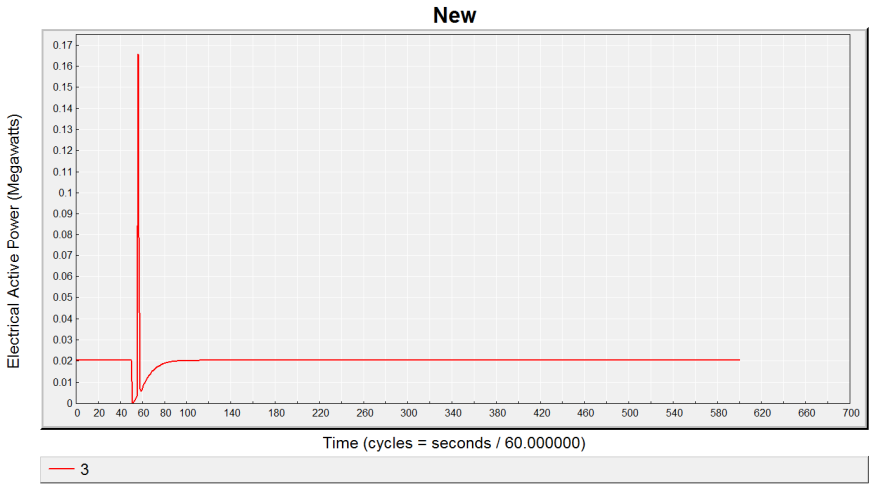

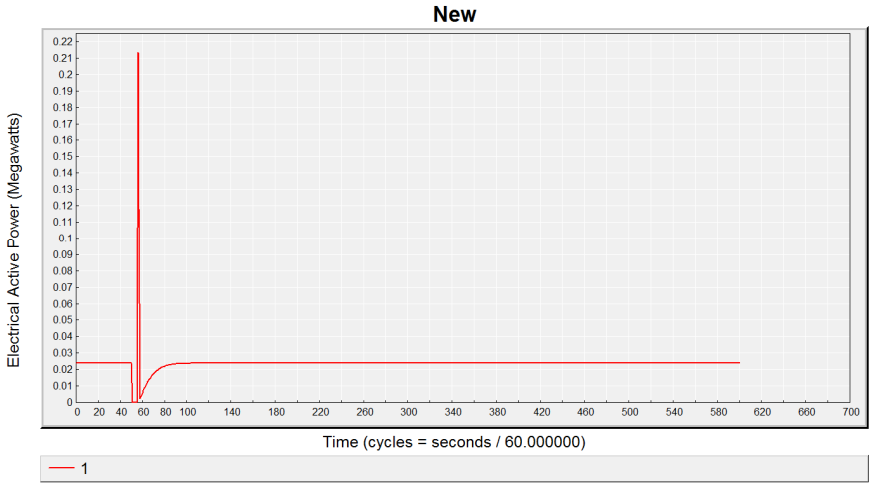


New
Frequency (hertz)
66
65
64
63
62
61
60
59
58
57
56
55
54
53
52
51
0 20 40 80 120 160 200 240 280 320 360 400 440 480 520 560 600 640 680
Time (cycles = seconds / 60.000000)
101
103
104
107
46

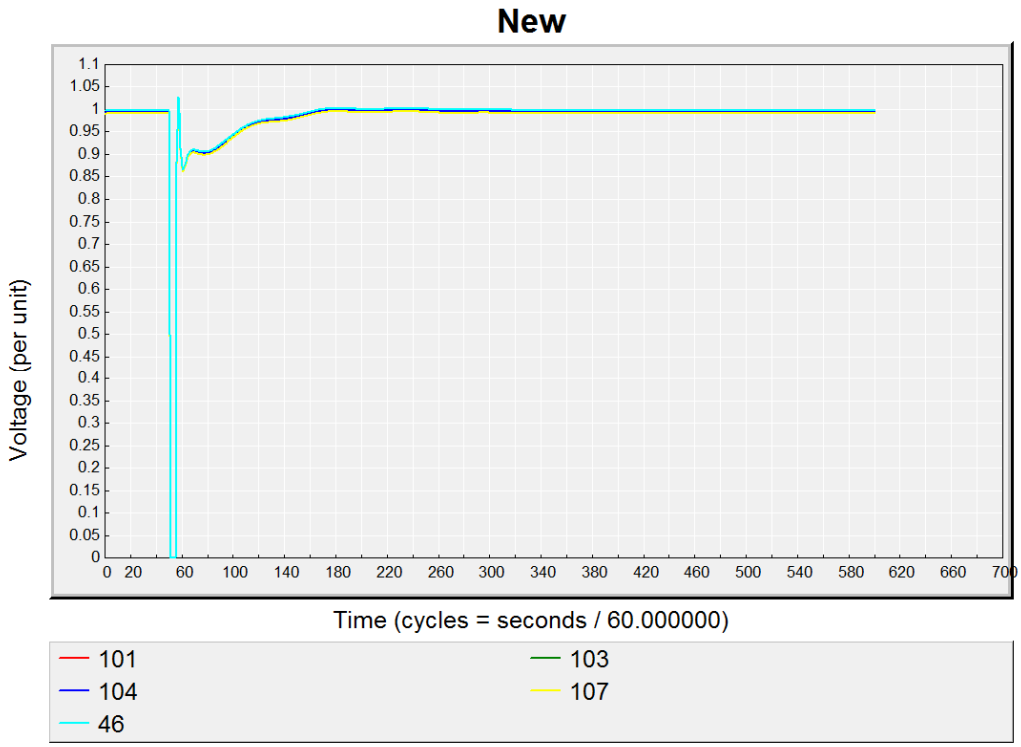
New
Voltage (per unit)
1.1
1.05
1
0.95
0.9
0.85
0.8
0.75
0.7
0.65
0.6
0.55
0.5
0.45
0.4
0.35
0.3
0.25
0.2
0.15
0.1
0.05
0
0 20 60 100 140 180 220 260 300 340 380 420 460 500 540 580 620 660 700
Time (cycles = seconds / 60.000000)
101
103
104
107
46

D.2.11 Loss of BESS PV System (1):

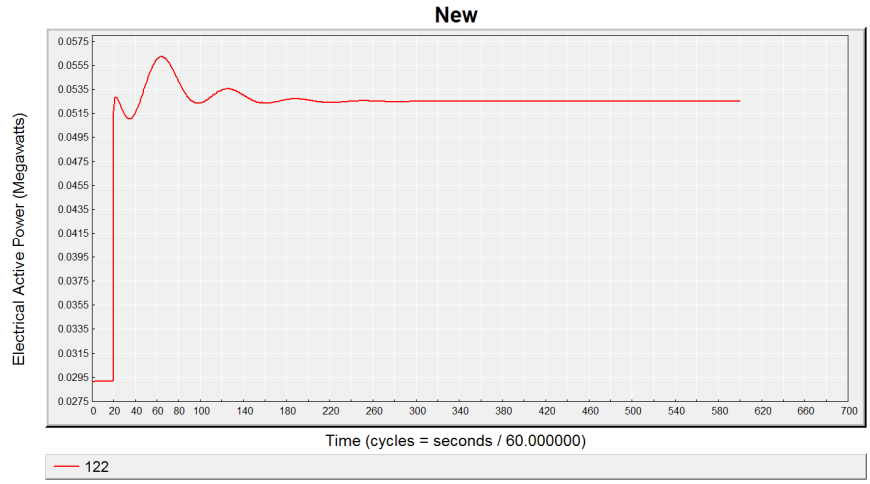

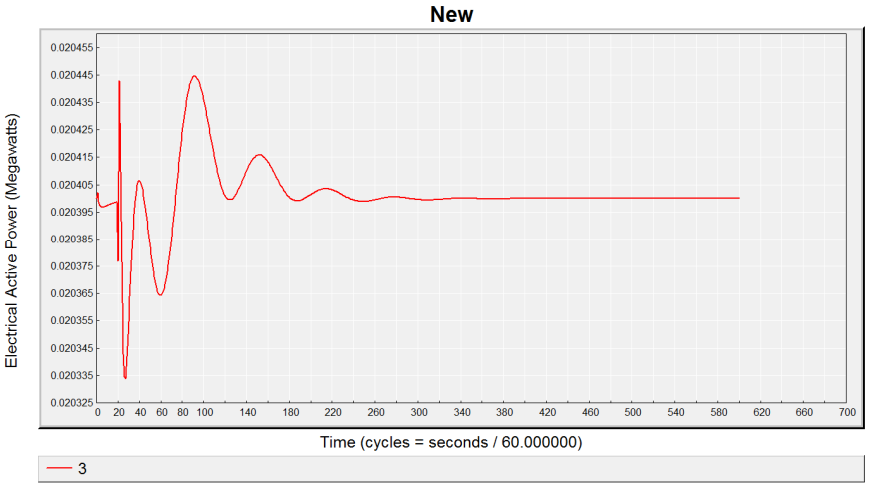

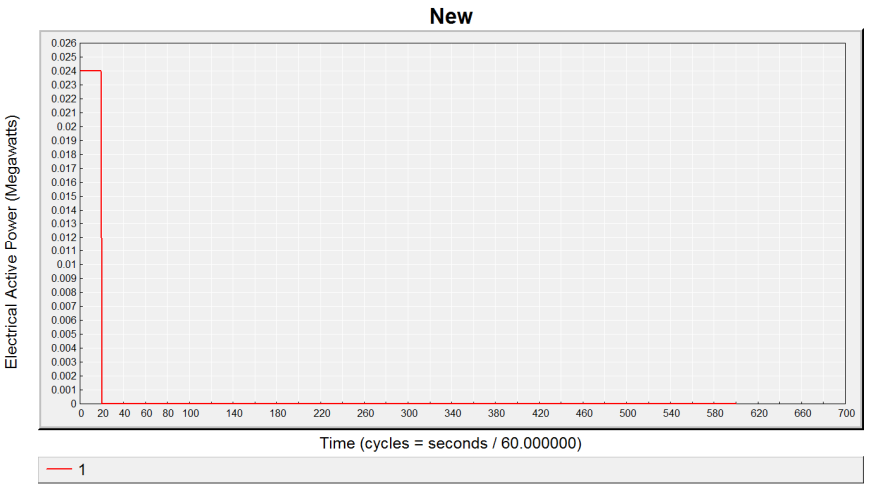

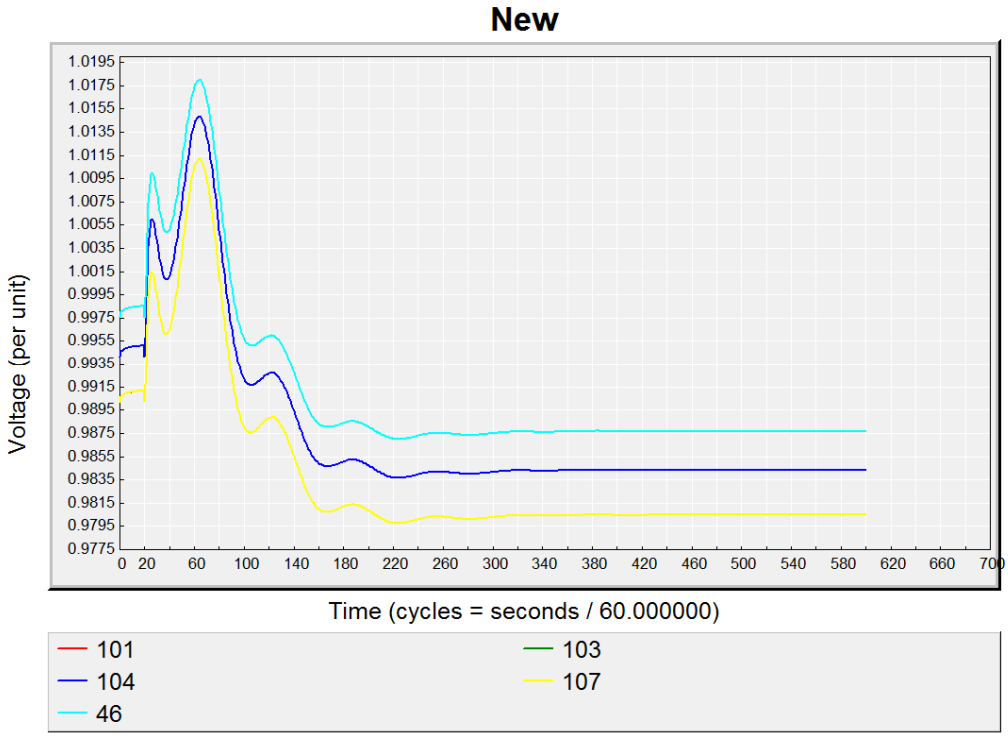
New
Voltage (per unit)
1.0195
1.0175
1.0155
1.0135
1.0115
1.0095
1.0075
1.0055
1.0035
1.0015
0.9995
0.9975
0.9955
0.9935
0.9915
0.9895
0.9875
0.9855
0.9835
0.9815
0.9795
0.9775
0 20 60 100 140 180 220 260 300 340 380 420 460 500 540 580 620 660 700
Time (cycles = seconds / 60.000000)
101
103
104
107
46


New
Frequency (hertz)
61
60.8
60.6
60.4
60.2
60
59.8
59.6
59.4
59.2
59
58.8
58.6
58.4
58.2
0 20 60 100 140 180 220 260 300 340 380 420 460 500 540 580 620 660 700
Time (cycles = seconds / 60.000000)
101
103
104
107
46

D.2.12 Disconnect PV Microinverter System (3):

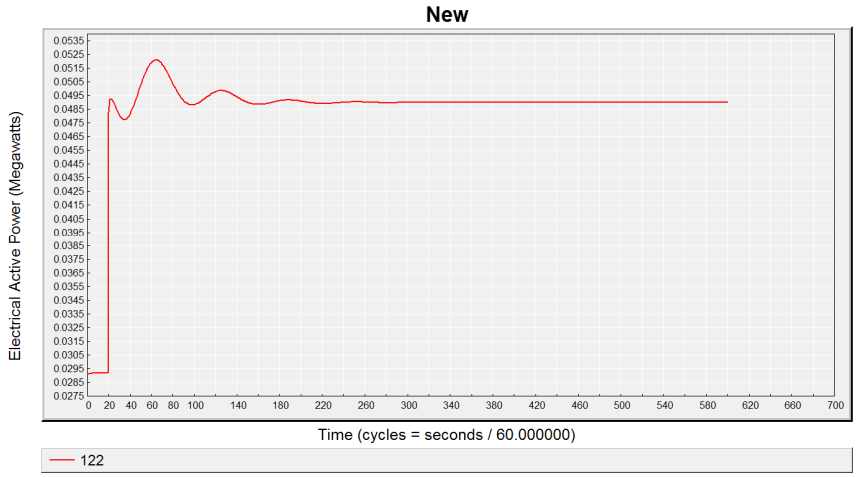

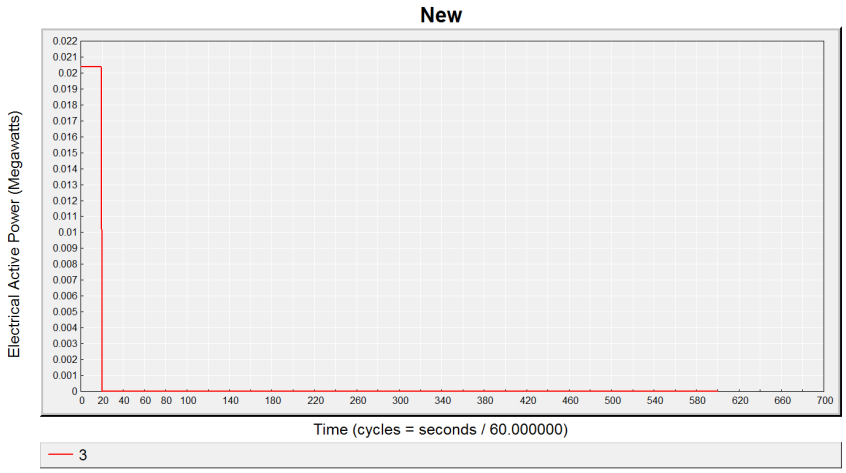

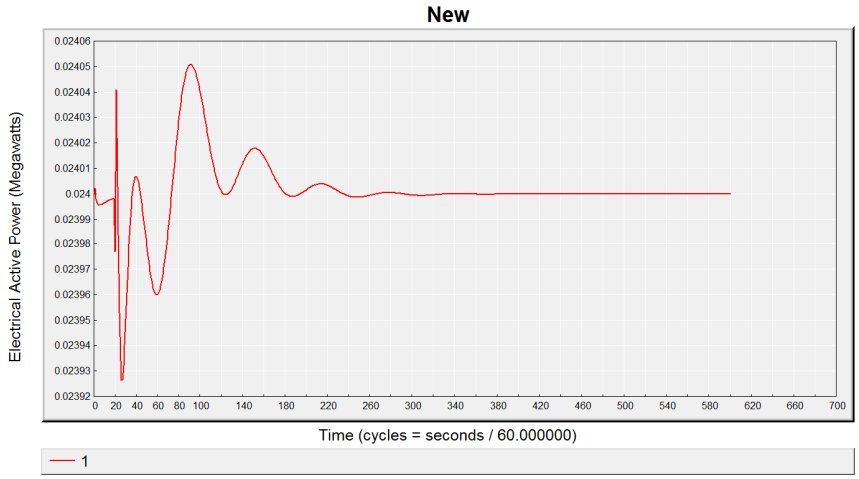

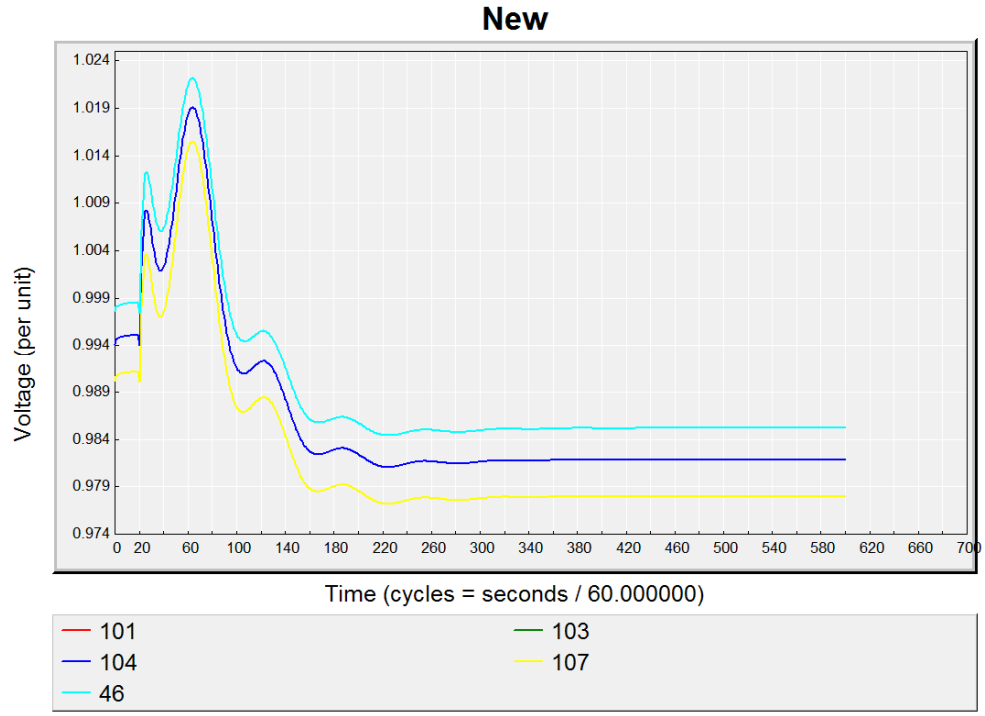
New
Voltage (per unit)
1.024
1.019
1.014
1.009
1.004
0.999
0.994
0.989
0.984
0.979
0.974
0 20 60 100 140 180 220 260 300 340 380 420 460 500 540 580 620 660 700
Time (cycles = seconds / 60.000000)
101
103
104
107
46


New
Frequency (hertz)
61.1
60.9
60.7
60.5
60.3
60.1
59.9
59.7
59.5
59.3
59.1
58.9
58.7
58.5
58.3
58.1
57.9
0 20 60 100 140 180 220 260 300 340 380 420 460 500 540 580 620 660 700
Time (cycles = seconds / 60.000000)
101
103
104
107
46

D.2.13 Simultaneous loss of 24kW BESS PV System and 21 kW Microinverter System

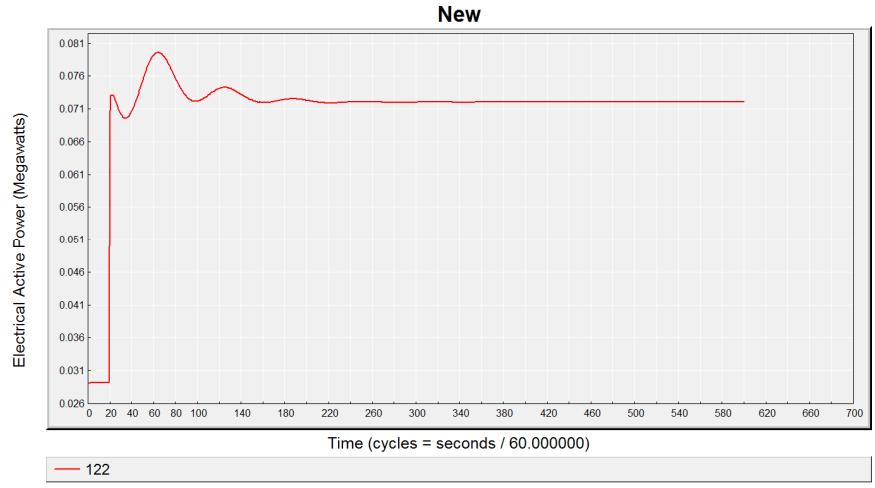

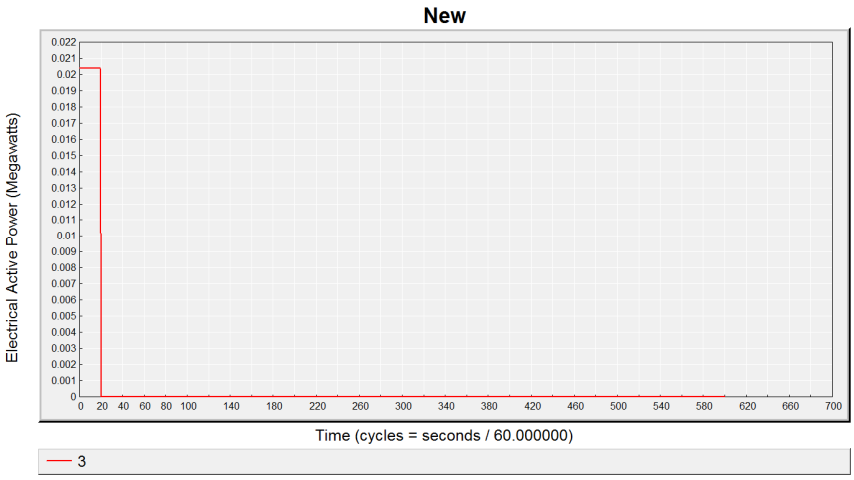

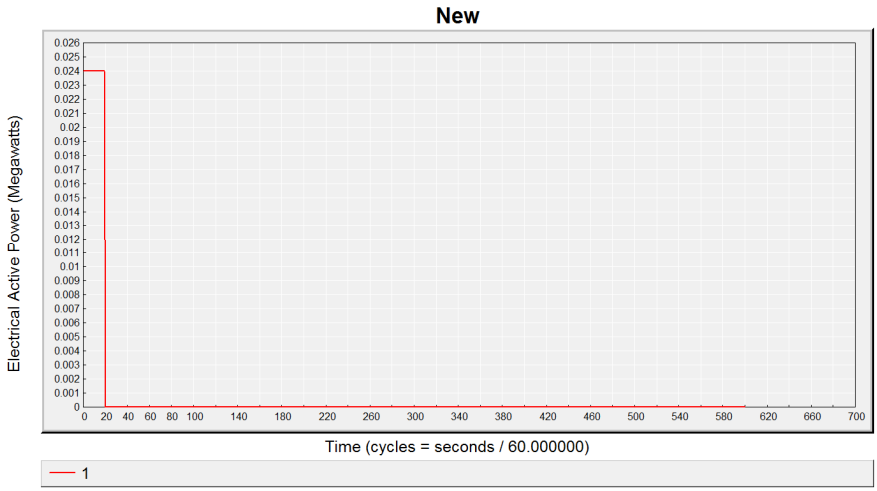

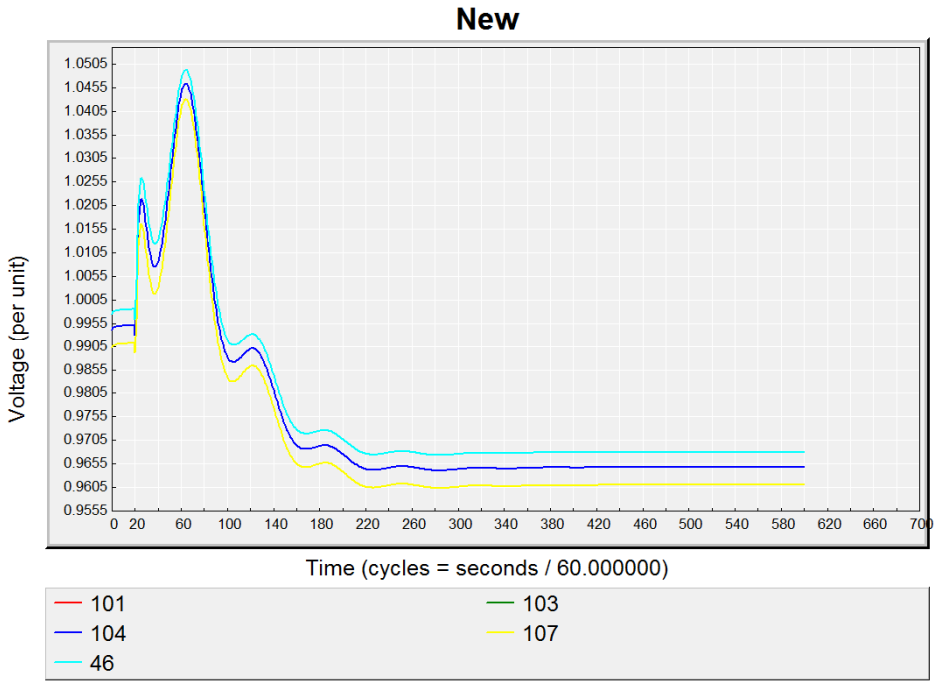
New
Voltage (per unit)
1.0505
1.0455
1.0405
1.0355
1.0305
1.0255
1.0205
1.0155
1.0105
1.0055
1.0005
0.9955
0.9905
0.9855
0.9805
0.9755
0.9705
0.9655
0.9605
0.9555
0 20 60 100 140 180 220 260 300 340 380 420 460 500 540 580 620 660 700
Time (cycles = seconds / 60.000000)
101
103
104
107
46

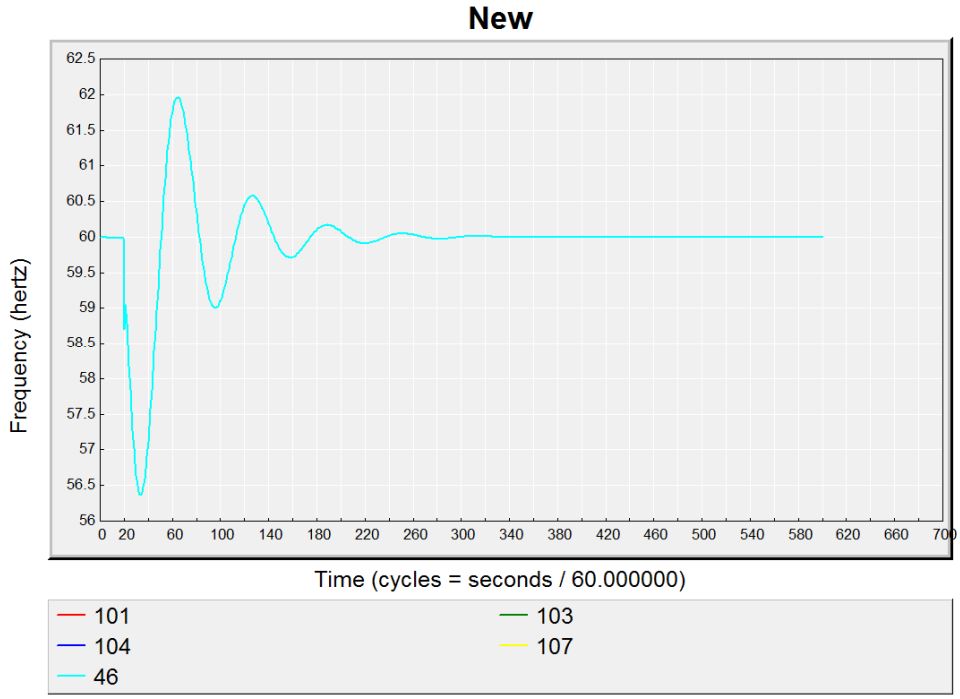
New
Frequency (hertz)
62.5
62
61.5
61
60.5
60
59.5
59
58.5
58
57.5
57
56.5
56
0 20 60 100 140 180 220 260 300 340 380 420 460 500 540 580 620 660 700
Time (cycles = seconds / 60.000000)
101
103
104
107
46

D.3 Matlab/Simpower Dynamic Stability Results

This appendix section provides all detailed Matlab/Simulink stability analysis results for all of the events mentioned in the table below.

Table D - 9: Matlab/Simulink Dynamic Stability Events and Results

Case #	Scenario	Conclusion
1	5 cycle fault at generator bus	Unstable, poorly damped response.
2	10 cycle fault at generator bus	Unstable, poorly damped response.
3	5 cycle fault at MV bus	Stable, poorly damped response.
4	10 cycle fault at MV bus	Unstable, poorly damped response.
5	5 cycle fault at Bldg. 3592 LV bus	Stable, poorly damped response.
6	10 cycle fault at Bldg. 3592 LV bus	Unstable, poorly damped response.
7	Loss of MI source	Stable
8	Step load increase at Bldg. 3592	Stable
9	Step load increase at Bldg. 3596	Stable

D.3.1 Normal Operation:

Case 0/Normal Operation	
Time (sec)	**Action/Event**
0	Power on to load 3592 and Power on to load 3596
5	UPS and MI contactor engages
15	PV engages @ I(ph)=25 A for both BESS and MI setup
20	Utility power interrupted
20	Bldg 3592 Breaker and Bldg 3592 Breaker opens
20	MI contactor isolates
27	Generator engages – picks up Bldg 3592 and Bldg 3596 Load
28	Bldg 3592 Breaker and Bldg 3592 Breaker closes
32	MI contactor engages
70	End of the simulation

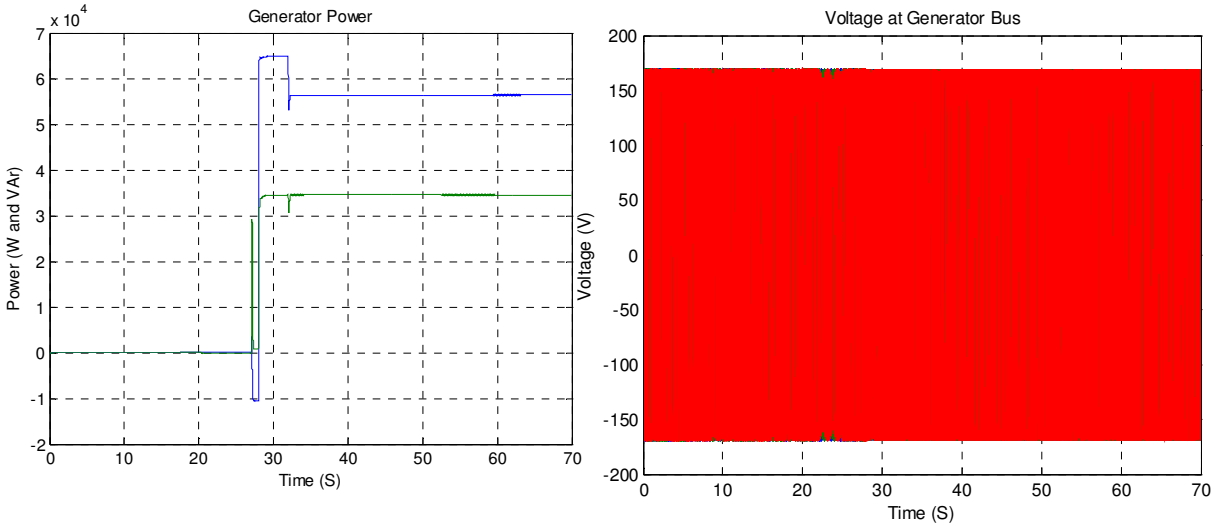

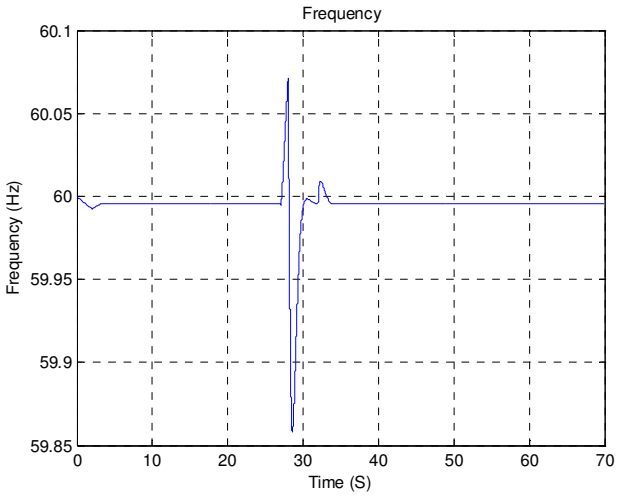
Frequency
Frequency (Hz)
Time (S)

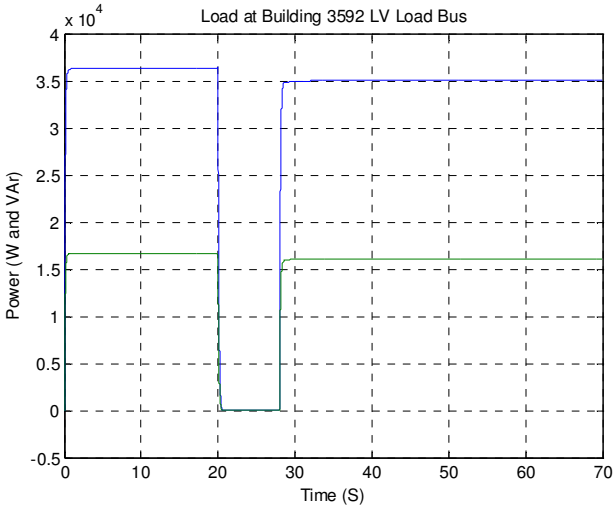
Load at Building 3592 LV Load Bus
x 10^4
Power (W and VAr)
Time (S)

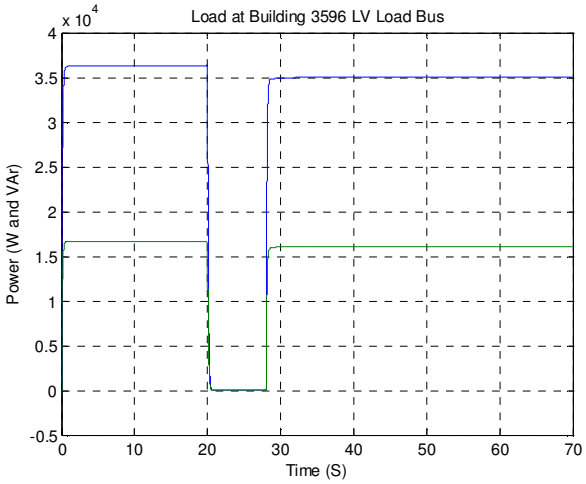
Load at Building 3596 LV Load Bus
x 10^4
Power (W and VAr)
Time (S)

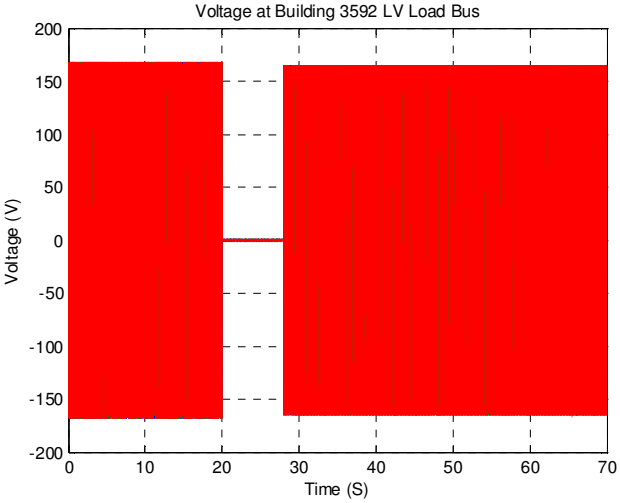
Voltage at Building 3592 LV Load Bus
Voltage (V)
Time (S)

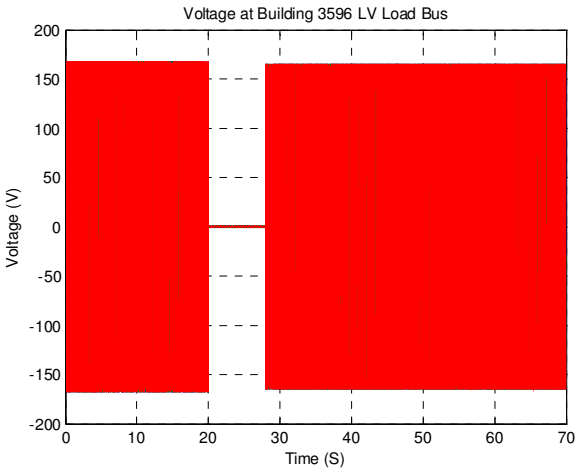
Voltage at Building 3596 LV Load Bus
Voltage (V)
Time (S)

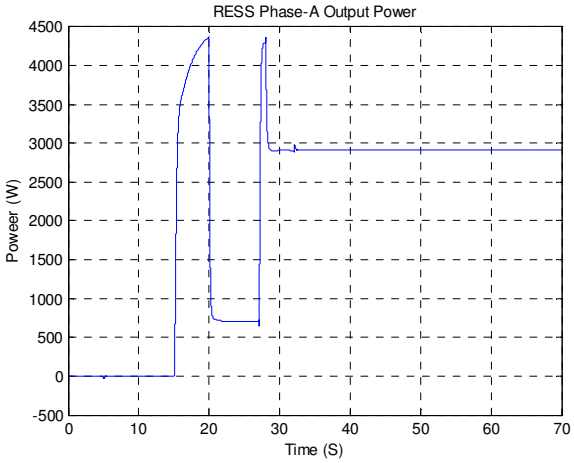
RESS Phase-A Output Power
Poweer (W)
Time (S)

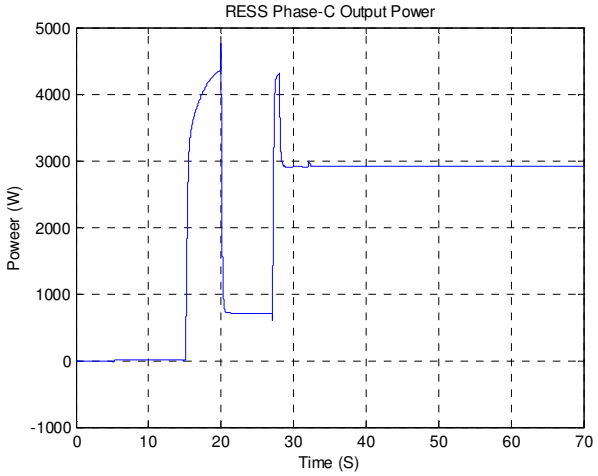
RESS Phase-C Output Power
Poweer (W)
Time (S)

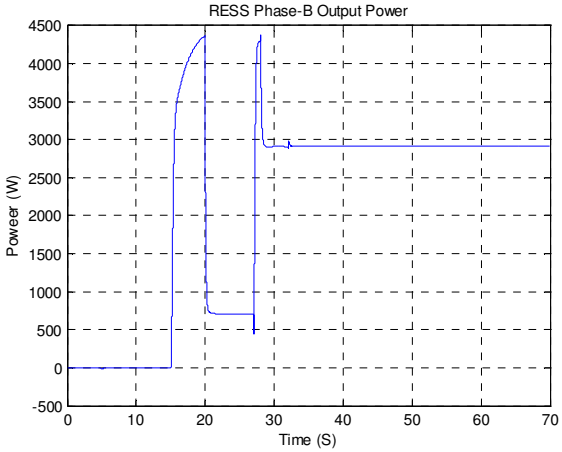
RESS Phase-B Output Power
Poweer (W)
Time (S)

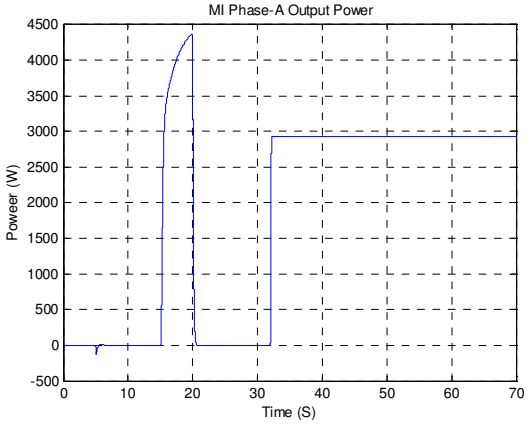
MI Phase-A Output Power
Poweer (W)
Time (S)

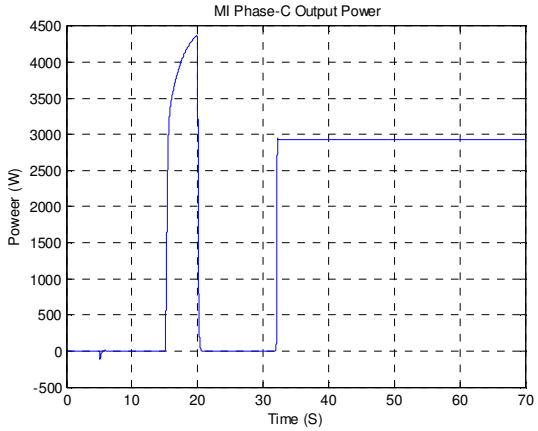
MI Phase-C Output Power
Poweer (W)
Time (S)

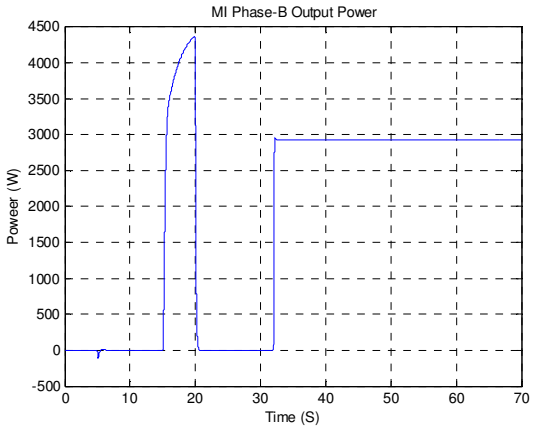
MI Phase-B Output Power
Poweer (W)
Time (S)

D.3 2 5 cycle 3-phase fault at Generator Bus

Case 1/5 cycle fault at generator bus	
Time (sec)	**Action/Event**
0	Power on to load 3592 and Power on to load 3596
5	UPS and MI contactor engages
15	PV engages @ I(ph)=25 A for both BESS and MI setup
20	Utility power interrupted
20	Bldg 3592 Breaker and Bldg 3592 Breaker opens
20	MI contactor isolates
27	Generator engages – picks up Bldg 3592 and Bldg 3596 Load
28	Bldg 3592 Breaker and Bldg 3592 Breaker closes
32	MI contactor engages
40	3-phase fault at generator bus
40+(5/60)	3-phase fault at generator bus clears
70	End of the simulation

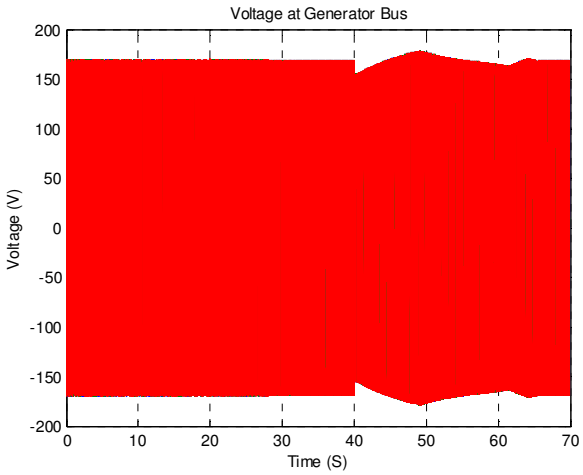
Voltage at Generator Bus
Voltage (V)
Time (S)

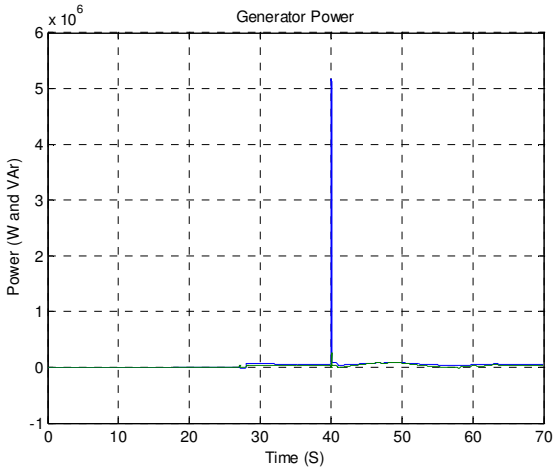
x 10^6
Generator Power
Power (W and VAr)
Time (S)

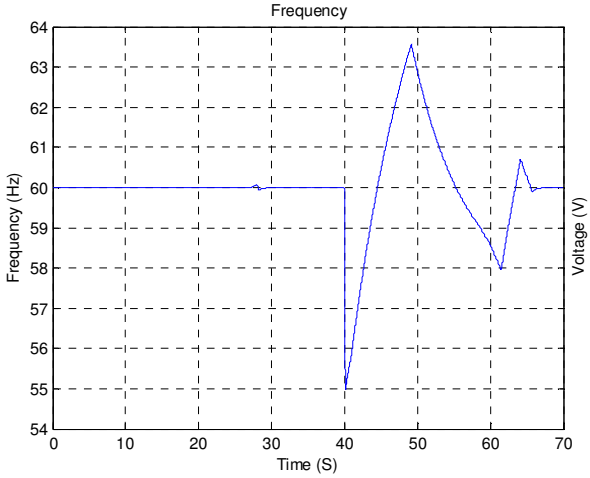
Frequency
Frequency (Hz)
Time (S)

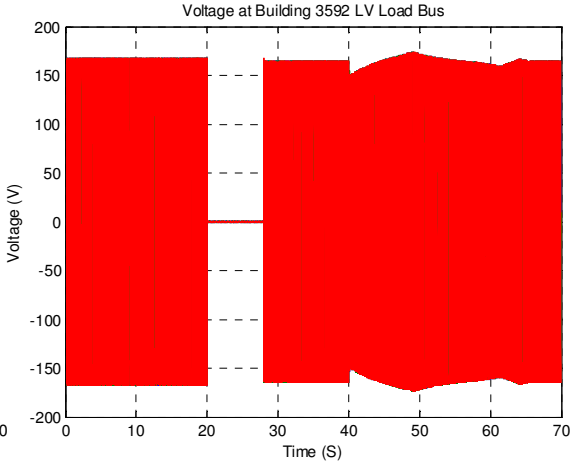
Voltage at Building 3592 LV Load Bus
Voltage (V)
Time (S)

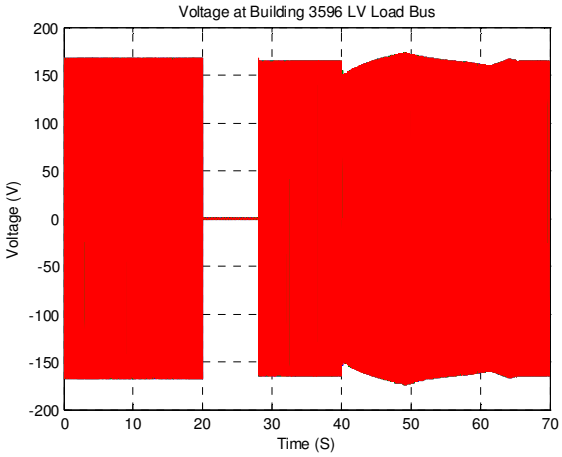
Voltage at Building 3596 LV Load Bus
Voltage (V)
Time (S)

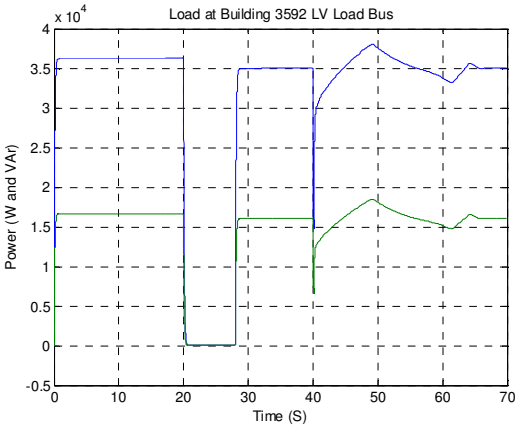
x 10^4
Load at Building 3592 LV Load Bus
Power (W and VAr)
Time (S)

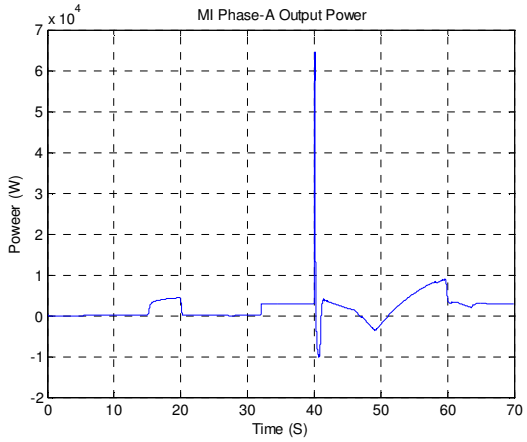
MI Phase-A Output Power
x 10^4
Powеer (W)
Time (S)

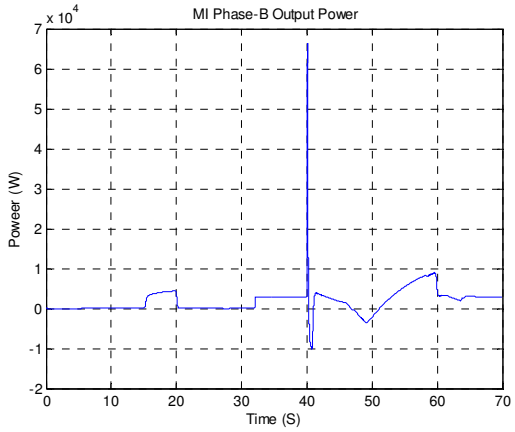
MI Phase-B Output Power
x 10^4
Powеer (W)
Time (S)

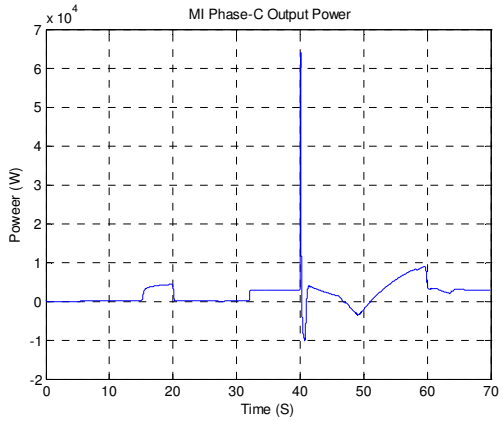
MI Phase-C Output Power
x 10^4
Powеer (W)
Time (S)

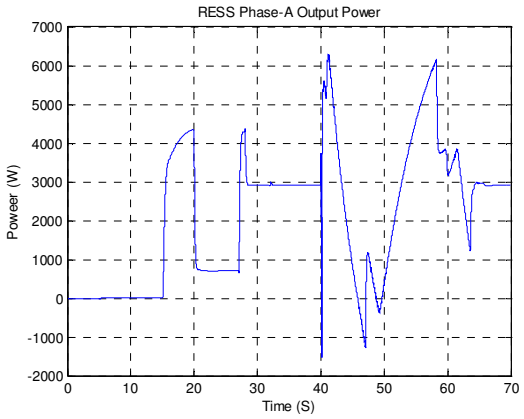
RESS Phase-A Output Power
Powеer (W)
Time (S)

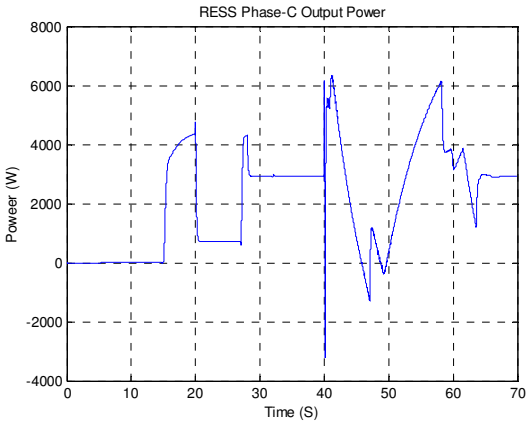
RESS Phase-C Output Power
Powеer (W)
Time (S)

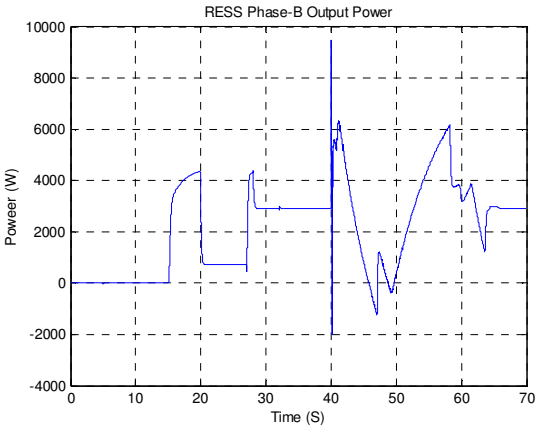
RESS Phase-B Output Power
Powеer (W)
Time (S)

D.3.3 10 cycle 3-phase fault at Generator Bus

Case 2/10 cycle fault at generator bus	
Time (sec)	**Action/Event**
0	Power on to load 3592 and Power on to load 3596
5	UPS and MI contactor engages
15	PV engages @ I(ph)=25 A for both BESS and MI setup
20	Utility power interrupted
20	Bldg 3592 Breaker and Bldg 3592 Breaker opens
20	MI contactor isolates
27	Generator engages – picks up Bldg 3592 and Bldg 3596 Load
28	Bldg 3592 Breaker and Bldg 3592 Breaker closes
32	MI contactor engages
40	3-phase fault at generator bus
40+(10/60)	3-phase fault at generator bus clears
70	End of the simulation

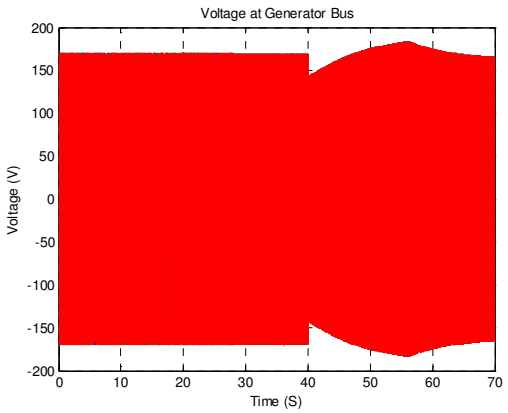
Voltage at Generator Bus
Voltage (V)
Time (S)

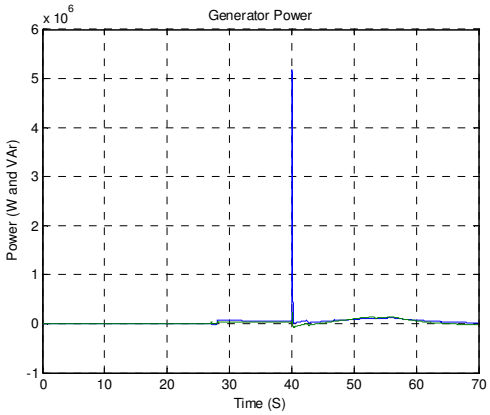
Generator Power
x 10^6
Power (W and VAr)
Time (S)

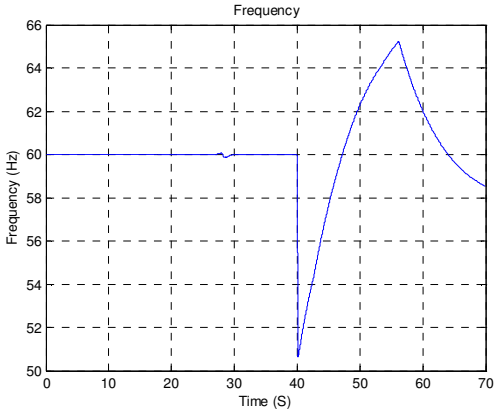
Frequency
Frequency (Hz)
Time (S)

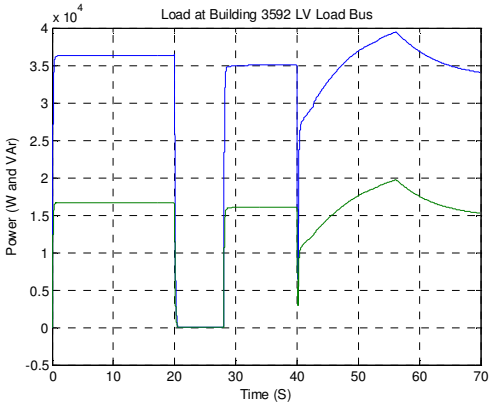
Load at Building 3592 LV Load Bus
x 10^4
Power (W and VAr)
Time (S)

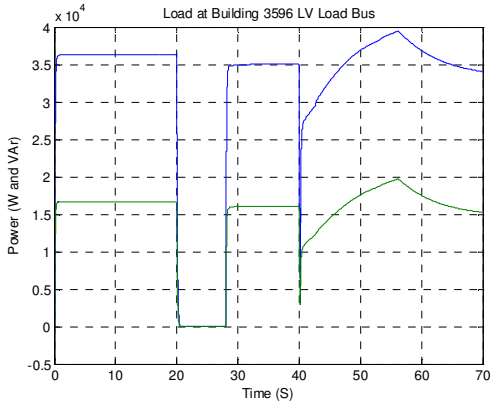
Load at Building 3596 LV Load Bus
x 10^4
Power (W and VAr)
Time (S)

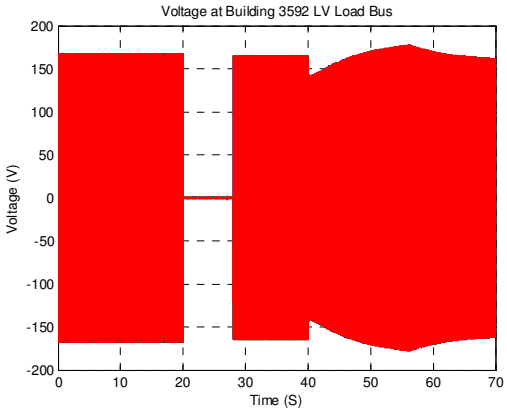
Voltage at Building 3592 LV Load Bus
Voltage (V)
Time (S)

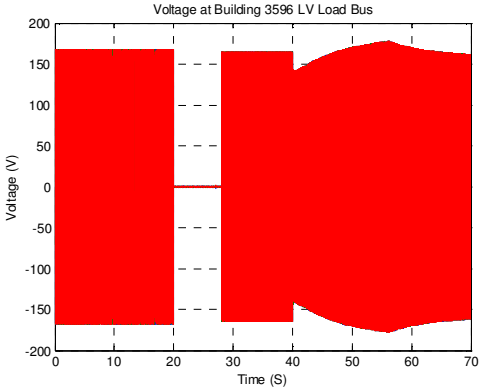
Voltage at Building 3596 LV Load Bus
Voltage (V)
Time (S)

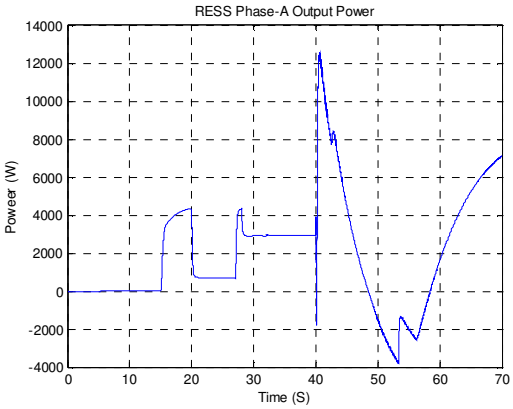
RESS Phase-A Output Power
Power (W)
Time (S)

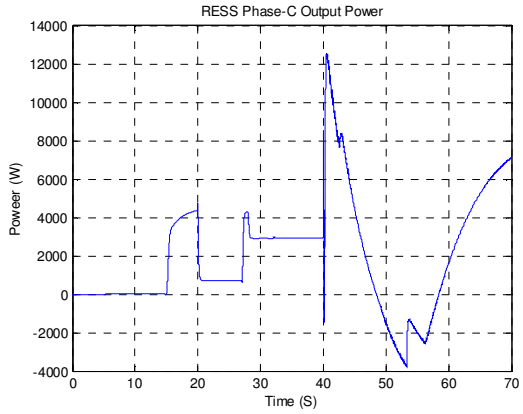
RESS Phase-C Output Power
Poweer (W)
Time (S)

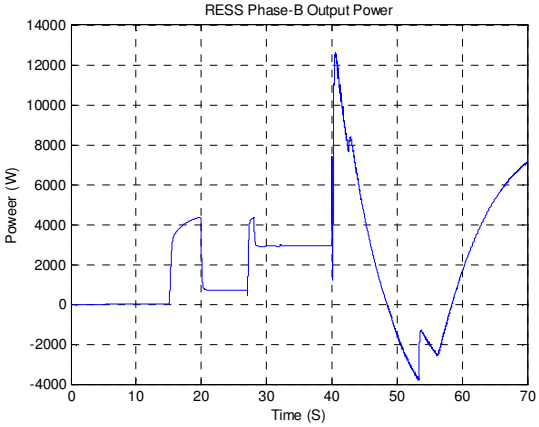
RESS Phase-B Output Power
Poweer (W)
Time (S)

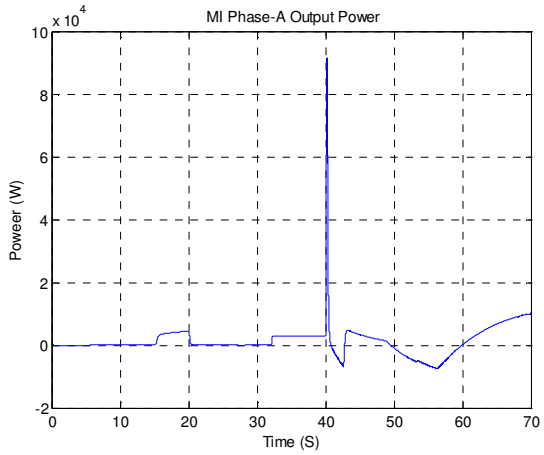
MI Phase-A Output Power
x 10^4
Poweer (W)
Time (S)

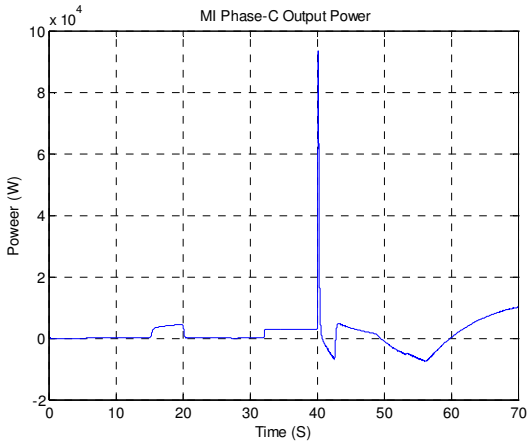
MI Phase-C Output Power
x 10^4
Poweer (W)
Time (S)

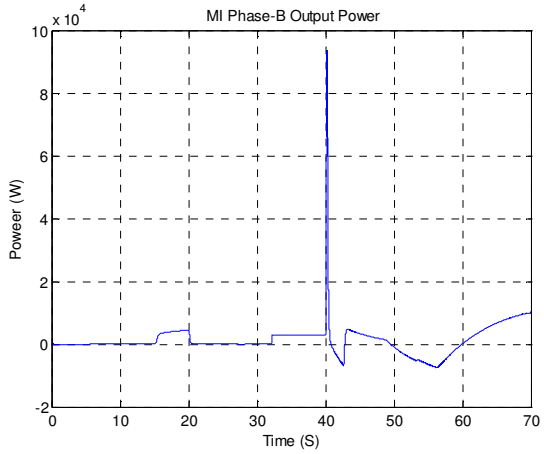
MI Phase-B Output Power
x 10^4
Poweer (W)
Time (S)

D.3.4 5 cycle 3-phase fault at MV Bus

Case 3/5 cycle fault at MV bus	
Time (sec)	**Action/Event**
0	Power on to load 3592 and Power on to load 3596
5	UPS and MI contactor engages
15	PV engages @ I(ph)=25 A for both BESS and MI setup
20	Utility power interrupted
20	Bldg 3592 Breaker and Bldg 3592 Breaker opens
20	MI contactor isolates
27	Generator engages – picks up Bldg 3592 and Bldg 3596 Load
28	Bldg 3592 Breaker and Bldg 3592 Breaker closes
32	MI contactor engages
40	3-phase fault at MV bus
40+(5/60)	3-phase fault at MV bus clears
70	End of the simulation

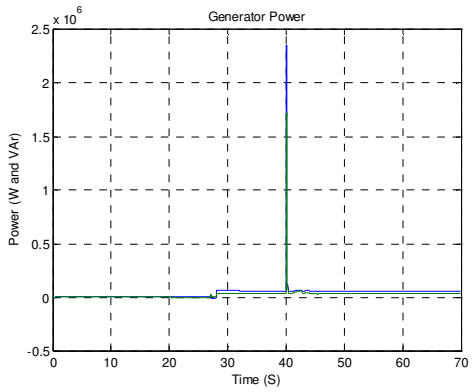
Generator Power
x 10^6
Power (W and VAr)
Time (S)

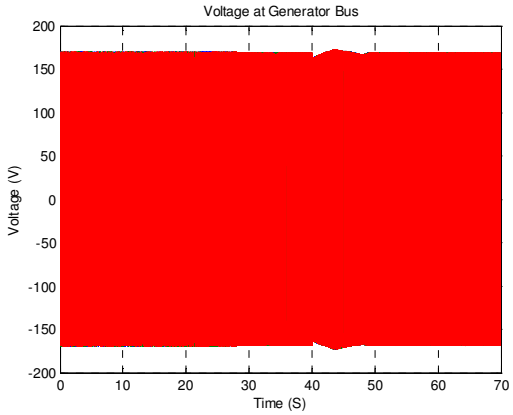
Voltage at Generator Bus
Voltage (V)
Time (S)

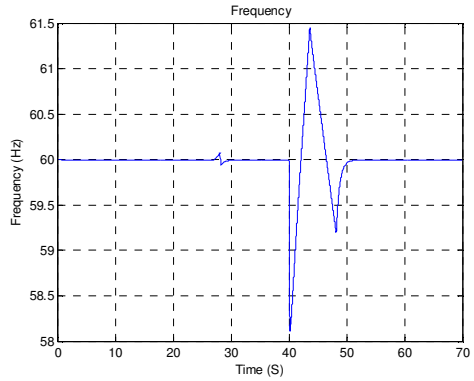
Frequency
Frequency (Hz)
Time (S)

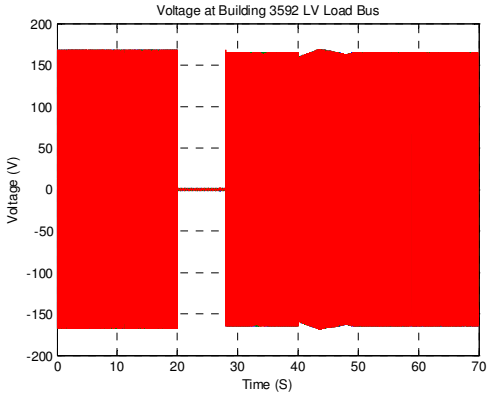
Voltage at Building 3592 LV Load Bus
Voltage (V)
Time (S)

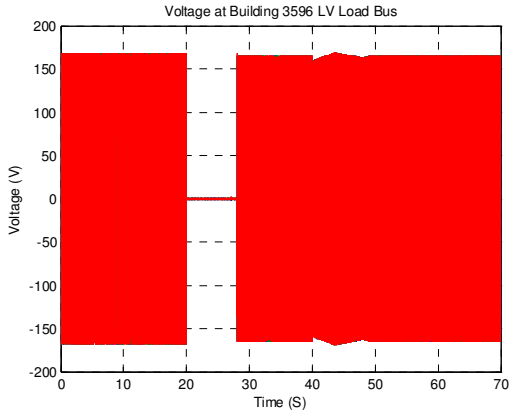
Voltage at Building 3596 LV Load Bus
Voltage (V)
Time (S)

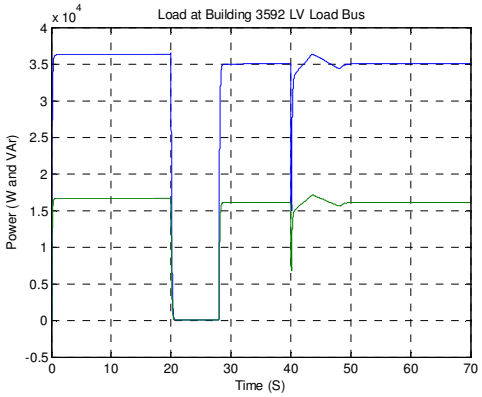
Load at Building 3592 LV Load Bus
x 10^4
Power (W and VAr)
Time (S)

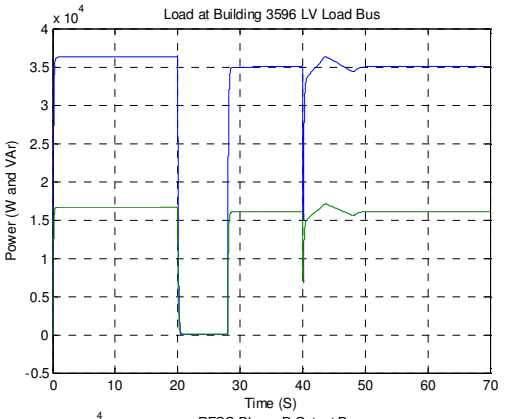
Load at Building 3596 LV Load Bus
x 10^4
Power (W and VAr)
Time (S)

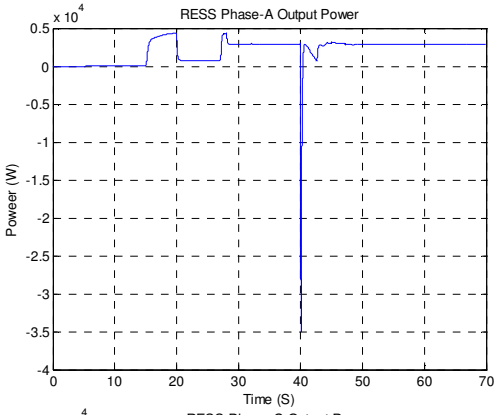
RESS Phase-A Output Power
x 10^4
Power (W)
Time (S)

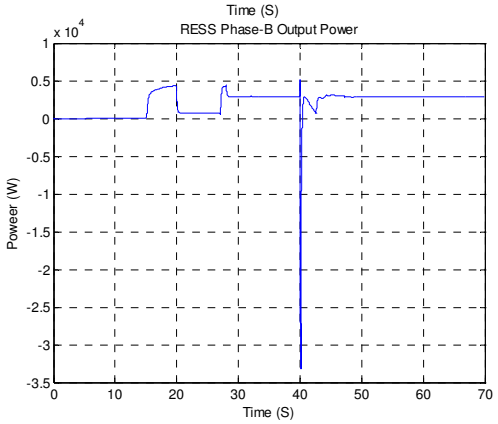
RESS Phase-B Output Power
x 10^4
Power (W)
Time (S)

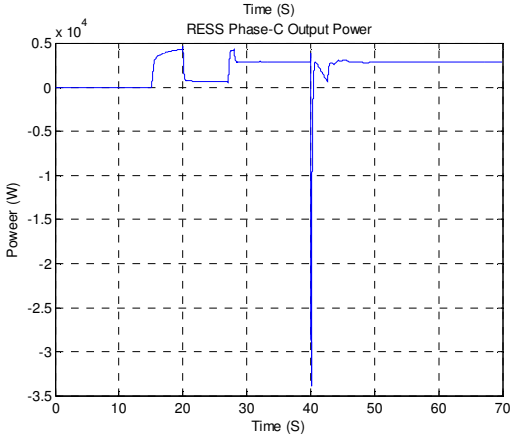
RESS Phase-C Output Power
x 10^4
Power (W)
Time (S)

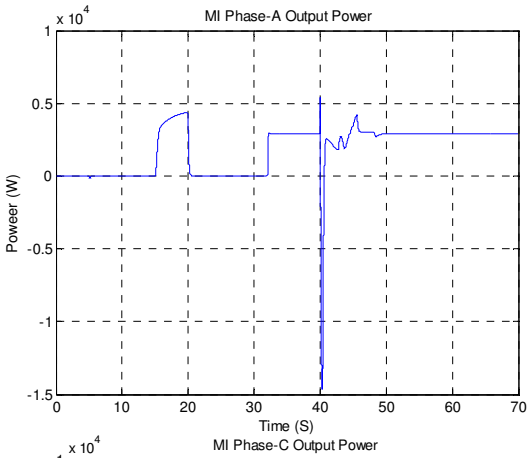
MI Phase-A Output Power
x 10^4
Power (W)
Time (S)

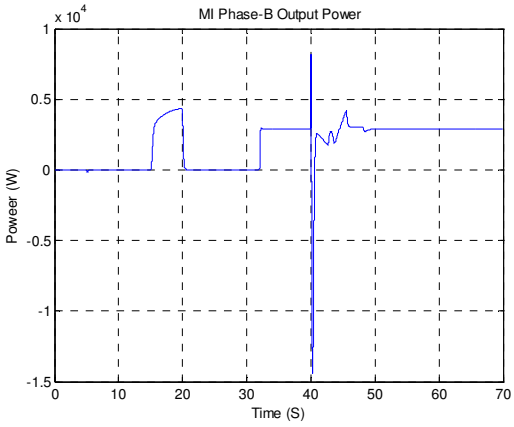
MI Phase-B Output Power
x 10^4
Power (W)
Time (S)

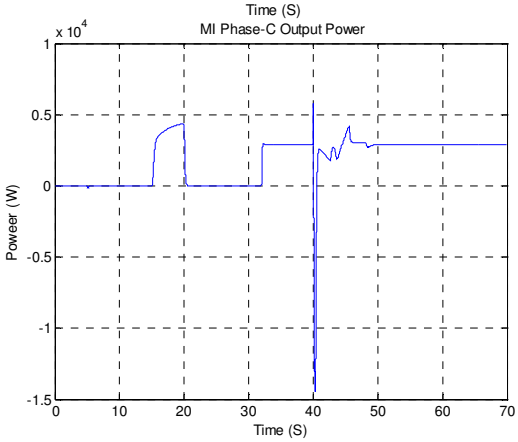
MI Phase-C Output Power
x 10^4
Power (W)
Time (S)

D.3.5 10 cycle 3-phase fault at MV Bus

Case 4/10 cycle fault at MV bus	
Time (sec)	**Action/Event**
0	Power on to load 3592 and Power on to load 3596
5	UPS and MI contactor engages
15	PV engages @ I(ph)=25 A for both BESS and MI setup
20	Utility power interrupted
20	Bldg 3592 Breaker and Bldg 3592 Breaker opens
20	MI contactor isolates
27	Generator engages – picks up Bldg 3592 and Bldg 3596 Load
28	Bldg 3592 Breaker and Bldg 3592 Breaker closes
32	MI contactor engages
40	3-phase fault at MV bus
40+(10/60)	3-phase fault at MV bus clears
70	End of the simulation

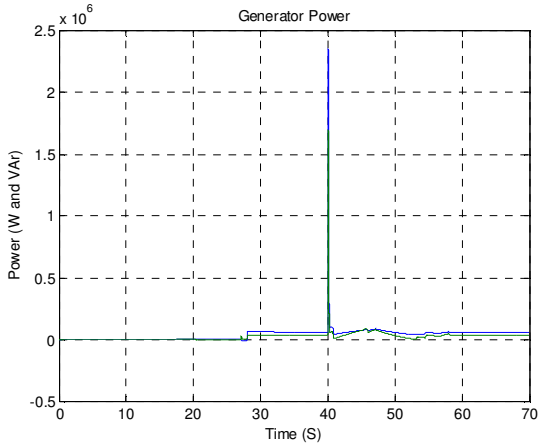
Generator Power
x 10^6
Power (W and VAr)
Time (S)

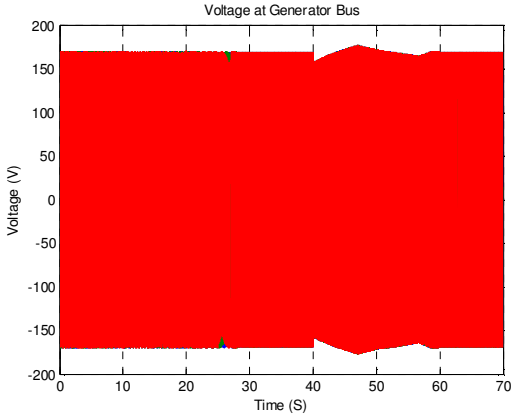
Voltage at Generator Bus
Voltage (V)
Time (S)

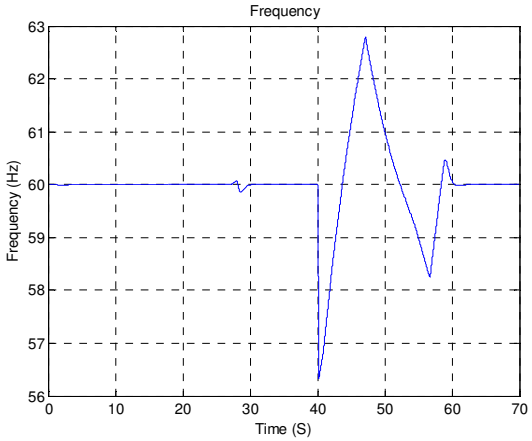
Frequency
Frequency (Hz)
Time (S)

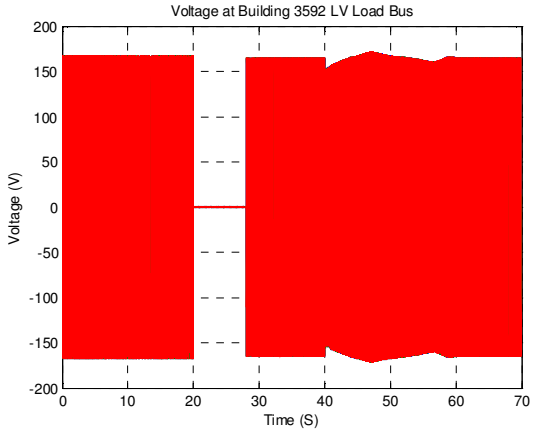
Voltage at Building 3592 LV Load Bus
Voltage (V)
Time (S)

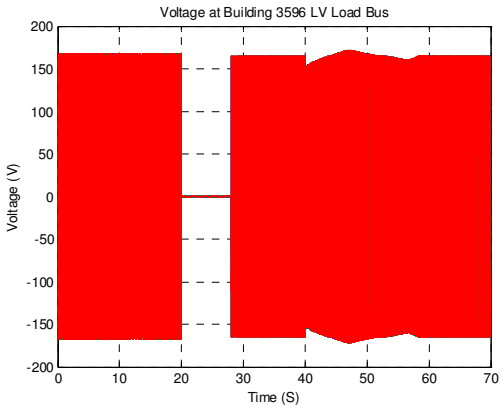
Voltage at Building 3596 LV Load Bus
Voltage (V)
Time (S)

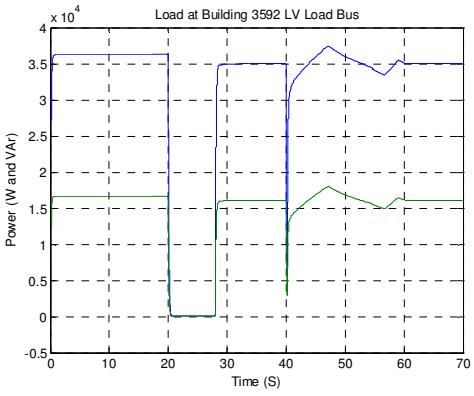
Load at Building 3592 LV Load Bus
x 10^4
Power (W and VAr)
Time (S)

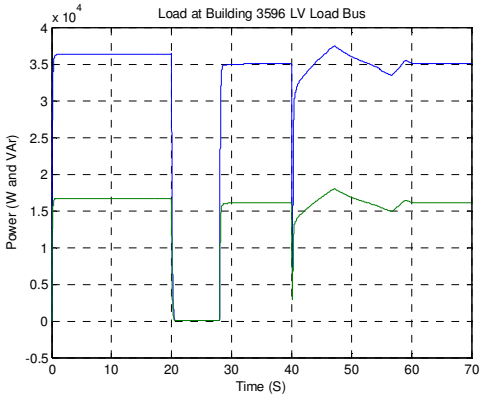
Load at Building 3596 LV Load Bus
x 10^4
Power (W and VAr)
Time (S)

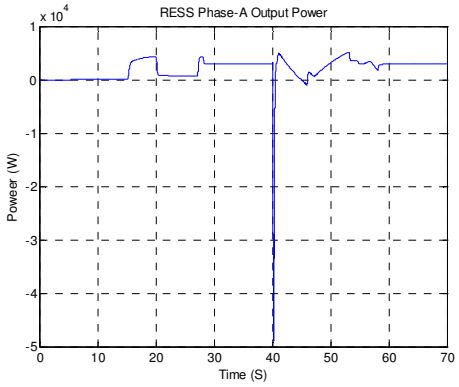
RESS Phase-A Output Power
x 10^4
Powеer (W)
Time (S)

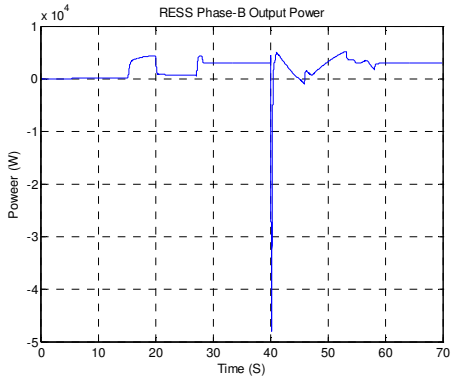
RESS Phase-B Output Power
x 10^4
Powеer (W)
Time (S)

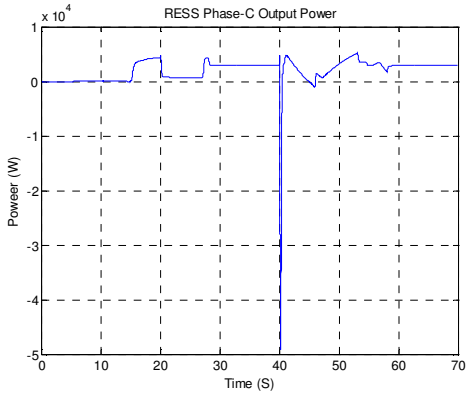
RESS Phase-C Output Power
x 10^4
Powеer (W)
Time (S)

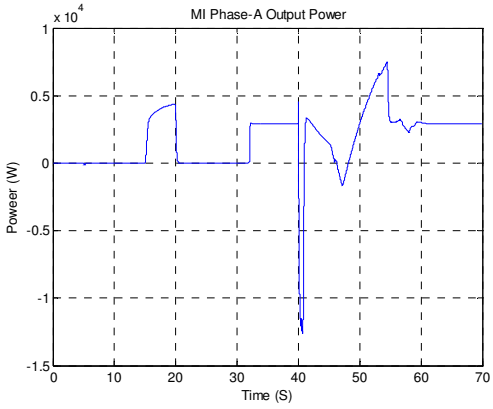
MI Phase-A Output Power
x 10^4
Powеer (W)
Time (S)

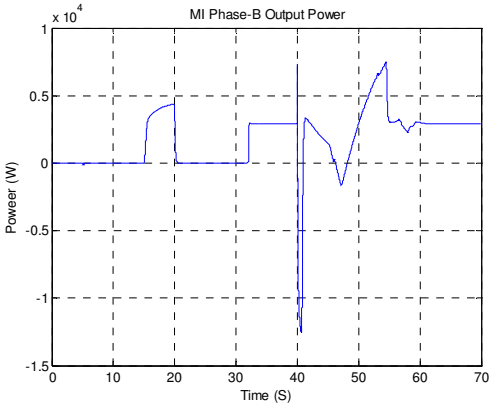
MI Phase-B Output Power
x 10^4
Powеer (W)
Time (S)

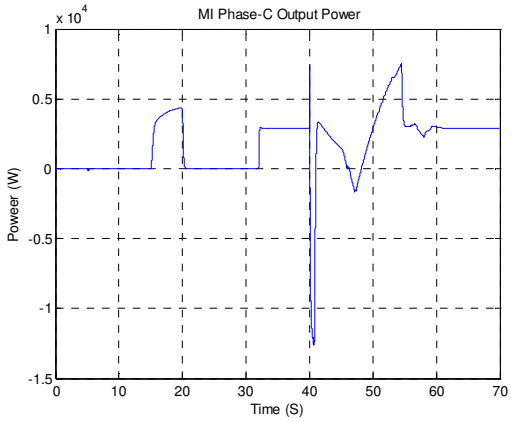
MI Phase-C Output Power
x 10^4
Powеer (W)
Time (S)

D.3.6 5 cycle 3-phase fault at Bldg. 3592 LV Bus

Case 5/5 cycle fault at Bldg 3592 LV bus	
Time (sec)	**Action/Event**
0	Power on to load 3592 and Power on to load 3596
5	UPS and MI contactor engages
15	PV engages @ I(ph)=25 A for both BESS and MI setup
20	Utility power interrupted
20	Bldg 3592 Breaker and Bldg 3592 Breaker opens
20	MI contactor isolates
27	Generator engages – picks up Bldg 3592 and Bldg 3596 Load
28	Bldg 3592 Breaker and Bldg 3592 Breaker closes
32	MI contactor engages
40	3-phase fault at MV bus
40+(5/60)	3-phase fault at MV bus clears
70	End of the simulation

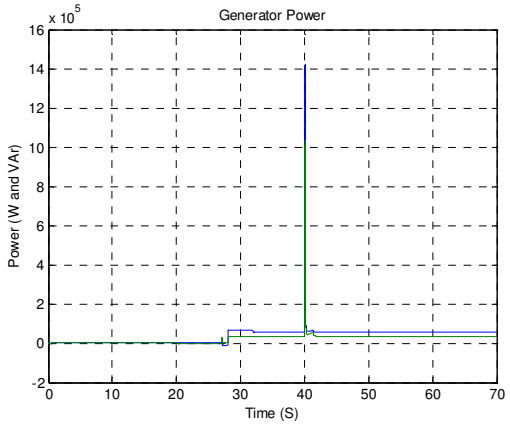
Generator Power
x 10^5
Power (W and VAr)
Time (S)

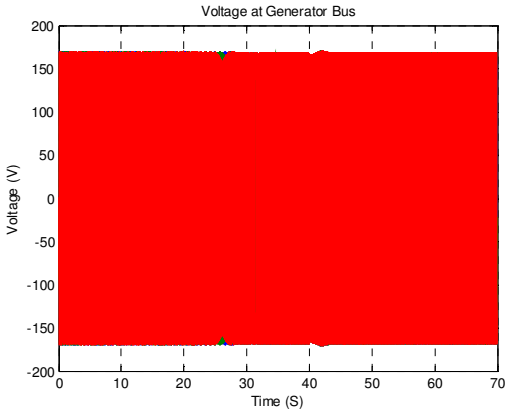
Voltage at Generator Bus
Voltage (V)
Time (S)

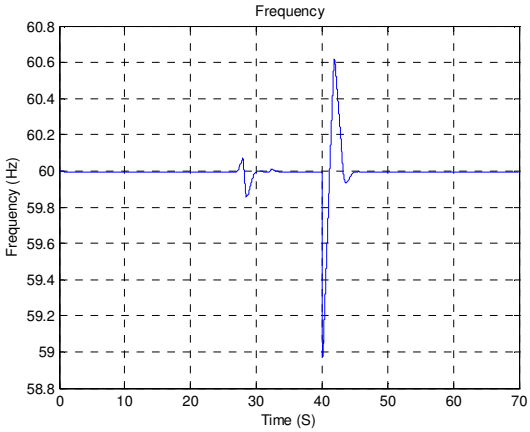
Frequency
Frequency (Hz)
Time (S)

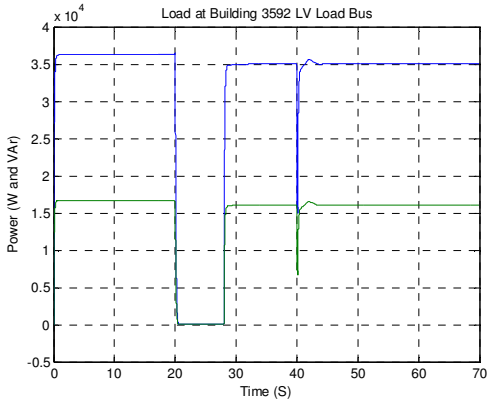
Load at Building 3592 LV Load Bus
x 10^4
Power (W and VAr)
Time (S)

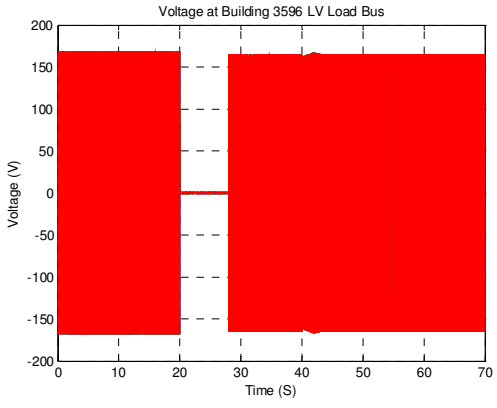
Voltage at Building 3596 LV Load Bus
Voltage (V)
Time (S)

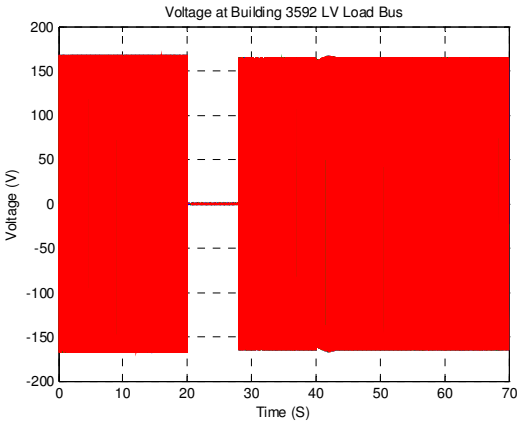
Voltage at Building 3592 LV Load Bus
Voltage (V)
Time (S)

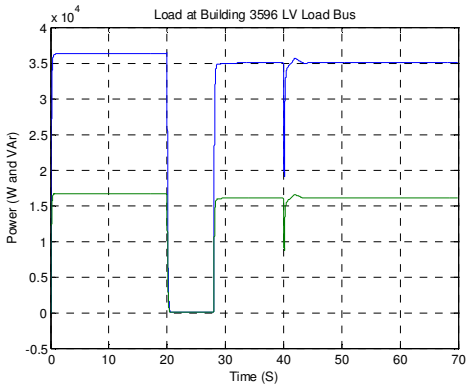
Load at Building 3596 LV Load Bus
x 10^4
Power (W and VAr)
Time (S)

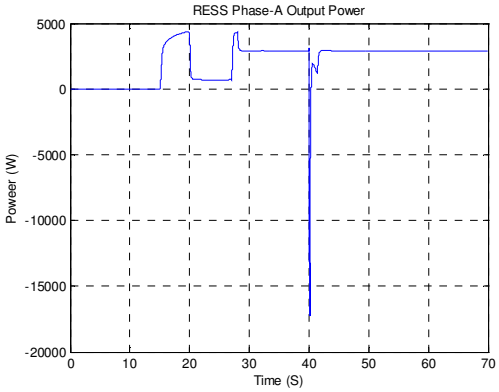
RESS Phase-A Output Power
Poweer (W)
Time (S)

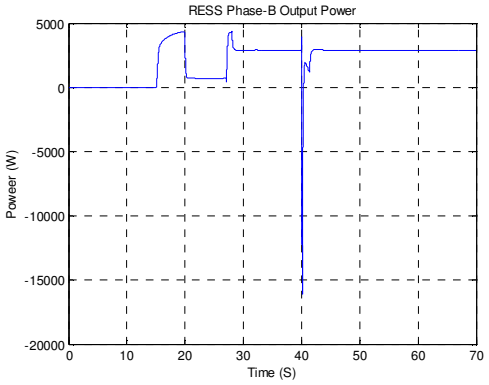
RESS Phase-B Output Power
Poweer (W)
Time (S)

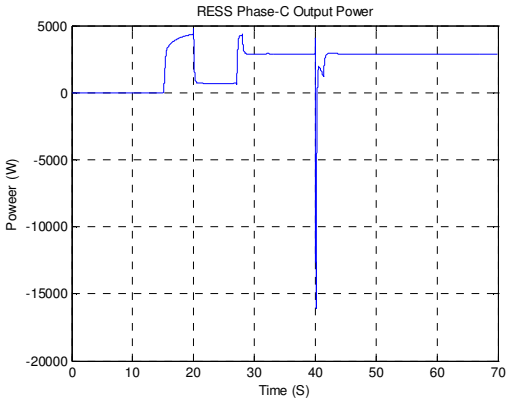
RESS Phase-C Output Power
Poweer (W)
Time (S)

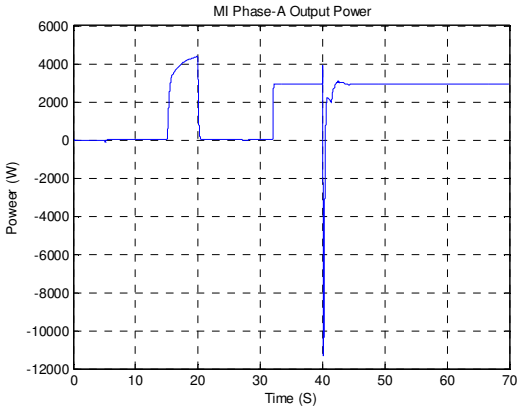
MI Phase-A Output Power
Poweer (W)
Time (S)

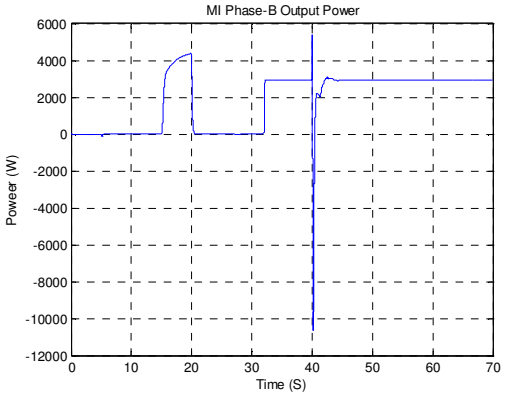
MI Phase-B Output Power
Poweer (W)
Time (S)

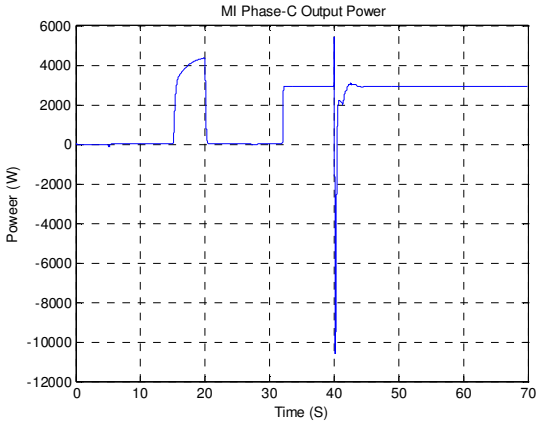
MI Phase-C Output Power
Poweer (W)
Time (S)

D.3.7 10 cycle 3-phase fault at Bldg. 3592 LV Bus

Case 6/10 cycle fault at Bldg 3592 LV bus	
Time (sec)	**Action/Event**
0	Power on to load 3592 and Power on to load 3596
5	UPS and MI contactor engages
15	PV engages @ I(ph)=25 A for both BESS and MI setup
20	Utility power interrupted
20	Bldg 3592 Breaker and Bldg 3592 Breaker opens
20	MI contactor isolates
27	Generator engages – picks up Bldg 3592 and Bldg 3596 Load
28	Bldg 3592 Breaker and Bldg 3592 Breaker closes
32	MI contactor engages
40	3-phase fault at MV bus
40+(10/60)	3-phase fault at MV bus clears
70	End of the simulation

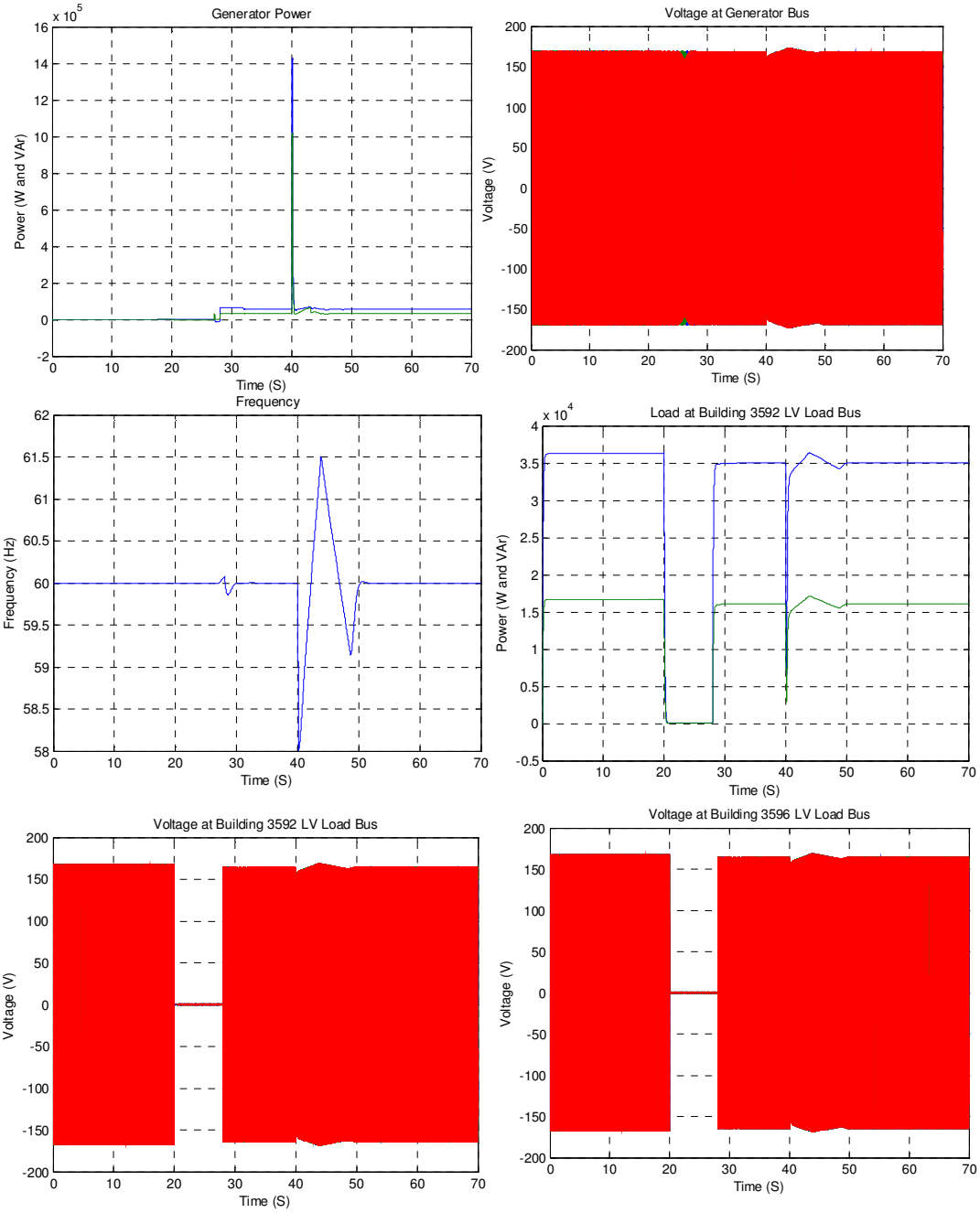
Generator Power
x 10^5
Power (W and VAr)
Time (S)
Voltage at Generator Bus
Voltage (V)
Time (S)
Frequency
Frequency (Hz)
Time (S)
Load at Building 3592 LV Load Bus
x 10^4
Power (W and VAr)
Time (S)
Voltage at Building 3592 LV Load Bus
Voltage (V)
Time (S)
Voltage at Building 3596 LV Load Bus
Voltage (V)
Time (S)

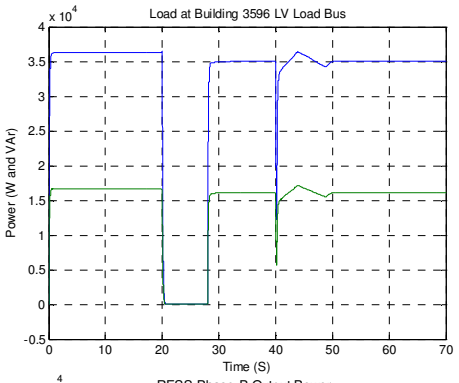
Load at Building 3596 LV Load Bus
x 10^4
Power (W and VAr)
Time (S)

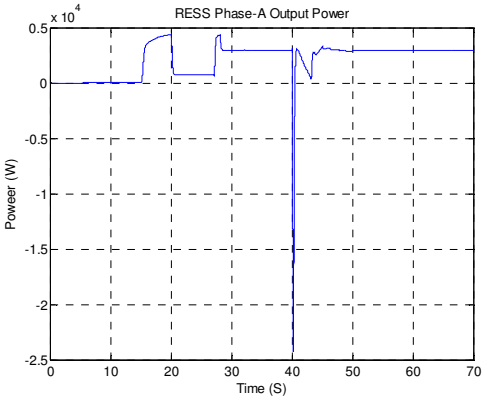
RESS Phase-A Output Power
x 10^4
Poweer (W)
Time (S)

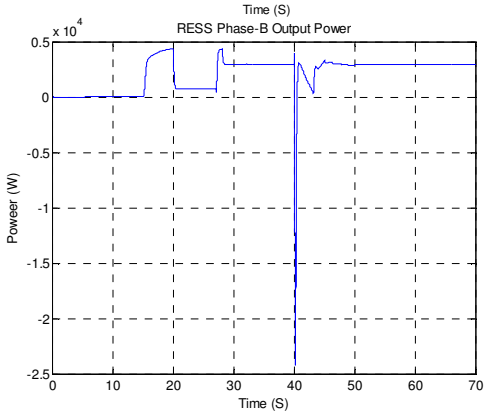
RESS Phase-B Output Power
x 10^4
Poweer (W)
Time (S)

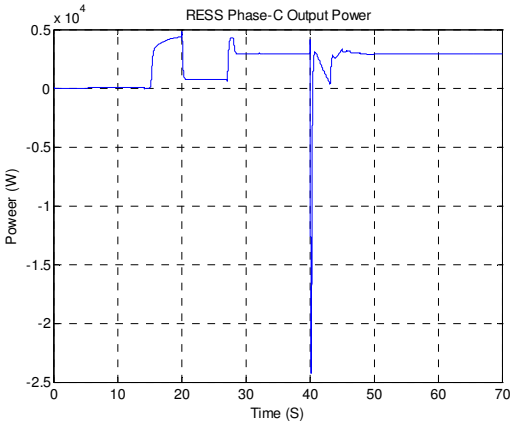
RESS Phase-C Output Power
x 10^4
Poweer (W)
Time (S)

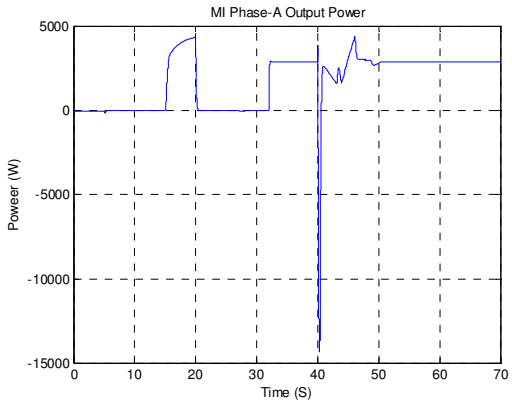
MI Phase-A Output Power
Poweer (W)
Time (S)

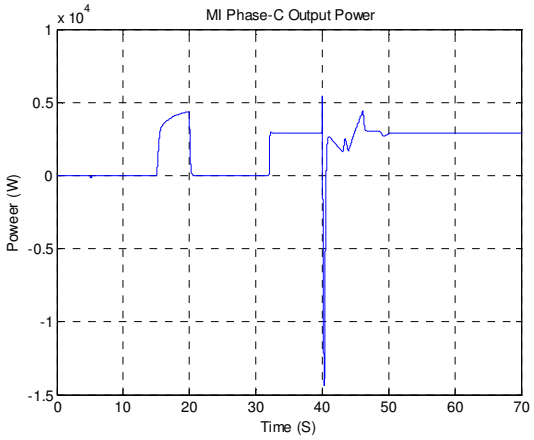
MI Phase-C Output Power
x 10^4
Poweer (W)
Time (S)

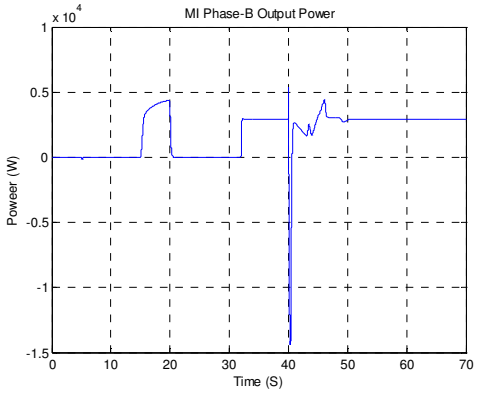
MI Phase-B Output Power
x 10^4
Poweer (W)
Time (S)

D.3.8 Loss of MI source from Microgrid

Case 7/Loss of MI source from Microgrid	
Time (sec)	**Action/Event**
0	Power on to load 3592 and Power on to load 3596
5	UPS and MI contactor engages
15	PV engages @ I(ph)=25 A for both BESS and MI setup
20	Utility power interrupted
20	Bldg 3592 Breaker and Bldg 3592 Breaker opens
20	MI contactor isolates
27	Generator engages – picks up Bldg 3592 and Bldg 3596 Load
28	Bldg 3592 Breaker and Bldg 3592 Breaker closes
32	MI contactor engages
40	Three phases of MI source are disconnected
70	End of the simulation

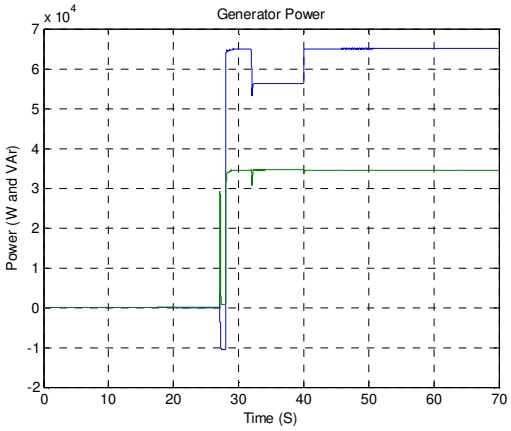
Generator Power
x 10^4
Power (W and VAr)
Time (S)

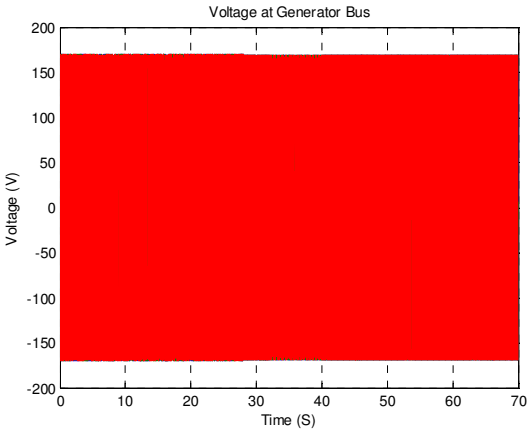
Voltage at Generator Bus
Voltage (V)
Time (S)

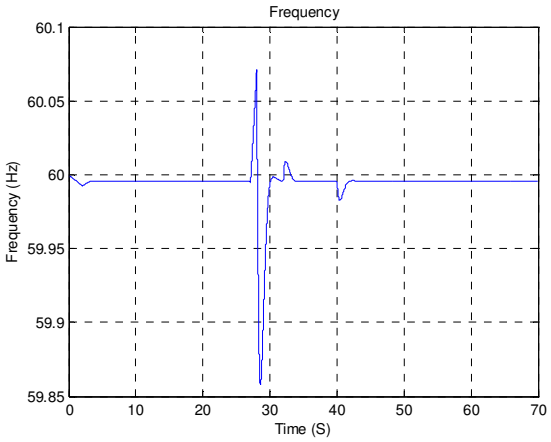
Frequency
Frequency (Hz)
Time (S)

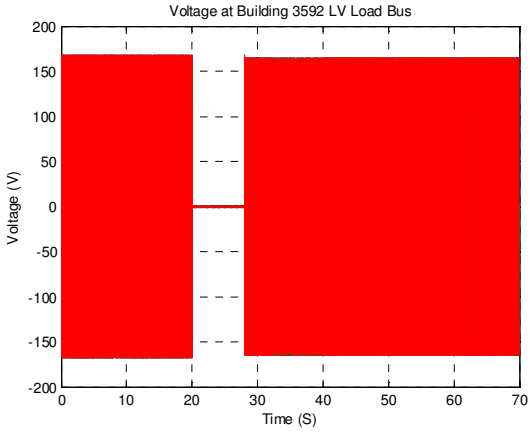
Voltage at Building 3592 LV Load Bus
Voltage (V)
Time (S)

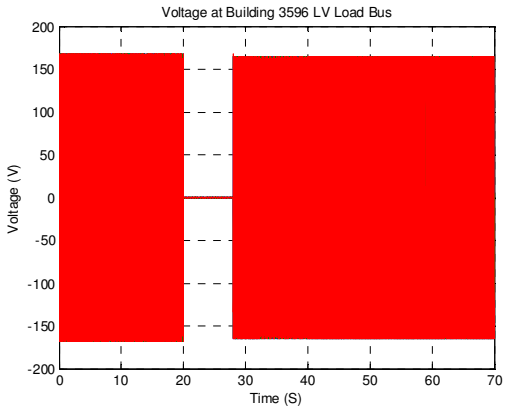
Voltage at Building 3596 LV Load Bus
Voltage (V)
Time (S)

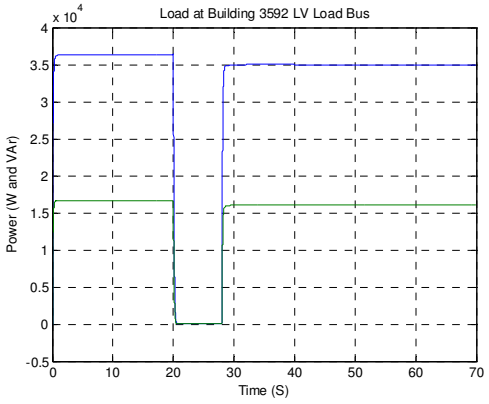
Load at Building 3592 LV Load Bus
x 10^4
Power (W and VAr)
Time (S)

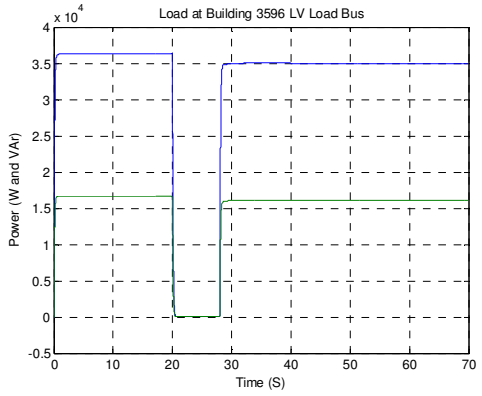
Load at Building 3596 LV Load Bus
x 10^4
Power (W and VAr)
Time (S)

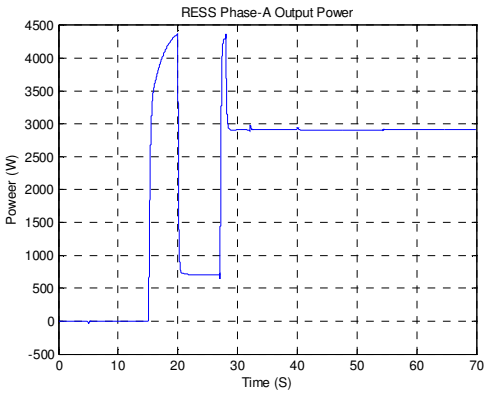
RESS Phase-A Output Power
Powoer (W)
Time (S)

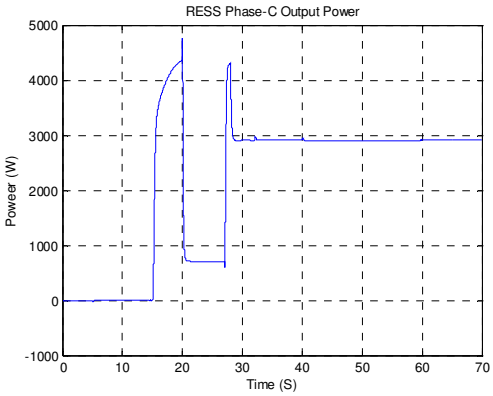
RESS Phase-C Output Power
Powoer (W)
Time (S)

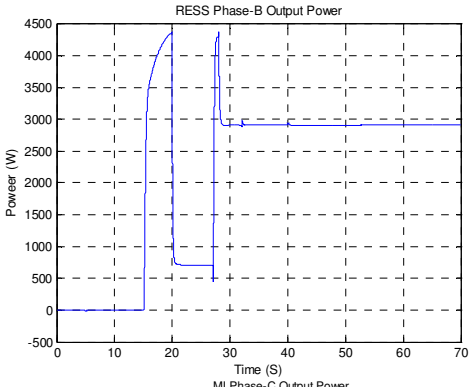
RESS Phase-B Output Power
Powoer (W)
Time (S)

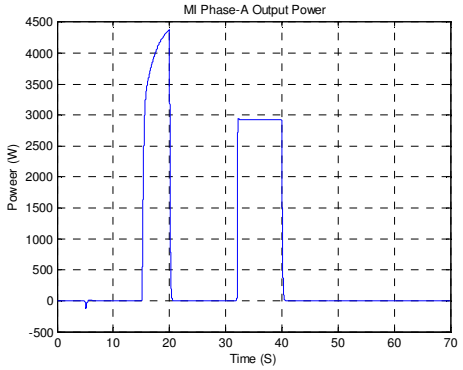
MI Phase-A Output Power
Powoer (W)
Time (S)

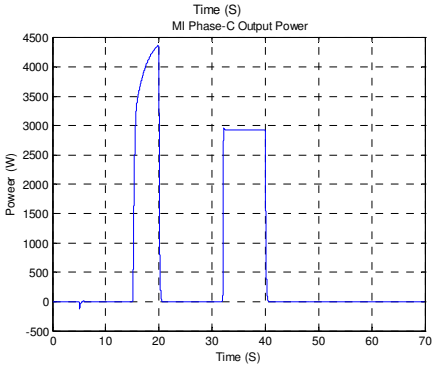
MI Phase-C Output Power
Powoer (W)
Time (S)

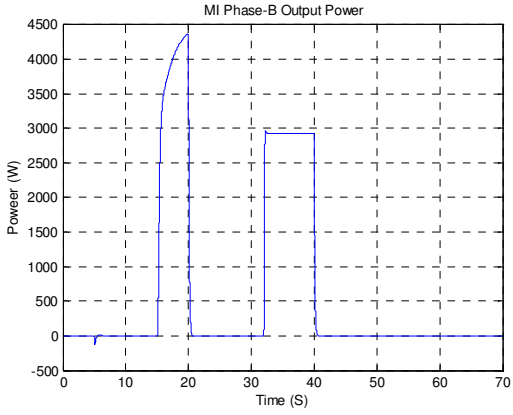
MI Phase-B Output Power
Powoer (W)
Time (S)

D.3.9 Step load increase (150%) at Bldg. 3592

Case 8/Step load increase at Bldg.3592	
Time (sec)	**Action/Event**
0	Power on to load 3592 and Power on to load 3596
5	UPS and MI contactor engages
15	PV engages @ I(ph)=25 A for both BESS and MI setup
20	Utility power interrupted
20	Bldg 3592 Breaker and Bldg 3592 Breaker opens
20	MI contactor isolates
27	Generator engages – picks up Bldg 3592 and Bldg 3596 Load
28	Bldg 3592 Breaker and Bldg 3592 Breaker closes
32	MI contactor engages
40	Step load increase (150%) at Bldg. 3592
70	End of the simulation

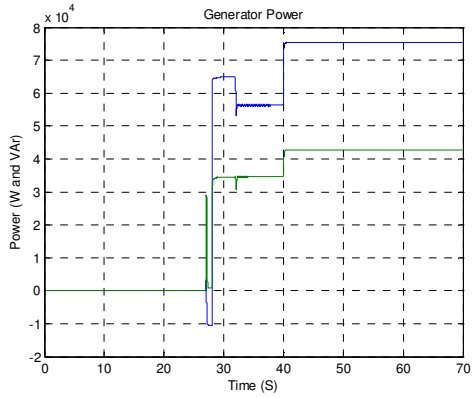
Generator Power
x 10^4
Power (W and VAr)
Time (S)

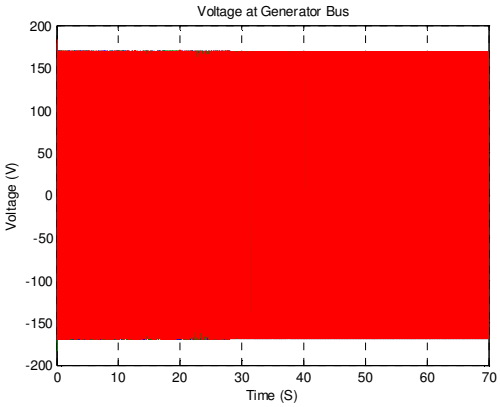
Voltage at Generator Bus
Voltage (V)
Time (S)

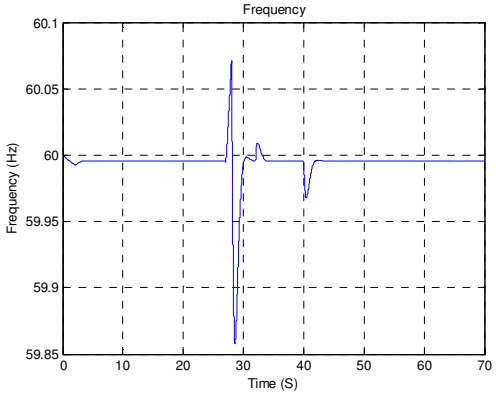
Frequency
Frequency (Hz)
Time (S)

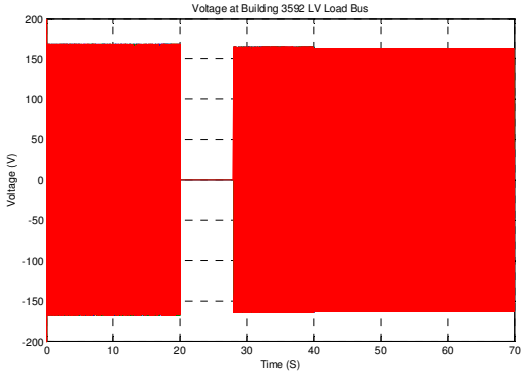
Voltage at Building 3592 LV Load Bus
Voltage (V)
Time (S)

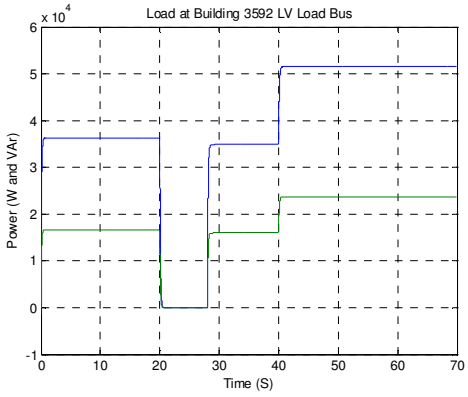
Load at Building 3592 LV Load Bus
x 10^4
Power (W and VAr)
Time (S)

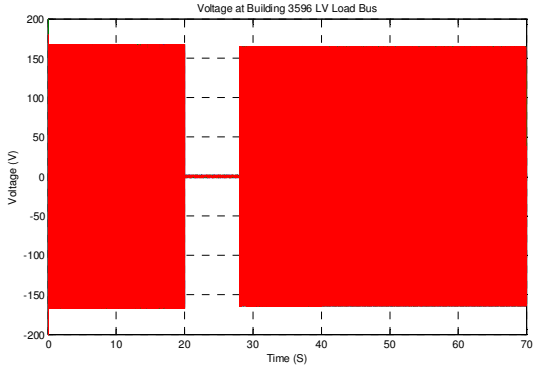
Voltage at Building 3596 LV Load Bus
Voltage (V)
Time (S)

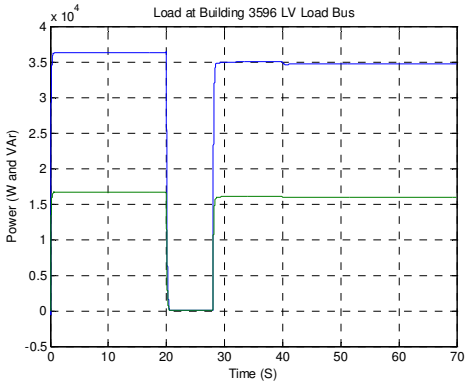
Load at Building 3596 LV Load Bus
x 10^4
Power (W and VAr)
Time (S)

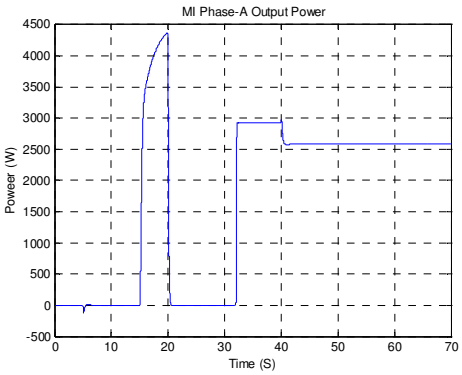
MI Phase-A Output Power
Poweer (W)
Time (S)

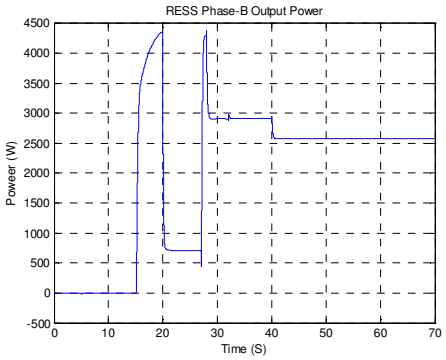
RESS Phase-B Output Power
Poweer (W)
Time (S)

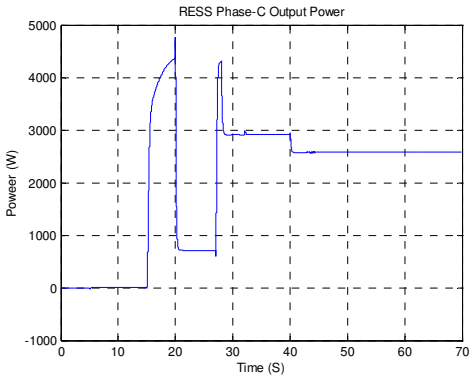
RESS Phase-C Output Power
Poweer (W)
Time (S)

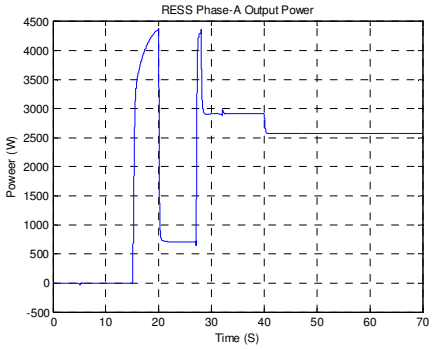
RESS Phase-A Output Power
Poweer (W)
Time (S)

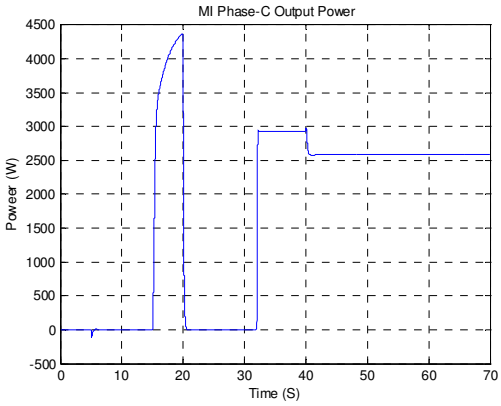
MI Phase-C Output Power
Power (W)
Time (S)

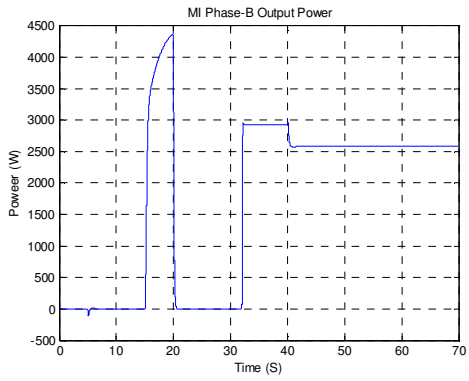
MI Phase-B Output Power
Poweer (W)
Time (S)

D.3.10 Step load increase (150%) at Bldg. 3596

Case 9/Step load increase at Bldg.3596	
Time (sec)	**Action/Event**
0	Power on to load 3592 and Power on to load 3596
5	UPS and MI contactor engages
15	PV engages @ I(ph)=25 A for both BESS and MI setup
20	Utility power interrupted
20	Bldg 3592 Breaker and Bldg 3592 Breaker opens
20	MI contactor isolates
27	Generator engages – picks up Bldg 3592 and Bldg 3596 Load
28	Bldg 3592 Breaker and Bldg 3592 Breaker closes
32	MI contactor engages
40	Step load increase (150%) at Bldg. 3596
70	End of the simulation

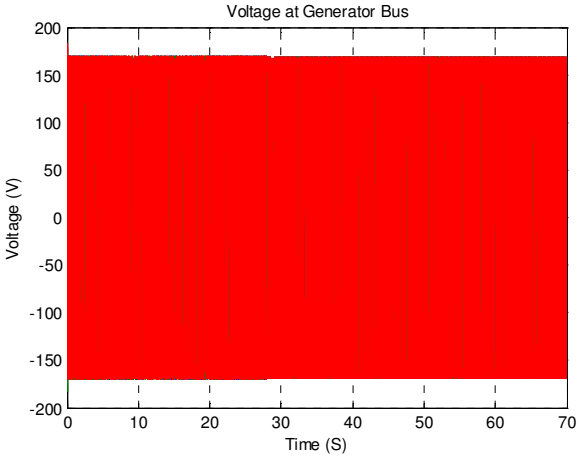
Voltage at Generator Bus
Voltage (V)
Time (S)

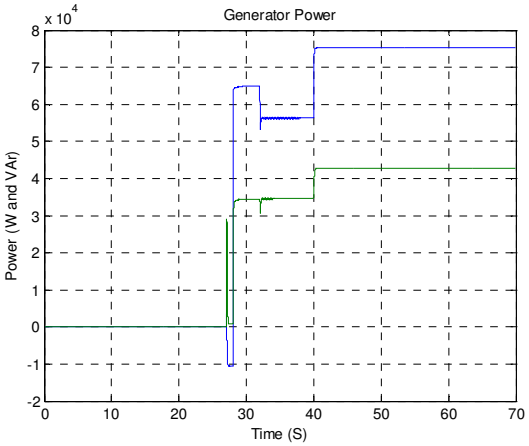
Generator Power
x 10^4
Power (W and VAr)
Time (S)

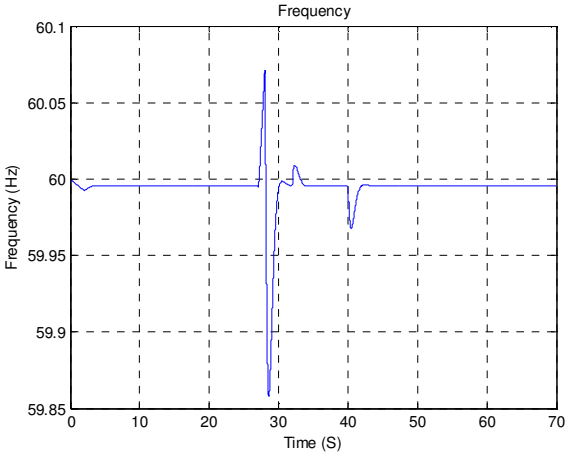
Frequency
Frequency (Hz)
Time (S)

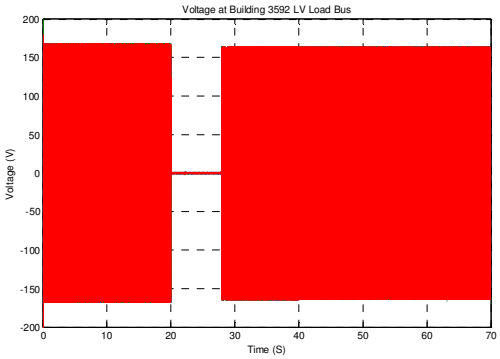
Voltage at Building 3592 LV Load Bus
Voltage (V)
Time (S)

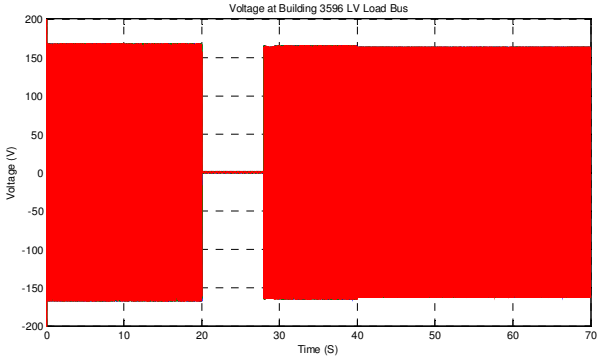
Voltage at Building 3596 LV Load Bus
Voltage (V)
Time (S)

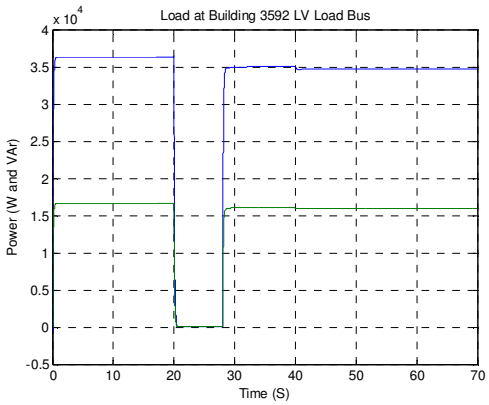
Load at Building 3592 LV Load Bus
x 10^4
Power (W and VAr)
Time (S)

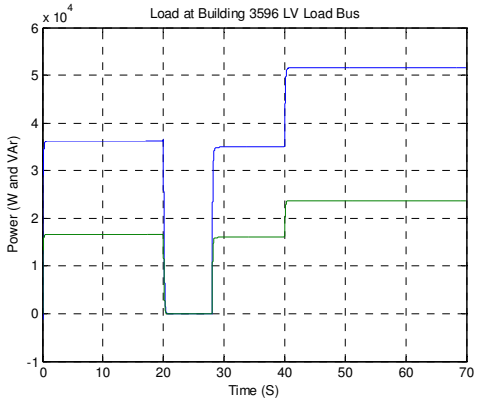
Load at Building 3596 LV Load Bus
x 10^4
Power (W and VAr)
Time (S)

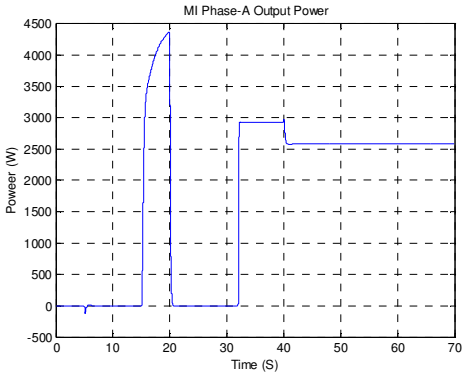
MI Phase-A Output Power
Poweer (W)
Time (S)

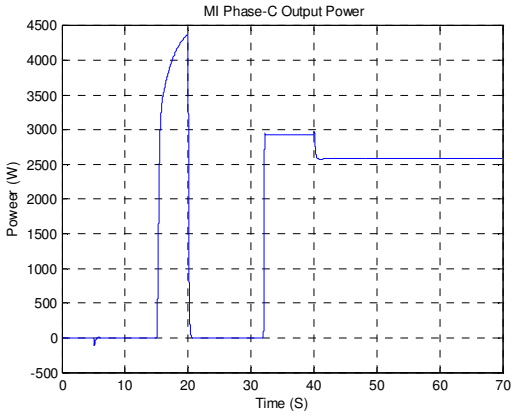
MI Phase-C Output Power
Poweer (W)
Time (S)

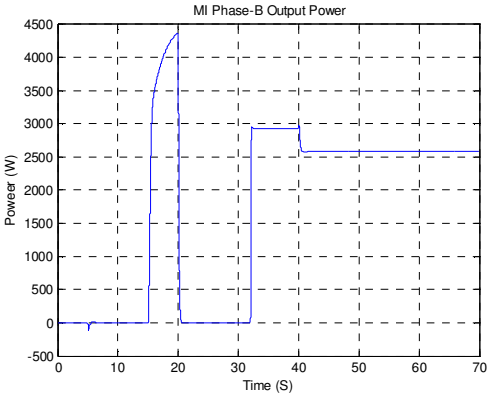
MI Phase-B Output Power
Poweer (W)
Time (S)

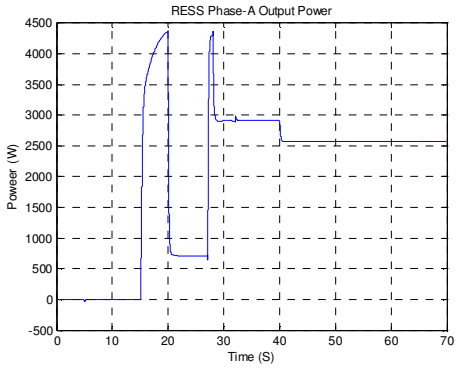
RESS Phase-A Output Power
Poweer (W)
Time (S)

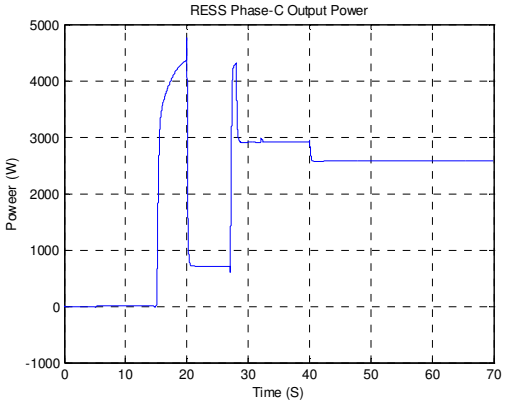
RESS Phase-C Output Power
Poweer (W)
Time (S)

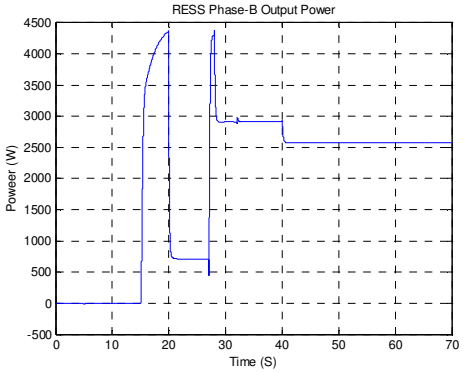
RESS Phase-B Output Power
Poweer (W)
Time (S)

D.4 Long-term Dynamic Analysis (time-series load flow) results

This appendix section presents detailed results of WVSC microgrid Long-term Dynamic Analysis (time-series load flow). The figures below show the feeder peak load profile, building load profiles, generator profile, and solar PV profiles that have been used in the model. In generator profile and Solar PV profile 100% represents the maximum nameplate generation.

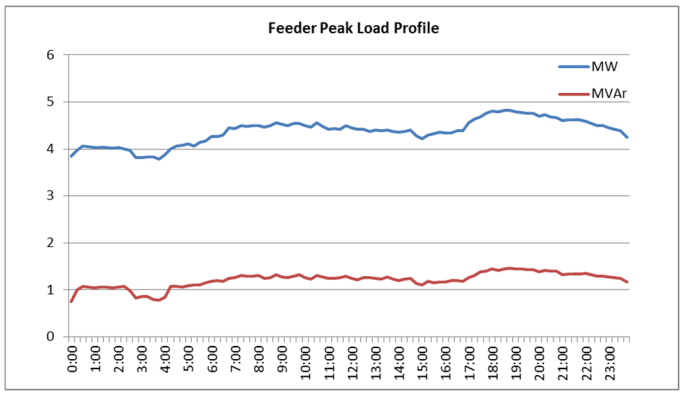

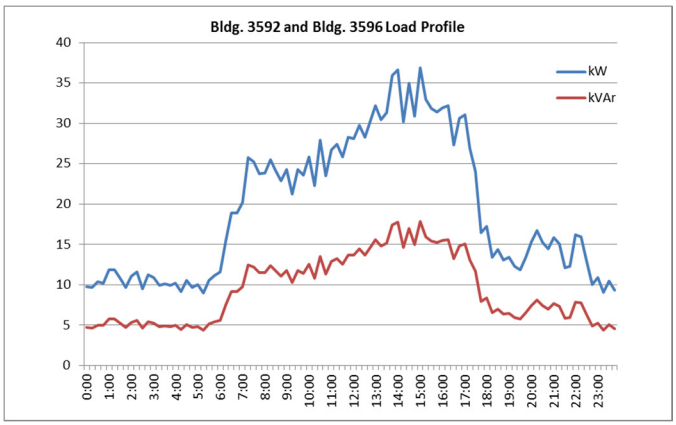

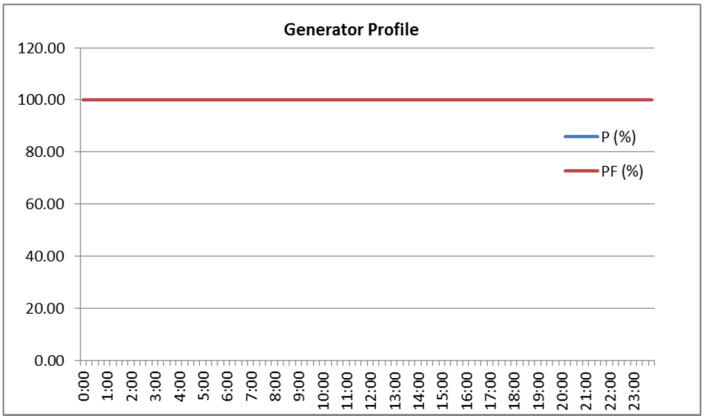

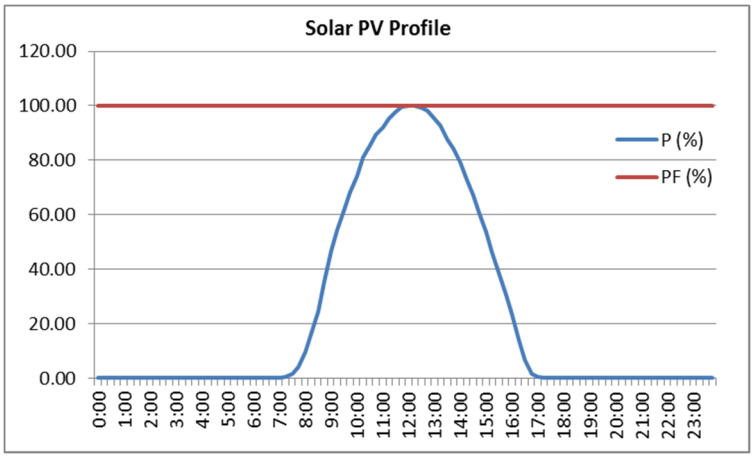

D.4.1 Grid connected microgrid time-series load flow results

Following figures show the time series load flow analysis results for a peak day feeder load profile. The X- axis represents 15 minute time intervals of an entire day starting from 0:00 time stamp and ending at 23:45 time stamp.

Feeder loading profile

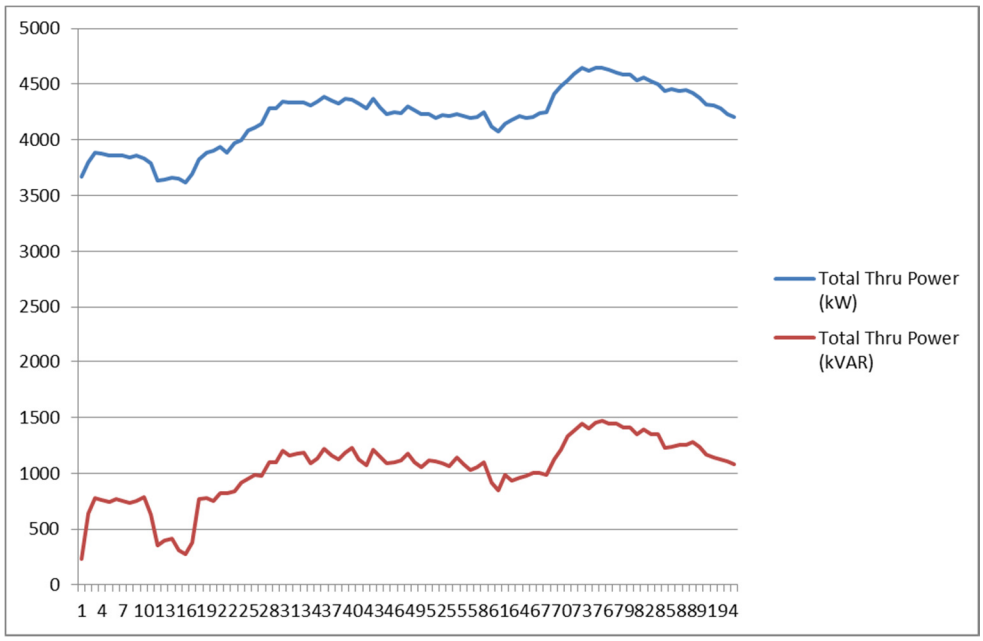

Substation secondary side voltage profile

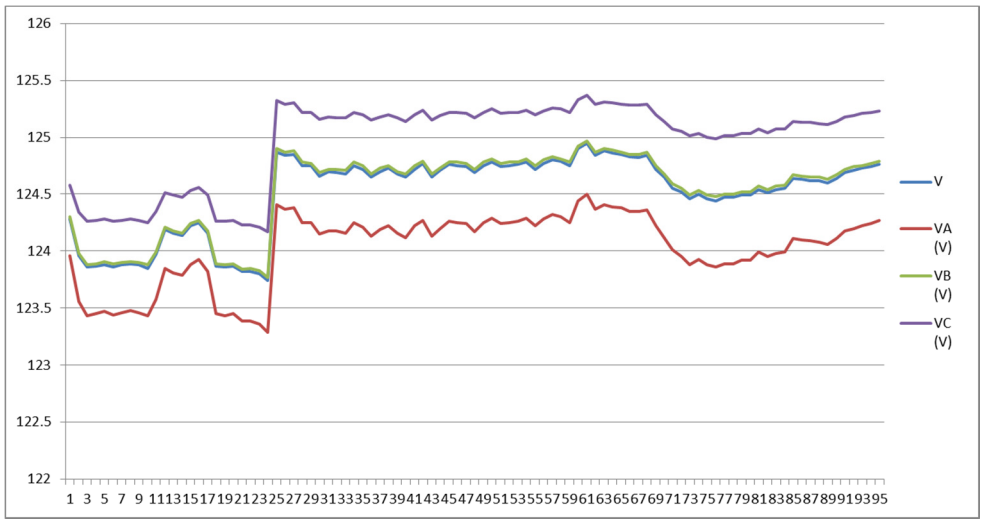

Building 3592 and 3596 loading profile

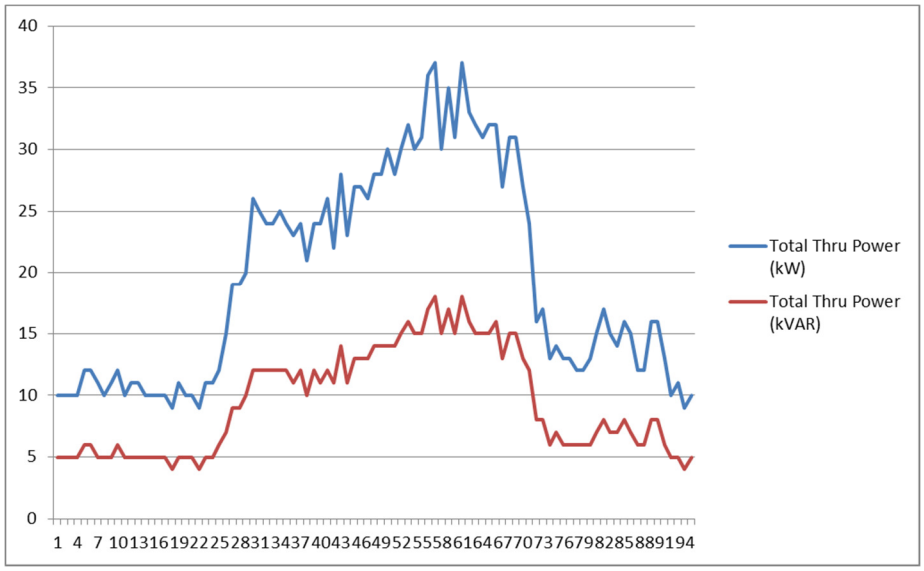

Total microgrid generation profile

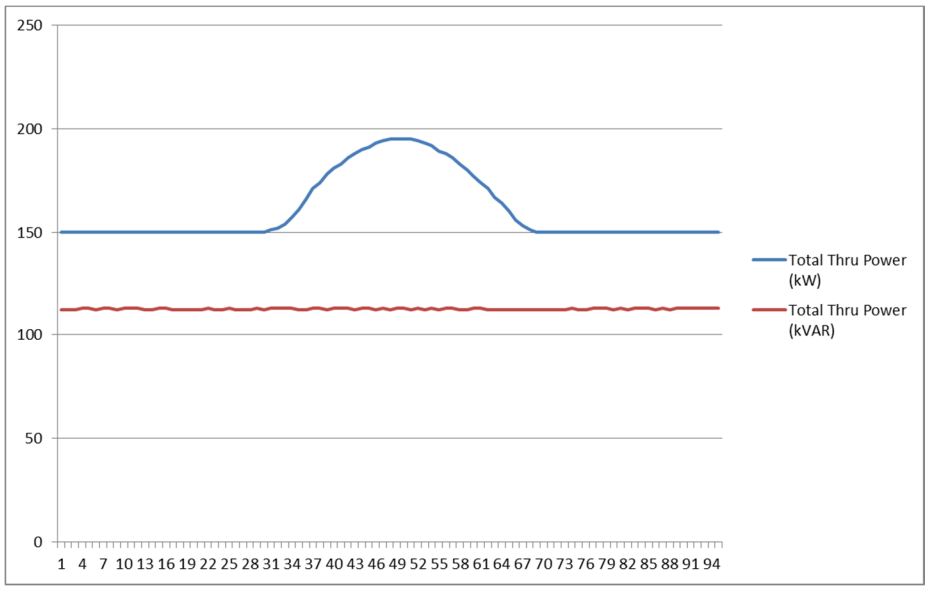

PCC Breaker voltage profile

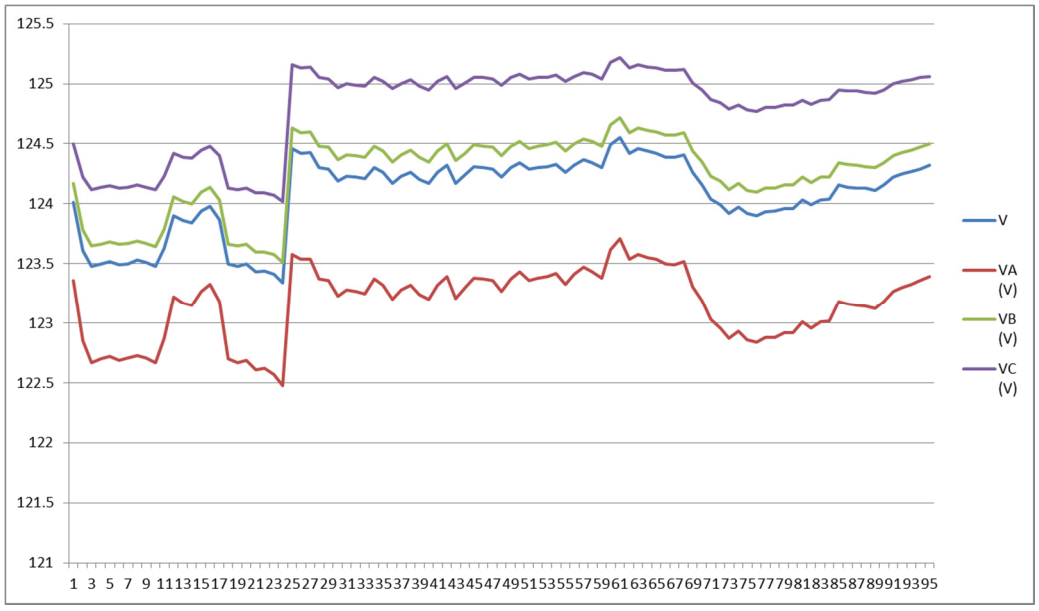

Generation connection Bus (MV) voltage profile

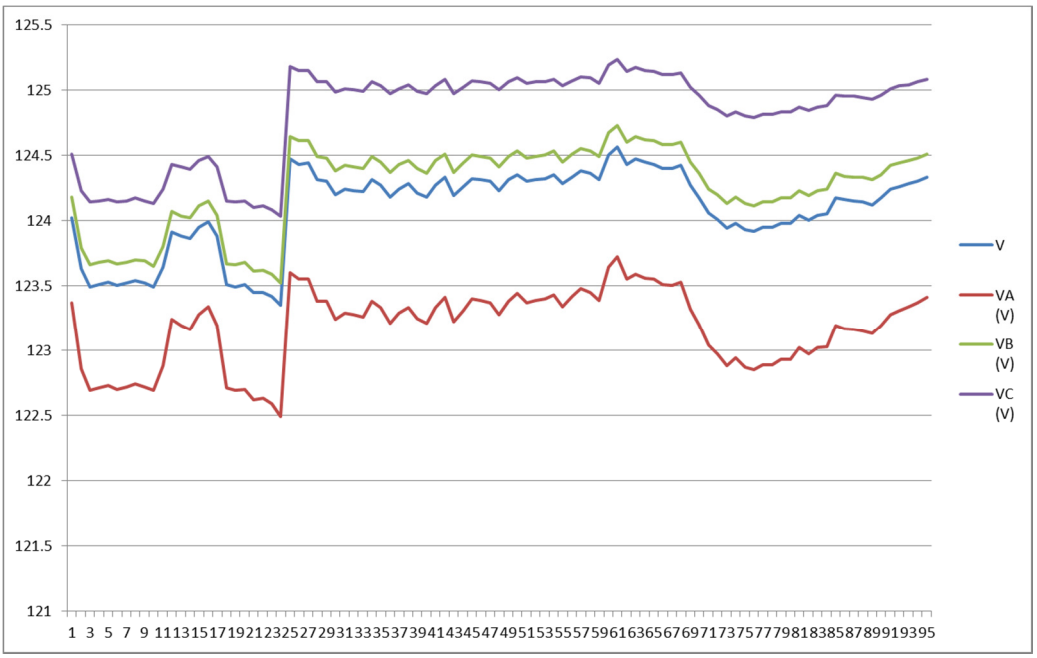

Bldg. 3592 voltage profile

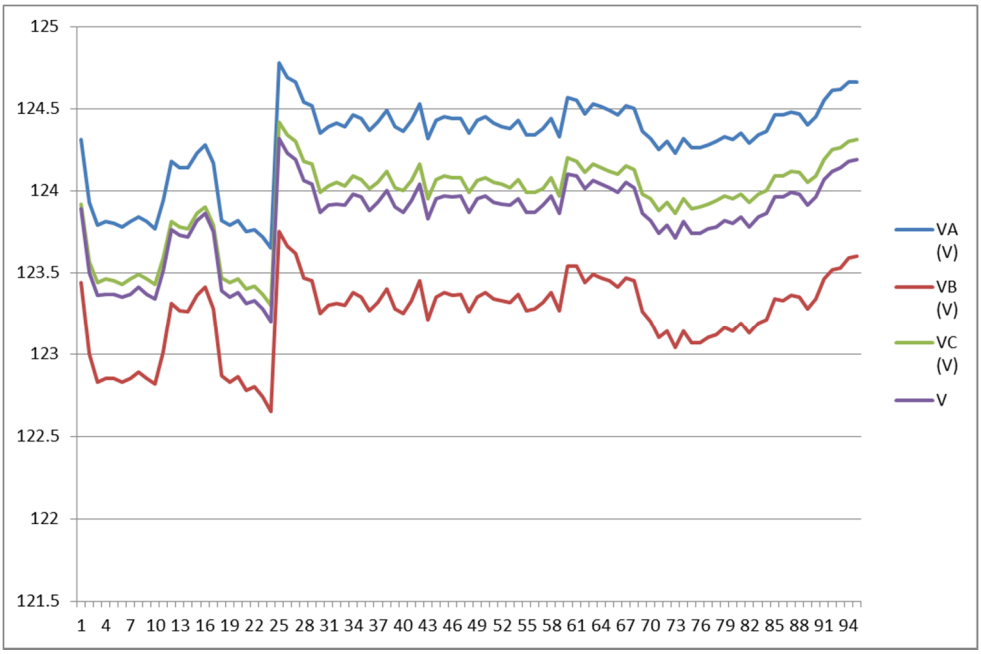

Bldg. 3596 voltage profile

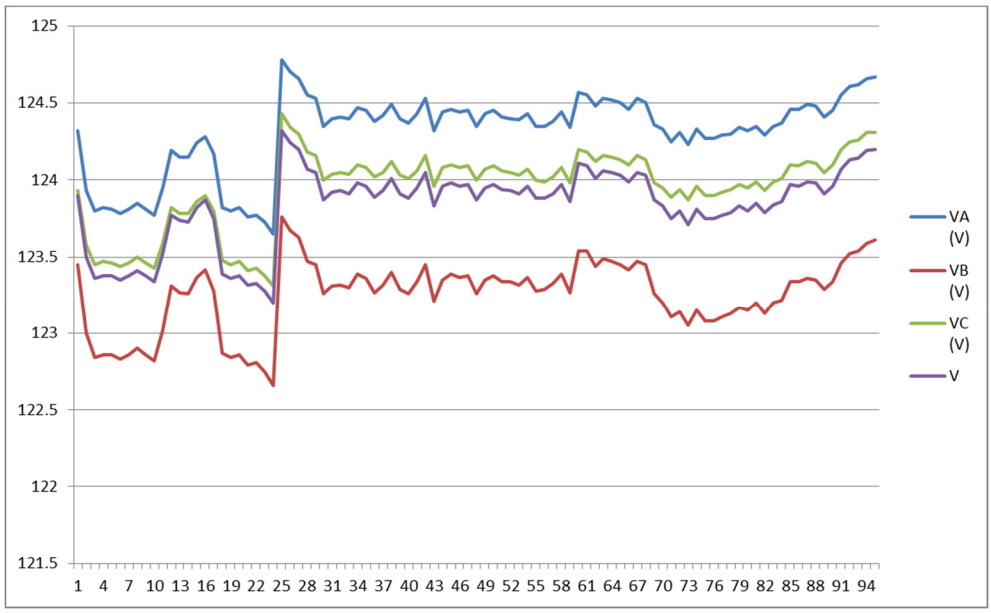

Feeder End of Line voltage profile

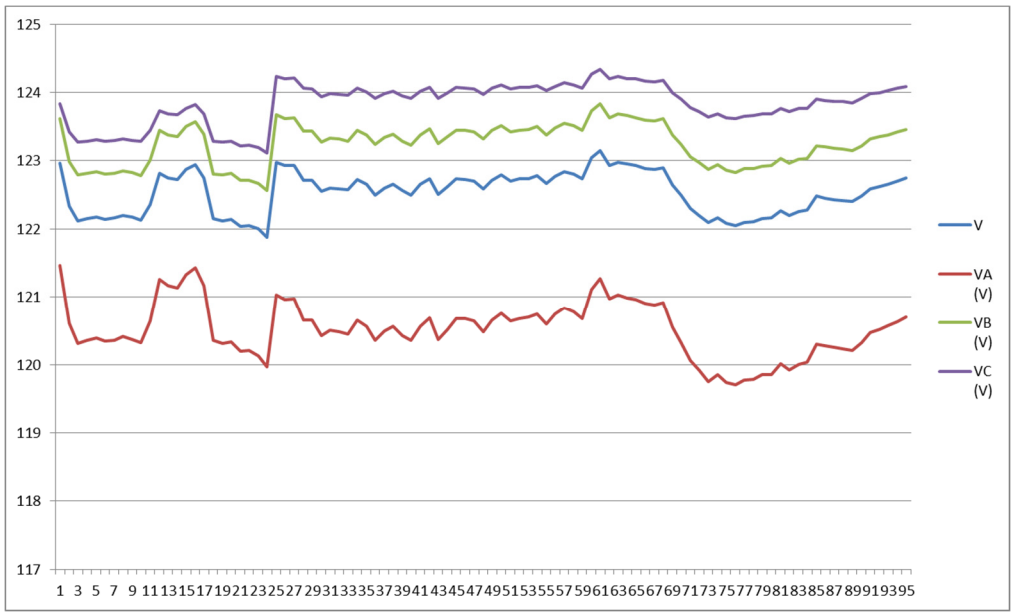

D.4.2 Islanded microgrid time-series load flow results

Following figures show the time series load flow analysis results for a peak day feeder load profile. The x-axis in the charts represents 15 minute time intervals of an entire day starting from 0:00 time stamp and ending at 23:45 time stamp.

Feeder loading profile

Building 3592 and 3596 loading profile

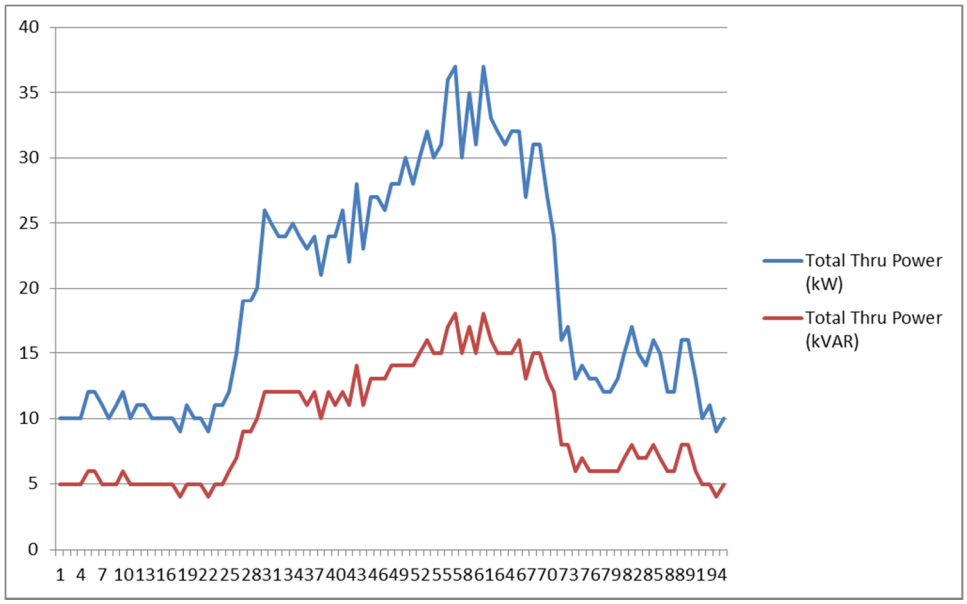

Total microgrid generation profile

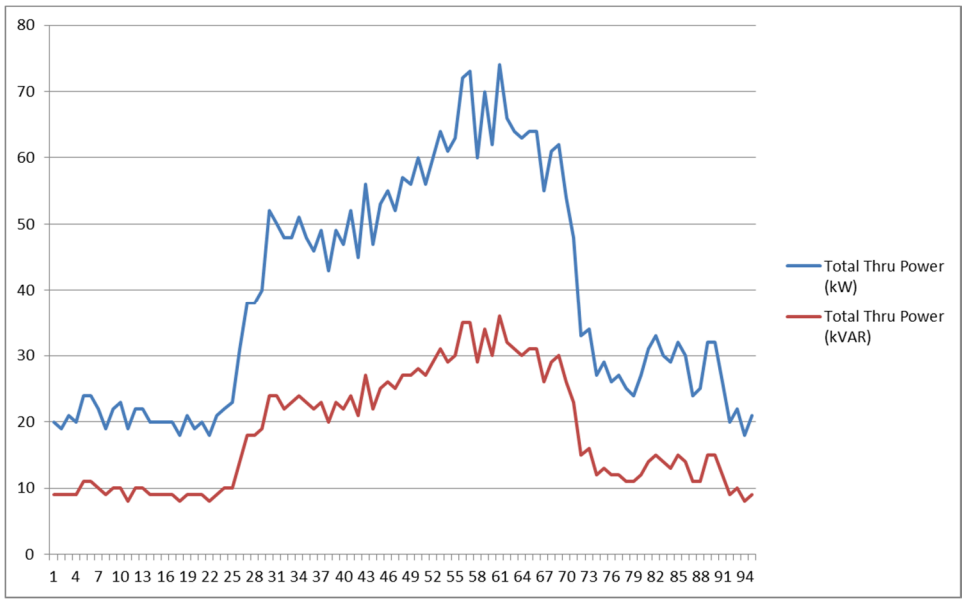

PCC Breaker voltage profile

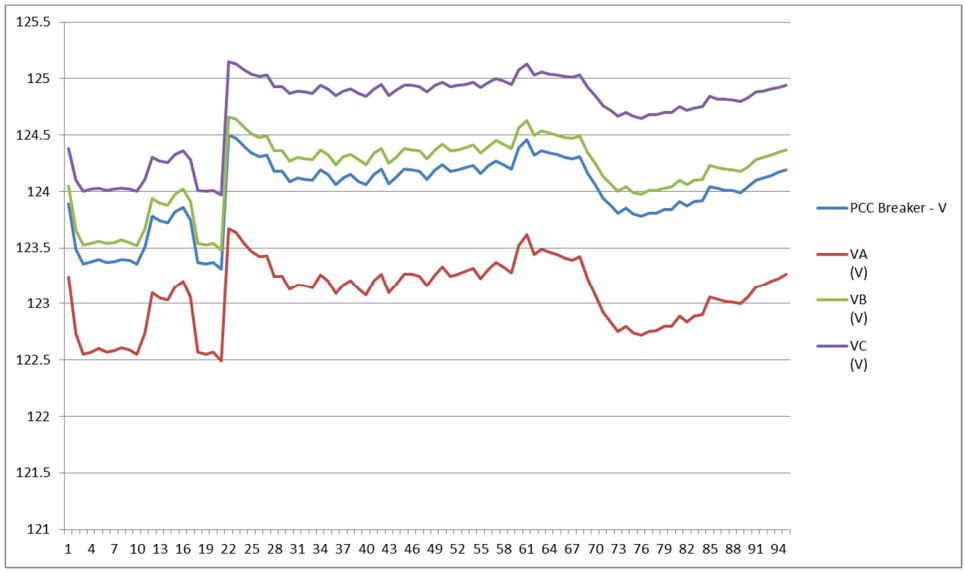

Generation connection Bus (MV) voltage profile

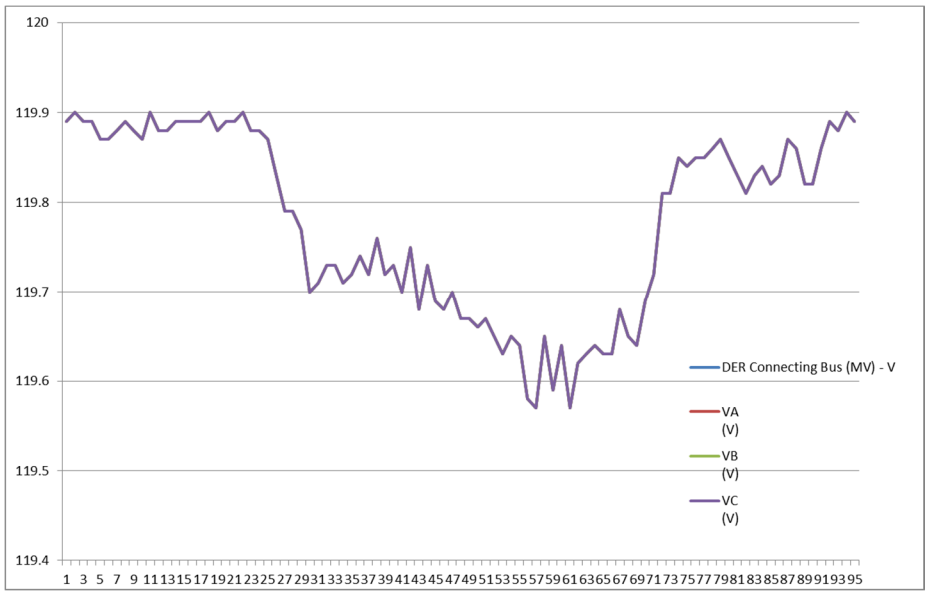

Bldg. 3592 voltage profile

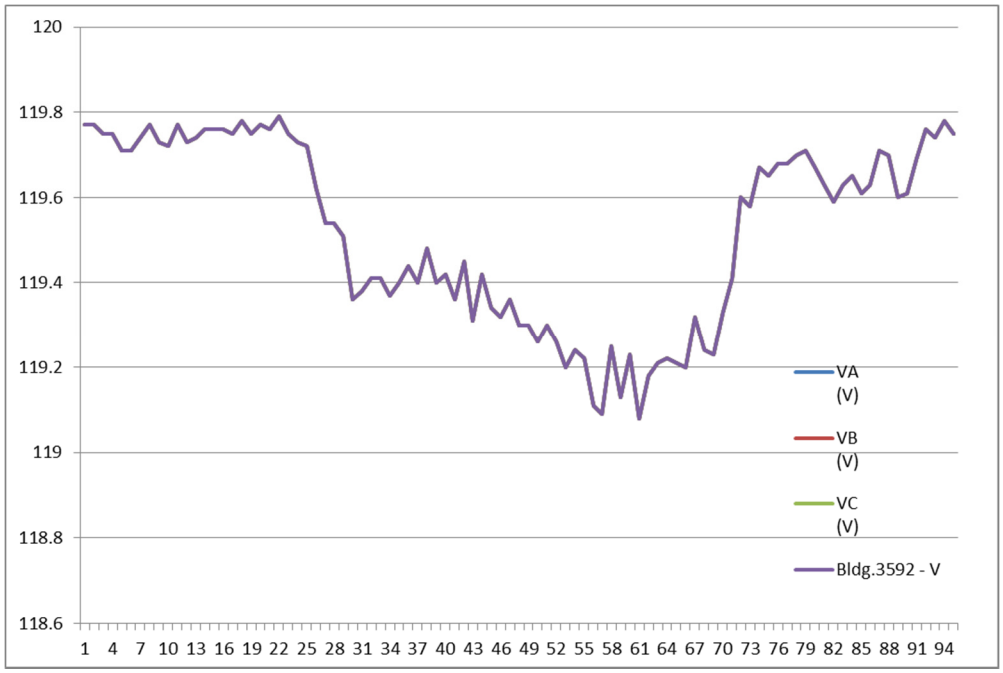

Bldg. 3596 voltage profile

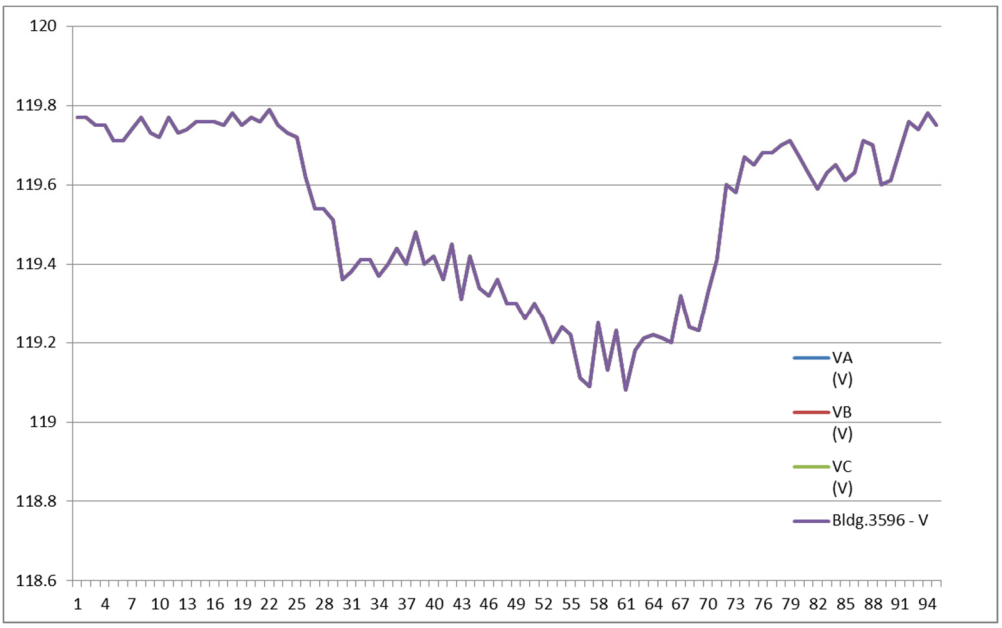

Appendix E-APERC Modeling and Simulation

E.1 Code to extract PV Module Parameters from a Data Sheet

```
% Program to obtain the PV parameters from  data Sheet
% Parameter of Polycrystalline PV Module 60 cells UP-M225P
voc=37.0;          % Open circuit voltage in V of the module
vm=29.2;           % voltage value @ MPP
Isc=8.27;          % Short Circuit current in A of the module
Im=7.71;           % current value at MPP
pm=225;            % Power value @ MPP
nc=60;             % number of cell in a module
K_i=5.5e-4;
K_v=-3.3e-3;
Tstc=25  ;          % In degree C
Iro= 1000;         % Irradiance at STC
Irr=Iro;
% Other papameter
Tr=273+Tstc;
Tref=Tr;
k=1.3806e-23;
q=1.602e-19;
a=1.5;
Vt=k*Tr/q;
% Initializing the unknown parameters;
Toler=0.0001;
Incr_rs=0.0001;
Err=50;
max_iter=1000000;
iter=0;

% Initial guess of Rp and Rs
rs=0;
rp=(vm/(Isc-Im))-((voc-vm)/Im);
% calculating the diode saturation current
Isat=Isc/(exp(voc/(nc*a*Vt))-1);
while (Err> Toler) && rp>0 && (iter<max_iter)
```

```
    iter=iter+1;
    Ipv=(rp+rs)*Isc/rp;
    rp_init=rp;
    rs=rs+Incr_rs;
    rp=vm*(vm+Im*rs)/(vm*Ipv-
vm*Isat*exp((vm+Im*rs)/(Vt*nc*a))+vm*Isat-pm);
    v=0:voc/100:voc;
    [q1,q2]=size(v);
    I=zeros(1,q2);
    % solving for I using newton rhapson
    for k=1:q2
        M=Ipv-Isat*(exp((v(k)+I(k)*rs)/(Vt*nc*a))-1)-
(v(k)+I(k)*rs)/rp-I(k);
        while (abs (M)> Toler)
            M=Ipv-Isat*(exp((v(k)+I(k)*rs)/(Vt*nc*a))-1)-
(v(k)+I(k)*rs)/rp-I(k);
            derivM=-Isat*rs/(Vt*nc*a)*exp((v(k)+I(k)*rs)/(Vt*nc*a))-
rs/rp-1;
            I_new=I(k)-M/derivM;
            I(k)=I_new;
        end;
    end;
    p=(Ipv-Isat*(exp((v+I.*rs)/(Vt*nc*a))-1)-(v+I.*rs)/rp).*v;
    pc=max(p);
    Err=abs(pc-pm);
end;
if rp<0;
    rp=rp_init;
end;
% To obtain the parameter for the panel;
 C2=(vm/voc-1)/log(1-Im/Isc);
C1=(1-Im/Isc)*exp(-vm/C2/voc);
V_panel=190;
Ns=5;
P_panel=10000;
P_string=Ns*pm;
```

```
Np=ceil(P_panel/P_string);
 Rs=rs*Ns;
Rp=rp*Ns;
A=nc*Ns*a;
Voc=voc*Ns;
Vm=vm*Ns;
Pm=Im*Vm;
Pa=Np*Pm;
Ts=1e-6;
```

E.2 Microgrid Simulink Models

Single Phase System

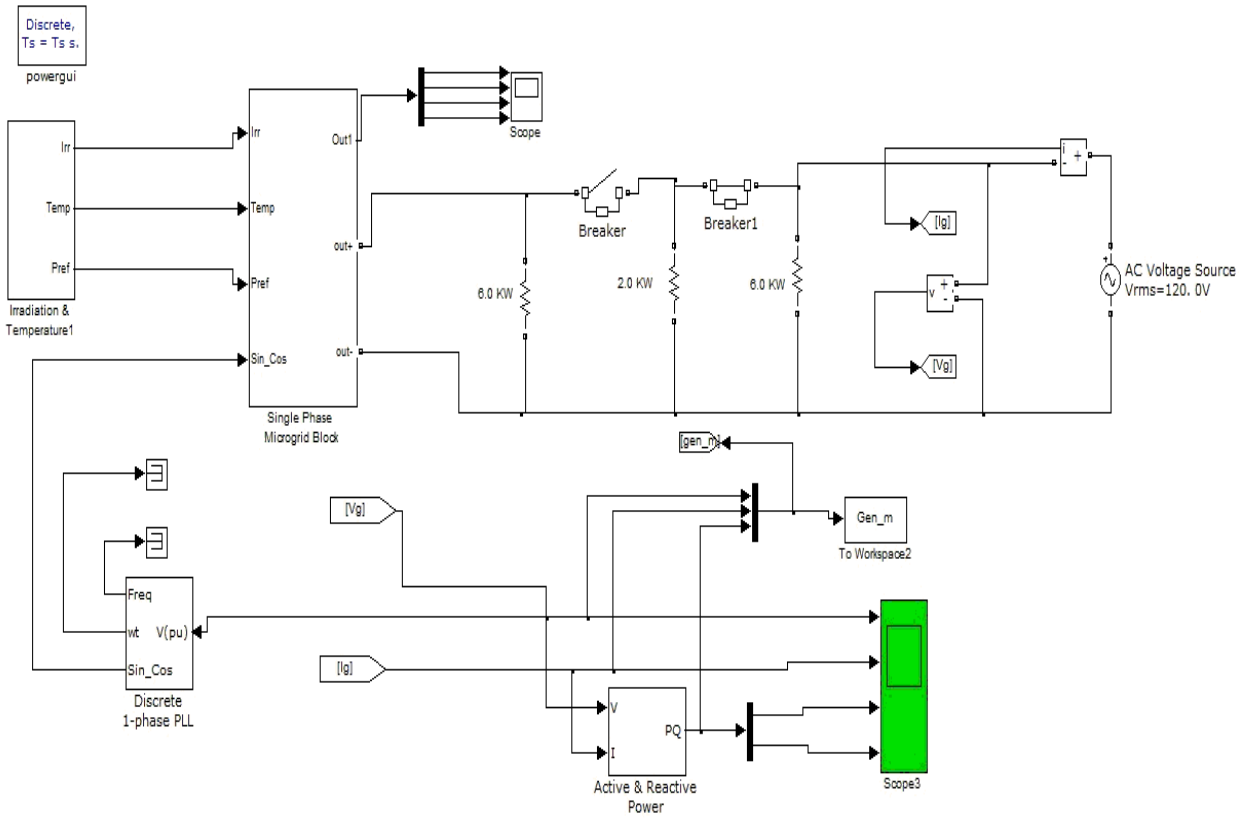

Figure E.1: Single Phase Microgrid System

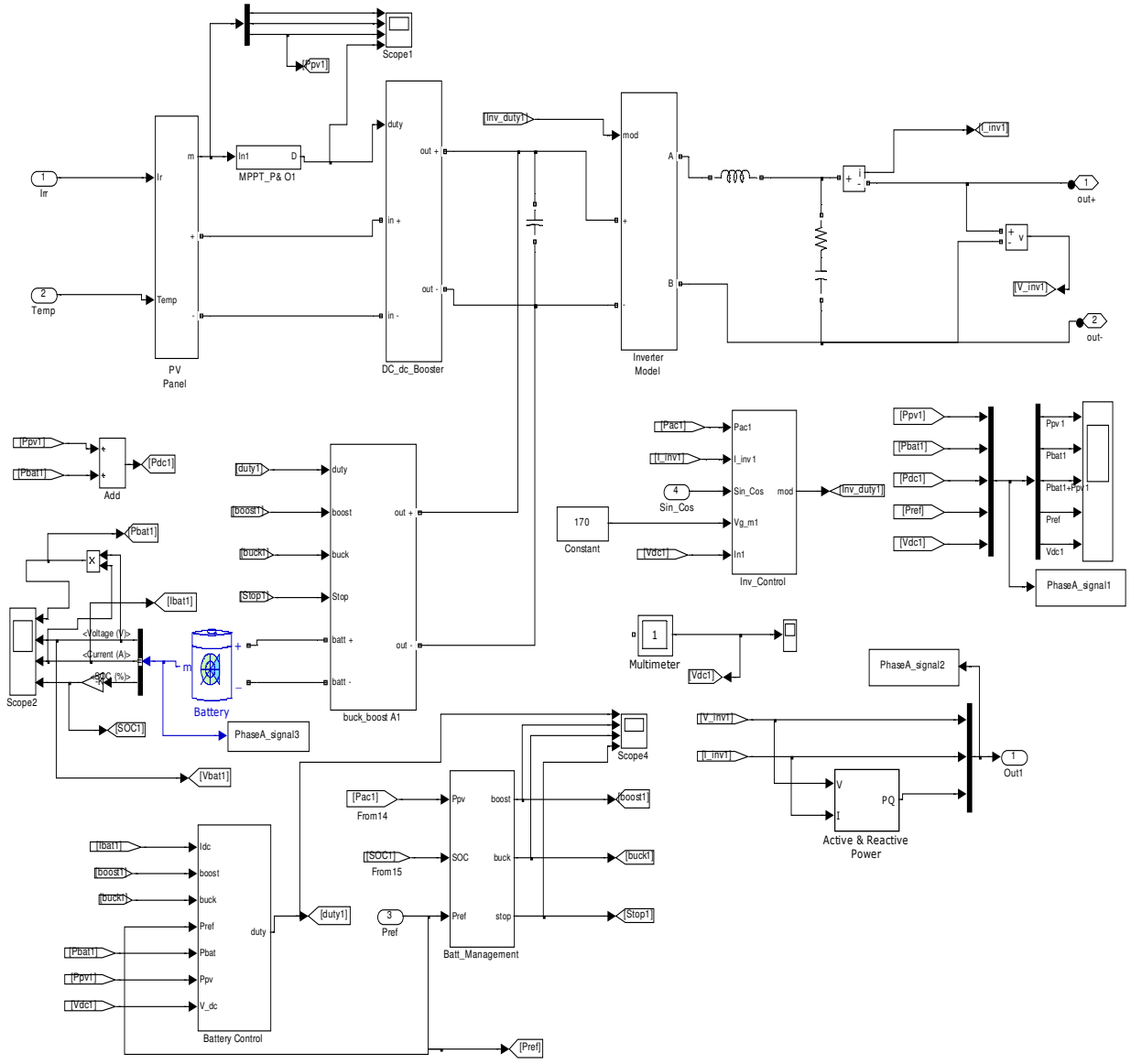

Figure E.2: Inside the Single Phase Microgrid Block

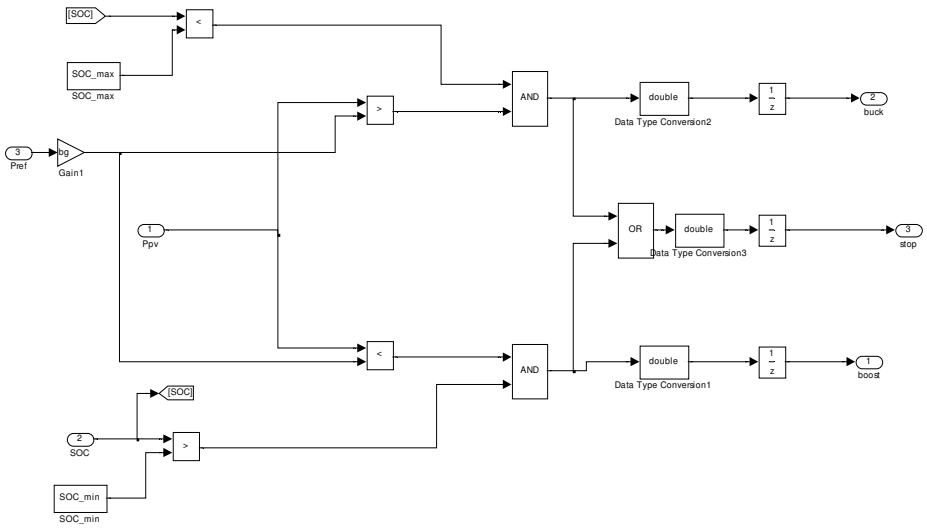

Figure E.3: Inside the Battery Management Block

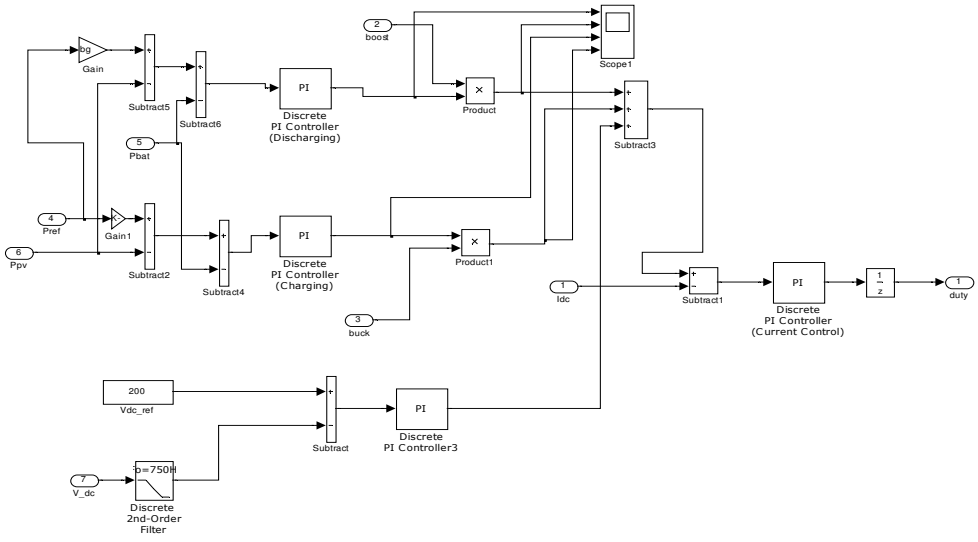

Figure E.4: Inside the Battery Control Block

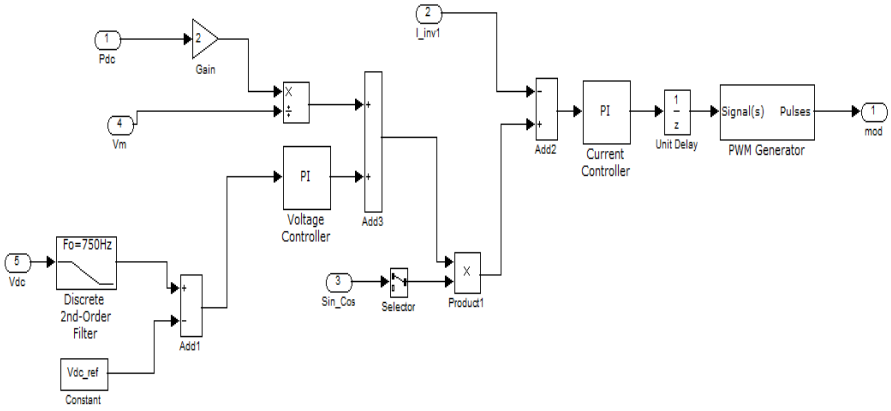

Figure E.5: Inside the Inverter Control Block

E.3 PSCAD Modeling

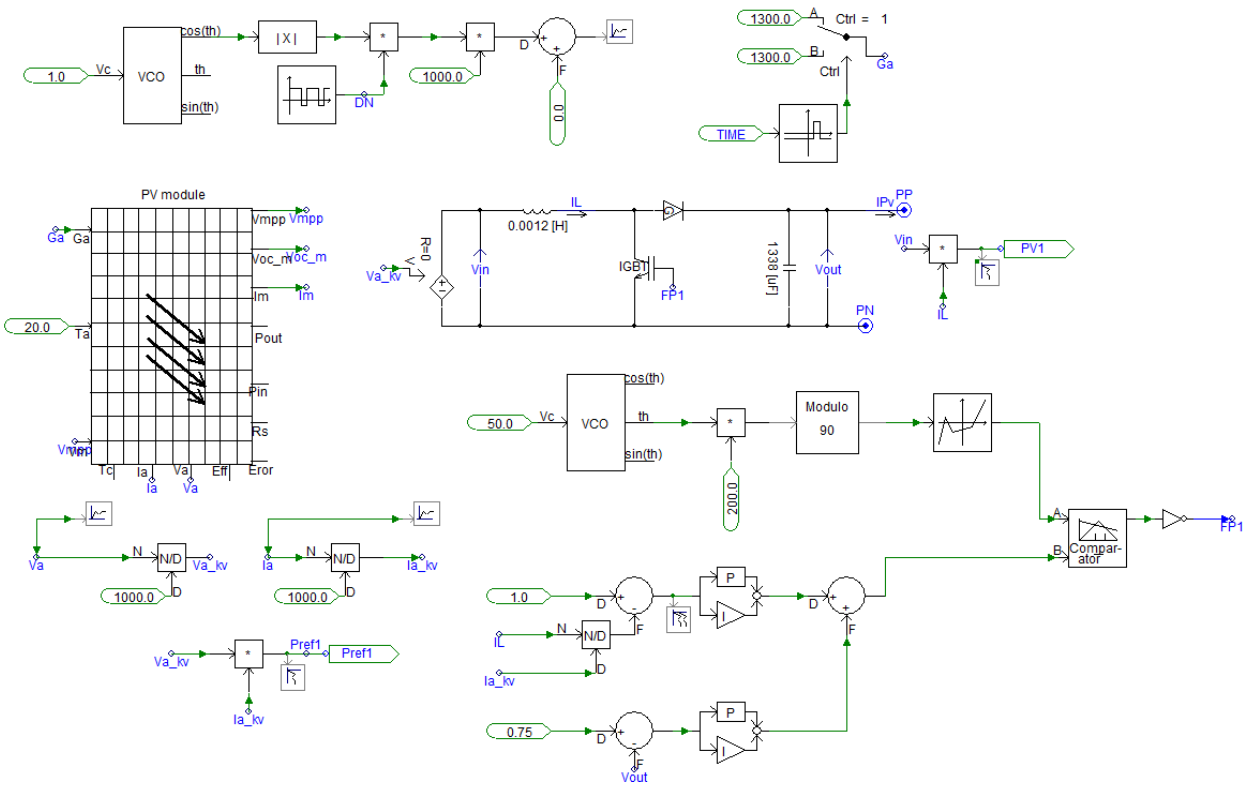

Figure E.6: Modeling of PV and DC/DC

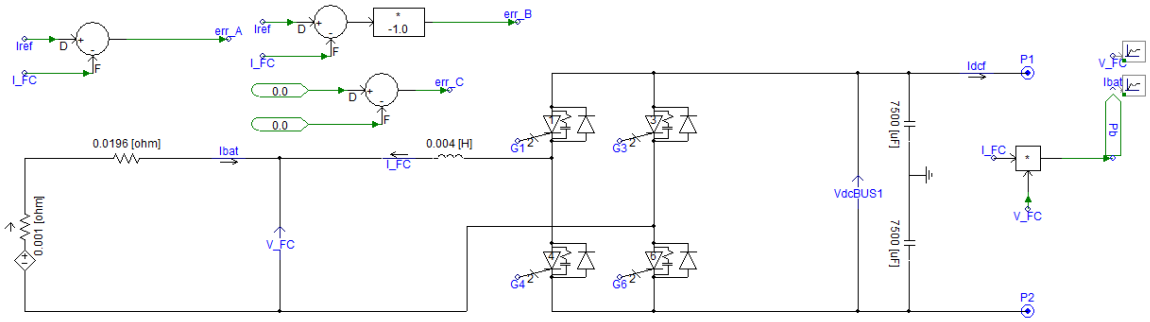

Figure E.7: Battery Simulation Modeling

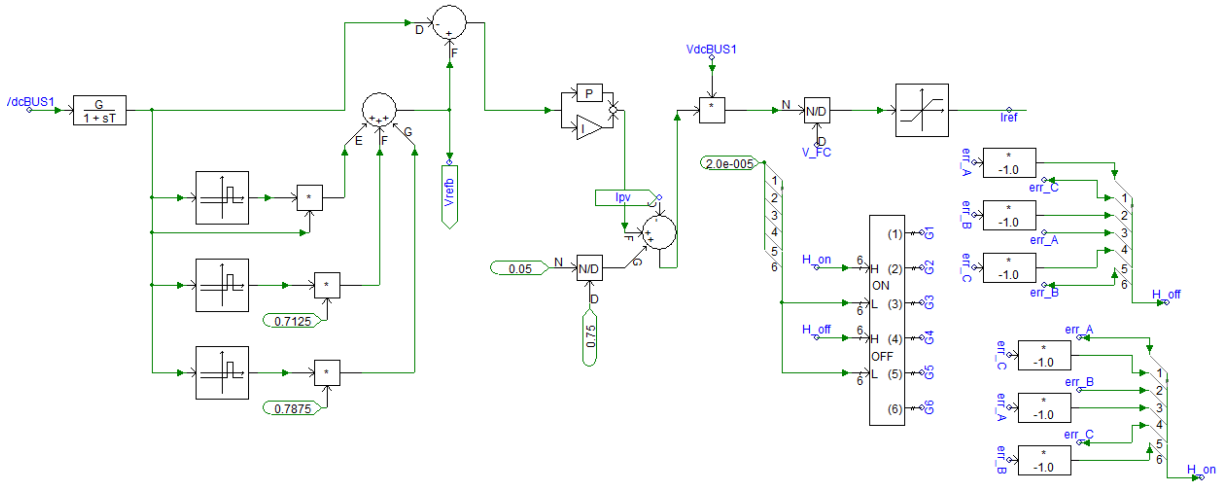

Figure E.8: Battery Control System

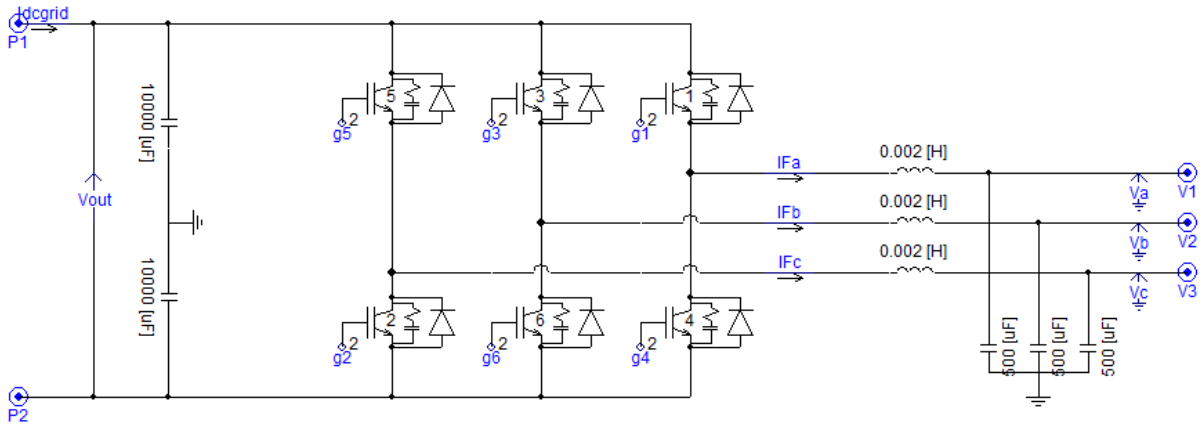

Figure E.9: System's Inverter

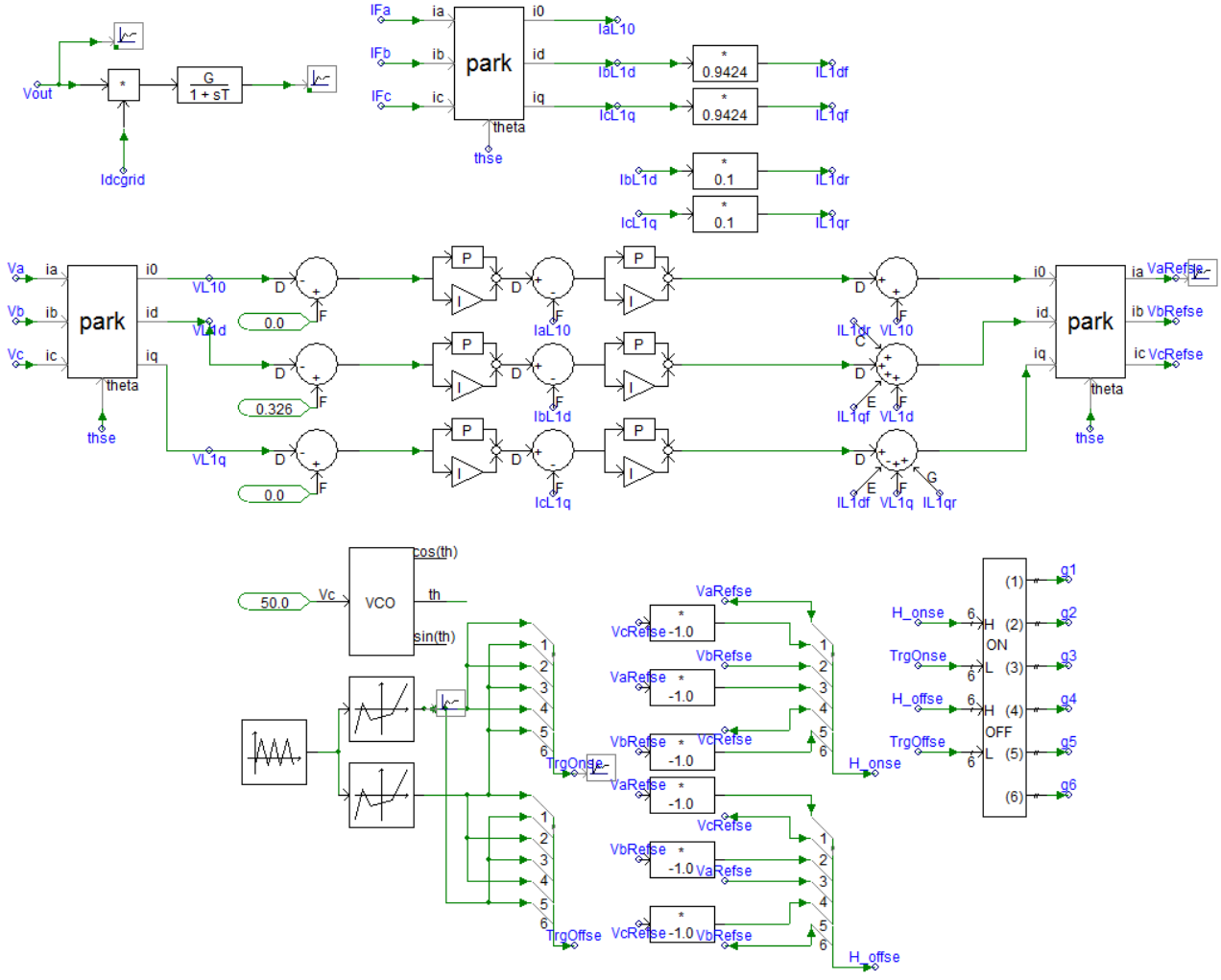

Figure E.10: Control Strategy of Inverter

E.4 Implementation on SCE's Circuit of the Future Model

The technique presented above is implemented on a model of a Southern California Edison (SCE) distribution feeder known as the Circuit of the Future. The project is designed to test new hardware and automation technologies for circuit construction. The system consists of 66 buses, one substation, 2 distributed generators and 14 residential loads with some capacitor banks scattered throughout the grid as shown in Figure E.11. The system is divided into 3 zones connected via controllable switches. In case of faults, these switches are operated to change or reconfigure the system in order to feed the loads and restore the power in the isolated areas.

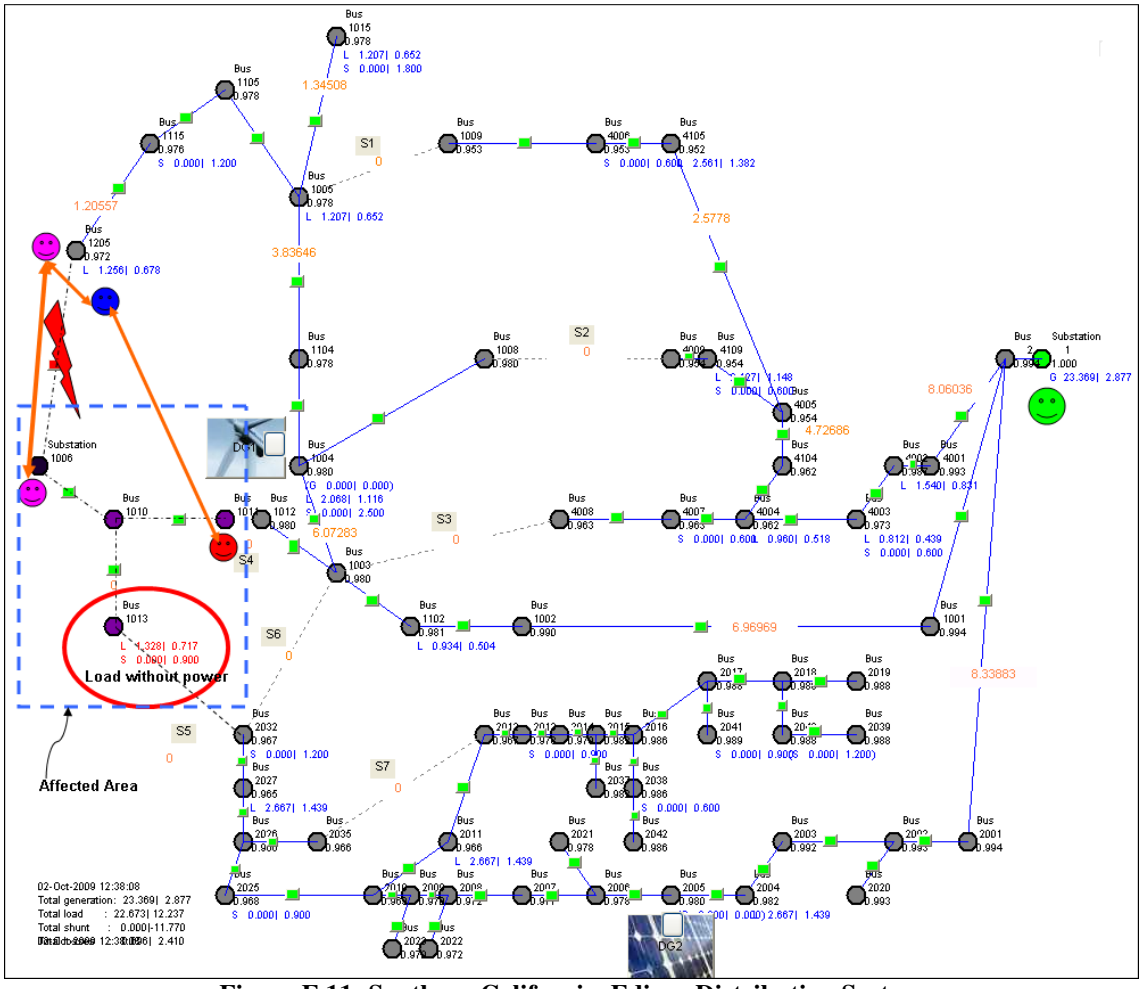

Figure E.11: Southern California Edison Distribution System

In the following, a line fault is simulated between bus number 1102 and 1002 (see Figure E.12). We can see from the figure the region which has been affected by the fault. The objective of the algorithm is to reroute the power or find the best reconfiguration to feed the faulted area. The algorithm takes into account the following constraints when searching for the suitable switching:

- Maximum loads
- Voltage constraints

- Minimum losses
- Capacity of the lines
- Minimum switching

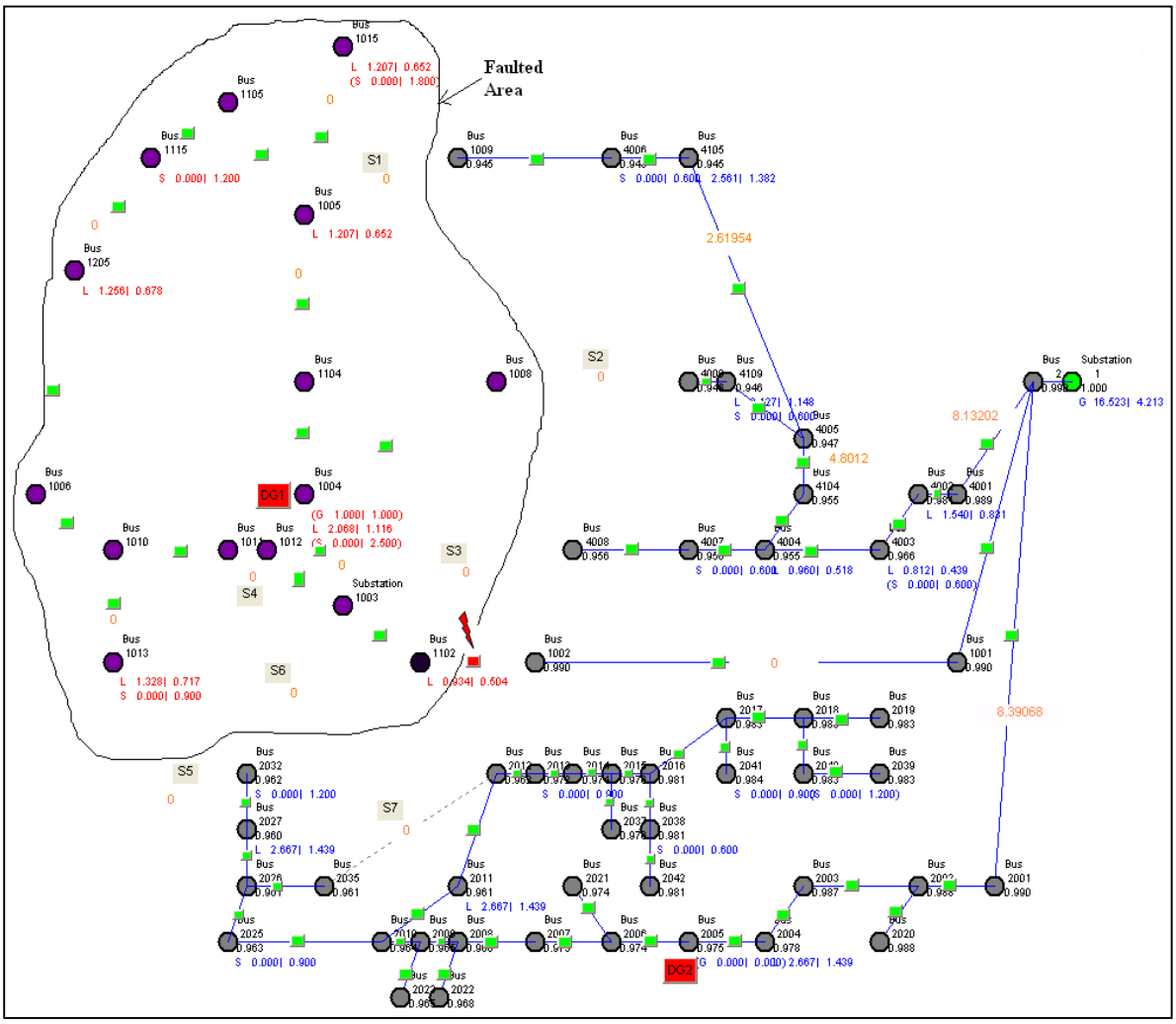

Figure E.12: Fault at Bus Number 1102

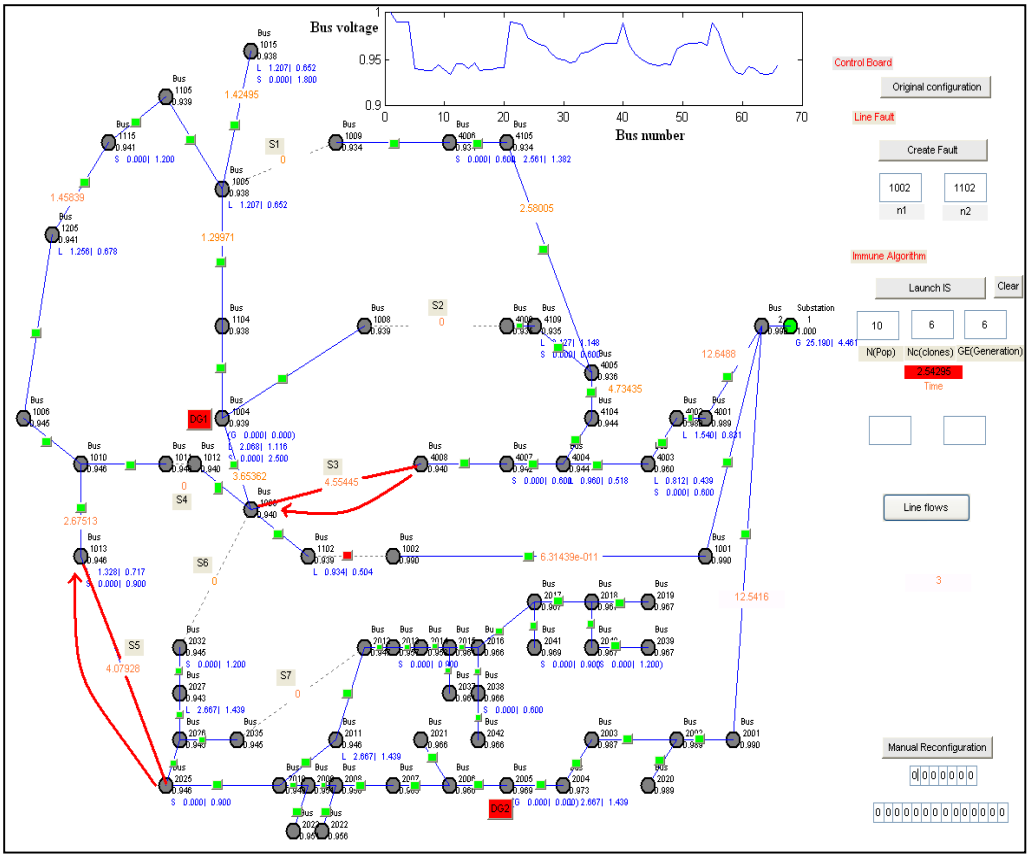

Figure E.13: Reconfiguration Using AIS Algorithm

All these constraints help the algorithm to compute the affinity and direct the algorithm towards the best reconfiguration solution.

In the biological immune system, the destruction of the antigen, once it faces the cell, is done by part.

The cell does partial damages or destruction to the antigen till its final annihilation. The same thing is happening in the case of reconfiguration using the AIS. A partial healing is applied first to the system to restore some part of grid, for example, or at least to bring the system to a better state by reducing the congestion of the lines by performing low priority load shedding. As the fault occurs the AIS is triggered, and starts rerouting the power to the outaged area. Figure E.13 shows the path found by the AIS algorithm. We notice in this case that the algorithm has chosen to get the power from two different zones by switching on the switch number 5 and 3. The figure shows also the voltage profile after performing the reconfiguration.

By analyzing different combination of switching, we found out the choice, or the strategy, taken by the algorithm. The algorithm divides the power through two feeders to relieve the feeders since the amount of the power needed to supply the faulted area is about 8 MW. If brought from one feeder, it will result in huge losses and the voltage will drop under the limit. In this scenario, the algorithm came up with a strategy in less than 3 seconds and by using the learning part of the algorithm, the same strategy is trigged instantly if the same fault occurs in the future. In Figure

E.14, we show a manual reconfiguration of the system which simulates the human intervention in the real system. We can see from the figure that the operator has chosen to switch on Switch number 1 for example, which is the simplest choice without any prior knowledge of the system. We can see that by choosing this combination, the whole power is traveling through one area which causes a loss of about 1.68 MW and bad voltage profile with a minimum voltage of 0.866pu. We realize that this action affects the whole grid and the entire system can collapse. In addition, even if the operator chooses to divide the power between the two feeders by using a combination other than the one applied by the AIS algorithm, in this case switch number 6 and any other switch, the voltage is still low (see Figure E.15).

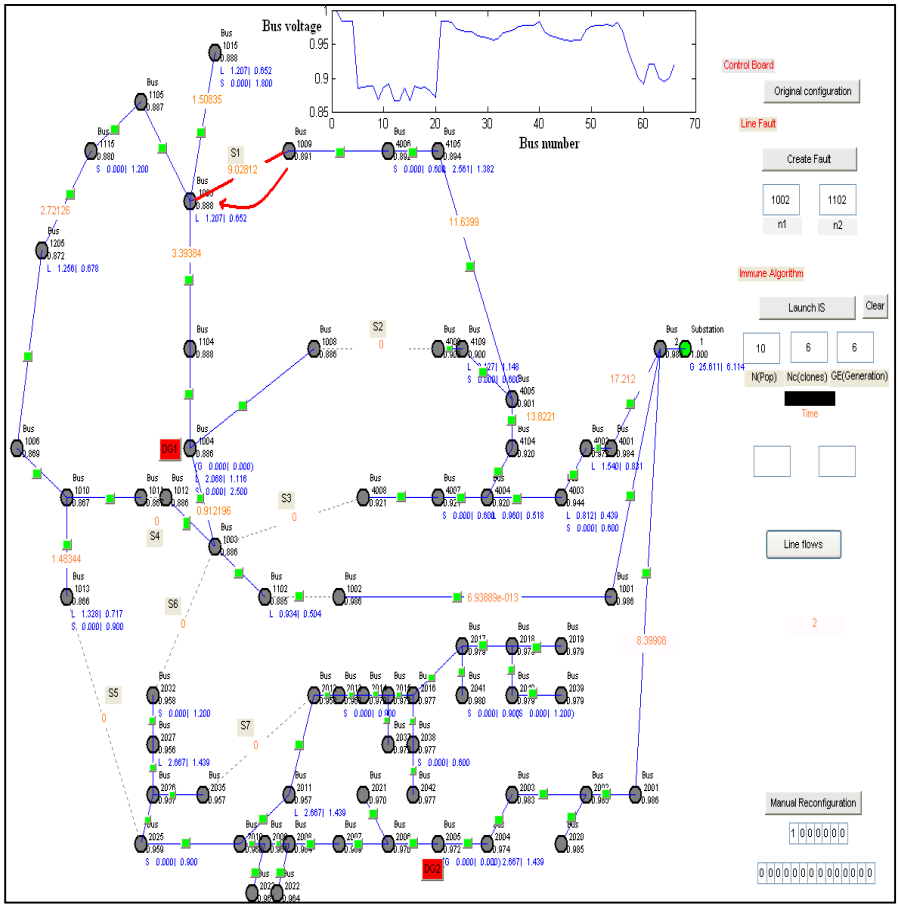

Figure E.14: Manual Reconfiguration (One Switch Operated)

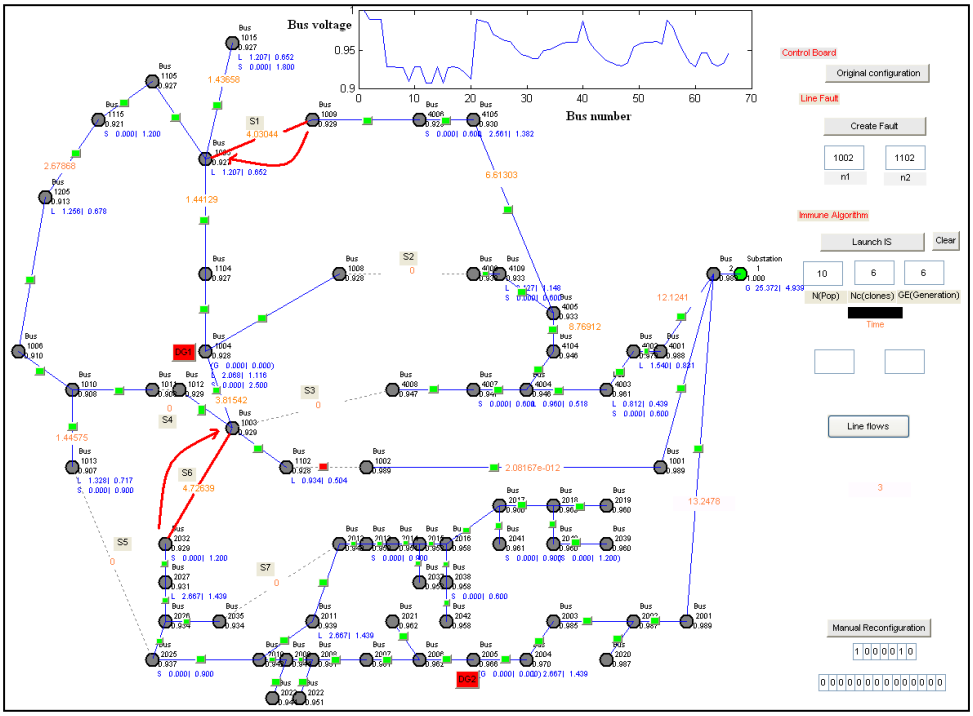

Figure E.15: Manual Reconfiguration (Two Switches Operated)

Appendix F – Cost Benefit Analysis – A University Study

This section on Cost Benefit Analysis was done as a University study using hypothetical values of benefits and estimated equipment costs. Due to significantly higher costs to utility level integration, the project team, with the DOE review team, determined at the conclusion of the project period to develop a final report on the work performed. Since no systems were deployed or operated, there is no actual data available to do the Cost Benefit Analysis. This analysis is based on hypothetical data from sources outside of the project.

Cost benefit analyses were performed on four operational use cases based on estimated data. Two microgrid cases were examined, one agent based Fault Location Isolation Restoration Agent (FLIR-A) / Fault Location Algorithm (FLA) / Fault Protection Algorithm (FPA) / Distributed Energy Resources (DER) dispatch case and one DER dispatch case. The WVSC microgrid was assumed to operate in two modes: grid connected mode and islanded mode. In the grid connected mode of operation the natural gas generators, energy storage units and solar PV arrays were assumed to operate in compliance with Mon Power's interconnection requirements. Energy storage units and PV's with micro-inverters were assumed to provide no frequency regulation or voltage support. The primary function of the microgrid in this mode of operation was to provide peak shaving support for the circuit. The microgrid was assumed to provide power to the grid for two hours in the morning and in the evening with no seasonal variations.

In the islanded mode of operation the primary function of the microgrid was to enhance reliability of service for the customers it supported. Reliability improvements were based upon circuit reliability measures provided by the utility and the assumption that outages would be eliminated for the microgrid when it went into islanding mode.

The DER dispatch case analysis focused on evaluating the economics of shaving peak demand by 15 percent by bringing privately owned backup generation units on line to address excessive peaks and on evaluating the potential reliability improvement through the implementation of an agent based distribution automation system. The peak shaving demonstration was to be performed on the West Run Number 8 Circuit. It should be noted that the capital investment related to this phase of the demonstration was not limited to the peak shaving application. A portion of the investment would also enhance reliability. Therefore the benefits derived for this investment are a result of both the ability to shave peak and improve reliability.

A list of technologies and their associated benefits were provided for each operational use case in the metrics and benefits report. A discussion of these benefits is provided for each use case along with a description of the monetization process used to assign values to indirect benefits. Additionally, each benefit is assigned to its respective beneficiary and a cost benefit ratio is calculated for each beneficiary. In instances where multiple beneficiaries may exist and no clear distribution can be derived with the available data, no attempts are made to allocate the benefits multiple beneficiaries. In these cases, the benefits were assumed to accrue to the beneficiary for whom the benefit could be calculated.

The cost benefit analyses were performed using 2013 as a base year therefore all figures are in 2013 dollars. In cases were 2013 data values were not available, they were adjusted using an average annual rate of inflation of 2.5 percent based upon US Bureau of Economic Analysis GDP Deflator. A project life of 10 years and a corporate required rate of return of 8 percent were used in the analysis.

A sensitivity analysis was performed for each operational use case to identify the inputs that have the greatest potential to impact the economics of each case. All inputs used in construction of the model were examined applying a range of plus or minus twenty percent.

F.1 Microgrid

F.1.1 Cost

The microgrid capital cost estimates were based on the premise that there were no preexisting DG's or connections within the microgrid. Additionally, it is assumed that there was not a point of common coupling. The system was designed for the specific application outlined in this research. Additional capital costs were therefore incurred due to the unique circumstances associated with the facility.

Under the contractual agreement with the owner of the facility at which the microgrid was to be constructed, the PV panels had to be mounted in a carport fashion and the natural gas generator, transformers and switch gear had to be pad mounted in an enclosed structure. These factors resulted in a capital cost of more than $1 million which is significantly higher than would be anticipated had these restrictions not been imposed. A breakdown of the capital costs is provided in Table F-1.

Table F-1: Detailed Microgrid Capital Cost Estimate

	Equipment	Installation	Installed Cost	No.	Total Cost
Microgrid					**$1,011,146**
Solar PV Assembly		**Included**			**$311,076**
Carport Structure					
PV Panels with Smart Energy					
PV Panels					
Switching/Mounting Hardware					
Design					
Build					
Installation					
Shipping					
Training					
Residential Energy Storage Assembly		**Included**			**$150,760**
Residential Energy Storage (Li-Ion,	$47,920	0	$47,920	3	$143,760
Onsite Commissioning Support	$5,000	0	$5,000	1	$5,000
Shipping	$2,000	0	$2,000	1	$2,000
Microgrid Switchgear and Controls		**Included**			**$489,310**
Pad mounted Breaker (PCC)					
Nat'l Gas Generator (150 kW) +					
Microgrid Switchboard and Control					
Microgrid Control Network					
Startup Commissioning					
Shipping					
DER Interconnection Assembly					**$60,000**
Pad mounted Xfmr (225kVA, 12.5/208V)	$25,000	$5,000	$30,000	1	$30,000
DER Interconnection (Cabling, etc.)	10,000	2,000	12,000	1	12,000
ENMAC Integration		0	180	100	18,000

From Table F-1 it can be seen that the microgrid switch gear and controls cost which include the natural gas generator account for nearly one half of the total capital cost. The solar PV assembly also accounted for a large portion of the capital cost. O&M, depreciation, interest and fuel costs were estimated and used in the analysis.

The O&M costs were assumed to be 4 percent of the total capital expenditures as described earlier in the report. Interest charges were included because it was assumed that the capital investment would be financed on the bases of the size of the investment and the size of the proposed microgrid. The facility at which the microgrid was to be installed would be considered to be in the Small C&I customer category based upon its annual load. A ten year bond rate of 3 percent was used to represent the cost of financing from either a community or a business perspective given the currently low interest rates.

Equipment was depreciated using the simple straight line method to allocate the capital cost over its useful life. The life of the PV was assumed to be 20 years and the batteries and microgrid switch gear and controls were assumed to have 10 year lives. This assumption is highly conservative for

the microgrid switch gear and controls. However the cost estimate for this portion of the microgrid provided by vendors did not contain sufficient detail to apply a more accurate estimate of these depreciation costs.

The present values of these annualized costs and the capital investments are presented for the two microgrid use cases in Table F-2.

Table F-2: Microgrid Use Case Costs

Microgrid Use Case Cost	PV $1000
Peak Shaving	
Total Capital Investment	468
O&M Cost	271
Annual Fuel Cost	162
Interest	204
Depreciation	462
Total	**1,567**
Islanding	
Total Capital Investment	468
O&M Cost	271
Annual Fuel Cost	52
Interest	204
Depreciation	462
Total	**1,457**
PV @ 8% for 10 yrs.	

The cost elements are the same for both cases except for the annual fuel cost. The variation in the fuel cost is a result of the difference in the number of hours that the natural gas generator operates. In the peak shaving use case the natural gas generator is assumed to run 4 hours per day for 365 days for a total of 1,460 hours per year while, in the islanding case the generator is assumed to be needed for 466 hours per year based upon outage data. The natural gas price was assumed to be the 2013 commercial price of $8 per MCF.[8]

F.1.2 Microgrid Benefits

The benefits anticipated from the operation of the microgrid for both the peak shaving and islanding modes are summarized in Table F-3. Each benefit listed in Table F-3 is discussed in more detail in the following sections. A description of the estimation of each benefit is also provided.

[8] http://www.eia.gov/dnav/ng/ng_pri_sum_dcu_nus_m.htm

Table F-3: Microgrid Benefits

Benefit Category	Benefit	Beneficiary		
		Utility	Consumers	Society
Economic	Reduced Electricity Losses	X	X	
	Economic Growth and Employment			X
Reliability	Reduced Sustained Outages & Major Outages		X	
Environmental	Reduced Carbon Dioxide Emissions			X
	Reduced SO_X, NO_X, and PM $_{2.5}$ Emissions			X

Reduced Electricity Losses

These benefits were assumed to accrue to the utility and were calculated based upon potential profit losses. Peak system loss savings from the microgrid simulation were estimated to be 0.76 kW while simulation results for islanding were slightly better at 0.85 kW.

The benefit of these savings was calculated by allocating the losses among the various customer classes based on the average load of each class. Losses were monetized by multiplying the allocated loss by the potential profit for each customer class. This benefit was estimated to be $37 and was assumed to grow annually at a rate of 1 percent which is equivalent to the circuit load growth. No value was calculated for the islanding case given the extremely low value of this benefit.

Economic Growth and Employment

Avoided power losses from islanding translate into additional revenue for commercial and industrial customers on the microgrid. These saving were multiplied by the WV GDP multiplier to estimate the potential benefit from the avoided power outages. The present value of this benefit is estimated to be $26,000 initially and it was assumed to grow at 2.5 percent annually. The only savings generated from the peak shaving case were from the utility's avoid profit losses which were extremely small and did not warrant calculation of this benefit. The results suggest that approximately one half of one job per year would be created as a result of the stimulus.

Reduced Sustained Outages & Major Outages

These benefits are only relevant for the islanding use case and were assumed to accrue to Small C&I customers. The grid connected peak shaving mode was assumed not to have an effect on outages. Benefits for the islanding application were determined using the same methodology employed to calculate these benefits for FLIR-A/FLA/FPA/DER Dispatch use case. The initial benefits estimates for small C&I customers was approximately $80 thousand. These benefits are assumed to increase over the life of the project at a rate of approximately 6 percent which is the estimated growth rate for the number of customers served by the circuit based on historical data**.**

Reduced Carbon Dioxide Emissions

There were 64 kW of renewable resources that could be dispatched under these use cases. However, 24 kW of these resources are provided by lithium ion batteries which are only available for a maximum of 2 hours before needing recharged. As with the FLIR-A/FLA/FPA/DER Dispatch use case, emissions reductions are possible assuming the power generated by the renewables and the natural gas generator are considered to offset an equivalent amount of coal fired generation.

Under the peak shaving scenario approximately 300 MWh per year would be supplied to the circuit by the microgrids DER's. Approximately two thirds of this power would be supplied by the natural gas generator which would provide a 45 percent reduction in CO_2 emissions over the coal fired generation that it assumed to offset. The remaining generation provided by the renewables would provide a 100 percent reduction in CO_2 emissions. The benefit from these reductions in CO_2 emissions is estimated to be $928 per year. This benefit is even lower for the islanding scenario.

Using historical reliability data for the circuit and average load profiles for the microgrid it was estimated that the microgrid would be required to provide approximately 100 MWh per year to avoid service disruptions. Emissions benefits that could be obtained while operating in this fashion are approximately $300 per year.

Reduced SO_X, NO_X, and $PM_{2.5}$ Emissions

The benefits associated with the reduction in SO_x emissions were found to be negligible in the FLIR-A/FLA/FPA/DER Dispatch use cases. The level of SO_x benefits would be essentially the same as the FLIR-A/FLA/FPA/DER Dispatch use cases for the peak shaving scenario and would be approximately one third lower for the islanding scenario. The assumption that there would be no net reduction in NO_x emissions was made based upon the currently low levels of NO_x emissions from coal fired units; low emissions permit prices and the lack of operation data from the diesel generator. $PM_{2.5}$ emissions benefits were not calculated due to low level of benefits associated with the other emissions.

F.1.3 Microgrid Benefits by beneficiaries

The benefits discussed in section 5.2.2.1 through 5.1.2.5 are reclassified and summarized by beneficiary class in Table F-4. These benefits are used to derive the benefits to cost ratio for each beneficiary.

Table F-4: Microgrid Benefits by Beneficiary Class

Beneficiary	PV Benefit Estimate $1000	
	Peak Shaving	Islanding
Consumers		
Residential	-	-
Medium & Large C&I	-	-
Small C&I	210	623
Total Consumers	**210**	**623**
Utility		
Avoided profit losses from line losses	0.3	0
Total Utility	**0.3**	**-**

Societal		
Reduced Emissions US & WV Emissions benefit from Microgrid	6	**2**
Reduce price of electricity Peak Shaving and load flattening Region	-57	-
Economic development/job creation WV	**-**	195
Total Societal	**-51**	**197**
Total Benefits	**159**	**820**

Consumer

The benefit for this beneficiary class is comprised solely of benefits that accrue to Small C&I customers. In the case of peak shaving, the benefit is derived from revenue payments made to the owners of the DER's. It was assumed that the utility would reimburse the DER owner their cost of generation for supplying peak shaving power. These costs were assumed to be based entirely on fuel cost. The cost of the DER's was assumed to be a sunk cost and it was assumed that there were no additional O&M cost associated with using the DER's in this capacity. The present value of these benefits is estimated to be $159 thousand.

Under the islanding scenario the benefits are assumed to be derived from avoided service interruptions for Small C&I customers. The microgrid was assumed to completely eliminate sustained interruption and therefore reliability was assumed to be 100 percent for the microgrid. The present value of the resulting improved reliability from islanding is estimated to be $623 thousand.

Utility

The utility did not receive any benefits from the microgrid under the islanding scenario and received very little benefit from the microgrid under the peak shaving scenario. A reduction in line losses attributed to the operation of the microgid under this scenario provided a benefit of avoided profit losses with a present value of less than $300.

Society

The estimation process used to calculate societal benefits was outlined in Section 5.1.3.3 The only societal benefits of any significance were the economic development benefits derived from avoided Small C&I customer interruption costs under the islanding scenario. The present value of these benefits is approximately $195 thousand.

Potential emission reductions benefits worth noting were from the reduction of CO_2. However, this benefit is insignificant in relation to other benefits in both microgrid scenarios. The present value of the emissions reduction benefit is approximately $6 thousand for the peak shaving scenario and $2 thousand for the islanding scenario.

There were no societal benefits associated with price reduction associated with peak shaving or load flattening for the region. In fact, based upon real time monthly futures prices for PJM there would be a negative benefit or a cost associated with using the distributed resources to offset peak demand because the average futures contract price of $55 MWh was significantly less than the cost of $77/MWh for power supplied by the DER's. This translated into a $5,500 per year social

cost. There are no price reduction benefits in islanding mode. The primary purpose for islanding was assumed to be for loss avoidance.

As noted in Section 5.1.3.3 societal benefits from lower electricity prices, public health and safety, and energy security were not estimated. The inclusion of these benefits would provide higher level of social benefits.

F.1.4 Microgrid Benefit Cost Analysis

The microgrid is not economically feasible under either scenario or from any beneficiary's perspective. As shown in Table F-5, all of the benefits to cost ratios are less than one. This is partially due to the high capital cost of the microgrid which was due to unusual installation requirements discussed in Section 5.2.1.

Table F - 5: Microgrid Benefit Cost Analysis Results

Beneficiary	Benefit/Cost Ratio	
	Peak Shaving	Islanding
Consumer	0.13	0.4
Utility	0.09	0.0
Society	0.00	0.1
Total Benefits	**0.1**	**0.5**

Peak Shaving

The underlying assumption for this use case is that all costs associated with providing power to the grid during peak demand periods would be accounted for in the analysis. This combined with the high capital cost resulted in an extremely uneconomical outcome. These high costs coupled with a low level of benefits led to extremely low benefits to cost ratios regardless of what perspective the scenario is analyzed. The most significant level of benefits was from savings from renewables which offset a portion of the cost of providing the peak power. The utility received very little benefit due to the low level of congestion on the circuit and low levels of line losses. It is anticipated that these factors would be more favorable for an application of this nature. However, the economics can be improved by relaxing the assumption that all cost associated with providing peak power are to be included. If the capital investment is treated as a sunk cost and all other costs except for fuel are ignored, the analysis yield a benefit of 1.3 to 1 suggesting that providing peak shaving power to the grid would be favorable for the microgrid owner's perspective. However from the utility's perspective this option remains uneconomical for the reason previously mentioned.

Islanding

In addition to the high capital cost associated with the microgrid design, circuit reliability contributes to the overall poor economic prospects of this scenario. Studies show that customers invest in backup generation to avoid interruptions just to the point at which the value of backup generation equals the economic cost of unreliability. To justify the large capital investment associated with this microgrid, the circuit to which the microgid is connected would need to experience more frequent or longer outages or the cost of service interruptions would need to be significantly higher.

However the economics of the microgrid may be favorable if it is assumed that the only capital investment need to operate in islanding mode is an isolation switch. Assuming that the generation and switch gear already exist on the microgrid, the only costs that are relevant under this scenario are the O&M costs and the generator fuel costs. Applying these assumptions the benefits to cost ratio would be 2 to 1 from the consumer or microgrid owner's perspective and 2.8 to 1 when all beneficiaries are considered

F.2 FLIR-A/FLA/FPA/DER Dispatch for Peak Shaving

F.2.1 Cost Estimates

Capital cost estimates were obtained from vendors based upon the engineering designs. Vendor quotes for hardware, software, communications, and installation for the FLIR-A/FLA/FPA/DER Dispatch case are $1,836,497. This capital investment is not amortized and is assumed to be made a lump sum investment at the beginning of the project. A more detailed presentation of these costs is provided in Table F-6.

Table F - 6: FLIR-A/FLA/FPA/DER Dispatch Capital Cost Estimates

	Equipment	Installation	Installed Cost	No.	Total Cost
FLIR-A/FLA/FPA/DER Dispatch					**$1,836,497**
FLA/FLIR Integration for existing switches					**$232,000**
PQ Monitors	$3,000	$2,000	$5,000	8	$40,000
Agent Platform	$10,000	$2,000	$12,000	16	$192,000
FLIR & expansion to West Run-8 circuit					**$1,030,000**
Recloser	$40,000	$10,000	$50,000	3	$150,000
15 kV Poletop Loadbreak Switch	$30,000	$10,000	$40,000	16	$640,000
3-phase Potential Transformer Set + Bypass switches	$10,000	$2,000	$12,000	16	$192,000
Switch Controller (Switch Controller Panel, Agent Platform, RTU, Battery Backup, PQ Monitor, Communication HW)	$20,000	$4,000	$24,000	16	$48,000
EMS Integration					**$228,000**
ENMAC integration		$180	$180	100	$18,000
Update master/slave RTU and IED configurations (DNP3/IP)		$180	$180	200	$36,000
Existing 14 switches (for new PQ equipment and agent platform)					
New 2 switches (Mon General)					
FLA/FPA software integration with legacy systems		$180	$180	300	$54,000
FLIR software integration with legacy systems		$180	$180	300	$54,000
Software license (CYMEDist and COM Module)					$30,000
Cyber security support		$180	$180	200	$36,000

Communications Hardware and Software					**$346,497**
Computing platforms + software					$177,815
Communications hardware					$128,682
Installation, commissioning, integration, etc.					$40,000

Actual operational and maintenance (O&M) cost data was not available. Therefore commonly accepted heuristic of annual O&M cost estimates used in the operations management discipline were employed. These estimates range between 2 and 4 percent of the total capital investment. A conservative estimate of 4 percent was used to derive the O&M cost for this operational case.[9] The O&M cost were estimated to be $73,460 per year.

Additionally, fuel cost paid to Mon General Hospital for approximately 300MW hours of peak power annually would be incurred. This cost was estimated to be $66,000 per year based upon fuel consumption obtained for similar size diesel generation units and a No. 2 fuel oil cost of $3.50 per gallon.

Total Cost

The total cost for the peak shaving phase of the project is simply the present value of the annual fuel payment plus the present value of the deferred capital investment. No additional capital costs were assumed to be associated with demonstrating the peak shaving aspect of the project on the West Run Number 8 circuit. The capital investment that would be required to address peak demand was estimated to be $1.2 million. The present value of this deferred capital investment and the annual fuel payment is equal to approximately $1 million as illustrated in Table F-7 below. The cost of the privately owned generation was assumed to be a sunk cost by nature of the contractual agreement with Mon General. Therefore no O&M costs or depreciation costs were factored into the analysis. It is highly unlikely that private entities would enter into an agreement of this nature because an agreement to provide peak shaving power would shorten the expected life of the generator and result in additional O&M. Additionally, there may be issues and additional costs with respect to emissions permitting because the original permits for the units are based on their function as backup emergency generation units with limited operation hours.

Table F - 7: Use Case Costs

Use Case Cost	PV $1000
DER Peak Shaving Only	
Mon General Annual Fuel Payment	444
Deferred Capital Investment	556
Total	**1,000**
FLIR-A/FLA/FPA/DER Dispatch	
Total Capital Investment	1,836

[9] Harvey Kaiser, Capital Renewal and Deferred Maintenance Programs, APPA Body of Knowledge, 2009, page 9.

O&M Cost	493
Mon General Annual Fuel Payment	444
Sub Total	**2,773**
Deferred Capital Investment	556
Total	**3,329**

PV @ 8% for 10 yrs.

While the present value of the total cost for the FLIR-A/FLA/FPA/DER Dispatch for the Peak Shaving operation case is estimated to be approximately $3.3 million assuming the intent is to defer the construction of a new circuit. However if the project is assumed to be independent the present value of the future expenditure to construct a new circuit can be ignored and the present value would be approximately $2.8 million dollars. The costs of the preventive measure are unusual in this case because they are lower than the cost they are intended to delay which is not typical.

F.2.2 Technology Benefits

The early termination of the project precludes the calculation of the actual total benefits. Therefore the benefits discussion is forced to rely on general inferences and results of similar studies to augment the benefit calculations when actual data was not available.

Deferred Distribution Capacity Investments

The dispatch of DER was employed to reduce energy usage for the identified major peaks on the circuit. It was established that DER dispatch would be required approximately 150 hours per year to reduce the demand by 15 percent when demand was at its greatest. Two megawatts of load would be offset by Mon General Hospital through the use of their backup generators.

Given the relative infrequency of the peak demand the potential to offset a portion of the load with local privately owned generation provides the distribution company with the opportunity to defer distribution capacity upgrades that would have been necessary without peak demand reduction. These upgrades were estimated to cost 1.2 million dollars. With peak shaving these upgrades can be deferred for 10 years providing savings of approximately $29,000 per year.

Reduced Equipment Failures

Fault Prediction is intended to identify faults before they happen and thus, provide a mechanism to identify potential equipment failures and take actions to repair and/or replace such equipment. No attempt was made to isolate these benefits. It is assumed that they accrue to the utility and to the customers and are captured in the estimated benefit of reliability and restoration cost reductions.

Reduced Distribution Operations Cost

FLIR, FPA, and FLA will all contribute to reducing the overall cost that is required to operate and maintain the distribution system. Fewer faults will lower the cost for staff activity that is necessary to locate and isolate faults along with the need to analyze equipment failures or misoperation. Faster location and or restoration times provide benefits to both utility and society. The utility's cost reductions are assumed to be in the form of avoided revenue losses due to outages. This benefit was estimated based on average customer usage profiles obtained from the Interruption

Cost Estimate (ICE) Calculator, reliability improvement estimates from circuit automation[10] and First Energy's potential profit per MWh derived from the companies published operating cost[11] and the average retail electricity price for West Virginia end users.[12] Avoided revenue losses were estimated to be approximately $142,000 initially and were assumed to grow at a rate of 1 percent annually based on the expected load growth for the circuit. The additional revenue generated translates into a societal benefit through its economic impact on the State and regional economies. The net societal benefit was estimate to be approximately $63,000 initially and it was assumed to grow at the average GDP growth rate for the state of 2.5 percent a year.

Reduced Electricity Losses

Dispatching the DER would benefit the distribution system by reducing the losses incurred by delivering the energy from the transmission system. The generator could supply energy locally reducing demand at peak times which could reduce losses throughout the distribution network. However the cost of these losses would need to exceed $240 per MWh in order, the cost per MW h to run the diesel generator, before any benefits could be obtained. It was determined that the losses on this circuit were not sufficient to generate any benefits therefore no attempt was made to estimate them directly.

Economic Growth and Employment

Avoided loses attributed to a more reliable power supply translates into additional revenue for commercial and industrial customers and into additional discretionary income for residential consumers. A portion of these monies are returned into the local economy generating income and revenue for other consumers. This spending has a multiplier effect that facilitates economic growth and job creation. The avoided losses were assumed to represent a stimulus to the State's economy and their economic impact was derived using IMPLAN software. IMPLAN is widely used by government agencies, colleges and universities, non-profit organizations, corporations, and business development and community planning organizations too quickly and efficiently model economic impacts. Using the IMPLAN model of the West Virginia economy the economic benefit would be approximately $218,000 initially and it was assumed to grow annually at a rate of 2.5 percent. Job creation can also be estimated using the IMPLAN model. The results suggest that approximately 4 jobs per year would be created as a result of the stimulus.

Reduced Sustained & Major Outages

Several of the technologies that would be demonstrated in the project would have a direct benefit in reducing distribution outages. By either enabling quicker reconfiguration and/or identifying the cause of a fault can aid in reducing the time to restore power to customers. The value of this benefit is determined by estimating the interruption costs to the various classes of customers and estimating the reduction in this cost that could be obtained by implementing these technologies. The costs of interruptions were calculated using the U.S. Department of Energy's Interruption Cost (ICE) Calculator. This tool provides the ability to calculate the costs of sustained interruptions

[10] The reliability improvement estimate is based upon a comparison of actual restoration times versus circuit automation restoration time for the DFT project.

[11] First Energy 2012 Annual Report page 23

[12] www.eia/gov/electricity/annual/html/epa_02_10.html

lasting up to 8 hours. Estimates of outage costs for residential and commercial customers in a given state are calculated based upon reliability data, and the number of customers entered by the user. The ICE calculator uses this information along with default data on customer characteristics and customer percentages for each state to derive interruption cost estimates.[13]

Historical circuit reliability data and reliability improvement estimates were entered into the tool for the circuit. The initial benefits estimates obtained were $20,375 for residential customers, $179,400 for Medium and Large Commercial and Industrial (C&I) customers and $235,500 for Small C&I customers. These benefits were assumed to increase over the life of the project at a rate of approximately 6 percent which is the estimated growth rate for the number of customers served by the circuit based on historical data**.**

Reduced Restoration Cost

The cost incurred during distribution feeder restoration after a fault can be time consuming and personnel intensive. FLIR, FPA, and FLA will all be instrumental in either increasing preventative measures and/or reducing the time and effort to return customers from sustained outages. These benefits were calculated based upon the avoided cost of service interruption responses following the methodology applied in the WV smart Grid Implementation Plan. The initial benefit is estimated to be $457,000 and increase at a rate of 6 percent annually based upon the average growth rate of the number of customers served on the circuit. As assumed in the WV Smart Grid Implementation plan[14], 67 percent of the service calls occur outside of business hours and a 10 percent reduction in these calls would be possible with automation of the circuit. The cost of each truck roll is estimated to be approximately $600 and the circuit SAIFI was estimated to be 0.97 based upon historical data.[15]

Reduced Carbon Dioxide Emissions

There were no renewable resources to be dispatched under this use case. CO_2 emissions were assumed to be lower based upon the carbon content of the fuels. However, a reduction of CO_2 emissions is possible assuming the 300 MWh of peak power that is provided by Mon General's diesel generators is considered to offset an equivalent amount of coal fired generation. Given the lower carbon content of the fuel oil on a MMBTU basis it would be possible to obtain a 24 percent reduction in CO_2 emissions. With annual coal fired emission of 1980 lbs. /MWh a potential reduction of approximately 475 lbs. per MWh in CO_2 emission would be possible for a total reduction in CO_2 emissions of approximately 71 tons annually. At a CO_2 price of $9.51 per ton a total benefit of approximately $678 would be generated.[16]

Reduced SO_X, NO_X, and PM2.5 Emissions

The benefits associated with the reduction in these emissions were found to be negligible. The potential emissions reduction benefits were assumed to be derived primarily from the reduction in

---

[13] Sullivan, Michael J. Matthew G. Mercurio, Josh A. Schellenberg, and Joseph H. Eto, "Estimated Value of Service Reliability for Electric Utility Customers in the United Sates," *LBNL Research Project Final Report*, June 2009

[14] https://www.smartgrid.gov/sites/default/files/pdfs/wv_smart_grid_implemenation_plan_09-2009.pdf

[15] Customers served * SAIFI*% DA penetration*5 service call outside business hrs.*% reduction in calls*cost per truck roll

[16] http://www.bloomberg.com/news/2014-02-19/carbon-bulls-at-three-year-high-in-options-market-on-surplus-fix.html

SO_x emissions resulting from the offset of 300 MWh of coal fire generation. The assumption that there would be no net reduction in NO_x emissions was made based upon the currently low levels of NO_x emissions; low emissions permit prices and the lack of operation data from the diesel generator.[17] Additionally, it was assumed that Mon General's diesel generators would operate using ultra-low sulfur fuel and as a result the SO_x emissions and $PM_{2.5}$ emissions from the diesel generator were assumed to be zero. Based upon these assumptions approximately 5.2 lbs. per MWh of SO_x emissions or 1500 lbs. of SO_x emissions would be offset. At an average cost of $0.28 per ton emission based on the latest EPA permit auction[18] these benefits were estimated to be approximately $0.20

F.2.3 Benefits by beneficiaries

The benefits discussed in section 5.1.2.1 through 5.1.2.9 are reclassified as illustrated in Table F-8 and examined by beneficiary class (utility, customer and societal) to derive the benefits to cost ratio for each beneficiary.

Table F - 8: Benefits Matrix

Benefit Category	Benefit	Beneficiary		
		Utility	Consumers	Society
Economic	Deferred Distribution Capacity Investments	X	X	
	Reduced Equipment Failures	X	X	
	Reduced Distribution Operations Cost	X		X
	Reduced Electricity Losses	X	X	
	Economic Growth and Employment			X
Reliability	Reduced Sustained Outages & Major Outages		X	
	Reduced Restoration Cost	X	X	X
Environmental	Reduced Carbon Dioxide Emissions			X
	Reduced SO_X, NO_X, and $PM_{2.5}$ Emissions			X

The automation of distribution feeders has a number of indirect benefits associated with it that can affect other enterprise activities making it difficult to allocate their contribution to specific functions or activities. Therefore the decision was made to conduct the cost benefit analysis using beneficiary classes. Additionally this method illustrates to whom the benefits accrue and can identify spillover benefits associated with the capital investment.

[17] http://www.epa.gov/reg3artd/globclimate/r3pplants.html
[18] http://www.epa.gov/airmarkets/trading/2013/13spotbids.html

Consumers

Studies suggest that the benefit that is most predominate is quality of service improvement measured by the reduction of SAIDI/customer minutes lost. [19,20] Achieving satisfactory SAIDA levels is crucial to maintaining customer loyalty. Research suggests that even partial automation can deliver up to a 25 percent improvement in increased customer satisfaction. Feeder automation has been shown to deliver flexibility and reliability in excess of the planned benefits. Reports indicate that customer minutes lost may be reduced by as much as 33 percent on MV circuits through distribution automation alone.[21, 22] The reduction may increase significantly when distributed generation and multi-agents are incorporated. The reduction of lost minutes with these technologies employed has been shown to be in the order of 80%. Data from a previous DOE study referred to as the Development Field Test (DFT) suggest that a 67 percent improvement would be anticipated for this circuit. This translates into an average annual benefit of $500 thousand based on the cost of power outages using the ICE Calculator. Under the current tariff structure in place in West Virginia these benefits would accrue to the consumers.

Utility

The benefits that accrue to the utility are calculated based on the loss of revenues associated with the outages on the circuit, reductions in congestion costs and saving from deferred circuit construction. The present value of these benefits is estimated to be approximately $4.8 million. Additional utility benefits that may be associated with reduced outage times such as reductions in work related injuries and reductions in operations staff were not calculated due to a lack of data. Studies suggest that these benefits account for less than one percent of the total operational benefits when estimated for a utility or a state with multiple utilities. Thus, they are negligible for a distribution circuit and would have virtually no impact on the results of the analysis.

Societal

The societal benefits were estimated based on the economic gains that would be obtainable with a more reliable power source and the potential environmental benefits from lower emissions of NO_x, SO_x, CO_2, and $PM_{2.5.}$ The societal benefits from improved reliability were estimated by considering the consumer savings and the Utility's avoided profit losses from reliability improvements as an economic stimulus. The effects of this stimulus on the West Virginia economy were estimated using the IMPLAN software as described in Section 5.1.2.5. The model provided a complex multiplier of 1.3 suggesting the expansionary effect of the stimulus would result in a net increase of approximately $1.6 million in the states GDP over the life of the project. However, the actual effect may be somewhat smaller due to linkages associated with the various sectors throughout the state's economy.

The only potential emission reductions benefit would be for the reduction of CO_2 emissions assuming the offset would result in lower output from coal fired units. However this may not be

---

[19] Walton, C.M. and Friel, R., Benefits of Large Scale Urban Distribution Network Automation and their Role in Meeting Enhanced Customer Expectation Regulator Regimes, CIRED, 2000.
[20] Cepedes, R., Mesa, L., and Schierenbeck, A., Distribution Management System at Epressas Publicas de Medellin (Columbia), CIRED 2000
[21] Walton, C.M. and Friel, R., Benefits of Large Scale Urban Distribution Network Automation and their Role in Meeting Enhanced Customer Expectation Regulator Regimes, CIRED, 2000.
[22] Cepedes, R., Mesa, L., and Schierenbeck, A., Distribution Management System at Epressas Publicas de Medellin (Columbia), CIRED 2000

the case given that the distributed resource is assumed to be employed to shave excessive peaks whose load would most likely be supplied by natural gas fired peaking plants. This benefit is insignificant in relation to other benefits and amount to only $630 per year which translates to a NPV of approximately $4,000 over the life of the project.

There were no societal benefits associated with price reduction associated with peak shaving or load flattening for the region. In fact based upon real time monthly futures prices for PJM there would be a negative benefit or a cost associated with using the distributed resource to offset peak demand because the average futures contract price of $55 MWh was significantly less than the $240/MWh cost to operate the DR.[23] This translated into a more than $50,000 per year social cost.

While the estimate of social benefits accounts for the reduction in power outages, emissions reductions and economic development and job creation, it fails to account for benefits derived from national security that result from improved energy efficiency or public health and safety benefits. The benefits derived from lower electricity prices are also excluded. An estimate of the level of price reduction was not obtainable due to early termination of the project. The inclusion of these benefits would have resulted in a higher level of social benefits. Thus, the estimated social benefit level of $1.3 million may be somewhat conservative.

Total Benefits

The present value of each benefit by beneficiary is presented in Table F-9. From this table it can be seen that most benefits are derived from the reduction in restoration cost and that these benefits accrue to the utility. Additionally, the beneficiary class with the highest level of overall benefits overall is the utility which is encouraging given the fact the utility is making the capital investment. However, there are a significant amount of benefits that accrue to consumers with the largest shares going to C&I customers. Thus the improved reliability could be used as a marketing tool to attempt to capture a share of these benefits.

[23] http://www.cmegroup.com/trading/energy/electricity/pjm-western-hub-peak-calendar-month-real-time-lmp_quotes_globex.html

Table F - 9: Benefits by Beneficiary Class

Beneficiary	PV Benefit Estimate $1000	
	FLIR-A/FLA/FPA/ DER Dispatch	DER Peak Shaving Only
Consumers		
Residential	171	0
Medium & Large C&I	1,204	0
Small C&I	1,982	0
Total Consumers	**3,357**	**0**
Utility		
Avoided profit losses	992	
Savings from avoided new substation construction cost	-128	242
Reduced Restoration Cost	3,901	
Total Utility	**4,764**	**242**
Societal		
Reduced Emissions US & WV Emissions benefit from Mon General	4	4
Reduce price of electricity Peak Shaving and load flattening Region	-358	-358
Economic development/job creation WV	$1,615	0
Total Societal	**1,261**	**-354**
Total Benefits	**9,383**	**-113**

The levels of societal benefits are small compared to similar smart grid studies. This is partially attributed to the relatively small amount of distributed resources, the types of distributed resources and the low level of congestion in the study area. Additionally some societal benefits as discussed in Section 5.1.3.3 were not estimated. Had these benefits been estimated the resultant societal benefit would have been higher.

F.2.4 FLIR-A/FLA/FPA/DER Dispatch Benefit Cost Analysis

DER Peak Shaving

Given the high fuel cost and the low level of benefits associated with this use case it is uneconomical to consider this option as a means to defer the construction of a new circuit. The only significant benefit is derived from the interest savings from the delayed construction. As indicated in Table F-10 the benefits to cost ratios are less than one for all classes of beneficiaries.

Table F - 10: Benefit Cost Analysis DER Peak Shaving

Beneficiary	Benefit Estimate $1000	Cost Estimate $1000	Benefit/Cost Ratio
Consumer	0	1,002	0.0
Utility	242	1,002	0.2
Society	-354	1,002	0.4
Total Benefits	-113	1,002	0.1
Benefits estimate based on PV @ 8% for 10 yrs.			

FLIR-A/FLA/FPA/DER Dispatch

The economic feasibility of implementing this technology is marginal from the Utility's perspective. From Table F-11, it can be seen that the benefit to cost ratio is 1.2 to 1 if the project is considered in the context of a deferred capital investment. If the assumption that the project would be undertaken for the purpose of delaying the construction of a new circuit is relaxed, the benefit to cost ratio improves slightly to 1.7. However the project will still remain questionable given the inherent uncertainty in the data. The economics improve if utility is capable of capturing a portion of the benefits that accrue to its customers.

Table F - 11: Benefit Cost Analysis FLIR-A/FLA/FPA/DER Dispatch

Beneficiary	Benefit Estimate $1000	Cost Estimate $1000		Benefit/Cost Ratio	
		Deferred Capital Investment	Stand Alone	Deferred Capital Investment	Stand Alone
Consumer	3,357	3,329	2,773	1.0	1.2
Utility	4,764	3,329	2,773	1.2	1.7
Society	1,261	3,329	2,773	0.4	0.5
Total	9,383	3,329	2,773	**2.8**	**3.4**
Based on PV @ 8% for 10 yrs.					

However, these benefits cannot be captured under the current tariff structure in West Virginia. Given the questionable economics based on the utility's numbers it is unlikely this type of investment would be economically feasible. Therefore, in order for utilities to implement FLIR-A/FLA/FPA/DER Dispatch, systemic revisions may need to be made to the tariff structure to provide recovery to utility for investments of this nature. Once again, caution is warranted given the uncertainty in data estimates.

The economics look more favorable when all benefits are factored into the analysis and the benefits to cost ratio increases to approximately 2.8 for the deferred investment case, and 3.4 for the stand alone case. Although on the surface this appears to make the FLIR-A/FLA/FPA/DER Dispatch even more attractive, it presents a new set of issues regarding the non-market aspects of some of the societal benefits. This refers to aspects of the automation process that do not produce a financial return, but are perceived by the public as being benefits. They can also be called "non-market benefits". They include benefits enjoyed by users and those valued by the general

population. These benefits can be extremely difficult to capture and would also require some form of rate restructuring or government incentive.

The business case developed in this study demonstrates the need for the utility to be able to capture at least a portion of the societal and/or the consumer benefits to ensure that the investment is economically feasible given the overshadowing market uncertainty. It is unlikely that sufficient amounts of capital investment in distribution infrastructure will take place to meet rising reliability concerns under current market conditions. Although some investments in grid modernization to enhance reliability are being made by the electricity industry, fundamental market failures make it difficult to recoup these investments. Therefore, regulatory intervention and/or financial incentives may be required to counter these market failures and promote wide scale modernization and reliability investments or consumers must be willing to pay for improvements in power quality and reliability.

F.2.5 Sensitivity Analysis

A sensitivity analysis was performed on the stand alone scenario which provides the most favorable results. A ±20 percent change in input values was used to conduct the analysis. The ten most significant inputs affecting the benefits to cost ratio that were obtained for the analysis were plotted for overall project and each beneficiary class.

Total Benefits to Cost Ratio Sensitivity

From Table F-1, it can be seen that the inputs that have the most significant impact on the total benefits to cost ratio are:

- the percentage of reliability improvements that would be achieved by automating the circuit,
- the State GDP Multiplier and
- the variables that factor into the reduction in restoration costs (darkly shaded bars in Figure F-1)

The pole-top load break switch cost and the Small C&I customer losses also have a significant impact on the benefits to cost ratio.

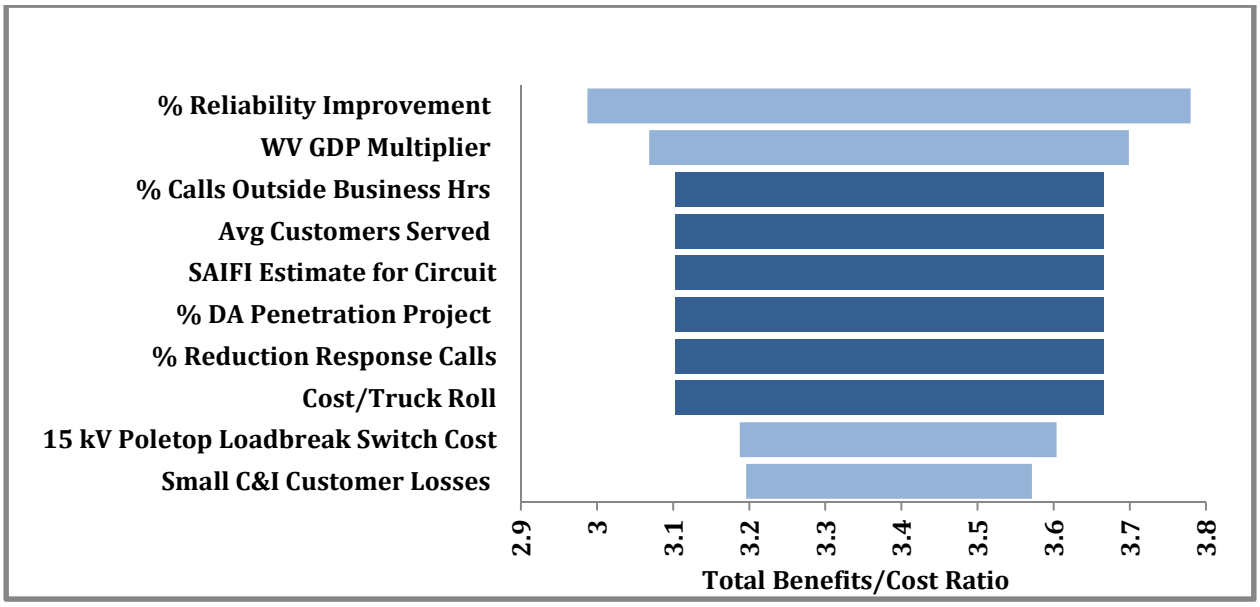

Figure F-1: FLIR-A/FLA/FPA/DER Dispatch Total Benefits / Cost Impact by Input

The percentage change in output for a given percentage in input value for each of the top inputs are illustrate in Figure F-1. From Figure F-2 it can be seen that a twenty percent increase or decrease in the level of reliability results in a corresponding 11.7 percent change in the benefits to cost ratio. The reliability estimate was derived using the result from the DFT project where the actual restoration time for three events was compared to the calculated restoration time from the automated circuit. From this data an average restoration time improvement of 67 percent was calculated. A larger sample size may improve the percentage. The State GDP multiplier also appeared to be quite significant. A twenty percent increase or decrease results in a corresponding 8 percent in the benefits to cost ratio.

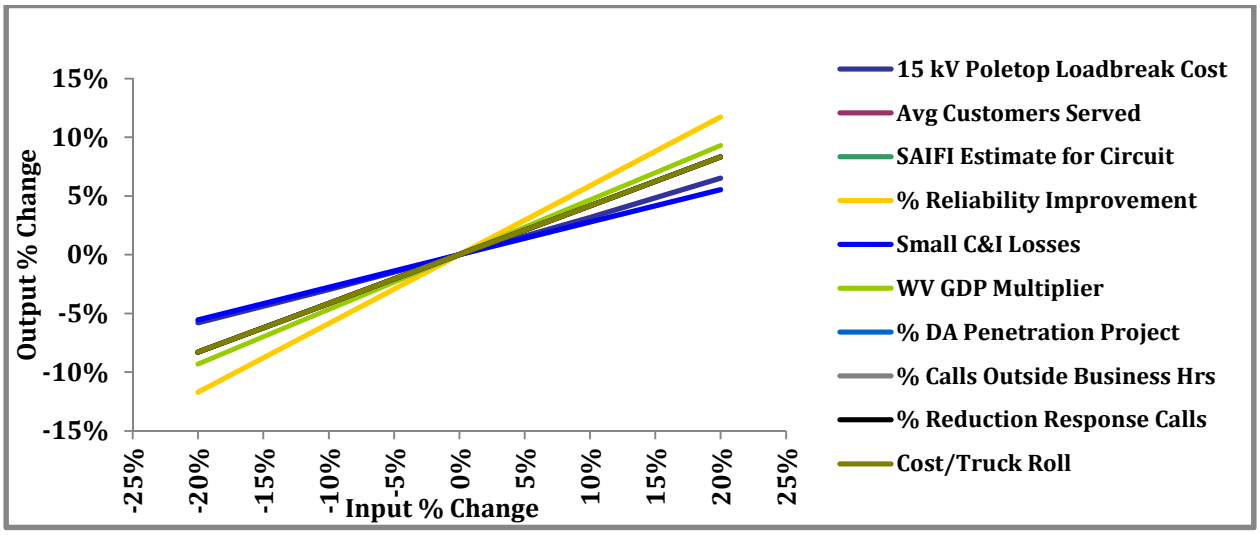

Figure F-2: FLIR-A/FLA/FPA/DER Dispatch Total Benefits / Cost Sensitivity

Detailed information regarding the types of customers and the standard industrial classifications for the C&I customers on the circuit could provide a more accurate estimate of the multiplier. As previously mentioned in the discussion of benefits, reduced restoration cost represents the highest level of benefits of overall. These benefits accrue to the Utility. Because the value of the inputs used to derive the benefit account for the top six inputs that impact the Utility's benefits to cost ratio their discussion is deferred to sensitivity analysis from the utility's perspective.

The cost of each switch was obtained from the vendor and therefore the cost estimate is not susceptible to question. As for the Small C&I customer losses, they were obtained for the ICE calculator based upon a survey used to construct a state profile. The accuracy of this estimate could be improved by adjusting the model parameters. However that would require additional information on these customers.

Consumers' Benefits to Cost Ratio Sensitivity

The benefits which have the most significant impact on the benefits to cost ratio for consumers are shown in Figure F-3. The ratio is most sensitive to changes in the percentage of reliability improvement followed by consumer losses. The remaining inputs while ranked among the top ten have little impact on the ratio.

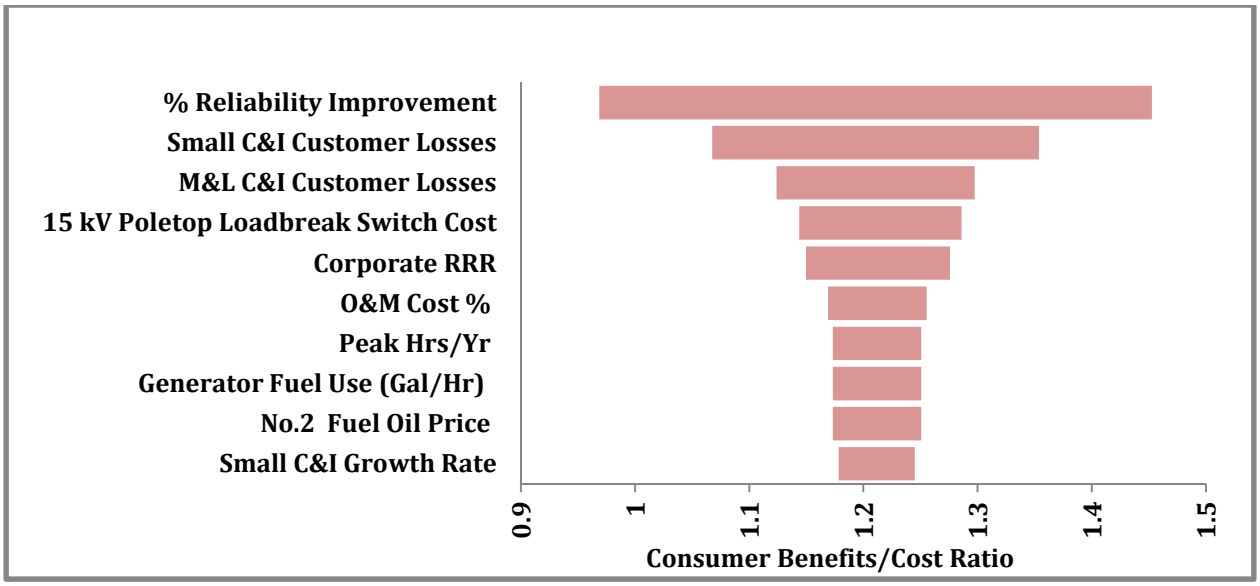

Figure F-3: FLIR-A/FLA/FPA/DER Dispatch Consumer Benefits / Cost Impact by Input

From Figure F-4 it can be seen that a twenty percent improvement in reliability is estimated to improve the benefits to cost ratio by 20 percent. It can also be seen that Small C&I and Medium and Large C&I customers impacts that result from a 20 percent increase in their respective input values results in improvements in the benefits to cost ratio of 12 and 7 percent, respectively. Keep in mind that increases in these losses represent potential savings or benefits that were assumed to be gained through reliability improvements. As stated in the previous section more accurate

estimates of these variables could be obtained with more detailed customer information. The remaining inputs while among the top ten most significant have little effect on the ratio as can been seen by the relatively flat lines representing them in Figure F-4.

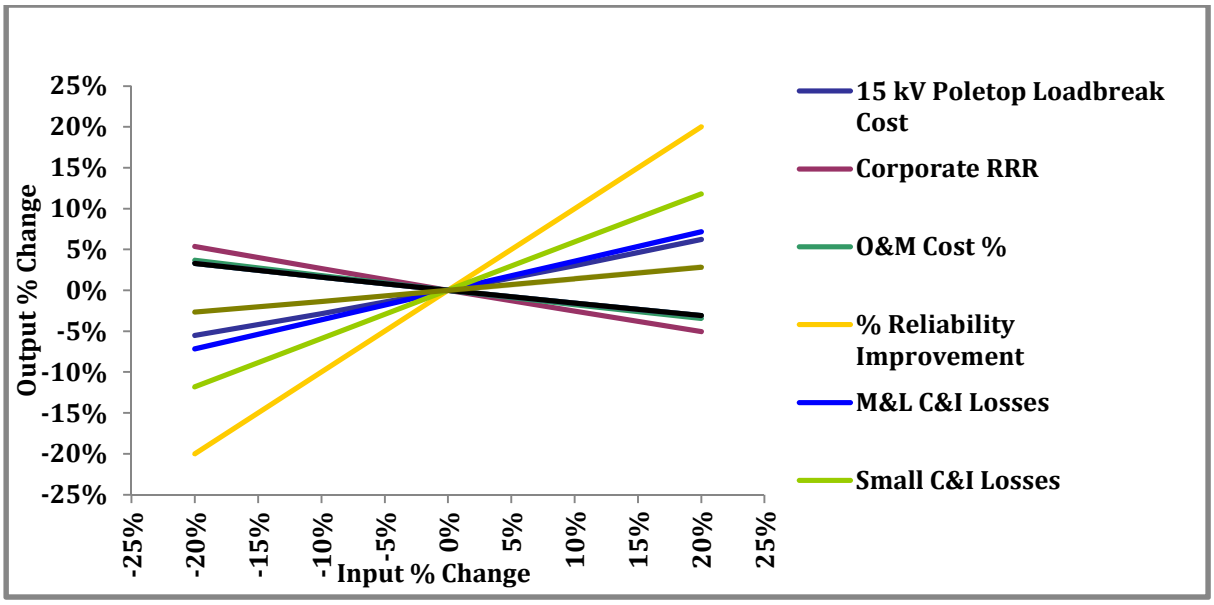

Figure F-4: FLIR-A/FLA/FPA/DER Dispatch Consumer Benefits / Cost Sensitivity

Utility's Benefits to Cost Ratio Sensitivity

From the utility's perspective, the variables associated with the calculation of the restoration cost savings are the most significant. The top six values represented in Figure G-5 were used in the calculation of this benefit. The average number of customers served and the SAIFI estimate were derived from historical data. The circuit automation was assumed to be 100 percent. The percentage of repair call outside normal business hours, percentage reduction in response call resulting from automation and the cost per truck roll were obtained from the West Virginia Smart Grid Implementation Plan due to the lack of actual data. Given the significance of this benefit additional resources should be devoted to obtain a more accurate estimate of the restoration cost savings. These inputs have a similar impact on the benefits to cost ratio as indicated by the length of the bar representing each of them. Favorable improvements in these variables can have a significant impact on the economics since a 20 percent change in their values transpires in approximately a 17 percent change in the output value as illustrated in Figure F-6.

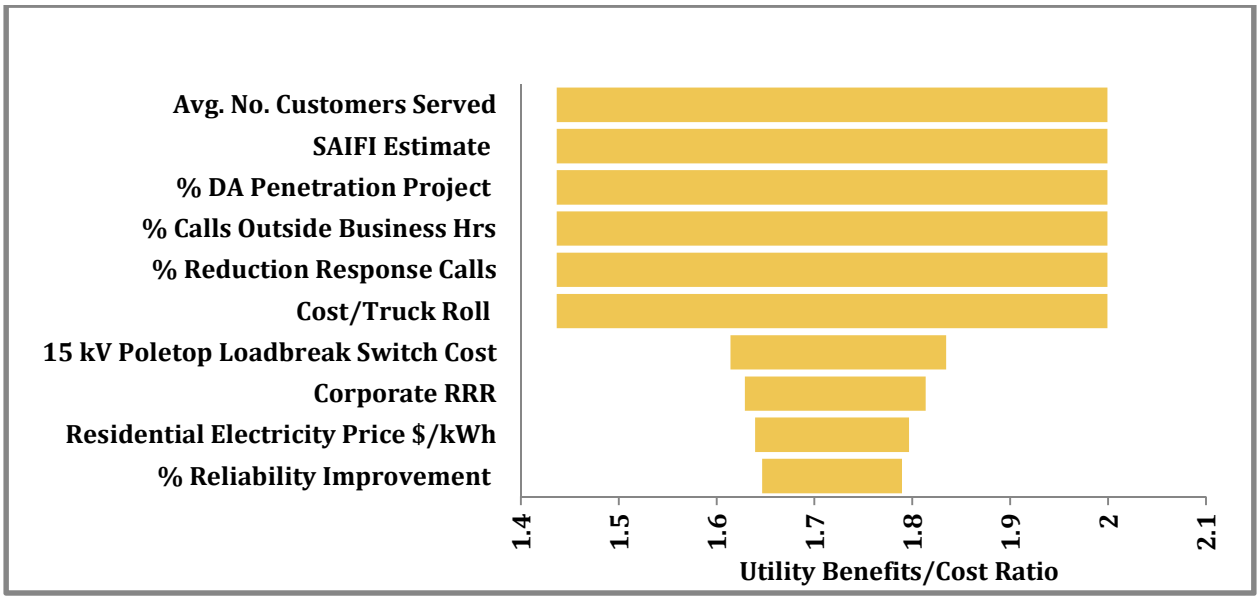

Figure F-5: Utility Benefits / Cost Impact by Input

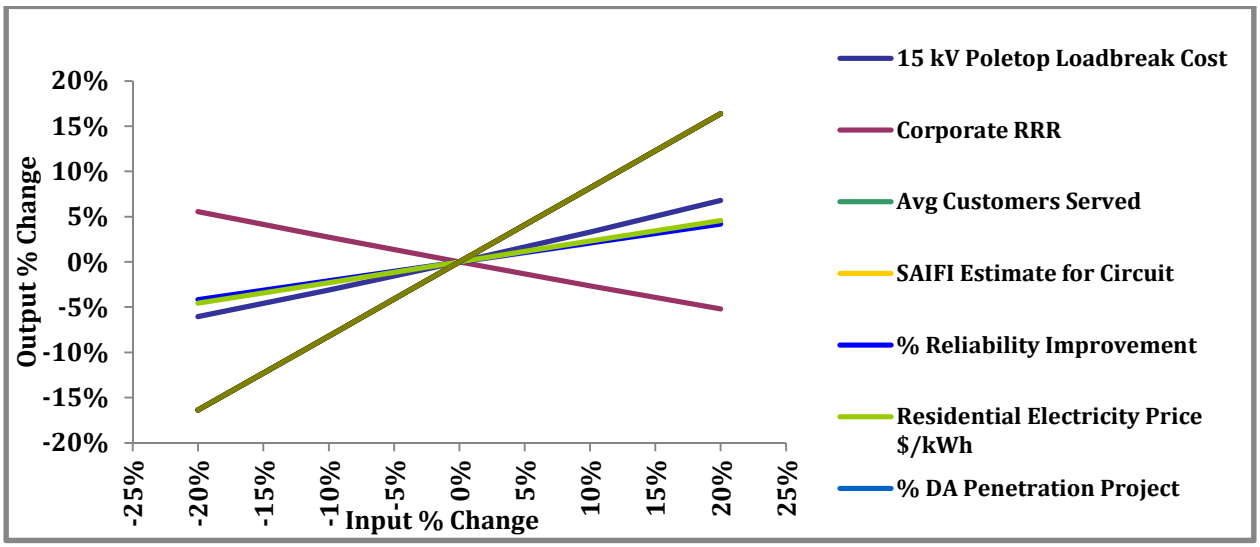

Figure F-6: FLIR-A/FLA/FPA/DER Dispatch Utility Benefits / Cost Sensitivity

Societal Benefits to Cost Ratio Sensitivity

As illustrated in Figure F-7, the multipliers used to determine the economic impacts of the savings from reliability improvements have the most significant impact on the societal benefits to cost ratio. However varying them favorably by twenty percent still results in a benefits to cost ratio of less than one. Although the project from a societal perspective may not be attractive, it is not necessarily a deterrent since the utility is the one making the investment. This simply means that there are fewer spillover benefits that the utility must try to capture. The remaining inputs have very little impact on the ratio and therefore are not addressed.

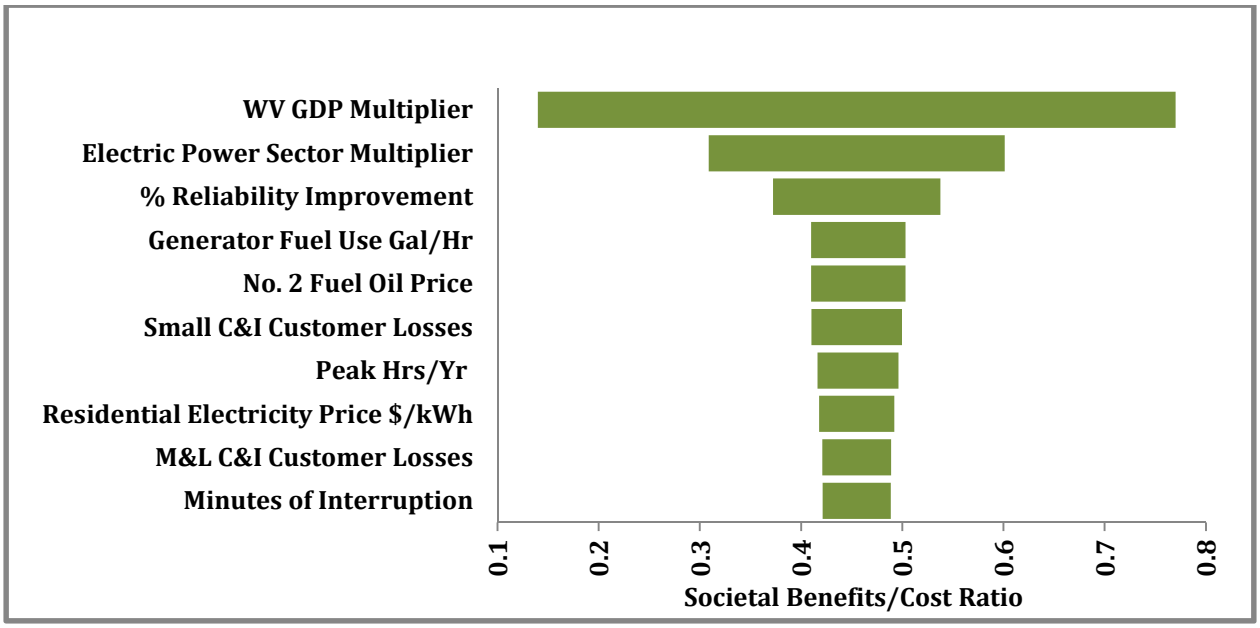

Figure F-7: Societal Benefits/Cost Impact by Input

Appendix G – Project Financial Report

Total Program Expenditures	Federal Cost Share	Mon Power Cost Share
$4,076,258.05	$2,831,452.48	$1,244,805.57

Project Cost Details

Category	Costs
Personnel	$296,963.37
Fringe Benefits	$113,569.06
Equipment	$343,300.00
Supplies	$71,281.11
Contractual	$3,249,970.02
Construction	$0.00
Other	$1,174.50
Total Direct Charges	$4,076,258.05

Appendix H - References

[1]. A. Keyhani, Design of Smart Power Grid Renewable Energy Systems, Wiley 2011

[2]. Polycrystalline PV Module 60 cells. Available at http://www.upsolar.com/usa/products/monocrystalline.aspx?type=4#135

[3]. K. Ishaque, Z. Salam, and H. Taheri, "Accurate MATLAB Simulink PV System Simulator Based on a Two-diode Model," *Journal of Power Electronics,* In Press, Corrected Proof

[4]. T. Esram and P. L. Chapman, "Comparison of Photovoltaic Array Maximum Power Point Tracking Technique," *IEEE Transaction on Energy Conversion, V*ol. 22, pp. 439-449, 2007.

[5]. Vieira, J.A.B., Mota, A.M., "Implementation of a stand-alone photovoltaic lighting system with MPPT battery charging and LED current control", *Proc. IEEE International Conference on Control Applications*, pp. 185 - 190, Pacifico Yokohama, Yokohama, Japan, Sept. 8-10, 2010.

[6]. C. Min and G. A. Rincon-Mora, "Accurate electrical battery model capable of predicting runtime and I-V performance," *IEEE Transactions on Energy Conversion,* vol. 21, pp. 504-511, 2006.

[7]. Mathworks. (2012). *Battery*. Available at :

http://www.mathworks.com/help/toolbox/physmod/powersys/ref/battery.html

[8]. A. Keyhani, "Design of Smart Power Grid Renewable Energy Systems," Wiley 2011

[9]. Mathworks. (2012) *Simplified Synchronous Machine*. Available at:

http://www.mathworks.com/help/toolbox/physmod/powersys/ref/simplifiedsynchronousmachine.html

[10]. A.P. Lopes, C. L. Moreira, A. G. Madureira, "Defining control strategies for MicroGrids islanded operation", IEEE Transactions on Power Systems, vol.21, no.2, May 2006.

[11]. Z. Jiang, X. Yu, "Active power Voltage control scheme for islanding operation of inverter-inter-faced microgrids," Proc. Power & Energy Society General Meeting, PES '09, pp. 1-7, 2009.

[12]. S. Ahn, J. Choi, "Power Sharing and Frequency Control of an Autonomous Microgrid Considering the Dynamic Characteristics of Distributed Generations", Journal of International Council on Electrical Engineering, vol. 2, no. 1, pp. 39-44, 2012.

[13]. T. Ota, K. Yukita, H. Nakano, Y. Goto, K. Ichiyanagi, "Study of load frequency control for a microgrid", Australasian Universities Power Engineering Conference, AUPEC 2007, pp. 1-6, Dec. 2007.

[14]. K. Sedghisigarchi, A. Feliachi, "Impact of fuel cells on load-frequency control in power distribution systems", IEEE Trans on Energy Conversion, vol. 21, no. 1, March 2006.

[15]. Y. Riffonneau, S. Bacha, F. Barruel, A. Delaille, "Energy flow management in grid connected PV systems with storage - A deterministic approach", IEEE International Conference on Industrial Technology, pp. 1-6, 2009.

[16]. I. Maity; S. Rao, "Simulation and Pricing Mechanism Analysis of a Solar-Powered Electrical Microgrid" IEEE Systems Journal, vol. 4, no. 3, September 2010.

[17]. A. Sinha, A.K. Basu, R.N. Lahiri; S. Chowdhury, S.P. Chowdhury, P.A. Crossley, " Setting of market clearing price (MCP) in microgrid power scenario," IEEE Power and Energy Society General Meeting - Conversion and Delivery of Electrical Energy in the 21st Century, pp. 1-8, 2008.

[18]. Weiss, "Multi-agent Systems: A Modern Approach to Distributed Artificial Intelligence", the MIT Press, 2000.

[19]. The Foundation for Physical Intelligent Agents, http://www.fipa.org

[20]. C. Sridhar, "Agent based modeling of Power Distribution system", M.S Thesis, West Virginia University, 2008

[21]. Seetaram Alwala, "Multi Agent System Based Fault Location and Isolation In a Smart Micro-Grid System", M.S Thesis, West Virginia University, 2008

[22]. Rabie Belkacemi, "Immune System Based Control and Intelligent-Agent Design for Power Systems Application", Ph.D. Thesis, West Virginia University, 2011.

[23]. Jawad Ghorbani, "A Multi-Agent Design for Power Distribution Systems Automation", Ph.D. Thesis, West Virginia University, 2014.

[24]. Chouhan, Sridhar, et al. "Smart MAS restoration for distribution system with Microgrids." *Power and Energy Society General Meeting (PES), 2013 IEEE*. IEEE, 2013.